SAND-75-0635

SPECIFIED DISTRIBUTION ONLY.

UGR Fil[illegible]
August [illegible] 1975
Sandia [illegible]

MASSIVE HYDRAULIC FRACTURE MAPPING AND CHARACTERIZATION PROGRAM

FIRST QUARTERLY REPORT: AUGUST THROUGH OCTOBER 1975

EDITED BY:
C. L. SCHUSTER, SUPERVISOR
SENSORS SYSTEMS DIVISION 5733

SF 2900-QQB(3-74)

Issued by Sandia Laboratories, operated for the United States Energy Research and Development Administration by Sandia Corporation.

NOTICE

This report was prepared as an account of work sponsored by the United States Government. Neither the United States nor the United States Energy Research and Development Administration, nor any of their employees, nor any of their contractors, subcontractors, or their employees, makes any warranty, express or implied, or assumes any legal liability or responsibility for the accuracy, completeness or usefulness of any information, apparatus, product or process disclosed, or represents that its use would not infringe privately owned rights.

Printed in the United States of America

Available from

National Technical Information Service

U.S. Department of Commerce

5285 Port Royal Road

Springfield, VA 22151

Price: Printed Copy $4.50; Microfiche $2.25

UGR File #C073/75Q4
August-Oct. 1975
Sandia Laboratories

SAND-75-0635
Specified Distribution

MASSIVE HYDRAULIC FRACTURE MAPPING AND CHARACTERIZATION PROGRAM

First Quarterly Report: August through October 1975

Edited by: C. L. Schuster, Supervisor
Sensor Systems Division
Sandia Laboratories
Albuquerque, New Mexico 87115

December 1975

ABSTRACT

The most significant event occurring during this quarter was the October '75 massive hydrofracture experiment conducted by Halliburton for El Paso Natural Gas Company at their Pinedale Well No. 5. Sandia supported this experiment with both surface and down-hole seismic arrays as well as the surface electrical potential data system.

This was the first use of the PDP-11 computer for the collection of electrical potential data.

TABLE OF CONTENTS

		Page
I.	INTRODUCTION	7
II.	BACKGROUND	8
	A. Nevada Test Site	8
	B. San Juan Basin	8
	C. Pinedale, Wyoming	8
III.	SEISMIC EXPERIMENT	9
	A. System Development	9
	B. Pinedale No. 5, October 1975	10
	C. Data Analysis	11
IV.	SURFACE POTENTIAL EXPERIMENT	15
	A. Equipment Development	15
	B. Pinedale No. 5, October 1975	15

I. INTRODUCTION

This is the first quarterly report for the Sandia Laboratories Program on Massive Hydraulic Fracture (MHF) Mapping and Characterization Program funded by the Oil and Gas Division of ERDA. This report summarizes the activities from August 1 through October 31, 1975, and also includes background information prior to this first reporting period. Previous work was also funded by ERDA and the AEC prior to its becoming a part of ERDA.

Activity occurring during this quarter is briefly described as follows:

(1) Data collected during the July 2, 1975, Pinedale No. 5 massive hydrofracture was returned to Albuquerque and data analysis commenced.

(2) The DECLAB-11/10E data acquisition system for the electrical surface potential data was received, checked out and deployed for the October experiment at Pinedale No. 5.

(3) An expanded seismic surface array was installed including a down-hole instrumentation system, and data was collected for several events associated with the October fracture.

Activities which can be expected during the next quarter (through January 1976) are as follows:

(1) Continued data analysis for both seismic and electrical data of the July and October Pinedale No. 5 fractures.

(2) Fielding of three electrical and one seismic experiment with Amoco in their Wattenberg field northeast of Denver, Colorado.

II. BACKGROUND

A. Nevada Test Site

Several hydrofracture experiments were conducted at the test site and some seismic data were collected during the spring of 1974. The experiments were conducted by Sandia's nuclear test department to study in-situ stress and fracture orientation, which was determined by mining into the area of the fracture. Seismic data was collected in a tunnel complex which was adjacent to the fracture and apparently signals associated with the fracture were recorded.

B. San Juan Basin

A second series of experiments were conducted in the San Juan Basin of New Mexico in the summer of 1974. In this gas field, hydraulic fracturing is extensively utilized in relatively shallow wells as a means of stimulation. Both surface electrical potential and seismic instrumentation techniques were deployed for evaluation of their fracture mapping capabilities. Since the main purpose of these experiments was to evaluate the instrumentation for subsequent deep-well tests, no major effort was applied to data analysis.

C. Pinedale, Wyoming

In September 1974, and July 1975, the El Paso Natural Gas Company conducted hydraulic fracturing experiments in their Pinedale unit in Wyoming. Sandia participated in these experiments again with the objective of evaluating geophysical methods for fracture location. Both seismic and surface potential techniques were applied.

Surface, subsurface and deep geophones were employed at several locations. A significant number of signals were recorded that appear to be associated with the fracturing event. Since analysis of this seismic data is extremely

complex and time-consuming, and the record electronics and transducer array used in the September exercise was not as well suited to mapping the fracture as that used in later experiments, only selected portions of that data has been studied. A more complete analysis has been deferred in favor of data from the more recent tests.

Electrical data was obtained through measurements of the surface potential gradient induced by a bipolar current pulse of 15-20 amps. Computerized analysis of the data and the development of associated numerical models is still in the initial stage. However, preliminary data analysis indicates that gradient changes did occur in the formation based on several sets of pre- and post-fracture measurements. Additional technique and equipment development for increased sensitivity along with continued field testing is required to make the surface potential measurements an operational tool.

III. SEISMIC EXPERIMENT

A. System Development

The spring and summer of 1974 were taken up entirely with obtaining and building the sensing and recording equipment for the Pinedale No. 7 fracture which took place September 1974. The seismic data collection system was characterized by wide bandwidths and dynamic range which was necessitated by the many unknowns such as signal present at the surface from the fracture and noise at the recording station due to the pumping operation. The experiment was designed to define some of the unknowns as much as it was to plot the fracture. All data was taken with logarithmic amplifiers in cased holes at various depths and distances from the fracture well.

The period of the late fall 1974 and early spring of 1975 was taken up with examining the data from the September 1974 fracture for frequency and amplitude content. As a result of this experiment it was learned that the predominant frequencies of signals believed to be fracture related in origin were low, on the order of a few hertz. The noise generated by the pumping operation was not as large as was previously feared it might be, and it appeared that very little was gained by having the instruments at several hundred-foot depths as opposed to twenty-foot holes. The late spring of 1975 was taken up with designing and preparing hardware for the second massive Pinedale fracture which finally took place at Pinedale Unit No. 5 in July of 1975. During this period all downhole amplifiers were linearized and the hardware needed for sensing and telemetering from an extensive surface array was constructed. This data acquisition system was expanded and used for a subsequent test in October 1975.

B. Pinedale No. 5, October 1975

El Paso conducted the second massive hydrofracture experiment on Well No. 5 of the Pinedale unit during October. Perforations for this fracture were at a mean depth of 10,355 feet and extended over a height of 648 feet. Prior to the operation a packer was set in the well case above the perforations used in the July operation.

The seismic instrumentation effort was very similar to that used in July with the exception that the surface array was expanded to include three subarrays of three closely spaced vertical elements, and the downhole instrumentation in water well No. 2 was expanded to include three hydrophone stations in a vertical array with 2,000-foot spacing. Emplacement of the seismic instrumentation was readily accomplished due to the fact that the surface cables and recording vans were left in place after the July exercise.

Figure 1 illustrates the physical layout of the experiment with the seismic stations and the surface potential probe (18-, 23-) locations shown.

Table I gives the exact location of each seismic site and the type of amplifier and transducer used.

Seismic data were recorded during several operational events throughout the fracture experiment. The first of these occurred on October 3 when the well case was perforated and a diagnostic pumping of 37 barrels of fluid took place. Several hours of information was recorded prior to and during the event to test the system and monitor the seismic background.

The second major event occurred on October 14 when the formation was initially broken down with a pump of 60,000 gallons of fluid.

The final exercise was on October 20 when the main fracture was pumped with a total volume of 468,000 gallons and 1,400,000 pounds of sand.

C. Data Analysis

Following the September '74 fracture at Pinedale No. 7, a considerable effort went into generating a suitable computer code to do bookkeeping and calculation of hypocenter locations once the time difference of arrivals at the various recording stations has been obtained. Time differences were obtained by computer plotting cross-correlation functions and hand-reading the times of peaks. This process was very slow and tedious, but it was accomplished for some of the breakdown data. The results were in general agreement with other mapping techniques being attempted. A problem area was identified with respect to periodicity of the correlation function which could hopefully be partially eliminated through the use of an expanded and more closely spaced monitor array.

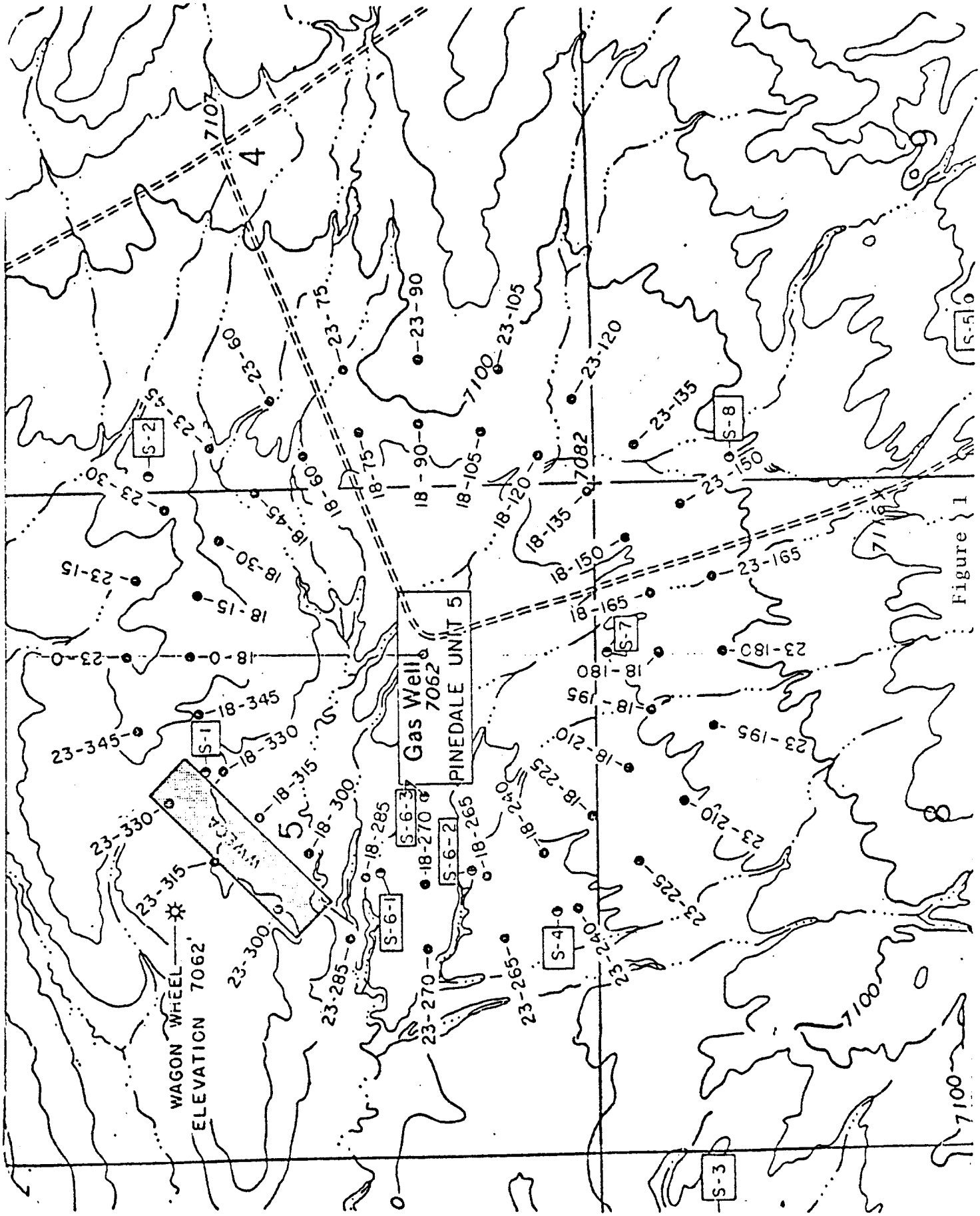
WAGON WHEEL
ELEVATION 7062'
Gas Well
7062
PINEDALE UNIT 5
S-1
S-2
S-3
S-4
S-5
S-6-1
S-6-2
S-6-3
S-7
S-8
7100
7082
23-345
23-330
23-315
23-300
23-285
23-270
23-265
23-225
23-210
23-195
23-180
23-165
23-150
23-135
23-120
23-105
23-90
23-75
23-60
23-45
23-30
23-15
23-0
18-345
18-330
18-315
18-300
18-285
18-270
18-265
18-225
18-210
18-195
18-180
18-165
18-150
18-135
18-120
18-105
18-90
18-75
18-60
18-45
18-30
18-15
18-0

Figure 1

TABLE I

SEISMIC ARRAY

SITE NUMBER	LOCATION E-W	LOCATION N-S	TRANSDUCER/ TYPE	AMPLIFIER
1	-900	1700	GEO SPACE HS-1	TELEDYNE AS-310
2.1	1400	2100	GEO SPACE HS-1	TELEDYNE AS-310
2.2	2027	2410	GEO SPACE HS-1	TELEDYNE EA-210A
2.3	1445	2799	GEO SPACE HS-1	TELEDYNE EA-210
3	-4440	-2221	GEO SPACE HS-1	TELEDYNE AS-310
4	-2000	-1000	GEO SPACE HS-1	TELEDYNE EA-210A
5	2707	-4232	GEO SPACE HS-1	TELEDYNE AS-310
6.1	-1100	0	GEO SPACE HS-1	TELEDYNE AS-310
6.2	-1706	350	GEO SPACE HS-1	TELEDYNE EA-310
6.3	-1706	-350	GEO SPACE HS-1	TELEDYNE AS-310
7.1	0	-1500	GEO SPACE HS-1	TELEDYNE AS-310
7.2	-350	-2106	GEO SPACE HS-1	TELEDYNE EA-210
7.3	350	-2106	GEO SPACE HS-1	TELEDYNE AS-310
8.1 (H)	1518	-2374	GEO SPACE HS-1	SANDIA T29769
8.2 (H)	1518	-2374	GEO SPACE HS-1	SANDIA T29769
8.3 (V)	1518	-2374	GEO SPACE HS-1	SANDIA T29769
8.4 (V)	1518	-2374	GEO SPACE HS-10	SANDIA T29769
WATER WELL (H)	-2750	2000	GEO SPACE HS-1	SANDIA T29769
WATER WELL (H)	-2750	2000	GEO SPACE HS-1	SANDIA T29769
WATER WELL (V)	-2750	2000	GEO SPACE HS-1	SANDIA T29769

During the current quarter a concentrated effort has been applied to improvement of the software support. A process of cross-correlating the seismic signals at two monitoring stations and then locating peaks in the correlation in order to find the time difference of signal arrival at the stations was automated on the 6600 computer system. This routine has been interfaced with locally developed software to check data consistency and to calculate hypocenter location resulting in a first-cut at completely automating the data reduction process from digitized data to location plotting. Although this process involves some rather simple procedures which may later need refinement, it does allow the handling of all the available digitized data in a short period of time. Four station data filtered to 10 Hz can be converted to locations at the rate of 10 minutes computer time per hour of analog data.

The problem of location images generated by data periodically, which was noted earlier in the hand-reduced Pinedale No. 7 data, has been found to exist with all of Pinedale No. 7 and No. 5 data which has been currently digitized. The most recent data reduction efforts have centered on finding some means of reducing this problem. Automated processing makes it possible to vary the criterions for accepting time differences for location calculation and seeing the effect on the plotted result. It also makes possible the handling of much larger quantities of data for trial situations.

Seismic data reduction efforts during October were slowed considerably since most of the project personnel were at the field test site.

Most of the data reduction and analysis activities have been centered on the breakdown data from the July experiment. Through examination of this data some problem areas have been identified in the automated reduction process which are currently being corrected.

IV. SURFACE POTENTIAL EXPERIMENT

A. Equipment Development

During the conceptual stages of the electrical experiment the potential data was collected sequentially from the pairs of potential probes. The September '74 Pinedale No. 7 fracture indicated that this technique had the possibilities of indicating the orientation of the fracture from the surface. Prior to the July '75 fracture the hardware was assembled that allowed all potential data to be collected simultaneously. Data from this fracture could not be analyzed in the field and was returned to Albuquerque. Later analysis indicated that the activity around the well-head greatly affects the potential field data.

B. Pinedale No. 5, October '75

An analog-to-digital converter with a PDP-11 computer was utilized to collect and analyze the potential data in the field in real-time for this experiment. This was the first experiment conducted by this organization in which a computer was used in the field to collect and analyze data. Discrepancies in the data collection system were discovered and corrected much faster than had been possible previously. Two specific examples were: 1) open wires caused by gnawing varmints (ground squirrels, etc.) and 2) a slow but intolerable drift in some of the potential measurements caused by the porous copper sulphate pots used initially for the potential probes.

The surface potential data was measured by 24 pairs of probes placed in a circular array around the wellhead at 15-degree spacings. The inner probe was 1800 feet from the wellhead, the outer probe was 2300 feet from the wellhead. A potential field was created by forcing current through the soil by connecting a current source between the well casings of Pinedale No. 5 and Pinedale No. 1. The potentials detected

by each of these probes were amplified and fed to a voltage controlled oscillator (VCO). Two coax cables with 12 multiplexed VCO's each (A-string and B-string) carried the data to the instrumentation van. The van contained twelve discriminators, the PDP-11 computer with analog multiplexer and A/D converter, and other associated equipment. The van also contained the current source.

During periods of interest, potential measurements were taken at regular intervals. Each time a potential measurement was taken the analog data was digitized and stored on disk in the PDP-11 computer. Figure 2 is a typical printout of one of the test measurements. This is only one sample of the over 180 sets of data that was collected. It contains the basic test information such as test, time of day, and the resistance table which is the normalized potential gradients.

Subsequent measurements taken on any day were normally compared to the first measurement of the day in order to identify trends or discrepancies in the data. Also a number of measurements were often averaged and compared to other sets.

The results thus far are inconclusive. Further analysis and modeling on the CDC 6600 may be required to determine the validity and practicality of the experiment.

```
RUN

PINDAL  18-OCT-75  BASIC V01-05

18-OCT-75

PINEDALE NO. 5 - BACKGROUND FOR HYDROFRACTURE NO. 2

TIME OF DAY:     ?11:45

DATA STRING:     ?0

TEST NO:         ?137

NUMBER OF BATTERIES:     ?5

DELAY TIME =  1 SECONDS
TIME BETWEEN SAMPLES =  8.333 MILLISECONDS
NUMBER OF SAMPLES =  20 PER CHANNEL

IF READY TYPE Y     ?Y
P1
N1

DATA FILE:  PINDAL.DAT

P1 VOLTS = 148.292
P1 AMPS = 9.39072
P1 VALUES
 41150        41134        33269        25333
 19073        14416        11983        22069
 19986        19819        22076        13438
 16340        18999        22481        21254

N1 VOLTS =-145.132
N1 AMPS =-9.05495
N1 VALUES
 40972        40976        48376        56254
 73968        62884        61885        73483
 66720        63854        68465        68501
 67111        69131        70213        71913

RESISTANCE TABLE
 3.63375      3.20831      3.30324      3.40332
 3.09353      2.91487      3.0707       3.64487
 3.36076      3.31846      3.15959      3.35335

READY
```

Figure 2

Org.	Bldg.	Name	Rec'd by*	Org.	Bldg.	Name	Rec'd by*

*Recipient must initial on classified documents.

SAND-77-1992
UNLIMITED RELEASE

Annual
Part 1

UGR-C073

ENHANCED GAS RECOVERY PROGRAM
SECOND ANNUAL REPORT - PART I
OCTOBER 1976 THROUGH SEPTEMBER 1977

EGSP
OPEN FILE # 073 9-77

D. A. NORTHROP AND C. L. SCHUSTER, EDITORS

Prepared by Sandia Laboratories, Albuquerque, NM 87115 and Livermore, CA 94550 for the United States Department of Energy under Contract AT (29-1)-789

PRINTED APRIL 1978

Open File
073/A77
Part I

SAND-77-1992

Unlimited Release

ENHANCED GAS RECOVERY PROGRAM
SECOND ANNUAL REPORT - PART I*

October 1976 through September 1977

ABSTRACT

Massive hydraulic fracture mapping field experiments continued in FY 77 with Sandia participating in fractures with G.P.E., Amoco, Shell and Conoco. The surface electrical potential system has demonstrated that the fracture orientation can be determined to within ± 5 degrees and has clearly shown that most fractures are asymmetrical. This system has been completely documented and has had wide exposure to the industry providing for the transfer of its technology. Improvements in the electrical system, its analytical model and the development of new systems for fracture diagnostics was also continuing.

Hydraulic and explosive fracturing experiments have been conducted adjacent to an existing tunnel complex at DOE's Nevada Test Site and have been directly observed by subsequent mineback activities. Evaluation of a proppant distribution experiment has revealed a very complex fracture system which differed significantly from design; additional in situ stress and material property measurements are being made to quantify observed behavior. An experiment has been designed and

* Part II of this publication is a separate volume and contains all the Appendices referred to in this publication, Part I.

conducted which will examine hydraulic fracture behavior at a geologic interface between formations with significantly different moduli, Poisson's ratios and porosities; mineback evaluation will occur next year. In conjunction with a nuclear containment program, the stresses surrounding a contained explosive detonation have been examined. A 256 lb TNT detonation produced no radial fractures extending from the main cavity, but gases escaping down a borehole did create a 30 x 75 ft fracture in a region of reduced overburden stress caused by the explosion.

Specific aid was provided in the planning and development of the Western Tight Gas Sands Project and DOE's Enhanced Gas Recovery Strategy Plan. A resource survey of the Greater Green River Basin was conducted as part of the latter activity.

TABLE OF CONTENTS

		Page
I.	Introduction and Summary	2
II.	Instrumentation Systems Development	6
	A. Surface Electrical Potential Method	6
	B. MHF Mapping Experiment Results	13
	C. Electrolytic Model Tank	29
	D. NTS Seismic Recording	43
	E. Borehole Seismic System	48
III.	Mine Back Stimulation Test Program	52
	A. G-Tunnel Site and Mine Back Operations	52
	B. Proppant Distribution Experiment: Hole 5	57
	C. Formation Interface Experiment: Hole 6	65
	D. Fracture Calculations	74
	E. Containment Program Activities	74
IV.	Additional Enhanced Gas Recovery Activities	78
	A. Green River Basin Resource Evaluation	78
	B. Program Planning	80
V.	Publications, Presentations and Other Communications	82

I. INTRODUCTION AND SUMMARY

Sandia Laboratories conducts two projects which are part of the United States Department of Energy's (DOE) Enhanced Gas Recovery Program. One is the Massive Hydraulic Fracture Characterization Project whose objective is to develop instrumentation systems for characterizing fracture systems, formations and other parameters contributing to enhanced gas recovery. The other is the Mineback Stimulation Test Project whose objective is to understand, and thus improve, fracturing processes for stimulation of natural gas production from low permeability formations which contain a high potential resource. This report summarizes activities conducted under these two projects during Fiscal Year 1977: October 1, 1976 through September 30, 1977.

The Massive Hydraulic Fracture Characterization Project began in 1974 with the initial application of Sandia's instrumentation capability in a joint experiment with El Paso Natural Gas in the Pinedale Field, Green River Basin, Wyoming. The initial effort was an attempt to measure the orientation and growth of a massive hydraulic fracture using both surface seismic recording and electrical potential mapping techniques. In the ensuing years, the surface seismic program has been discontinued because of its inability to map fractures from the surface. The electrical potential technique has grown and has been fielded on several experiments over the past three years. This instrumentation system has been deployed on both joint DOE-industry funded and private industry experiments on a non-transfer of funds basis. These experiments have covered a range of stimulation techniques in natural gas, petroleum and tar sands recovery.

The electrical potential technique is based upon the surface measurement of potential changes caused by a changing current electrode geometry. The current electrode is the fracture well and the conductive frac fluid introduced into the subsurface formation causes the geometry to change during the fracture operation. These potential changes are small and require extensive data collection and analysis to ascertain fracture orientation. Model calculations aid in the interpretation of fracture orientation and symmetry.

Recent program activities have focused upon the continued development and application of the surface electrical potential technique as well as a broadening of scope to develop other instrumentation systems

and techniques for characterizing geological features such as sand lenses and natural fracture systems, effects due to different stimulation processes, and other factors affecting enhanced gas recovery. A continuing close relationship with industry is anticipated in these activities.

The Mineback Stimulation Test Project was initiated in FY77. However, the program has built upon fracturing and mineback activities which have been conducted since 1974 in G-tunnel, at the Nevada Test Site, as part of a nuclear containment program sponsored by the Division of Military Applications under ERDA. The commonality of objectives between the containment and enhanced gas recovery activities is striking and the continued close relationship between the two programs will be mutually beneficial.

Various stimulation techniques have been applied to the so-called unconventional natural gas resources, such as the western tight sands basins and the eastern Devonian shale formations, with varying, but generally non-economic, results. Massive hydraulic fracturing (MHF) as being practiced is based upon extensive "conventional" fracturing experience, laboratory testing, and empirical design models; the extrapolation to the massive scale has not been generally successful. Dendritic, foam, gas and chemical explosive fracturing techniques have been applied and successes or failures are not well understood. Industry has often stated the need to perform experiments in an environment which allows for direct examination and evaluation.

Mineback evaluation provides this opportunity. A detailed physical description can be obtained directly and which can be correlated with measured geologic material properties, in situ stress distributions, fluid behavior, and the operational parameters of the test. Supportive rock and fluid mechanics laboratory and modeling work will be performed to aid in this interpretation. The mineback also provides the opportunity for the calibration of instrumentation techniques under known conditions. Thus, mineback testing provides significantly more information than the evaluation of a commercial stimulation job which is based primarily upon gas production. Industry and service company participation in the program will ensure that the results will impact the experience and knowledge base used in production; such industry interest has been high. The program will provide a unique opportunity to quantify and understand fracture behavior.

Sandia's projects derive their support from both the Eastern Gas Shales Project and Western Gas Sands Project which are major parts of DOE's Enhanced Gas Recovery Program. Sandia's projects provide a broad supporting research and development capability. Activities are planned, conducted, and reported with the aim of contributing to the objectives of both the Eastern and Western Projects and to the overall development of Enhanced Gas Recovery technology.

The surface electrical potential experiments have covered a wide range of testing situations and have undergone a more intensive analytical study. Sandia participated in fracturing experiments with G.P.E., Amoco, Shell and Conoco. Documentation was completed for the electronic system and several presentations of its capabilities have been made facilitating the transfer of this new technology to industry. For reservoir planning and well placement, the system has demonstrated that fracture orientation can be determined to $\pm$ 5 degrees and that most fractures are asymmetrical. Mapping experiments included 1) a very shallow test for model verification, 2) an enhanced oil recovery fracture, 3) a very tight gas sand, and 4) two Mesa Verde multi zone fractures. Each of these experiments contributed to our overall understanding of the capabilities and limitation of the surface electrical potential technique. Formalization of the analytical work, coupled with an in-house model facility, was initiated and should lead to an even better understanding of these field results. Hole 6 fracture experiment at NTS was instrumented with a seismic recording system and produced several seismic signals during pumping. The analysis of this data could reveal not only fracture locations but the nature of the source mechanisms. Extensive analysis of this data will be persued in FY 78 both in-house and with consultants. The receiving of seismic signals associated with fracturing increases our expectations for the borehole seismic system that currently is under development.

The mineback experiments have provided considerable information during the past year. Fracture evaluation methods have been demonstrated and local geological descriptions have been developed. Mineback evaluation of a propped hydraulic fracture experiment indicated a very complex fracture system was created. Observed fracture lengths were only 5 and 25 ft at the depth of the fracture interval which differs significantly from the design length of 175 ft. The top of the fracture has

been delineated and fracture growth must be downwards. No distinct patterns of the different colored proppant were found. Examples of interactions of the fracture with faults and formation bedding are numerous. Additional material property and in situ stress data in this region are being obtained. An experiment to examine the behavior of hydraulic fractures at an interface between different geologic formations has been designed and the first of two fractures has been created. The ashfall tuff and the welded tuff have significant differences in their elastic moduli (0.24×10^6 and 3.8×10^6 psi), Poisson's ratio (0.312 and 0.238) and porosity (45 and 13%). Conventional fracture calculations were used to design fractures of 50 ft height and 600 ft total length. Evaluation will occur next year. In a containment program activity, evaluation of the region surrounding a 256 lb TNT detonation indicated that no radial fractures extended from the main cavity. However, explosive gases escaping along a borehole from the cavity produced a fracture estimated at 75 ft high in the region of altered in situ stress approximately 10 to 40 ft from the cavity.

Contributions were also made to the development of the Management Plan for Enhanced Gas Recovery and in the Program Plan for the Western Gas Sands Project. A resource evaluation of the Green River Basin was conducted as part of these efforts.

II. INSTRUMENTATION SYSTEMS DEVELOPMENT (C. L. Schuster, Editor)

A. Surface Electrical Potential Method[1]

The surface electrical potential data are taken by periodically recording the potential difference at the earth's surface between 24 data probes, placed every 15° circumferentially around the fracture well, and a reference probe. This potential field is created by injecting electrical current flow through the earth between the fracture well and a return or sink well (Fig. II-1). The current is of a pulse form and the direction is reversed during each measurement period to minimize the effects of induced polarization. The current pulse generator is earth isolated. Electrical connections are made directly to the casings of the fracture and sink wells. Prior to hydraulic fracture initiation, background data are taken to establish the potential levels around the fracture well at the 24 data probes. This then becomes the reference data levels for detecting the changes produced when the conductive fracture fluid alters the electrical geometry of the fracture well. This change in the fracture well current distribution, caused by fracture growth, alters the surface electrical potential around the fracture well. The change influence on the surface potentials tend to be greatest in and opposite the direction(s) of the fracture orientation and is the basis of this development effort.

The instrumentation[2] layout around the fracture well (Fig. II-2) represents the present usage. This layout has evolved from early experiments. Changes which have been made include the replacement of the outer probe by the reference circle. This reference circle is an electrical conductor having the same layout radius as the data probes. The reference circle is connected to the reference probe located a distance of 5 to 10 times the data probe radius from the fracture well and in a direction usually opposite the sink well. This type of layout yields the same basic information but greatly simplifies the fracture well instrumentation set up since only half as many data probe sites need to be surveyed and placed. The data probe radius ranges from 1000 to 1800 ft and is determined from

1. Bartel, L. C., McCann, R. P., Keck, L. J., "Use of Potential Gradients in Massive Hydraulic Fracture Mapping and Characterization," SPE 6090, presented at the SPE 51st Annual Fall Meeting, New Orleans, October 3-6, 1976.

2. Keck, L. J., and Seavey, R. W., "Instrumentation System for Massive Hydraulic Fracture Mapping," SAND-77-0195, April 1977.

a mathematical model[1] which considers such parameters as fracture depth and expected fracture length(s). The instrumentation van is usually placed at a radius approximately equal to the data probe radius and can occupy any one of 24 positions around the fracture well. The location is usually determined, however, by the fracture well access road location.

The instrumentation to sense and transfer the 24 data source pair potentials to the instrumentation van is broken into two parts referred to as the A string (A1 through A12) and the B string (B1 through B12). The electrical potential between each data probe and the common reference circle is input to a Potential Measurement Box (PMB). Each data probe potential source undergoes earth reference isolation, passband limiting, gain, and impression on a FM multiplex subcarrier. The 12 different subcarriers are mixed in a common data cable (A string) for transfer to the instrumentation van. The B string is a duplicate of the A string. The A and B string data cables, in addition, transfer DC power to the PMB's from the instrumentation van.

The 24 data probe potentials are implicitly earth related and some special isolation hardware is necessary to insure against the unintentional relocation of the reference probe. This is accomplished by the isolation amplifier in the PMB whose output has no electrical common tie to the reference circle but is electrically connected to all of the remaining hardware of the data system. The PMB has a passband of .001 to 10 HZ and calibrated gains of 1, 3, 10, 30, 100, 300, and 1000 can be selected. The gain required is dependent on well geometry, data probe radius from fracture well, distance to the reference probe, and pulse current injection level. After undergoing the necessary gain, the surface potential is input to a Voltage Controlled Oscillator (VCO). This FM carrier is combined with the other carriers.

The coaxial cables from the A and B strings enter the instrumentation van from opposite halves of the fracture well circle and connect to the power multiplex filters. These filters route the two sets of 12 incoming carriers to the FM subcarrier discriminators and connect the DC power onto the A and B string cables. The output from each of the 24 discriminators is connected to one of the 64 channels of the analog multiplex portion of the Laboratory Perhipheral System (Fig. II-3). The voltage and current monitor terminals of the pulse current generator are also input to the L.P.S.

1. Bartel, L. C., "Model Calculation of the Potential Gradients Used in Massive Hydraulic Fracture Mapping and Characterization," presented at the 46th Annual International Meeting of the Society of Exploration Geophysicists, Houston, TX, October 24-28, 1976.

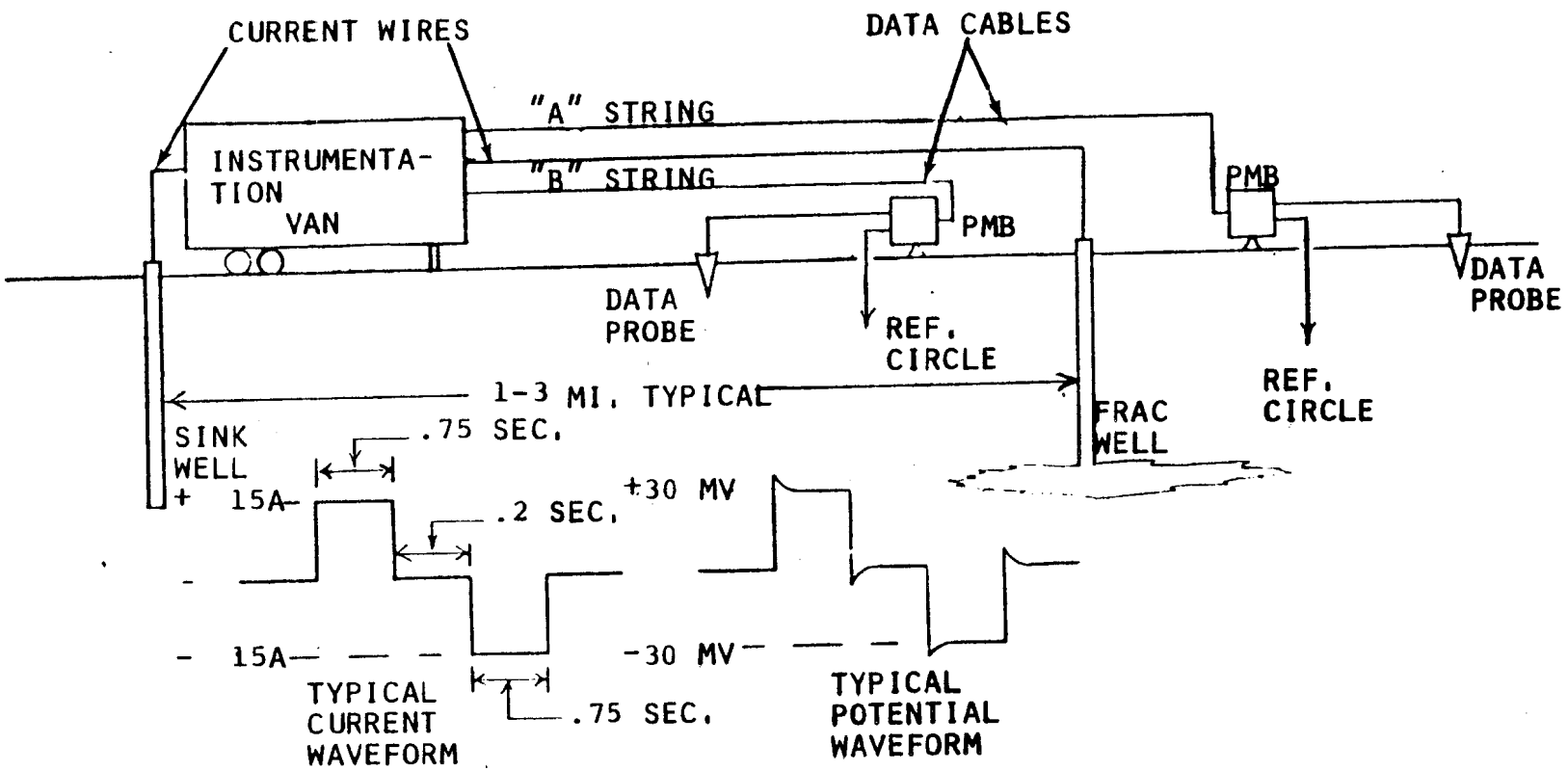

Fig. II-1 - Equipment Layout and Typical Current and Potential Waveforms

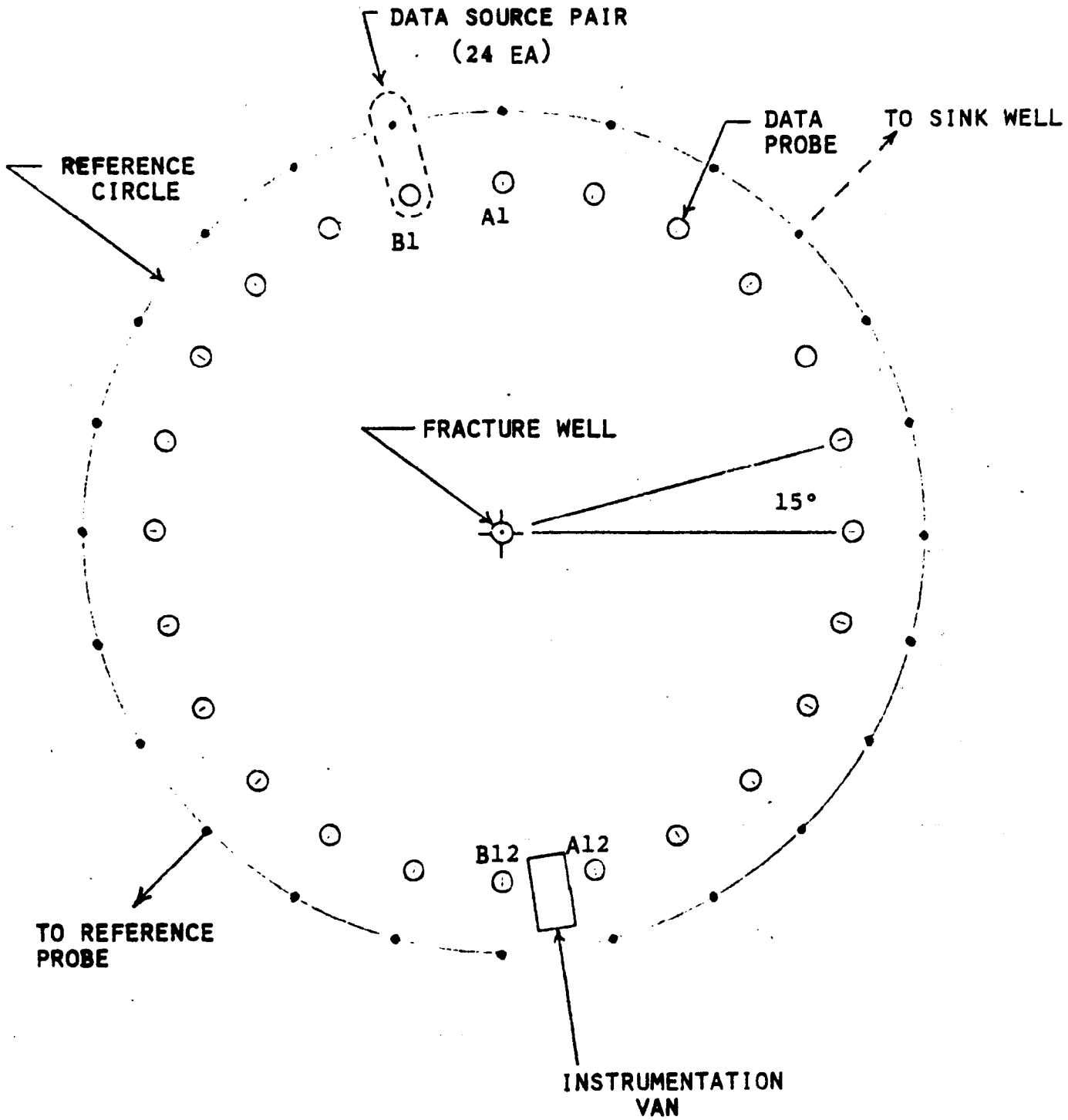

Fig. II-2 - Instrumentation Layout Around Fracture Well

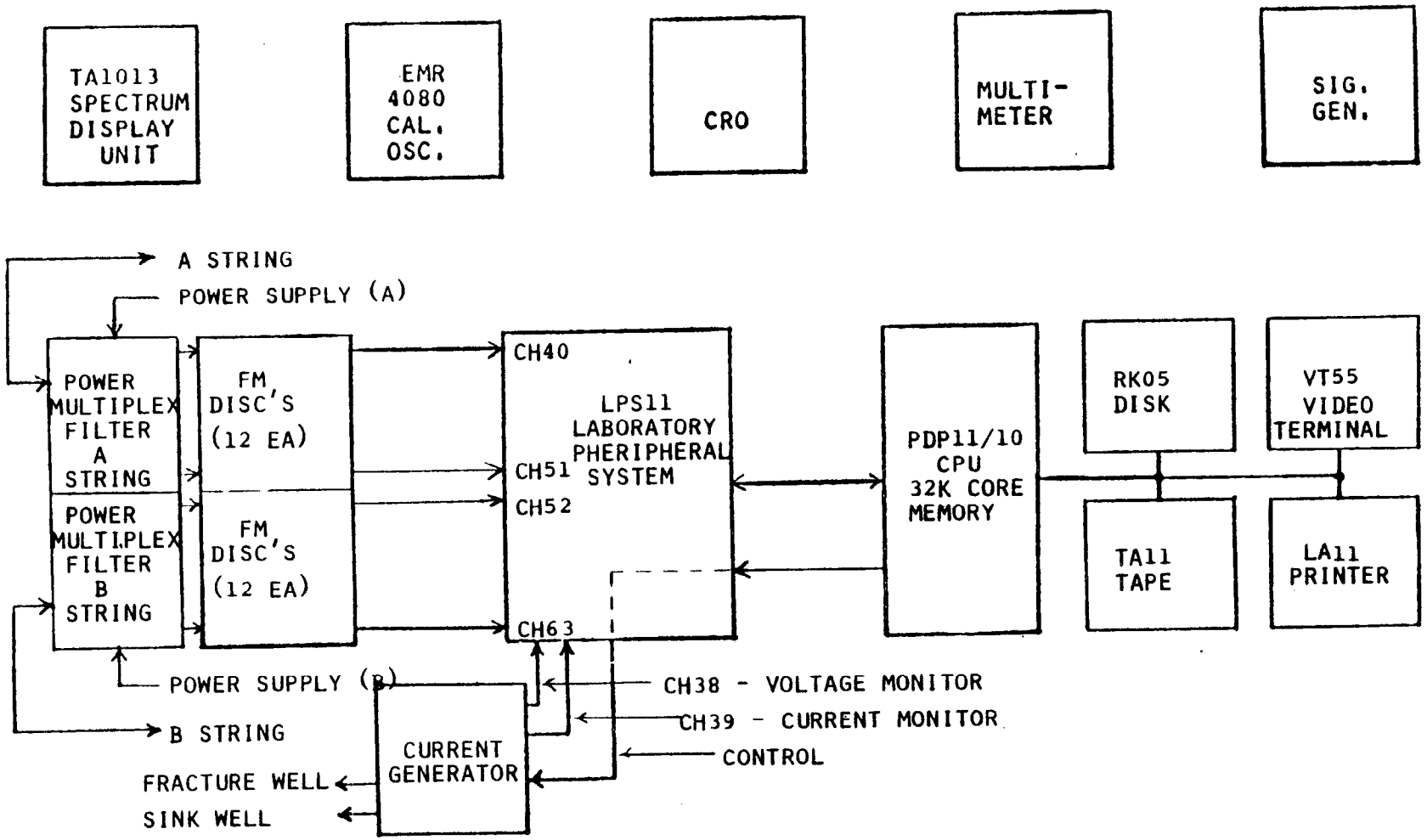

Fig. II-3 - Instrumentation Van

The heart of the current pulse control and data acquisition system is a PDP 11/10 minicomputer with a 32 K core memory. The minicomputer operates under the RT11 operating system and all application programs are written in BASIC.

In a typical fracture mapping test start up, the appropriate data acquisition program is called from the RK05 disk into memory. An example is LARFR1 BAS (Laredo, Texas fracture, version 1 in BASIC), Fig. II-4. The test run is initiated and certain special conditions such as test number, start time, time between tests and the PMB located at north are input to the VT55 computer console. The test number may be the first

```
26-AUG-77
STATE OF DATA RUN
FIELD BOX GAIN:  30
VOLTAGE MONITOR GAIN:  HI
CURRENT MONITOR GAIN:  HI
START TIME:  630
TIME BETWEEN TESTS (MINUTES):  1
POTENTIAL MEASUREMENT BOX AT NORTH IS A3
NOTE:  LIVE RUN, 2ND DAY

TEST NO.  283              TIME:  6:30:26
VOLTS =   185.677    AMPS =  19.3081     RESISTANCE = 9.61651
VOLTS =   179.705    AMPS = -18.9862     RESISTANCE = 9.46503
POTENTIAL, MILLIVOLTS (A1 > A2 & B12 > B1)
 55.8591     54.4213     55.0574     52.153     49.6034     47.8003
 49.5824     51.6115     54.8261     56.0168    57.3862     61.0344
 62.3854     62.8585     64.7536     62.9505    71.0828     68.2441
 69.8764     67.7001     69.4112     59.8096    67.2585     61.0134

U S G S SURFACE TILT DATA - A/D VALUES
 2051   2051   2052   2051   2707   2246      0   1959   4095   3387   2843
 2031   2128   1872   2048   2047   2148   1436   2046   2047   2047   2047
 2664    545

PRESSURE & FLOW DATA, MV. - AC LINE, VOLTS
 50.7813    -87.8908     2.68555     -1.62761     122.607
```

Fig. II-4 - Computer Printout Example

test of a series or it may be a number appropriate after some fracture procedure shut-down and restart. Start time is that future time, one minute or several hours from the present time, when the automated test sequence is to start (the computer has an internal 24 hour clock). Time between test sets the test repetition rate with a range of 30 seconds to several hours. The instrumentation van can be located in any one of 24 positions around the fracture well. When plotting on the VT55 video terminal it is a convention to begin the plot with north and proceed

clockwise through east, south, and west back to north. Since the data is not necessarily acquired in this sequence, the "PMB at North" console input is used to rotate the data before plotting. These input conditions are then echoed on the LA11 printer and the software enters the phase of pulsed current application and simultaneous acquisition of the 24 PMB, pulse current, and pulse voltage data values. The peak-to-peak potentials in millivolts input to each PMB is computed using gain correction factors for each PMB data channel. The millivolt level data is written into a data file on the RK05 disk for future evaluation and then listed on the LA11 printer. When the time delay specified by "time between tests" has elapsed, the sequence will repeat with the application of another current pulse.

The surface potential data written onto the RK05 disk can be accessed for many special purposes. Programs to plot this data on the VT55 video console have been written. One such program will compress the fracture time of several hours into a few minutes and quickly indicate fracture progress and direction, if detected. Another program plots the changes in potential at each of the 24 PMB's in reference to time on the LA11 printer.

All of the computer software written for use with the surface electrical potential method of fracture mapping is constantly undergoing changes and improvements. This applies to the hardware as well. These changes are dictated by field experience and the evaluation of the surface electrical potential data in conjunction with other related data sources.

B. MHF Mapping Experiment Results

During FY'77, Sandia Laboratories participated in five MHF experiments and was preparing for a sixth for natural gas and oil recovery stimulation. The first of these (near Tulsa, Oklahoma) was a joint AMOCO/ERDA mini-frac experiment with AMOCO conducting the fracture and Sandia and the USGS participating in the fracture diagnostic instrumentation. Gas Producing Enterprises (GPE) conducted two experiments in the Natural Buttes field south of Vernal, Utah, and a fourth was conducted by CONOCO as a part of their tertiary oil recovery experiment in the Big Muddy field east of Casper, Wyoming. The fifth MHF test was conducted by Shell Oil Company near Laredo, Texas. Preparation was also started for an experiment with AMOCO in the tar sands of Canada.

AMOCO Mini-Frac Experiment -- On November 4, 1976, AMOCO Production Company conducted a small scale hydrofracture experiment located on the Williams Lease site approximately five miles northeast of Tulsa, Oklahoma. The purpose of the experiment was to test various methods of hydrofracture mapping instrumentation. The fracture well was approximately 80 feet depth with an open hole fracture zone in shaly limestone between 40 and 80 feet. The experiment was designed to produce a fracture 40 feet high and 600 feet in length.

The surface electrical potential data was taken by recording the potential differences between 24 pairs of probes placed circumferentially around the test well with an inner probe radius of 150 feet and an outer probe radius of 350 feet. The current pulse was induced directly into the wellhead (source) at the surface of the earth.[1] The return line (sink) was attached to the casing of an abandoned test hole located approximately 1400 feet distance from the test well. Data readings were taken every two minutes from prior to pumping until after flowback. Sandia also digitized and recorded the USGS data on the mini computer concurrently with the potential data.

Surface potential data were recorded prior to, during, and after pumping. Pumping for the fracture occurred in two stages. The first commenced at 0828 hours and stopped at 0842 hours. The second started

[1] L. J. Keck and R. W. Seavey, "Instrumentation System for Massive Hydraulic Fracture Mapping", SAND-77-0195, April 1977.

at 0910 hours and continued until 1002 hours. A constant rate of 2 bbl per min was held for both stages.

The data for the operation are presented in Table I, Appendix A. The electrical potential data was taken at approximately two-minute intervals beginning at 0540 hours and continuing through 1324 hours. Approximately 25 data points taken prior to pumping were averaged and used as the before fracture reference measurement. Figure II-5 shows the potential comparison, V(θ), for data points taken at the noted time points beginning early in the fracturing sequence through its completion at 1000 hours. The potential comparison, V(θ), was multiplied by a factor of 10 in order to facilitate computer plotting. The data appear to provide a one-cycle change in the normalized potential differences, thus indicating an asymmetrical fracture was created. When compared with the model calculations[2] the cycle minima appears to lie in the easterly direction, indicating that the fracture is asymmetric with the major wing in that direction. Data taken from the downhole TV camera and the USGS tiltmeters seem to verify this conclusion.

GPE Experiments --

1. Natural Buttes Unit No. 14 -- Sandia participated in the GPE MHF experiment in the Natural Buttes No. 14 well located approximately 40 miles south of Vernal, Utah. The MHF was performed by Dowell for GPE.

The MHF experiment was designed for eight stages of pad, proppant, and balls to fracture 15 zones. The intention was that each stage would treat two zones. At the end of each stage balls would seal the perforation taking fluid and new zones would then be treated.

The fracture zones for the experiment began at a depth of 6294 feet and extended to 8010 feet. The pay interval varied in thickness from 8 feet to 38 feet and the separating shale layers varied from 4 feet to 250 feet. Natural Buttes #14 is an "old" well. Breakdown on the first 12 zones, extending in depth from 6825 feet to 8010 feet, occurred on October 10, 1976 with 10,000 gallons of 15% HCl in 500 gallon stages.

[2] L. C. Bartel, "Model Calculations of the Potential Gradients Used In Massive Hydraulic Fracture Mapping and Characterization," presented at the 46th Annual International Meeting of the Society of Exploration Geophysicists, Houston, TX, October 24-28, 1976 (submitted for publication).

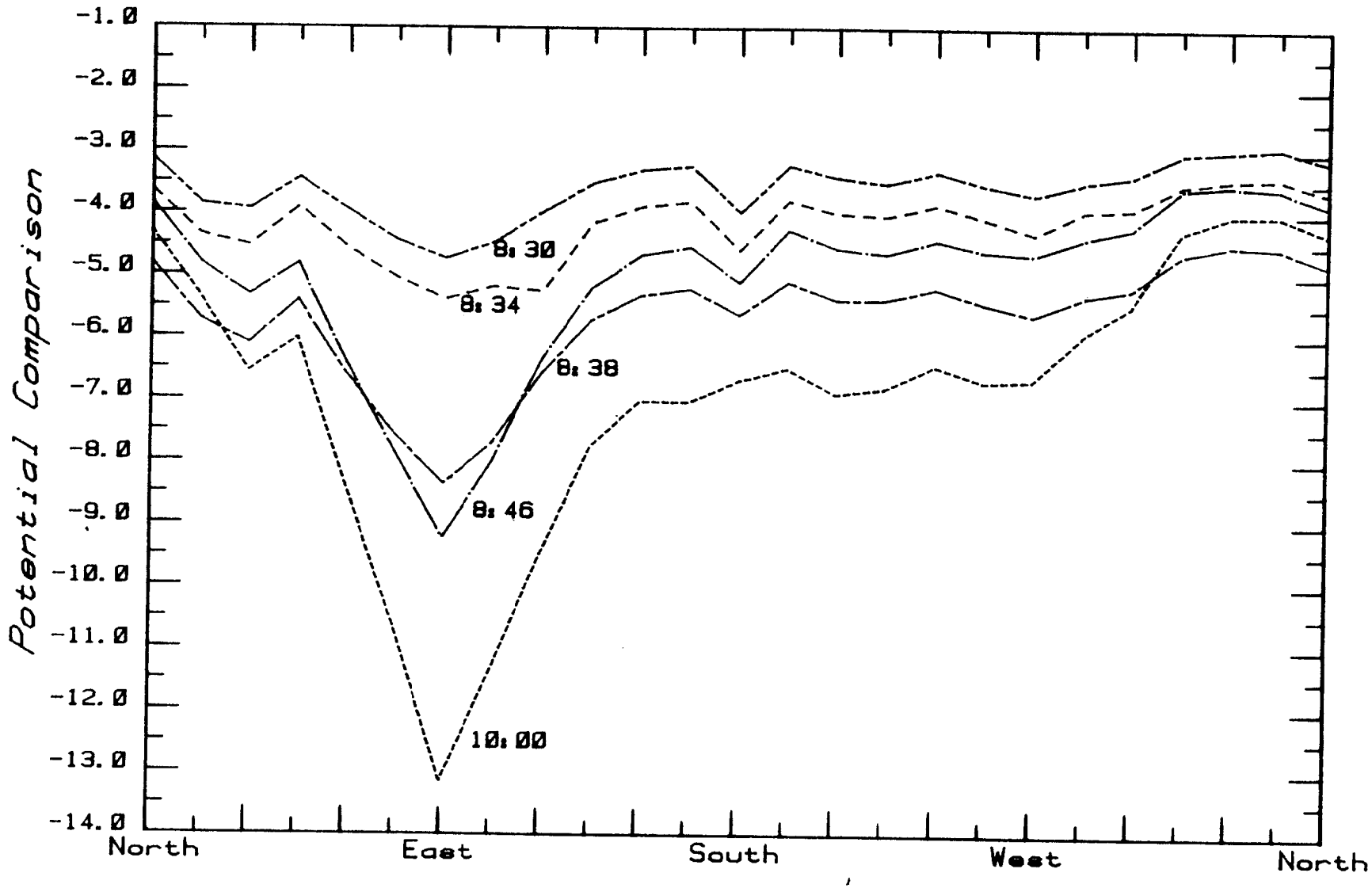

Fig. II-5 - Potential Comparison as a Function of Direction of the AMOCO Mini-Frac Experiment, November 4, 1976.

Perforations were made on three additional zones in February 1977. These zones, extending from a depth of 6294 feet to 6648 feet, did not experience breakdown prior to the MHF experiment on March 15, 1977.

Pumping started at approximately 0715 hours and continued through 1800 hours at a near constant rate of 25 barrels per minute. Approximately 640,000 gallons of fluid and 1.1 million pounds of proppant were injected in the multilayered pay zone.

The electrical potential measurement system included 24 pairs of potential probes placed circumferentially around the well with an inner radius of 1800 feet and an outer radius of 3800 feet. Injection of the induced current into the frac zone by means of a downhole current probe had been planned for this test, however, because a 4-1/2 inch casing was already installed in the well the downhole current probe could not be utilized and the current was injected into the casing at the surface. Field data were collected at two minute intervals starting at 0650 hours and continuing through 1815 hours. The data are presented in Table I, Appendix B. Figures II-6 and II-7 show the potential comparison, $V(\theta)$, for data points coincident with the end of each pre-planned pumping stage compared to data taken prior to the initial start of pumping. For convenience a multiplying factor of 100 was used. Very little change was observed after the fourth stage. The potential changes that occurred did not agree with the eight stage fracturing plan. Indications are that fracturing occurred in a near east-west orientation. The data suggests that early in the pumping process an asymmetric fracture was developing. However, on the basis of a two-cycle recurrence, the data collected at later times (1230 hours through 1800 hours) suggest that a more nearly symmetrical fracture was created. The interpretation may be misleading because of the extreme range in depth of the fracturing zones. The distributions of the fractures and their directions can lead to ambiguous interpretations on the orientation and symmetry. As an example, single asymmetric fractures, one easterly at one depth, and another westerly at a different depth, could be interpreted as a single symmetrical fracture oriented in the east-west direction.

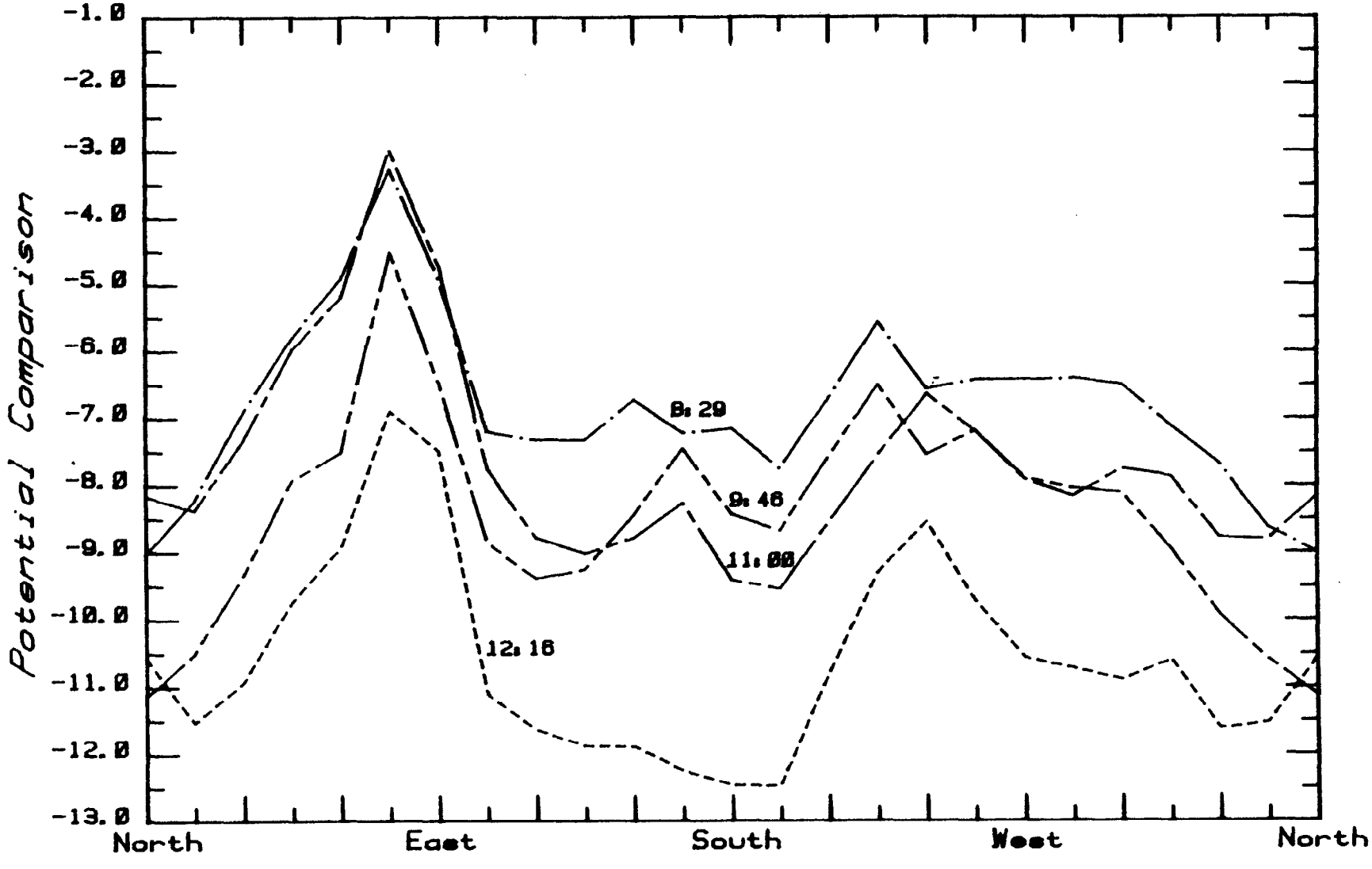

Fig. II-6 - Potential Comparison as a Function of Direction of First Four Stages of the GPE Natural Buttes Unit No. 14 Hydrofracture, March 15, 1977.

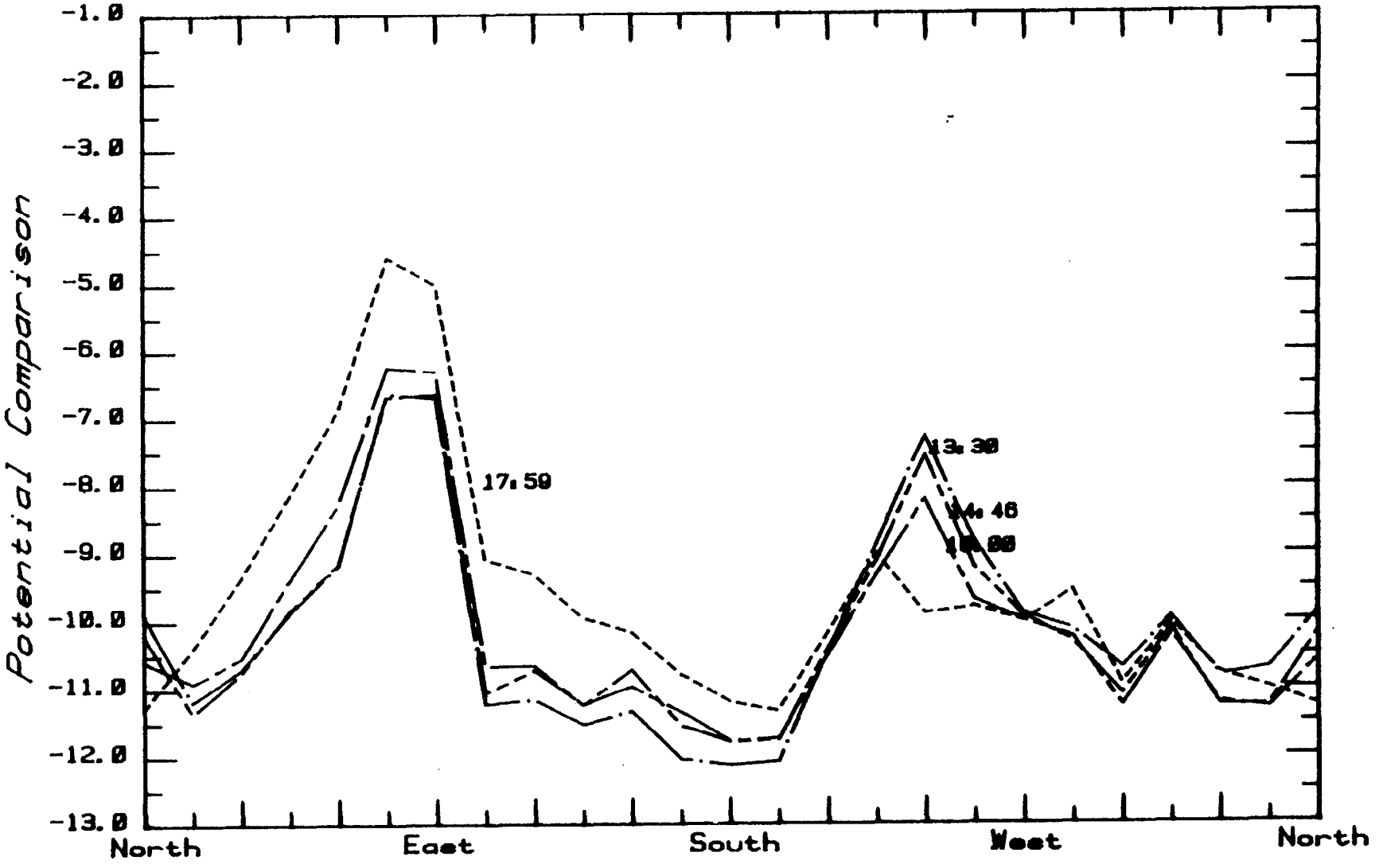

Fig. II-7 - Potential Comparison as a Function of Direction of the Last Four Stages of the GPE Natural Buttes Unit No. 14 Hydrofracture, March 15, 1977.

2. Natural Buttes Unit No. 20 -- Sandia participated in the GPE MHF experiment on their Natural Buttes Unit No. 20 well located approximately 40 miles south of Vernal, Utah. The fracture was performed by Dowell for GPE on June 22, 1977.

The MHF was designed for the limited entry technique. Eight pay zones were selected between depths of 8498 feet and 9476 feet. Approximately 350,000 gallons of fluid and 825,000 pounds of proppant were injected into the multilayered gas pay zone. Pumping started at approximately 0900 hours and continued through 1250 hours at a rate of approximately 40 barrels per minute.

The electrical potential measurement system included 24 probes placed around the well at a radius of 1800 feet on 15 degree intervals. A well casing approximately five miles distant (UT52X) was used as the other voltage probe for the potential measurements. The current was induced into the NB #20 well casing at the surface of the earth. The current return line was attached to NB #4 well casing located to the east at a distance of approximately two miles. The potential field data were collected at one minute intervals starting at 0857 hours and continued through 1307 hours. The data are presented in Table II, Appendix B. Figure II-8 shows the potential comparison, $V(\theta)$, for data points at various times through pumping compared to an average of 51 data points taken prior to pumping. The dashed curve represents the result when approximately 20 data points averaged after pumping are compared to the 51 points averaged before pumping. A multiplying factor of 100 has been used for convenience. The analysis of the data thus far has not produced any definite fracture orientation. It is possible that the electrical length of the fracture is very short and the effect is not large enough to be detected in the surface potential measurements.

CONOCO Experiment -- On March 22, 1977, the Continental Oil Company (CONOCO) conducted a small fracture as a part of a tertiary oil recovery experiment in the Big Muddy Field east of Casper, Wyoming. Sandia Laboratories' objective in the experiment was to test the effectiveness of the surface potential measurement system on a small open hole hydrofracture. In addition to the Sandia surface potential instrumentation,

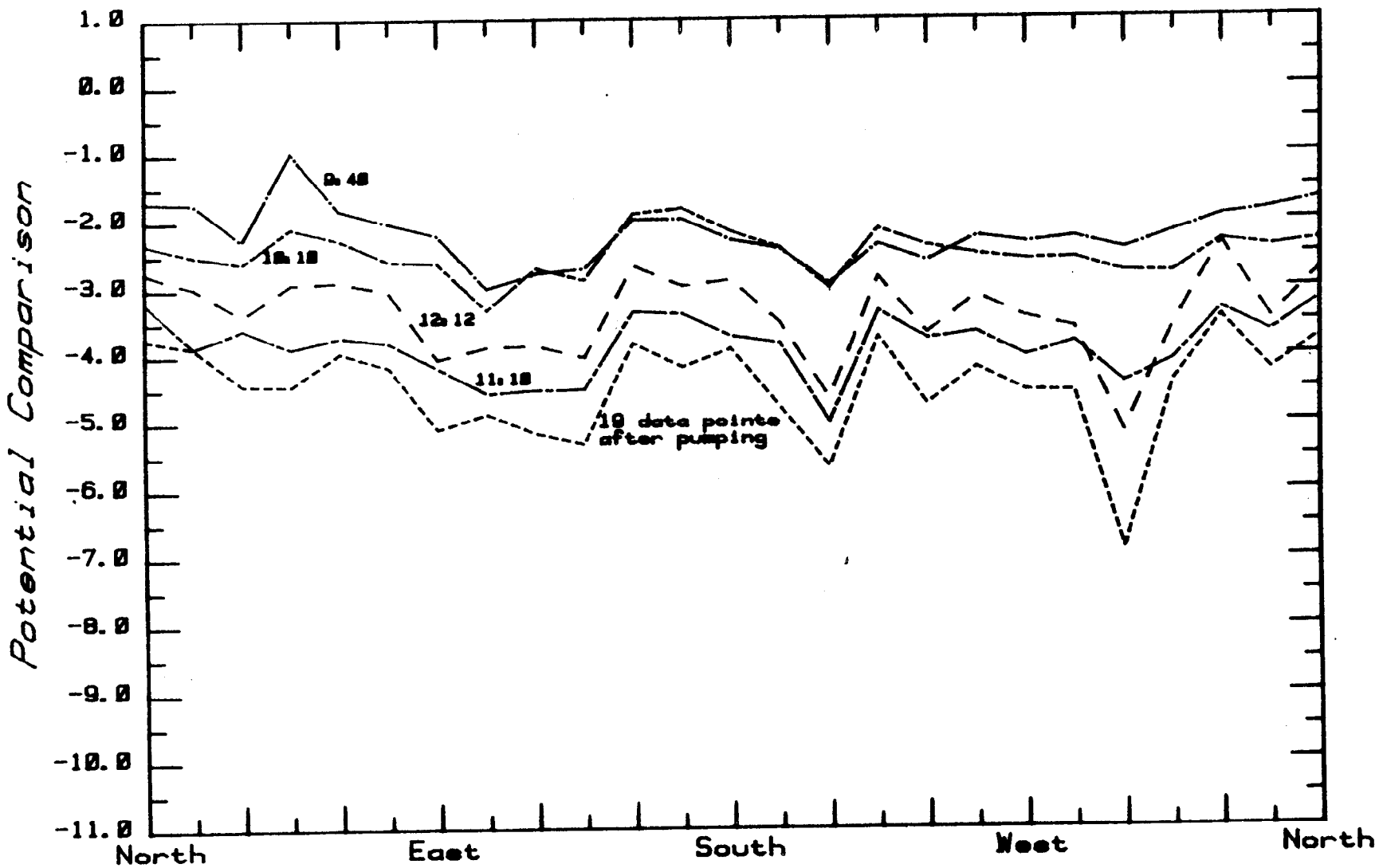

Fig. II-8 - Potential Comparison as a Function of Direction for the GPE Natural Buttes Unit No. 20 Hydrofracture, June 22, 1977.

CONOCO had installed several pressure gages in nearby surrounding wells as a diagnostic tool to assist in determining fracture orientation. The fracture zone consisted of a section of open hole located at a depth of approximately 3500 feet. Approximately 12,000 gallons of conductive fluid was pumped which was calculated to produce a fracture length of approximately 500 feet.

Electrical potential measurements were taken by recording the potentials at 24 locations around the well before, during, and after the fracture. Eighteen pairs of potential probes were placed circumferentially around the well at 20 degree spacing with an inner radius of 1000 feet and an outer radius of 2000 feet. In addition, the relative potential was measured by using as probes the casing of six wells located adjacent to the fracture well. In all cases the distance to any one of the six wells was less than 1000 feet from the fracture well. A downhole sinker bar in the fractured well and at the fracture depth served as the induced current probe. The casing of a well approximately 1.5 miles distance was used as the current return. Electrical potential data were taken at 40 second intervals commencing prior to pumping (1113 hours) and continuing through fracture completion (1143 hours).

The electrical potential data are presented in Table I, Appendix C. Approximately seven data points taken just prior to pumping were averaged and used as a before reference measurement. Measurements taken at indicated times shown in Figs. II-9 and II-10 were compared to the before reference data and are plotted versus azimuth. For convenience, a multiplying factor of 100 was used. The data obtained on the northern side of the array was compromised by a high degree of external noise and is, therefore, excluded from the plot.

Data analysis based on the fracture model calculations indicates that the fracture is asymmetric and that the azimuthal direction is from nearly east to west with the major extension primarily to the east. Also fracture growth can be recognized by a decreasing potential thus the data suggest the major growth (at least the electrical length) occurred within the first few minutes of pumping.

Shell Oil Company Experiment -- On August 25 and 26, 1977, Sandia participated in the Shell Oil Company MHF test in the Rachel Foundation No. 2 well located approximately 40 miles northwest of Laredo, Texas. The fracture was performed by Halliburton for the Shell Oil Company.

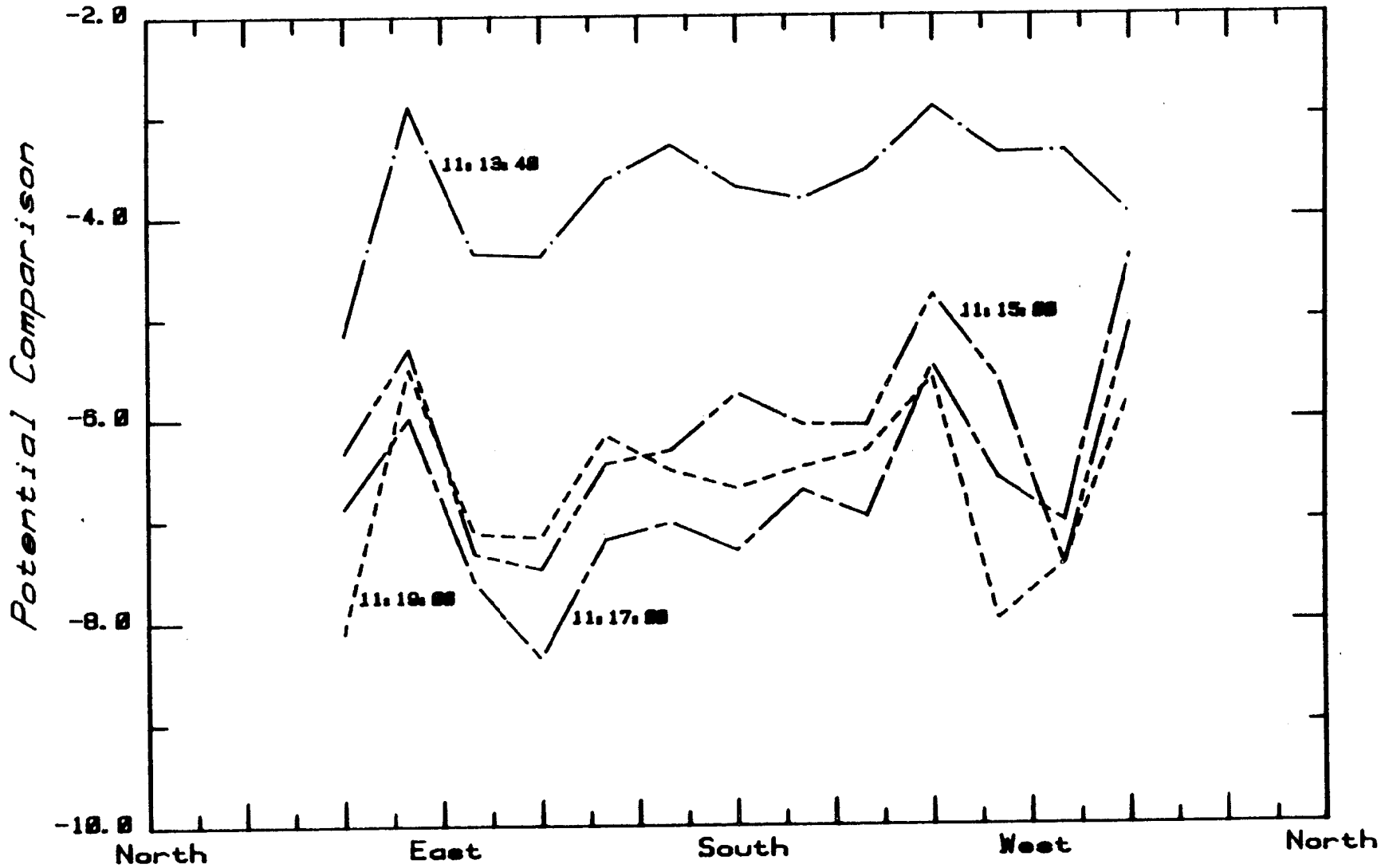

Fig. II-9 - Potential Comparison as a Function of Direction for the CONOCO RBW #80 Hydrofracture. Eighteen Stake Pair. March 22, 1977.

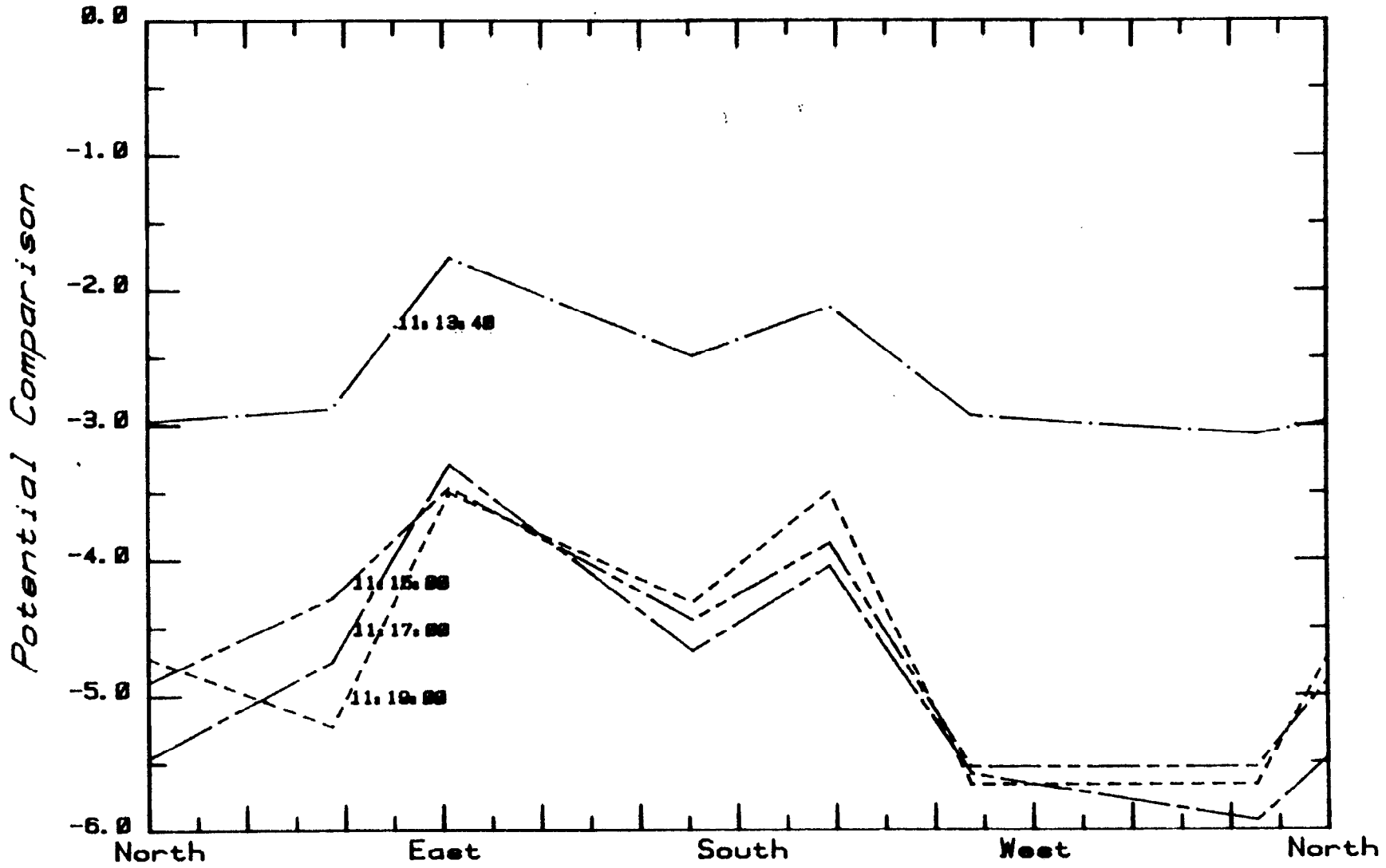

Fig. II-10 - Potential Comparison as a Function of Direction for the CONOCO RBW #80 Hydrofracture. Six Well Casings. March 22, 1977.

The experiment was designed in two pumping stages, the first occurring on August 25, 1977 and the second on August 26, 1977. This was done in order to obtain some logging diagnostics before completion of the fracture.

Three major pay zones were selected between the depth of 5345 feet and 5515 feet. The entry technique was designed such that all zones would take fluid simultaneously.

Pumping for the first stage commenced on August 25, 1977 at 1040 hours and continued through 1325 hours at an average rate of approximately 12.5 barrels per minute. Approximately 80,000 gallons of fluid and 98,000 pounds of proppant were pumped. Surface electrical potential data were recorded at intervals of two minutes starting at 0826 hours and continuing through 1405 hours.

The second stage pumping occurred on August 26, 1977 when approximately 200,000 gallons of fluid and 280,000 pounds of proppant were pumped. The operations started at 0830 hours and continued through 1330 hours. Surface electrical potential data were taken at one minute intervals beginning at 0630 hours and continuing through 1437 hours.

Figures II-11 through II-13 show the results of the data acquired during pumping on August 26, 1977. Each curve is labeled as to the time during pumping when data has been analyzed. The 800 before pumping reference was obtained by averaging the data taken between 0730 hours and 0800 hours. The time shown for data comparison is an average of the data taken during the period of one-half hour prior to that time indicated on the curve. The data was normalized by the induced current for each data point and after the average over a specified time the difference of the "after" and the "before" plotted. For convenience a multiplying factor of 100 was used. When compared to the mathematical model an asymmetric fracture in the northeast-southwest direction is indicated with the major wing oriented to the northeast.

The data are presented in Table I and II, Appendix D.

Surmont Project -- During September 1977, trailer B-59 was installed at the Numac Oil and Gas Ltd. Project Site about 40 miles south of Ft. McMurray, Alberta, Canada.

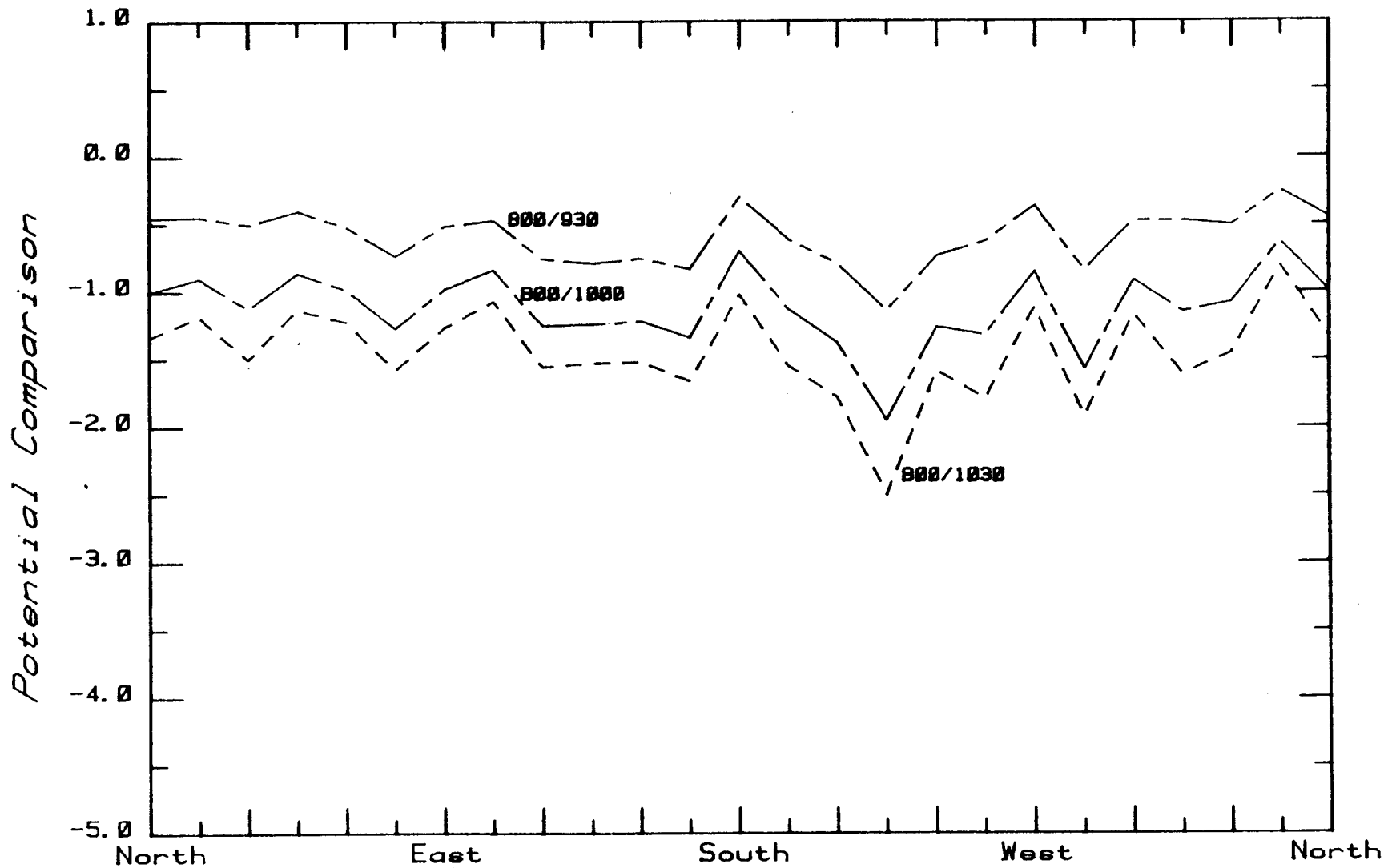

Fig. II-11 - Potential Comparison as a Function of Direction for the Shell Oil Company Hydrofracture, Rachal Foundation No. 2, August 26, 1977. Comparison from 0930 hours through 1030 hours.

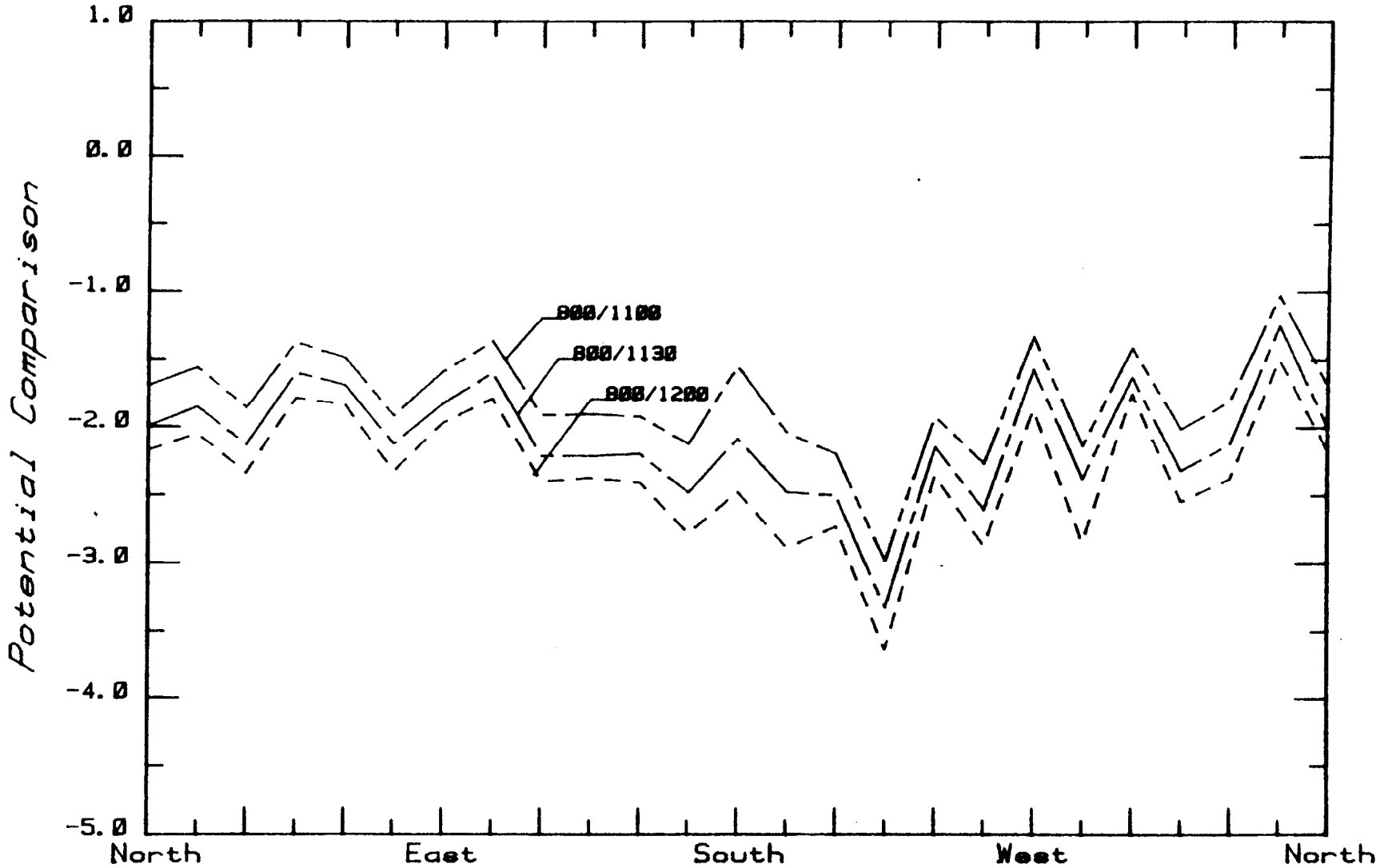

Fig. II-12 - Potential Comparison as a Function of Direction for the Shell Oil Company Hydrofracture, Rachal Foundation No. 2, August 26, 1977. Comparison from 1100 hours through 1200 hours.

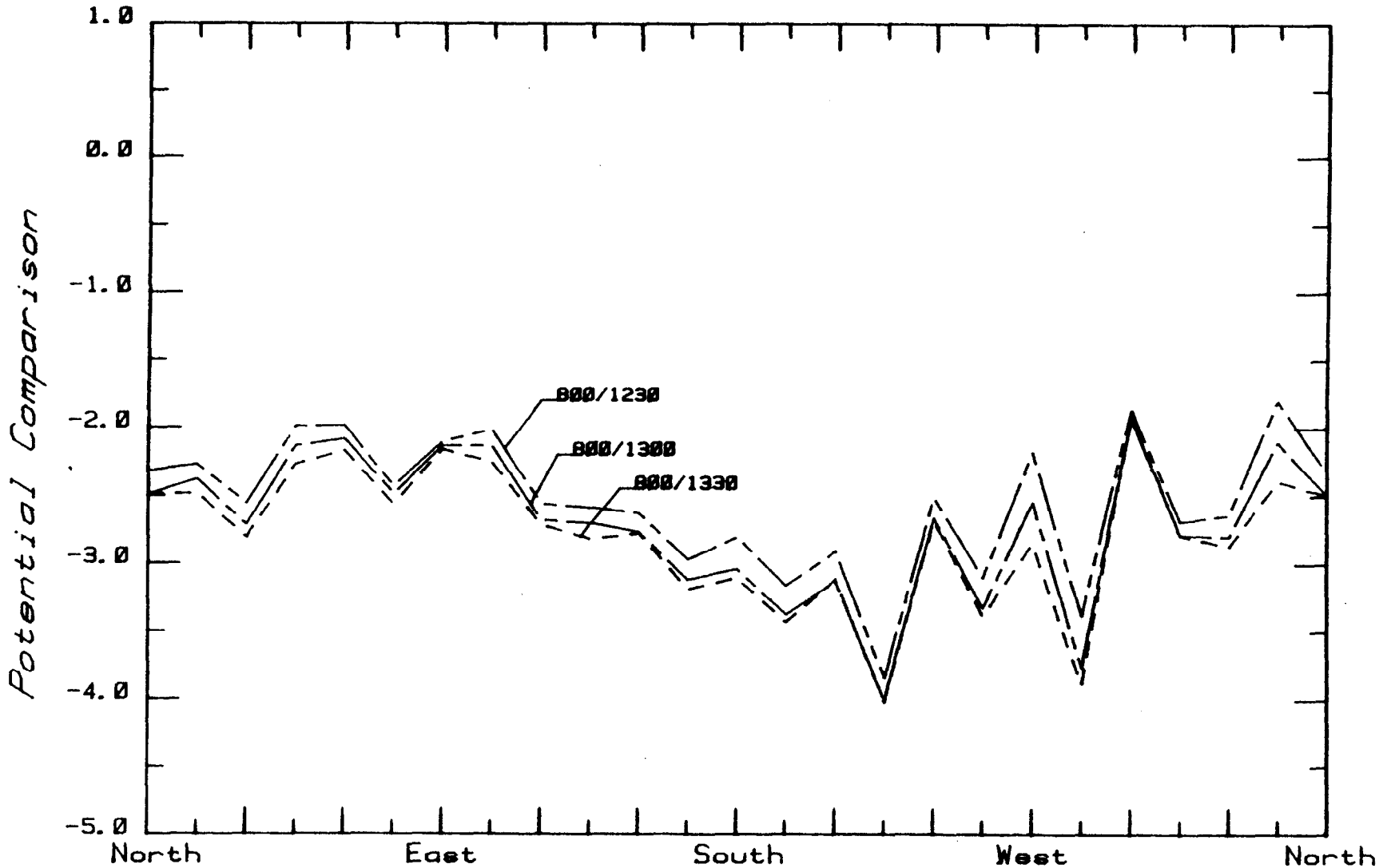

Fig. II-13 - Potential Comparison as a Function of Direction for the Shell Oil Company Hydrofracture, Rachal Foundation No. 2, August 26, 1977. Comparison from 1230 hours through 1330 hours.

Well F-1 will be the fracture well in which two fractures at depths of 1150 and 1100 feet will be performed. The lower zone is at the interface between the tar sands and the Devonian shale. The upper zone is within the tar sands. Pumping rates will be very low in order to initiate a horizontal fracture in the order of 500 feet.

During the fracture current will be injected alternately between the fracture well casing, a downhole current probe and the return well. Additional measurements will include monitoring the potential between the two well casings which should provide a better normalizer base.

The casing potential will also be monitored as the downhole current probe is lowered in order to provide voltage gradient information to verify modeling.

All equipment has been installed and checked out for the fracture which is scheduled for early October, 1977.

C. Electrolytic Model Tank

To date, the primary field technique employed for monitoring the effectiveness of massive hydraulic fracture (MHF) programs has been the surface measurement of induced electrical potentials when the fracture, or fracture plus well casing, are charged with electrical current. Mathematical modeling of this boundary value problem[1] has been performed for the case of an homogeneous earth with an uniform casing/fracture source electrode. However, the introduction of layering and lateral inhomogeneity (both in terms of electrical resistivity) in the earth model, imperfect or variable casing-earth electrical contact, or the presence of man-made distortions (e.g., other metal well casing in the area) produce mathematical rigors which are not tractable by techniques presently available. These situations are typically the rule rather than the exception in actual field locations. As an accurate, quantitative description of the fracture system (length, height, etc.) is desired, an alternate modeling technique was sought which could accommodate those situations met in the field which reduce the applicablity of mathematical synthesis. This was the rationale behind the development of an electrolytic model tank.

An electrolytic model tank is basically a brinewater-filled tank with water of variable salinity representing the homogeneous earth. Layering may be simulated by the introduction of sheets of material of varied resistivity into the water.[2] Similarly, casing, ore bodies, cavities or other size-limited bodies may be modeled and placed in appropriate positions within the tank. Scaling of lengths, resistivities, and frequency of applied current from the field to the model is dictated by the following relation (assuming magnetic permeability of model and full-scale materials is the same):

$$\frac{\omega' L'^2}{\rho'} = \frac{\omega L^2}{\rho}$$

[1] McCann, R. P., Hay, R. G., and Bartel, L. C.: "Massive Hydraulic Fracture Mapping and Characterization Program, First Annual Report," SAND-77-0286, 1977.

[2] Frischknecht, Frank C., USGS, Denver, Personal Communication.

where

ρ' = model resistivity	ρ = full scale resistivity
ω' = model current frequency	ω = full scale current frequency
L' = characteristic model length	L = corresponding full scale length

Our initial interest was to locate an existing model facility and arrange for its use for modeling MHF experiments. To this end, R. P. McCann and T. L. Dobecki visited the electrolytic model facilities at the United States Geological Survey (USGS), Denver and at the Colorado School of Mines (CSM), Golden, Colorado. Both tanks were massive poured cement structures, rectangular in shape, and typically 10 ft x 15 ft x 5 to 8 ft deep (3 x 4.6 x 1.5 to 2.4 m). Both tanks were fitted for the performance of electromagnetic model experiments and would, therefore, require retooling for our galvanic experiments, thereby interrupting the progress of on-going tests. The USGS facility is in current use with projected heavy use by USGS personnel in the near future. The CSM facility, on the other hand, is being terminated for future office space and will not be available. The situation, therefore, dictated construction of a model tank at Sandia.

After consideration of the varied tank designs currently in use, space limitations at the SLA test facility, and the particular field procedure which we intended to model, we developed a unique tank design which approximates an infinite sized tank while being significantly smaller than any of those visited. To accomplish this, the tank employs a conductive, hemispherical shell as one current electrode; the other current electrode is placed at the center of the hemisphere, and all potential measurements are made within the hemisphere (Fig. II-14). The reasoning behind the choice of an hemispherical electrode may be explained as follows:

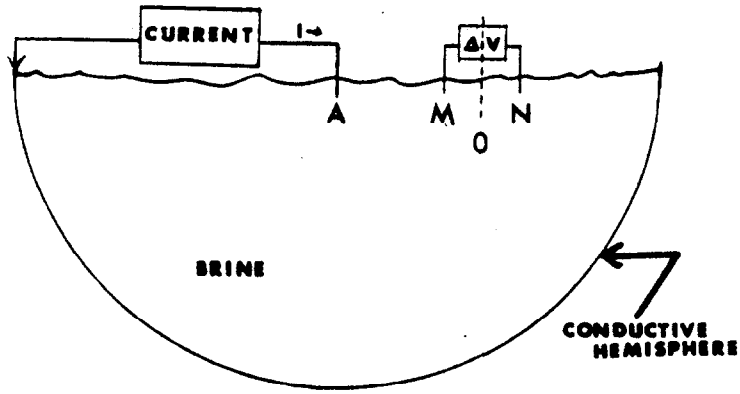

Fig. II-14 - Schematic illustrating an electrolytic model tank design employing an hemispherical return current electrode.

The electrical potential field about a point electrode at the earth's surface, if the return electrode is an infinite distance away, is given by

$$V = \frac{I\rho}{2\pi R} \qquad (2)$$

where

I = impressed current

ρ = resistivity of earth material

R = distance from point electrode to observation point

All equipotential surfaces are given by R = constant which are hemispheres centered on the point source. If, on the other hand, the return electrode is made a hemisphere centered on the point source, it necessarily becomes an equipotential surface and current flow remains radial from the point source to the shell. Therefore, again all equipotential surfaces are hemispheres with the same potential distribution as a point source except for an additive constant. For potential difference measurements, this technique is equivalent to having a return electrode at infinity while maintaining a reasonably small sized tank.

The electrolytic model tank (Fig. II-15) consists of four basic units: 1) a wooden exterior tank, 2) the aluminum hemisphere, 3) an aluminum probe track, and 4) the resistivity measurement system.

The wooden tank measures 5 x 5 x 3 ft deep (1.5 x 1.5 x 0.9 m) and is constructed of 0.75 in. (1.9 cm) plywood with suitable structural bracing to withstand stresses applied when filled with water. A sealant was applied to the interior to prevent water leakage, and a standard water bibcock was bottom mounted for ease in tank drainage. When filled, the tank holds 75 ft^3 (2124 ℓ), or 2.33 tons (2124 kg) of water. The purpose of this exterior tank is twofold. Firstly, by placing the water-filled hemisphere in a water-filled tank, the differential pressures on the aluminum shell are minimized reducing the chance of warping or collapse. Secondly, for standard four electrode experiments (Wenner or Schlumberger arrays, for example), the aluminum hemisphere may be removed, and experiments are performed in the wooden tank.

The aluminum hemisphere (Fig. II-16) is a 1/16 in. (.16 cm) shell of 47.75 in. (121.3 cm) nominal I.D. After initial testing, the aluminum required an alodine coating to prevent formation of unknown chemical or organic precipitates in the brine solution. This represents the maximum size aluminum hemisphere which could be fabricated in the Albuquerque area, and, therefore, was the main size limiting factor in the tank design.

The aluminum probe track is a slotted, moveable unit which holds the current and potential probes and allows for their precise location.

An advantage of a large tank is that high precision in placement of electrodes or in lengths of models is not critical. As the size of the tank is decreased, the scaling relation requires greater precision in

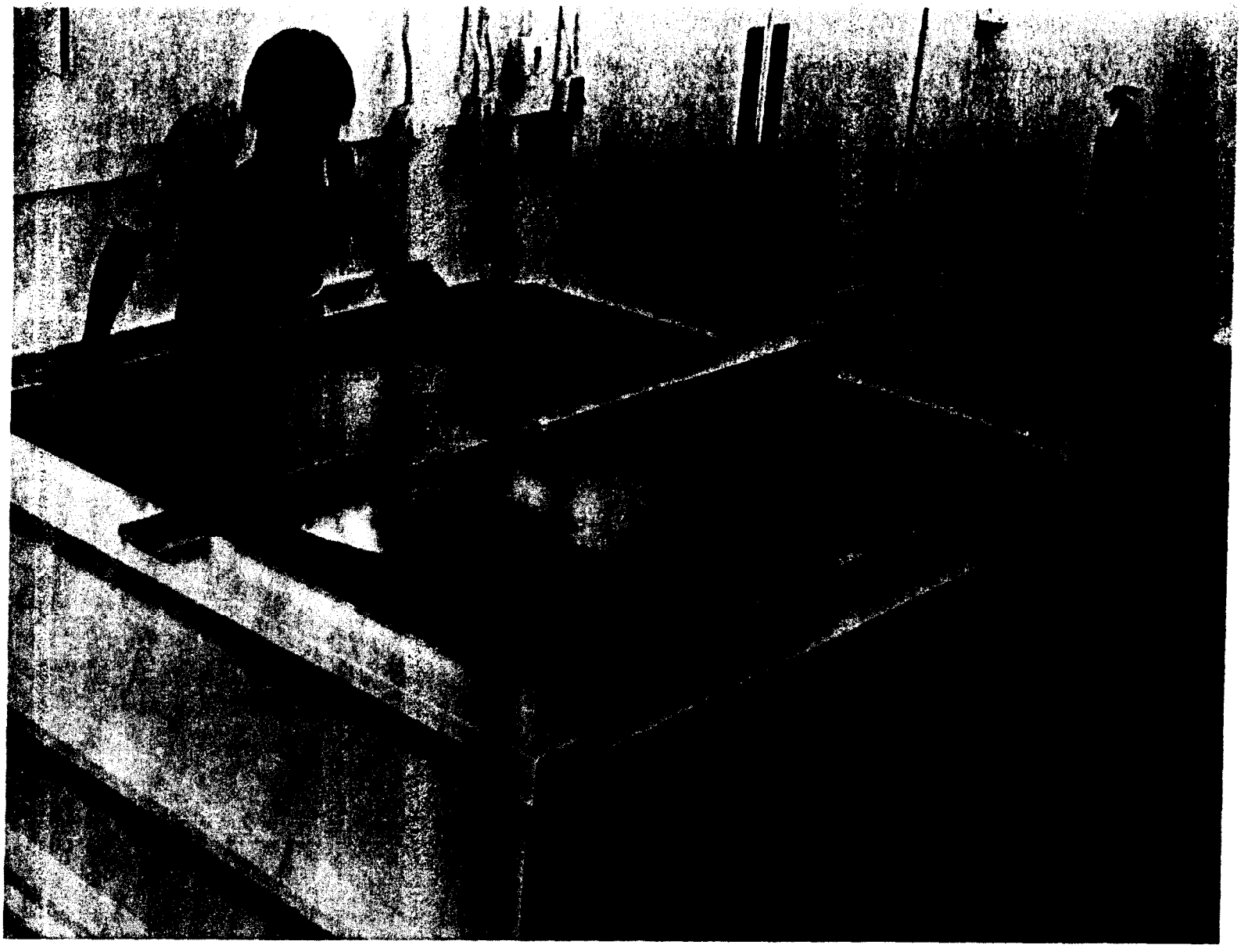

Fig. II-15 - Electrolytic Model Tank Facility at Sandia Laboratories.

Fig. II-16 - Aluminum Hemisphere Used as Current Return Electrode in Model Tank.

the measurement of lengths. A scaled track is fit to the top of the hemisphere upon which moveable potential-measuring electrodes may be located with an accuracy of ± 0.005 in. (± 0.13 mm).

The potential measuring probes are held in spring-loaded holders which slide in a scale calibrated slot (Fig. II-17). The central current probe, which represents the fracture well, is held in a rotatable, protractor calibrated mount (Fig. II-18). By holding the potential probe positions fixed and rotating the fracture through 360°, the effect of a fixed fracture surrounded by potential probes is achieved. This is the field situation of radial dipoles used in the MHF mapping program which we intended to model.

Several probe materials have been tried including stainless steel hypodermic stock of several diameters, high carbon steel drill stem rod of varied diameter, and Kovar rods. Typical diameter used is in the 0.046-0.050 in. (0.117-0.127 cm) range. In addition, copper and gold platings of these probes are being evaluated. Evidence of instrumental drift suggests instability of the probes tested which may require consideration of platinum or platinized platinum as probe material. The observed drift is slight and decreases with time which, although an inconvenience, may be more attractive than the more expensive platinum alternative.

The resistivity system utilized to date at SLA has been the BISON Model 2350A resistivity meter. This is a bridge null unit which reads directly in units of $2\pi\frac{V}{I}$ in response to a nominal 23 mamp, 10 HZ square wave current.

To date, experiments utilizing the described electrolytic model tank have been of two types: 1) tests to verify the "infinite" size objective in the tank design, and 2) parametric studies of anomaly size and shape for various fracture depths and lengths. These tests will be discussed separately.

As noted in published test results by Goudswaard[3], in a finite sized, box-shaped electrolytic tank, experiments must be limited in

[3] Goudswaard, W.: "On The Effect of the Tank Wall Material in Geoelectric Model Experiments," Geophysical Prospecting, Vol 5, No. 3, pp 272-281, 1957.

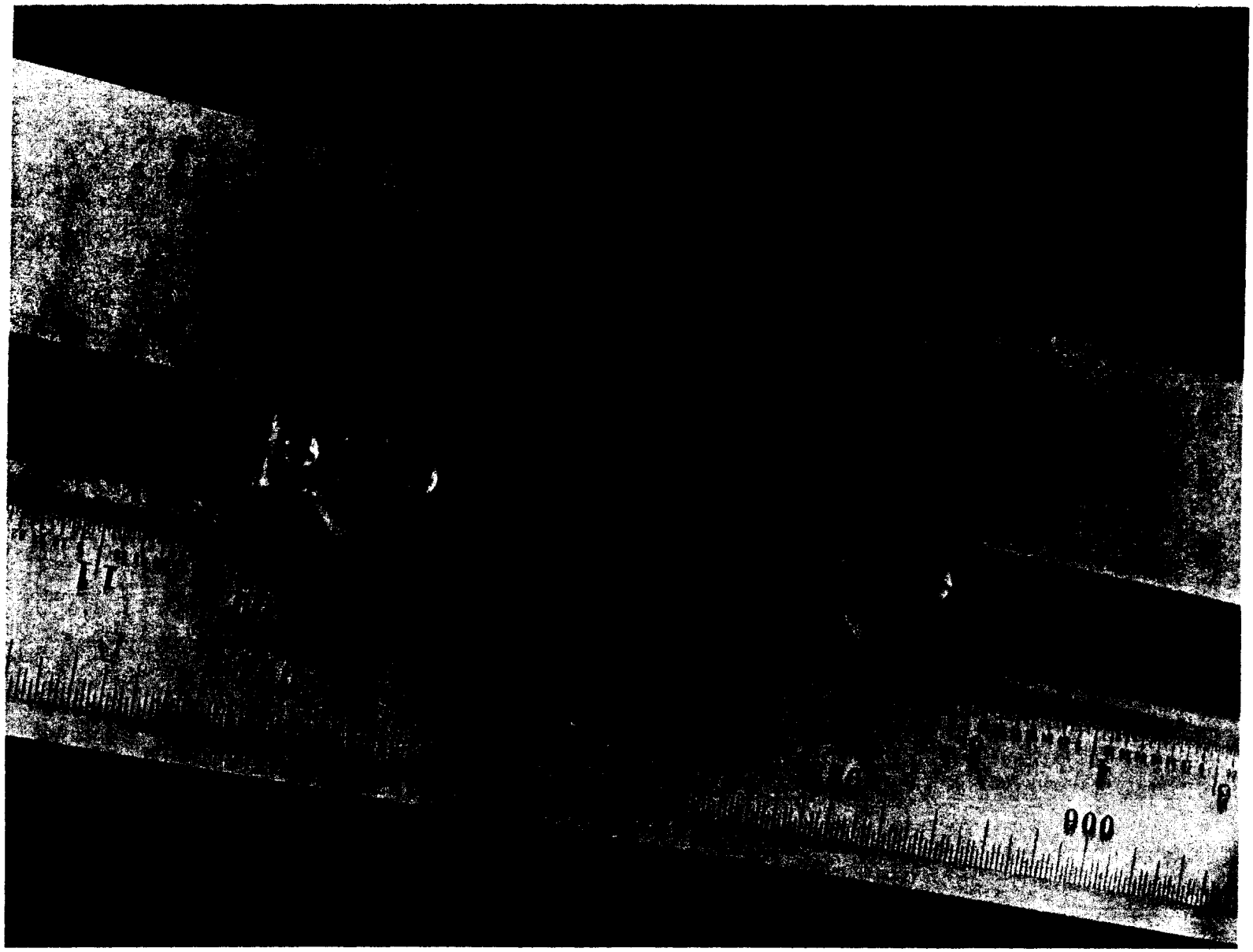

Fig. II-17 - Potential Electrode Holders and Calibrated Slide Track.

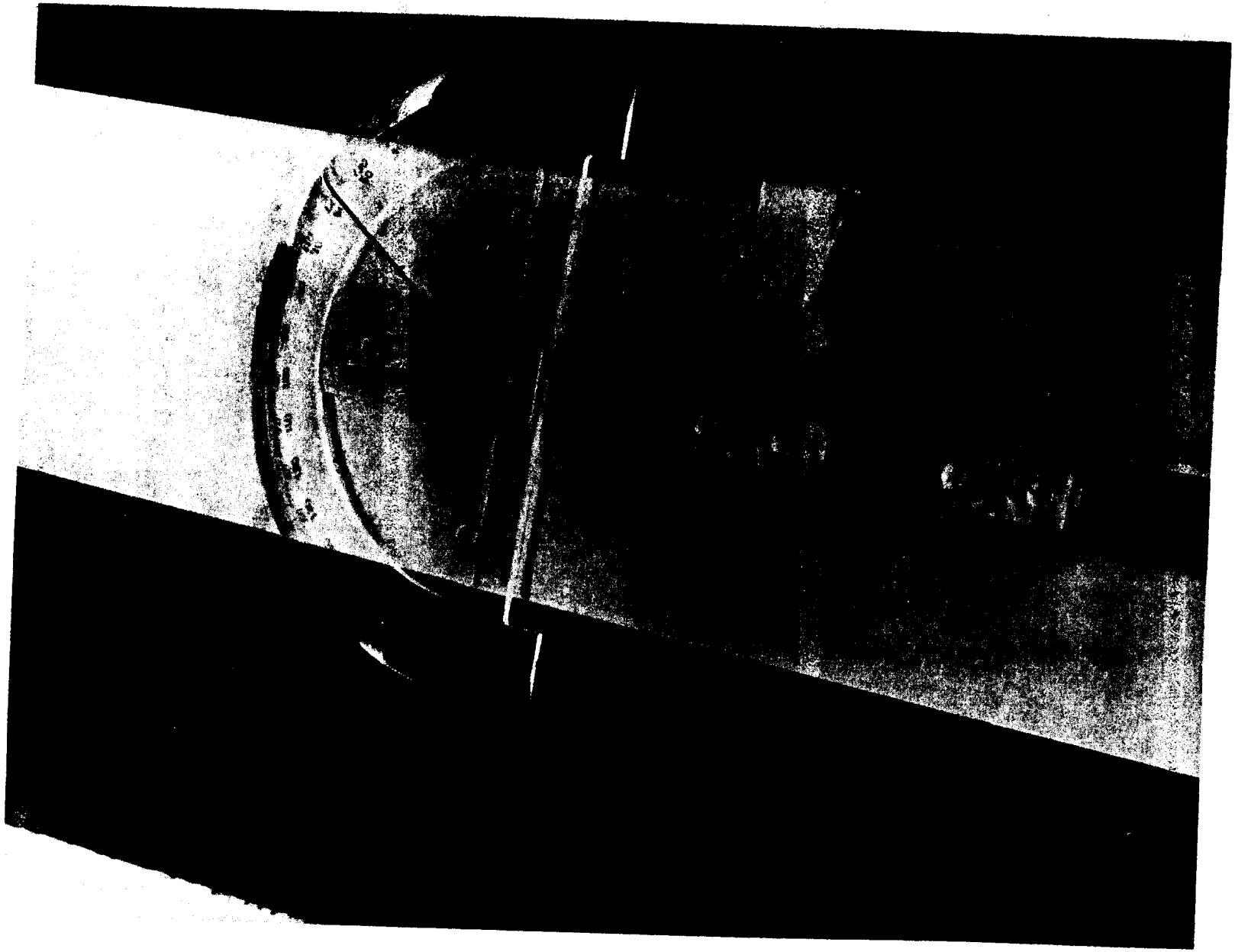

Fig. II-18 - Calibrated, Rotating Central Current Electrode Unit.

laterial dimensions and located near the tank center or else the experiment "sees" the walls and bottom of the tank. Goudswaard eliminated these errors by lining the walls with a conductive grid to enlarge the usable area of the tank. Our use of a conducting hemispheric electrode is intended to accomplish the same results.

The first set of tests were to establish, for a given $\overline{MN}$ spacing (see Fig. II-14), how close we would approach the aluminum shell before our data became inaccurate. For each test, a constant $\overline{MN}$ value was chosen while the $\overline{AO}$ value was varied from its minimum to maximum values. Apparent resistivity was calculated using

$$\rho_a = 2\pi\frac{V}{I}/\left(\frac{1}{\overline{AM}} - \frac{1}{\overline{AN}}\right) \qquad (3)$$

True brine resistivity, ρ, was determined using a conductivity bridge. Values of $\frac{\rho_a}{\rho}$ versus $\overline{AO}$ were then plotted as shown in Fig. II-19. Note that in the worst case the outermost potential electrode can come to within 3 in. (7.5 cm) of the shell before deterioration in data accuracy is observed. The data show an average ρ_a/ρ value near 0.95 rather than 1.0 which we attribute to the 1 kHZ frequency utilized by the conductivity bridge being substantially higher than the 10 HZ used by our system. In addition, the dip cell constant for the conductivity bridge is itself

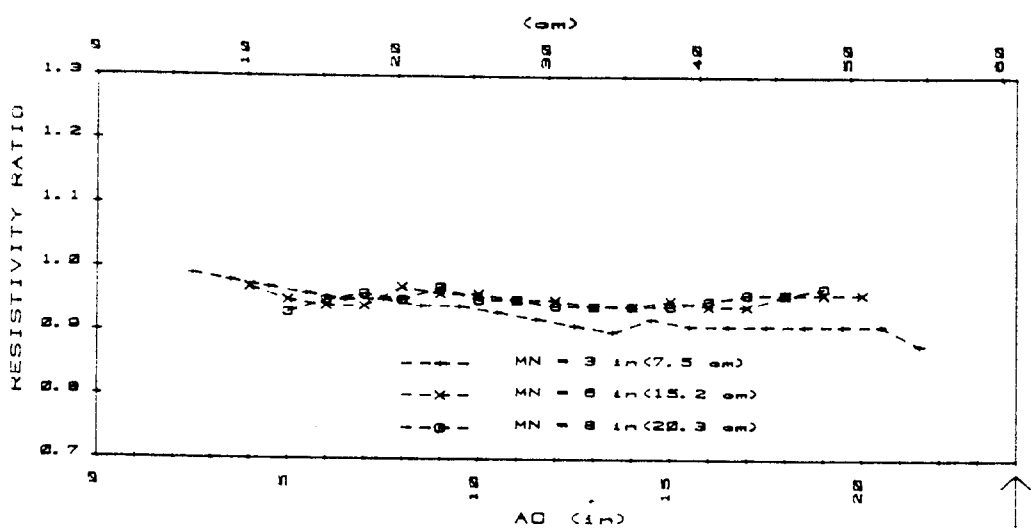

Fig. II-19 Results of experiment demonstrating the effect of the aluminum hemisphere on resistivity measurements. The position of the arrow marks the hemisphere wall.

± 1.0% at best. It was felt that these test results established that we may assume that the return current electrode is effectively at an infinite distance from the center of the hemisphere.

A second test of tank design involved determination of the maximum length central current electrode which could be used in model experiments before experimental accuracy is reduced. Inherent in the tank design is that the central current probe is a point source. At distances greater than a few times the length of a line source, the line source still appears to be a point source. Therefore, line sources at the central tank position may be used only up to a length where the hemisphere "sees" the line nature of the source. This test simply measured the apparent resistivity versus line electrode length at various $\overline{AO}$ positions and compared these values to those which would be measured if a point source had been used. The results (Fig. II-20) show that for near field measurements ($\overline{AO}$ = 3 in.) the measured apparent resistivity drops rapidly as electrode penetration is increased. At a large distance from the central probe ($\overline{AO}$ = 19 in.; near the hemisphere) the change is slight and is only 11% down at an electrode penetration of 8 in. (20.3 cm).

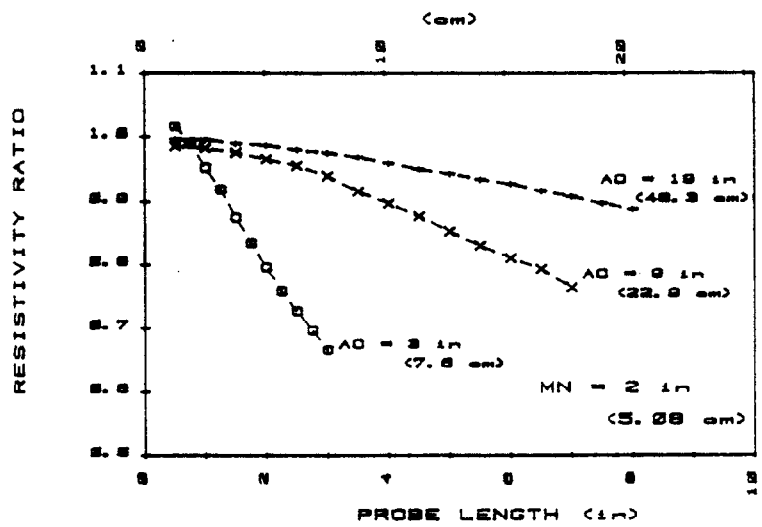

Fig. II-20 - Results of experiment demonstrating the effect of increasing the length of the central current probe upon resistivity measurements.

From these results it is felt safe to use central electrodes up to a penetration of 6 in. (15.2 cm) without fear of violating the central point electrode assumption of the tank design.

The experiment described exemplifies the on-going series of tests being performed to characterize the nature of potential field variation as related to fracture geometry. The experimental set-up is shown schematically in Fig. II-21. In this configuration, both the return electrode and the outer potential electrode are attached to the hemisphere. By placing the outer potential electrode at a practical infinite distance from the center of the tank, we are actually measuring the value

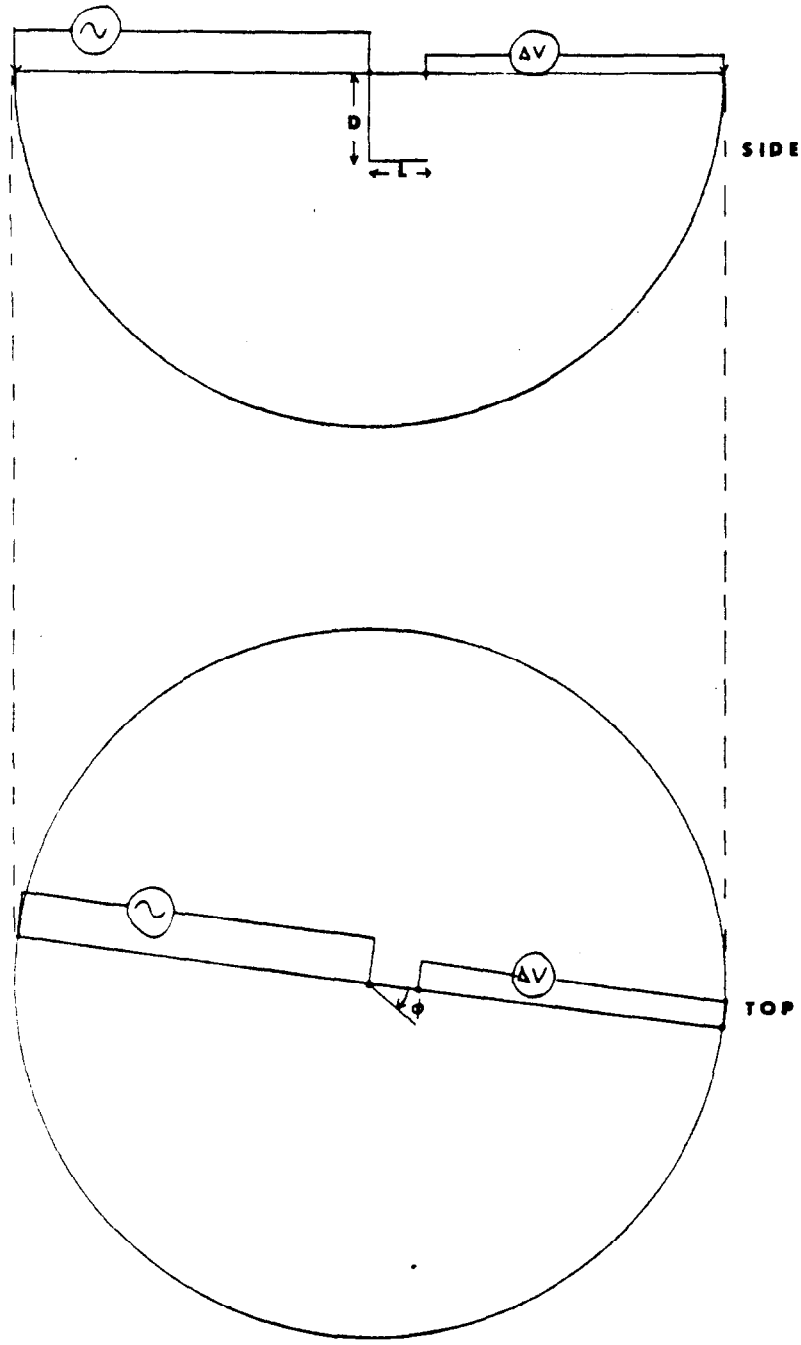

Fig. II-21 - Schematic illustrating the experimental set-up to determine the potential field distribution around an "L" shaped fracture of length, L, at depth, D.

of potential at the position of the inner potential probe. The fracture/well casing is represented by a length of Kovar rod. By putting a right angle bend in the rod, an asymmetric ("L" shaped) fracture may be modeled. Similarly, symmetric ("T" shaped) and various types of asymmetric fractures may be modeled by soldering various length pieces of Kovar to the tip of the Kovar rod representing the well casing. It is important to note that these are preliminary models and do not model relative heights, thicknesses, and resistivity contrast between the casing material and the fluid-filled fracture. These tests are concerned primarily with the effect of fracture length on observed potential distributions.

Figure II-22 shows the results of an experiment for an "L" fracture for fracture length varied from 0 up to one-half the depth of burial (0 to 7.5 cm in model dimensions). Considering the symmetry of the set-up, we would expect the same potential value when the fracture azimuth is ± 90° from the measuring point. Similarly, we expect a maximum in the field when the fracture azimuth is 0° (directly beneath the measuring point) and a minimum value when pointing away (azimuth = 180°). The only correction necessary is to account for a skew in the potential field caused by the casing part of the model not being perfectly straight. Performing the test with zero fracture length with measurements made at 10° intervals completely describes the field of the casing. This measurement allows correction of those tests made with finite fracture lengths to eliminate the effect of bending in the rod. As shown in Fig. II-22, the absolute value of the potential field (actually $\frac{2\pi}{I}*V$) decreases as the fracture length increases. In addition, the amplitude of the potential distribution (maximum value-minimum value) for a given fracture length increases with increasing fracture length as shown in Fig. II-23. From this result, it is suggested that given some knowledge of fracture asymmetry, the amplitude of the potential distribution surrounding the fracture well may provide the information required to deduce fracture length.

Similar parametric studies for other degrees of asymmetry and for symmetric models are presently underway at Sandia. As testing continues, models employed will increase in complexity to more accurately model the fracture/casing situation and to determine the effects of subsurface layering, lateral resistivity variation, etc.

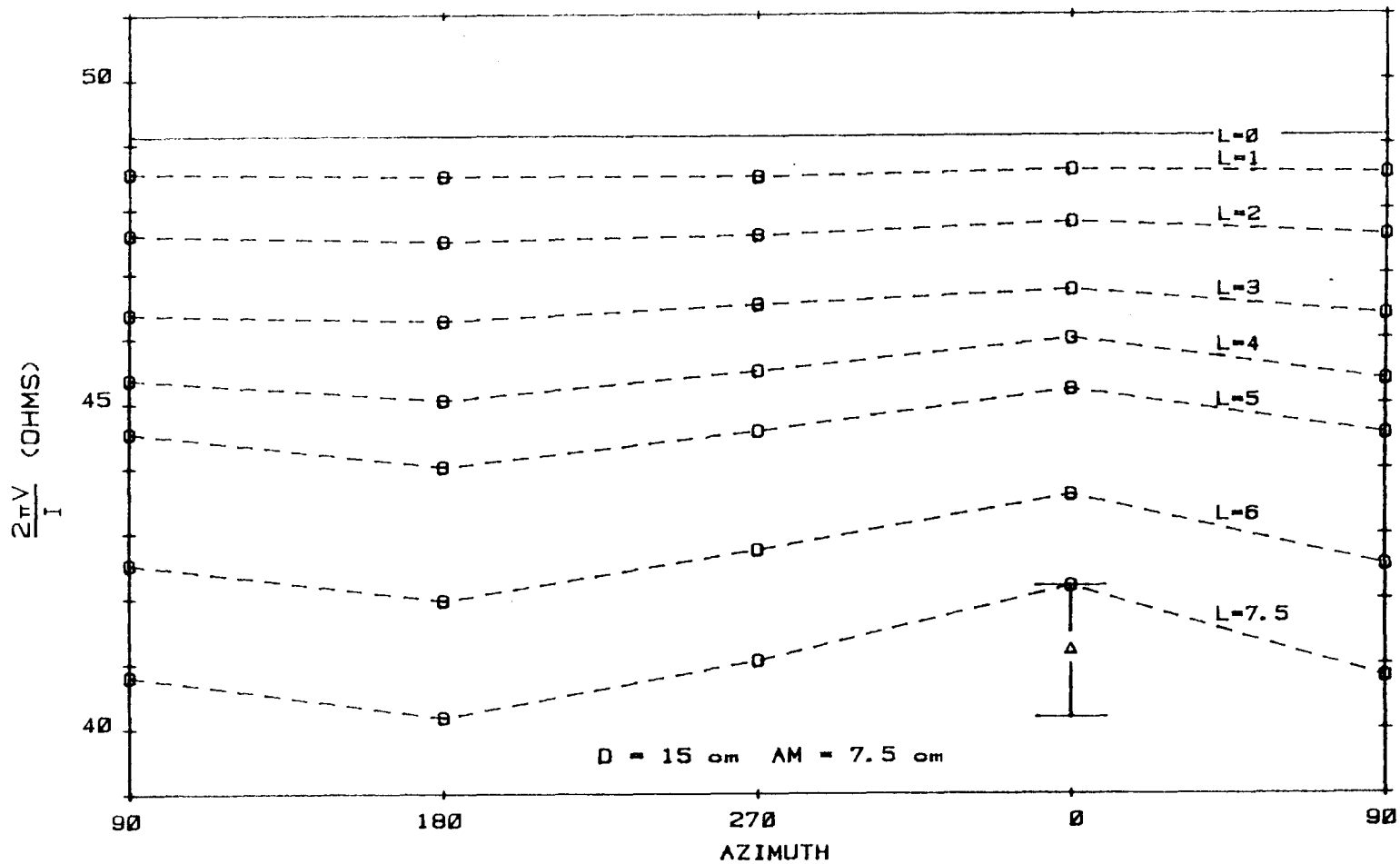

Fig. II-22 - Azimuthal Variation of Normalized Potential for Various Length "L" Shaped Fractures. Fracture lengths (L) in centimeters.

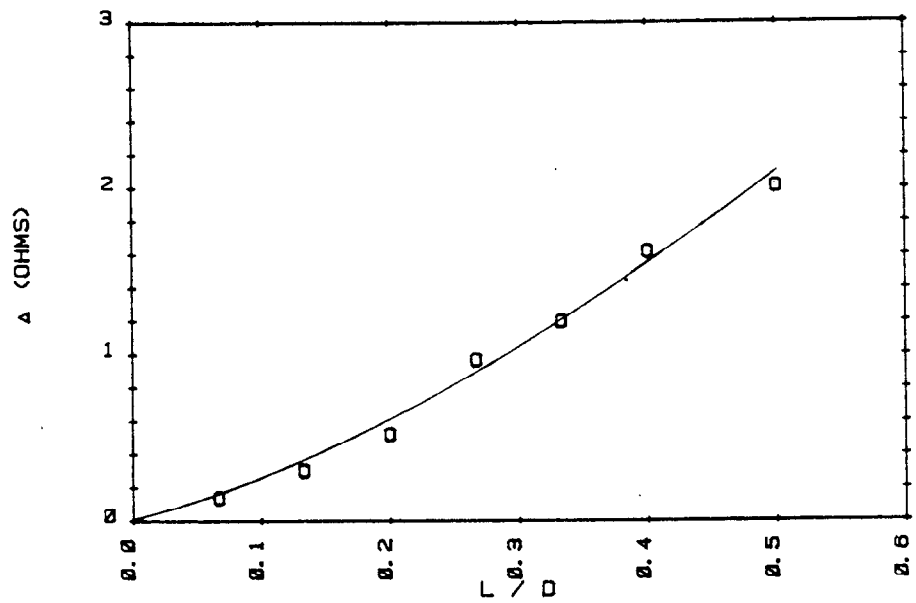

Fig. II-23 - Variation of Δ (maximum to minimum potential values) with increasing fracture length.

D. NTS Seismic Recording

A seismic monitoring system was installed in G-Tunnel at the Nevada Test Site to record seismic signals generated from hydrofractures in well Uel2gl0#6. The seismic monitoring system consisted of four triaxial geophone packages placed in holes in G-tunnel such that the geophones were in a vertical plane and spaced to form a fifty foot square approximately 215 feet from the fracture well. Figure II-24 shows the location of the well and geophones. Geophones are in instrumentation holes 5 to 8.

The instrumentation system consisted of four triaxial geophones (Mark Products L25A), amplifiers, power supplies, and line drivers placed at the end of G-tunnel and a magnetic tape recorder located at the G-tunnel portal as shown in Fig. II-25. The geophone signal was amplified by 100 db and modulated voltage controlled oscillators (VCO's) and the mixed VCO signals sent to the tape recorder via a line drive and long cable. Not shown in Fig. II-25 is the power supplies for the amplifiers which are connected to each instrument box and the DC/signal splitting circuits. Power was supplied to the boxes from this instrumentation van at the portal.

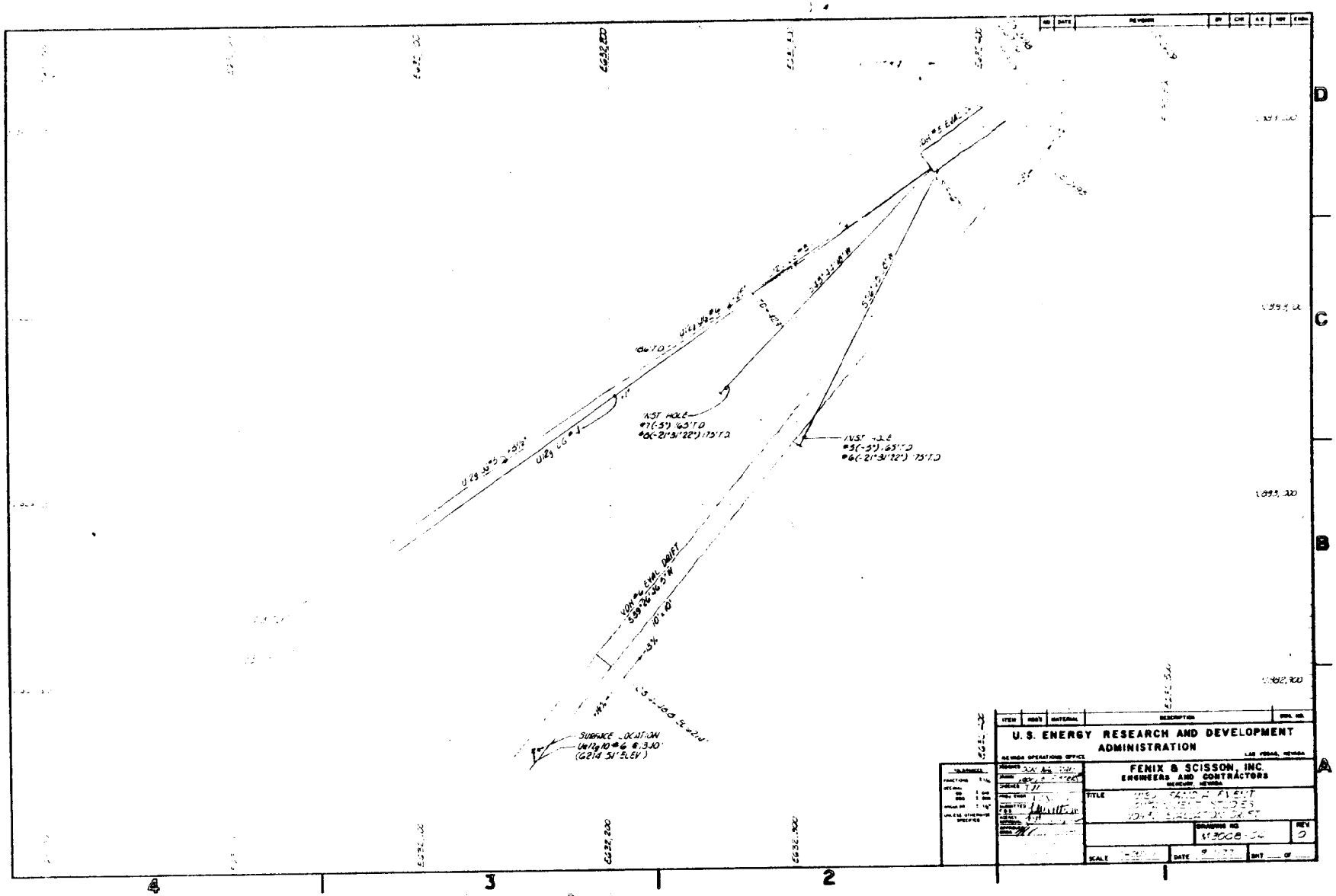
U.S. ENERGY RESEARCH AND DEVELOPMENT ADMINISTRATION
FENIX & SCISSON, INC.
ENGINEERS AND CONTRACTORS
SURFACE LOCATION
INST. HOLE
INST. HOLE

Fig. II-24

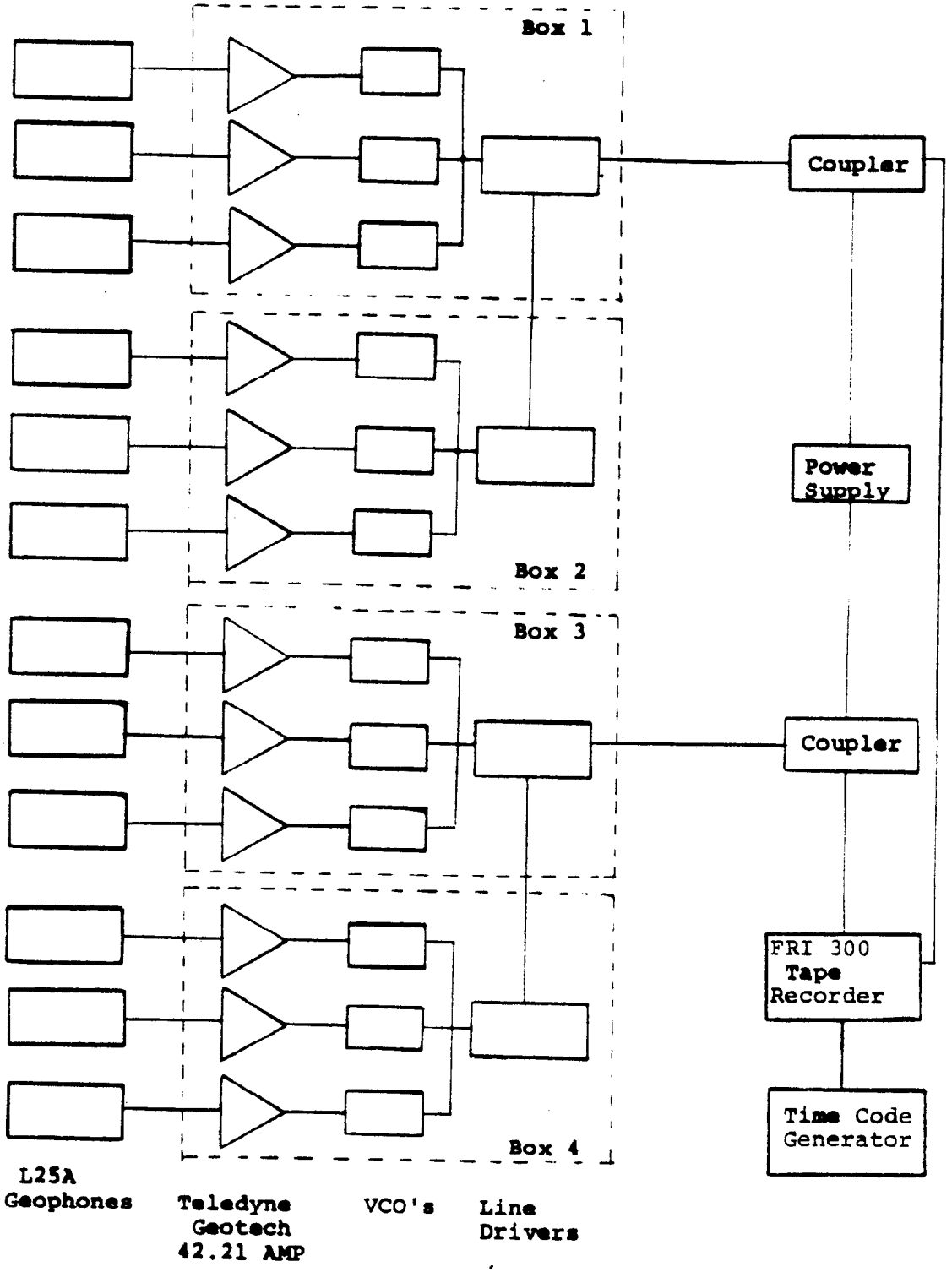

Fig. II-25 - Instrumentation System

Prior to recording the hydrofracture signals, the P-wave and S-wave velocities were measured at the end of G-tunnel, a 100 V, 100 Hz calibration signal was recorded, hammer blows on the drift faces (front, right and left faces) were recorded and the seismic signal generated by setting the packer was recorded.

On August 23, 1977 hole #6 was fractured at the 1352 to 1364 foot zone in ash fall tuff. A number of fracture related seismic signals were recorded. A total of 91 seismic events were noticeable upon initial examination of the data. A typical seismic signal appears in Fig. II-26. Each set of traces consist of two horizontal and one vertical geophone - the vertical geophone in the center trace. The first arrow on each trace indicates the P-wave arrival and the second arrow indicates the S-wave arrival.

Approximately 30 to 35 of the signals will be analyzed for wave content and recognition, amplitudes, frequency content and source location information. The source locations will be calculated using the following techniques.

1. Vector solutions from each triaxial package[1]
   four solutions

2. P-wave arrival times at four stations[2]
   one solution

3. S-wave, P-wave difference times at four stations[3]
   one solution

4. S-wave, P-wave difference times at three stations
   four solutions

---

[1] Los Alamos Scientific Laboratory Progress Report - LA6525PR, "LASL Hot Dry Rock Geothermal Project, July 1, 1975 - June 30, 1976", compiled by A. G. Blair, J. W. Tester and J. J. Mortensen.

[2] E. D'Appolonia Consulting Engineers, Inc., "Manual of Event Recognition and Interpretation Microearthquake Survey", T. L. Dobecki, January 1976.

[3] Bureau of Mines Bulletin 665, "Microseismic Techniques for Monitoring

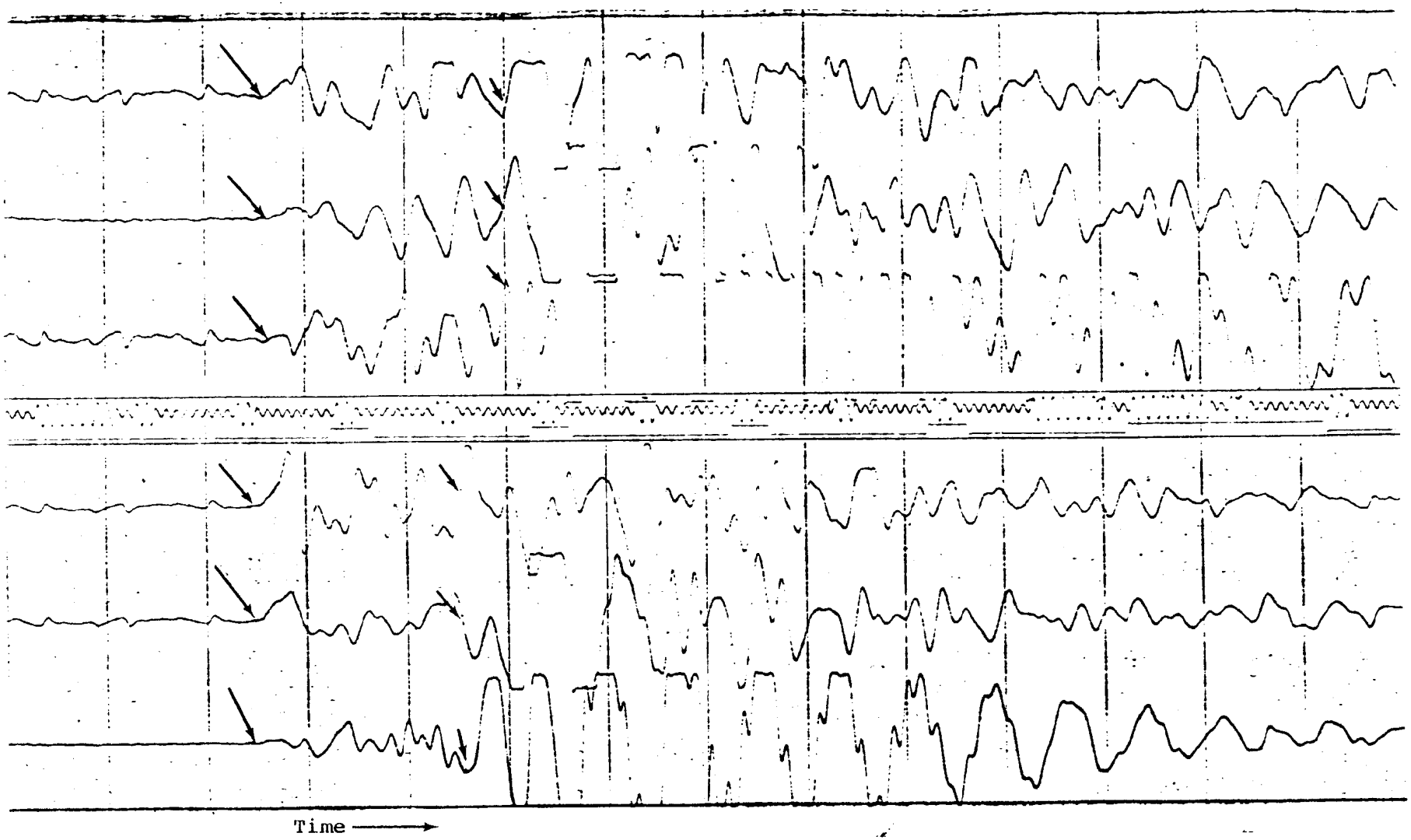

Fig. II-26 - Example of Observed Seismic Signals

The first calculations will also aid in evaluating the Borehole Seismic Locator since mineback will locate the fracture and accuracies can be estimated.

E. Borehole Seismic System

Examination of arrival times and polarization of seismic signals generated by hydraulic fractures may be used to map the size and orientation of those fractures. By employing a triaxial geophone package which is clamped to the borehole near the start of the fracture, the direction and distance to the seismic events created by the fracturing can be determined. Examination of a sufficient quantity of these seismic events may be used to determine the profile and orientation of the fracture near the wellbore.

The signals from two horizontal geophones may be used to calculate the azimuth direction of the event. A vertical geophone in conjunction with the horizontal geophones may be used to determine the angle of inclination to the source. Measurement of the difference in arrival times of the compressional wave (p-wave) and the shear wave (s-wave) may be used to calcualte the distance to the seismic event if the velocities of these waves are known. The addition of a package orientation device permits mapping of the fractures with respect to some geophysical reference.

A Borehole Seismic Locator (BSL) has been designed and has been fabricated. A triaxial geophone system has been incorporated with a mechanism to clamp the BSL to the wall of the borehole. The BSL is 3-5/8 inches in diameter and up to 16 feet long, capable of being locked to boreholes from 4-1/2 inches to 15 inches in diameter.

Figure II-27 shows component arrangement of the BSL. Power is supplied to the unit by means of a single conductor logging cable. Signals are sent to the surface over the same cable. The electronics package provides amplification for the geophone signal and controls for the clamping mechanism. The motor, arm drive, and clamping arm is the means for clamping the BSL to the wall. This unit is a portion of Geo Space Corporation Wall Lock Geophone System. The triaxial geophones are two horizontal and one vertical L-25A geophone produced by Mark Products. Orientation of the BSL is determined by using a photographic compass unit in open holes or a gyro unit in cased holes. The compass

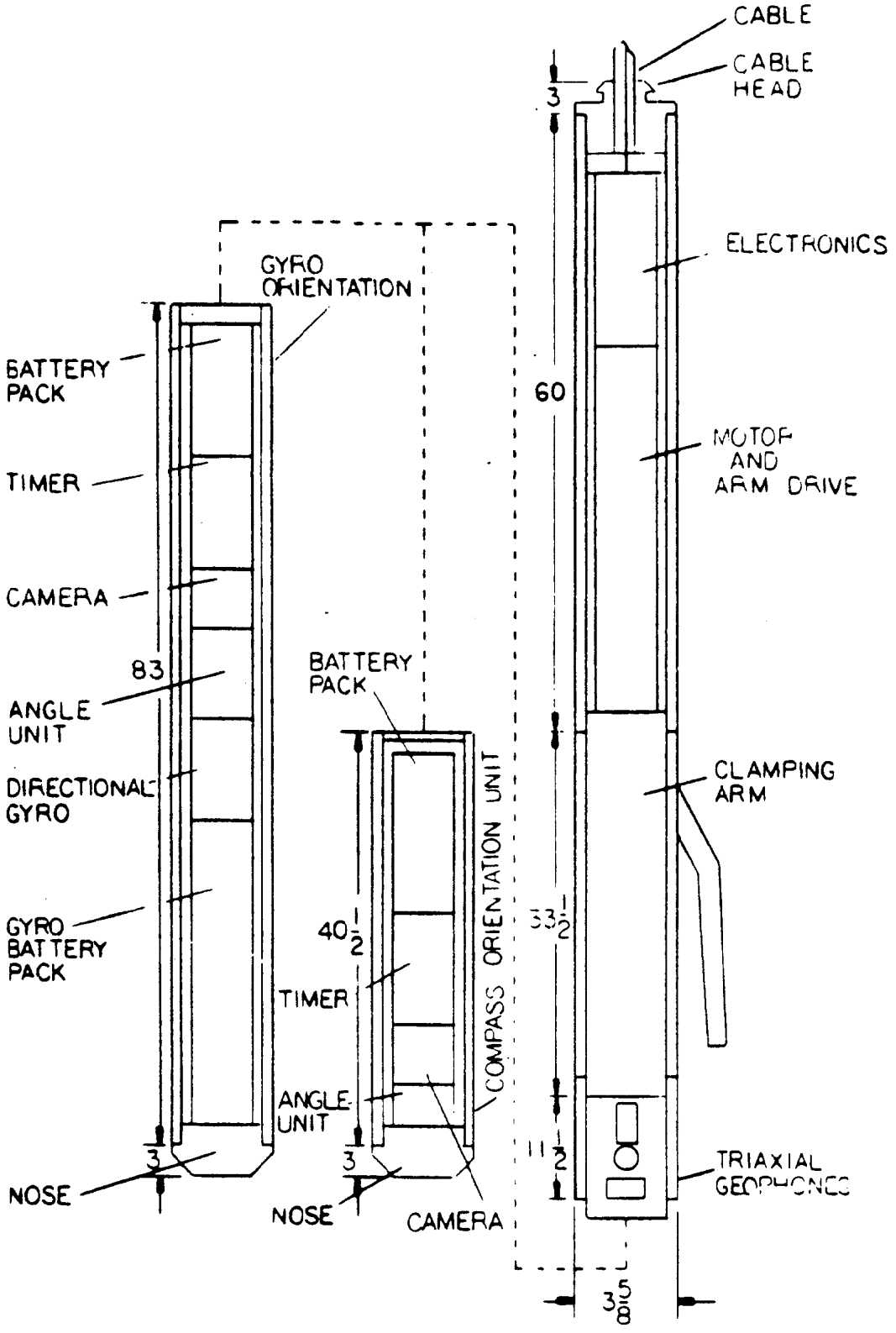

Fig. II-27 - Borehole Seismic Locator

unit contains a timed camera and a magnetic angle unit. Periodic photographs will be taken giving magnetic bearings and angle of inclination of the BSL. The gyro unit utilizes the same photographic unit in conjunction with a directional gyro and a gyro angle unit. The photographs will be developed after the BSL has been removed from the borehole. Both orientation devices have been purchased from Humphrey, Inc. Figure II-28 is a block diagram of the BSL electronics.

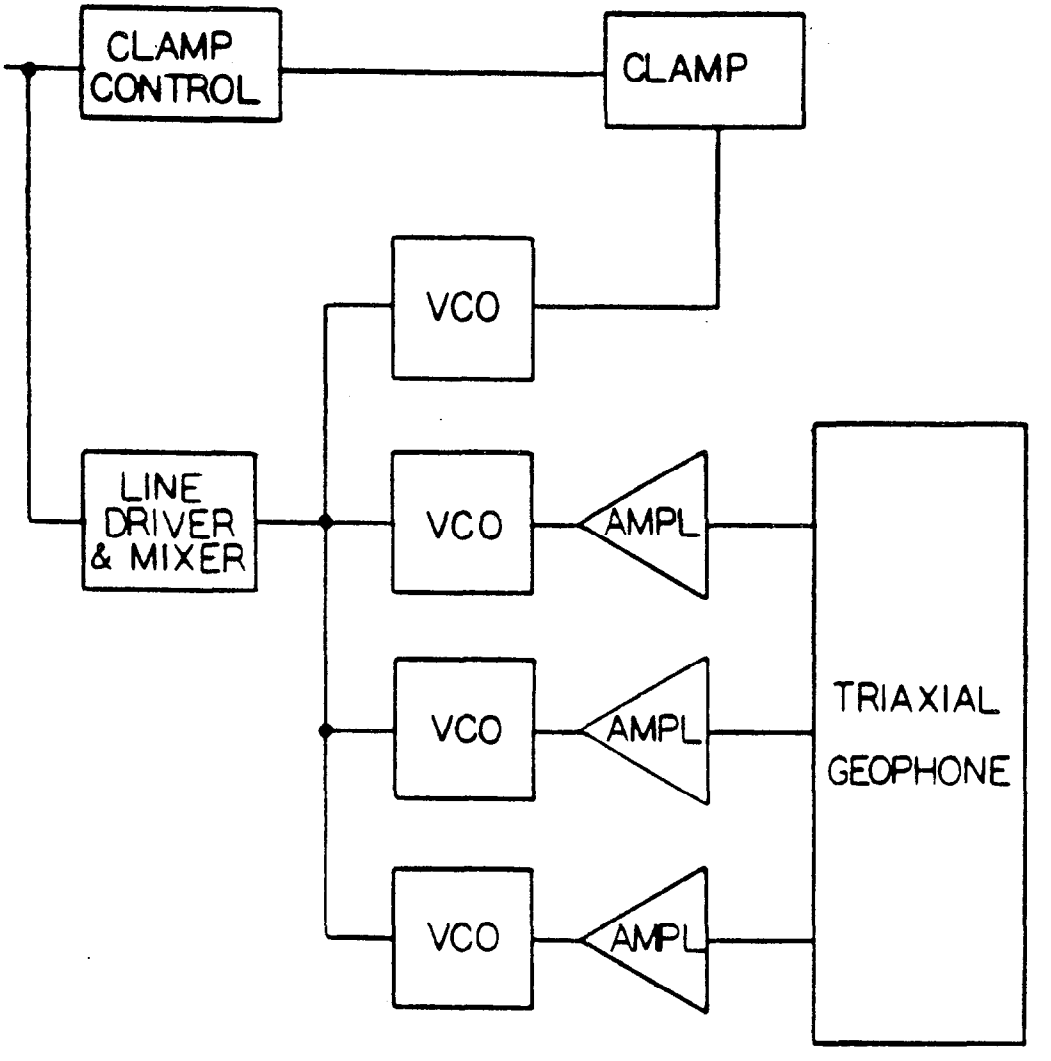

Fig. II-28 - Borehole Seismic Locator Electronics

The signals from the triaxial geophone array are amplified in Sandia Laboratories designed amplifier and modulate voltage controlled oscillation (VCO's). The VCO signals are multiplexed and transmitted to the surface through a line driven and a single wire line. At the

surface, these signals will be recorded on a magnetic tape recorder. Power to the system will be supplied from the surface over the same single wire line.

The Borehole Seismic Locator (BSL) was assembled and pressure tested at Southwest Research Institute in San Antonio, Texas. The geophone section which was fabricated from 304 stainless steel failed at 12,000 psi. This housing has been remade from 4340 steel. Stainless steel was initially used because of its proximity to the compass orientation unit. However, it is felt that because of the battery pack separating it from the compass unit, 4340 steel can be used.

During April, surface explosive tests were performed at the test well recently drilled on Kirtland Air Force Base. A number of charges were detonated at the surface in a number of locations. The charge sites were in contact with the limestone bed to which the BSL was coupled. These received signals will be analyzed for wave content and recognition, amplitudes, frequency contact and source location information. Because of the size and weight of the BSL, handling techniques were also evaluated and procedures refined.

Calibration data has been recorded for the electronic portion of the BSL. Gain and phase characteristics of the amplifiers and voltage controlled oscillators will be determined.

During FY 78, the BSL will be used for recording seismic signals from a hydrofracture of an AMOCO well in the Wattenberg Oil Field in Colorado.

Tests were conducted with triaxial geophones at the Nevada Test Site during hydraulic fracturing experiments. Recordings made during these tests will provide fracture seismic signal characterization and provide further information as to the accuracy of the system since mineback is planned in order to determine the size and extent of the fracture.

III. MINEBACK STIMULATION TEST PROGRAM (Edited by D. A. Northrop, 5732)

A. G-Tunnel Site and Mineback Operations
(G. B. Griswold, 5732, and W. C. Vollendorf, 1133)

G Tunnel is one of a number of tunnels that have been driven into Rainier Mesa at the Nevada Test Site for the purpose of conducting underground nuclear tests. This tunnel complex is shown in Fig. III-1. The mesa has strong topographic relief, ranging from an elevation of 6114 ft at the portal of G tunnel, which was driven into the base of the escarpment, to 7600 ft at the crest. The end of the tunnel complex is under 1000 to 1400 feet of cover, and thereby provides an effective maximum overburden stress in the range of 1000 to 1400 psi.

The geologic formations underlying Rainier Mesa are entirely of volcanic origin and a geologic cross section is shown in Fig. III-2. The majority of the section is composed of fairly flat-lying, ash-fall and welded tuffs. In the vicinity of G tunnel, this sequence of volcanic beds have been divided into four major geologic units. In descending order they are: Rainer Mesa Member (∿ 400 ft thick) consisting mostly of dense gray welded tuff, Survey Butte Member (∿ 850 ft) of gray to brown ash-fall tuff, Grouse Canyon Member (∿ 150 ft) of dense gray to reddish welded and ash-fall tuff, and the Tunnel Beds (∿ 1000 ft) of well-layered gray to pinkish brown ash-fall tuff.

The G tunnel complex was driven entirely in bedded ash-fall tuff. It is a near ideal medium to conduct fracture studies because of its uniformity in physical characteristics and absence of zones of native fracturing. Faults are present, but typically are of small displacement and rehealed. Figure III-3 is an enlarged view of the region where these experiments are being conducted. The locations of the Hole 5 (proppant distribution) and Hole 6 (formation interface) experiments are shown. The contact between the bedded and welded tuffs in the Grouse Canyon Member was the interface used in the Hole 6 test and occurred at a depth of 1346 ft.

The in situ examination of created fractures is provided by mining operations. A self-advancing, Alpine miner is used to make successive cuts at the working face. As seen in Fig. III-4, the mining head produces an exceptionally clean face which allows for detailed evaluation. Fracture descriptions are obtained via colored photography and detailed

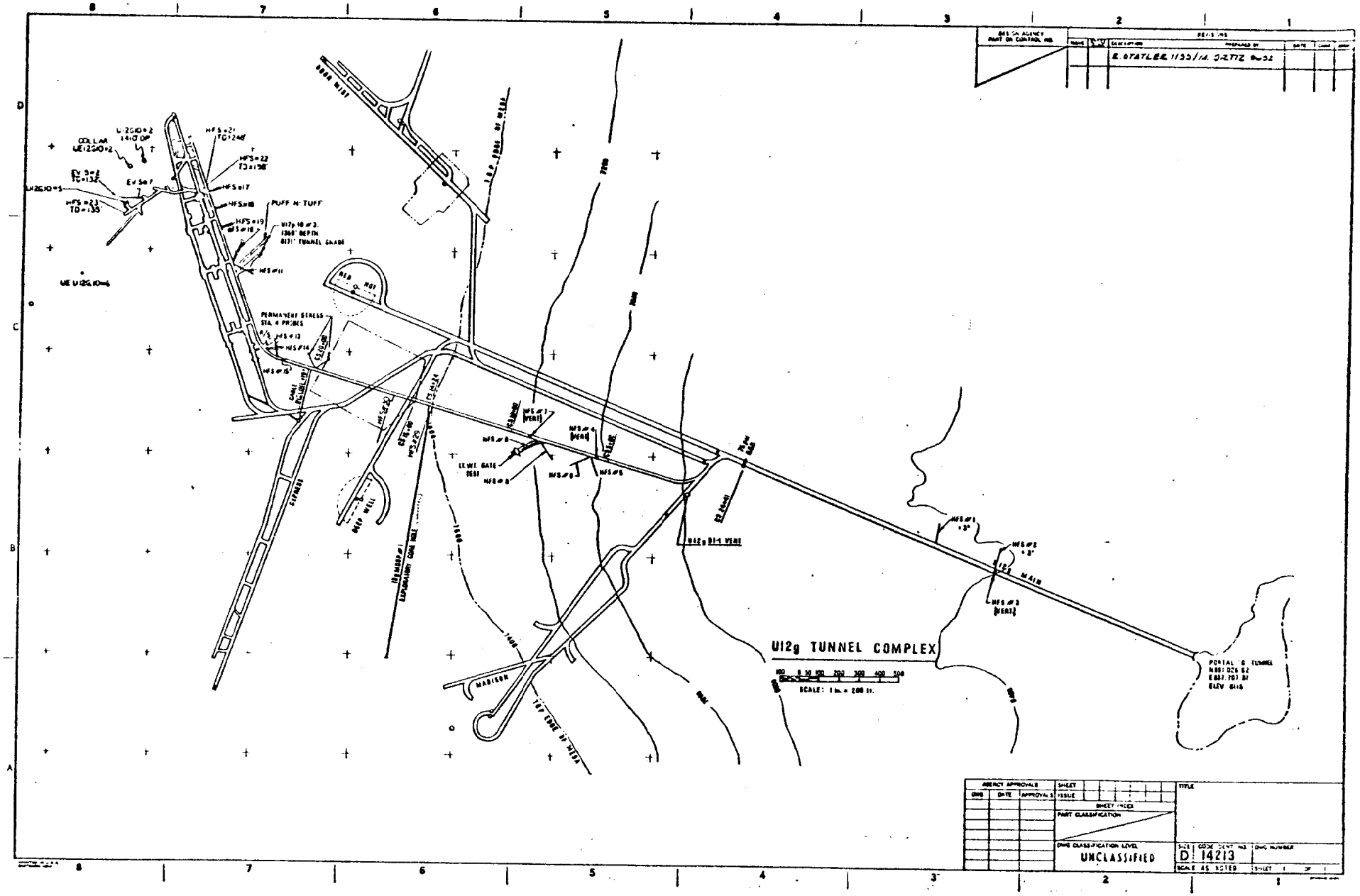

Fig. III-1 - Plan View of the U12g Tunnel Complex

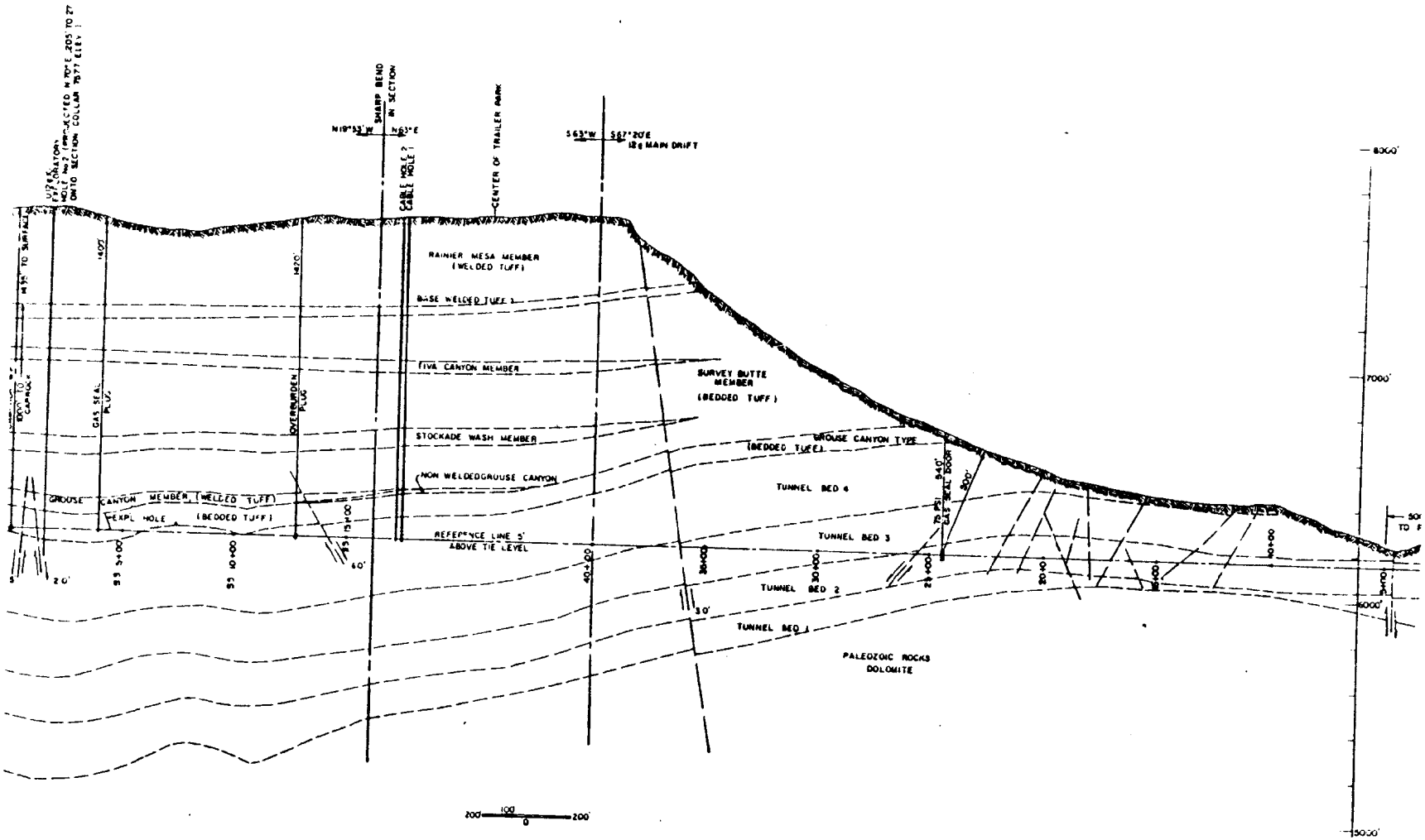

Fig. III-2 - Geologic Cross-Section of the U12g Tunnel Complex

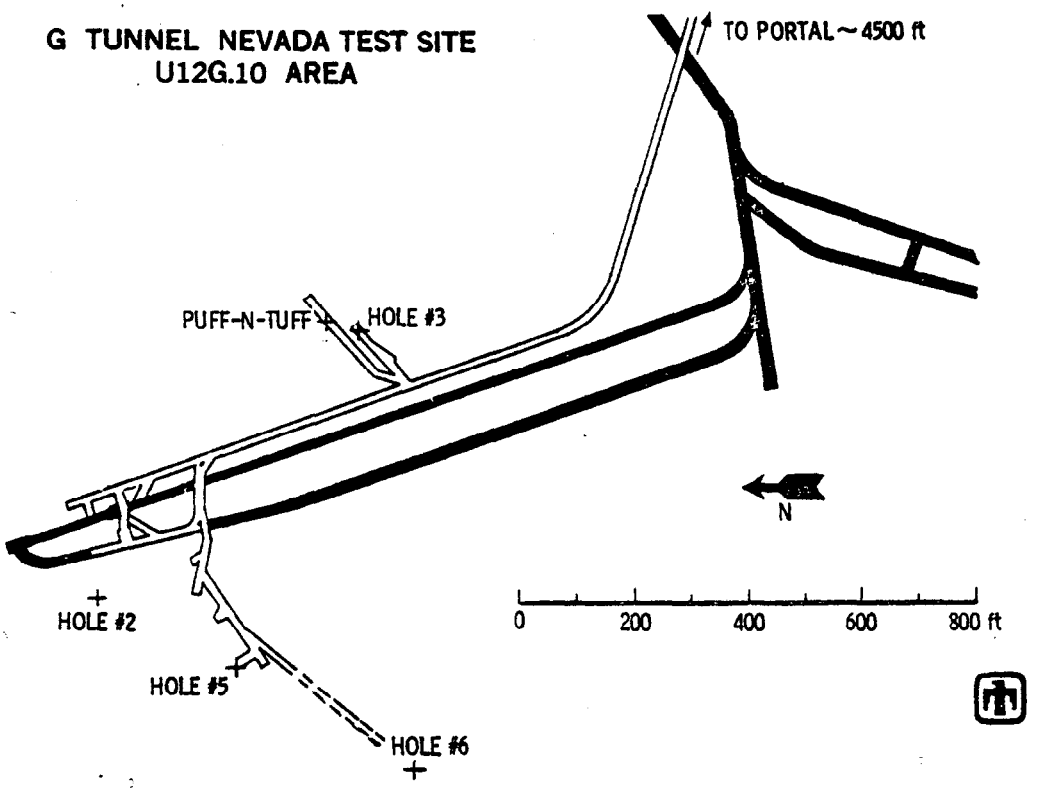

Fig. III-3 - Close-up of Mineback Experiment Sites

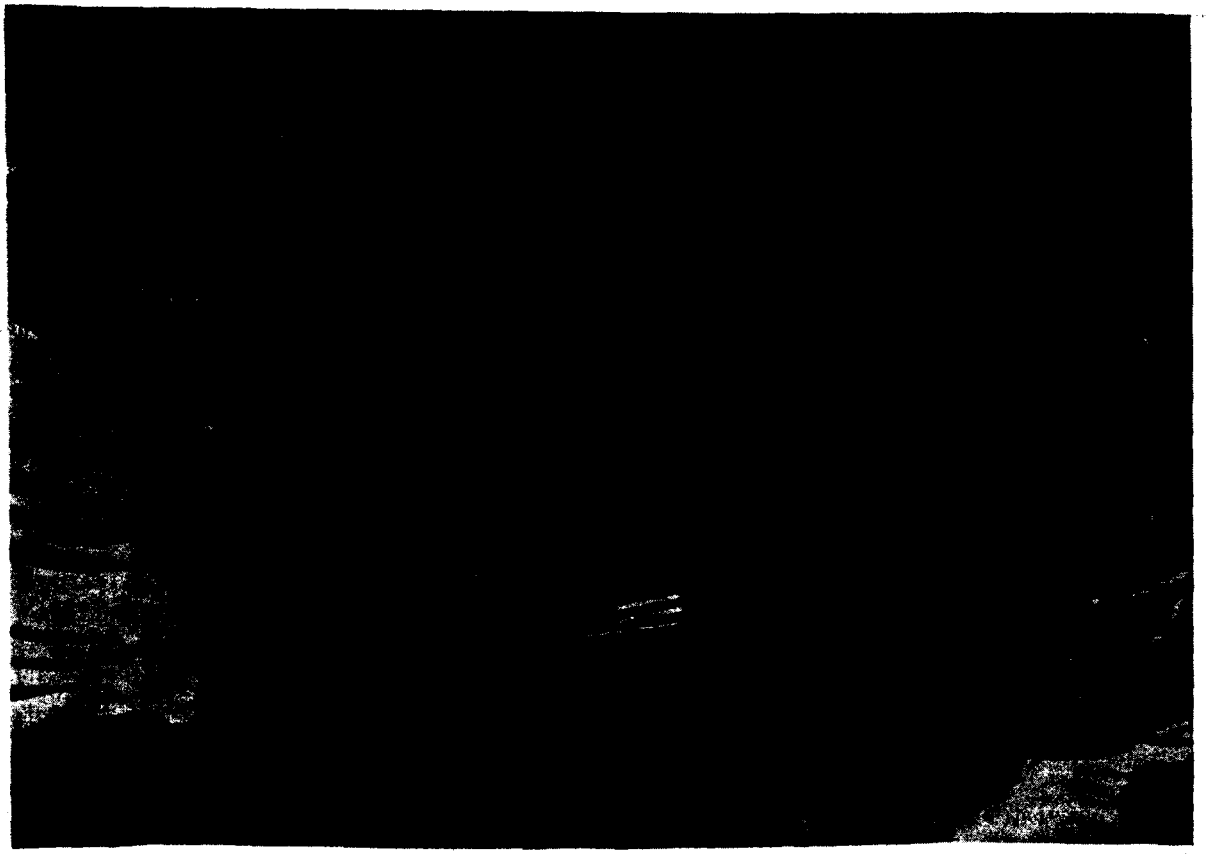

Fig. III-4 - View of Alpine Miner's Cutting Head and Uncovered Grout-Filled Fracture and Borehole.

geologic notes and maps. Recently, stereophotography and computer reduction of these photographs have been investigated for additional data presentations. In addition, coreholes are drilled from existing drifts to further delineate the created fracture system. Rock samples can be obtained for material property measurements at specific regions of interest. In situ stress measurements are made via both overcore and small hydraulic fracture techniques*. The latter technique is particularly convenient, as subsequent mineback examination yields the orientation normal to the minimum principle stress.

B. Proppant Distribution Experiment: Hole 5
(L. D. Tyler, 1111, and G. B. Griswold, 5732)

The basic objective of the test was to study sand proppant transport and deposition in a hydraulically-induced fracture. The fracture treatment design was a joint effort between Sandia and technical representatives of Halliburton, Inc., the latter being the service company who actually conducted the fracture operations.

The proper identification code number of the test hole is UE12g10 No. 5. (The code reads that the hole was drilled in Area 12, in G tunnel, in the vicinity of the 10th drift, and is hole No. 5 of a sequence.) The exact location by the NTS coordinate system is 883,237 N and 632,370 E. The collar elevation is 7570 ft and the total depth was 1400 ft. The hole was drilled during 1976. The core log indicated characteristics typical of the Tunnel Beds tuff with a fracture in the zone where the test was to be conducted.

The fracture design is shown schematically in Fig. III-5 and involved the following sequence of operations:

1. Place an HQ rod (3-1/8" ID) inside hole with the packer element on bottom.
2. Circulate the hole with clean water.
3. Set the packer at 1395 feet.
4. Run a string of NQ rod (2-3/8" ID)
5. Conduct the fracture treatment by pumping fluid down the center rod with the annulus between the two rod strings packed off at the surface.

*Haimson, B. C. et al, "Deep Stress Measurements in Tuff at the Nevada Test Site," Proc. of the Third Conference, International Society of Rock Mechanics, Denver, CO, 1974.

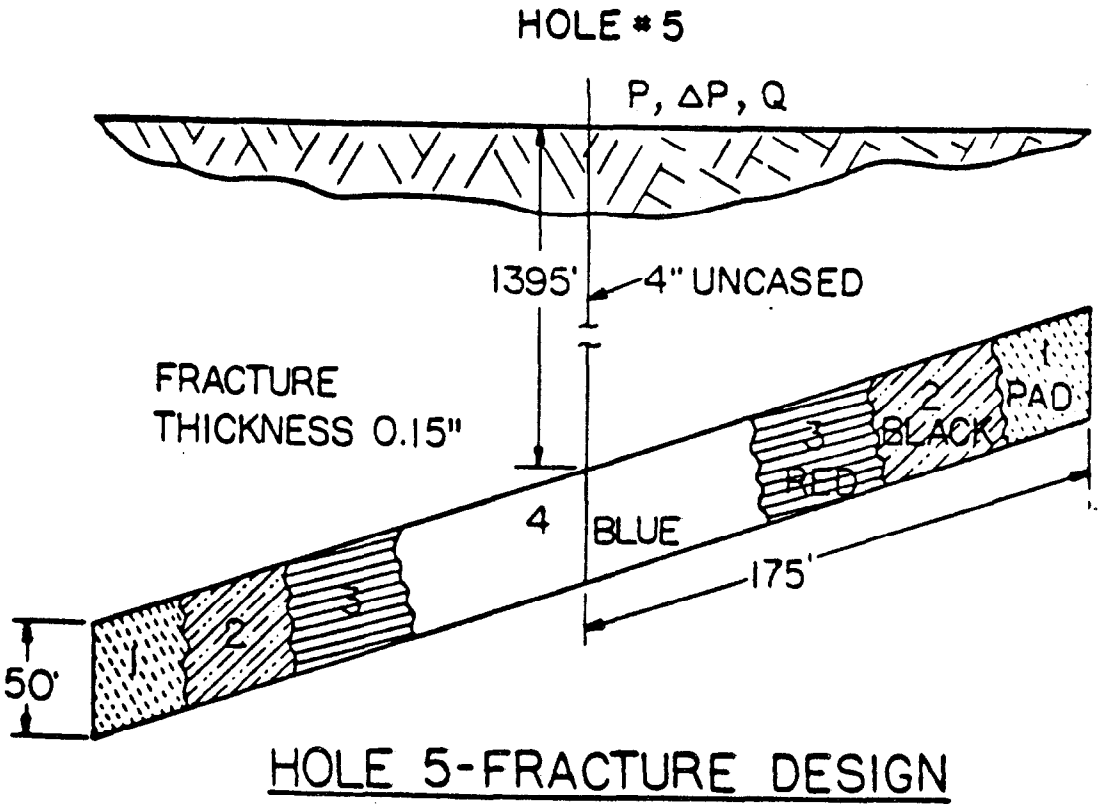

Fig. III-5

6. During breakdown and treatment, the pressure inside the NQ rod string and the static pressure on the annulus would be measured with high sensitivity pressure transducers.
7. Fracture initiation would be under open hole conditions in the 5 foot zone from the packer to the bottom of the hole.

The fracture fluid was specially tailored to the test requirements and was scheduled as follows:

1. Breakdown - 350 gallons of water-based gel
2. 1st Stage - 450 gallons of water-based gel with black-dyed, 20-40 mesh sand at 1 lb per gallon concentration.
3. 2nd Stage - 400 gallons as above but with red sand at 2 lb per gallon.
4. 3rd Stage - 400 gallons as above but with blue sand at 3 lb per gallon.
5. Flush - 320 gallons of clear water to flush the 3rd stage clear of the drill rod.

All fluids were premixed. Once injection commenced, it was to be maintained at a constant rate as possible with no shutdown between

stages other than valve switching. The injection rate was to be 4 bbls per minute. The design of the water-base gel (designation PWG/FR26L) called for a viscosity in the range of 30 to 100 cp. Fracture design calculations predicted a distribution of colored sand proppants as shown in Fig. III-5.

The test occurred on August 23, 1976 and proceeded as planned. The results from the pressure and injection rate sensors are shown on Fig. III-6. Significant operational events are also noted on the diagram.

An array of acoustic signal detectors had been placed underground in the tunnel to detect acoustic signals related to fracture propagation. Seismic signals were recorded, but data analysis has revealed that all of the decipherable signals originated from the vicinity of the wellbore; none were detected that could be associated with a growing crack.*

An analysis of the injection records as exhibited in Fig. III-6 has led to these observations:

(1) The pressure spike at point 1 indicates that the formation may have broken down while circulating clear water. The maximum pressure recorded was 975 psi, but this pressure may not represent true breakdown. The record does indicate that the annulus was prematurely closed while pumping. The instantaneous shut-in pressure (point 2) was ~850 psi. Another pressure spike was recorded (point 3) upon initiation of pad injection; this peak was 1060 psi.

(2) Rapid pressure increase was observed during pad injection. At point 4, the pressure was 820 psi and by the time the first stage started to enter the hole, the pressure had climbed to 1100 psi (point 5). The injection pressure continued to climb until the completion of injection (1425 psi at point 6).

(3) An excellent record of the instantaneous shut-in pressure was recorded after shut down (point 7).

*Further details of this aspect of the experiment are given in the first Annual Report of this program: Sandia Laboratories Report, SAND-77-0286, June 1977, p. 62.

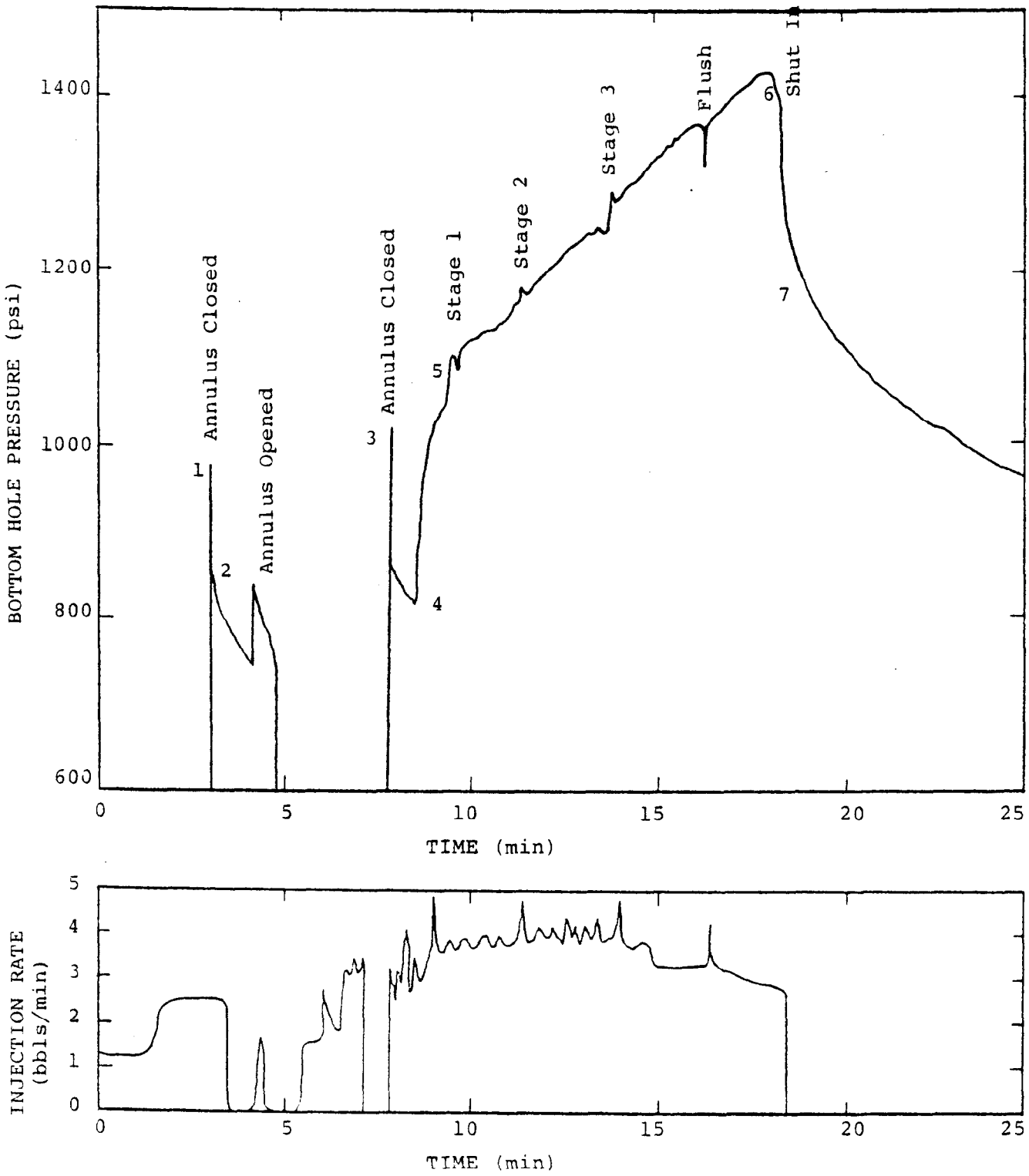

Fig. III-6 - Injection Pressures and Rates, Hole 5 Test

(4) The gross shape of the pressure plot between points 4 and 6 is exponential while the injection rate remained nearly constant. Such behavior should be expected from a constantly growing radial fracture being fed from the wellbore. However, the final injection pressure was 1425 psi versus a minimum rock stress of $\sim$ 850 psi. The 575 psi pressure difference must be ascribed to friction losses, probably very near to the wellbore, because theory states that the pressure required to propagate a fracture is only slightly over the minimum stress.

(5) Seismic signals related to fracture propagation were not detected and this suggests that a normal fracture was not formed.

(6) The friction loss down the pipe, as measured by taking the difference between the surface injection and annulus pressures, of the frac fluid were similar to those for the water flush. Therefore, the conclusion is that the actual frac fluid viscosity was about 1 centipoise. The low viscosity is in agreement with the composition of the frac fluid which contained a friction reducing agent. Under turbulent flow conditions experienced in the pipe the fluid has low ($\sim$ 1 cp) viscosity. Under laminar flow conditions expected in the fracture, the viscosity rapidly increases. The design viscosity for laminar flow was 79 centipoise.

Mineback operations commenced from the end of the then existing tunnel, approximately 200 ft from Hole 5 (see Fig. III-3). A number of mini-breakdown tests were accomplished ahead of the mining sequence for in situ stress measurements. A long horizontal hole had been previously drilled and six breakdown tests conducted prior to fracing Hole 5. The mining plan therefore included mining along that hole while advancing towards the Hole 5 region.

No evidence of the Hole 5 fracture was found in the main drift even after it was driven to a position some 60 ft from the borehole. An exploratory coring program was then conducted to search for the fracture. Seven holes were drilled from stations in the drift or short cross-cuts off the main drift. Evidence of the fracture was obtained only in three of the holes and the decision was then made to cross-cut directly to the borehole. Eventual mineback operations resulted in creating a small gallery in the vicinity of the borehole as shown in Fig. III-7.

A simple fracture was not created by the staged proppant experiment. Details of the fractures are shown in Figs. III-8, 9, and 10. The mine-back has indicated that the main course of the fracture was downward and to the south. The primary fracture was steep but sinuous. A secondary fracture branched off the main zone and its orientation was about 30° from horizontal. Both fractures cut bedding and minor fault planes for most of their course except in two significant cases. Upward growth of the main fracture terminated against a flat bedding plane or parting forcing the fracture to propagate downward. The secondary fracture was effectively terminated by a high angle fault. No distinct distribution pattern of the three stages of colored sand proppant was witnessed during mineback. In most instances the three colors were mixed. The fracture width varied from 1 to 5 mm.

This experiment was conducted closer to a nuclear event than the Hole 3 experiment conducted in 1975 and which produced a more "classical" fracture.* Thus, the results from the Hole 5 test may be confounded by effects from the nuclear event. Nonetheless, significant observations can be made:

(1) fracture growth was limited and affected by faults,
(2) the fracture did not penetrate, and sand proppant was not found in, an open fracture about 3-5 from the borehole,
(3) upwards growth of the fracture was limited by a parting plane (essentially a no strength interface),
(4) no distinct patterns of the three stages of colored sand proppant were observed,
(5) orientation of the minor fracture changes as it passed through different bedding planes, and
(6) observed fracture is dramatically different than the design fracture.

No simple explanation can be given for the fracture complexity observed in this test. Work is now underway to study the in situ stress distribution in the region as well as obtaining a comprehensive set of rock properties. This work will hopefully contribute to our understanding of this complex fracture experiment.

*Tyler, L. D. and Vollendorf, W. C. "Physical Observations and Mapping of Cracks Resulting from Hydraulic Fracturing In Situ Stress Measurements," SPE Paper 5542, 50th Annual Technical Conference and Exhibition, Society of Petroleum Engineers of AIME, Dallas, TX, September 30-October 1, 1975.

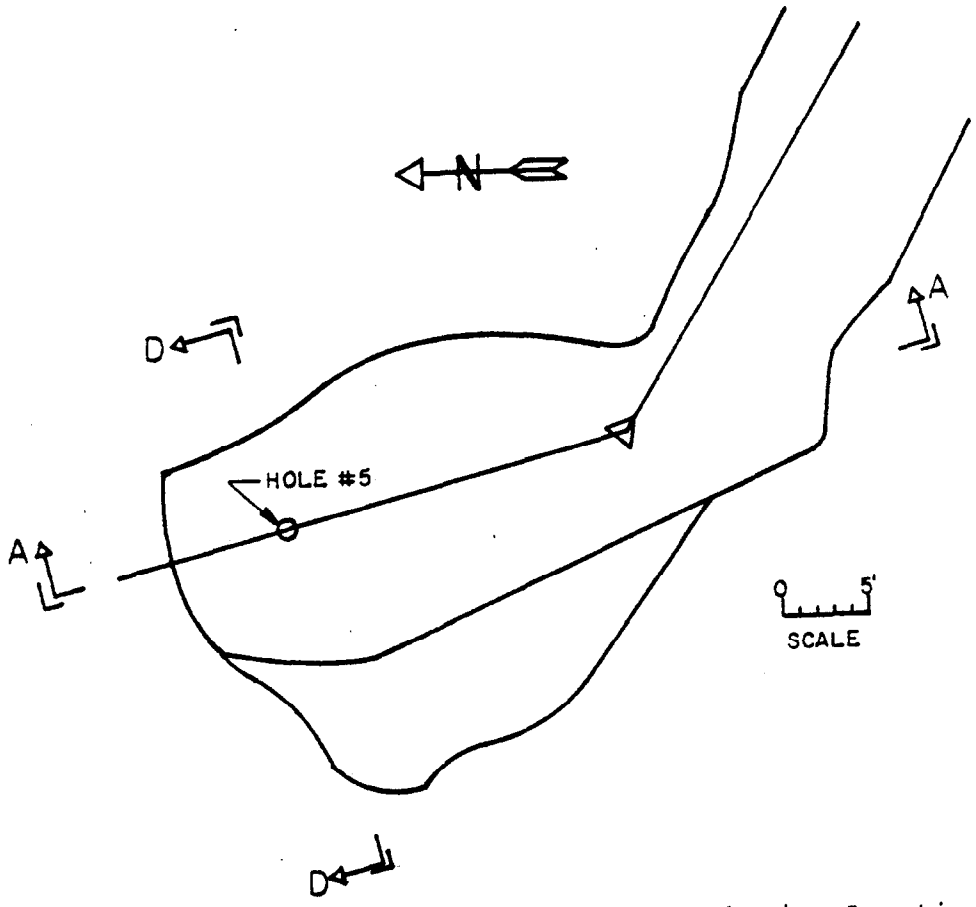

Fig. III-7 - Plan View of Hole No. 5 Mineback Showing Locations of Vertical Sections.

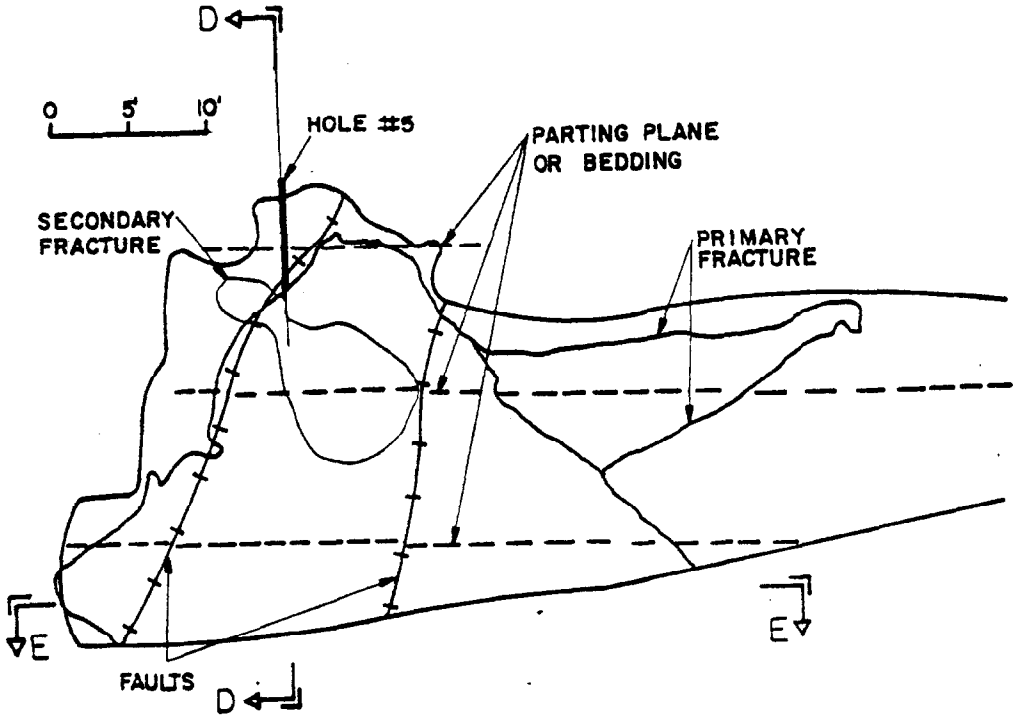

Fig. III-8 - Longitudinal Cross-Section A-A

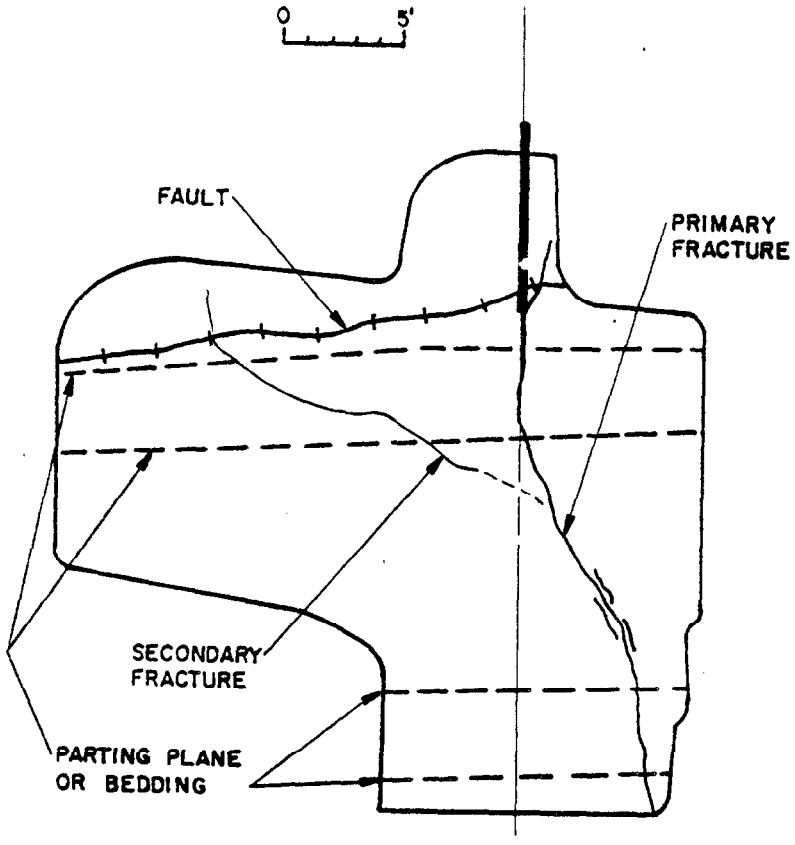

Fig. III-9 - Cross Section D-D, Looking North

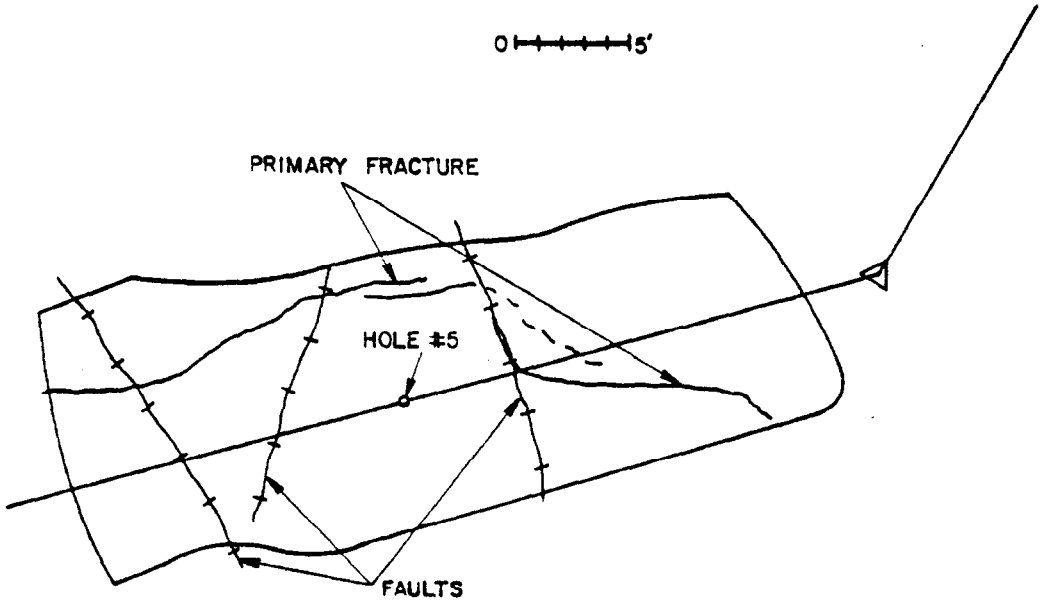

Fig. III-10 - Plan View E-E of Fractures 15 ft Below Bottom of Hole No. 5.

C. Formation Interface Experiment: Hole 6
(N. R. Warpinski, 5732, L. D. Tyler, 1111, and G. B. Griswold, 5732)

The behavior of hydraulic fractures at formation interfaces is not well understood and its investigation is of prime interest to industry. A formation interface between the ash fall and welded tuffs is available in G tunnel and was utilized in the design and conduction of the Hole 6 experiment. The initial test design was formulated at a meeting of Amoco, Dowell, Halliburton, and Sandia representatives in Tulsa, OK on February 22, 1977. Specific fracture design was performed by Dowell and they conducted the actual frac jobs at the Nevada Test Site.

The location of the test hole was chosen at a site 425 feet south southwest of Hole 5. Hole 6, which is officially designated UE12g10#6, is shown in Figure III-3; the exact location is N882,870.34, E632,160.37 referenced to the NTS coordinate system. The hole's collar elevation is 7554.76 feet and its total depth is 1455 ft. The hole was cored and nuclear, density and caliper logs were run. The dense welded tuff unit was encountered from 1320 to 1336 feet as can be seen from a section of the density log in Figure III-11. From 1336 to 1352 feet is a transition region where there are many voids, fractures and breccia. Below 1352, the ash fall tuff is easily identified. The location of the welded tuff unit in the hole is about 50 feet higher than was originally anticipated and will necessitate uphill inclined mining to expose the interface. Table III-1 shows the properties of the various formations as determined from cores of Hole 5 nearby.

On July 8, 1977, a second meeting with Dowell was held in Albuquerque to finalize the design of the experiment. It was decided that each zone of the tuff be fractured separately with Class "A" cement containing 1% D-60 mixed at 15.4 lbs/gal. The properties of the grout are shown in Table III-2. Different colored grouts would be used in each formation to allow easy mineback identification of the cement-filled fractures. Fifty foot vertical fractures with 300 foot wings appeared sufficient for the purposes of the experiment. Given the average reservoir properties shown in Table III-3, Dowell provided a fracture design calling for 8000 gallons of grout pumped at 6 bbls/min for the ash fall tuff and 5000 gallons of grout at the same flow rate for the welded tuff. These designs would produce widths of 0.4 in. and 0.15 in. respectively.

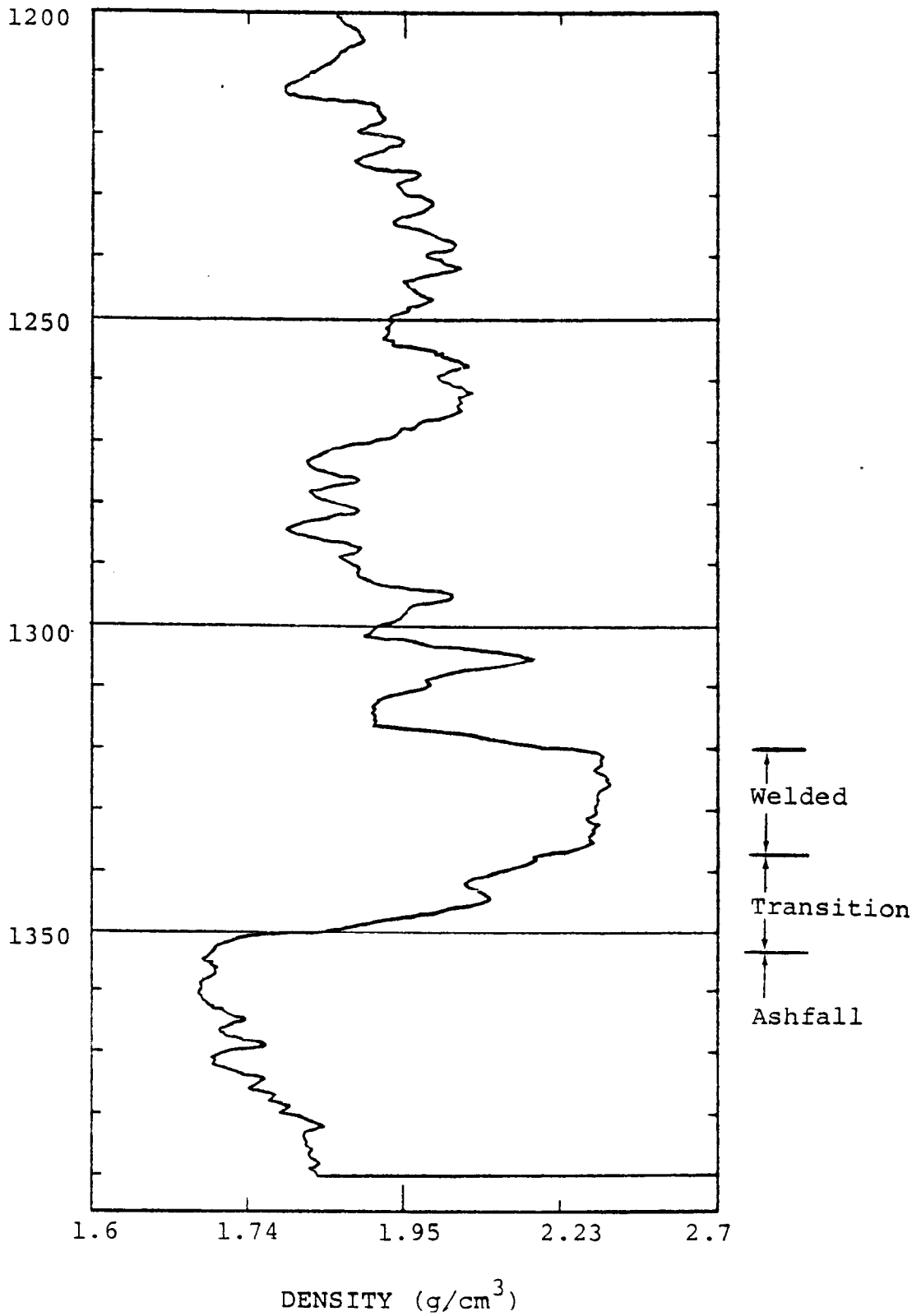

Figure III-11 - Density Log of Hole 6

TABLE III-1

Material Properties

Obtained From Hole 5 Cores

Depth Interval (ft)	Description	Permeability Horiz. (md)	Permeability Vert. (md)	Porosity (%)	Grain Density (g/cm^3)	Bulk Density (g/cm^3)	E (10^6 psi)	Poisson's Ratio
1303.0 1304.0	Upper Transition	0.01	<0.01	13.8	2.30	1.91	2.01	0.13
1338.3 1339.4	Welded Vapor	0.04	0.04	15.1	2.58	2.29	4.94	0.22
1358.8 1359.8	Dense Welded	<0.01	<0.01	9.8	2.50	2.23	Test Failure	
1364.1 1365.6	Lower Transition	0.82	0.88	21.1	2.60	2.12	3.79	0.15
1383.0 1384.3	Ash Fall	1.4	1.4	39.2	2.20	1.39	0.45	0.17

TABLE III-2

Properties of Class "A" Cement
With 1% D-60 @ 15.4 lbs/gal

Yield	1.21 ft^3/sack	
Viscosity	128 cps	
n'	0.86	Pseudo Plastic
k' (not corrected)	0.0031 lb-$sec^{n'}/ft^2$	Pseudo Plastic
η	0.07 lbm/ft-sec	Bingham Plastic
τy	0.23 lb/ft^2	Bingham Plastic
Cw	4.1×10^{-3} ft/$\sqrt{min}$	
Spurt	0	

TABLE III-3

Reservoir Properties

	Ash Fall Tuff	Welded Tuff
Bulk Density (g/cm^3)	1.77	2.37
Grain Density (g/cm^3)	2.42	2.6
Porosity (%)	44.6	13.0
Water Saturation (%)	100.0	100.0
Modulus of Elasticity (10^6 psi)	0.236	3.8
Poisson's Ratio	0.312	0.238
Permeability (md)	0.01	0.022-2.2
Bulk Modulus (10^6 psi)	0.221	2.44
Shear Modulus (10^6 psi)	0.111	1.5

Details of the fracturing operations were finalized in August and are shown in Figure III-12. The first fracture would be initiated in the ash fall tuff. The well would be back filled with pea gravel to 1364 ft and an inflatable packer would be set with the bottom of the element at 1352 ft. This would provide a 12 foot isolated zone just below the transition region. Downhole pressures would be monitored with an Amerada bomb on a wireline in the open zone and a transducer hardwired to the surface situated in a sub directly above the packer. Wellhead pressure would be obtained from a transducer at the surface and the flow rate would be taken from Dowell's instrumentation. The formation would be broken down with 30 bbls of water. After a short quiet time for acoustic measurements, 4000 gal of green grout followed by 4000 gal of black grout would be injected. This would be displaced from the well bore with 10 bbls of water and then shut in for another quiet period.

The second fracture, also shown in Figure III-12, would be initiated in the dense welded tuff region. The hole would be back filled to 1331 feet and the packer set at 1323.5 feet, leaving an open interval of 7.5 feet. A notch, cut at 1328.5 feet would reduce breakdown pressure and insure that the fracture would initiate at that point. The same pressure and flow rate measurements would be obtained and the same fracturing operation followed, with the exception that only 5000 gal of blue grout would be injected.

An array of four triaxial geophone assemblies were emplaced in coreholes near the fracture region. Further details of this part of the experiment can be found in Section II-C.

The ash fall tuff zone of Hole 6 was fraced on August 23, 1977. A few items on the operational plan were modified as the experiment progressed. The pea gravel was tagged at 1358 feet instead of 1365 ft, leaving an open interval of only 4 feet. This required that the six foot long Amerada bomb be positioned above the packer at 1337 feet. The quiet time after breakdown was eliminated and the fracturing commenced immediately. Dowell injected 128 bbls of green grout and 90 bbls of black grout instead of the original design volume of 96 bbls of each. The pressure transducer at the surface malfunctioned and, consequently, no well head pressure data was obtained. Without this data, the friction losses through the pipe could not be determined. Figure III-13 shows the flow rate and downhole pressure data that were obtained as well as the location and number density of acoustic signals that are believed

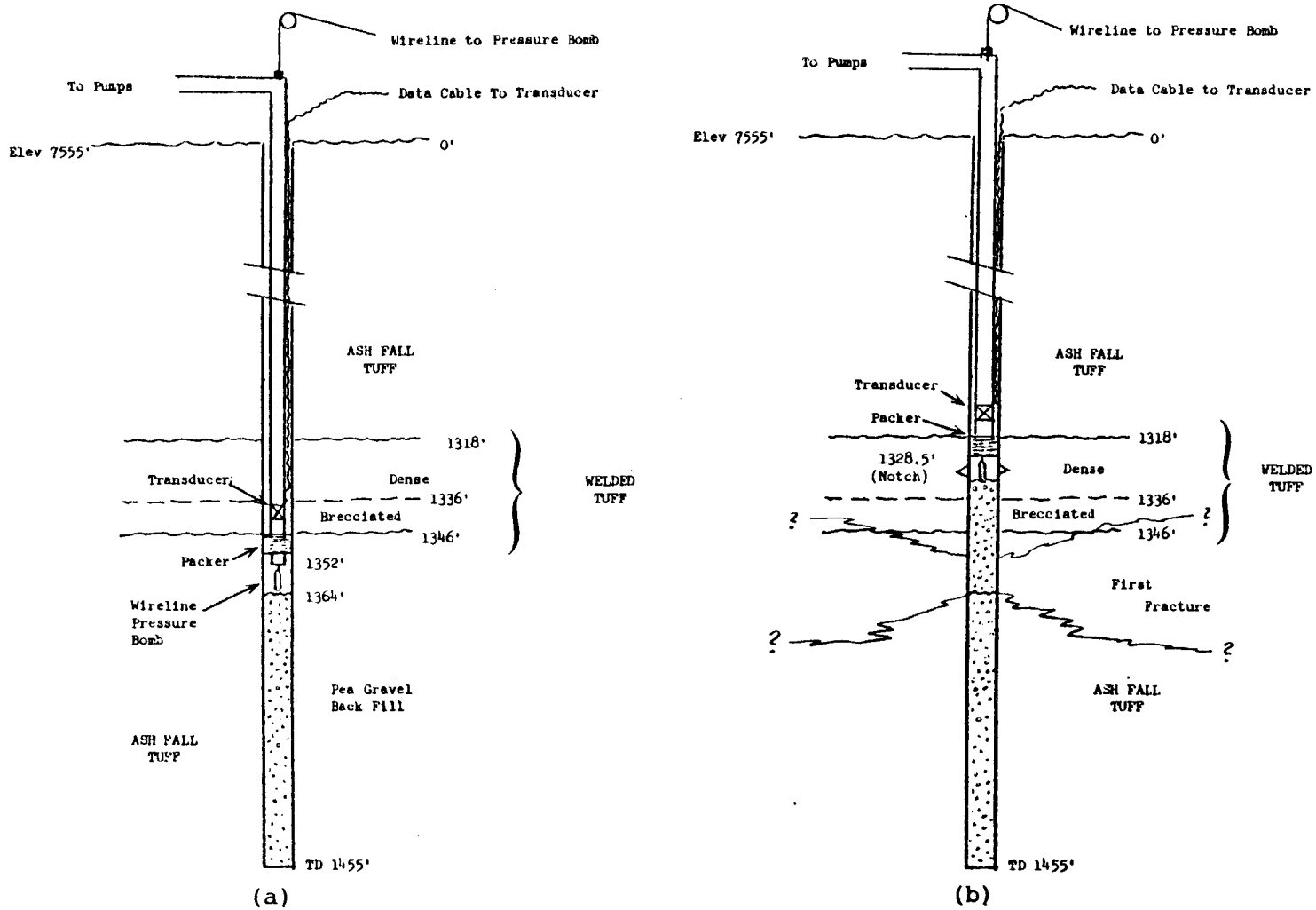

Figure III-12 - Fracture Locations, Formation Interface Test, Hole 6: (a) Lower Frac, (b) Upper Frac

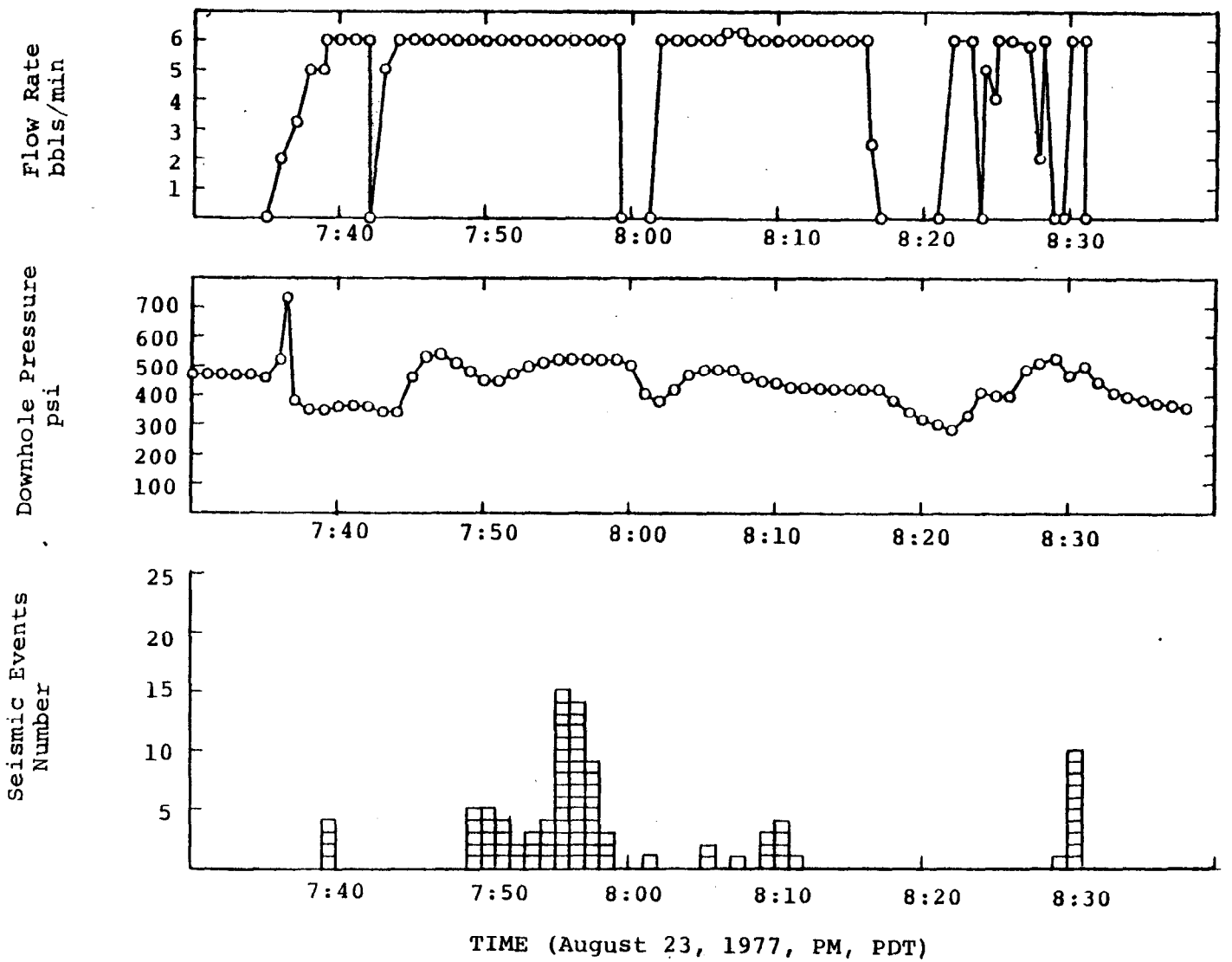

Figure III-13 - Flow, Pressure, and Seismic Data Recorded During the Lower Frac Job in Hole 6

to be fracture related. Not shown on the pressure record are severe fluctuations that are thought to be a result of a water hammer effect. These fluctuations occurred at approximately 7:40 and 8:28 for a duration of about 2 minutes each.

In order to translate the specific results of this experiment into general "fracture-interface interaction" criteria it is necessary to relate the results to their hydraulic fracturing history. For example, filling open fractures will provide no fracture-interface confrontation and unusual in situ stress distributions might produce unexpected results. It is expected that the pressure and flow measurements, as well as the acoustic measurements, can provide information to characterize the fracturing process prior to mineback. A number of preliminary observations have been based on these data.

As indicated in Figure III-13, the bottom hole pressure (BHP) before fracturing was constant at 465 psi. This demonstrates that fluid was not flowing into the formation and the zone was tight. The 730 psi pressure spike at 7:35.30 was coincident with the start of pumping and probably indicates breakdown. Although this is somewhat lower than expected, the minimum in situ stress (σ_{min}) cannot be greater than the smallest pressure (340 psi) observed during fracturing and a breakdown pressure that is 390 psi above σ_{min} is not unreasonable. If it is assumed that the maximum principle in situ stress (σ_{max}) can be calculated from

$$\sigma_{max} = 3\ \sigma_{min} - P_c + \sigma_t\ ,$$

where P_c is the breakdown pressure and σ_t is the tensile strength, and further, that the tensile strength is on the order of 300 psi, then an upper limit on σ_{max} can be placed at 590 psi.

Given the material properties in Tables III-1 and III-3, it is expected that a significant pressure rise would have been observed if the fracture had broken into the welded tuff formation. No such pressure increase is evident in Figure III-13. However, as shown by Simonson et.al.*, tectonic stress variations can also affect fracture propagation. If the in situ stresses in the welded tuff are lower than

---

*Simonson, E. R., Abou-Sayed, A. S. and Clifton, R. J. "Containment of Massive Hydraulic Fractures," SPE 6089, 51st Annual Conference and Exhibition, Society of Petroleum Engineers of AIME, New Orleans, LA, October, 1976.

those in the ash fall tuff, the effect would be just the opposite expected from the inherent material property variations. Thus, it is very important that in situ stress measurements be made in both formations at various locations around the fracture. Finally, in order to observe this interaction, it is mandatory that the fracture "climb" as it propagates. This is usually expected in fracturing operations since the fracturing fluid's hydrostatic pressure gradient is less than the lithostatic pressure gradient. In the present case, the lithostatic pressure is due entirely to the overburden and the gradient in the ash fall tuff region is proportional to the tuff density which varies from 1.4 to 2.0 g/cm^3. The hydrostatic gradient, which is proportional to the fluid density (1.90 g/cm^3) is, in general, larger than the lithostatic. This suggests that the fractures may propagate downward.

It should be mentioned that shutdowns must be avoided if the pressure record is to be used for diagnostic information. Interpretation of the BHP in Figure III-13 is quite difficult due to the numerous interuptions in the flow rate. On the other hand, valving was not evident in the BHP record and presented no complications.

A definite shut-in pressure was not obtained because the Amerada pressure bomb surpassed its time limit (1-1/2 hrs) at 8:37. This pressure, which should be equal to σ_{min}, probably is not greater than 340 psi as previously discussed. Knowledge of friction losses through both the drill pipe and the fracture is also quite important. It is estimated that this slurry, which behaves like a Bingham plastic, has a friction loss of 755 psi/1000 ft through the 2-3/8 in. tubing at 6 bbls/min. The pressure gradient through the fracture has not yet been determined.

After completion of the first fracturing operation, fracing of the second zone was delayed when a string of drill pipe was lost in the hole during the notching operation. A fishing operation was successfully completed in September and the second zone will be fraced in late October, 1977. An operational plan has been devised that will insure that the instantaneous shut-in pressure (σ_{min}) and the friction losses through the drill pipe are obtained. Mineback operations have already begun towards the Hole 6 region, but not to an extent that will interfere with the second fracture.

D. Fracture Calculations
(N. R. Warpinski, 5732)

The interface between the welded and ash fall tuffs is not well defined and the rock properties vary widely over a ten foot range. In this region, the rock characteristics are not uniform and there are many voids, fractures and breccia. Since it is imperative to extend the fracture far enough in the ash fall tuff to allow interaction with the welded tuff, the fracture models of Geertsma and de Klerk* and Perkins and Kern** have been employed to study the effect of variations of bulk and matrix rock properties on fracture propagation.

Figure III-14 shows how the fracture length increases with injected volume. The design calls for a 50 ft high fracture with a flow rate of 6 bbls/min and a fluid viscosity of 128 cp. The fracture propagates in a medium where Young's modulus (E) is 2.36×10^5 psi and Poisson's ratio (ν) is 0.312. The fluid loss coefficient (CVW) is as shown on the graph and Dowell's predicted curve is shown for comparison. The two curves with CVW calculated use a porosity of 44.6% and a permeability of 0.01 md.

The effect of Young's modulus (E) on fracture length is shown in Figure III-15. For larger E, the fractures are longer but not as wide. Therefore, no problems are expected as the welded interface is approached since E for the welded tuff is larger than for the ash fall tuff. Figure III-16 shows that variations in ν have a negligible effect on the fracture.

The permeability has a pronounced effect on fracture length as demonstrated in Figure III-17. It is important to remember that even though matrix permeability may be low, a large fracture permeability can greatly reduce the length of the fracture. This is certainly the situation in the interface where voids, fractures and breccia are widespread.

E. Containment Program Activities: Puff-N-Tuff Experiment
(L. D. Tyler, 1111)

The Puff-N-Tuff experiment was conducted in G tunnel for the purpose

*Geertsma, J. and de Klerk, F., "A Rapid Method of Predicting Width and Extent of Hydraulically Induced Fractures," Journal of Petroleum Technology, December, 1969, Vol. 21, pp. 1571-1581.

**Perkins, T. K. and Kern, L. R., " Widths of Hydraulic Fractures," Journal of Petroleum Technology, September, 1961, Vol. 13, pp. 937-949.

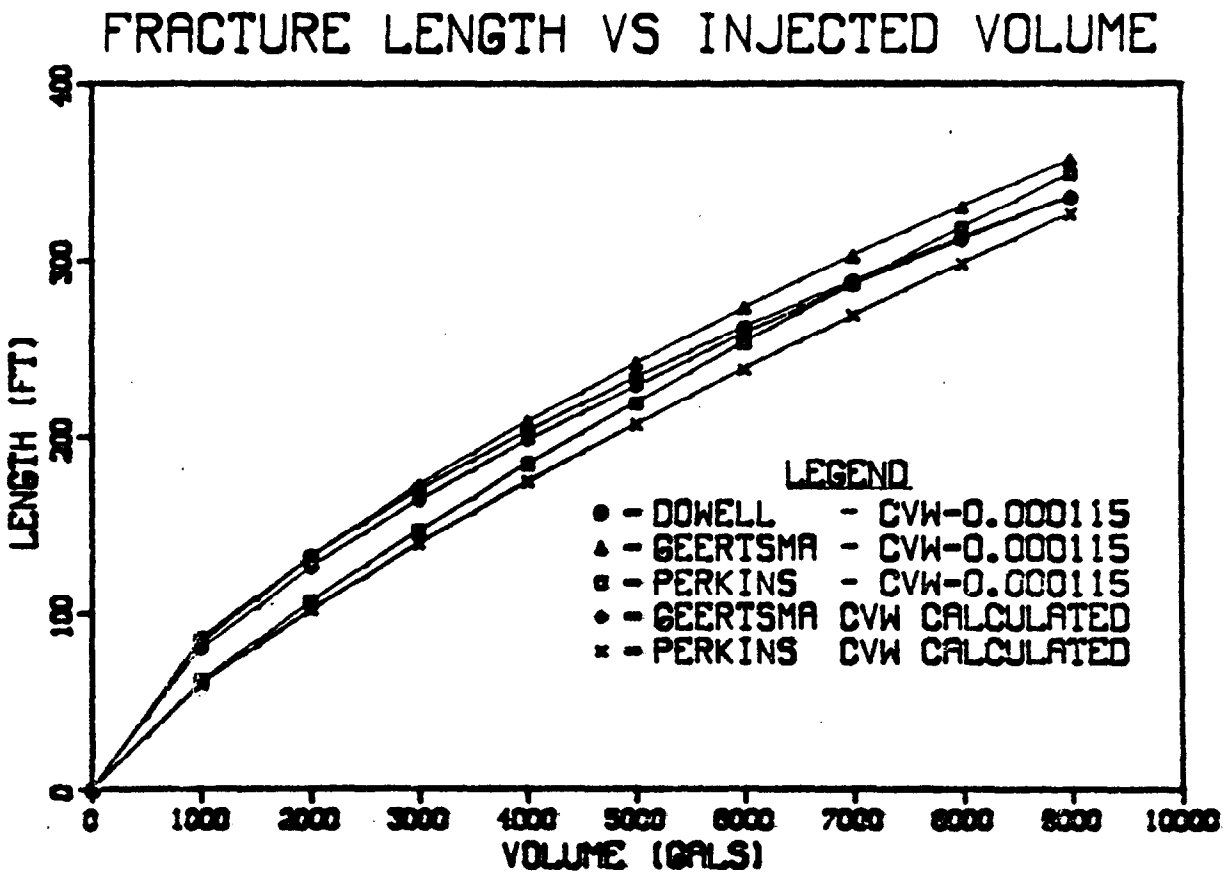

Figure III-14

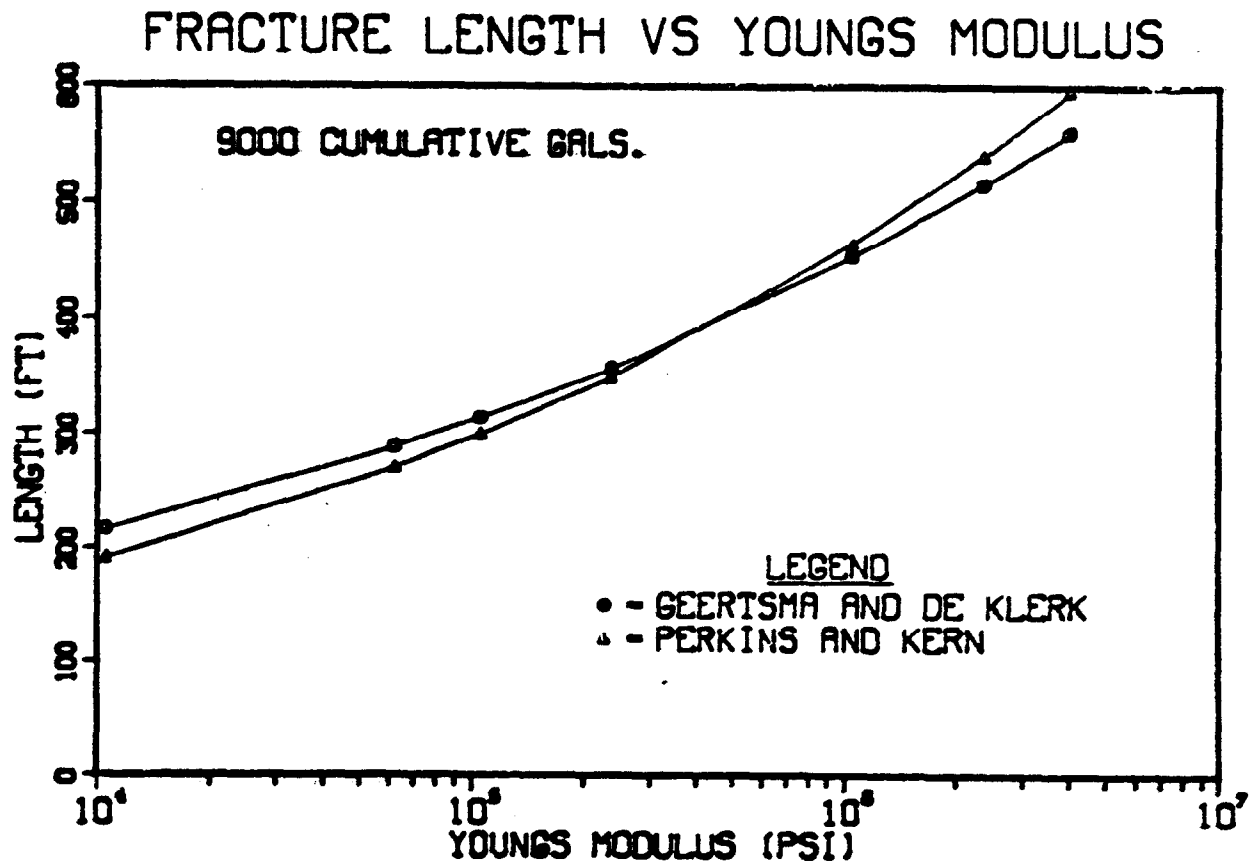

Figure III-15

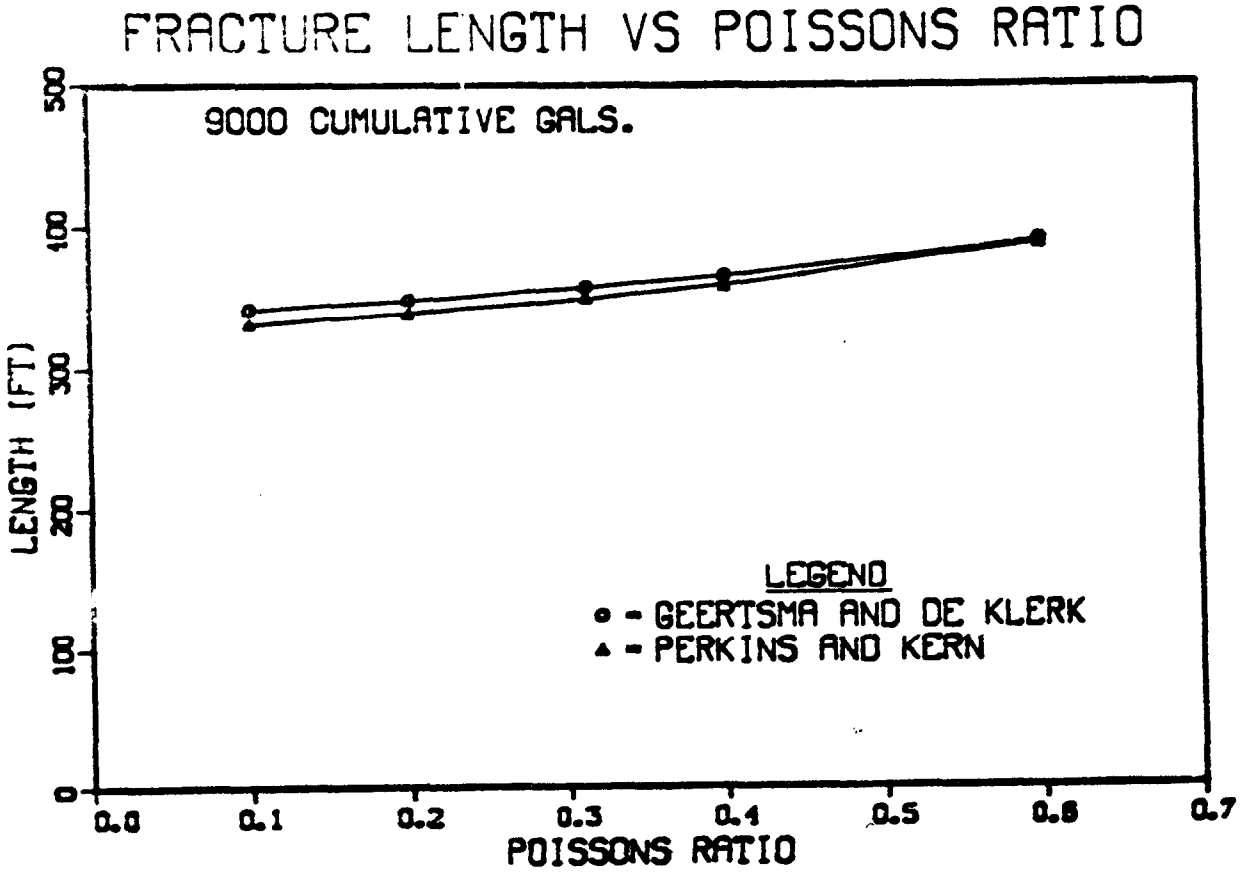

Figure III-16

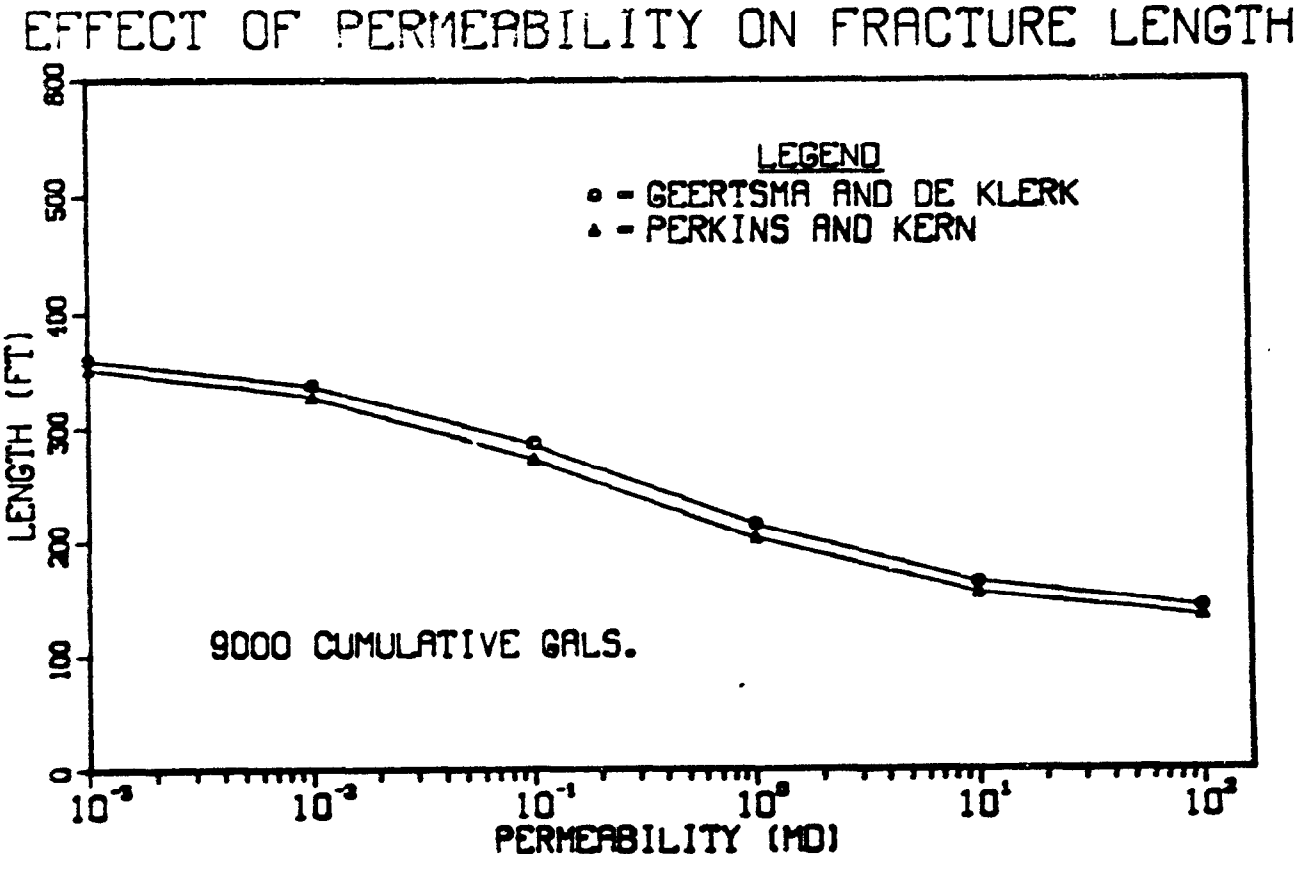

Figure III-17

of studying the effects from an explosion of a spherical charge of high explosive. The principal objective was to study the effect of post-detonation high pressure gases on containment. The work was sponsored by the Division of Military Applications as part of a continuing program to study the containment of nuclear test experiments.

The initial configuration of the explosive test is shown in Figure III-18. A 256 lb spherical charge was placed at the end of a drift 4 x 4 ft cross-section. The charge was then stemmed into the drift with cement grout which closely matched the physical properties of tuff. Two open 6 in. transite pipes extended in opposite directions from the spherical charge; the pipe in the tuff was not grouted. Conical "transition" cones were placed at the junction of the pipes and the sphere. The purpose of these cones was to delay collapse of the open pipes during the short-lived hydrodynamic phase immediately following the detonation. Once the shock waves had dissipated, it was expected that the high pressure gases would escape down the open pipes.

Figure III-19 illustrates the results of the post-detonation mine-back operation in the tuff region "in back of" the explosive cavity. The crosshatched area shows a vertical fracture produced by the explosive gases from the pipe and borehole which extended into the tuff. The pipe that was grouted into the stemmed drift apparently collapsed during the hydrodynamic phase.

The fracture initiated in the tuff is remarkably similar in orientation to that induced by conventional hydraulic fracture techniques at Hole No. 3 which is located nearby. The radial extent of the fracture is in close agreement with a hydrodynamic calculation showing that residual stresses lower than the overburden stress exist in this region. Fracture widths of 2-3 mm filled with black explosive debris were observed. While not uncovered, rough calculations suggest a fracture height of 75 ft.

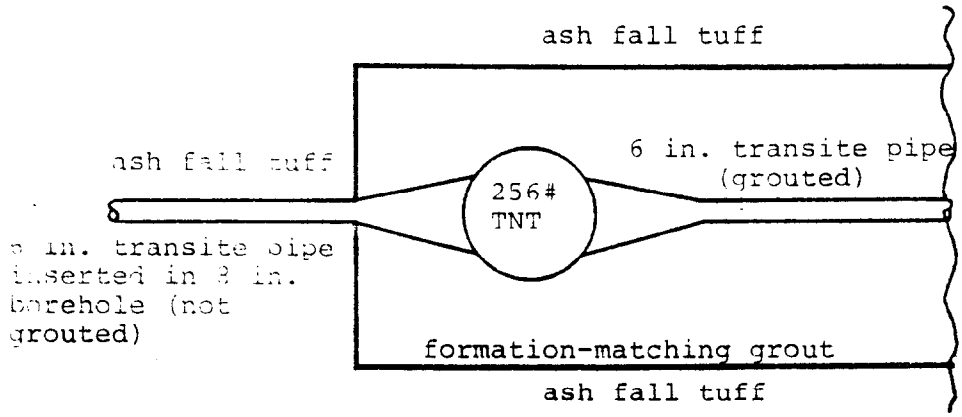

Figure III-18 - Test Configuration, Puff-N-Tuff

IV. ADDITIONAL ENHANCED GAS RECOVERY ACTIVITIES

A. Green River Basin Resource Evaluation
(G. B. Griswold, 5732, and N. R. Warpinski, 5732)

An evaluation of the natural gas resources of the tight gas sands of the Wyoming Greater Green River Basin was conducted in June and July, 1977. The particular gas sands under consideration were the Paleocene Fort Union formation and the Upper Cretaceous Mesaverde group which is comprised of the Almond, Ericson, Rock Springs and Blair formations. The areal extend of the basin is approximately 20,000 square miles and is delineated in Figure III-20. After consultations with the United States Geological Survey (USGS), Amoco, Davis and Colorado Interstate Gas, approximately fifty wells were selected that were considered to be representative of their region and from which considerable information could be derived. The individual well file of each of these wells was obtained from the USGS district office at Rock Springs and the files were searched for information from electric logs, drill stem tests, cores and mud logs that would aid in characterizing the reservoir. In particular, it was necessary to estimate the average depth, gross and net pays, gas porosity, permeability and bottom hole pressure and temperature of the reservoir for each formation at each location. The basin was subsequently divided into a number of subregions and volumetric calculations of the gas in place were performed by extrapolating the information from the individual well files.

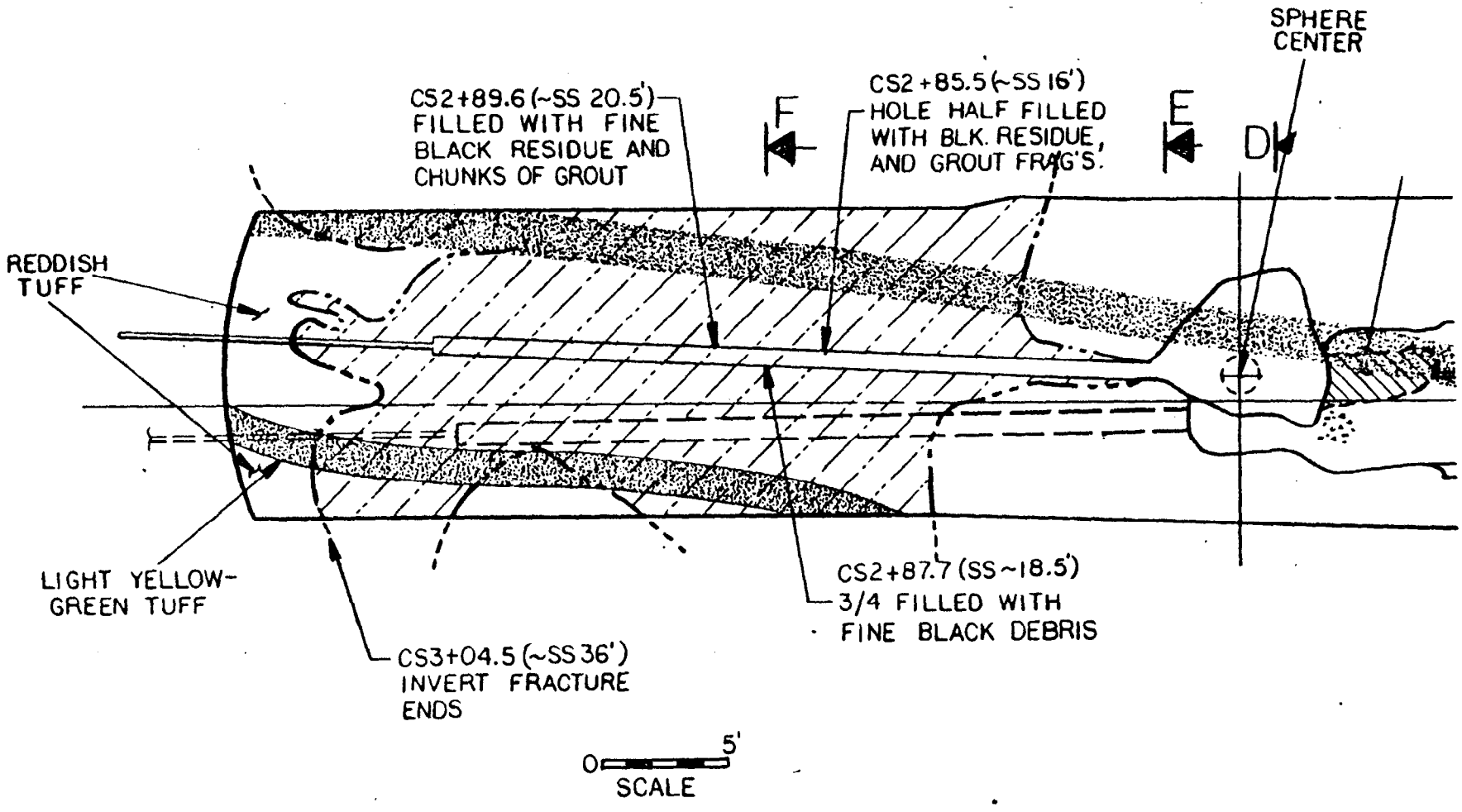

Figure III-19 - Gas Fracture Produced in the Puff-N-Tuff Experiment

Production records of various wells dating back to 1968 were obtained from the Wyoming Oil and Gas Conservation Commission. Production decline curves were computed so that estimates of recoverable gas could be calculated. The recovery factors of various completion techniques (particularly MHF) could then be computed and an estimate of recoverable gas could be presented. For the tight gas sands, however, this data was quite limited and it was suggested that the recovery factors be obtained from other tight gas sand basins where more data has been accumulated.

All of the preliminary results have been sent to an independent consulting geologist for further evaluation and refinement. The final values for the estimated resource will be derived by Lewin & Associates who is combining the results from this study with similar studies in other areas under DOE's enhanced gas recovery program.

B. Program Planning

1. David A. Northrop is a member of a formal working group charged with providing technical direction to the development of a Program Strategy Plan for Enhanced Gas Recovery being prepared for DOE by Booz. Allen and Hamilton, Inc. and Lewin and Associates. Meetings have been held in Washington on April 18-19, May 12-13, June 27-28, August 4-5, and September 19-22, 1977. The Green River Basin Resource Survey described above was conducted for this strategy plan.

2. Sandia personnel participated in the design and development of the program plan for DOE's Western Gas Sands Project which was initiated during the past year. Numerous reviews and revisions were prepared with particular emphasis placed upon the laboratory research and development activities. G. B. Griswold spent a week with CER and TRW in Las Vegas in December 1976 in the actual drafting of the plan.

Figure III-20

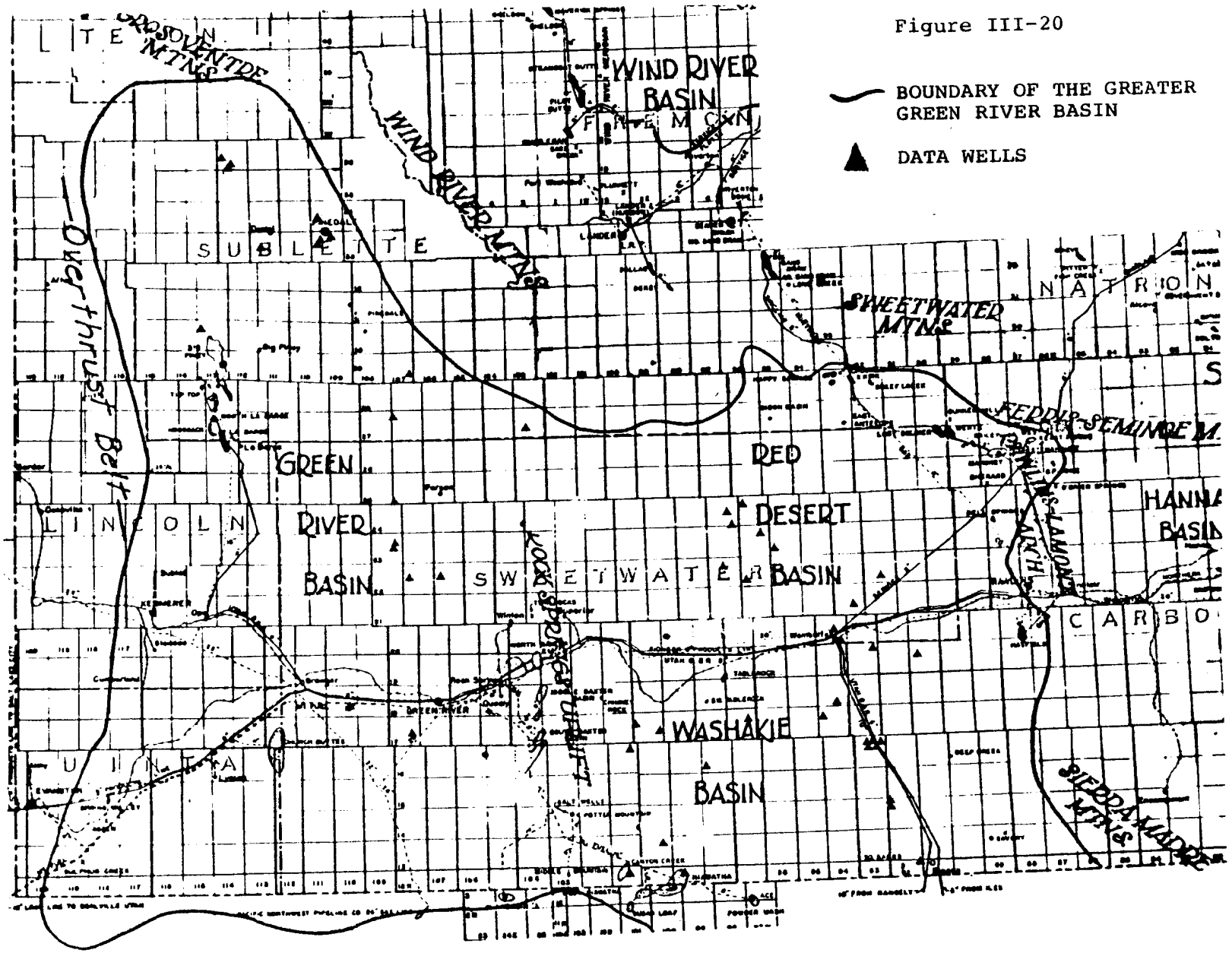

V. PUBLICATIONS, PRESENTATIONS, AND OTHER COMMUNICATIONS

A. Publications and Presentations

1. L. D. Tyler, W. C. Vollendorf, and D. A. Northrop, "In Situ Examination of Hydraulic Fractures," presented by L. D. Tyler and D. A. Northrop at the Third DOE Symposium on Enhanced Oil and Gas Recovery and Improved Drilling Methods, Tulsa OK, August 30-September 1, 1977. Paper published in the Proceedings, Volume 2, p. F-4/1.

2. C. L. Schuster, "A Status Report on the MHF Mapping and Characterization Program," presented at the Third DOE Symposium on Enhanced Oil and Gas Recovery and Improved Drilling Methods, Tulsa OK, August 30-September 1, 1977. Paper published in the Proceedings, Volume 2, p. F-5/1.

3. C. L. Schuster and R. P. McCann, "Frac Mapping by Surface Electrical Techniques," presented by C. L. Schuster at the Massive Hydraulic Fracturing Symposium, University of Oklahoma, Norman OK, February 28-March 1, 1977. Published in the Proceedings, p. 323.

4. L. J. Keck and R. W. Seavey, "Instrumentation for Massive Hydraulic Fracture Mapping," Sandia Laboratories Report, SAND77-0195, April 1977.

5. R. P. McCann, R. G. Hay, and L. C. Bartel, "Massive Hydraulic Fracture Mapping and Characterization Program: First Annual Report: Augsut 1975 through July 1976," Sandia Laboratories Report, SAND77-0286, June 1977.

6. R. P. McCann, L. C. Bartel, and L. J. Keck, "Massive Hydraulic Fracture Mapping and Characterization Program: Surface Potential Data for Wattenburg 1975-76 Experiments," Sandia Laboratories Report, SAND77-0396, August 1977.

7. C. L. Schuster and D. A. Northrop, editors, "Natural Gas Massive Hydraulic Fracture Research and Advanced Technology Project, Quarterly Report: February through April, 1977," Sandia Laboratories Report, SAND77-1132, July 1977.

8. L. J. Keck and C. L. Schuster, "Shallow Formation Hydrofracture Mapping Experiment," presented by C. L. Schuster at the Energy Technology

Conference and Exhibition, ASME, Houston TX, September 18-23, 1977. Published as ASME paper 77-Pet-51.

9. C. L. Schuster, editor, "Natural Gas Massive Hydraulic Fracture Research and Advanced Technology Project, Quarterly Report: November 1976 through January 1977," Sandia Laboratories Report, SAND77-0475, April 1977.

10. L. C. Bartel, R. P. McCann, and L. J. Keck, "Use of Potential Gradients in Massive Hydraulic Fracture Mapping and Characterization," presented by L. C. Bartel at the 51st Annual Fall Technical Conference and Exhibition of the Society of Petroleum Engineers of AIME, New Orleans LA, October 3-6 1977, published as paper SPE 6090.

B. Other Communications

1. D. A. Northrop, L. D. Tyler, and G. B. Griswold met with representatives from Halliburton, Dowell, and AMOCO to review present activites and discuss future directions of the mineback fracture test program; meeting was held in Tulsa OK, February 22, 1977.

2. Project reviews were presented at the 2nd DOE Natural Gas Working Group Meeting, Sandia Laboratories, Albuquerque NM, January 13, 1977: L. D. Tyler "NTS/MHF Simulation Studies," and C. L. Schuster "Electrical Results from Controlled Fracture Experiment."

3. Project reviews were presented at the 3rd DOE Natural Gas Working Group Meeting, Lawrence Livermore Laboratory, Livermore CA, July 12, 13, 1977: L. D. Tyler "NTS Mineback Experiments," and C. L. Schuster "Results of Electrical Mapping Experiments."

4. L. D. Tyler and D. A. Northrop presented a program briefing for H. C. Walther, H. A. Wahl and other personnel at Continental Oil Company, Ponca City OK, May 19, 1977.

5. D. A. Northrop and L. D. Tyler presented a mineback program review for Alex B. Crawley, Fossil Energy/DOE, at the Nevada Test Site, July 14, 1977.

6. D. A. Northrop, C. L. Schuster, and L. D. Tyler visited the Morgantown Energy Research Center to review Sandia's and the Eastern Gas' Shales Program's activities, in Morgantown WV, September 29-30, 1977.

7. Sandia personnel participated in the MHF-3 (Rio Blanco) Technical Committee meeting in Las Vegas NV, April 5, 1977. L. D. Tyler and D. A. Northrop gave presentations on G tunnel mineback experiments and plans for the mineback stimulation test project. The following day, Sandia sponsored a tour of NTS and G tunnel for approximately 30 of the industry representatives.

8. L. D. Tyler briefed E. Smith and S. McKetta of Columbia Gas Company on the mineback testing activities, Nevada Test Site, April 19, 1977.

9. C. L. Schuster presented project review at the Annual Meeting of the Solution Mining Research Institute, Atlanta GA, December 2, 1976.

DISTRIBUTION:

G. Fumich
Acting Program Manager
Fossil Energy
U. S. Department of Energy
Washington, DC 20545

H. D. Guthrie, Director
J. W. Watkins, Deputy Director
J. D. Ham, Assistant Director
D. C. Ward
J. B. Smith
A. B. Crawley (10)
Division of Oil, Gas, Shale
and In Situ Technology
U. S. Department of Energy
400 First St. NW
Washington, DC 20545

E. Lievens, Acting Director
Office of Program Planning
and Analysis
U. S. Department of Energy
20 Massachusetts Ave. NW
Washington, DC 20545

A. A. Pitrolo, Director
L. A. Schrider
W. K. Overbey, Jr.
U. S. Department of Energy
Morgantown Energy Research Center
P. O. Box 880
Morgantown, WV 26505

C. H. Atkinson
U. S. Department of Energy
Nevada Operations Office
P. O. Box 14100
Las Vegas, NV 89114

G. R. Leutkenhans
R. L. Mann
CER Corporation
P. O. Box 15090
Las Vegas, NV 89114

J. S. Ball, Director
R. T. Johansen
U. S. Department of Energy
Bartlesville Energy Research Center
Bartlesville, OK 74003

D. K. Nowlin, Director
Special Programs Division
U. S. Department of Energy
Albuquerque Operations Office
Albuquerque, NM 87185

M. E. Hanson
Lawrence Livermore Laboratory
Livermore, CA 94550

R. Brownlee G-Division
W. G. Davey Q-Division
Los Alamos Scientific Laboratory
Los Alamos, NM 87545

A. B. Waters
A. A. Daneshy
Halliburton Services
Research Center
Duncan, OK 73533

W. B. Bradley
Shell Development Co.
3737 Bellaire Boulevard
Houston, TX 77001

J. Fitch
W. L. Medlin
Mobil Research and
Development Corporation
Field Research Laboratory
P. O. Box 900
Dallas, TX 75211

H. C. Walther
H. Wahl
Production Research Division
Continental Oil Company
Ponca City, OK 74601

L. S. Cook
Columbia Gas System Service Corp.
1600 Dublin Road
Columbus, OH 43215

J. Short
Gas Producing Enterprises, Inc.
2100 Prudential Plaza
P. O. Box 749
Denver, CO 80201

Distribution, continued

T. Nyquist
Dowell
P. O. Box 21
Tulsa, OK 74102

J. P. Pavlich
Dowell
Division of Dow Chemical
220 W. Loop S
Houston, TX 77027

R. L. Huggins
R. W. Veatch
M. B. Smith
Amoco Production Co.
P. O. Box 591
Tulsa, OK 74102

M. D. Woods
131 Mimosa Way
Portola Valley, CA 94025

R. P. Trump
Gulf Research and
Development Company
P. O. Drawer 2038
Pittsburgh, PA 15230

1 M. Sparks
1000 G. A. Fowler
1100 C. D. Broyles
1110 J. D. Kennedy
Attn: C. R. Mehl, 1111
C. W. Smith, 1111

1120 G. E. Hansche
1130 H. E. Viney
Attn: W. D. Statler, 1133
W. C. Vollendorf, 1133

5100 J. K. Galt
Attn: W. Herrmann, 5160

5163 D. E. Munson
5200 E. H. Beckner
5337 L. D. Tyler
5400 A. W. Snyder
5700 J. H. Scott
5710 G. E. Brandvold
5730 H. M. Stoller
5731 R. K. Traeger
5732 D. A. Northrop (25)
5733 C. L. Schuster (15)
5734 A. L. Stevens
5735 S. G. Varnado
5736 A. F. Veneruso
5740 V. L. Dugan
5800 R. S. Claassen
8266 E. A. Aas (1)
9420 T. L. Pace
3141 C. A. Pepmueller (5)
3151 W. L. Garner (3)
for DOE/TIC (25)
Attn: R. P. Campbell, 3173-2

SAND-77-1992
UNLIMITED RELEASE

EGSP Files
UGR-C073

UGR File #c073/A77, part 2
SAND-77-1992
Oct. 1976-Sept. 1977

ENHANCED GAS RECOVERY PROGRAM
SECOND ANNUAL REPORT - PART II
OCTOBER 1976 THROUGH SEPTEMBER 1977

D. A. NORTHROP AND C. L. SCHUSTER, EDITORS

Prepared by Sandia Laboratories, Albuquerque, NM 87115 and Livermore, CA 94550 for the United States Department of Energy under Contract AT (29-1)-789

PRINTED APRIL 1978

EGSP
OPEN FILE # 0731

Sandia Laboratories
energy research

UGR File #c073/A77, part 2
SAND-77-1992
Oct. 1976-Sept. 1977

Issued by Sandia Laboratories, operated for the United States Department of Energy by Sandia Corporation

---

NOTICE

This report was prepared as an account of work sponsored by the United States Government. Neither the United States nor the United States Department of Energy, nor any of their employees, nor any of their contractors, subcontractors, or their employees, makes any warranty, express or implied, or assumes any legal liability or responsibility for the accuracy, completeness or usefullness of any information, apparatus, product or process disclosed, or represents that its use would not infringe privately owned rights.

NOTICE

Reference to a company or product name does not imply endorsement or recommendation of the product by Sandia Laboratories or the U.S. Department of Energy to the exclusion of others that may be suitable.

Printed in the United States of America
Available from:
National Technical Information Service
U.S. Department of Commerce
5285 Port Royal Road
Springfield, VA 22151
Price: Printed Copy $5.00; Microfiche $3.00

*Add $2.50 per copy for foreign price.

UGR File #c073/A77, part 2
SAND-77-1992
Oct. 1976-Sept. 1977

SAND-77-1992

Unlimited Release
Printed

ENHANCED GAS RECOVERY PROGRAM

SECOND ANNUAL REPORT - PART II*

OCTOBER 1976 THROUGH SEPTEMBER 1977

D. A. Northrop and C. L. Schuster, Editors

* Part I of this publication is a separate volume and contains a summary and overview of the year's activities.

This page left intentionally blank

TABLE OF CONTENTS

	Page
APPENDIX A	
Table I. Amoco Hydrofracture Experiment	3
APPENDIX B	
Table I. GPE Natural Buttes No. 14 Hydrofracture	13
Table II. GPE Natural Buttes No. 20 Hydrofracture	29
APPENDIX C	
Table I. Conoco Hydrofracture	43
APPENDIX D	
Table I. Shell Oil Company - Rachal No. 1	51
Table II. Shell Oil Company - Rachal No. 1	59

This page intentionally left blank

APPENDIX A

TABLE I

AMOCO HYDROFRACTURE EXPERIMENT-TULSA,OK

FRACTURE-NOV. 4,1976

TIME	0°	15°	30°	45°	60°	75°	90°	105°	120°	135°	150°	165°
5:40	8.1790	8.7912	9.6821	8.8152	9.8863	10.6527	11.1563	10.3875	10.4430	9.4328	9.1015	9.6991
5:45	8.1372	8.7646	9.6484	8.7861	9.8486	10.6112	11.1121	10.9433	10.4101	9.3568	9.0664	9.6652
5:50	8.1832	8.7995	9.6596	8.8208	9.8866	10.6647	11.1570	10.9902	10.4527	9.4357	9.1067	9.7230
5:55	8.1320	8.7454	9.6291	8.7688	9.8267	10.5906	11.0397	10.9191	10.3917	9.3302	9.0451	9.6494
6:00	8.2147	8.8283	9.7201	8.8569	9.9246	10.6370	11.1934	11.0271	10.4880	9.4707	9.1394	9.7338
6:05	8.1598	8.7648	9.6631	8.7994	9.8651	10.6298	11.1335	10.9618	10.4283	9.4159	9.0833	9.6840
6:10	8.2194	8.8232	9.7321	8.8610	9.9276	10.6997	11.1946	11.0329	10.4940	9.4402	9.1470	9.7463
6:15	8.1336	8.7345	9.6310	8.7681	9.8279	10.5903	11.0841	10.9199	10.3938	9.3832	9.0544	8.6619
6:20	8.1382	8.7536	9.6442	8.7802	9.8400	10.6048	11.0992	10.9375	10.4023	9.3973	9.0647	9.6664
6:25	8.1154	8.7255	9.5939	8.7403	9.7910	10.5454	11.0414	10.3871	10.3545	9.3514	9.0229	8.6288
6:30	8.1517	8.7472	9.6519	8.7933	9.8523	10.6168	11.1104	10.9534	10.4230	9.4080	9.0739	8.6522
6:35	8.1753	8.7799	9.6646	8.8075	9.8589	10.6211	11.1127	10.9579	10.4246	9.4139	9.0916	9.6855
6:40	8.1480	8.7523	9.6387	8.7797	9.8306	10.5944	11.0862	10.9239	10.3994	9.3889	9.0553	8.6617
6:45	8.1311	8.7302	9.6177	8.7603	9.8097	10.5660	11.0574	10.9020	10.3726	9.3656	9.0384	8.6543
6:50	8.1497	8.7712	9.6488	8.7906	9.8348	10.5928	11.0892	10.9333	10.3971	9.3825	9.0543	8.6672
6:55	8.2897	8.9032	9.7925	8.9120	9.9653	10.7428	11.2297	11.3694	10.5159	9.4945	9.1586	8.7721
7:24	8.3691	8.6577	9.5261	8.6746	9.6981	10.4492	10.9331	10.7789	10.2541	9.2546	8.9321	8.5465
7:29	8.3216	8.6086	9.4582	8.6214	9.6447	10.3364	10.8728	10.7228	10.1973	9.1399	8.8332	8.4393
7:34	5.1604	5.4979	5.9859	5.4676	6.0427	6.4555	6.7453	6.6846	6.4921	5.8271	5.6573	5.4117
7:36	6.2262	6.8222	7.3684	6.7451	7.7148	8.6340	9.3274	8.9664	8.2658	7.2654	6.9541	6.6952
7:38	6.2527	7.2579	7.5136	6.8882	8.1794	9.5540	10.4151	10.3264	8.8221	7.4961	7.0576	6.7752
7:40	6.1708	6.9116	7.5135	6.8665	8.1571	9.5283	10.7878	9.9933	8.7619	7.4628	7.0270	6.7464
7:42	6.2179	6.7742	7.5339	6.9267	8.2478	9.6523	10.9226	10.1155	8.8238	7.5334	7.0927	6.7989
7:44	6.2383	6.8386	7.4105	6.9403	8.2555	9.6521	10.9287	10.1306	8.9114	7.5674	7.1257	6.8375
7:46	6.3175	6.9457	7.5025	7.0251	8.3578	9.7744	11.3756	10.2499	8.9924	7.6543	7.2089	6.9259
7:48	6.3421	6.8639	7.5507	7.0692	8.4063	9.8252	11.1033	10.3124	9.0631	7.7005	7.2501	6.9593
7:50	6.2461	6.7081	7.4203	6.9567	8.2840	9.6994	10.9872	10.1744	8.9431	7.5879	7.1427	6.8535
7:52	6.3395	6.7723	7.4987	7.0156	8.3550	9.7712	11.0684	10.2543	8.9973	7.6515	7.2064	6.9194
7:54	6.3419	6.8157	7.5449	7.0658	8.4134	9.8428	11.1537	10.3319	9.0950	7.7143	7.2669	6.9732
7:56	6.3425	6.8064	7.5444	7.0611	8.4161	9.8428	11.1466	10.3356	9.0729	7.7377	7.2942	7.0118
7:58	6.3645	6.8502	7.5772	7.1034	8.4603	9.8943	11.1847	10.3957	9.1459	7.7818	7.3349	7.0369
8:00	6.5411	7.0403	7.8009	7.3075	8.7183	10.1962	11.5334	10.7375	9.3874	8.0142	7.5511	7.2533
8:02	6.3802	6.3471	7.5834	7.1074	8.4461	9.9147	11.2385	10.4143	9.1916	7.7968	7.3449	7.0526
8:04	6.4235	6.3256	7.6686	7.1915	8.5690	10.0144	11.3212	10.5219	9.2535	7.8765	7.4257	7.1296
8:06	6.3440	6.8179	7.5695	7.0863	8.4529	9.8855	11.1791	10.3857	9.1532	7.7736	7.3245	7.0409
8:08	6.4503	6.9400	7.6984	7.2148	8.6009	10.0501	11.3567	10.5558	9.2940	7.9052	7.4476	7.1521
8:10	6.3950	6.8846	7.6323	7.1550	8.5243	9.9708	11.2817	10.4769	9.2236	7.8349	7.3855	7.0876
8:12	6.4653	6.9563	7.7314	7.2043	8.5343	9.9888	11.1660	10.4144	9.2430	7.8819	7.4431	7.1564
8:14	6.4857	6.9629	7.7325	7.2491	8.6450	10.1104	11.4536	10.6270	9.3657	7.9575	7.4918	7.1914
8:16	6.3767	6.8574	7.6663	7.1313	8.4947	9.9366	11.2474	10.4399	9.1876	7.8398	7.3597	7.0643
8:18	6.4429	6.9278	7.6836	7.1991	8.5778	10.0306	11.3473	10.5438	9.2793	7.8892	7.4329	7.1330
8:20	6.4260	6.9127	7.6597	7.1776	8.5530	10.0080	11.3285	10.5114	9.2439	7.8636	7.4085	7.1071
8:22	6.3921	6.8713	7.6277	7.1406	8.5135	9.9589	11.2646	10.4686	9.2375	7.8325	7.3798	7.0784

UGR File #c073/A77, part 2
SAND-77-1992
Oct. 1976-Sept. 1977

TABLE I (Continued)

AMOCO HYDROFRACTURE EXPERIMENT-TULSA, OK

FRACTURE-NOV. 4, 1976

TIME		0°	15°	30°	45°	60°	75°	90°	105°	120°	135°	150°	165°
3:24		6.4153	6.3901	7.6439	7.1653	8.5336	9.3847	11.3330	10.4927	9.2334	7.8466	7.3954	7.3950
3:26		6.3450	6.3166	7.5092	7.0913	8.4483	9.8139	11.1865	10.3906	9.1478	7.7726	7.3239	7.2238
3:28	Start pumping	6.4331	6.3285	7.6796	7.1997	8.5759	10.3358	11.3617	10.5485	9.2322	7.8399	7.4294	7.1293
3:30	Rate - 2 bbl/min	5.9948	6.4302	7.1266	6.6771	7.9346	9.2375	10.4077	9.7355	8.5014	7.3170	6.9047	6.6210
3:32		6.0282	6.4790	7.1745	6.7256	7.9855	9.3212	10.5477	9.7999	8.6179	7.3613	6.9476	6.6528
3:34		5.9444	6.3847	7.0692	6.6334	7.8739	9.1369	10.4121	9.6074	8.4621	7.2521	6.8456	6.5642
3:36		6.0229	6.4501	7.1202	6.6446	7.7862	8.9570	10.0214	9.4257	8.4593	7.2589	6.8346	6.6193
3:38		5.9782	6.2533	6.9115	6.4805	7.6705	8.9430	10.1049	9.4126	8.3325	7.0961	6.7017	6.4231
3:40		5.8009	6.2370	6.8797	6.4494	7.6266	8.8308	10.0443	9.3439	8.2832	7.0532	6.6705	6.3370
3:42	Stop pumping	5.9064	6.2312	6.8762	6.4468	7.6167	8.8633	10.0194	9.3343	8.2748	7.0555	6.6729	6.3327
3:44		5.7436	6.1910	6.7300	6.3583	7.5394	8.7336	9.8400	9.1912	8.1454	6.9667	6.5346	6.3333
3:46		5.9030	6.3445	6.9394	6.5398	7.6390	8.9156	10.1175	9.3823	8.3532	7.1481	6.7679	6.4914
3:48		5.9234	6.3226	6.9566	6.4977	7.6334	8.7640	9.8322	9.2162	8.2479	7.0319	6.7214	6.4536
3:50		5.8745	6.2600	6.9345	6.4950	7.6563	8.8375	10.0100	9.3584	8.3039	7.0867	6.7039	6.4269
3:52		5.9596	6.3900	7.0342	6.5874	7.7688	9.0258	10.1374	9.4393	8.3966	7.1872	6.8215	6.5155
3:54		5.8469	6.3183	6.9633	6.5209	7.6924	8.9463	10.0910	9.4111	8.3338	7.1159	6.7291	6.4521
3:56		5.8476	6.3262	6.9679	6.5144	7.6303	8.8223	9.8933	9.2941	8.2635	7.0948	6.7231	6.4525
3:58		5.9452	6.3760	7.0236	6.5837	7.7621	9.0233	10.1723	9.4958	8.3796	7.1769	6.7893	6.5354
4:00		5.9508	6.3916	7.0360	6.5897	7.7692	9.0329	10.1429	9.5000	8.3880	7.1823	6.7952	6.5383
4:02		5.9494	6.3779	7.0349	6.5386	7.7707	9.0375	10.1562	9.5104	8.4165	7.1886	6.7981	6.5375
4:04		5.9452	6.3787	7.0262	6.5860	7.7654	9.0258	10.1670	9.5009	8.4089	7.1922	6.7908	6.5309
4:06		5.9481	6.3981	7.0416	6.5993	7.7816	9.0547	10.1998	9.5283	8.4302	7.1983	6.8060	6.5188
4:08		5.9316	6.3296	6.9758	6.5350	7.7294	8.9693	10.1835	9.4332	8.3448	7.1274	6.7397	6.4578
4:10	Start pumping	5.8757	6.2960	6.9389	6.5065	7.6627	8.9127	10.0134	9.3709	8.2985	7.0923	6.7072	6.4203
4:12	Rate - 2 bbl/min	5.8993	6.2944	6.9123	6.4779	7.6156	8.8427	9.9422	9.2982	8.2414	7.0517	6.6751	6.3902
4:14		5.8838	6.3032	6.9224	6.4850	7.6206	8.8445	9.9577	9.3027	8.2235	7.0473	6.6733	6.3875
4:16		5.9324	6.3557	6.9763	6.5266	7.6503	8.8566	9.9436	9.3050	8.2420	7.0776	6.7050	6.4197
4:18		5.9855	6.3770	6.9822	6.5406	7.6329	8.8063	9.8489	9.2414	8.2002	7.0472	6.6816	6.3937
4:20		5.9164	6.3423	6.9322	6.4940	7.5751	8.7381	9.7774	9.1784	8.1534	6.9916	6.6285	6.3459
4:22		5.9434	6.3596	6.9410	6.5117	7.5927	8.7528	9.7832	9.1757	8.1549	7.0125	6.6337	6.3550
4:24		5.9459	6.3653	6.9604	6.5173	7.5923	8.7461	9.7677	9.1659	8.1563	6.9866	6.6365	6.3497
4:26		5.9798	6.4018	6.9851	6.5440	7.6181	8.7695	9.8089	9.1993	8.1819	7.0188	6.6592	6.3709
4:28		5.9391	6.3483	6.9402	6.4951	7.5665	8.7138	9.7491	9.1189	8.1038	6.9609	6.6035	6.3157
4:30		5.9769	6.3879	6.9736	6.5292	7.5605	8.7386	9.7723	9.1571	8.1422	6.9922	6.6311	6.3454
4:32		5.9729	6.3921	6.9777	6.5327	7.5948	8.7231	9.7392	9.1441	8.1392	6.9829	6.6259	6.3373
4:34		5.9477	6.3656	6.9399	6.4935	7.5546	8.6846	9.6941	9.0917	8.0847	6.9417	6.5855	6.2972
4:36		5.9250	6.3341	6.9046	6.4661	7.5163	8.6330	9.6621	9.0405	8.0451	6.8947	6.5472	6.2584
4:38		5.9743	6.3956	6.9630	6.5152	7.5810	8.7126	9.7202	9.1076	8.1018	6.9574	6.6008	6.3143
4:40		5.9870	6.3919	6.9683	6.5193	7.5711	8.6933	9.7102	9.0961	8.0933	6.9514	6.5961	6.3077
4:42		5.9602	6.3630	6.9609	6.4654	7.4815	8.4366	9.3632	8.8949	8.0392	6.9190	6.5818	6.3157
4:44		5.9415	6.2965	6.8527	6.4184	7.5251	8.6910	9.7124	9.1143	8.3751	6.9358	6.5353	6.2531
4:46		5.9630	6.4550	7.0014	6.5675	7.6057	8.8368	9.8936	9.2650	8.2229	7.0431	6.6521	6.3893
4:48		5.9444	6.3056	6.9515	6.5367	7.5977	8.7454	9.7633	9.1678	8.1423	6.9894	6.6264	6.3375
4:50													
4:52													

TABLE I (Continued)

AMOCO HYDROFRACTURE EXPERIMENT-TULSA,OK

FRACTURE-NOV. 4,1976

TIME	0°	15°	30°	45°	60°	75°	90°	105°	120°	135°	150°	165°
9:54	5.9361	6.3565	6.9407	6.4910	7.5754	8.7269	9.7855	9.1373	8.3371	6.9021	6.6136	6.3117
9:56	5.9711	6.3933	6.9721	6.5246	7.6182	8.7735	9.8122	9.1373	8.1383	7.0314	6.6370	6.3439
9:58	6.0271	6.4199	7.0106	6.5584	7.5594	8.8215	9.3413	9.2456	8.2156	7.0450	6.6797	6.3427
10:00	5.9781	6.2896	6.8670	6.4166	7.4927	8.6366	9.6254	9.0401	8.1337	6.8926	6.5318	6.2439
10:02 Stop pumping	5.9323	6.4407	7.0804	6.6153	7.7828	8.9342	10.0345	9.4286	8.3693	7.1527	6.7615	6.4086
10:04	6.0184	6.4652	7.1071	6.6464	7.8599	9.1310	10.2678	9.5873	8.4283	7.2032	6.8015	6.4089
10:06	5.8649	6.3609	6.9166	6.4735	7.6360	8.8673	9.9442	9.3118	8.1704	7.0283	6.6322	6.3358
10:08	5.9754	6.4095	7.0311	6.5782	7.7466	8.9790	10.0521	9.4287	8.3367	7.1318	6.7476	6.4475
10:10	5.9369	6.3721	6.9749	6.5149	7.6636	8.8674	9.9165	9.3125	8.2593	7.0726	6.6922	6.3946
10:12	5.9746	6.4686	7.0390	6.5453	7.6880	8.8943	9.9443	9.3379	8.2872	7.1013	6.7232	6.4242
10:14	5.9307	6.3788	6.9824	6.5112	7.6504	8.8404	9.9194	9.2978	8.2464	7.0540	6.6352	6.3849
10:16	5.9396	6.4165	7.0218	6.5520	7.6907	8.8877	9.9353	9.3246	8.2188	7.0915	6.7229	6.4252
10:18	5.9899	6.4177	7.0162	6.5524	7.6857	8.8365	9.9538	9.3279	8.2734	7.0894	6.7155	6.4149
10:20	5.9422	6.3579	6.9573	6.4955	7.6133	8.7976	9.8389	9.2362	8.1932	7.0242	6.6542	6.3536
10:22	6.0036	6.4337	7.0244	6.5596	7.6913	8.8869	9.9239	9.3198	8.2703	7.0833	6.7060	6.4352
10:24	5.9573	6.3865	6.9744	6.5093	7.6352	8.8206	9.8811	9.2573	8.2114	7.0274	6.6502	6.3498
10:26	6.0162	6.4444	7.0431	6.5726	7.7059	8.8943	9.9332	.0004	8.2819	7.0883	6.7105	6.4363
10:28	6.0292	6.4551	7.0569	6.5841	7.7175	8.9218	9.9906	.0025	8.2987	7.1034	6.7225	6.4173
10:30	6.0236	6.4486	7.0330	6.5293	7.5616	8.6389	9.5215	-.0014	8.0641	7.0256	6.6794	6.4031
10:32	5.9154	6.3428	6.9341	6.4663	7.5843	8.7659	9.8389	.0014	8.1832	6.9823	6.6355	6.3324
10:34	5.9832	6.4224	7.0147	6.5447	7.6770	8.8644	9.9167	.0018	8.2861	7.0739	6.6932	6.3331
10:36	5.9924	6.4147	7.0136	6.5452	7.6843	8.8342	9.9532	-.0014	8.2921	7.0826	6.7029	6.3383
10:38	5.9722	6.3942	6.9943	6.5239	7.6561	8.8560	9.9244	-.0068	8.2434	7.0944	6.6830	6.3781
10:40	5.9936	6.4359	7.0272	6.5443	7.6687	8.8492	9.9362	9.2669	8.1895	7.0767	6.7057	6.4069
10:42	6.0297	6.4356	7.0396	6.5644	7.7056	8.9129	9.9731	9.3507	8.3177	7.1093	6.7253	6.4191
10:44	5.9971	6.4241	7.0201	6.5463	7.6940	8.8975	9.9768	9.3335	8.3110	7.0925	6.7101	6.4045
10:46	6.0079	6.4309	7.0517	6.5684	7.7329	8.9537	10.0119	9.4011	8.3430	7.1285	6.7447	6.4352
10:48	5.9982	6.4320	7.0465	6.5670	7.7368	8.9702	10.0599	9.4144	8.3451	7.1318	6.7425	6.4330
10:50	6.0264	6.4641	7.0496	6.6060	7.7812	9.0226	10.1319	9.4713	8.3767	7.1672	6.7726	6.4688
10:52	5.9639	6.3937	7.0190	6.5384	7.7104	8.9389	10.0047	9.3861	8.3028	7.1019	6.7147	6.4036
10:54	5.9793	6.4191	7.0434	6.5648	7.7392	8.9724	10.0545	9.4202	8.3226	7.1231	6.7313	6.4241
10:56	6.0078	6.5584	7.1355	6.6523	7.8451	9.1047	10.1927	9.5567	8.4469	7.2229	6.8269	6.5129
10:58	6.0163	6.4573	7.0361	6.5965	7.7309	9.0452	10.1324	9.4910	8.3831	7.1690	6.7745	6.4625
11:00	6.0556	6.4998	7.1364	6.6482	7.8512	9.1322	10.2051	9.5642	8.4496	7.2226	6.8247	6.5078
11:02	5.9632	6.3975	7.0218	6.5406	7.7227	8.9653	10.0379	9.4054	8.3152	7.1077	6.7170	6.4043
11:04	6.0722	6.5211	7.1565	6.6700	7.8731	9.1426	10.2378	9.5852	8.4763	7.2437	6.8465	6.5274
11:06	6.0659	6.5113	7.1511	6.6635	7.8674	9.1304	10.2207	9.5841	8.4663	7.2414	6.8416	6.5211
11:08	6.0126	6.4524	7.0888	6.6071	7.8041	9.0610	10.1512	9.5265	8.3712	7.1778	6.7803	6.4568
11:10	5.9523	6.3844	7.0139	6.5357	7.7181	8.9682	10.0692	9.4119	8.3112	7.1046	6.7099	6.3844
11:12	6.0195	6.4585	7.0928	6.6126	7.8108	9.0715	10.1754	9.5162	8.3531	7.1941	6.7892	6.4729
11:14	6.0541	6.4900	7.1326	6.6516	7.8602	9.1311	10.2553	9.5884	8.4555	7.2339	6.8326	6.5122
11:16	5.9953	6.4338	7.0760	6.5919	7.7983	9.0612	10.1703	9.5140	8.3661	7.1681	6.7721	6.4528
11:18	6.0862	6.5232	7.1709	6.6844	7.8948	9.1662	10.2874	9.5224	8.4934	7.2736	6.8695	6.5449
11:20												

UGR File #C075/A77, part 2
SAND-77-1992
Oct. 1976-Sept. 1977

TABLE I (Continued)

AMOCO HYDROFRACTURE EXPERIMENT-TULSA,OK

FRACTURE-NOV. 4,1976

TIME	0°	15°	30°	45°	60°	75°	90°	105°	120°	135°	150°	165°
11:22	6.2430	6.4838	7.1318	6.6479	7.8593	9.1264	10.2503	9.5629	8.4504	7.2347	6.8336	6.5094
11:24	6.1434	6.5454	7.2018	6.7375	7.9329	9.2229	10.3535	9.6798	8.5335	7.3017	6.8355	6.5711
11:26	6.0945	6.4377	7.0724	6.5944	7.7990	9.0623	10.1834	9.5137	8.3941	7.1772	6.7739	6.4579
11:28	5.9983	6.4420	7.0771	6.5986	7.8361	9.0695	10.1899	9.5182	8.3350	7.1305	6.7841	6.4622
11:30	6.0053	6.5171	7.1565	6.6726	7.9303	9.1762	10.3353	9.6293	8.4469	7.2623	6.8614	6.5356
11:32	5.9884	6.4251	7.0587	6.5662	7.7333	8.9264	9.9833	9.3536	8.2444	7.1339	6.7534	6.4429
11:34	6.0372	6.4753	7.1267	6.6433	7.8643	9.1441	10.2694	9.5962	8.4113	7.2326	6.8328	6.5136
11:36	6.1024	6.5571	7.2332	6.7172	7.9334	9.2453	10.3628	9.6992	8.5168	7.3147	6.9033	6.5734
11:38	6.0353	6.4034	7.1043	6.6217	7.8479	9.1239	10.2532	9.5422	8.4439	7.2212	6.8159	6.4355
11:40	6.0838	6.5346	7.1823	6.6914	7.9154	9.1906	10.2934	9.6530	8.5161	7.2399	6.8429	6.5543
11:42	6.1267	6.5651	7.2261	6.7272	7.9676	9.2632	10.4262	9.7239	8.5676	7.3313	6.9131	6.5849
11:44	6.0447	6.4959	7.1353	6.6567	7.8829	9.1742	10.3194	9.6295	8.4727	7.2523	6.8440	6.5142
11:46	6.0690	6.5142	7.1336	6.6261	7.7495	8.8645	9.9834	9.3303	8.3343	7.2005	6.8341	6.5335
11:48	6.0557	6.5333	7.1877	6.6863	7.8733	9.0946	10.1655	9.5457	8.4449	7.2765	6.8333	6.5672
11:50	6.0712	6.5171	7.1613	6.6839	7.9211	9.2393	10.3463	9.6563	8.4485	7.2309	6.8772	6.5447
11:52	6.1209	6.5542	7.2279	6.7216	7.9673	9.2694	10.3941	9.7219	8.5656	7.3312	6.9182	6.5867
11:54	6.1.9.	6.5661	7.2205	6.7292	7.9307	9.2810	10.4135	9.7365	8.5703	7.3376	6.9253	6.5832
11:56	5.9617	6.3856	7.0292	6.5452	7.7369	8.9594	10.0436	9.4108	8.3146	7.1427	6.7578	6.4342
11:58	3.3031	4.2561	4.6531	4.3425	5.0715	5.8362	6.4997	6.1153	5.4310	4.6306	4.4512	4.2313
12:00	2.6325	3.3939	3.3670	3.1430	3.6544	4.1858	4.6571	4.3884	3.9161	3.3966	3.2299	3.0561
12:02	2.5735	2.7644	3.3011	2.8033	3.2499	3.7100	4.1314	3.3951	3.4813	3.1275	2.8320	2.7329
12:04	2.5735	2.7644	3.3011	2.8033	3.2499	3.7100	4.1314	3.3951	3.4813	3.1275	2.8320	2.7329
12:06	2.7276	2.9172	3.1724	2.9848	3.4422	3.9395	4.3328	4.1277	3.6384	3.2033	3.0463	2.8381
12:08	2.3112	2.9065	3.2698	3.0552	3.5472	4.0636	4.5150	4.2634	3.8310	3.2974	3.1397	2.9762
12:10	2.9374	3.2026	3.4945	3.2596	3.7922	4.3456	4.8313	4.5678	4.0071	3.5225	3.3491	3.1769
12:12	3.3251	3.5525	3.8314	3.6299	4.2189	4.8466	5.3658	5.2795	4.5143	3.9100	3.7143	3.5037
12:14	3.5064	4.1355	4.5183	4.2155	4.9249	5.6646	6.3114	5.9362	5.2734	4.5519	4.3143	4.0356
12:16	4.3291	4.6257	5.0213	4.7217	5.5319	6.3759	7.0366	6.6745	5.9152	5.1027	4.8337	4.5923
12:18	4.5115	4.9126	5.2652	4.9216	5.7556	6.6425	7.3393	6.9552	6.1628	5.3205	5.0270	4.7739
12:20	4.5167	4.9325	5.2694	4.9317	5.7867	6.6778	7.4565	6.9894	6.1361	5.3230	5.0451	4.7923
12:22	4.7742	5.1197	5.5091	5.2294	6.1389	7.0335	7.9111	7.4221	6.5292	5.6432	5.3458	5.2749
12:24	5.3697	5.7515	6.3048	5.8754	6.3147	7.9372	8.3353	8.3545	7.3562	6.3409	5.9036	5.6580
12:26	5.4534	5.8215	6.4393	5.9598	6.9640	8.0357	8.4643	8.4362	7.4575	6.4329	6.0319	5.7126
12:28	5.7194	6.1375	6.7356	6.2673	7.4154	8.5316	9.5325	8.9774	7.9232	6.7832	6.4336	6.2357
12:30	5.9211	6.3135	6.9564	6.4766	7.5119	8.7365	9.3031	9.1978	8.1332	6.9889	6.6155	6.2763
12:32	6.1048	6.5447	7.3043	6.8111	8.0546	9.3447	10.4663	9.7729	8.6332	7.3602	6.9461	6.5945
12:34	6.2232	6.6605	7.3257	6.8337	8.0882	9.3355	10.5336	9.8279	8.6410	7.3372	6.9617	6.6256
12:36	6.6273	7.1107	7.8366	7.3105	8.6629	10.0697	11.2917	10.5345	9.2509	7.9286	7.4493	7.0035
12:38	6.7443	7.1916	7.9269	7.3955	8.7653	10.2328	11.4439	10.6643	9.3514	7.9972	7.5337	7.1775
12:40	6.8320	7.3341	8.1429	7.5904	9.0368	10.4375	11.7572	10.9666	9.6265	8.2154	7.7325	7.3603
12:42	7.1530	7.5903	8.4168	7.9174	9.4021	10.9590	12.3126	11.4673	10.2462	8.6682	8.0559	7.6711
12:44	7.2546	7.6373	8.6502	8.0708	9.5904	11.1323	12.5498	11.6887	10.2473	8.7232	8.2036	7.7815
12:46	7.4271	7.8636	8.8186	8.2114	9.7647	11.3744	12.7635	11.8713	10.3931	8.8335	8.3067	7.8768
12:55	7.6044	8.2638	9.0656	8.4198	9.9400	11.5390	12.8863	11.9875	10.4830	8.8804	8.3355	7.9259
12:55												

TABLE I (Continued)

AMOCO HYDROFRACTURE EXPERIMENT-TULSA,OK

FRACTURE-NOV. 4,1976

TIME	0°	15°	30°	45°	60°	75°	90°	105°	120°	135°	150°	165°
13:[illegible]	7.7[illegible]	8.2967	9.1142	8.4193	9.8949	11.4674	12.7855	11.8813	10.3958	8.8317	8.2913	7.8515
13:14	8.[illegible]	9.3422	10.2364	9.4685	11.1506	12.9565	14.4747	13.3858	11.5837	9.8261	9.1995	8.7273
13:16	7.3396	8.4623	9.2595	8.5004	9.8867	11.3362	12.5213	11.6375	10.2977	8.7805	8.2712	7.8564
13:17	7.2003	7.7698	8.4265	7.7518	8.9937	10.3575	11.5[illegible]54	10.7309	9.3867	7.9967	7.6243	7.1338
13:19	6.1932	6.5736	7.1695	6.9925	7.6215	8.7372	9.6833	9.0311	7.9958	6.7903	6.4019	6.3632
13:21	5.3277	5.6666	6.1348	5.6873	6.5428	7.4352	8.2767	7.7323	6.8332	5.8478	5.5295	5.2354
13:22	4.5612	4.8729	5.2662	4.8671	5.5762	6.3627	7.0175	6.5769	5.8306	5.0342	4.7362	4.4355
13:24	3.5257	3.8669	4.1921	3.8594	4.4169	5.0223	5.5491	5.1974	4.6239	3.9792	3.7695	3.5658

USGS File #c075/A77, part 2
SAND-77-1992
Oct. 1976-Sept. 1977

TABLE I (Continued)

AMOCO HYDROFRACTURE EXPERIMENT-TULSA,OK

FRACTURE-NOV. 4,1976

TIME	180°	195°	210°	225°	240°	255°	270°	285°	300°	315°	330°	345°
5:40	8.0383	8.0396	9.1043	8.5739	8.8402	9.1536	8.9862	8.7609	8.5254	7.7835	7.5445	7.6656
5:45	8.0375	8.0286	9.1315	8.5330	8.8472	9.1196	8.9431	8.7245	8.4959	7.7614	7.5248	7.6382
5:50	8.0336	8.0436	9.1797	8.5687	8.8457	9.1579	8.9675	8.7517	8.5269	7.7383	7.5536	7.6759
5:55	7.9926	8.0951	9.1155	8.5127	8.8259	9.1317	8.9335	8.7396	8.4798	7.7476	7.5052	7.6247
6:00	8.0033	8.0305	9.0126	8.6003	8.8144	9.1068	9.0133	8.7884	8.5621	7.8172	7.5745	7.5943
6:05	8.0247	8.0233	9.1022	8.5495	8.8571	9.1389	8.3663	8.7381	8.5331	7.7653	7.5397	7.6499
6:10	8.0735	8.0920	9.2128	8.6077	8.9163	9.1055	9.0213	8.7388	8.5651	7.8294	7.5886	7.7146
6:15	7.9956	8.0001	9.1199	8.5191	7.2469	9.1162	8.9319	8.7266	8.4761	7.7513	7.5375	7.6226
6:20	8.0041	8.0116	9.1325	8.5295	7.6168	9.1161	8.9442	8.7224	8.4892	7.7551	7.5153	7.6147
6:25	7.9675	8.0724	9.0960	8.4921	7.3748	9.0756	8.9026	8.6742	8.4511	7.7205	7.4864	7.5945
6:30	8.0132	8.0267	9.1454	8.5453	7.8568	9.1368	8.9556	8.7328	8.4976	7.7663	7.5235	7.6746
6:35	8.0239	8.0351	9.1557	8.5595	8.4299	9.1568	8.9835	8.7573	8.5297	7.7946	7.5528	7.6622
6:40	8.0014	8.0039	9.1329	8.5374	8.4343	9.1296	8.9623	8.7435	8.5291	7.7762	7.5378	7.6409
6:45	7.9803	8.0932	9.1190	8.5136	8.3764	9.1055	8.9391	8.7178	8.4852	7.7536	7.5138	7.6141
6:50	8.0001	8.0195	9.1261	8.5384	8.4582	9.1296	8.9651	8.7416	8.5164	7.7769	7.5349	7.6436
6:55	8.0990	9.0249	9.2594	8.6666	8.5895	9.2874	9.1313	8.9116	8.6659	7.9263	7.6784	7.7315
7:00	7.8792	8.0067	9.0235	8.4253	8.5526	9.0461	8.8979	8.6758	8.4543	7.7241	7.4746	7.5561
7:05	7.8299	8.7559	8.9723	8.3752	8.4420	8.9335	8.8654	8.6309	8.4159	7.6723	7.4314	7.5266
7:10	4.9393	5.9861	5.0851	5.2854	5.3423	5.6757	5.5832	5.4348	5.3644	4.9351	4.7312	4.8478
7:20	6.0694	6.7329	6.8735	6.3445	6.5797	6.8660	6.7522	6.6322	6.4707	5.9427	5.7679	5.8432
7:30	5.9353	6.7174	6.8247	6.3364	6.5785	6.7935	6.6896	6.5618	6.4155	5.8827	5.7223	5.9343
7:40	6.0336	6.9913	6.7945	6.3133	6.5783	6.7749	6.6013	6.5305	6.4336	5.8623	5.6943	5.7319
7:45	6.0134	6.7910	6.8565	6.3656	6.6366	6.8389	6.7361	6.5933	6.4650	5.9214	5.7469	5.8344
7:50	6.0210	6.7859	6.8555	6.3895	6.6053	6.8549	6.7535	6.6173	6.4332	5.9353	5.7674	5.8495
7:55	6.0619	6.8012	6.9647	6.4611	6.7349	6.9389	6.8263	6.6977	6.5644	6.0142	5.8344	5.9195
8:00	6.2259	6.9157	7.0299	6.5325	6.7837	6.9932	6.9180	6.7400	6.5943	6.0426	5.8723	5.9544
8:05	6.3652	6.7962	6.9306	6.3962	6.6772	6.8791	6.7743	6.6113	6.4938	5.9469	5.7402	5.8636
8:10	5.9651	6.8679	6.9997	6.4328	6.7362	6.9365	6.8253	6.6372	6.5542	6.0140	5.8282	5.9141
8:15	6.0284	6.8211	7.0215	6.5513	6.7813	6.9891	6.8724	6.7346	6.5302	6.0371	5.8593	5.9591
8:20	6.0422	6.8622	7.0475	6.5209	6.7999	7.0011	6.8762	6.7377	6.5961	6.0372	5.8607	5.9.6[illegible]
8:25	6.0730	6.8844	7.0621	6.5466	6.8311	7.0239	6.9354	6.7794	6.6195	6.0623	5.8641	5.9757
8:30	6.2425	7.1910	7.2442	6.7363	7.0234	7.2371	7.1049	6.9531	6.8159	6.2241	6.0413	6.1345
8:35	6.0733	6.8676	7.0648	6.5466	6.8295	7.0300	6.9038	6.7572	6.6119	6.0741	5.8742	5.9589
8:40	6.1353	7.0639	7.1034	6.6155	6.9323	7.1076	6.9787	6.8297	6.6754	6.1125	5.9359	6.0346
8:45	6.0491	6.8651	7.0638	6.5193	6.8351	7.0256	6.8817	6.7356	6.5813	6.0259	5.8554	5.9531
8:50	6.1544	7.0656	7.1031	6.6307	6.9243	7.1323	7.0319	6.8503	6.6984	6.1342	5.9572	6.0591
8:55	6.1349	7.0256	7.1217	6.5693	6.8039	7.0536	6.9411	6.7332	6.5437	6.0845	5.8369	5.9939
9:00	6.2729	7.1512	7.2024	6.6403	6.9429	7.1903	7.0222	6.9727	6.7183	6.1512	5.9705	6.0504
9:05	6.3057	7.1251	7.2243	6.6583	6.9533	7.1315	7.1035	6.8949	6.7390	6.1551	5.9374	6.1453
9:10	6.2442	7.1019	7.0495	6.5420	6.8413	7.0454	6.9157	6.7678	6.5241	6.0624	5.8446	5.9736
9:15	6.1133	7.0712	7.1700	6.6376	6.9095	7.1166	6.9966	6.8368	6.5924	6.1257	5.9439	6.0394
9:20	6.1054	7.0481	7.1457	6.5835	6.8972	7.1073	7.0553	6.8319	6.6749	6.1111	5.9255	6.0232
9:22	6.0941	7.0240	7.1168	6.5573	6.8549	7.0769	7.0239	6.7982	6.6433	6.0792	5.9322	6.0024

SAND-77-1992
Oct. 1976-Sept. 1977

TABLE I (Continued)

AMOCO HYDROFRACTURE EXPERIMENT-TULSA,OK

FRACTURE-NOV. 4,1976

TIME		180°	195°	210°	225°	240°	255°	270°	285°	300°	315°	330°	345°
8:24		6.5595	7.0376	7.1324	6.5722	6.8801	7.0977	7.0339	6.3145	6.5626	6.2939	5.9163	6.0114
8:26		6.9957	6.8657	7.0596	6.4974	6.8554	7.0113	6.8759	6.7315	6.5848	6.0272	5.8575	5.9476
8:28	Start pumping	6.5763	7.0708	7.1862	6.5915	6.9015	7.1145	6.9791	6.8361	6.6828	6.1172	5.9435	6.0415
8:30	Rate - 2 bbl/min	6.5594	6.5763	6.6576	6.1212	6.4167	6.6284	6.5847	6.3520	6.2172	5.7119	5.5327	5.6273
8:32		6.5725	6.5154	6.6974	6.1601	6.4534	6.6498	6.5258	6.3925	6.2551	5.7340	5.5696	5.6362
8:34		6.5982	6.5196	6.6001	6.1688	6.3637	6.5551	6.4215	6.3059	6.1643	5.6519	5.4863	5.5774
8:36		6.5472	6.5932	6.6805	6.1405	6.4397	6.6383	6.5139	6.3765	6.2458	5.7189	5.5544	5.6383
8:38		6.4835	6.3852	6.4601	5.9343	6.2286	6.4169	6.2995	6.1669	6.0352	5.5392	5.3813	5.4655
8:40		6.4639	6.3631	6.4346	5.9118	6.1998	6.3869	6.2659	6.1449	6.0159	5.5238	5.3674	5.4527
8:42	Stop pumping	6.4544	6.3626	6.4327	5.9055	6.2023	6.3862	6.2654	6.1442	6.0202	5.5269	5.3639	5.4515
8:44		6.3884	6.2645	6.3536	5.8303	6.1256	6.3100	6.1912	6.0763	5.9468	5.4668	5.3061	5.3932
8:46		6.5450	6.4722	6.5431	6.0076	6.3063	6.5016	6.3875	6.2619	6.1335	5.6453	5.4773	5.5596
8:48		6.5139	6.4424	6.5150	5.9787	6.2562	6.4771	6.3630	6.2400	6.1191	5.6279	5.4659	5.5500
8:50		6.4925	6.4050	6.4703	5.9394	6.2351	6.4387	6.3179	6.2079	6.0767	5.5907	5.4297	5.5165
8:52		6.5587	6.4929	6.5685	6.0203	6.3246	6.5296	6.4071	6.2915	6.1672	5.6727	5.5164	5.5913
8:54		6.5007	6.4259	6.4378	5.9568	6.2597	6.4626	6.3403	6.2237	6.1029	5.6076	5.4471	5.5309
8:56		6.5156	6.4344	6.5097	5.9665	6.2675	6.4740	6.3533	6.2390	6.1281	5.6172	5.4593	5.5454
8:58		6.5510	6.4838	6.5547	6.0085	6.3247	6.5165	6.3974	6.2764	6.1515	5.6564	5.4933	5.5830
9:00		6.5572	6.4906	6.5601	6.0127	6.3245	6.5239	6.4030	6.2858	6.1610	5.6621	5.5029	5.5883
9:02		6.5562	6.4930	6.5635	6.0131	6.3276	6.5249	6.4052	6.2876	6.1584	5.6644	5.4998	5.5872
9:04		6.5507	6.4827	6.5566	6.0036	6.2997	6.5180	6.3951	6.2801	6.1510	5.6577	5.4944	5.5771
9:06		6.5574	6.4976	6.5691	6.0131	6.3372	6.5326	6.4163	6.2920	6.1619	5.6723	5.5075	5.5946
9:08		6.5022	6.4321	6.5029	5.9541	6.2664	6.4668	6.3545	6.2282	6.1325	5.6177	5.4545	5.5390
9:10	Start pumping	6.4723	6.4041	6.4723	5.9235	6.2410	6.4343	6.3161	6.1961	6.0801	5.5970	5.4303	5.5172
9:12	Rate - 2 bbl/min	6.4611	6.3780	6.4437	5.8959	6.2225	6.4125	6.2949	6.1947	6.0681	5.5938	5.4255	5.5118
9:14		6.4596	6.3787	6.4445	5.8911	6.2189	6.4123	6.2943	6.1915	6.0701	5.5996	5.4338	5.5270
9:16		6.5241	6.4165	6.4812	5.9274	6.2596	6.4530	6.3364	6.2320	6.1180	5.6425	5.4803	5.5667
9:18		6.5694	6.4050	6.4697	5.9102	6.2463	6.4416	6.3307	6.2339	6.1260	5.6599	5.5122	5.5996
9:20		6.5136	6.3518	6.4108	5.8620	6.1910	6.3866	6.2762	6.1886	6.0773	5.6218	5.4691	5.5569
9:22		6.4965	6.3649	6.4204	5.8734	6.2062	6.4017	6.2889	6.2005	6.0930	5.6383	5.4862	5.5735
9:24		6.4535	6.3621	6.4169	5.8692	6.2033	6.4010	6.2921	6.2076	6.0944	5.6464	5.4979	5.5881
9:26		6.4933	6.3612	6.4379	5.8872	6.2259	6.4216	6.3078	6.2238	6.1222	5.6721	5.5223	5.6152
9:28		6.4455	6.3262	6.3853	5.8510	6.1773	6.3591	6.2628	6.1752	6.0763	5.6320	5.4313	5.5502
9:30		6.4712	6.3556	6.4104	5.8646	6.2038	6.3974	6.2845	6.2101	6.1072	5.6652	5.5123	5.6117
9:32		6.4640	6.3496	6.4062	5.8605	6.1999	6.3928	6.2875	6.2091	6.1077	5.6658	5.5207	5.6111
9:34		6.4257	6.3084	6.3671	5.8258	6.1626	6.3569	6.2493	6.1735	6.0762	5.6337	5.4928	5.5997
9:36		6.3735	6.2643	6.3235	5.7881	6.1267	6.3217	6.2348	6.1362	6.0433	5.6163	5.4597	5.5607
9:38		6.4447	6.3224	6.3798	5.8404	6.1769	6.3765	6.2736	6.1979	6.0969	5.6642	5.5194	5.6142
9:40		6.4444	6.3208	6.3766	5.8384	6.1764	6.3718	6.2630	6.1933	6.0989	5.6634	5.5208	5.6204
9:42		6.4478	6.3296	6.3931	5.8583	6.1869	6.3860	6.2795	6.1967	6.0941	5.6445	5.5050	5.5994
9:44		6.3076	6.2515	6.3146	5.7829	6.1063	6.2953	6.1924	6.1099	5.9856	5.5447	5.3911	5.4791
9:46		6.5386	6.3939	6.4575	5.9154	6.2454	6.4403	6.3282	6.2371	6.1350	5.6825	5.5354	5.6171
9:48		6.4050	6.3470	6.4344	5.8676	6.1937	6.3916	6.2737	6.1962	6.0967	5.6523	5.4993	5.5914
9:50													
9:52													

UGR File #c073/A77, part 2
SAND-77-1992
Oct. 1976-Sept. 1977

TABLE I (Continued)

AMOCO HYDROFRACTURE EXPERIMENT-TULSA,OK

FRACTURE-NOV. 4,1976

TIME		180°	195°	210°	225°	240°	255°	270°	285°	300°	315°	330°	345°
9:54		5.6444	6.3255	6.3844	5.9512	6.1779	6.3699	6.2612	6.1744	6.2798	5.6400	5.4952	5.5761
9:56		5.4780	6.3534	6.4148	5.8765	6.2063	6.3969	6.2860	6.2130	6.1138	5.6648	5.5245	5.6174
9:58		5.5[illegible]6	6.3793	6.4522	5.9163	6.2421	6.4363	6.3266	6.2406	6.1449	5.7123	5.5516	5.6433
10:00		5.3376	6.2433	6.3190	5.7915	6.1347	6.2315	6.1337	6.1058	6.0884	5.5753	5.4291	5.5152
10:02	Stop pumping	5.5343	6.4540	6.5365	6.0084	6.3134	6.5127	6.3927	6.2767	6.1582	5.6819	5.5373	5.6194
10:04		5.5551	6.4864	6.5624	6.0275	6.3379	6.5337	6.4112	6.3012	6.1378	5.7391	5.5576	5.6346
10:06		5.3474	6.3238	6.3965	5.8785	6.1675	6.3724	6.2556	6.1363	6.2237	5.5798	5.4392	5.5118
10:08		5.5431	6.4501	6.5177	5.9861	6.2998	6.4939	6.3689	6.2643	6.1524	5.6908	5.5318	5.6133
10:10		5.5530	6.4613	6.4658	5.9455	6.2601	6.4411	6.3213	6.2246	6.1389	5.6549	5.4981	5.5344
10:12		5.5326	6.4295	6.4964	5.9716	6.2775	6.4710	6.3674	6.2570	6.1485	5.6971	5.5356	5.6139
10:14		5.4339	6.3874	6.4518	5.9371	6.2565	6.4291	6.3248	6.2216	6.1435	5.6663	5.5174	5.5951
10:16		5.5526	6.4330	6.4355	5.9776	6.2814	6.4683	6.3572	6.2617	6.1573	5.7136	5.5449	5.6245
10:18		5.5287	6.4192	6.4346	5.9716	6.2667	6.4616	6.3466	6.2565	6.1537	5.6968	5.5452	5.6297
10:20		5.4352	6.3614	6.4251	5.9153	6.2110	6.4025	6.2889	6.1989	6.0957	5.6511	5.4952	5.5777
10:22		5.5304	6.4232	6.5067	5.9946	6.2993	6.4869	6.3751	6.2811	6.1669	5.7168	5.5564	5.6436
10:24		5.4943	6.3758	6.4577	5.9594	6.2658	6.4495	6.3352	6.2427	6.1374	5.6815	5.5224	5.6039
10:26		5.5420	6.4353	6.5124	6.0147	6.3136	6.5174	6.3916	6.2945	6.1936	5.7375	5.5742	5.6559
10:28		5.5495	6.4411	6.5220	6.0234	6.3222	6.5224	6.4017	6.3052	6.2004	5.7438	5.5815	5.6670
10:30		5.5423	6.4355	6.5240	6.0267	6.3249	6.5168	6.4244	6.3159	6.2038	5.7471	5.5835	5.6665
10:32		5.4465	6.3235	6.4026	5.9200	6.2550	6.3331	6.2805	6.1855	6.0532	5.6346	5.4777	5.5595
10:34		5.5324	6.4127	6.4814	5.9964	6.2811	6.4636	6.3534	6.2618	6.1592	5.7082	5.5490	5.6302
10:36		5.5520	6.4197	6.4366	6.0111	6.2839	6.4773	6.3586	6.2653	6.1580	5.7104	5.5456	5.6285
10:38		5.5415	6.3995	6.4736	5.9954	6.2641	6.4533	6.3366	6.2480	6.1365	5.6879	5.5298	5.6144
10:40		5.5552	6.4341	6.5119	6.0269	6.2994	6.4903	6.3721	6.2779	6.1033	5.7149	5.5516	5.6397
10:42		5.5224	6.4424	6.5177	6.0348	6.3269	6.4937	6.3783	6.2815	6.1746	5.7232	5.5611	5.6414
10:44		5.5470	6.4259	6.5241	6.0235	6.2902	6.4752	6.3509	6.2603	6.1596	5.7115	5.5434	5.6301
10:46		5.5514	6.4553	6.5357	6.0596	6.3199	6.5356	6.3832	6.2811	6.1602	5.7239	5.5619	5.6435
10:48		5.5495	6.4531	6.5343	6.0657	6.3173	6.5366	6.3802	6.2718	6.1727	5.7163	5.5544	5.6337
10:50		5.5241	6.4896	6.5726	6.1004	6.3569	6.5377	6.4236	6.3184	6.2112	5.7421	5.5752	5.6594
10:52		5.5717	6.4237	6.5346	6.0429	6.2892	6.4755	6.3513	6.2417	6.1367	5.6951	5.5231	5.6349
10:54		5.5317	6.4428	6.5249	6.0653	6.3057	6.4923	6.3643	6.2555	6.1579	5.6925	5.5397	5.6121
10:56		5.5734	6.5233	6.5156	6.1521	6.3956	6.5815	6.4564	6.3447	6.2349	5.7753	5.6120	5.6840
10:58		5.6266	6.4801	6.5619	6.1031	6.3433	6.5275	6.4077	6.2938	6.1596	5.7261	5.5633	5.6411
11:00		5.5082	6.5249	6.6093	6.1517	6.3856	6.5758	6.4536	6.3372	6.2317	5.7712	5.6002	5.6832
11:02		5.5473	6.4210	6.5377	6.0555	6.2893	6.4694	6.3524	6.2383	6.1299	5.6776	5.5141	5.5957
11:04		5.5966	6.5492	6.6324	6.1787	6.4088	6.5948	6.4770	6.3585	6.2438	5.7345	5.6182	5.7026
11:06		5.6332	6.5333	6.6253	6.1704	6.4009	6.5885	6.4501	6.3481	6.2414	5.7792	5.6176	5.6941
11:08		5.5694	6.4752	6.5743	6.1284	6.3510	6.5382	6.4170	6.3312	6.1930	5.7203	5.5675	5.6447
11:10		5.5321	6.4151	6.5343	6.0653	6.2844	6.4650	6.3547	6.2248	6.1246	5.6638	5.5257	5.6345
11:12		5.5776	6.4967	6.5874	6.1448	6.3653	6.5458	6.4260	6.3347	6.1389	5.7325	5.5727	5.6522
11:14		5.7123	6.5321	6.6237	6.1831	6.3985	6.5825	6.4577	6.3450	6.2318	5.7601	5.5994	5.6708
11:16		5.6[illegible]	6.4762	6.5648	6.1318	6.3384	6.5222	6.3988	6.2752	6.1728	5.7124	5.5446	5.6264
11:18		5.7356	6.5730	6.6629	6.2232	6.4343	6.6183	6.4956	6.3740	6.2619	5.7922	5.6322	5.7253

TABLE I (Continued)

AMOCO HYDROFRACTURE EXPERIMENT-TULSA,OK

FRACTURE-NOV. 4,1976

TIME	180°	195°	210°	225°	240°	255°	270°	285°	300°	315°	330°	345°
11:22	5.7164	6.5345	6.6257	6.1926	6.3986	6.5818	6.4579	6.3376	6.2318	5.7591	5.6014	5.6784
11:24	5.7514	6.5964	6.6859	6.2563	6.4593	6.6404	6.5176	6.3941	6.2819	5.8142	5.6455	5.7181
11:26	5.6917	6.4031	6.5731	6.1488	6.3451	6.5299	6.3977	6.2775	6.1740	5.7111	5.5479	5.6254
11:28	5.6347	6.4658	6.5773	6.1560	6.3481	6.5319	6.4258	6.2847	6.1823	5.7115	5.5517	5.6263
11:30	5.7523	6.5607	6.6545	6.2320	6.4250	6.6374	6.4353	6.3590	6.2517	5.7811	5.6177	5.6950
11:32	5.5720	6.4766	6.5713	6.1591	6.3431	6.5274	6.4203	6.2729	6.1739	5.7066	5.5443	5.6181
11:34	5.7295	6.5309	6.6253	6.2124	6.3943	6.5766	6.4542	6.3221	6.2208	5.7545	5.5890	5.6612
11:36	5.7495	6.6071	6.7214	6.2865	6.4616	6.6320	6.5263	6.3992	6.2392	5.8127	5.6514	5.7253
11:38	5.7152	6.5116	6.6046	6.2013	6.3791	6.5543	6.4410	6.3038	6.2020	5.7346	5.5652	5.6481
11:40	5.7745	6.5846	6.6819	6.2705	6.4473	6.6314	6.5359	6.3755	6.2694	5.7979	5.6296	5.7279
11:42	5.6088	6.5138	6.7192	6.3057	6.4732	6.6577	6.5313	6.4033	6.2960	5.8184	5.6526	5.7316
11:44	5.7454	6.5396	6.6367	6.2371	6.4014	6.5830	6.4613	6.3291	6.2294	5.7567	5.5956	5.6729
11:46	5.7452	6.5738	6.6755	6.2789	6.4443	6.6322	6.5324	6.3693	6.2665	5.7896	5.6201	5.6949
11:48	5.7783	6.6129	6.7173	6.3203	6.4817	6.6695	6.5387	6.4058	6.2985	5.8181	5.6457	5.7224
11:50	5.7524	6.5639	6.6853	6.2954	6.4495	6.6359	6.5229	6.3794	6.2660	5.7918	5.6203	5.6948
11:52	5.6175	6.6230	6.7241	6.3315	6.4929	6.6718	6.5449	6.4123	6.3013	5.8244	5.6525	5.7281
11:54	5.8218	6.6286	6.7318	6.3433	6.4989	6.6848	6.5587	6.4198	6.3109	5.8233	5.6589	5.7337
11:56	5.7116	6.4937	6.6004	6.2148	6.3561	6.5261	6.3969	6.2566	6.1463	5.6771	5.5378	5.5834
11:58	3.7703	4.2754	4.3356	4.0913	4.1975	4.3210	4.2423	4.1733	4.1103	3.8381	3.7316	3.7423
12:00	2.7446	3.1978	3.1348	2.9513	3.1323	3.1186	3.0599	3.1211	2.9815	2.7741	2.6397	2.7211
12:02	2.4543	2.7616	2.7919	2.6313	2.7031	2.7764	2.7246	2.6942	2.6573	2.4684	2.3335	2.4243
12:04	2.5337	2.9193	2.9516	2.7824	2.8536	2.9360	2.8792	2.8394	2.8060	2.6082	2.5368	2.5335
12:06	2.6765	3.0078	3.0430	2.8676	2.9402	3.0273	2.9675	2.9283	2.8885	2.6876	2.6123	2.6425
12:08	2.8566	3.2120	3.2508	3.0695	3.1416	3.2331	3.1725	3.1242	3.0868	2.8654	2.7973	2.9166
12:10	3.1365	3.5612	3.6371	3.4566	3.4891	3.5486	3.5193	3.4710	3.4227	3.1958	3.0873	3.1257
12:12	3.6069	4.1301	4.1956	3.9685	4.0642	4.1822	4.1031	4.0468	3.9738	3.6932	3.5864	3.6279
12:14	4.1131	4.6356	4.7034	4.4513	4.5557	4.6973	4.6335	4.5242	4.4616	4.1313	4.0157	4.0636
12:16	4.2736	4.8209	4.8921	4.6331	4.7394	4.8778	4.7943	4.7034	4.6383	4.2975	4.1768	4.2236
12:18	4.2303	4.8363	4.9143	4.6537	4.7583	4.8963	4.8139	4.7230	4.6534	4.3129	4.1920	4.2427
12:20	4.5434	5.1200	5.2259	4.9310	5.0411	5.1883	5.0949	5.0023	4.9337	4.5673	4.4330	4.4871
12:22	5.0372	5.7573	5.8526	5.5461	5.6652	5.8360	5.7314	5.6210	5.5409	5.1174	4.9713	5.0352
12:24	5.1769	5.8543	5.9535	5.6483	5.7631	5.9363	5.8325	5.7208	5.6379	5.2943	5.0593	5.1169
12:26	5.4343	6.1459	6.2517	5.9264	6.0493	6.2344	6.1230	6.0011	5.9138	5.4593	5.3667	5.3683
12:28	5.5976	6.3399	6.4538	6.1235	6.2473	6.4306	6.3160	6.1992	6.1035	5.6393	5.4763	5.5330
12:30	5.8759	6.6527	6.7754	6.4292	6.5541	6.7631	6.6389	6.5205	6.4014	5.9364	5.7394	5.8053
12:32	5.8607	6.6652	6.7874	6.4454	6.5672	6.7730	6.6508	6.5123	6.4118	5.9154	5.7469	5.8167
12:34	6.2028	7.1292	7.2544	6.9026	7.0270	7.2464	7.1210	6.9719	6.8573	6.3217	6.1412	6.2161
12:36	6.3432	7.2892	7.3454	6.9802	7.1063	7.3282	7.1944	7.0475	6.9311	6.3843	6.2043	6.2773
12:38	6.5363	7.3967	7.5384	7.1717	7.2948	7.5274	7.3913	7.2352	7.1128	6.5524	6.3666	6.4392
12:40	6.7874	7.7033	7.8596	7.4756	7.6928	7.8406	7.7037	7.5287	7.4069	6.8204	6.6210	6.6971
12:42	6.8331	7.8463	8.0379	7.6173	7.7457	7.9313	7.8502	7.6741	7.5464	6.9442	6.7429	6.8263
12:44	6.9331	7.9076	8.1513	7.7742	7.9156	8.1779	8.0417	7.8580	7.7278	7.0944	6.8846	6.9551
12:46	7.2184	7.9396	8.1999	7.8408	8.0327	8.3197	8.2233	8.0647	7.9647	7.3328	7.1254	7.2362

UGR File #c075/A77, part 2
SAND-77-1992
Oct. 1976-Sept. 1977

TABLE I (Continued)

AMOCO HYDROFRACTURE EXPERIMENT-TULSA, OK

FRACTURE-NOV. 4,1976

TIME	180°	195°	210°	225°	240°	255°	270°	285°	300°	315°	330°	345°
13:12	6.4649	7.3638	8.1629	7.8163	7.0628	8.2739	8.1931	8.0427	7.3546	7.3328	7.1439	7.2372
13:14	7.7519	8.3544	9.1238	8.7754	8.9193	9.2980	9.2252	9.0387	8.9453	8.2242	8.2177	8.1345
13:16	8.3391	7.4949	8.2166	7.8965	8.0455	8.3793	8.3113	8.1716	8.1031	7.4759	7.2883	7.3391
13:17	6.3503	7.2555	7.4411	7.1491	7.2742	7.5319	7.5277	7.4155	7.3545	6.8196	6.6492	6.7421
13:19	5.4275	6.1739	6.3204	6.0660	6.1809	6.4347	6.3923	6.3021	6.2638	5.8053	5.6778	5.7533
13:21	4.6710	5.3255	5.4512	5.2264	5.3283	5.5351	5.4972	5.4322	5.4036	5.0150	4.8768	4.8340
13:22	4.3351	4.5650	4.6029	4.4898	4.5523	4.7320	4.6935	4.6494	4.6248	4.3127	4.2122	4.2732
13:24	3.2147	3.5251	3.6392	3.5417	3.6114	3.7469	3.7171	3.6843	3.6712	3.4238	3.3481	3.3394

APPENDIX B

TABLE I

GPE NATURAL BUTTES NO.14-HYDROFRACTURE

FRACTURE-MARCH 15,1977

TIME		0°	15°	30°	45°	60°	75°	90°	105°	120°	135°	150°	165°
6:59		1.9417	2.0346	2.1047	2.2417	2.2500	2.2501	2.2998	2.1437	2.0405	2.0208	2.0344	2.0228
7:01		1.9407	2.0317	2.1042	2.2416	2.2484	2.2508	2.3305	2.1436	2.0393	2.0190	2.0322	2.0224
7:03		1.9405	2.0208	2.1045	2.2426	2.2508	2.2483	2.2980	2.1441	2.0411	2.0212	2.0342	1.9990
7:05		1.9431	2.0395	2.1087	2.2457	2.2528	2.2466	2.2962	2.1435	2.0419	2.0202	2.0316	1.9933
7:07		1.9447	2.0279	2.1074	2.2451	2.2521	2.2460	2.2956	2.1441	2.0398	2.0187	2.0313	2.0249
7:09		1.9403	2.0277	2.1069	2.2432	2.2516	2.2469	2.2966	2.1486	2.0435	2.0232	2.0359	2.0226
7:14	Stage 1 - Start pumping	1.9407	2.0401	2.1061	2.2432	2.2501	2.2384	2.2879	2.1421	2.0378	2.0173	2.0304	1.9977
7:16		1.9413	2.0228	2.1062	2.2413	2.2479	2.2384	2.2879	2.1398	2.0354	2.0149	2.0277	1.9953
7:18	Start pre-pad	1.9409	2.0205	2.1061	2.2422	2.2488	2.2396	2.2891	2.1414	2.0382	2.0171	2.0307	1.9984
7:20		1.9236	2.0077	2.0879	2.2239	2.2315	2.2399	2.2871	2.1269	2.0223	2.0029	2.0161	1.9944
7:22		1.9221	2.0248	2.0845	2.2198	2.2286	2.2390	2.2834	2.1235	2.0195	1.9999	2.0137	1.9906
7:24		1.9197	2.0181	2.0800	2.2233	2.2309	2.2405	2.2895	2.1280	2.0233	2.0021	2.0141	1.9905
7:26		1.9069	2.0063	2.0718	2.2065	2.2176	2.2274	2.2720	2.1135	2.0106	1.9906	2.0043	1.9715
7:28		1.9151	2.0152	2.0822	2.2201	2.2269	2.2357	2.2798	2.1175	2.0114	1.9899	1.9979	1.9632
7:30		1.9137	2.0123	2.0813	2.2172	2.2252	2.2352	2.2768	2.1165	2.0121	1.9909	2.0010	1.9665
7:32		1.9092	2.0106	2.0786	2.2144	2.2230	2.2332	2.2737	2.1137	2.0091	1.9869	1.9983	1.9639
7:34		1.9095	2.0093	2.0772	2.2122	2.2245	2.2316	2.2725	2.1116	2.0078	1.9867	1.9986	1.9638
7:36		1.9002	2.0000	2.0687	2.2045	2.2149	2.2245	2.2786	2.1083	2.0059	1.9853	1.9999	1.9667
7:38		1.9028	2.0026	2.0714	2.2061	2.2179	2.2241	2.2739	2.1085	2.0051	1.9846	1.9980	1.9657
7:40		1.9036	2.0048	2.0748	2.2096	2.2209	2.2312	2.2692	2.1094	2.0056	1.9842	1.9971	1.9624
7:42		1.8949	1.9930	2.0634	2.1982	2.2098	2.2193	2.2645	2.1021	1.9989	1.9792	1.9924	1.9588
7:44		1.9037	2.0041	2.0734	2.2072	2.2150	2.2240	2.2736	2.1353	1.9983	1.9743	1.9840	1.9482
7:46		1.8882	1.9902	2.0619	2.1977	2.2098	2.2202	2.2648	2.0994	1.9971	1.9760	1.9885	1.9540
7:48		1.8824	1.9936	2.0649	2.2002	2.2195	2.2181	2.2666	2.1009	1.9962	1.9737	1.9845	1.9494
7:50		1.8846	1.9958	2.0675	2.2007	2.2097	2.2183	2.2624	2.1095	1.9928	1.9690	1.9794	1.9439
7:52		1.8830	1.9931	2.0625	2.1953	2.2027	2.2113	2.2569	2.0935	1.9883	1.9674	1.9772	1.9426
7:54		1.8881	1.9901	2.0626	2.1984	2.2086	2.2176	2.2668	2.0961	1.9916	1.9683	1.9791	1.9419
7:56		1.8849	1.9833	2.0532	2.1863	2.1957	2.2053	2.2493	2.0833	1.9801	1.9591	1.9742	1.9390
7:58		1.8737	1.9709	2.0405	2.1745	2.1854	2.1955	2.2408	2.0757	1.9741	1.9548	1.9706	1.9369
8:00	46,000 gal.	1.8796	1.9796	2.0533	2.1922	2.2013	2.2096	2.2548	2.0873	1.9821	1.9595	1.9736	1.9349
8:02		1.8591	1.9686	2.0369	2.1779	2.1859	2.1950	2.2396	2.0735	1.9716	1.9547	1.9732	1.9381
8:04		1.8693	1.9744	2.0483	2.1923	2.2024	2.2107	2.2527	2.0850	1.9808	1.9603	1.9763	1.9382
8:06		1.8731	1.9759	2.0523	2.1962	2.2046	2.2131	2.2524	2.0824	1.9781	1.9567	1.9716	1.9329
8:08		1.8676	1.9726	2.0511	2.1980	2.2059	2.2165	2.2526	2.0866	1.9818	1.9617	1.9773	1.9405
8:10		1.8648	1.9734	2.0489	2.1934	2.1990	2.2097	2.2441	2.0765	1.9746	1.9559	1.9733	1.9356
8:12		1.8686	1.9765	2.0550	2.2035	2.2102	2.2211	2.2513	2.0862	1.9809	1.9602	1.9756	1.9352
8:14		1.8727	1.9818	2.0578	2.2065	2.2149	2.2221	2.2540	2.0851	1.9793	1.9565	1.9721	1.9316
8:16		1.8657	1.9733	2.0508	2.1986	2.2062	2.2171	2.2456	2.0828	1.9773	1.9570	1.9748	1.9370
8:18		1.8652	1.9734	2.0527	2.2022	2.2112	2.2212	2.2532	2.0858	1.9799	1.9591	1.9752	1.9370
8:20		1.8561	1.9656	2.0456	2.1958	2.2056	2.2178	2.2435	2.0807	1.9757	1.9550	1.9722	1.9350
8:22		1.8669	1.9754	2.0553	2.2055	2.2133	2.2240	2.2530	2.0838	1.9755	1.9529	1.9663	1.9273
8:24		1.8591	1.9648	2.0454	2.1963	2.2073	2.2172	2.2501	2.0814	1.9759	1.9553	1.9751	1.9355
8:26		1.8587	1.9675	2.0463	2.1961	2.2052	2.2153	2.2464	2.0771	1.9704	1.9489	1.9664	1.9297
8:28													

UGR File #c073/A77, part 2
SAND-77-1992
Oct. 1976-Sept. 1977

TABLE I (Continued)

GPE NATURAL BUTTES NO.14-HYDROFRACTURE

FRACTURE-MARCH 15,1977

TIME		0°	15°	30°	45°	60°	75°	90°	105°	120°	135°	150°	165°
8:29		1.8506	1.9577	2.0370	2.1853	2.2010	2.2058	2.2387	2.0701	1.9645	1.9440	1.9632	1.9255
8:31	78,000 gal.	1.8443	1.9530	2.0309	2.1808	2.1936	2.2057	2.2346	2.0659	1.9603	1.9391	1.9579	1.9211
8:33	Stage 2	1.8520	1.9549	2.0328	2.1817	2.1907	2.2025	2.2281	2.0613	1.9557	1.9355	1.9531	1.9166
8:35		1.8395	1.9513	2.0301	2.1816	2.1931	2.2029	2.2342	2.0636	1.9555	1.9332	1.9483	1.9121
8:37	Start pre-pad	1.8322	1.9416	2.0230	2.1755	2.1922	2.2030	2.2339	2.0632	1.9572	1.9343	1.9517	1.9122
8:39		1.8349	1.9435	2.0243	2.1738	2.1876	2.1991	2.2253	2.0575	1.9533	1.9253	1.9456	1.9051
8:41		1.8354	1.9489	2.0307	2.1843	2.1969	2.2081	2.2352	2.0675	1.9583	1.9348	1.9494	1.9149
8:44		1.8338	1.9430	2.0246	2.1751	2.1865	2.1999	2.2258	2.0590	1.9502	1.9278	1.9443	1.9066
8:46		1.8337	1.9420	2.0224	2.1726	2.1874	2.1952	2.2253	2.0570	1.9480	1.9264	1.9427	1.9062
8:48		1.8337	1.9429	2.0241	2.1759	2.1880	2.2012	2.2299	2.0595	1.9504	1.9274	1.9446	1.9073
8:50		1.8347	1.9443	2.0263	2.1774	2.1905	2.2075	2.2333	2.0629	1.9536	1.9300	1.9473	1.9092
8:52		1.8364	1.9462	2.0274	2.1783	2.1901	2.2040	2.2321	2.0617	1.9522	1.9300	1.9489	1.9109
8:54		1.8352	1.9443	2.0253	2.1770	2.1910	2.2022	2.2307	2.0610	1.9520	1.9302	1.9483	1.9106
8:56		1.8372	1.9452	2.0260	2.1777	2.1897	2.2032	2.2310	2.0615	1.9511	1.9298	1.9490	1.9112
8:58		1.8378	1.9453	2.0263	2.1765	2.1974	2.2032	2.2310	2.0612	1.9513	1.9297	1.9486	1.9112
9:00		1.8321	1.9435	2.0255	2.1770	2.1991	2.2051	2.2357	2.0646	1.9555	1.9346	1.9533	1.9181
9:02		1.8404	1.9476	2.0276	2.1779	2.1909	2.2023	2.2340	2.0590	1.9498	1.9283	1.9476	1.9153
9:04	110,000 gal.	1.8383	1.9481	2.0293	2.1812	2.1926	2.2084	2.2321	2.0644	1.9544	1.9330	1.9510	1.9130
9:06		1.8357	1.9453	2.0246	2.1775	2.1887	2.2029	2.2320	2.0620	1.9526	1.9320	1.9513	1.9139
9:08		1.8416	1.9506	2.0312	2.1826	2.1946	2.2094	2.2356	2.0650	1.9538	1.9316	1.9517	1.9152
9:10		1.8355	1.9422	2.0218	2.1725	2.1845	2.1988	2.2265	2.0573	1.9488	1.9296	1.9521	1.9176
9:12		1.8392	1.9499	2.0312	2.1833	2.1961	2.2123	2.2365	2.0694	1.9581	1.9369	1.9562	1.9183
9:14		1.8426	1.9528	2.0279	2.1775	2.1904	2.2017	2.2332	2.0591	1.9478	1.9267	1.9475	1.9126
9:15		1.8433	1.9537	2.0348	2.1873	2.2022	2.2144	2.2410	2.0680	1.9564	1.9333	1.9536	1.9132
9:18		1.8442	1.9511	2.0281	2.1775	2.1881	2.2001	2.2271	2.0558	1.9449	1.9239	1.9449	1.9127
9:20		1.8462	1.9530	2.0333	2.1856	2.1960	2.2113	2.2332	2.0659	1.9548	1.9321	1.9517	1.9151
9:22		1.8372	1.9424	2.0190	2.1682	2.1805	2.1931	2.2193	2.0481	1.9369	1.9159	1.9365	1.9037
9:24		1.8319	1.9414	2.0220	2.1760	2.1902	2.2030	2.2296	2.0592	1.9466	1.9223	1.9416	1.9027
9:26		1.8237	1.9328	2.0127	2.1651	2.1764	2.1947	2.2250	2.0519	1.9421	1.9213	1.9409	1.9063
9:28		1.8391	1.9512	2.0343	2.1893	2.2024	2.2169	2.2453	2.0713	1.9566	1.9297	1.9424	1.9113
9:30		1.8379	1.9443	2.0216	2.1704	2.1869	2.1930	2.2186	2.0475	1.9348	1.9121	1.9312	1.8964
9:32		1.8329	1.9420	2.0216	2.1733	2.1957	2.1995	2.2282	2.0581	1.9456	1.9247	1.9424	1.9079
9:34		1.8385	1.9466	2.0361	2.1782	2.1898	2.2051	2.2315	2.0597	1.9467	1.9227	1.9403	1.9032
9:36		1.8323	1.9359	2.0130	2.1629	2.1743	2.1917	2.2186	2.0491	1.9404	1.9215	1.9433	1.9112
9:38		1.8331	1.9410	2.0205	2.1737	2.1854	2.2024	2.2296	2.0595	1.9487	1.9260	1.9459	1.9106
9:40		1.8372	1.9475	2.0289	2.1818	2.1957	2.2099	2.2382	2.0660	1.9546	1.9306	1.9494	1.9111
9:42		1.8402	1.9508	2.0318	2.1856	2.1972	2.2133	2.2343	2.0609	1.9543	1.9292	1.9452	1.9068
9:44	157,000 gal.	1.8277	1.9354	2.0155	2.1690	2.1797	2.1982	2.2280	2.0596	1.9499	1.9285	1.9477	1.9137
9:46		1.8293	1.9351	2.0128	2.1642	2.1751	2.1932	2.2233	2.0536	1.9439	1.9249	1.9461	1.9232
9:48		1.8384	1.9435	2.0211	2.1715	2.1897	2.1962	2.2253	2.0532	1.9411	1.9193	1.9383	1.9163
9:50	Stage 3	1.8373	1.9467	2.0256	2.1795	2.1932	2.2064	2.2331	2.0642	1.9533	1.9297	1.9476	1.9137
9:52		1.8386	1.9467	2.0271	2.1803	2.1929	2.2054	2.2376	2.0642	1.9513	1.9280	1.9461	1.9064
9:54	Start pre-pad	1.8331	1.9390	2.0176	2.1691	2.1843	2.1967	2.2248	2.0569	1.9469	1.9250	1.9462	1.9134

TABLE I (Continued)

GPE NATURAL BUTTES NO.14-HYDROFRACTURE

FRACTURE-MARCH 15,1977

TIME		0°	15°	30°	45°	60°	75°	90°	105°	120°	135°	150°	165°
9:56		1.8372	1.9451	2.0236	2.1763	2.1905	2.2024	2.2333	2.0612	1.9493	1.9262	1.9434	1.9034
9:58		1.8360	1.9451	2.0246	2.1765	2.1907	2.2048	2.2339	2.0626	1.9497	1.9275	1.9439	1.9080
10:00		1.8371	1.9460	2.0243	2.1775	2.1915	2.2062	2.2368	2.0632	1.9515	1.9281	1.9445	1.9076
10:02		1.8403	1.9482	2.0252	2.1770	2.1894	2.2048	2.2323	2.0617	1.9492	1.9264	1.9450	1.9085
10:04		1.8398	1.9484	2.0269	2.1784	2.1925	2.2057	2.2352	2.0616	1.9487	1.9261	1.9427	1.9063
10:06		1.8434	1.9469	2.0242	2.1725	2.1850	2.1961	2.2280	2.0546	1.9423	1.9237	1.9375	1.9116
10:08		1.8355	1.9438	2.0223	2.1750	2.1916	2.2041	2.2376	2.0639	1.9527	1.9300	1.9465	1.9113
10:10		1.8431	1.9490	2.0254	2.1746	2.1571	2.1991	2.2307	2.0558	1.9431	1.9199	1.9383	1.9032
10:12	184,000 gal.	1.8373	1.9455	2.0231	2.1761	2.1911	2.2026	2.2363	2.0638	1.9510	1.9292	1.9469	1.9114
10:14		1.8375	1.9454	2.0226	2.1751	2.1892	2.2024	2.2343	2.0603	1.9471	1.9248	1.9429	1.9027
10:16		1.8394	1.9449	2.0212	2.1695	2.1836	2.1950	2.2317	2.0536	1.9423	1.9194	1.9371	1.9034
10:20		1.8387	1.9442	2.0204	2.1704	2.1841	2.1972	2.2293	2.0552	1.9439	1.9206	1.9416	1.9024
10:22		1.8386	1.9456	2.0236	2.1743	2.1896	2.1992	2.2300	2.0586	1.9463	1.9228	1.9403	1.9055
10:24		1.8395	1.9444	2.0211	2.1706	2.1836	2.1992	2.2308	2.0545	1.9421	1.9206	1.9338	1.9052
10:26		1.8404	1.9445	2.0238	2.1745	2.1878	2.1991	2.2330	2.0611	1.9480	1.9263	1.9428	1.9081
10:30		1.8472	1.9456	2.0237	2.1737	2.1891	2.1984	2.2337	2.0576	1.9457	1.9238	1.9398	1.9075
10:34		1.8418	1.9412	2.0184	2.1704	2.1887	2.1994	2.2371	2.0618	1.9503	1.9289	1.9473	1.9091
10:36		1.8476	1.9463	2.0226	2.1742	2.1887	2.2003	2.2298	2.0611	1.9477	1.9246	1.9411	1.9137
10:38		1.8476	1.9458	2.0226	2.1742	2.1914	2.1977	2.2349	2.0601	1.9471	1.9252	1.9420	1.9125
10:44		1.8476	1.9455	2.0232	2.1748	2.1920	2.2029	2.2414	2.0633	1.9521	1.9300	1.9470	1.9125
10:48		1.8517	1.9488	2.0248	2.1747	2.1910	2.2015	2.2321	2.0594	1.9461	1.9235	1.9431	1.9071
10:50		1.8480	1.9438	2.0209	2.1715	2.1894	2.2042	2.2398	2.0624	1.9522	1.9311	1.9513	1.9228
10:52		1.8532	1.9515	2.0279	2.1771	2.1955	2.2041	2.2406	2.0620	1.9497	1.9268	1.9437	1.9139
10:54		1.8512	1.9439	2.0249	2.1737	2.1906	2.2009	2.2381	2.0600	1.9481	1.9277	1.9442	1.9095
10:56		1.8531	1.9500	2.0257	2.1752	2.1910	2.2028	2.2353	2.0601	1.9476	1.9257	1.9427	1.9136
10:59		1.8529	1.9494	2.0263	2.1788	2.1962	2.2072	2.2449	2.0654	1.9538	1.9315	1.9483	1.9199
11:00		1.8590	1.9563	2.0328	2.1834	2.1982	2.2088	2.2408	2.0646	1.9500	1.9272	1.9428	1.9151
11:02		1.8539	1.9500	2.0263	2.1772	2.1944	2.2035	2.2420	2.0623	1.9519	1.9302	1.9470	1.9188
11:04		1.8504	1.9437	2.0182	2.1685	2.1850	2.1958	2.2350	2.0576	1.9471	1.9278	1.9472	1.9222
11:06	237,000 gal.	1.8510	1.9462	2.0217	2.1725	2.1874	2.1995	2.2375	2.0587	1.9477	1.9271	1.9453	1.9185
11:08	Stage 4	1.8551	1.9503	2.0263	2.1763	2.1924	2.2047	2.2460	2.0627	1.9518	1.9308	1.9491	1.9233
11:10		1.8519	1.9449	2.0204	2.1703	2.1879	2.1993	2.2372	2.0580	1.9471	1.9261	1.9448	1.9171
11:12	Start pre-pad	1.8512	1.9465	2.0230	2.1736	2.1909	2.2006	2.2392	2.0602	1.9486	1.9264	1.9431	1.9152
11:14		1.8507	1.9453	2.0201	2.1701	2.1860	2.1969	2.2379	2.0566	1.9468	1.9249	1.9445	1.9177
11:16		1.8554	1.9530	2.0306	2.1818	2.1983	2.2077	2.2498	2.0664	1.9543	1.9315	1.9478	1.9182
11:18		1.8547	1.9517	2.0267	2.1774	2.1923	2.2044	2.2417	2.0608	1.9496	1.9266	1.9447	1.9159
11:20		1.8575	1.9542	2.0290	2.1807	2.1954	2.2041	2.2449	2.0631	1.9504	1.9292	1.9452	1.9150
11:22		1.8552	1.9521	2.0282	2.1793	2.1969	2.2047	2.2458	2.0626	1.9501	1.9276	1.9451	1.9138
11:24		1.8517	1.9460	2.0226	2.1739	2.1910	2.2023	2.2428	2.0613	1.9514	1.9296	1.9477	1.9173
11:26		1.8544	1.9505	2.0265	2.1775	2.1938	2.2042	2.2452	2.0637	1.9518	1.9298	1.9468	1.9180
11:28		1.8583	1.9551	2.0304	2.1800	2.1954	2.2043	2.2452	2.0611	1.9491	1.9269	1.9449	1.9127
11:30		1.8562	1.9517	2.0265	2.1792	2.1949	2.2054	2.2463	2.0643	1.9544	1.9320	1.9492	1.9179
11:32		1.8555	1.9496	2.0261	2.1761	2.1917	2.2030	2.2465	2.0616	1.9518	1.9299	1.9479	1.9160

USGS File #c073/A77, part 2
SAND-77-1992
Oct. 1976-Sept. 1977

TABLE I (Continued)

GPE NATURAL BUTTES NO.14-HYDROFRACTURE

FRACTURE-MARCH 15,1977

TIME		0°	15°	30°	45°	60°	75°	90°	105°	120°	135°	150°	165°
11:34		1.8470	1.9509	2.0249	2.1752	2.1927	2.2010	2.2363	2.0585	1.9495	1.9282	1.9450	1.9164
11:36		1.8543	1.9487	2.0248	2.1751	2.1991	2.2041	2.2450	2.0627	1.9533	1.9325	1.9501	1.9189
11:38		1.8557	1.9535	2.0286	2.1785	2.1948	2.2063	2.2468	2.0649	1.9542	1.9321	1.9436	1.9132
11:40		[illegible]	[illegible]	2.0270	2.1759	2.1901	2.1992	2.2410	2.0577	1.9475	1.9253	1.9433	1.9136
11:42		1.8542	1.9539	[illegible]	2.1798	2.1951	[illegible]	[illegible]	2.0645	1.9541	1.9322	1.9467	1.9124
11:44		1.8573	1.9513	[illegible]	2.1743	2.1879	2.1967	2.2412	2.0571	1.9459	1.9248	1.9426	1.9119
11:46		1.8548	1.9476	2.0216	[illegible]	[illegible]	2.1999	2.2412	2.0560	1.9473	1.9271	1.9443	1.9173
11:48		1.8542	1.9527	2.0263	[illegible]	2.1968	2.2059	2.2475	2.0607	1.9511	1.9294	1.9464	[illegible]
11:50		1.8551	1.9477	2.0202	2.1726	2.1869	2.1966	2.2439	2.0574	1.9491	1.9266	1.9431	1.9127
11:52		1.8565	1.9514	2.0262	2.1775	2.1921	2.2039	2.2442	2.0627	1.9523	1.9305	1.9481	1.9135
11:54		1.8572	1.9494	2.0233	2.1734	2.1881	2.1987	2.2398	2.0502	1.9472	1.9264	1.9440	[illegible]
11:56		1.8558	1.9514	2.0250	2.1767	2.1936	2.2050	2.2496	2.0638	1.9525	1.9319	1.9479	1.9139
11:58		1.8616	1.9584	2.0327	2.1828	2.1994	2.2066	2.2439	2.0635	1.9539	1.9327	1.9477	1.9142
12:00		1.8581	1.9516	2.0235	2.1753	2.1891	2.2001	2.2392	2.0577	1.9481	1.9278	1.9443	[illegible]
12:02		1.8571	1.9524	2.0269	2.1786	2.1950	2.2051	2.2485	2.0660	1.9566	1.9365	1.9530	1.9194
12:04		1.8540	1.9435	2.0161	2.1653	2.1797	2.1921	2.2378	2.0468	1.9393	1.9193	1.9373	[illegible]
12:06		1.8431	1.9343	2.0069	2.1565	2.1728	2.1837	2.2277	2.0441	1.9349	1.9133	1.9303	1.8939
12:08		1.8422	1.9317	2.0046	2.1541	2.1698	2.1832	2.2236	2.0385	1.9285	1.9078	1.9216	1.8858
12:10		1.8357	1.9275	2.0009	2.1501	2.1703	2.1796	2.2267	2.0376	1.9257	1.9069	1.9219	1.8857
12:12		1.8319	1.9215	1.9942	2.1425	2.1608	2.1728	2.2140	2.0346	1.9257	1.9046	1.9219	1.8864
12:14		1.8349	1.9267	1.9969	2.1459	2.1609	2.1695	2.2131	2.0311	1.9214	1.8935	1.9116	1.8753
12:16		1.8355	1.9254	1.9973	2.1460	2.1618	2.1742	2.2190	2.0322	1.9245	1.9014	1.9152	1.8782
12:18		1.8389	1.9196	1.9932	2.1433	2.1612	2.1761	2.2207	2.0364	1.9276	1.9063	1.9206	1.8827
12:20	316,000 gal.	1.8384	1.9282	1.9998	2.1464	2.1629	2.1736	2.2232	2.0306	1.9214	1.8954	1.9112	1.8756
12:22		1.8343	1.9233	1.9964	2.1426	2.1586	2.1699	2.2145	2.0295	1.9220	1.9003	1.9147	1.8788
12:24	Stage 5	1.8353	1.9249	1.9977	2.1462	2.1630	2.1742	2.2184	2.0329	1.9258	1.9038	1.9177	1.8735
12:26		1.8342	1.9222	1.9972	2.1438	2.1599	2.1730	2.2243	2.0320	1.9249	1.9037	1.9194	1.8821
12:28	Start pre-pad	1.8340	1.9241	1.9983	2.1479	2.1656	2.1770	2.2197	2.0373	1.9313	1.9080	1.9228	1.8833
12:30		1.8381	1.9269	2.0007	2.1506	2.1685	2.1810	2.2234	2.0408	1.9302	1.9111	1.9236	1.8873
12:32		1.8365	1.9257	1.9988	2.1453	2.1649	2.1703	2.2196	2.0314	1.9240	1.9031	1.9174	1.8803
12:34		1.8368	1.9245	1.9991	2.1481	2.1655	2.1777	2.2229	2.0394	1.9313	1.9092	1.9232	1.8849
12:36		1.8363	1.9243	1.9966	2.1460	2.1669	2.1769	2.2204	2.0349	1.9282	1.9077	1.9222	1.8838
12:38		1.8367	1.9276	2.0003	2.1498	2.1663	2.1790	2.2225	2.0372	1.9303	1.9068	1.9212	1.8837
12:40		1.8344	1.9223	1.9955	2.1435	2.1664	2.1758	2.2207	2.0349	1.9299	1.9069	1.9232	1.8873
12:42		1.8387	1.9294	2.0014	2.1511	2.1700	2.1793	2.2279	2.0398	1.9334	1.9101	1.9247	1.8854
12:44		1.8442	1.9340	2.0063	2.1520	2.1673	2.1807	2.2252	2.0358	1.9282	1.9047	1.9171	[illegible]
12:46		1.8387	1.9273	1.9987	2.1443	2.1609	2.1730	2.2206	2.0303	1.9242	1.9026	1.9167	1.8734
12:48		1.8390	1.9296	2.0013	2.1478	2.1654	2.1781	2.2183	2.0346	1.9288	1.9056	1.9135	1.8826
12:50		1.8364	1.9239	1.9970	2.1416	2.1566	2.1736	2.2136	2.0297	1.9268	1.9042	1.9150	1.8814
12:52		1.8376	1.9292	2.0006	2.1470	2.1640	2.1773	2.2236	2.0333	1.9237	1.9057	1.9192	1.8796
12:54		1.8422	1.9280	2.0005	2.1463	2.1627	2.1764	2.2195	2.0319	1.9273	1.9047	1.9130	[illegible]
12:56		1.8375	1.9262	1.9984	2.1443	2.1603	2.1749	2.2204	2.0311	1.9265	1.9049	1.9192	1.8739
12:58		1.8410	1.9300	2.0016	2.1480	2.1629	2.1771	2.2239	2.0338	1.9279	1.9056	1.9198	1.8813

SAND-77-1992
Oct. 1976-Sept. 1977

TABLE I (Continued)

GPE NATURAL BUTTES NO.14-HYDROFRACTURE

FRACTURE-MARCH 15,1977

TIME		0°	15°	30°	45°	60°	75°	90°	105°	120°	135°	150°	165°
13:08		1.8380	1.9270	1.9989	2.1446	2.1605	2.1746	2.2171	2.0326	1.9275	1.9061	1.9205	1.8794
13:10		1.8410	1.9311	2.0023	2.1482	2.1655	2.1797	2.2240	2.0344	1.9296	1.9066	1.9196	1.8739
13:12		1.8398	1.9273	1.9976	2.1429	2.1587	2.1716	2.2176	2.0292	1.9251	1.9039	1.9173	1.8737
13:14	378,000 gal.	1.8433	1.9322	2.0016	2.1461	2.1614	2.1730	2.2195	2.0294	1.9245	1.9029	1.9148	1.8749
13:16		1.8418	1.9293	2.0002	2.1457	2.1618	2.1745	2.2198	2.0314	1.9264	1.9033	1.9176	1.8755
13:18		1.8439	1.9331	2.0055	2.1510	2.1677	2.1801	2.2229	2.0359	1.9318	1.9066	1.9182	1.8793
13:20		1.8410	1.9279	1.9998	2.1449	2.1615	2.1723	2.2169	2.0324	1.9280	1.9047	1.9198	1.8836
13:22		1.8417	1.9289	2.0002	2.1447	2.1606	2.1733	2.2187	2.0311	1.9277	1.9042	1.9185	1.8796
13:24		1.8432	1.9318	2.0011	2.1467	2.1599	2.1734	2.2206	2.0315	1.9275	1.9037	1.9176	1.8796
13:26	Stage 6	1.8405	1.9303	2.0011	2.1471	2.1635	2.1767	2.2243	2.0349	1.9306	1.9069	1.9205	1.8839
13:28		1.8391	1.9273	1.9981	2.1423	2.1575	2.1727	2.2169	2.0318	1.9279	1.9041	1.9185	1.8796
13:30	Start pre-pad	1.8417	1.9284	1.9991	2.1446	2.1585	2.1723	2.2211	2.0299	1.9263	1.9021	1.9172	1.8773
13:32		1.8397	1.9254	1.9970	2.1417	2.1585	2.1720	2.2203	2.0317	1.9245	1.9051	1.9205	1.8815
13:34		1.8410	1.9283	2.0009	2.1467	2.1621	2.1744	2.2236	2.0347	1.9305	1.9054	1.9185	1.8781
13:36		1.8368	1.9264	1.9995	2.1467	2.1634	2.1796	2.2273	2.0385	1.9342	1.9109	1.9231	1.8828
13:38		1.8398	1.9267	1.9998	2.1447	2.1610	2.1744	2.2239	2.0336	1.9293	1.9047	1.9186	1.8807
13:40		1.8373	1.9278	2.0005	2.1486	2.1659	2.1782	2.2287	2.0391	1.9353	1.9120	1.9249	1.8842
13:42		1.8415	1.9291	1.9982	2.1433	2.1575	2.1727	2.2179	2.0298	1.9266	1.9024	1.9171	1.8791
13:44		1.8410	1.9281	2.0010	2.1479	2.1636	2.1771	2.2291	2.0366	1.9326	1.9064	1.9204	1.8797
13:46		1.8389	1.9266	1.9980	2.1419	2.1582	2.1714	2.2290	2.0313	1.9240	1.9042	1.9188	1.8808
13:48		1.8406	1.9310	2.0020	2.1464	2.1619	2.1736	2.2220	2.0325	1.9287	1.9042	1.9180	1.8787
13:50		1.8416	1.9230	1.9993	2.1437	2.1569	2.1698	2.2192	2.0285	1.9237	1.8998	1.9146	1.8764
13:52		1.8412	1.9247	1.9995	2.1444	2.1618	2.1711	2.2215	2.0321	1.9287	1.9052	1.9196	1.8812
13:54		1.8369	1.9261	1.9980	2.1433	2.1595	2.1733	2.2219	2.0319	1.9298	1.9062	1.9198	1.8837
13:56		1.8381	1.9267	1.9980	2.1435	2.1595	2.1731	2.2252	2.0329	1.9298	1.9054	1.9207	1.8839
13:58		1.8369	1.9257	1.9967	2.1423	2.1573	2.1708	2.2205	2.0316	1.9285	1.9046	1.9202	1.8819
14:00		1.8404	1.9303	2.0015	2.1465	2.1655	2.1769	2.2270	2.0379	1.9349	1.9098	1.9246	1.8855
14:02		1.8392	1.9273	2.0002	2.1461	2.1623	2.1745	2.2268	2.0357	1.9328	1.9080	1.9214	1.8822
14:04		1.8388	1.9274	1.9985	2.1427	2.1583	2.1713	2.2245	2.0309	1.9281	1.9037	1.9195	1.8813
14:06		1.8395	1.9271	1.9970	2.1429	2.1586	2.1717	2.2223	2.0318	1.9291	1.9048	1.9202	1.8820
14:08		1.8399	1.9284	2.0014	2.1453	2.1634	2.1729	2.2278	2.0344	1.9322	1.9072	1.9226	1.8848
14:10		1.8386	1.9272	1.9973	2.1444	2.1579	2.1713	2.2228	2.0312	1.9292	1.9054	1.9207	1.8837
14:12		1.8412	1.9310	2.0016	2.1473	2.1615	2.1764	2.2203	2.0320	1.9285	1.9032	1.9182	1.8818
14:14		1.8387	1.9286	2.0002	2.1455	2.1640	2.1745	2.2216	2.0348	1.9315	1.9064	1.9214	1.8834
14:16		1.8384	1.9277	1.9985	2.1448	2.1582	2.1734	2.2258	2.0340	1.9312	1.9058	1.9226	1.8846
14:18	438,000 gal.	1.8379	1.9270	1.9977	2.1441	2.1604	2.1730	2.2222	2.0341	1.9333	1.9082	1.9249	1.8876
14:20		1.8423	1.9335	2.0024	2.1481	2.1623	2.1747	2.2239	2.0346	1.9295	1.9041	1.9184	1.8764
14:22		1.8402	1.9287	1.9992	2.1443	2.1602	2.1709	2.2233	2.0325	1.9274	1.9032	1.9192	1.8822
14:24		1.8387	1.9300	2.0020	2.1492	2.1648	2.1762	2.2253	2.0367	1.9327	1.9082	1.9225	1.8840
14:26		1.8387	1.9280	1.9987	2.1460	2.1604	2.1742	2.2216	2.0343	1.9307	1.9056	1.9202	1.8825
14:28		1.8383	1.9277	1.9996	2.1463	2.1602	2.1753	2.2272	2.0362	1.9334	1.9092	1.9246	1.8849
14:30		1.8401	1.9318	2.0046	2.1522	2.1569	2.1785	2.2329	2.0411	1.9374	1.9098	1.9249	1.8853
14:32		1.8402	1.9295	2.0019	2.1493	2.1636	2.1755	2.2238	2.0387	1.9349	1.9094	1.9246	1.8849

UGR File #c073/A77, part 2
SAND-77-1992
Oct. 1976-Sept. 1977

TABLE I (Continued)

GPE NATURAL BUTTES NO.14-HYDROFRACTURE

FRACTURE-MARCH 15,1977

TIME		0°	15°	30°	45°	60°	75°	90°	105°	120°	135°	150°	165°
14:34		1.8380	1.9293	2.0005	2.1482	2.1626	2.1760	2.2272	2.0364	1.9338	1.9071	1.9242	1.8851
14:38		1.8441	1.9324	2.0014	2.1467	2.1593	2.1713	2.2225	2.0308	1.9267	1.9016	1.9168	1.8792
14:40		1.8405	1.9287	1.9978	2.1432	2.1572	2.1714	2.2176	2.0291	1.9260	1.9035	1.9176	1.8822
14:42	Stage 7	1.8398	1.9249	2.0013	2.1487	2.1641	2.1804	2.2291	2.0379	1.9359	1.9035	1.9233	1.8852
14:44		1.8417	1.9305	2.0009	2.1467	2.1617	2.1717	2.2243	2.0326	1.9301	1.9027	1.9199	1.8801
14:46	Start pre-pad	1.8333	1.9265	1.9987	2.1453	2.1588	2.1718	2.2217	2.0317	1.9306	1.9049	1.9234	1.8423
14:48		1.8405	1.9298	1.9999	2.1463	2.1609	2.1707	2.2238	2.0310	1.9293	1.9036	1.9161	1.8523
14:50		1.8425	1.9309	2.0007	2.1456	2.1609	2.1713	2.2179	2.0295	1.9266	1.9007	1.9165	1.8782
14:52		1.8422	1.9310	2.0014	2.1478	2.1636	2.1707	2.2216	2.0332	1.9298	1.9045	1.9195	1.8827
14:54		1.8430	1.9314	1.9977	2.1443	2.1580	2.1672	2.2188	2.0281	1.9246	1.8988	1.9135	1.8763
14:56		1.8410	1.9318	2.0030	2.1506	2.1662	2.1777	2.2299	2.0362	1.9357	1.9089	1.9244	1.8852
14:58		1.8425	1.9311	1.9997	2.1458	2.1592	2.1722	2.2172	2.0307	1.9247	1.9030	1.9187	1.8529
15:00		1.8367	1.9272	1.9990	2.1471	2.1639	2.1754	2.2273	2.0370	1.9352	1.9083	1.9253	1.8836
15:02		1.8414	1.9329	2.0004	2.1472	2.1605	2.1715	2.2225	2.0323	1.9289	1.9028	1.9179	1.8815
15:04		1.8417	1.9312	1.9991	2.1433	2.1596	2.1694	2.2167	2.0289	1.9263	1.9014	1.9158	1.8815
15:06		1.8410	1.9329	2.0027	2.1513	2.1649	2.1773	2.2300	2.0369	1.9356	1.9086	1.9207	1.8834
15:08		1.8401	1.9343	2.0070	2.1575	2.1718	2.1861	2.2367	2.0468	1.9394	1.9113	1.9265	1.8856
15:10		1.8421	1.9332	2.0004	2.1463	2.1617	2.1715	2.2266	2.0335	1.9331	1.9052	1.9211	1.8828
15:12		1.8395	1.9304	1.9994	2.1477	2.1637	2.1744	2.2264	2.0360	1.9328	1.9068	1.9223	1.8849
15:14		1.8376	1.9320	2.0042	2.1534	2.1693	2.1817	2.2331	2.0439	1.9373	1.9107	1.9245	1.8857
15:16		1.8367	1.9292	1.9993	2.1475	2.1641	2.1756	2.2281	2.0378	1.9332	1.9073	1.9229	1.8855
15:18		1.8369	1.9297	1.9997	2.1474	2.1641	2.1761	2.2262	2.0384	1.9338	1.9077	1.9242	1.8853
15:20		1.8379	1.9299	1.9992	2.1467	2.1642	2.1747	2.2271	2.0362	1.9316	1.9067	1.9211	1.8824
15:22		1.8354	1.9295	1.9989	2.1451	2.1615	2.1734	2.2249	2.0344	1.9301	1.9055	1.9215	1.8845
15:24		1.8389	1.9311	2.0000	2.1479	2.1646	2.1744	2.2250	2.0369	1.9325	1.9065	1.9214	1.8844
15:26		1.8413	1.9367	2.0065	2.1534	2.1679	2.1820	2.2301	2.0406	1.9349	1.9076	1.9215	1.8833
15:28		1.8369	1.9283	1.9976	2.1431	2.1625	2.1736	2.2257	2.0342	1.9321	1.9060	1.9229	1.8677
15:30	522,000 gal.	1.8351	1.9306	1.9985	2.1450	2.1618	2.1727	2.2249	2.0343	1.9290	1.9054	1.9210	1.8829
15:32		1.8377	1.9306	2.0001	2.1471	2.1655	2.1772	2.2337	2.0380	1.9331	1.9083	1.9237	1.8874
15:34		1.8368	1.9320	2.0015	2.1502	2.1678	2.1761	2.2293	2.0391	1.9345	1.9086	1.9225	1.8856
15:36		1.8361	1.9294	1.9987	2.1461	2.1628	2.1735	2.2245	2.0341	1.9303	1.9038	1.9176	1.8837
15:38		1.8364	1.9310	2.0014	2.1509	2.1679	2.1794	2.2322	2.0398	1.9362	1.9096	1.9237	1.8861
15:40		1.8372	1.9335	2.0029	2.1521	2.1683	2.1791	2.2313	2.0379	1.9329	1.9060	1.9207	1.8817
15:42		1.8390	1.9336	2.0042	2.1519	2.1701	2.1773	2.2324	2.0364	1.9322	1.9062	1.9190	1.8837
15:44		1.8374	1.9308	1.9989	2.1453	2.1626	2.1730	2.2232	2.0311	1.9232	1.9022	1.9183	1.8526
15:46		1.8387	1.9332	2.0033	2.1528	2.1709	2.1793	2.2353	2.0379	1.9335	1.9067	1.9195	1.8324
15:48		1.8375	1.9310	2.0001	2.1465	2.1612	2.1717	2.2226	2.0304	1.9265	1.9016	1.9160	1.8812
15:50		1.8352	1.9330	2.0022	2.1510	2.1682	2.1745	2.2302	2.0358	1.9318	1.9047	1.9211	1.8829
15:52		1.8343	1.9301	1.9994	2.1473	2.1651	2.1759	2.2274	2.0356	1.9326	1.9062	1.9214	1.8957
15:54		1.8342	1.9315	2.0025	2.1510	2.1706	2.1806	2.2328	2.0396	1.9362	1.9079	1.9228	1.8854
15:56		1.8360	1.9327	2.0017	2.1485	2.1664	2.1757	2.2282	2.0341	1.9289	1.9042	1.9176	1.8811
15:58		1.8370	1.9339	2.0027	2.1512	2.1690	2.1762	2.2321	2.0362	1.9315	1.9056	1.9211	1.8816
16:00		1.8349	1.9310	2.0009	2.1494	2.1673	2.1761	2.2250	2.0355	1.9312	1.9050	1.9208	1.8843

SAND-77-1992
Oct. 1976-Sept. 1977

TABLE I (Continued)

GPE NATURAL BUTTES NO.14-HYDROFRACTURE

FRACTURE-MARCH 15,1977

TIME		0°	15°	30°	45°	60°	75°	90°	105°	120°	135°	150°	165°
15:02		1.8346	1.9331	2.0030	2.1524	2.1692	2.1789	2.2322	2.0387	1.9339	1.9062	1.9218	1.8843
15:04		1.8339	1.9315	2.0009	2.1471	2.1650	2.1744	2.2236	2.0326	1.9290	1.9034	1.9187	1.8831
15:06		1.8348	1.9320	2.0019	2.1512	2.1674	2.1782	2.2313	2.0370	1.9309	1.9048	1.9219	1.8847
15:08		1.8315	1.9310	2.0004	2.1493	2.1657	2.1764	2.2260	2.0343	1.9303	1.9043	1.9199	1.8836
15:10	554,000 gal.	1.8322	1.9300	2.0012	2.1494	2.1660	2.1784	2.2304	2.0361	1.9327	1.9056	1.9233	1.8860
15:12		1.8308	1.9321	2.0022	2.1492	2.1691	2.1779	2.2329	2.0356	1.9301	1.9038	1.9201	1.8837
15:14	Stage 8	1.8354	1.9318	2.0041	2.1532	2.1710	2.1819	2.2319	2.0394	1.9348	1.9084	1.9225	1.8865
15:16		1.8345	1.9320	2.0028	2.1520	2.1697	2.1820	2.2328	2.0374	1.9336	1.9077	1.9223	1.8867
15:18		1.8334	1.9293	1.9979	2.1434	2.1603	2.1716	2.2209	2.0270	1.9239	1.8995	1.9165	1.8829
15:20		1.8360	1.9341	2.0033	2.1503	2.1679	2.1763	2.2271	2.0335	1.9287	1.9033	1.9171	1.8800
15:22		1.8344	1.9332	2.0044	2.1549	2.1727	2.1843	2.2333	2.0404	1.9348	1.9079	1.9226	1.8853
15:24		1.8315	1.9288	1.9996	2.1488	2.1669	2.1775	2.2286	2.0325	1.9333	1.9053	1.9214	1.8861
15:26		1.8335	1.9313	2.0015	2.1494	2.1669	2.1768	2.2307	2.0330	1.9301	1.9031	1.9209	1.8847
15:28		1.8337	1.9314	2.0016	2.1499	2.1682	2.1799	2.2285	2.0340	1.9302	1.9049	1.9217	1.8849
15:30		1.8339	1.9307	1.9986	2.1469	2.1629	2.1732	2.2234	2.0297	1.9265	1.9018	1.9179	1.8832
15:32		1.8323	1.9332	2.0040	2.1534	2.1723	2.1814	2.2298	2.0390	1.9350	1.9079	1.9233	1.8863
15:34		1.8369	1.9357	2.0062	2.1555	2.1726	2.1823	2.2332	2.0388	1.9349	1.9093	1.9237	1.8865
15:36		1.8345	1.9335	2.0036	2.1519	2.1720	2.1825	2.2321	2.0360	1.9328	1.9058	1.9212	1.8840
15:38	585,000 gal.	1.8335	1.9315	2.0018	2.1484	2.1660	2.1770	2.2248	2.0301	1.9273	1.9032	1.9176	1.8819
15:40		1.8346	1.9320	2.0033	2.1526	2.1704	2.1787	2.2306	2.0359	1.9318	1.9074	1.9217	1.8855
15:42		1.8349	1.9323	2.0016	2.1486	2.1669	2.1758	2.2252	2.0304	1.9271	1.9029	1.9174	1.8824
15:44		1.8355	1.9329	2.0030	2.1519	2.1694	2.1811	2.2269	2.0356	1.9307	1.9067	1.9217	1.8854
15:46		1.8323	1.9324	2.0047	2.1560	2.1748	2.1840	2.2339	2.0395	1.9345	1.9088	1.9234	1.8856
15:48		1.8327	1.9335	2.0066	2.1579	2.1767	2.1865	2.2378	2.0424	1.9387	1.9136	1.9268	1.8839
15:50		1.8330	1.9328	2.0038	2.1525	2.1710	2.1819	2.2310	2.0364	1.9314	1.9069	1.9220	1.8845
15:52		1.8342	1.9340	2.0051	2.1523	2.1724	2.1812	2.2335	2.0368	1.9334	1.9094	1.9229	1.8876
15:54		1.8343	1.9344	2.0053	2.1539	2.1708	2.1817	2.2311	2.0349	1.9325	1.9066	1.9222	1.8842
15:56		1.8317	1.9340	2.0053	2.1562	2.1739	2.1864	2.2343	2.0362	1.9361	1.9115	1.9246	1.8831
15:58		1.8334	1.9330	2.0049	2.1535	2.1736	2.1826	2.2325	2.0362	1.9336	1.9098	1.9231	1.8863
17:00		1.8317	1.9322	2.0039	2.1533	2.1717	2.1817	2.2298	2.0373	1.9342	1.9097	1.9243	1.8877
17:02		1.8327	1.9326	2.0053	2.1546	2.1721	2.1838	2.2329	2.0385	1.9347	1.9096	1.9241	1.8860
17:04		1.8329	1.9323	2.0043	2.1538	2.1711	2.1840	2.2354	2.0384	1.9359	1.9108	1.9247	1.8836
17:06		1.8327	1.9337	2.0066	2.1574	2.1746	2.1862	2.2323	2.0410	1.9366	1.9128	1.9261	1.8833
17:08		1.8325	1.9329	2.0055	2.1554	2.1738	2.1841	2.2348	2.0393	1.9355	1.9100	1.9246	1.8875
17:10		1.8348	1.9367	2.0090	2.1578	2.1754	2.1855	2.2332	2.0399	1.9351	1.9094	1.9233	1.8858
17:13		1.8322	1.9311	2.0028	2.1488	2.1666	2.1757	2.2251	2.0316	1.9295	1.9049	1.9199	1.8861
17:15		1.8315	1.9335	2.0066	2.1561	2.1753	2.1854	2.2363	2.0431	1.9368	1.9114	1.9255	1.8875
17:17		1.8313	1.9319	2.0044	2.1531	2.1695	2.1808	2.2290	2.0365	1.9324	1.9079	1.9220	1.8860
17:19		1.8334	1.9347	2.0080	2.1563	2.1755	2.1853	2.2357	2.0424	1.9374	1.9120	1.9257	1.8883
17:21		1.8317	1.9354	2.0088	2.1578	2.1757	2.1849	2.2356	2.0418	1.9365	1.9096	1.9239	1.8852
17:23		1.8320	1.9342	2.0079	2.1567	2.1752	2.1864	2.2332	2.0411	1.9363	1.9110	1.9227	1.8861
17:25		1.8315	1.9346	2.0084	2.1570	2.1762	2.1886	2.2363	2.0437	1.9337	1.9127	1.9253	1.8850
17:27		1.8313	1.9350	2.0093	2.1584	2.1763	2.1860	2.2397	2.0436	1.9387	1.9141	1.9250	1.8884
17:29													

UGR File #c073/A77, part 2
SAND-77-1992
Oct. 1976-Sept. 1977

TABLE 1 (Continued)

GPE NATURAL BUTTES NO.14-HYDROFRACTURE

FRACTURE-MARCH 15,1977

TIME		0°	15°	30°	45°	60°	75°	90°	105°	120°	135°	150°	165°
17:31		1.8291	1.9344	2.0089	2.1585	2.1776	2.1889	2.2604	2.0454	1.9386	1.9125	1.9257	1.8367
17:33		1.8311	1.9363	2.0113	2.1609	2.1798	2.1929	2.2383	2.0464	1.9400	1.9138	1.9263	1.8394
17:35		1.8317	1.9342	2.0097	2.1592	2.1791	2.1904	2.2342	2.0479	1.9437	1.9159	1.9266	1.8484
17:37		1.8301	1.9346	2.0089	2.1564	2.1764	2.1869	2.2352	2.0448	1.9395	1.9131	1.9256	1.8367
17:39		1.8311	1.9366	2.0110	2.1601	2.1797	2.1892	2.2371	2.0472	1.9401	1.9146	1.9264	1.8367
17:41		1.8295	1.9355	2.0089	2.1575	2.1764	2.1878	2.2356	2.0461	1.9401	1.9133	1.9262	1.8379
17:43		1.8312	1.9364	2.0104	2.1595	2.1787	2.1907	2.2355	2.0475	1.9407	1.9157	1.9273	1.8395
17:45		1.8317	1.9376	2.0139	2.1631	2.1837	2.1928	2.2403	2.0518	1.9443	1.9189	1.9326	1.8921
17:47		1.8300	1.9354	2.0097	2.1573	2.1782	2.1880	2.2348	2.0458	1.9394	1.9142	1.9265	1.8338
17:49		1.8290	1.9343	2.0104	2.1585	2.1773	2.1881	2.2348	2.0466	1.9397	1.9137	1.9269	1.8377
17:51		1.8311	1.9342	2.0143	2.1634	2.1818	2.1946	2.2407	2.0518	1.9420	1.9166	1.9274	1.8385
17:53		1.8263	1.9338	2.0111	2.1613	2.1816	2.1933	2.2411	2.0539	1.9463	1.9211	1.9321	1.8327
17:55	Shut down	1.8274	1.9354	2.0125	2.1614	2.1784	2.1929	2.2389	2.0519	1.9435	1.9184	1.9300	1.8357
17:57	640,000 gal. (Total Vol.)	1.8287	1.9368	2.0130	2.1635	2.1811	2.1948	2.2436	2.0540	1.9461	1.9211	1.9311	1.8357
17:59		1.8278	1.9363	2.0127	2.1613	2.1814	2.1925	2.2379	2.0514	1.9447	1.9179	1.9289	1.8399
18:01		1.8287	1.9350	2.0110	2.1590	2.1775	2.1877	2.2334	2.0473	1.9411	1.9153	1.9278	1.8399
18:03		1.8272	1.9368	2.0114	2.1597	2.1769	2.1896	2.2362	2.0480	1.9411	1.9147	1.9272	1.8397
18:05		1.8275	1.9351	2.0131	2.1633	2.1808	2.1929	2.2393	2.0518	1.9441	1.9187	1.9302	1.8918
18:07		1.8275	1.9349	2.0115	2.1621	2.1789	2.1905	2.2361	2.0509	1.9447	1.9190	1.9310	1.8327
18:09		1.8275	1.9409	2.0140	2.1649	2.1813	2.1944	2.2389	2.0549	1.9481	1.9222	1.9338	1.8352
18:11		1.8293	1.9384	2.0145	2.1641	2.1786	2.1945	2.2330	2.0528	1.9449	1.9203	1.9315	1.8343
18:13		1.8264	1.9365	2.0144	2.1663	2.1826	2.1964	2.2402	2.0550	1.9478	1.9216	1.9336	1.8339

TABLE I (Continued)

GPE NATURAL BUTTES NO.14-HYDROFRACTURE

FRACTURE-MARCH 15,1977

TIME		180°	195°	210°	225°	240°	255°	270°	285°	300°	315°	330°	345°
6:59		1.9261	1.9832	1.7940	1.3785	1.7999	1.7833	1.5848	1.6569	1.7314	1.6857	1.7488	1.8997
7:01		1.9231	1.9775	1.7921	1.3778	1.7958	1.7770	1.5871	1.6560	1.7339	1.6878	1.7500	1.8914
7:03		1.9242	1.9772	1.7900	1.3761	1.7978	1.7810	1.5837	1.6551	1.7300	1.6854	1.7472	1.8893
7:05		1.9206	2.1429	1.7857	1.3724	1.7943	1.7778	1.5815	1.6530	1.7300	1.6861	1.7497	1.8920
7:07		1.9210	1.9746	1.7838	1.3741	1.7966	1.7791	1.5827	1.6555	1.7309	1.6872	1.7498	1.8923
7:09		1.9255	1.9742	1.3567	1.3758	1.7980	1.7792	1.5828	1.6547	1.7301	1.6857	1.7476	1.8896
7:14	Stage 1 - Start pumping	1.9222	1.9771	1.3101	1.3740	1.7971	1.7774	1.5838	1.6559	1.7323	1.6862	1.7476	1.8898
7:16		1.9194	1.9730	1.3349	1.3759	1.7981	1.7796	1.5850	1.6572	1.7326	1.6874	1.7506	1.8922
7:18	Start pre-pad	1.9223	1.9770	1.1474	1.3771	1.7979	1.7786	1.5843	1.6557	1.7322	1.6866	1.7487	1.8939
7:20		1.9291	1.9631	.9306	1.3677	1.7864	1.7680	1.5725	1.6430	1.7176	1.6719	1.7340	1.8729
7:22		1.9046	1.9583	1.1409	1.3631	1.7807	1.7626	1.5674	1.6388	1.7130	1.6674	1.7294	1.8699
7:24		1.9022	1.9544	1.0302	1.3589	1.7768	1.7654	1.5639	1.6364	1.7098	1.6648	1.7278	1.8693
7:26		1.8961	1.9491	.9810	1.3582	1.7735	1.7577	1.5603	1.6235	1.7047	1.6577	1.7190	1.8582
7:30		1.8846	1.9364	1.0410	1.3447	1.7599	1.7433	1.5512	1.6262	1.6998	1.6570	1.7215	1.8620
7:32		2.2764	1.9409	1.0930	1.3497	1.7650	1.7492	1.5554	1.6286	1.7029	1.6575	1.7212	1.8610
7:34		1.8865	1.9375	1.2230	1.3486	1.7643	1.7478	1.5545	1.6355	1.7017	1.6560	1.7196	1.8605
7:36		1.8879	1.9401	1.0382	1.3498	1.7654	1.7484	1.5552	1.6349	1.7024	1.6554	1.7184	1.8571
7:38		2.2786	1.9441	1.4541	1.3545	1.7697	1.7539	1.5564	1.6298	1.7013	1.6533	1.7142	1.8522
7:40		2.2733	[illegible]	1.0628	1.3533	1.7683	1.7534	1.5509	1.6100	1.7027	1.6547	1.7159	1.8537
7:42		2.2695	1.9373	[illegible]	1.3477	1.7620	1.7468	1.5524	1.6180	1.6996	1.6517	1.7146	1.8532
7:44		2.2695	1.9369	[illegible]	1.3475	1.7609	1.7431	1.5439	1.6233	1.6935	1.6452	1.7061	1.8432
7:46		1.8701	1.9203	1.3022	[illegible]	1.7531	1.7384	1.5462	1.6193	1.6968	1.6514	1.7139	1.8545
7:48		1.8772	1.9277	1.594[illegible]	[illegible]	1.7505	1.7323	1.5391	1.6092	1.6841	1.6364	1.6999	1.8374
7:50		1.8703	1.9208	1.5449	1.3344	1.7472	1.7298	1.5377	1.6085	1.6854	1.6385	1.7024	1.8398
7:52		1.8652	1.9156	1.3440	1.3317	1.7446	1.7284	1.5377	1.6118	1.6871	1.6413	1.7046	1.8453
7:54		1.8659	1.9171	1.2412	1.3357	1.7504	1.7354	1.5428	1.6154	1.6915	1.6448	1.7054	1.8455
7:56		1.8633	1.9113	1.1182	1.3266	1.7394	1.7230	1.5322	1.6225	1.6837	1.6347	1.6971	1.8369
7:58		1.8625	1.9156	1.1076	1.3304	1.7495	1.7339	1.5421	1.6145	1.6899	1.6404	1.7010	1.8382
7:59		1.8625	1.9165	1.0762	1.3367	1.7481	1.7321	1.5335	1.6096	1.6836	1.6316	1.6910	1.8256
8:01	46,000 gal.	1.8579	1.9053	1.1175	1.3220	1.7333	1.7142	1.5255	1.5978	1.6734	1.6254	1.6888	1.8257
8:03		1.8653	1.9196	1.1300	1.3399	1.7524	1.7341	1.5423	1.6130	1.6860	1.6327	1.6906	1.8225
8:05		1.8605	1.9105	1.2069	1.3271	1.7377	1.7189	1.5282	1.6001	1.6747	1.6252	1.6853	1.8212
8:07		1.8571	1.9059	1.0795	1.3254	1.7372	1.7203	1.5294	1.6017	1.6771	1.6280	1.6878	1.8222
8:09		1.8623	1.9108	1.3134	1.3240	1.7363	1.7183	1.5254	1.5972	1.6715	1.6221	1.6835	1.8183
8:11		1.8625	1.9121	1.7338	1.3304	1.7445	1.7289	1.5345	1.6076	1.6818	1.6296	1.6886	1.8212
8:13		1.8577	1.9062	1.7279	1.3209	1.7332	1.7150	1.5233	1.5959	1.6716	1.6226	1.6846	1.8189
8:15		1.8534	1.9022	1.7248	1.3193	1.7326	1.7149	1.5244	1.5988	1.6749	1.6264	1.6831	1.8214
8:17		1.8609	1.9106	1.7326	1.3268	1.7399	1.7216	1.5282	1.6003	1.6754	1.6245	1.6839	1.8156
8:19		1.8594	1.9094	1.7168	1.3229	1.7358	1.7174	1.5253	1.5975	1.6730	1.6217	1.6829	1.8161
8:21		1.8591	1.9067	1.1252	1.3202	1.7322	1.7138	1.5200	1.5914	1.6664	1.6152	1.6792	1.8284
8:23		1.8479	1.8966	1.1323	1.3133	1.7255	1.7084	1.5172	1.5913	1.6680	1.6196	1.6820	1.8153
8:25		1.8587	1.9074	1.0645	1.3216	1.7327	1.7132	1.5189	1.5909	1.6651	1.6138	1.6733	1.8081
8:27		1.8527	1.9015	1.2673	1.3196	1.7320	1.7142	1.5214	1.5948	1.6701	1.6194	1.6794	1.8118

UGR File #CU/S/A//, part 2
SAND-77-1992
Oct. 1976-Sept. 1977

TABLE I (Continued)

GPE NATURAL BUTTES NO.14-HYDROFRACTURE

FRACTURE-MARCH 15,1977

TIME		180°	195°	210°	225°	240°	255°	270°	285°	300°	315°	330°	345°
8:29		1.8597	1.8996	1.2424	1.3192	1.7315	1.7132	1.5196	1.5919	1.6670	1.6151	1.6728	1.8134
8:31	78,000 gal.	1.8453	1.8933	1.2726	1.3142	1.7247	1.7066	1.5129	1.5848	1.6590	1.6071	1.6659	1.7972
8:33	Stage 2	1.8415	1.8917	1.3884	1.3158	1.7278	1.7118	1.5185	1.5931	1.6665	1.6142	1.6727	1.8027
8:35		1.8324	1.8793	1.2941	1.3018	1.7110	1.6935	1.5018	1.5717	1.6497	1.5987	1.6596	1.7921
8:37	Start pre-pad	1.8347	1.8817	1.4839	1.3009	1.7077	1.6383	1.4962	1.5672	1.6413	1.5893	1.6439	1.7810
8:39		1.8314	1.8798	1.1732	1.3037	1.7125	1.6956	1.5035	1.5728	1.6496	1.5978	1.6574	1.7882
8:41		1.8304	1.8747	1.1216	1.2941	1.7023	1.6838	1.4922	1.5653	1.6405	1.5923	1.6531	1.7856
8:44		1.8299	1.8769	1.1303	1.3005	1.7096	1.6911	1.4996	1.5733	1.6468	1.5952	1.6549	1.7864
8:46		1.8295	1.8776	1.0674	1.3014	1.7111	1.6935	1.5012	1.5759	1.6475	1.5959	1.6555	1.7858
8:48		1.8321	1.8773	1.1165	1.2983	1.7093	1.6909	1.4985	1.5670	1.6453	1.5931	1.6526	1.7844
8:50		1.8310	1.8773	1.2091	1.2973	1.7074	1.6897	1.4956	1.5687	1.6431	1.5925	1.6516	1.7848
8:52		1.8349	1.8830	1.1365	1.3040	1.7152	1.6975	1.5037	1.5758	1.6501	1.5992	1.6575	1.7834
8:54		1.8354	1.8834	1.1083	1.3058	1.7172	1.6962	1.5046	1.5773	1.6506	1.5981	1.6568	1.7880
8:56		1.8344	1.8820	1.1964	1.3037	1.7154	1.6947	1.5026	1.5742	1.6495	1.5990	1.6576	1.7895
8:58		1.8351	1.8838	1.2440	1.3040	1.7164	1.6954	1.5027	1.5757	1.6507	1.5973	1.6579	1.7882
9:00		1.8423	1.8888	1.2026	1.3067	1.7189	1.6977	1.5032	1.5736	1.6491	1.5962	1.6539	1.7852
9:02		1.8358	1.8850	1.3121	1.3066	1.7205	1.7025	1.5079	1.5807	1.6562	1.6037	1.6612	1.7930
9:04	110,000 gal.	1.8364	1.8847	1.2733	1.3026	1.7152	1.6957	1.5023	1.5742	1.6493	1.5985	1.6554	1.7894
9:06		1.8375	1.8859	1.2553	1.3062	1.7191	1.6996	1.5032	1.5755	1.6509	1.5990	1.6559	1.7892
9:08		1.8387	1.8877	1.2571	1.3061	1.7211	1.7016	1.5060	1.5787	1.6548	1.6033	1.6615	1.7952
9:10		1.8444	1.8961	1.1530	1.3162	1.7314	1.7121	1.5138	1.5843	1.6592	1.6043	1.6599	1.7921
9:12		1.8406	1.8886	1.2226	1.3031	1.7173	1.6973	1.5019	1.5734	1.6491	1.5975	1.6567	1.7904
9:14		1.8346	1.8901	1.1868	1.3129	1.7281	1.7100	1.5136	1.5861	1.6621	1.6078	1.6658	1.7965
9:16		1.8353	1.8844	1.3013	1.3002	1.7163	1.6969	1.5024	1.5751	1.6521	1.6021	1.6603	1.7943
9:18		1.8371	1.8897	1.3328	1.3111	1.7265	1.7107	1.5143	1.5866	1.6637	1.6112	1.6672	1.7991
9:20		1.8376	1.8871	1.4196	1.3053	1.7228	1.7034	1.5080	1.5811	1.6575	1.6054	1.6633	1.7976
9:22		1.8232	1.8738	1.2136	1.3068	1.7227	1.7051	1.5039	1.5818	1.6580	1.6040	1.6597	1.7899
9:24		1.8248	1.8720	1.3785	1.2915	1.7079	1.6851	1.4917	1.5632	1.6401	1.5906	1.6476	1.7836
9:26		1.8296	1.8805	1.2621	1.2989	1.7118	1.6906	1.4943	1.5644	1.6396	1.5881	1.6433	1.7812
9:28		1.8197	1.8638	1.0597	1.2790	1.6921	1.6704	1.4794	1.5521	1.6337	1.5846	1.6451	1.7949
9:30		1.8222	1.8733	1.3924	1.3008	1.7190	1.7014	1.5055	1.5796	1.6568	1.6047	1.6609	1.7947
9:32		1.8307	1.8833	1.3605	1.2999	1.7159	1.6966	1.4993	1.5719	1.6474	1.5959	1.6520	1.7894
9:34		1.8274	1.8767	1.3784	1.2968	1.7130	1.6931	1.4970	1.5700	1.6472	1.5967	1.6571	1.7929
9:36		1.8382	1.8911	1.3379	1.3141	1.7326	1.7117	1.5112	1.5826	1.6571	1.6029	1.6597	1.7876
9:38		1.8341	1.8849	1.4508	1.3019	1.7179	1.6953	1.4985	1.5699	1.6465	1.5943	1.6513	1.7865
9:40		1.8337	1.8826	1.1728	1.2966	1.7141	1.6942	1.4962	1.5679	1.6446	1.5942	1.6531	1.7890
9:42		1.8294	1.8755	1.2405	1.2921	1.7096	1.6885	1.4935	1.5602	1.6439	1.5948	1.6536	1.7922
9:44	157,000 gal.	1.8378	1.8882	1.2220	1.3034	1.7204	1.6973	1.4981	1.5681	1.6434	1.5919	1.6472	1.7814
9:46		1.8379	1.8903	1.2130	1.3099	1.7217	1.7056	1.5049	1.5755	1.6516	1.5987	1.6503	1.7839
9:48		1.8235	1.8632	1.2279	1.3031	1.7223	1.7035	1.5055	1.5776	1.6556	1.6038	1.6546	1.7938
9:50	Stage 3	1.8340	1.8829	1.4300	1.2995	1.7179	1.6966	1.4977	1.5691	1.6462	1.5954	1.6536	1.7893
9:52		1.8323	1.8796	1.3821	1.2981	1.7159	1.6953	1.4967	1.5691	1.6469	1.5957	1.6543	1.7911
9:54	Start pre-pad	1.8360	1.8876	1.1353	1.3059	1.7247	1.7018	1.5029	1.5733	1.6496	1.5971	1.6554	1.7869

TABLE I (Continued)

GPE NATURAL BUTTES NO.14-HYDROFRACTURE

FRACTURE-MARCH 15,1977

TIME		180°	195°	210°	225°	240°	255°	270°	285°	300°	315°	330°	345°
9:56		1.8307	1.8313	1.2190	1.2989	1.7198	1.6363	1.4984	1.5694	1.6475	1.5966	1.6527	1.7835
9:58		1.8322	1.8825	1.4613	1.2996	1.7209	1.6962	1.4999	1.5705	1.6491	1.5967	1.6544	1.7911
10:00		1.8308	1.8802	1.4358	1.2964	1.7181	1.6935	1.4961	1.5672	1.6452	1.5950	1.6527	1.7897
10:02		1.8326	1.8846	1.4158	1.3013	1.7243	1.6993	1.5025	1.5736	1.6523	1.6008	1.6571	1.7936
10:04		1.8297	1.8800	1.4698	1.2990	1.7217	1.6970	1.4997	1.5707	1.6497	1.5994	1.6557	1.7946
10:06		1.8291	1.8815	1.2498	1.3041	1.7287	1.7052	1.5074	1.5793	1.6585	1.6041	1.6627	1.7982
10:08		1.8336	1.8837	1.2473	1.2994	1.7210	1.6956	1.4977	1.5671	1.6449	1.5948	1.6516	1.7872
10:10		1.8292	1.8813	1.1346	1.3034	1.7288	1.7068	1.5062	1.5788	1.6570	1.6062	1.6618	1.7990
10:12	184,000 gal.	1.8349	1.8868	1.2668	1.3022	1.7256	1.7000	1.5033	1.5697	1.6482	1.5973	1.6534	1.7901
10:14		1.8279	1.8791	1.2900	1.2962	1.7196	1.6968	1.4975	1.5677	1.6469	1.5975	1.6532	1.7901
10:16		1.8299	1.8818	1.1499	1.3035	1.7280	1.7049	1.5056	1.5768	1.6556	1.6061	1.6592	1.7979
10:20		1.8300	1.8834	1.1961	1.3035	1.7282	1.7037	1.5062	1.5751	1.6543	1.6038	1.6579	1.7924
10:22		1.8291	1.8815	1.1972	1.2990	1.7234	1.6986	1.5008	1.5712	1.6501	1.6009	1.6557	1.7926
10:24		1.8287	1.8823	1.2316	1.3031	1.7277	1.7037	1.5045	1.5744	1.6535	1.6025	1.6551	1.7930
10:26		1.8306	1.8831	1.4161	1.3007	1.7261	1.7012	1.5012	1.5714	1.6502	1.6020	1.6547	1.7951
10:30		1.8270	1.8797	1.4179	1.2983	1.7236	1.6997	1.5006	1.5701	1.6495	1.6001	1.6542	1.7929
10:34		1.8359	1.8868	1.5771	1.3015	1.7307	1.7004	1.4995	1.5672	1.6451	1.5950	1.6485	1.7869
10:36		1.8283	1.8809	1.4259	1.2981	1.7234	1.6975	1.4986	1.5674	1.6474	1.5987	1.6516	1.7912
10:38		1.8294	1.8824	1.2273	1.3005	1.7264	1.7003	1.5016	1.5710	1.6492	1.6017	1.6544	1.7924
10:44		1.8334	1.8865	1.5737	1.3008	1.7267	1.6996	1.4992	1.5673	1.6459	1.5980	1.6511	1.7888
10:48		1.8283	1.8817	1.1453	1.3012	1.7292	1.7035	1.5049	1.5739	1.6532	1.6042	1.6576	1.7975
10:50		1.8385	1.8940	1.9982	1.3065	1.7335	1.7063	1.5048	1.5723	1.6503	1.5996	1.6534	1.7936
10:52		1.8317	1.8858	1.1015	1.3023	1.7321	1.7061	1.5059	1.5748	1.6541	1.6051	1.6581	1.7986
10:54		1.8334	1.8886	1.2521	1.3040	1.7463	1.7104	1.5070	1.5754	1.6546	1.6050	1.6584	1.7987
10:56		1.8316	1.8871	1.2348	1.3034	1.7348	1.7076	1.5057	1.5756	1.6544	1.6061	1.6580	1.7993
10:58		1.8337	1.8886	1.4647	1.3009	1.7298	1.7022	1.5011	1.5699	1.6481	1.6004	1.6546	1.7955
11:00		1.8281	1.8817	1.4389	1.2993	1.7307	1.7059	1.5047	1.5743	1.6545	1.6075	1.6618	1.8018
11:02		1.8349	1.8901	1.3636	1.3049	1.7353	1.7083	1.5068	1.5752	1.6530	1.6024	1.6590	1.7983
11:04		1.8386	1.8952	1.4936	1.3130	1.7434	1.7150	1.5119	1.5804	1.6567	1.6054	1.6577	1.7945
11:06	237,000 gal.	1.8336	1.8911	1.4546	1.3078	1.7373	1.7088	1.5060	1.5748	1.6525	1.6029	1.6547	1.7956
11:08	Stage 4	1.8394	1.8971	1.3618	1.3126	1.7442	1.7152	1.5127	1.5814	1.6587	1.6087	1.6613	1.7992
11:10		1.8327	1.8890	1.4825	1.3052	1.7371	1.7073	1.5060	1.5741	1.6509	1.6016	1.6545	1.7959
11:12	Start pre-pad	1.8303	1.8856	1.4823	1.2990	1.7313	1.7010	1.5007	1.5691	1.6474	1.5980	1.6536	1.7946
11:14		1.8341	1.8903	1.4174	1.3009	1.7417	1.7109	1.5083	1.5768	1.6537	1.6052	1.6564	1.7966
11:16		1.8306	1.8849	1.3873	1.2976	1.7317	1.7009	1.4994	1.5679	1.6475	1.6001	1.6556	1.7954
11:18		1.8314	1.8858	1.4667	1.3028	1.7362	1.7070	1.5054	1.5745	1.6524	1.6039	1.6587	1.8006
11:20		1.8284	1.8847	1.1945	1.3016	1.6966	1.6976	1.5041	1.5734	1.6515	1.6034	1.6599	1.8012
11:22		1.8287	1.8846	1.4272	1.3002	1.7323	1.7029	1.5025	1.5706	1.6494	1.6018	1.6568	1.7999
11:24		1.8324	1.8886	1.4678	1.3019	1.7356	1.7042	1.5015	1.5668	1.6459	1.5973	1.6523	1.7940
11:26		1.8320	1.8877	1.4365	1.3014	1.7338	1.7049	1.5027	1.5721	1.6488	1.6012	1.6560	1.7988
11:28		1.8305	1.8868	1.4298	1.3038	1.7389	1.7077	1.5071	1.5765	1.6547	1.6070	1.6627	1.8048
11:30		1.8337	1.8892	1.4828	1.3029	1.7397	1.7044	1.5029	1.5722	1.6490	1.6019	1.6563	1.7997
11:32		1.8339	1.8903	1.3917	1.3051	1.7372	1.7061	1.5054	1.5733	1.6505	1.6023	1.6565	1.7983

UGR File #c073/A77, part 2
SAND-77-1992
Oct. 1976-Sept. 1977

TABLE I (Continued)

SPE NATURAL BUTTES NO.14-HYDROFRACTURE

FRACTURE-MARCH 15,1977

TIME		180°	195°	210°	225°	240°	255°	270°	285°	300°	315°	330°	345°
11:34		1.8376	1.8927	1.2428	1.3092	1.7417	1.7129	1.5092	1.5786	1.6552	1.6065	1.6603	1.9028
11:36		1.8356	1.8933	1.1548	1.3058	1.7410	1.7105	1.5054	1.5735	1.6503	1.6019	1.6559	1.7963
11:38		1.8353	1.8919	1.2558	1.3060	1.7412	1.7104	1.5054	1.5753	1.6524	1.6043	1.6589	1.8024
11:40		1.8297	1.8852	1.2351	1.3052	1.7409	1.7111	1.5065	1.5764	1.6531	1.6052	1.6600	1.8012
11:42		1.8303	1.8859	1.2418	1.3011	1.7335	1.7027	1.5005	1.5700	1.6476	1.6009	1.6560	1.7932
11:44		1.8292	1.8878	1.2705	1.3051	1.7405	1.7098	1.5072	1.5775	1.6538	1.6063	1.6595	1.8017
11:46		1.8313	1.8890	1.1471	1.3064	1.7407	1.7093	1.5052	1.5749	1.6502	1.6041	1.6575	1.7961
11:48		1.8305	1.8878	1.2391	1.3024	1.7392	1.7058	1.5022	1.5721	1.6488	1.6034	1.6571	1.7977
11:50		1.8306	1.8865	1.1683	1.3054	1.7371	1.7078	1.5024	1.5726	1.6486	1.6024	1.6546	1.7969
11:52		1.8328	1.8892	1.4106	1.3042	1.7376	1.7074	1.5024	1.5725	1.6485	1.6026	1.6566	1.7999
11:54		1.8314	1.8896	1.3798	1.3063	1.7417	1.7115	1.5072	1.5766	1.6526	1.6060	1.6585	1.8009
11:56		1.8335	1.8907	1.4255	1.3022	1.7375	1.7046	1.5030	1.5694	1.6450	1.6026	1.6536	1.7965
11:58		1.8329	1.8924	1.4564	1.3062	1.7432	1.7131	1.5076	1.5783	1.6550	1.6100	1.6644	1.8071
12:00		1.8320	1.8899	1.4111	1.3096	1.7457	1.7137	1.5096	1.5790	1.6548	1.6074	1.6610	1.8030
12:02		1.8389	1.8983	1.3598	1.3093	1.7464	1.7137	1.5092	1.5742	1.6497	1.6336	1.6571	1.8023
12:04		1.8244	1.8818	1.3706	1.3021	1.7402	1.7081	1.5068	1.5714	1.6473	1.6226	1.6531	1.7924
12:06		1.8132	1.8711	1.3657	1.2935	1.7244	1.6942	1.4893	1.5596	1.6337	1.5887	1.6424	1.7846
12:08		1.8075	1.8632	1.3348	1.2878	1.7178	1.6860	1.4866	1.5561	1.6314	1.5873	1.6397	1.7803
12:10		1.8058	1.8613	1.3689	1.2846	1.7134	1.6812	1.4792	1.5494	1.6230	1.5797	1.6327	1.7715
12:12		1.8062	1.8623	1.4590	1.2878	1.7181	1.6857	1.4806	1.5496	1.6230	1.5777	1.6314	1.7723
12:14		1.7976	1.8524	1.3728	1.2819	1.7113	1.6802	1.4792	1.5487	1.6231	1.5813	1.6334	1.7744
12:16		1.7983	1.8535	1.3538	1.2834	1.7139	1.6818	1.4803	1.5504	1.6233	1.5824	1.6341	1.7747
12:18		1.8053	1.8600	1.4243	1.2833	1.7117	1.6793	1.4755	1.5434	1.6160	1.5727	1.6263	1.7660
12:20	316,000 gal.	1.7955	1.8508	1.3582	1.2803	1.7109	1.6803	1.4766	1.5503	1.6235	1.5809	1.6346	1.7770
12:22		1.8012	1.8577	1.3935	1.2867	1.7174	1.6804	1.4840	1.5530	1.6258	1.5824	1.6347	1.7744
12:24	Stage 5	1.8015	1.8570	1.4300	1.2829	1.7141	1.6816	1.4796	1.5492	1.6219	1.5805	1.6325	1.7726
12:26		1.8049	1.8605	1.3582	1.2864	1.7155	1.6832	1.4808	1.5499	1.6224	1.5790	1.6319	1.7714
12:28	Start pre-pad	1.8050	1.8594	1.4065	1.2832	1.7139	1.6811	1.4773	1.5459	1.6184	1.5767	1.6296	1.7714
12:30		1.8054	1.8605	1.3809	1.2820	1.7140	1.6791	1.4757	1.5447	1.6176	1.5760	1.6289	1.7743
12:32		1.8032	1.8591	1.4311	1.2882	1.7223	1.6892	1.4849	1.5546	1.6271	1.5836	1.6364	1.7753
12:34		1.8063	1.8629	1.4589	1.2848	1.7181	1.6832	1.4794	1.5483	1.6210	1.5786	1.6313	1.7731
12:36		1.8067	1.8628	1.3317	1.2873	1.7173	1.6844	1.4806	1.5505	1.6221	1.5797	1.6323	1.7735
12:38		1.8046	1.8596	1.2589	1.2870	1.7171	1.6836	1.4792	1.5495	1.6226	1.5799	1.6326	1.7758
12:40		1.8052	1.8644	1.4197	1.2896	1.7194	1.6854	1.4806	1.5492	1.6206	1.5772	1.6306	1.7713
12:42		1.8057	1.8602	1.3279	1.2868	1.7158	1.6827	1.4785	1.5480	1.6204	1.5782	1.6334	1.7756
12:44		1.8212	1.8572	1.4127	1.2843	1.7175	1.6866	1.4842	1.5550	1.6246	1.5878	1.6426	1.7839
12:46		1.8225	1.8583	1.4198	1.2879	1.7203	1.6882	1.4837	1.5545	1.6271	1.5845	1.6373	1.7790
12:48		1.8033	1.8590	1.3558	1.2862	1.7168	1.6845	1.4829	1.5522	1.6248	1.5834	1.6376	1.7782
12:51		1.8043	1.8613	1.4583	1.2891	1.7215	1.6891	1.4856	1.5545	1.6261	1.5842	1.6363	1.7775
12:53		1.8028	1.8586	1.4979	1.2855	1.7177	1.6848	1.4805	1.5508	1.6234	1.5820	1.6350	1.7771
12:55		1.8024	1.8585	1.4322	1.2868	1.7209	1.6876	1.4837	1.5536	1.6264	1.5850	1.6384	1.7795
12:57		1.8035	1.8596	1.3141	1.2874	1.7212	1.6885	1.4845	1.5548	1.6265	1.5851	1.6382	1.7779
12:59		1.8028	1.8576	1.3859	1.2860	1.7206	1.6871	1.4833	1.5533	1.6251	1.5851	1.6396	1.7798
13:05													

TABLE I (Continued)

GPE NATURAL BUTTES NO.14-HYDROFRACTURE

FRACTURE-MARCH 15,1977

TIME		180°	195°	210°	225°	240°	255°	270°	285°	300°	315°	330°	345°
13:08		1.8047	1.8603	1.2576	1.2880	1.7215	1.6876	1.4827	1.5523	1.6240	1.5833	1.6375	1.7762
13:10		1.8010	1.8565	1.5232	1.2836	1.7188	1.6841	1.4805	1.5509	1.6227	1.5837	1.6378	1.7795
13:12		1.8030	1.8607	1.5576	1.2899	1.7243	1.6909	1.4858	1.5564	1.6269	1.5874	1.6390	1.7790
13:14	378,000 gal.	1.7988	1.8542	1.5600	1.2856	1.7204	1.6862	1.4854	1.5567	1.6287	1.5894	1.6436	1.7840
13:16		1.8019	1.8566	1.5261	1.2859	1.7209	1.6875	1.4810	1.5542	1.6256	1.5872	1.6402	1.7812
13:18		1.8006	1.8548	1.5725	1.2806	1.7151	1.6822	1.4794	1.5503	1.6213	1.5845	1.6399	1.7820
13:20		1.8039	1.8597	1.5752	1.2877	1.7214	1.6866	1.4833	1.5530	1.6240	1.5852	1.6390	1.7762
13:22		1.8023	1.8583	1.5795	1.2879	1.7225	1.6881	1.4855	1.5550	1.6257	1.5863	1.6398	1.7779
13:24		1.8015	1.8576	1.5811	1.2879	1.7222	1.6887	1.4861	1.5564	1.6270	1.5886	1.6429	1.7822
13:26	Stage 6	1.8031	1.8545	1.5711	1.2842	1.7177	1.6839	1.4812	1.5509	1.6212	1.5844	1.6398	1.7790
13:28		1.8032	1.8583	1.5389	1.2861	1.7212	1.6873	1.4833	1.5529	1.6232	1.5885	1.6384	1.7785
13:30	Start pre-pad	1.8009	1.8564	1.5353	1.2863	1.7245	1.6892	1.4849	1.5546	1.6250	1.5867	1.6414	1.7826
13:32		1.8046	1.8594	1.4296	1.2875	1.7203	1.6864	1.4819	1.5507	1.6209	1.5833	1.6365	1.7757
13:34		1.8001	1.8538	1.2470	1.2813	1.7208	1.6821	1.4790	1.5488	1.6198	1.5829	1.6387	1.7778
13:36		1.8038	1.8564	1.3611	1.2794	1.7113	1.6766	1.4744	1.5423	1.6128	1.5744	1.6314	1.7733
13:38		1.8025	1.8568	1.4086	1.2841	1.7190	1.6840	1.4818	1.5499	1.6208	1.5840	1.6385	1.7782
13:40		1.8051	1.8579	1.3422	1.2812	1.7126	1.6769	1.4742	1.5427	1.6127	1.5774	1.6316	1.7739
13:42		1.7999	1.8549	1.4281	1.2849	1.7209	1.6869	1.4852	1.5536	1.6248	1.5850	1.6425	1.7793
13:44		1.8038	1.8570	1.3218	1.2823	1.7155	1.6836	1.4781	1.5474	1.6173	1.5808	1.6354	1.7767
13:46		1.8011	1.8575	1.3226	1.2880	1.7204	1.6867	1.4857	1.5543	1.6238	1.5863	1.6399	1.7780
13:48		1.8012	1.8560	1.3022	1.2895	1.7191	1.6847	1.4834	1.5524	1.6231	1.5862	1.6400	1.7815
13:50		1.8003	1.8558	1.3363	1.2855	1.7226	1.6887	1.4865	1.5559	1.6263	1.5878	1.6429	1.7812
13:52		1.8027	1.8576	1.2355	1.2737	1.7259	1.6876	1.4836	1.5523	1.6219	1.5854	1.6384	1.7791
13:54		1.8037	1.8576	1.3527	1.2822	1.7195	1.6836	1.4818	1.5506	1.6197	1.5825	1.6366	1.7761
13:56		1.8045	1.8603	1.2875	1.2848	1.7196	1.6844	1.4827	1.5510	1.6194	1.5827	1.6363	1.7751
13:58		1.8045	1.8591	1.3693	1.2843	1.7211	1.6857	1.4834	1.5512	1.6203	1.5838	1.6364	1.7763
14:00		1.8069	1.8601	1.4307	1.2845	1.7195	1.6836	1.4813	1.5493	1.6189	1.5823	1.6359	1.7787
14:02		1.8035	1.8577	1.3653	1.2825	1.7168	1.6811	1.4803	1.5490	1.6184	1.5817	1.6353	1.7755
14:04		1.8041	1.8583	1.3797	1.2866	1.7221	1.6877	1.4861	1.5543	1.6236	1.5856	1.6394	1.7779
14:06		1.8045	1.8586	1.4301	1.2870	1.7220	1.6867	1.4851	1.5538	1.6228	1.5850	1.6378	1.7785
14:08		1.8054	1.8606	1.4433	1.2860	1.7204	1.6852	1.4846	1.5529	1.6218	1.5855	1.6376	1.7774
14:10		1.8054	1.8599	1.4164	1.2889	1.7231	1.6886	1.4869	1.5553	1.6237	1.5868	1.6386	1.7806
14:12		1.8021	1.8561	1.4945	1.2849	1.7187	1.6852	1.4854	1.5549	1.6235	1.5876	1.6406	1.7814
14:14		1.8046	1.8593	1.6318	1.2834	1.7185	1.6835	1.4836	1.5522	1.6215	1.5852	1.6377	1.7790
14:16		1.8052	1.8600	1.6909	1.2852	1.7204	1.6853	1.4839	1.5525	1.6219	1.5845	1.6367	1.7783
14:18	438,000 gal.	1.8094	1.8626	1.6800	1.2861	1.7207	1.6854	1.4839	1.5524	1.6202	1.5825	1.6354	1.7740
14:20		1.7993	1.8258	1.6710	1.2789	1.7194	1.6857	1.4854	1.5551	1.6241	1.5891	1.6413	1.7807
14:22		1.8038	1.8580	1.6824	1.2853	1.7214	1.6862	1.4857	1.5542	1.6236	1.5866	1.6360	1.7795
14:24		1.8028	1.8573	1.6795	1.2811	1.7169	1.6804	1.4798	1.5488	1.6173	1.5827	1.6353	1.7790
14:26		1.8032	1.8574	1.6791	1.2815	1.7178	1.6811	1.4805	1.5499	1.6186	1.5827	1.6358	1.7775
14:28		1.8046	1.8581	1.6806	1.2818	1.7185	1.6804	1.4794	1.5481	1.6162	1.5804	1.6333	1.7739
14:30		1.8056	1.8583	1.6767	1.2785	1.7152	1.6783	1.4773	1.5464	1.6148	1.5811	1.6344	1.7776
14:32		1.8061	1.8594	1.6721	1.2806	1.7185	1.6799	1.4796	1.5478	1.6171	1.5813	1.6345	1.7763

UGR File #c075/A77, part 2
SAND-77-1992
Oct. 1976-Sept. 1977

TABLE I (Continued)

GPE NATURAL BUTTES NO.14-HYDROFRACTURE

FRACTURE-MARCH 15,1977

TIME		180°	195°	210°	225°	240°	255°	270°	285°	300°	315°	330°	345°
14:34		1.8048	1.8579	1.6385	1.2816	1.7198	1.6913	1.4797	1.5485	1.6165	1.5817	1.6343	1.7799
14:38		1.7987	1.8532	1.5421	1.2828	1.7241	1.6966	1.4854	1.5551	1.6249	1.5892	1.6411	1.7810
14:40		1.8025	1.8583	1.4272	1.2833	1.7233	1.6884	1.4870	1.5563	1.6248	1.5864	1.6409	1.7782
14:42	Stage 7	1.8053	1.8596	1.3771	1.2814	1.7189	1.6809	1.4854	1.5480	1.6176	1.5826	1.6346	1.7773
14:44		1.8010	1.8548	1.4024	1.2821	1.7199	1.6837	1.4837	1.5520	1.6222	1.5864	1.6392	1.7783
14:46	Start pre-pad	1.8043	1.8596	1.4244	1.2838	1.7219	1.6853	1.4844	1.5528	1.6211	1.5850	1.6369	1.7772
14:48		1.8016	1.8569	1.4782	1.2831	1.7206	1.6843	1.4853	1.5536	1.6229	1.5866	1.6393	1.7798
14:50		1.8005	1.8567	1.4971	1.2846	1.7220	1.6870	1.4878	1.5572	1.6265	1.5905	1.6421	1.7827
14:52		1.8027	1.8569	1.5166	1.2823	1.7212	1.6851	1.4855	1.5556	1.6236	1.5877	1.6401	1.7812
14:54		1.7981	1.8525	1.5418	1.2843	1.7230	1.6872	1.4880	1.5581	1.6279	1.5943	1.6428	1.7833
14:56		1.8059	1.8630	1.5831	1.2818	1.7192	1.6815	1.4821	1.5506	1.6192	1.5832	1.6367	1.7756
14:58		1.8043	1.8635	1.5899	1.2854	1.7236	1.6877	1.4881	1.5561	1.6250	1.5886	1.6417	1.7777
15:00		1.8133	1.8728	1.5816	1.2842	1.7161	1.6776	1.4777	1.5459	1.6134	1.5786	1.6335	1.7685
15:02		1.8033	1.8595	1.5878	1.2844	1.7215	1.6855	1.4857	1.5553	1.6240	1.5879	1.6401	1.7815
15:04		1.8032	1.8594	1.6341	1.2865	1.7243	1.6891	1.4891	1.5585	1.6270	1.5905	1.6427	1.7713
15:06		1.8039	1.8522	1.5909	1.2795	1.7171	1.6799	1.4811	1.5499	1.6179	1.5832	1.6376	1.7781
15:08		1.8025	1.8554	1.6077	1.2741	1.7190	1.6721	1.4736	1.5424	1.6109	1.5776	1.6324	1.7774
15:10		1.8045	1.8592	1.6290	1.2841	1.7206	1.6855	1.4864	1.5550	1.6232	1.5869	1.6391	1.7799
15:12		1.8053	1.8613	1.6119	1.2843	1.7198	1.6816	1.4839	1.5523	1.6204	1.5843	1.6376	1.7891
15:14		1.8025	1.8569	1.6066	1.2763	1.7104	1.6722	1.4747	1.5445	1.6123	1.5781	1.6325	1.7725
15:16		1.8052	1.8589	1.6092	1.2805	1.7166	1.6776	1.4787	1.5474	1.6146	1.5806	1.6339	1.7759
15:18		1.8049	1.8598	1.6210	1.2802	1.7165	1.6787	1.4789	1.5477	1.6157	1.5811	1.6336	1.7778
15:20		1.8039	1.8594	1.6112	1.2813	1.7166	1.6796	1.4810	1.5498	1.6173	1.5813	1.6361	1.7775
15:22		1.8046	1.8603	1.6090	1.2844	1.7199	1.6837	1.4843	1.5541	1.6210	1.5856	1.6374	1.7765
15:24		1.8040	1.8596	1.6085	1.2818	1.7156	1.6801	1.4818	1.5512	1.6184	1.5829	1.6374	1.7784
15:26		1.8010	1.8540	1.6044	1.2795	1.7140	1.6791	1.4807	1.5518	1.6194	1.5859	1.6403	1.7819
15:28		1.8098	1.8671	1.6186	1.2874	1.7200	1.6849	1.4856	1.5539	1.6203	1.5845	1.6368	1.7772
15:30	522,000 gal.	1.8056	1.8645	1.6216	1.2840	1.7161	1.6819	1.4829	1.5519	1.6196	1.5840	1.6365	1.7778
15:32		1.8054	1.8633	1.6105	1.2830	1.7166	1.6807	1.4828	1.5524	1.6186	1.5834	1.6361	1.7774
15:34		1.8075	1.8644	1.6094	1.2823	1.7142	1.6792	1.4804	1.5505	1.6170	1.5833	1.6366	1.7776
15:36		1.8023	1.8572	1.6156	1.2829	1.7174	1.6833	1.4844	1.5541	1.6203	1.5842	1.6371	1.7774
15:38		1.8093	1.8592	1.6173	1.2798	1.7129	1.6784	1.4786	1.5483	1.6141	1.5794	1.6345	1.7747
15:40		1.8037	1.8564	1.6171	1.2779	1.7111	1.6769	1.4792	1.5498	1.6174	1.5827	1.6367	1.7782
15:42		1.8001	1.8552	1.6191	1.2796	1.7136	1.6793	1.4824	1.5528	1.6196	1.5856	1.6397	1.7785
15:44		1.8040	1.8609	1.6197	1.2844	1.7169	1.6840	1.4860	1.5559	1.6229	1.5864	1.6393	1.7783
15:46		1.8015	1.8554	1.6120	1.2769	1.7113	1.6764	1.4794	1.5492	1.6170	1.5829	1.6372	1.7786
15:48		1.8010	1.8575	1.6183	1.2845	1.7209	1.6871	1.4885	1.5585	1.6255	1.5891	1.6415	1.7837
15:50		1.8033	1.8598	1.6133	1.2795	1.7123	1.6780	1.4794	1.5506	1.6170	1.5828	1.6359	1.7749
15:52		1.8057	1.8630	1.6166	1.2782	1.7152	1.6804	1.4825	1.5528	1.6183	1.5829	1.6356	1.7747
15:54		1.8029	1.8558	1.6103	1.2798	1.7121	1.6773	1.4791	1.5505	1.6164	1.5810	1.6344	1.7751
15:56		1.8014	1.8566	1.5952	1.2821	1.7139	1.6831	1.4844	1.5555	1.6226	1.5869	1.6397	1.7786
15:58		1.8002	1.8551	1.5924	1.2812	1.7136	1.6819	1.4833	1.5539	1.6209	1.5846	1.6388	1.7794
16:00		1.8045	1.8598	1.6011	1.2817	1.7150	1.6805	1.4838	1.5535	1.6194	1.5842	1.6374	1.7766

UGR [illegible]
SAND-77-1992
Oct., 1976-Sept., 197[illegible]

TABLE I (Continued)

GPE NATURAL BUTTES NO.14-HYDROFRACTURE

FRACTURE-MARCH 15,1977

TIME		180°	195°	210°	225°	240°	255°	270°	285°	300°	315°	330°	345°
16:02		1.8034	1.8586	1.5898	1.2805	1.7128	1.6892	1.4800	1.5521	1.6179	1.5825	1.6352	1.7787
16:04		1.8030	1.8570	1.5420	1.2829	1.7168	1.6931	1.4844	1.5560	1.6210	1.5851	1.6378	1.7786
16:06		1.8034	1.8594	1.5387	1.2819	1.7139	1.6812	1.4831	1.5543	1.6199	1.5844	1.6373	1.7783
16:08		1.8036	1.8595	1.5256	1.2831	1.7145	1.6823	1.4836	1.5552	1.6196	1.5849	1.6370	1.7763
16:10	554,000 gal.	1.8069	1.8634	1.5298	1.2826	1.7127	1.6795	1.4808	1.5519	1.6172	1.5819	1.6344	1.7749
16:12		1.8040	1.8630	1.2313	1.2840	1.7150	1.6826	1.4843	1.5562	1.6215	1.5821	1.6382	1.7779
16:14	Stage 8	1.8047	1.8617	1.4857	1.2825	1.7117	1.6800	1.4815	1.5539	1.6185	1.5847	1.6361	1.7777
16:16		1.8047	1.8672	1.4574	1.2828	1.7130	1.6785	1.4808	1.5523	1.6170	1.5815	1.6343	1.7759
16:18		1.8068	1.8636	1.4511	1.2887	1.7195	1.6800	1.4879	1.5605	1.6257	1.5893	1.6405	1.7790
16:20		1.7960	1.8482	1.4971	1.2818	1.7136	1.6833	1.4863	1.5595	1.6249	1.5899	1.6415	1.7630
16:22		1.8027	1.8575	1.4968	1.2789	1.7072	1.6753	1.4784	1.5513	1.6156	1.5824	1.6346	1.7769
16:24		1.8087	1.8702	1.4519	1.2857	1.7130	1.6839	1.4830	1.5558	1.6204	1.5844	1.6357	1.7757
16:26		1.8054	1.8639	1.4979	1.2847	1.7136	1.6827	1.4842	1.5571	1.6220	1.5861	1.6370	1.7785
16:28		1.8055	1.8654	1.4789	1.2841	1.7139	1.6921	1.4838	1.5563	1.6217	1.5848	1.6369	1.7783
16:30		1.8074	1.8647	1.5135	1.2875	1.7159	1.6851	1.4859	1.5602	1.6242	1.5866	1.6386	1.7752
16:32		1.8029	1.8578	1.4794	1.2812	1.7061	1.6770	1.4806	1.5529	1.6182	1.5823	1.6344	1.7762
16:34		1.8049	1.8604	1.3863	1.2838	1.7140	1.6847	1.4860	1.5591	1.6245	1.5885	1.6404	1.7821
16:36		1.8038	1.8593	1.3724	1.2830	1.7119	1.6824	1.4833	1.5574	1.6218	1.5861	1.6379	1.7773
16:38	585,000 gal.	1.8015	1.8594	1.3337	1.2851	1.7138	1.6837	1.4867	1.5604	1.6249	1.5883	1.6394	1.7800
16:40		1.8041	1.8603	1.2524	1.2834	1.7107	1.6811	1.4830	1.5559	1.6219	1.5851	1.6369	1.7774
16:42		1.8030	1.8598	1.2139	1.2868	1.7151	1.6865	1.4877	1.5617	1.6265	1.5891	1.6413	1.7799
16:44		1.8051	1.8612	1.3773	1.2849	1.7109	1.6840	1.4860	1.5599	1.6243	1.5875	1.6396	1.7795
16:46		1.8047	1.8588	1.2186	1.2793	1.7037	1.6739	1.4782	1.5520	1.6167	1.5818	1.6338	1.7772
16:48		1.8067	1.8605	1.3425	1.2797	1.7035	1.6748	1.4769	1.5501	1.6154	1.5804	1.6329	1.7762
16:50		1.8049	1.8603	1.2298	1.2835	1.7077	1.6797	1.4833	1.5573	1.6220	1.5859	1.6384	1.7782
16:54		1.8074	1.8631	1.4554	1.2855	1.7096	1.6840	1.4843	1.5580	1.6223	1.5862	1.6380	1.7790
16:56		1.8050	1.8605	1.5007	1.2835	1.7077	1.6816	1.4837	1.5582	1.6230	1.5874	1.6388	1.7795
16:58		1.8070	1.8617	1.1030	1.2818	1.7039	1.6783	1.4798	1.5545	1.6183	1.5833	1.6354	1.7746
17:00		1.8065	1.8603	1.2520	1.2829	1.7054	1.6777	1.4819	1.5557	1.6209	1.5844	1.6359	1.7780
17:02		1.8064	1.8619	1.3521	1.2840	1.7054	1.6798	1.4832	1.5569	1.6209	1.5854	1.6370	1.7793
17:04		1.8054	1.8591	1.3257	1.2826	1.7038	1.6777	1.4814	1.5559	1.6195	1.5837	1.6358	1.7784
17:06		1.8090	1.8655	1.4022	1.2853	1.7057	1.6806	1.4830	1.5582	1.6215	1.5854	1.6369	1.7779
17:08		1.8097	1.8652	1.4428	1.2846	1.7043	1.6796	1.4825	1.5574	1.6206	1.5848	1.6377	1.7780
17:10		1.8067	1.8624	1.3727	1.2837	1.7030	1.6791	1.4818	1.5566	1.6205	1.5836	1.6363	1.7793
17:13		1.8059	1.8631	1.4070	1.2842	1.7032	1.6805	1.4849	1.5602	1.6249	1.5887	1.6410	1.7826
17:15		1.8072	1.8643	1.4612	1.2918	1.7108	1.6898	1.4922	1.5688	1.6303	1.5919	1.6427	1.7827
17:17		1.8069	1.8610	1.4235	1.2828	1.7001	1.6787	1.4812	1.5564	1.6194	1.5839	1.6363	1.7790
17:19		1.8063	1.8639	1.4513	1.2863	1.7043	1.6831	1.4849	1.5601	1.6227	1.5867	1.6388	1.7798
17:21		1.8069	1.8634	1.3354	1.2835	1.7001	1.6792	1.4820	1.5571	1.6200	1.5846	1.6376	1.7792
17:23		1.8051	1.8576	1.3059	1.2838	1.7013	1.6794	1.4833	1.5590	1.6221	1.5886	1.6400	1.7811
17:25		1.8047	1.8589	1.4585	1.2834	1.7005	1.6789	1.4827	1.5588	1.6221	1.5893	1.6387	1.7826
17:27		1.8073	1.8614	1.4664	1.2840	1.7008	1.6800	1.4833	1.5593	1.6217	1.5864	1.6394	1.7803
17:29		1.8061	1.8614	1.3802	1.2842	1.7000	1.6790	1.4825	1.5593	1.6222	1.5863	1.6391	1.7804

SAND-77-1992
Oct. 1976-Sept. 1977

TABLE I (Continued)

GPE NATURAL BUTTES NO.14-HYDROFRACTURE

FRACTURE-MARCH 15,1977

TIME		180°	195°	210°	225°	240°	255°	270°	285°	300°	315°	330°	345°
17:31		1.8069	1.8620	1.4250	1.2802	1.6977	1.6792	1.4837	1.5562	1.6186	1.5828	1.6368	1.7791
17:33		1.8072	1.8621	1.3939	1.2835	1.6993	1.6796	1.4815	1.5585	1.6213	1.5855	1.6397	1.7809
17:35		1.8066	1.8596	1.2890	1.2825	1.6964	1.6735	1.4739	1.5548	1.6174	1.5820	1.6396	1.7775
17:37		1.8077	1.8620	1.3720	1.2844	1.7012	1.6807	1.4837	1.5598	1.6222	1.5859	1.6386	1.7800
17:39		1.8079	1.8625	1.4162	1.2850	1.7001	1.6798	1.4836	1.5602	1.6229	1.5868	1.6401	1.7823
17:41		1.8082	1.8622	1.3035	1.2854	1.7004	1.6803	1.4839	1.5602	1.6221	1.5849	1.6382	1.7793
17:43		1.8083	1.8632	1.3551	1.2856	1.7014	1.6816	1.4849	1.5613	1.6235	1.5864	1.6402	1.7807
17:45		1.8114	1.8659	1.3252	1.2850	1.7005	1.6795	1.4839	1.5604	1.6223	1.5869	1.6413	1.7819
17:47		1.8294	1.8641	1.4658	1.2844	1.7032	1.6948	1.4873	1.5643	1.6263	1.5891	1.6423	1.7829
17:49		1.8084	1.8636	1.3108	1.2862	1.7005	1.6826	1.4854	1.5623	1.6238	1.5866	1.6403	1.7807
17:51		1.8043	1.8618	1.3869	1.2833	1.6970	1.6795	1.4826	1.5596	1.6223	1.5870	1.6418	1.7821
17:53		1.8121	1.8654	1.4250	1.2825	1.6961	1.6764	1.4792	1.5591	1.6168	1.5814	1.6359	1.7758
17:55	Shut down	1.8109	1.8644	1.2865	1.2862	1.6978	1.6792	1.4833	1.5591	1.6212	1.5847	1.6424	1.7786
17:57	640,000 gal. (Total Vol.)	1.8111	1.8646	1.4127	1.2841	1.6970	1.6778	1.4817	1.5581	1.6203	1.5838	1.6404	1.7795
17:59		1.8103	1.8638	1.3209	1.2848	1.6963	1.6795	1.4837	1.5605	1.6227	1.5859	1.6415	1.7797
18:01		1.8115	1.8658	1.3559	1.2891	1.7031	1.6852	1.4878	1.5656	1.6277	1.5900	1.6446	1.7836
18:03		1.8097	1.8653	1.3344	1.2889	1.7019	1.6841	1.4873	1.5647	1.6263	1.5893	1.6444	1.7838
18:05		1.8119	1.8657	1.3614	1.2876	1.7007	1.6828	1.4856	1.5625	1.6245	1.5888	1.6433	1.7819
18:07		1.8223	1.8677	1.3223	1.2893	1.7033	1.6836	1.4864	1.5631	1.6247	1.5887	1.6425	1.7815
18:09		1.8157	1.8676	1.3459	1.2869	1.7011	1.6829	1.4837	1.5604	1.6223	1.5865	1.6422	1.7801
18:11		1.8142	1.8685	1.3260	1.2907	1.7050	1.6859	1.4908	1.5670	1.6292	1.5924	1.6475	1.7843
18:13		1.8136	1.8665	1.6849	1.2853	1.6988	1.6730	1.4832	1.5590	1.6214	1.5849	1.6415	1.7795

APPENDIX B

TABLE II

GPE NATURAL BUTTES NO.20-HYDROFRACTURE

FRACTURE-JUNE 22,1977

TIME	0°	15°	30°	45°	60°	75°	90°	105°	120°	135°	150°	165°
8:05	3.1424	3.1648	2.9956	2.8945	2.8335	2.9108	3.0120	3.1259	3.2689	3.1922	3.4006	3.3693
8:06	3.1473	3.1717	2.9398	2.9017	2.8360	2.9157	3.0180	3.1298	3.2743	3.1970	3.4066	3.3737
8:07	3.1417	3.1666	2.9838	2.8846	2.8312	2.9091	3.0121	3.1236	3.2653	3.1875	3.3982	3.3649
8:08	3.1469	3.1708	2.9899	2.8979	2.8368	2.9153	3.0147	3.1288	3.2731	3.1983	3.4072	3.3733
8:09	3.1399	3.1653	2.9859	2.8944	2.8303	2.9091	3.0099	3.1217	3.2677	3.1905	3.4014	3.3679
8:10	3.1443	3.1696	2.9874	2.8947	2.8392	2.9115	3.0147	3.1250	3.2700	3.1926	3.4037	3.3695
8:11	3.1497	3.1726	2.9491	2.9032	2.8421	2.9165	3.0187	3.1315	3.2751	3.1972	3.4071	3.3744
8:12	3.1501	3.1758	2.9970	2.9023	2.8385	2.9179	3.0197	3.1317	3.2766	3.1996	3.4108	3.3751
8:13	3.1550	3.1805	3.0003	2.9089	2.8447	2.9212	3.0240	3.1372	3.2802	3.2026	3.4122	3.3792
8:14	3.1470	3.1697	2.9877	2.9017	2.8343	2.9117	3.0120	3.1257	3.2708	3.1930	3.4044	3.3696
8:15	3.1519	3.1758	2.9956	2.9036	2.8415	2.9167	3.0167	3.1284	3.2722	3.1932	3.4055	3.3716
8:16	3.1445	3.1674	2.9818	2.8976	2.8343	2.9115	3.0117	3.1234	3.2668	3.1906	3.4026	3.3684
8:17	3.1535	3.1779	2.9976	2.9061	2.8429	2.9210	3.0201	3.1319	3.2770	3.1999	3.4120	3.3747
8:18	3.1585	3.1836	3.0011	2.9062	2.8486	2.9253	3.0227	3.1395	3.2803	3.2026	3.4156	3.3814
8:19	3.1341	3.1567	2.9807	2.8871	2.8199	2.8998	3.0011	3.1116	3.2541	3.1794	3.3990	3.3587
8:20	3.1440	3.1691	2.9928	2.8964	2.8350	2.9107	3.0111	3.1234	3.2648	3.1922	3.4002	3.3683
8:21	3.1387	3.1609	2.9820	2.8919	2.8303	2.9063	3.0071	3.1181	3.2621	3.1842	3.3971	3.3643
8:22	3.1401	3.1646	2.9802	2.8909	2.8262	2.9045	3.0059	3.1185	3.2605	3.1836	3.3963	3.3647
8:23	3.1452	3.1660	2.9851	2.8947	2.8345	2.9077	3.0101	3.1227	3.2643	3.1847	3.3995	3.3666
8:24	3.1481	3.1699	2.9877	2.8973	2.8348	2.9112	3.0117	3.1243	3.2702	3.1907	3.4034	3.3699
8:25	3.1497	3.1726	2.9893	2.8923	2.8324	2.9120	3.0145	3.1277	3.2698	3.1919	3.4053	3.3711
8:26	3.1515	3.1747	2.9908	2.8990	2.8386	2.9150	3.0169	3.1270	3.2695	3.1924	3.4066	3.3728
8:27	3.1501	3.1740	2.9930	2.8956	2.8379	2.9162	3.0150	3.1291	3.2722	3.1945	3.4085	3.3739
8:28	3.1513	3.1746	2.9912	2.9101	2.8379	2.9164	3.0140	3.1303	3.2721	3.1951	3.4099	3.3759
8:29	3.1443	3.1708	2.9871	2.8878	2.8349	2.9113	3.0088	3.1219	3.2643	3.1869	3.4024	3.3692
8:30	3.1471	3.1713	2.9838	2.8982	2.8365	2.9115	3.0117	3.1231	3.2668	3.1896	3.4051	3.3705
8:31	3.1509	3.1774	2.9905	2.9029	2.8418	2.9141	3.0131	3.1289	3.2704	3.1917	3.4059	3.3721
8:32	3.1555	3.1789	2.9952	2.9056	2.8364	2.9197	3.0196	3.1300	3.2742	3.1964	3.4125	3.3758
8:33	3.1478	3.1714	2.9865	2.8985	2.8340	2.9109	3.0133	3.1232	3.2657	3.1892	3.4051	3.3704
8:34	3.1487	3.1719	2.9842	2.8971	2.8376	2.9119	3.0119	3.1238	3.2653	3.1896	3.4042	3.3712
8:35	3.1418	3.1644	2.9754	2.8897	2.8239	2.9044	3.0052	3.1161	3.2602	3.1831	3.3972	3.3637
8:36	3.1482	3.1714	2.9867	2.9032	2.8375	2.9120	3.0116	3.1233	3.2661	3.1895	3.4047	3.3701
8:37	3.1390	3.1628	2.9740	2.8899	2.8264	2.9019	3.0017	3.1144	3.2573	3.1814	3.3967	3.3627
8:38	3.1454	3.1670	2.9880	2.8932	2.8357	2.9073	3.0059	3.1188	3.2606	3.1845	3.4007	3.3679
8:39	3.1582	3.1774	3.0007	2.9083	2.8419	2.9193	3.0196	3.1322	3.2763	3.1931	3.4151	3.3790
8:40	3.1494	3.1730	2.9878	2.8991	2.8348	2.9113	3.0107	3.1236	3.2690	3.1895	3.4077	3.3745
8:41	3.1426	3.1670	2.9826	2.8922	2.8293	2.9054	3.0074	3.1174	3.2615	3.1852	3.4001	3.3665
8:42	3.1472	3.1671	2.9923	2.8956	2.8302	2.9059	3.0075	3.1204	3.2646	3.1870	3.4035	3.3675
8:43	3.1348	3.1582	2.9750	2.8825	2.8206	2.8978	2.9986	3.1118	3.2533	3.1785	3.3942	3.3600
8:44	3.1305	3.1557	2.9736	2.8883	2.8197	2.8946	2.9933	3.1067	3.2489	3.1735	3.3913	3.3562
8:45	3.1411	3.1633	2.9832	2.8865	2.8316	2.9072	3.0080	3.1182	3.2616	3.1850	3.4033	3.3681
8:57	3.1393	3.1630	2.9843	2.8913	2.8296	2.9066	3.0053	3.1160	3.2621	3.1846	3.4038	3.3687
8:58	3.1338	3.1559	2.9717	2.8867	2.8233	2.8971	3.0003	3.1110	3.2553	3.1771	3.3969	3.3628

UGR File #c073/A77, part 2
SAND-77-1992
Oct. 1976-Sept. 1977

TABLE II (Continued)

GPE NATURAL BUTTES NO.20-HYDROFRACTURE

FRACTURE-JUNE 22,1977

TIME		0°	15°	30°	45°	60°	75°	90°	105°	120°	135°	150°	165°
8:59		3.1374	3.1577	2.9746	2.8900	2.8176	2.8959	2.9945	3.1094	3.2510	3.1746	3.3936	3.3587
9:00		3.1326	3.1516	2.9582	2.8843	2.8196	2.8932	2.9931	3.1052	3.2469	3.1707	3.3898	3.3543
9:01		3.1254	3.1466	2.9664	2.8753	2.8101	2.8854	2.9849	3.0970	3.2416	3.1632	3.3827	3.3491
9:02		3.1199	3.1430	2.9590	2.8630	2.8088	2.8831	2.9831	3.0934	3.2365	3.1577	3.3802	3.3444
9:03		3.1316	3.1508	2.9676	2.8720	2.8170	2.8920	2.9911	3.1031	3.2473	3.1724	3.3888	3.3534
9:04		3.1177	3.1404	2.9571	2.8656	2.8011	2.8815	2.9731	3.0957	3.2343	3.1593	3.3772	3.3429
9:05		3.1243	3.1488	2.9659	2.8693	2.8144	2.8873	2.9850	3.0979	3.2391	3.1625	3.3812	3.3476
9:06		3.1392	3.1569	2.9739	2.8691	2.8257	2.9045	3.0002	3.1137	3.2583	3.1824	3.4020	3.3654
9:07	Start pumping	3.1123	3.1347	2.9517	2.8572	2.7972	2.8748	2.9729	3.0854	3.2276	3.1493	3.3719	3.3371
9:08		3.1179	3.1405	2.9556	2.8681	2.8085	2.8799	2.9804	3.0999	3.2332	3.1532	3.3733	3.3433
9:09		3.1207	3.1393	2.9564	2.8660	2.8041	2.8840	2.9817	3.0935	3.2368	3.1595	3.3803	3.3439
9:10		3.1132	3.1362	2.9497	2.8639	2.7973	2.8726	2.9752	3.0813	3.2267	3.1518	3.3706	3.3385
9:11		3.1183	3.1408	2.9597	2.8727	2.8043	2.8840	2.9817	3.0923	3.2386	3.1605	3.3805	3.3454
9:12		3.1021	3.1210	2.9389	2.8479	2.7874	2.8633	2.9647	3.0742	3.2184	3.1399	3.3612	3.3261
9:13		3.1259	3.1473	2.9653	2.8685	2.8098	2.8854	2.9832	3.0915	3.2370	3.1610	3.3807	3.3460
9:14		3.1184	3.1379	2.9551	2.8706	2.8069	2.8787	2.9799	3.0885	3.2333	3.1573	3.3770	3.3423
9:15		3.1143	3.1333	2.9520	2.8635	2.7977	2.8750	2.9736	3.0849	3.2280	3.1559	3.3770	3.3395
9:16		3.1166	3.1249	2.9433	2.8580	2.7935	2.8689	2.9701	3.0764	3.2199	3.1445	3.3639	3.3304
9:17		3.1166	3.1274	2.9529	2.8586	2.7905	2.8660	2.9708	3.0784	3.2220	3.1477	3.3653	3.3323
9:18		3.1081	3.1203	2.9348	2.8518	2.7865	2.8614	2.9591	3.0683	3.2146	3.1376	3.3577	3.3241
9:19		3.1037	3.1212	2.9406	2.8522	2.7846	2.8640	2.9612	3.0692	3.2141	3.1372	3.3572	3.3221
9:20		3.1047	3.1241	2.9409	2.8541	2.7939	2.8662	2.9659	3.0773	3.2200	3.1442	3.3603	3.3291
9:21		3.0722	3.1025	2.9073	2.8177	2.7593	2.8334	2.9355	3.0440	3.1858	3.1113	3.3302	3.2973
9:22		3.0921	3.1123	2.9241	2.8439	2.7772	2.8523	2.9503	3.0599	3.2030	3.1276	3.3479	3.3140
9:23		3.1592	3.1730	2.9885	2.9021	2.8400	2.9109	3.0125	3.1292	3.2641	3.1845	3.4089	3.3732
9:24		3.1615	3.1836	3.0000	2.9184	2.8472	2.9197	3.0205	3.1286	3.2772	3.1985	3.4230	3.3854
9:25		3.1369	3.1544	2.9680	2.8880	2.8192	2.8945	2.9933	3.1015	3.2478	3.1699	3.3958	3.3600
9:26		3.1219	3.1419	2.9574	2.8682	2.8018	2.8751	2.9757	3.0826	3.2277	3.1518	3.3758	3.3414
9:27		3.1229	3.1450	2.9616	2.8775	2.8075	2.8809	2.9799	3.0885	3.2341	3.1587	3.3815	3.3467
9:28		3.1486	3.1709	2.9913	2.9042	2.8324	2.9092	3.0104	3.1152	3.2650	3.1864	3.4144	3.3748
9:29		3.1227	3.1428	2.9618	2.8739	2.8023	2.8799	2.9799	3.0887	3.2344	3.1561	3.3798	3.3436
9:30		3.1254	3.1458	2.9653	2.8763	2.8100	2.8851	2.9848	3.0923	3.2397	3.1589	3.3851	3.3493
9:31		3.1314	3.1509	2.9703	2.8816	2.8148	2.8909	2.9896	3.0974	3.2445	3.1682	3.3943	3.3545
9:32		3.0992	3.1153	2.9348	2.8485	2.7804	2.8594	2.9591	3.0651	3.2104	3.1368	3.3574	3.3220
9:33		3.1130	3.1311	2.9513	2.8673	2.7956	2.8755	2.9720	3.0761	3.2214	3.1463	3.3690	3.3347
9:34	42,000 gal.	3.1274	3.1461	2.9613	2.8755	2.8118	2.8839	2.9842	3.0904	3.2395	3.1644	3.3879	3.3528
9:35		3.1348	3.1543	2.9723	2.8873	2.8150	2.8929	2.9922	3.0980	3.2443	3.1673	3.3925	3.3554
9:36		3.1105	3.1314	2.9463	2.8510	2.7964	2.8688	2.9630	3.0752	3.2205	3.1447	3.3635	3.3307
9:37		3.1260	3.1451	2.9662	2.8715	2.8073	2.8832	2.9799	3.0873	3.2344	3.1615	3.3817	3.3436
9:38		3.1427	3.1622	2.9868	2.8926	2.8306	2.9012	2.9991	3.1036	3.2549	3.1760	3.3999	3.3638
9:39		3.1076	3.1252	2.9441	2.8526	2.7990	2.8674	2.9671	3.0709	3.2187	3.1431	3.3660	3.3315
9:40		3.1262	3.1491	2.9612	2.8837	2.8127	2.8872	2.9857	3.0903	3.2358	3.1594	3.3812	3.3472
9:41		3.1180	3.1399	2.9710	2.8701	2.8027	2.8787	2.9808	3.0865	3.2343	3.1567	3.3807	3.3462

TABLE II (Continued)

GPE NATURAL BUTTES NO.29-HYDROFRACTURE

FRACTURE-JUNE 22,1977

TIME		0°	15°	30°	45°	60°	75°	90°	105°	120°	135°	150°	165°
9:42		3.1296	3.1488	2.9571	2.8827	2.8163	2.8939	2.9884	3.0955	3.2417	3.1643	3.3877	3.3525
9:43		3.0994	3.1167	2.9369	2.8485	2.7846	2.8605	2.9614	3.0686	3.2127	3.1387	3.3610	3.3265
9:44		3.1056	3.1264	2.9420	2.8634	2.7869	2.8620	2.9643	3.0713	3.2146	3.1384	3.3615	3.3278
9:45		3.0903	3.1069	2.9256	2.8376	2.7725	2.8478	2.9472	3.0520	3.1983	3.1266	3.3464	3.3128
9:46	62,000 gal.	3.0984	3.1178	2.9346	2.8483	2.7807	2.8563	2.9583	3.0619	3.2098	3.1309	3.3567	3.3225
9:47		3.1077	3.1278	2.9459	2.8546	2.7945	2.8694	2.9699	3.0723	3.2215	3.1468	3.3677	3.3328
9:48		3.1354	3.1548	2.9677	2.8875	2.8225	2.8951	2.9954	3.0992	3.2479	3.1716	3.3943	3.3587
9:49		3.1023	3.1219	2.9366	2.8533	2.7846	2.8626	2.9643	3.0695	3.2159	3.1401	3.3636	3.3324
9:50		3.1227	3.1441	2.9603	2.8794	2.8098	2.8866	2.9831	3.0911	3.2378	3.1597	3.3842	3.3496
9:51		3.1192	3.1380	2.9512	2.8700	2.8056	2.8786	2.9794	3.0870	3.2335	3.1560	3.3799	3.3437
9:52		3.0995	3.1211	2.9369	2.8541	2.7896	2.8637	2.9619	3.0671	3.2113	3.1359	3.3605	3.3255
9:53		3.1051	3.1251	2.9391	2.8577	2.7929	2.8677	2.9667	3.0711	3.2174	3.1389	3.3623	3.3296
9:54		3.0999	3.1161	2.9344	2.8435	2.7826	2.8589	2.9586	3.0655	3.2116	3.1360	3.3602	3.3255
9:55		3.1088	3.1255	2.9401	2.8512	2.7917	2.8662	2.9667	3.0680	3.2167	3.1399	3.3635	3.3283
9:56		3.1015	3.1155	2.9362	2.8551	2.7842	2.8609	2.9612	3.0629	3.2108	3.1344	3.3582	3.3233
9:57		3.1211	3.1375	2.9600	2.8715	2.8049	2.8794	2.9784	3.0845	3.2314	3.1537	3.3773	3.3423
9:58		3.1017	3.1199	2.9299	2.8629	2.7840	2.8609	2.9591	3.0644	3.2130	3.1419	3.3595	3.3259
9:59		3.0995	3.1077	2.9257	2.8328	2.7724	2.8478	2.9491	3.0544	3.2014	3.1279	3.3487	3.3151
10:00		3.1148	3.1336	2.9550	2.8723	2.8026	2.8779	2.9770	3.0818	3.2272	3.1525	3.3794	3.3392
10:01		3.0474	3.1074	2.9299	2.8376	2.7737	2.8468	2.9472	3.0501	3.1972	3.1208	3.3420	3.3090
10:02		3.1090	3.1292	2.9528	2.8650	2.7930	2.8694	2.9688	3.0747	3.2226	3.1437	3.3694	3.3355
10:03		3.0996	3.1190	2.9321	2.8505	2.7794	2.8536	2.9572	3.0645	3.2100	3.1344	3.3598	3.3257
10:04		3.1434	3.1618	2.9789	2.8920	2.8248	2.8995	2.9991	3.1014	3.2531	3.1744	3.4035	3.3650
10:05	93,500 gal.	3.0999	3.1166	2.9405	2.8472	2.7820	2.8580	2.9569	3.0608	3.2091	3.1350	3.3575	3.3230
10:06		3.0890	3.1074	2.9190	2.8396	2.7732	2.8486	2.9473	3.0525	3.1999	3.1227	3.3476	3.3145
10:07		3.1101	3.1268	2.9369	2.8604	2.7960	2.8687	2.9662	3.0728	3.2183	3.1422	3.3652	3.3321
10:08		3.1081	3.1276	2.9483	2.8511	2.7910	2.8636	2.9652	3.0697	3.2176	3.1374	3.3640	3.3293
10:09		3.1106	3.1285	2.9458	2.8661	2.7968	2.8703	2.9714	3.0754	3.2223	3.1441	3.3607	3.3364
10:10		3.1200	3.1413	2.9578	2.8725	2.8084	2.8817	2.9815	3.0870	3.2365	3.1577	3.3821	3.3485
10:11		3.1212	3.1409	2.9570	2.8727	2.8094	2.8817	2.9793	3.0816	3.2315	3.1529	3.3781	3.3440
10:12		3.1047	3.1236	2.9476	2.8475	2.7859	2.8601	2.9631	3.0647	3.2299	3.1339	3.3566	3.3262
10:13		3.1107	3.1289	2.9400	2.8636	2.7943	2.8711	2.9693	3.0779	3.2220	3.1466	3.3695	3.3348
10:14		3.1093	3.1290	2.9370	2.8627	2.7905	2.8681	2.9684	3.0699	3.2192	3.1429	3.3678	3.3316
10:15		3.1066	3.1225	2.9412	2.8562	2.7852	2.8634	2.9612	3.0641	3.2120	3.1357	3.3590	3.3258
10:16		3.1039	3.1222	2.9425	2.8554	2.7883	2.8618	2.9605	3.0653	3.2112	3.1364	3.3588	3.3266
10:17		3.0948	3.1143	2.9331	2.8462	2.7798	2.8566	2.9562	3.0578	3.2069	3.1336	3.3547	3.3209
10:18		3.1047	3.1210	2.9427	2.8562	2.7944	2.8669	2.9649	3.0697	3.2206	3.1415	3.3679	3.3329
10:19		3.1168	3.1366	2.9641	2.8719	2.8037	2.8785	2.9792	3.0812	3.2293	3.1504	3.3757	3.3411
10:20		3.1248	3.1462	2.9664	2.8843	2.8104	2.8887	2.9872	3.0908	3.2395	3.1609	3.3861	3.3507
10:21		3.1255	3.1442	2.9644	2.8799	2.8094	2.8895	2.9866	3.0919	3.2379	3.1591	3.3866	3.3500
10:22		3.1091	3.1330	2.9468	2.8634	2.7962	2.8759	2.9740	3.0781	3.2232	3.1471	3.3712	3.3374
10:23		3.1132	3.1321	2.9439	2.8616	2.7972	2.8755	2.9725	3.0758	3.2243	3.1510	3.3724	3.3374
10:24		3.0950	3.1146	2.9341	2.8465	2.7810	2.8575	2.9553	3.0598	3.2076	3.1235	3.3549	3.3217

UGR File #c073/A77, part 2
SAND-77-1992
Oct 1976-Sept. 1977

TABLE II (Continued)

GPE NATURAL BUTTES NO.20-HYDROFRACTURE

FRACTURE-JUNE 22,1977

TIME		0°	15°	30°	45°	60°	75°	90°	105°	120°	135°	150°	165°
10:25		3.1070	3.1287	2.9556	2.8605	2.8002	2.8692	2.9687	3.0741	3.2208	3.1448	3.3671	3.3337
10:26		3.1406	3.1617	2.9775	2.8934	2.8298	2.9021	3.0035	3.1345	3.2547	3.1720	3.4000	3.3639
10:27		3.1178	3.1373	2.9547	2.8688	2.8111	2.8839	2.9813	3.0859	3.2331	3.1557	3.3779	3.3430
10:28		3.1008	3.1216	2.9372	2.8574	2.7865	2.8655	2.9616	3.0672	3.2141	3.1359	3.3612	3.3281
10:29		3.1262	3.1472	2.9635	2.8763	2.8085	2.8881	2.9853	3.0903	3.2377	3.1589	3.3334	3.3004
10:30		3.0972	3.1142	2.9394	2.8467	2.7886	2.8638	2.9620	3.0674	3.2132	3.1382	3.3629	3.3260
10:31		3.1247	3.1319	2.9536	2.8612	2.7982	2.8729	2.9736	3.0761	3.2229	3.1432	3.3700	3.3373
10:32		3.1139	3.1312	2.9499	2.8622	2.8003	2.8775	2.9758	3.0922	3.2207	3.1492	3.3739	3.3400
10:33		3.1384	3.1269	2.9448	2.8655	2.7961	2.8710	2.9710	3.0765	3.2229	3.1463	3.3698	3.3359
10:34		3.1096	3.1299	2.9433	2.8593	2.7950	2.8714	2.9671	3.0759	3.2205	3.1406	3.3662	3.3311
10:35		3.0957	3.1129	2.9336	2.8506	2.7812	2.8583	2.9566	3.0636	3.2072	3.1292	3.3551	3.3216
10:36		3.1084	3.1270	2.9494	2.8571	2.7986	2.8735	2.9725	3.0761	3.2217	3.1417	3.3678	3.3356
10:37		3.1050	3.1242	2.9410	2.8533	2.7895	2.8676	2.9643	3.0708	3.2161	3.1379	3.3619	3.3289
10:38		3.1033	3.1235	2.9417	2.8524	2.7867	2.8684	2.9655	3.0708	3.2181	3.1407	3.3628	3.3326
10:39	148.000 gal.	3.1108	3.1318	2.9485	2.8575	2.7975	2.8721	2.9699	3.0784	3.2215	3.1443	3.3682	3.3359
10:40		3.1319	3.1557	2.9644	2.8803	2.8164	2.8357	2.9916	3.0973	3.2442	3.1674	3.3927	3.3588
10:41		3.1004	3.1219	2.9364	2.8483	2.7825	2.8519	2.9568	3.0631	3.2073	3.1322	3.3552	3.3222
10:42		3.1017	3.1205	2.9388	2.8493	2.7868	2.8640	2.9619	3.0672	3.2131	3.1339	3.3599	3.3243
10:43		3.0930	3.1162	2.9311	2.8484	2.7769	2.8585	2.9550	3.0595	3.2052	3.1290	3.3516	3.3235
10:44		3.0995	3.1129	2.9278	2.8433	2.7785	2.8534	2.9482	3.0553	3.2003	3.1220	3.3478	3.3136
10:45		3.1014	3.1217	2.9365	2.8544	2.7864	2.8647	2.9602	3.0656	3.2107	3.1322	3.3580	3.3248
10:46		3.1187	3.1375	2.9552	2.8733	2.8025	2.8902	2.9742	3.0827	3.2265	3.1498	3.3743	3.3405
10:47		3.1002	3.1238	2.9364	2.8553	2.7862	2.8625	2.9589	3.0653	3.2082	3.1323	3.3584	3.3242
10:48		3.0966	3.1156	2.9375	2.8482	2.7820	2.8581	2.9537	3.0596	3.2041	3.1254	3.3507	3.3177
10:49		3.1145	3.1356	2.9640	2.8648	2.7973	2.8761	2.9725	3.0772	3.2233	3.1457	3.3725	3.3381
10:50		3.1027	3.1228	2.9378	2.8492	2.7864	2.8632	2.9607	3.0671	3.2118	3.1327	3.3573	3.3267
10:51		3.0966	3.1043	2.9249	2.8360	2.7717	2.8495	2.9444	3.0500	3.1951	3.1181	3.3436	3.3108
10:52		3.1021	3.1228	2.9377	2.8518	2.7811	2.8628	2.9598	3.0644	3.2087	3.1305	3.3570	3.3246
10:53		3.1061	3.1257	2.9417	2.8579	2.7951	2.8717	2.9659	3.0753	3.2195	3.1413	3.3661	3.3329
10:54		3.1135	3.1319	2.9427	2.8614	2.7981	2.8748	2.9701	3.0768	3.2212	3.1474	3.3713	3.3386
10:55		3.1025	3.1192	2.9362	2.8461	2.7353	2.8605	2.9563	3.0641	3.2099	3.1306	3.3569	3.3224
10:56		3.0987	3.1177	2.9358	2.8452	2.7425	2.8594	2.9539	3.0628	3.2072	3.1294	3.3534	3.3195
10:57		3.1064	3.1256	2.9570	2.8519	2.7878	2.8686	2.9629	3.0745	3.2168	3.1368	3.3653	3.3326
10:58		3.1138	3.1323	2.9401	2.8627	2.8025	2.8792	2.9740	3.0813	3.2236	3.1459	3.3722	3.3337
10:59		3.0991	3.1084	2.9152	2.8361	2.7708	2.8405	2.9469	3.0530	3.1973	3.1218	3.3472	3.3133
11:00		3.1051	3.1244	2.9282	2.8540	2.7878	2.8651	2.9621	3.0701	3.2135	3.1364	3.3657	3.3281
11:01		3.0988	3.1205	2.9337	2.8505	2.7848	2.8612	2.9576	3.0651	3.2084	3.1319	3.3579	3.3210
11:02		3.1261	3.1461	2.9609	2.8714	2.8067	2.8834	2.9792	3.0875	3.2329	3.1564	3.3825	3.3473
11:03		3.1151	3.1344	2.9515	2.8618	2.8041	2.8767	2.9710	3.0805	3.2246	3.1453	3.3729	3.3393
11:04		3.1147	3.1374	2.9549	2.8671	2.8033	2.8814	2.9756	3.0840	3.2278	3.1535	3.3793	3.3424
11:05		3.1070	3.1279	2.9402	2.8485	2.7894	2.8662	2.9629	3.0692	3.2152	3.1352	3.3642	3.3306
11:06		3.1084	3.1269	2.9436	2.8538	2.7932	2.8678	2.9645	3.0726	3.2171	3.1405	3.3658	3.3329
11:07		3.1230	3.1436	2.9615	2.8698	2.8058	2.8822	2.9771	3.0860	3.2332	3.1545	3.3806	3.3464

SAND-77-1992
Oct. 1976-Sept. 1977

TABLE II (Continued)

GPE NATURAL BUTTES NO.20-HYDROFRACTURE

FRACTURE-JUNE 22,1977

TIME		0°	15°	30°	45°	60°	75°	90°	105°	120°	135°	150°	165°
11:08		3.1107	3.1277	2.9459	2.8594	2.7929	2.8700	2.9656	3.0740	3.2174	3.1385	3.3666	3.3328
11:09		3.1241	3.1424	2.9567	2.8694	2.8039	2.8310	2.9754	3.0879	3.2289	3.1536	3.3785	3.3427
11:10		3.1113	3.1276	2.9481	2.8545	2.7939	2.8696	2.9659	3.0745	3.2183	3.1414	3.3676	3.3332
11:11		3.0975	3.1158	2.9307	2.8481	2.7826	2.8566	2.9512	3.0598	3.2043	3.1266	3.3536	3.3196
11:12		3.0819	3.1041	2.9181	2.8308	2.7639	2.8441	2.9391	3.0473	3.1922	3.1122	3.3335	3.3052
11:13		3.1040	3.1236	2.9382	2.8495	2.7809	2.8638	2.9536	3.0697	3.2127	3.1315	3.3598	3.3258
11:14		3.0949	3.1063	2.9191	2.8312	2.7689	2.8446	2.9415	3.0518	3.1946	3.1195	3.3444	3.3124
11:15		3.1161	3.1362	2.9516	2.8641	2.8008	2.8773	2.9722	3.0821	3.2259	3.1470	3.3739	3.3385
11:16		3.0977	3.1195	2.9304	2.8411	2.7759	2.8559	2.9520	3.0611	3.2046	3.1291	3.3556	3.3206
11:17		3.0833	3.1063	2.9182	2.8305	2.7713	2.8429	2.9384	3.0471	3.1898	3.1147	3.3394	3.3044
11:18		3.1009	3.1180	2.9341	2.8495	2.7863	2.8619	2.9561	3.0667	3.2078	3.1290	3.3572	3.3208
11:19		3.0972	3.1167	2.9266	2.8451	2.7832	2.8590	2.9526	3.0625	3.2028	3.1281	3.3531	3.3199
11:20		3.1312	3.1514	2.9694	2.8812	2.8172	2.8948	2.9891	3.0993	3.2426	3.1643	3.3889	3.3536
11:21		3.0933	3.1102	2.9255	2.8375	2.7724	2.8510	2.9469	3.0577	3.2006	3.1235	3.3509	3.3157
11:22		3.0860	3.1062	2.9220	2.8365	2.7758	2.8487	2.9414	3.0538	3.1935	3.1167	3.3445	3.3107
11:23		3.1142	3.1362	2.9508	2.8632	2.7960	2.8754	2.9691	3.0783	3.2221	3.1421	3.3702	3.3156
11:24		3.0942	3.1129	2.9271	2.8424	2.7800	2.8570	2.9487	3.0620	3.2032	3.1256	3.3528	3.3189
11:25		3.0902	3.1066	2.9218	2.8358	2.7751	2.8495	2.9431	3.0549	3.1944	3.1195	3.3447	3.3117
11:26		3.1177	3.1329	2.9529	2.8616	2.8013	2.8771	2.9700	3.0816	3.2240	3.1476	3.3743	3.3379
11:27		3.1207	3.1372	2.9547	2.8662	2.8063	2.8799	2.9729	3.0826	3.2239	3.1454	3.3723	3.3363
11:28		3.1187	3.1381	2.9533	2.8675	2.8033	2.8785	2.9753	3.0841	3.2275	3.1495	3.3773	3.3412
11:29		3.0917	3.1121	2.9304	2.8419	2.7751	2.8529	2.9444	3.0575	3.1993	3.1218	3.3496	3.3144
11:30		3.1255	3.1418	2.9592	2.8693	2.8108	2.8341	2.9770	3.0870	3.2310	3.1543	3.3913	3.3442
11:31		3.1083	3.1259	2.9408	2.8528	2.7931	2.8631	2.9616	3.0702	3.2173	3.1413	3.3654	3.3301
11:32		3.0953	3.1140	2.9304	2.8410	2.7790	2.8556	2.9487	3.0629	3.1999	3.1251	3.3499	3.3156
11:33		3.0963	3.1157	2.9329	2.8404	2.7761	2.8557	2.9509	3.0621	3.2045	3.1312	3.3527	3.3191
11:34	239,000 gal.	3.1046	3.1281	2.9424	2.8533	2.7951	2.8711	2.9640	3.0738	3.2145	3.1354	3.3551	3.3278
11:35		3.1240	3.1436	2.9552	2.8673	2.8094	2.8824	2.9774	3.0873	3.2286	3.1527	3.3788	3.3439
11:36		3.0967	3.1151	2.9279	2.8439	2.7781	2.8572	2.9506	3.0609	3.2001	3.1247	3.3504	3.3136
11:37		3.1099	3.1305	2.9449	2.8547	2.7946	2.8717	2.9657	3.0779	3.2186	3.1397	3.3681	3.3314
11:38		3.1357	3.1551	2.9684	2.8795	2.8213	2.8988	2.9904	3.1032	3.2440	3.1626	3.3927	3.3558
11:39		3.1189	3.1373	2.9519	2.8625	2.8013	2.8778	2.9715	3.0832	3.2242	3.1444	3.3720	3.3375
11:40		3.1648	3.1821	2.9933	2.9062	2.8484	2.9248	3.0170	3.1308	3.2727	3.1934	3.4239	3.3845
11:41		3.1158	3.1344	2.9592	2.8613	2.7980	2.8752	2.9690	3.0817	3.2225	3.1442	3.3725	3.3364
11:42		3.1236	3.1453	2.9571	2.8719	2.8026	2.8829	2.9749	3.0862	3.2303	3.1502	3.3782	3.3412
11:43		3.1246	3.1450	2.9669	2.8733	2.8128	2.8870	2.9781	3.0901	3.2347	3.1554	3.3824	3.3442
11:44		3.1074	3.1254	2.9273	2.8542	2.7921	2.8685	2.9613	3.0711	3.2153	3.1379	3.3669	3.3290
11:45		3.1302	3.1523	2.9766	2.8779	2.8171	2.8947	2.9863	3.0976	3.2387	3.1623	3.3897	3.3517
11:46		3.1075	3.1239	2.9412	2.8531	2.7930	2.8686	2.9600	3.0742	3.2146	3.1382	3.3659	3.3285
11:47		3.1106	3.1274	2.9464	2.8539	2.7956	2.8719	2.9629	3.0767	3.2178	3.1394	3.3675	3.3307
11:48		3.1291	3.1516	2.9527	2.8779	2.8198	2.8916	2.9852	3.0978	3.2385	3.1626	3.3922	3.3529
11:49		3.1075	3.1259	2.9454	2.8523	2.7870	2.8692	2.9618	3.0705	3.2132	3.1349	3.3628	3.3280
11:50		3.1069	3.1257	2.9426	2.8482	2.7941	2.8678	2.9620	3.0716	3.2101	3.1310	3.3634	3.3256

UGR File #c073/A77, part 2
SAND-77-1992
Oct. 1976-Sept. 1977

TABLE II (Continued)

GPE NATURAL BUTTES NO.20-HYDROFRACTURE

FRACTURE-JUNE 22,1977

TIME		0°	15°	30°	45°	60°	75°	90°	105°	120°	135°	150°	165°
11:51		3.1014	3.1212	2.9341	2.8462	2.7841	2.8632	2.9561	3.0675	3.2089	3.1302	3.3607	3.3247
11:52		3.1163	3.1368	2.9458	2.8685	2.8022	2.8775	2.9697	3.0803	3.2202	3.1450	3.3721	3.3351
11:53		3.1092	3.1261	2.9429	2.8564	2.7902	2.8707	2.9615	3.0742	3.2157	3.1384	3.3670	3.3312
11:54		3.1064	3.1276	2.9424	2.8519	2.7950	2.8709	2.9604	3.0757	3.2155	3.1362	3.3674	3.3298
11:55		3.1167	3.1386	2.9507	2.8669	2.8086	2.8803	2.9705	3.0926	3.2261	3.1503	3.3760	3.3401
11:56		3.0933	3.1131	2.9391	2.8416	2.7823	2.8593	2.9477	3.0616	3.2016	3.1235	3.3526	3.3178
11:57		3.1069	3.1276	2.9439	2.8532	2.7951	2.8691	2.9599	3.0746	3.2149	3.1366	3.3662	3.3232
11:58		3.1229	3.1427	2.9667	2.8660	2.8075	2.8828	2.9743	3.0879	3.2289	3.1495	3.3799	3.3412
11:59		3.1187	3.1386	2.9509	2.8625	2.7986	2.8760	2.9677	3.0850	3.2237	3.1458	3.3756	3.3377
12:00		3.0973	3.1087	2.9204	2.8346	2.7755	2.8481	2.9407	3.0510	3.1918	3.1149	3.3423	3.3063
12:01		3.1136	3.1328	2.9472	2.8585	2.7971	2.8743	2.9646	3.0780	3.2188	3.1412	3.3692	3.3351
12:02		3.1334	3.1535	2.9695	2.8731	2.8173	2.8912	2.9843	3.0977	3.2399	3.1621	3.3832	3.3525
12:03		3.1163	3.1367	2.9574	2.8650	2.8085	2.8785	2.9832	3.0843	3.2268	3.1472	3.3761	3.3382
12:04		3.1041	3.1296	2.9410	2.8578	2.7943	2.8637	2.9627	3.0753	3.2164	3.1366	3.3663	3.3237
12:05		3.1033	3.1238	2.9367	2.8478	2.7937	2.8656	2.9573	3.0699	3.2110	3.1336	3.3627	3.3252
12:06		3.1076	3.1264	2.9418	2.8471	2.7961	2.8699	2.9586	3.0747	3.2172	3.1374	3.3695	3.3316
12:07		3.0942	3.1124	2.9280	2.8381	2.7782	2.8549	2.9457	3.0558	3.1967	3.1200	3.3476	3.3135
12:08		3.1117	3.1320	2.9459	2.8575	2.7997	2.8725	2.9621	3.0741	3.2165	3.1385	3.3693	3.3326
12:09		3.1185	3.1409	2.9526	2.8603	2.8006	2.8792	2.9698	3.0818	3.2252	3.1472	3.3759	3.3379
12:10		3.1264	3.1471	2.9599	2.8713	2.8192	2.8895	2.9816	3.0973	3.2357	3.1578	3.3859	3.3445
12:11		3.0964	3.1231	2.9399	2.8521	2.7891	2.8634	2.9554	3.0674	3.2083	3.1267	3.3580	3.3209
12:12		3.1157	3.1366	2.9501	2.8641	2.8021	2.8772	2.9673	3.0816	3.2250	3.1462	3.3744	3.3373
12:13		3.1002	3.1216	2.9363	2.8463	2.7868	2.8614	2.9525	3.0676	3.2049	3.1267	3.3553	3.3179
12:14		3.1190	3.1393	2.9441	2.8587	2.7961	2.8741	2.9640	3.0206	3.2195	3.1410	3.3697	3.3305
12:15		3.1483	3.1737	2.9834	2.8661	2.8356	2.9146	3.0143	3.1240	3.2644	3.1858	3.4151	3.3769
12:16		3.1166	3.1355	2.9506	2.8619	2.8036	2.8767	2.9673	3.0831	3.2231	3.1420	3.3735	3.3382
12:17		3.1215	3.1328	2.9378	2.8506	2.7986	2.8725	2.9623	3.0768	3.2164	3.1367	3.3687	3.3319
12:18		3.1294	3.1514	2.9609	2.8708	2.8094	2.8901	2.9773	3.0939	3.2337	3.1553	3.3862	3.3474
12:19		3.1160	3.1396	2.9312	2.8642	2.8073	2.8814	2.9705	3.0828	3.2217	3.1443	3.3759	3.3361
12:20		3.1133	3.1334	2.9459	2.8568	2.7978	2.8748	2.9643	3.0812	3.2196	3.1432	3.3717	3.3355
12:21		3.1135	3.1336	2.9474	2.8640	2.7979	2.8747	2.9644	3.0804	3.2188	3.1413	3.3724	3.3315
12:22		3.1083	3.1303	2.9445	2.8522	2.7926	2.8727	2.9622	3.0757	3.2148	3.1423	3.3665	3.3294
12:23		3.1269	3.1490	2.9529	2.8721	2.8169	2.8931	2.9824	3.0961	3.2357	3.1562	3.3888	3.3477
12:24		3.1237	3.1465	2.9580	2.8691	2.8127	2.8866	2.9761	3.0906	3.2302	3.1516	3.3840	3.3444
12:25	327,000 gal.	3.1263	3.1478	2.9581	2.8764	2.8144	2.8958	2.9788	3.0935	3.2328	3.1523	3.3829	3.3443
12:26		3.1336	3.1550	2.9650	2.8723	2.8152	2.8922	2.9836	3.0966	3.2399	3.1613	3.3926	3.3532
12:27		3.1207	3.1419	2.9555	2.8676	2.8094	2.8828	2.9722	3.0870	3.2262	3.1483	3.3825	3.3434
12:28		3.1247	3.1472	2.9561	2.8711	2.8083	2.8887	2.9701	3.0930	3.2333	3.1544	3.3854	3.3462
12:29		3.1122	3.1320	2.9467	2.8473	2.7976	2.8722	2.9656	3.0822	3.2181	3.1398	3.3699	3.3322
12:30		3.1332	3.1546	2.9661	2.8755	2.8202	2.8983	2.9871	3.1016	3.2434	3.1653	3.3959	3.3571
12:31		3.1336	3.1630	2.9716	2.8600	2.8225	2.9010	2.9927	3.1060	3.2522	3.1712	3.4024	3.3639
12:32		3.1315	3.1534	2.9633	2.8731	2.8161	2.8966	2.9826	3.0983	3.2372	3.1596	3.3945	3.3554
12:33		3.1369	3.1597	2.9689	2.8845	2.8197	2.8983	2.9887	3.1060	3.2453	3.1686	3.3970	3.3591

TABLE II (Continued)

GPE NATURAL BUTTES NO.20-HYDROFRACTURE

FRACTURE-JUNE 22,1977

TIME		0°	15°	30°	45°	60°	75°	90°	105°	120°	135°	150°	165°
12:34		3.1106	3.1347	2.9453	2.8565	2.7956	2.8738	2.9632	3.0785	3.2179	3.1407	3.3735	3.3334
12:35		3.1497	3.1754	2.9836	2.8891	2.8372	2.9109	3.0009	3.1188	3.2594	3.1800	3.4076	3.3737
12:36		3.1745	3.1965	3.0053	2.9221	2.8551	2.9324	3.0251	3.1403	3.2853	3.2046	3.4368	3.3967
12:37		3.1526	3.1764	2.9368	2.8908	2.8365	2.9133	3.0037	3.1200	3.2634	3.1839	3.4165	3.3774
12:38		3.1206	3.1451	2.9546	2.8648	2.8049	2.8803	2.9709	3.0860	3.2293	3.1590	3.3813	3.3426
12:39		3.1118	3.1307	2.9444	2.8540	2.7899	2.8700	2.9588	3.0739	3.2182	3.1394	3.3690	3.3315
12:40		3.0788	3.1031	2.9128	2.8311	2.7648	2.8393	2.9316	3.0425	3.1851	3.1058	3.3345	3.2973
12:41		3.1025	3.1258	2.9369	2.8478	2.7878	2.8626	2.9553	3.0681	3.2088	3.1297	3.3577	3.3219
12:42		3.0987	3.1208	2.9347	2.8464	2.7835	2.8591	2.9492	3.0614	3.2030	3.1249	3.3532	3.3167
12:43		3.0884	3.1115	2.9211	2.8313	2.7781	2.8492	2.9409	3.0529	3.1941	3.1169	3.3458	3.3086
12:44		3.1175	3.1371	2.9500	2.8573	2.8017	2.8746	2.9667	3.0825	3.2187	3.1408	3.3704	3.3333
12:45		3.1361	3.1578	2.9664	2.8726	2.8180	2.8949	2.9855	3.1026	3.2437	3.1668	3.3964	3.3576
12:46		3.0854	3.1083	2.9227	2.8362	2.7761	2.8504	2.9427	3.0562	3.1967	3.1172	3.3452	3.3092
12:47		3.1191	3.1411	2.9538	2.8659	2.8057	2.8782	2.9674	3.0826	3.2221	3.1407	3.3721	3.3327
12:48	Shut down	3.1080	3.1288	2.9400	2.8510	2.7926	2.8691	2.9586	3.0752	3.2121	3.1352	3.3654	3.3269
12:49	362,000 gal. (Total Vol.)	3.1177	3.1400	2.9547	2.8613	2.8003	2.8778	2.9668	3.0823	3.2247	3.1443	3.3771	3.3371
12:50		3.1023	3.1242	2.9369	2.8476	2.7853	2.8639	2.9528	3.0664	3.2095	3.1308	3.3617	3.3256
12:51		3.1269	3.1494	2.9574	2.8700	2.8091	2.8844	2.9762	3.0904	3.2303	3.1509	3.3825	3.3454
12:52		3.0826	3.1038	2.9151	2.8213	2.7714	2.8446	2.9333	3.0517	3.1886	3.1104	3.3400	3.3025
12:53		3.1058	3.1260	2.9402	2.8479	2.7969	2.8646	2.9573	3.0707	3.2134	3.1355	3.3639	3.3229
12:54		3.1195	3.1400	2.9526	2.8506	2.8048	2.8776	2.9708	3.0847	3.2259	3.1466	3.3776	3.3389
12:55		3.0914	3.1135	2.9256	2.8361	2.7811	2.8549	2.9458	3.0632	3.2007	3.1226	3.3521	3.3152
12:56		3.1092	3.1308	2.9434	2.8526	2.7932	2.8656	2.9588	3.0774	3.2141	3.1372	3.3626	3.3298
12:57		3.1104	3.1308	2.9444	2.8484	2.7968	2.8715	2.9613	3.0742	3.2161	3.1374	3.3672	3.3267
12:58		3.0614	3.0835	2.8980	2.8042	2.7508	2.8275	2.9159	3.0253	3.1701	3.0926	3.3142	3.2337
12:59		3.0565	3.0767	2.8909	2.8043	2.7503	2.8202	2.9084	3.0202	3.1623	3.0872	3.3116	3.2747
13:00		3.0452	3.0652	2.8827	2.7930	2.7415	2.8095	2.9982	3.0142	3.1522	3.0757	3.3017	3.2650
13:01		3.0306	3.0498	2.8780	2.7758	2.7228	2.7940	2.8863	2.9984	3.1373	3.0626	3.2863	3.2521
13:02		3.0733	3.0932	2.9076	2.8176	2.7619	2.8304	2.9268	3.0435	3.1803	3.1039	3.3295	3.2937
13:03		3.0695	3.0904	2.9057	2.8136	2.7587	2.8293	2.9213	3.0342	3.1755	3.0962	3.3253	3.2889
13:04		3.0774	3.0976	2.9118	2.8232	2.7619	2.8361	2.9273	3.0400	3.1835	3.1079	3.3334	3.2958
13:05		3.0863	3.1066	2.9200	2.8325	2.7739	2.8455	2.9374	3.1523	3.1926	3.1136	3.3430	3.3026
13:06		3.0916	3.1118	2.9265	2.8322	2.7771	2.8522	2.9393	3.0561	3.1982	3.1223	3.3458	3.3064
13:07		3.0815	3.1038	2.9155	2.8234	2.7695	2.8403	2.9322	3.0482	3.1882	3.1128	3.3395	3.3005

SAND-77-1992
Oct. 1976-Sept. 1977

TABLE II (Continued)

GPE NATURAL BUTTES NO.20-HYDROFRACTURE

FRACTURE-JUNE 22,1977

TIME	180°	195°	210°	225°	240°	255°	270°	285°	300°	315°	330°	345°
8:05	3.3952	3.2709	3.4162	3.4224	3.0666	3.1067	3.1822	3.1980	3.2081	2.9537	3.1255	3.1434
8:05	3.4029	3.2759	3.4202	3.4275	3.0651	3.1113	3.1879	3.1129	3.2021	2.9588	3.1298	3.1437
8:07	3.3949	3.2684	3.4136	3.4196	3.0595	3.1055	3.1822	3.1074	3.2002	2.9548	3.1253	3.1429
8:08	3.4004	3.2760	3.4211	3.4291	3.0665	3.1106	3.1875	3.1124	3.2043	2.9594	3.1297	3.1493
8:09	3.3975	3.2696	3.4158	3.4225	3.0592	3.1045	3.1811	3.1061	3.1981	2.9537	3.1223	3.1399
8:10	3.3995	3.2724	3.4182	3.4243	3.0626	3.1082	3.1852	3.1097	3.2020	2.9571	3.1283	3.1506
8:11	3.4020	3.2753	3.4220	3.4288	3.0655	3.1117	3.1896	3.1138	3.2076	2.9615	3.1324	3.1512
8:12	3.4047	3.2780	3.4237	3.4297	3.0671	3.1127	3.1897	3.1147	3.2069	2.9625	3.1321	3.1513
8:13	3.4067	3.2805	3.4270	3.4347	3.0716	3.1163	3.1954	3.1192	3.2140	2.9655	3.1427	3.1563
8:14	3.3981	3.2730	3.4183	3.4262	3.0636	3.1090	3.1860	3.1127	3.2064	2.9570	3.1284	3.1488
8:15	3.3986	3.2729	3.4202	3.4262	3.0653	3.1113	3.1833	3.1147	3.2073	2.9619	3.1338	3.1546
8:16	3.3964	3.2712	3.4177	3.4260	3.0638	3.1095	3.1851	3.1122	3.2052	2.9581	3.1247	3.1469
8:17	3.4062	3.2788	3.4293	3.4333	3.0697	3.1143	3.1928	3.1190	3.2095	2.9643	3.1351	3.1562
8:18	3.4091	3.2834	3.4295	3.4383	3.0739	3.1193	3.1985	3.1219	3.2132	2.9686	3.1405	3.1617
8:19	3.3816	3.2607	3.4049	3.4128	3.0522	3.0985	3.1745	3.1322	3.1394	2.9474	3.1194	3.1361
8:20	3.3947	3.2681	3.4157	3.4230	3.0599	3.1067	3.1842	3.1091	3.1955	2.9554	3.1275	3.1448
8:21	3.3912	3.2651	3.4114	3.4194	3.0579	3.1046	3.1825	3.1073	3.1950	2.9498	3.1224	3.1426
8:22	3.3916	3.2656	3.4114	3.4210	3.0591	3.1038	3.1821	3.1071	3.1954	2.9520	3.1222	3.1426
8:23	3.3946	3.2677	3.4131	3.4219	3.0587	3.1062	3.1823	3.1093	3.1982	2.9545	3.1272	3.1447
8:24	3.3985	3.2719	3.4175	3.4260	3.0625	3.1088	3.1866	3.1128	3.2024	2.9589	3.1302	3.1485
8:25	3.4002	3.2735	3.4196	3.4286	3.0645	3.1110	3.1883	3.1155	3.2035	2.9612	3.1336	3.1514
8:26	3.4001	3.2737	3.4209	3.4286	3.0646	3.1119	3.1896	3.1150	3.2024	2.9582	3.1337	3.1527
8:27	3.4004	3.2738	3.4202	3.4277	3.0653	3.1114	3.1895	3.1155	3.2049	2.9594	3.1331	3.1526
8:28	3.4043	3.2768	3.4229	3.4331	3.0686	3.1126	3.1917	3.1173	3.2080	2.9619	3.1365	3.1536
8:29	3.3963	3.2690	3.4143	3.4240	3.0612	3.1073	3.1857	3.1107	3.1987	2.9563	3.1292	3.1483
8:30	3.3976	3.2725	3.4190	3.4271	3.0634	3.1092	3.1869	3.1114	3.1996	2.9573	3.1284	3.1465
8:31	3.3997	3.2719	3.4191	3.4262	3.0640	3.1098	3.1846	3.1141	3.2031	2.9593	3.1351	3.1542
8:32	3.4053	3.2774	3.4237	3.4335	3.0695	3.1137	3.1932	3.1176	3.2074	2.9649	3.1372	3.1563
8:33	3.3975	3.2714	3.4183	3.4275	3.0617	3.1079	3.1863	3.1114	3.2026	2.9574	3.1295	3.1485
8:34	3.3983	3.2714	3.4174	3.4268	3.0628	3.1086	3.1863	3.1122	3.2014	2.9563	3.1302	3.1501
8:35	3.3899	3.2637	3.4113	3.4190	3.0562	3.1025	3.1804	3.1061	3.1939	2.9518	3.1234	3.1434
8:36	3.3984	3.2728	3.4189	3.4293	3.0643	3.1085	3.1865	3.1119	3.2054	2.9572	3.1297	3.1476
8:37	3.3956	3.2634	3.4087	3.4199	3.0542	3.0997	3.1783	3.1044	3.1932	2.9496	3.1223	3.1388
8:38	3.3938	3.2661	3.4127	3.4228	3.0569	3.1043	3.1812	3.1076	3.1977	2.9546	3.1267	3.1464
8:39	3.4059	3.2795	3.4247	3.4361	3.0715	3.1169	3.1949	3.1200	3.2124	2.9643	3.1391	3.1574
8:40	3.4013	3.2739	3.4213	3.4325	3.0650	3.1104	3.1879	3.1145	3.2015	2.9573	3.1325	3.1519
8:41	3.3946	3.2661	3.4119	3.4210	3.0575	3.1042	3.1839	3.1058	3.1967	2.9505	3.1254	3.1447
8:42	3.3928	3.2701	3.4159	3.4279	3.0617	3.1066	3.1836	3.1102	3.1992	2.9545	3.1285	3.1472
8:43	3.3879	3.2636	3.4053	3.4165	3.0521	3.0982	3.1755	3.1007	3.1939	2.9466	3.1175	3.1374
8:44	3.3797	3.2542	3.3990	3.4074	3.0464	3.0931	3.1731	3.0970	3.1823	2.9411	3.1130	3.1323
8:45	3.3944	3.2671	3.4120	3.4216	3.0578	3.1033	3.1799	3.1072	3.1950	2.9503	3.1237	3.1428
8:57	3.3950	3.2660	3.4105	3.4213	3.0555	3.1015	3.1785	3.1030	3.1941	2.9465	3.1209	3.1414
8:58	3.3984	3.2618	3.4052	3.4160	3.0517	3.0954	3.1729	3.0990	3.1891	2.9442	3.1143	3.1346

TABLE II (Continued)

GPE NATURAL BUTTES NO.20-HYDROFRACTURE

FRACTURE-JUNE 22,1977

TIME		180°	195°	210°	225°	240°	255°	270°	285°	300°	315°	330°	345°
8:59		3.3849	3.2610	3.4052	3.4202	3.0523	3.0969	3.1748	3.1011	3.1312	2.9427	3.1160	3.1354
9:00		3.3310	3.2556	3.3969	3.4093	3.0468	3.0936	3.1737	3.0969	3.1371	2.9410	3.1159	3.1344
9:01		3.3743	3.2475	3.3909	3.4006	3.0387	3.0837	3.1621	3.0883	3.1766	2.9348	3.1068	3.1268
9:02		3.3709	3.2444	3.3967	3.3993	3.0365	3.0816	3.1581	3.0851	3.1717	2.9276	3.1025	3.1209
9:03		3.3821	3.2553	3.4009	3.4147	3.0465	3.0918	3.1676	3.0932	3.1825	2.9391	3.1102	3.1322
9:04		3.3713	3.2440	3.3889	3.4038	3.0371	3.0810	3.1573	3.0842	3.1715	2.9260	3.1004	3.1175
9:05		3.3733	3.2464	3.3876	3.3981	3.0365	3.0841	3.1601	3.0856	3.1751	2.9324	3.1050	3.1268
9:06		3.3963	3.2656	3.4105	3.4256	3.0551	3.0986	3.1763	3.0990	3.1903	2.9440	3.1167	3.1359
9:07	Start pumping	3.3648	3.2383	3.3793	3.3943	3.0311	3.0755	3.1513	3.0774	3.1670	2.9232	3.0955	3.1131
9:08		3.3675	3.2413	3.3832	3.3929	3.0305	3.0773	3.1541	3.0806	3.1694	2.9245	3.0981	3.1199
9:09		3.3748	3.2479	3.3924	3.4116	3.0404	3.0836	3.1533	3.0838	3.1744	2.9274	3.1030	3.1199
9:10		3.3631	3.2382	3.3796	3.3924	3.0289	3.0753	3.1516	3.0771	3.1635	2.9213	3.0944	3.1138
9:11		3.3735	3.2457	3.3988	3.4013	3.0366	3.0814	3.1583	3.0836	3.1734	2.9278	3.1012	3.1210
9:12		3.3509	3.2273	3.3685	3.3834	3.0210	3.0646	3.1402	3.0678	3.1577	2.9111	3.0957	3.1037
9:13		3.3703	3.2453	3.3694	3.4031	3.0400	3.0358	3.1838	3.0898	3.1775	2.9350	3.1076	3.1279
9:14		3.3685	3.2430	3.3845	3.3994	3.0341	3.0785	3.1557	3.0805	3.1706	2.9238	3.0988	3.1164
9:15		3.3642	3.2383	3.3909	3.3968	3.0306	3.0756	3.1519	3.0770	3.1675	2.9201	3.0946	3.1153
9:16		3.3556	3.2298	3.3713	3.3856	3.0225	3.0681	3.1431	3.0681	3.1604	2.9124	3.0874	3.1062
9:17		3.3572	3.2311	3.3746	3.3863	3.0236	3.0675	3.1429	3.0701	3.1583	2.9128	3.0895	3.1087
9:18		3.3587	3.2251	3.3662	3.3827	3.0177	3.0622	3.1362	3.0614	3.1525	2.9066	3.0816	3.0979
9:19		3.3476	3.2234	3.3645	3.3796	3.0168	3.0628	3.1372	3.0640	3.1535	2.9074	3.0841	3.1023
9:20		3.3569	3.2312	3.3727	3.3886	3.0233	3.0679	3.1433	3.0697	3.1573	2.9131	3.0868	3.1045
9:21		3.3250	3.2003	3.3399	3.3548	2.9955	3.0376	3.1125	3.0392	3.1254	2.8907	3.0551	3.0732
9:22		3.3402	3.2155	3.3545	3.3684	3.0073	3.0533	3.1286	3.0555	3.1429	2.8997	3.0740	3.0932
9:23		3.3984	3.2692	3.4115	3.4240	3.0589	3.1061	3.1829	3.1079	3.1964	2.9514	3.1331	3.1490
9:24		3.4167	3.2839	3.4262	3.4431	3.0733	3.1186	3.1945	3.1208	3.2104	2.9629	3.1415	3.1625
9:25		3.3978	3.2599	3.4025	3.4222	3.0523	3.0968	3.1731	3.0974	3.1880	2.9416	3.1188	3.1341
9:26		3.3671	3.2424	3.3853	3.4032	3.0341	3.0808	3.1568	3.0834	3.1737	2.9252	3.1033	3.1218
9:27		3.3723	3.2451	3.3871	3.4012	3.0366	3.0839	3.1593	3.0849	3.1750	2.9300	3.1050	3.1253
9:28		3.4004	3.2719	3.4142	3.4281	3.0605	3.1065	3.1829	3.1077	3.1970	2.9497	3.1278	3.1494
9:29		3.3693	3.2438	3.3854	3.4025	3.0360	3.0819	3.1577	3.0837	3.1724	2.9308	3.1036	3.1251
9:30		3.3755	3.2488	3.3890	3.4031	3.0377	3.0852	3.1594	3.0856	3.1737	2.9295	3.1061	3.1232
9:31		3.3816	3.2537	3.3963	3.4128	3.0455	3.0904	3.1672	3.0926	3.1827	2.9331	3.1123	3.1322
9:32		3.3509	3.2239	3.3694	3.3835	3.0178	3.0618	3.1370	3.0642	3.1501	2.9056	3.0805	3.0902
9:33		3.3694	3.2338	3.3755	3.3927	3.0271	3.0737	3.1494	3.0747	3.1629	2.9204	3.0962	3.1143
9:34	42,000 gal.	3.3763	3.2512	3.3926	3.4097	3.0422	3.0870	3.1630	3.0888	3.1772	2.9311	3.1081	3.1266
9:35		3.3899	3.2547	3.3955	3.4142	3.0460	3.0916	3.1685	3.0936	3.1852	2.9367	3.1153	3.1340
9:36		3.3595	3.2344	3.3753	3.3920	3.0268	3.0704	3.1465	3.0593	3.1613	2.9169	3.0923	3.1107
9:37		3.3755	3.2462	3.3873	3.4070	3.0397	3.0855	3.1623	3.0859	3.1772	2.9319	3.1083	3.1246
9:38		3.3883	3.2609	3.4036	3.4208	3.0517	3.0978	3.1756	3.1008	3.1919	2.9473	3.1233	3.1427
9:39		3.3572	3.2320	3.3722	3.3901	3.0237	3.0679	3.1453	3.0701	3.1579	2.9134	3.0903	3.1074
9:40		3.3715	3.2437	3.3840	3.3992	3.0329	3.0823	3.1586	3.0851	3.1734	2.9311	3.1060	3.1202
9:41		3.3701	3.2431	3.3850	3.4008	3.0344	3.0793	3.1559	3.0807	3.1673	2.9250	3.0985	3.1174

USGS Open File Report 78-[illegible], part 4
SAND-77-1992
Oct. 1976-Sept. 1977

TABLE II (Continued)

GPE NATURAL BUTTES NO.20-HYDROFRACTURE

FRACTURE-JUNE 22,1977

TIME		180°	195°	210°	225°	240°	255°	270°	285°	300°	315°	330°	345°
9:42		3.3766	3.2495	3.3893	3.4073	3.0361	3.0830	3.1602	3.0856	3.1737	2.9299	3.1077	3.1264
9:43		3.3546	3.2271	3.3664	3.3872	3.0191	3.0632	3.1375	3.0546	3.1503	2.9348	3.0620	3.0934
9:44		3.3529	3.2244	3.3635	3.3783	3.0166	3.0639	3.1432	3.0661	3.1539	2.9119	3.0861	3.1074
9:45		3.3332	3.2125	3.3524	3.3699	3.0268	3.0512	3.1274	3.0538	3.1412	2.8975	3.0747	3.0929
9:46	62,000 gal.	3.3475	3.2233	3.3613	3.3814	3.0156	3.0605	3.1359	3.0617	3.1495	2.9046	3.0874	3.0946
9:47		3.3583	3.2311	3.3709	3.3889	3.0230	3.0691	3.1454	3.0739	3.1578	2.9145	3.0921	3.1081
9:48		3.3423	3.2543	3.3945	3.4145	3.0448	3.0898	3.1672	3.0924	3.1828	2.9357	3.1152	3.1344
9:49		3.3543	3.2243	3.3672	3.3850	3.0193	3.0651	3.1403	3.0663	3.1547	2.9062	3.0955	3.1157
9:50		3.3702	3.2479	3.3862	3.4038	3.0367	3.0823	3.1591	3.0851	3.1717	2.9275	3.1031	3.1225
9:51		3.3669	3.2421	3.3803	3.3975	3.0320	3.0776	3.1540	3.0796	3.1649	2.9222	3.0988	3.1186
9:52		3.3509	3.2235	3.3629	3.3799	3.0153	3.0609	3.1365	3.0629	3.1501	2.9041	3.0831	3.1027
9:53		3.3543	3.2264	3.3664	3.3850	3.0195	3.0657	3.1427	3.0681	3.1567	2.9135	3.0889	3.1083
9:54		3.3508	3.2248	3.3648	3.3850	3.0173	3.0615	3.1368	3.0621	3.1494	2.9052	3.0811	3.0967
9:55		3.3533	3.2268	3.3665	3.3849	3.0184	3.0640	3.1411	3.0660	3.1545	2.9109	3.0876	3.1052
9:56		3.3473	3.2224	3.3615	3.3804	3.0153	3.0599	3.1350	3.0617	3.1470	2.9042	3.0781	3.0973
9:57		3.3661	3.2378	3.3785	3.3981	3.0317	3.0763	3.1531	3.0789	3.1695	2.9222	3.1013	3.1209
9:58		3.3515	3.2246	3.3635	3.3837	3.0176	3.0626	3.1381	3.0630	3.1503	2.9059	3.0831	3.1019
9:59		3.3393	3.2140	3.3535	3.3709	3.0064	3.0502	3.1267	3.0522	3.1409	2.8976	3.0703	3.0931
10:00		3.3642	3.2370	3.3770	3.3950	3.0265	3.0726	3.1489	3.0748	3.1617	2.9183	3.0968	3.1142
10:01		3.3344	3.2070	3.3448	3.3650	3.0015	3.0461	3.1219	3.0481	3.1369	2.8931	3.0702	3.0864
10:02		3.3610	3.2329	3.3698	3.3870	3.0212	3.0671	3.1435	3.0687	3.1571	2.9125	3.0911	3.1102
10:03		3.3534	3.2255	3.3650	3.3827	3.0166	3.0627	3.1375	3.0629	3.1509	2.9057	3.0829	3.1012
10:04		3.3905	3.2623	3.4021	3.4240	3.0515	3.0972	3.1755	3.1008	3.1895	2.9438	3.1221	3.1417
10:05	93,500 gal.	3.3497	3.2229	3.3615	3.3818	3.0159	3.0608	3.1356	3.0620	3.1497	2.9042	3.0807	3.0993
10:06		3.3397	3.2144	3.3516	3.3715	3.0071	3.0521	3.1279	3.0537	3.1403	2.8958	3.0717	3.0836
10:07		3.3561	3.2283	3.3690	3.3877	3.0208	3.0655	3.1420	3.0682	3.1571	2.9112	3.0894	3.1083
10:08		3.3542	3.2274	3.3668	3.3853	3.0205	3.0651	3.1414	3.0683	3.1569	2.9116	3.0896	3.1101
10:09		3.3665	3.2317	3.3717	3.3914	3.0216	3.0668	3.1429	3.0694	3.1586	2.9143	3.0919	3.1092
10:10		3.3727	3.2439	3.3833	3.4014	3.0352	3.0796	3.1561	3.0820	3.1707	2.9251	3.1023	3.1226
10:11		3.3715	3.2439	3.3813	3.4008	3.0342	3.0790	3.1549	3.0810	3.1703	2.9233	3.1019	3.1235
10:12		3.3475	3.2240	3.3612	3.3795	3.0162	3.0623	3.1363	3.0641	3.1524	2.9076	3.0864	3.1045
10:13		3.3597	3.2337	3.3722	3.3908	3.0234	3.0690	3.1442	3.0709	3.1603	2.9165	3.0918	3.1109
10:14		3.3589	3.2295	3.3698	3.3875	3.0213	3.0669	3.1417	3.0699	3.1579	2.9113	3.0921	3.1093
10:15		3.3524	3.2244	3.3626	3.3825	3.0171	3.0621	3.1376	3.0647	3.1542	2.9099	3.0869	3.1052
10:16		3.3521	3.2245	3.3644	3.3843	3.0162	3.0605	3.1366	3.0643	3.1521	2.9101	3.0862	3.1027
10:17		3.3465	3.2211	3.3583	3.3785	3.0121	3.0564	3.1318	3.0574	3.1441	2.9011	3.0753	3.0932
10:18		3.3572	3.2302	3.3701	3.3882	3.0196	3.0657	3.1391	3.0650	3.1540	2.9067	3.0858	3.1035
10:19		3.3669	3.2382	3.3765	3.3960	3.0263	3.0738	3.1494	3.0758	3.1653	2.9196	3.0975	3.1152
10:20		3.3780	3.2462	3.3857	3.4044	3.0357	3.0822	3.1591	3.0828	3.1719	2.9275	3.1063	3.1246
10:21		3.3750	3.2463	3.3843	3.4034	3.0343	3.0806	3.1585	3.0824	3.1722	2.9278	3.1066	3.1249
10:22		3.3615	3.2331	3.3720	3.3899	3.0231	3.0688	3.1447	3.0692	3.1576	2.9136	3.0919	3.1115
10:23		3.3624	3.2344	3.3736	3.3920	3.0244	3.0697	3.1450	3.0711	3.1609	2.9154	3.0923	3.1130
10:24		3.3469	3.2185	3.3567	3.3742	3.0088	3.0537	3.1293	3.0558	3.1413	2.9012	3.0755	3.0944

TABLE II (Continued)

GPE NATURAL BUTTES NO.20-HYDROFRACTURE

FRACTURE-JUNE 22,1977

TIME		180°	195°	210°	225°	240°	255°	270°	285°	300°	315°	330°	345°
10:25		3.3549	3.2299	3.3675	3.3851	3.0171	3.0628	3.1382	3.1652	3.1531	2.9374	3.0872	3.1051
10:26		3.3479	3.2591	3.3986	3.4198	3.0485	3.0316	3.1682	3.1942	3.1845	2.9386	3.1182	3.1366
10:27		3.3684	3.2349	3.3753	3.3932	3.0264	3.0736	3.1486	3.1742	3.1633	2.9198	3.0994	3.1166
10:28		3.3521	3.2252	3.3632	3.3827	3.0134	3.0607	3.1353	3.1603	3.1483	2.9054	3.0849	3.1034
10:29		3.3730	3.2444	3.3941	3.4030	3.0339	3.0784	3.1555	3.0817	3.1732	2.9258	3.1061	3.1246
10:30		3.3514	3.2234	3.3621	3.3827	3.0140	3.0573	3.1327	3.0585	3.1462	2.9009	3.0833	3.0952
10:31		3.3591	3.2306	3.3680	3.3849	3.0196	3.0668	3.1420	3.0668	3.1555	2.9152	3.0908	3.1085
10:32		3.3655	3.2355	3.3757	3.3930	3.0240	3.0683	3.1431	3.0711	3.1565	2.9136	3.0927	3.1125
10:33		3.3601	3.2318	3.3716	3.3903	3.0218	3.0652	3.1414	3.0666	3.1568	2.9109	3.0900	3.1059
10:34		3.3572	3.2280	3.3676	3.3896	3.0200	3.0648	3.1390	3.0670	3.1584	2.9084	3.0890	3.1071
10:35		3.3473	3.2187	3.3564	3.3756	3.0095	3.0547	3.1288	3.0559	3.1419	2.9013	3.0794	3.0961
10:36		3.3577	3.2304	3.3682	3.3866	3.0200	3.0660	3.1405	3.0664	3.1543	2.9099	3.0892	3.1054
10:37		3.3530	3.2268	3.3658	3.3861	3.0171	3.0620	3.1373	3.0638	3.1520	2.9076	3.0862	3.1028
10:38		3.3569	3.2262	3.3662	3.3888	3.0193	3.0627	3.1363	3.0635	3.1534	2.9073	3.0859	3.1035
10:39	148,000 gal.	3.3601	3.2322	3.3656	3.3900	3.0241	3.0679	3.1441	3.0708	3.1583	2.9143	3.0918	3.1087
10:40		3.3838	3.2525	3.3879	3.4148	3.0426	3.0878	3.1632	3.0874	3.1788	2.9316	3.1127	3.1284
10:41		3.3461	3.2225	3.3534	3.3798	3.0146	3.0598	3.1344	3.0613	3.1491	2.9049	3.0815	3.1002
10:42		3.3511	3.2220	3.3554	3.3804	3.0166	3.0605	3.1359	3.0629	3.1490	2.9045	3.0862	3.1005
10:43		3.3445	3.2170	3.3508	3.3749	3.0116	3.0554	3.1334	3.0556	3.1420	2.8996	3.0755	3.0932
10:44		3.3390	3.2128	3.3445	3.3704	3.0049	3.0500	3.1259	3.0516	3.1412	2.8971	3.0749	3.0925
10:45		3.3479	3.2228	3.3547	3.3802	3.0146	3.0610	3.1369	3.0620	3.1500	2.9054	3.0828	3.1008
10:46		3.3695	3.2366	3.3691	3.3969	3.0289	3.0742	3.1520	3.0758	3.1656	2.9225	3.0992	3.1146
10:47		3.3491	3.2220	3.3544	3.3795	3.0139	3.0593	3.1354	3.0597	3.1516	2.9060	3.0858	3.1010
10:48		3.3402	3.2150	3.3462	3.3750	3.0098	3.0545	3.1312	3.0557	3.1444	2.9025	3.0804	3.0936
10:49		3.3614	3.2340	3.3679	3.3942	3.0290	3.0730	3.1457	3.0714	3.1607	2.9170	3.0961	3.1135
10:50		3.3496	3.2225	3.3546	3.3820	3.0156	3.0602	3.1364	3.0616	3.1495	2.9083	3.0833	3.0987
10:51		3.3351	3.2105	3.3414	3.3697	3.0046	3.0483	3.1239	3.0489	3.1397	2.8925	3.0712	3.0852
10:52		3.3501	3.2227	3.3564	3.3824	3.0156	3.0599	3.1359	3.0599	3.1479	2.9039	3.0853	3.1007
10:53		3.3596	3.2307	3.3627	3.3909	3.0207	3.0651	3.1411	3.0655	3.1539	2.9115	3.0878	3.1042
10:54		3.3617	3.2333	3.3682	3.3940	3.0263	3.0717	3.1478	3.0723	3.1607	2.9172	3.0954	3.1123
10:55		3.3473	3.2200	3.3526	3.3790	3.0132	3.0590	3.1347	3.0592	3.1484	2.9017	3.0813	3.0982
10:56		3.3459	3.2177	3.3520	3.3757	3.0101	3.0559	3.1323	3.0567	3.1449	2.9030	3.0806	3.0973
10:57		3.3555	3.2297	3.3630	3.3886	3.0199	3.0642	3.1392	3.0642	3.1514	2.9088	3.0871	3.1031
10:58		3.3569	3.2335	3.3673	3.3935	3.0265	3.0716	3.1493	3.0724	3.1611	2.9151	3.0974	3.1124
10:59		3.3391	3.2119	3.3450	3.3716	3.0133	3.0490	3.1244	3.0490	3.1354	2.8950	3.0759	3.0869
11:00		3.3535	3.2257	3.3590	3.3839	3.0175	3.0628	3.1372	3.0617	3.1492	2.9061	3.0828	3.1033
11:01		3.3479	3.2211	3.3530	3.3771	3.0118	3.0578	3.1331	3.0578	3.1435	2.9039	3.0826	3.0962
11:02		3.3703	3.2454	3.3798	3.4083	3.0352	3.0799	3.1560	3.0810	3.1723	2.9270	3.1235	3.1235
11:03		3.3634	3.2352	3.3662	3.3919	3.0240	3.0710	3.1465	3.0740	3.1591	2.9177	3.0978	3.1132
11:04		3.3670	3.2352	3.3752	3.3987	3.0285	3.0756	3.1530	3.0740	3.1624	2.9212	3.1000	3.1146
11:05		3.3543	3.2280	3.3621	3.3879	3.0188	3.0643	3.1397	3.0645	3.1537	2.9123	3.0839	3.1037
11:06		3.3575	3.2291	3.3634	3.3898	3.0202	3.0676	3.1423	3.0682	3.1547	2.9113	3.0917	3.1062
11:07		3.3722	3.2434	3.3783	3.4058	3.0342	3.0822	3.1576	3.0834	3.1682	2.9253	3.1034	3.1214

USR File #C075/A77, part 2
SAND-77-1992
Oct. 1976-Sept. 1977

TABLE II (Continued)

GPE NATURAL BUTTES NO.20-HYDROFRACTURE

FRACTURE-JUNE 22,1977

TIME		180°	195°	210°	225°	240°	255°	270°	285°	300°	315°	330°	345°
11:08		3.4962	3.2303	3.3637	3.3914	3.0234	3.0692	3.1450	3.0692	3.1552	2.9117	3.0952	3.1176
11:09		3.3681	3.2393	3.3754	3.4073	3.0308	3.0775	3.1520	3.0777	3.1658	2.9211	3.1041	3.1178
11:10		3.3572	3.2297	3.3633	3.3893	3.0215	3.0680	3.1418	3.0697	3.1534	2.9121	3.0922	3.1079
11:11		3.3444	3.2177	3.3519	3.3762	3.0104	3.0560	3.1314	3.0572	3.1434	2.9002	3.0792	3.0952
11:12		3.3312	3.2054	3.3373	3.3635	2.9963	3.0441	3.1175	3.0443	3.1289	2.8878	3.0673	3.0795
11:13		[illegible]	[illegible]	3.3545	3.3822	3.0145	3.0611	3.1358	3.0630	3.1498	2.9071	3.0868	3.1019
11:14		[illegible]	[illegible]	[illegible]	3.3694	3.0009	3.0475	3.1221	3.0467	3.1336	2.8939	3.0715	3.0864
11:15		3.3627	3.2349	[illegible]	3.3545	3.0259	3.0729	3.1444	3.0733	3.1621	2.9150	3.1008	3.1123
11:16		3.3445	3.2200	3.3550	[illegible]	[illegible]	3.0599	3.1335	3.0588	3.1453	2.9044	3.0820	3.0979
11:17		[illegible]	3.2030	3.3349	[illegible]	2.9952	3.0438	3.1109	3.0444	3.1261	2.8839	3.0669	3.0833
11:18		3.3470	3.2196	3.3525	3.3794	3.0107	3.0583	3.1335	3.0589	3.1422	2.9083	3.0834	3.0966
11:19		3.3450	3.2155	3.3486	3.3755	3.0088	3.0571	3.1316	3.0577	3.1391	2.9003	3.0811	3.0929
11:20		3.3305	3.2479	3.3841	3.4082	3.0378	3.0850	3.1618	3.0664	3.1724	2.9323	3.1123	3.1255
11:21		3.3439	3.2149	3.3503	3.3813	3.0096	3.0544	3.1292	3.0540	3.1379	2.8968	3.0762	3.0872
11:22		3.3374	3.2088	3.3416	3.3697	3.0004	3.0485	3.1220	3.0491	3.1308	2.8896	3.0736	3.0846
11:23		3.3572	3.2293	3.3649	3.3900	3.0188	3.0677	3.1439	3.0699	3.1527	2.9149	3.0970	3.1095
11:24		3.3464	3.2177	3.3519	3.3811	3.0088	3.0551	3.1309	3.0573	3.1394	2.8978	3.0787	3.0911
11:25		3.3375	3.2089	3.3433	3.3701	2.9995	3.0468	3.1217	3.0490	3.1323	2.8926	3.0735	3.0875
11:26		3.3654	3.2348	3.3729	3.4022	3.0272	3.0759	3.1507	3.0765	3.1588	2.9191	3.0983	3.1122
11:27		3.3607	3.2316	3.3684	3.3962	3.0230	3.0716	3.1497	3.0736	3.1601	2.9200	3.0997	3.1141
11:28		3.3697	3.2363	3.3732	3.4041	3.0305	3.0784	3.1529	3.0775	3.1613	2.9188	3.1014	3.1118
11:29		3.3419	3.2117	3.3445	3.3751	3.0047	3.0528	3.1278	3.0532	3.1333	2.8951	3.0778	3.0936
11:30		3.3713	3.2403	3.3764	3.4051	3.0320	3.0796	3.1567	3.0827	3.1625	2.9250	3.1057	3.1153
11:31		3.3599	3.2287	3.3648	3.3913	3.0200	3.0675	3.1426	3.0677	3.1503	2.9067	3.0916	3.1024
11:32		3.3471	3.2135	3.3474	3.3719	3.0046	3.0535	3.1235	3.0553	3.1350	2.8956	3.0776	3.0916
11:33		3.3480	3.2170	3.3537	3.3814	3.0102	3.0576	3.1322	3.0589	3.1395	2.9030	3.0809	3.0925
11:34	239,000 gal.	3.3555	3.2255	3.3602	3.3850	3.0149	3.0649	3.1401	3.0673	3.1468	2.9098	3.0897	3.1011
11:35		3.3683	3.2392	3.3744	3.4004	3.0296	3.0779	3.1550	3.0806	3.1619	2.9238	3.1049	3.1189
11:36		3.3428	3.2115	3.3456	3.3734	3.0060	3.0551	3.1298	3.0555	3.1344	2.9016	3.0819	3.0935
11:37		3.3583	3.2276	3.3624	3.3881	3.0185	3.0685	3.1430	3.0697	3.1460	2.9131	3.0920	3.1040
11:38		3.3837	3.2503	3.3864	3.4164	3.0422	3.0920	3.1681	3.0932	3.1759	2.9337	3.1196	3.1317
11:39		3.3642	3.2342	3.3691	3.3967	3.0202	3.0764	3.1513	3.0777	3.1587	2.9198	3.1007	3.1136
11:40		3.4119	3.2790	3.4164	3.4452	3.0663	3.1157	3.1930	3.1184	3.2005	2.9596	3.1443	3.1558
11:41		3.3640	3.2341	3.3679	3.3948	3.0237	3.0721	3.1469	3.0739	3.1546	2.9185	3.0979	3.1107
11:42		3.3682	3.2368	3.3749	3.4025	3.0298	3.0797	3.1561	3.0821	3.1584	2.9244	3.1079	3.1201
11:43		3.3734	3.2414	3.3798	3.4032	3.0318	3.0811	3.1583	3.0835	3.1613	2.9274	3.1083	3.1211
11:44		3.3574	3.2249	3.3601	3.3873	3.0161	3.0643	3.1395	3.0662	3.1473	2.9095	3.0901	3.1025
11:45		3.3791	3.2471	3.3807	3.4089	3.0371	3.0857	3.1640	3.0892	3.1664	2.9313	3.1135	3.1274
11:46		3.3549	3.2247	3.3598	3.3871	3.0166	3.0652	3.1415	3.0671	3.1452	2.9173	3.0919	3.1039
11:47		3.3585	3.2284	3.3626	3.3906	3.0194	3.0683	3.1446	3.0699	3.1484	2.9134	3.0936	3.1061
11:48		3.3823	3.2456	3.3814	3.4085	3.0375	3.0872	3.1632	3.0954	3.1653	2.9290	3.1119	3.1225
11:49		3.3544	3.2232	3.3591	3.3861	3.0174	3.0654	3.1429	3.0687	3.1437	2.9115	3.0916	3.1091
11:50		3.3546	3.2222	3.3574	3.3857	3.0154	3.0656	3.1417	3.0667	3.1441	2.9115	3.0922	3.1132

TABLE II (Continued)

GPE NATURAL BUTTES NO.21-HYDROFRACTURE

FRACTURE-JUNE 22,1977

TIME		180°	195°	210°	225°	240°	255°	270°	285°	300°	315°	330°	345°
11:51		3.3525	3.2261	3.3549	3.3923	3.0113	3.0601	3.1351	3.0630	3.1376	2.9061	3.0465	3.0951
11:52		3.3621	3.2300	3.3656	3.3938	3.0235	3.0719	3.1497	3.0742	3.1511	2.9192	3.0937	3.1100
11:53		3.3586	3.2267	3.3623	3.3914	3.0174	3.0672	3.1423	3.0675	3.1443	2.9125	3.0924	3.1034
11:54		3.3574	3.2260	3.3613	3.3883	3.0177	3.0657	3.1419	3.0663	3.1422	2.9101	3.0900	3.1025
11:55		3.3654	3.2349	3.3703	3.3983	3.0239	3.0740	3.1497	3.0742	3.1525	2.9200	3.1006	3.1120
11:56		3.3460	3.2139	3.3472	3.3754	3.0049	3.0540	3.1290	3.0560	3.1319	2.8978	3.0789	3.0910
11:57		3.3609	3.2233	3.3580	3.3842	3.0127	3.0627	3.1382	3.0646	3.1380	2.9088	3.0920	3.1030
11:58		3.3691	3.2358	3.3707	3.3995	3.0277	3.0764	3.1513	3.0779	3.1566	2.9233	3.1049	3.1169
11:59		3.3705	3.2338	3.3713	3.3995	3.0277	3.0760	3.1531	3.0772	3.1543	2.9196	3.1024	3.1134
12:00		3.3345	3.2025	3.3374	3.3638	2.9953	3.0440	3.1186	3.0457	3.1210	2.8921	3.0731	3.0854
12:01		3.3619	3.2302	3.3655	3.3956	3.0209	3.0698	3.1445	3.0706	3.1475	2.9154	3.0956	3.1089
12:02		3.3816	3.2473	3.3827	3.4106	3.0378	3.0871	3.1638	3.0887	3.1628	2.9344	3.1170	3.1263
12:03		3.3677	3.2334	3.3704	3.3970	3.0249	3.0737	3.1505	3.0743	3.1486	2.9193	3.1001	3.1120
12:04		3.3586	3.2254	3.3594	3.3878	3.0172	3.0665	3.1427	3.0684	3.1441	2.9129	3.0937	3.1054
12:05		3.3547	3.2221	3.3578	3.3861	3.0140	3.0632	3.1389	3.0630	3.1375	2.9076	3.0882	3.1006
12:06		3.3613	3.2305	3.3642	3.3937	3.0210	3.0702	3.1438	3.0689	3.1430	2.9096	3.0921	3.1032
12:07		3.3426	3.2114	3.3464	3.3781	3.0056	3.0548	3.1284	3.0554	3.1282	2.8965	3.0790	3.0884
12:08		3.3603	3.2266	3.3603	3.3863	3.0177	3.0690	3.1433	3.0678	3.1418	2.9139	3.0946	3.1065
12:09		3.3671	3.2328	3.3690	3.3944	3.0230	3.0751	3.1509	3.0757	3.1503	2.9188	3.1029	3.1140
12:10		3.3740	3.2429	3.3809	3.4064	3.0337	3.0834	3.1592	3.0823	3.1576	2.9277	3.1108	3.1201
12:11		3.3556	3.2175	3.3541	3.3812	3.0114	3.0625	3.1369	3.0615	3.1402	2.9079	3.0894	3.0996
12:12		3.3656	3.2328	3.3670	3.3943	3.0223	3.0736	3.1477	3.0717	3.1482	2.9172	3.1021	3.1099
12:13		3.3543	3.2160	3.3501	3.3788	3.0096	3.0598	3.1351	3.0590	3.1327	2.9047	3.0883	3.0972
12:14		3.3598	3.2245	3.3614	3.3896	3.0180	3.0671	3.1414	3.0669	3.1430	2.9119	3.0970	3.1055
12:15		3.4065	3.2685	3.4060	3.4329	3.0579	3.1072	3.1831	3.1061	3.1821	2.9477	3.1347	3.1449
12:16		3.3678	3.2332	3.3686	3.3955	3.0248	3.0745	3.1490	3.0747	3.1484	2.9177	3.1035	3.1123
12:17		3.3623	3.2283	3.3625	3.3900	3.0183	3.0694	3.1433	3.0682	3.1414	2.9117	3.0973	3.1104
12:18		3.3761	3.2431	3.3749	3.4041	3.0311	3.0828	3.1579	3.0828	3.1571	2.9301	3.1128	3.1247
12:19		3.3662	3.2306	3.3652	3.3939	3.0230	3.0746	3.1493	3.0746	3.1474	2.9186	3.1023	3.1136
12:20		3.3623	3.2303	3.3656	3.3943	3.0212	3.0711	3.1453	3.0699	3.1428	2.9143	3.0999	3.1095
12:21		3.3625	3.2272	3.3632	3.3913	3.0192	3.0698	3.1433	3.0700	3.1412	2.9139	3.0966	3.1079
12:22		3.3565	3.2224	3.3579	3.3846	3.0127	3.0638	3.1387	3.0650	3.1367	2.9107	3.0956	3.1067
12:23		3.3769	3.2426	3.3785	3.4073	3.0324	3.0846	3.1581	3.0831	3.1587	2.9284	3.1141	3.1244
12:24		3.3770	3.2399	3.3764	3.4037	3.0280	3.0798	3.1543	3.0800	3.1535	2.9260	3.1097	3.1196
12:25	327,000 gal.	3.3739	3.2392	3.3757	3.4022	3.0281	3.0801	3.1546	3.0811	3.1523	2.9236	3.1111	3.1215
12:26		3.3867	3.2499	3.3885	3.4162	3.0412	3.0921	3.1656	3.0909	3.1630	2.9341	3.1194	3.1305
12:27		3.3694	3.2354	3.3722	3.4035	3.0258	3.0766	3.1503	3.0761	3.1499	2.9224	3.1064	3.1164
12:28		3.3748	3.2411	3.3761	3.4047	3.0287	3.0807	3.1554	3.0790	3.1519	2.9257	3.1093	3.1210
12:29		3.3621	3.2234	3.3656	3.3923	3.0201	3.0707	3.1451	3.0688	3.1402	2.9171	3.0990	3.1089
12:30		3.3859	3.2485	3.3850	3.4146	3.0370	3.0884	3.1632	3.0882	3.1610	2.9333	3.1170	3.1256
12:31		3.3923	3.2576	3.3906	3.4236	3.0462	3.0976	3.1706	3.0964	3.1667	2.9426	3.1237	3.1330
12:32		3.3751	3.2448	3.3321	3.4103	3.0349	3.0849	3.1600	3.0847	3.1579	2.9328	3.1156	3.1267
12:33		3.3886	3.2519	3.3867	3.4166	3.0414	3.0916	3.1661	3.0930	3.1628	2.9376	3.1237	3.1332

SAND-77-1992
Oct. 1976-Sept. 1977

TABLE II (Continued)

GPE NATURAL BUTTES NO.20-HYDROFRACTURE

FRACTURE-JUNE 22,1977

TIME		180°	195°	210°	225°	240°	255°	270°	285°	300°	315°	330°	345°
12:34		3.3632	3.2267	3.3630	3.3896	3.0175	3.0686	3.1433	3.0698	3.1394	2.9159	3.0989	3.1071
12:35		3.4025	3.2664	3.4039	3.4317	3.0546	3.1056	3.1804	3.1058	3.1752	2.9527	3.1367	3.1483
12:36		3.4271	3.2834	3.4277	3.4562	3.0743	3.1231	3.1994	3.1243	3.1972	2.9715	3.1548	3.1700
12:37		3.4021	3.2708	3.4085	3.4369	3.0564	3.1077	3.1828	3.1083	3.1775	2.9516	3.1365	3.1476
12:38		3.3724	3.2371	3.3726	3.4009	3.0279	3.0780	3.1515	3.0790	3.1488	2.9260	3.1076	3.1159
12:39		3.3522	3.2259	3.3626	3.3910	3.0173	3.0673	3.1421	3.0671	3.1365	2.9133	3.0965	3.1054
12:40		3.3263	3.1931	3.3282	3.3576	2.9882	3.0384	3.1101	3.0382	3.1047	2.8854	3.0666	3.0763
12:41		3.3511	3.2152	3.3515	3.3791	3.0348	3.0595	3.1338	3.0599	3.1312	2.9060	3.0889	3.0974
12:42		3.3462	3.2108	3.3470	3.3717	2.9996	3.0524	3.1263	3.0542	3.1187	2.9012	3.0823	3.0920
12:43		3.3397	3.2048	3.3404	3.3667	2.9975	3.0474	3.1230	3.0474	3.1131	2.8941	3.0756	3.0855
12:44		3.3658	3.2280	3.3652	3.3915	3.0162	3.0714	3.1463	3.0714	3.1392	2.9181	3.1017	3.1132
12:45		3.3820	3.2442	3.3835	3.4254	3.0432	3.0931	3.1673	3.0914	3.1600	2.9348	3.1174	3.1295
12:46		3.3478	3.2054	3.3392	3.3664	2.9962	3.0469	3.1203	3.0475	3.1112	2.8916	3.0723	3.0840
12:47		3.3634	3.2275	3.3636	3.3915	3.0192	3.0705	3.1463	3.0715	3.1357	2.9190	3.1038	3.1166
12:48	Shut down	3.3594	3.2214	3.3572	3.3853	3.0142	3.0639	3.1375	3.0626	3.1292	2.9105	3.0929	3.1041
12:49	362,000 gal. (Total Vol.)	3.3565	3.2313	3.3707	3.3985	3.0219	3.0736	3.1495	3.0728	3.1396	2.9196	3.1037	3.1119
12:50		3.3543	3.2251	3.3566	3.3855	3.0107	3.0619	3.1343	3.0604	3.1266	2.9072	3.0893	3.1002
12:51		3.3730	3.2387	3.3761	3.4050	3.0294	3.0826	3.1569	3.0814	3.1494	2.9296	3.1127	3.1257
12:52		3.3332	3.1989	3.3344	3.3645	2.9912	3.0416	3.1150	3.0407	3.1084	2.8899	3.0682	3.0803
12:53		3.3547	3.2204	3.3586	3.3895	3.0142	3.0639	3.1373	3.0631	3.1272	2.9087	3.0885	3.1048
12:54		3.3692	3.2346	3.3731	3.4038	3.0260	3.0767	3.1497	3.0742	3.1396	2.9211	3.1051	3.1133
12:55		3.3444	3.2088	3.3451	3.3741	3.0017	3.0516	3.1248	3.0508	3.1149	2.8959	3.0772	3.0816
12:56		3.3583	3.2234	3.3593	3.3896	3.0149	3.0658	3.1401	3.0640	3.1304	2.9108	3.0953	3.1059
12:57		3.3569	3.2220	3.3577	3.3889	3.0115	3.0643	3.1306	3.0627	3.1300	2.9111	3.0918	3.1044
12:58		3.3090	3.1749	3.3094	3.3360	2.9704	3.0212	3.0952	3.0206	3.0814	2.8671	3.0472	3.0602
12:59		3.3042	3.1699	3.3067	3.3343	2.9654	3.0159	3.0891	3.0161	3.0763	2.8639	3.0410	3.0567
13:00		3.2942	3.1617	3.2961	3.3254	2.9575	3.0089	3.0806	3.0072	3.0679	2.8538	3.0322	3.0441
13:01		3.2795	3.1478	3.2814	3.3105	2.9439	2.9955	3.0665	2.9920	3.0539	2.8402	3.0174	3.0291
13:02		3.3214	3.1873	3.3239	3.3544	2.9809	3.0323	3.1051	3.0300	3.0944	2.8781	3.0571	3.0711
13:03		3.3170	3.1849	3.3203	3.3506	2.9781	3.0295	3.1011	3.0270	3.0904	2.8741	3.0549	3.0685
13:04		3.3255	3.1917	3.3292	3.3569	2.9865	3.0371	3.1116	3.0367	3.0989	2.8852	3.0640	3.0768
13:05		3.3343	3.1963	3.3337	3.3643	2.9906	3.0436	3.1171	3.0418	3.1045	2.8942	3.0727	3.0814
13:06		3.3348	3.2040	3.3421	3.3722	2.9972	3.0438	3.1235	3.0476	3.1093	2.8961	3.0746	3.0870
13:07		3.3315	3.1952	3.3331	3.3633	2.9886	3.0400	3.1147	3.0379	3.1029	2.8870	3.0658	3.0794

APPENDIX C

TABLE I

CONOCO HYDROFRACTURE-CASPER,WYO

FRACTURE-MARCH 22,1977

TIME	0°	20°	40°	Well 39	60°	80°	Well 55	100°	120°	140°	160°	Well 68
10:03:00	.0112	.0769	.1310	.1277	.0938	.0538	.1127	.1105	.1347	.1432	.1648	.1519
10:03:40	.0216	.0857	.1556	.1296	.0995	.0560	.1126	.1162	.1357	.1440	.1657	.1521
10:04:20	.0155	.0792	.1269	.1267	.0920	.0531	.1126	.1143	.1357	.1442	.1661	.1521
10:05:00	.0198	.0811	.1373	.1269	.0928	.0519	.1118	.1119	.1350	.1438	.1660	.1525
10:05:40	.0251	.0864	.1547	.1283	.0983	.0557	.1121	.1252	.1362	.1443	.1655	.1523
10:06:20	.0198	.0822	.1422	.1276	.0950	.0535	.1120	.1308	.1349	.1436	.1655	.1518
10:10:00	.0136	.0767	.1243	.1267	.0922	.0541	.1128	.1322	.1361	.1440	.1659	.1525
10:10:40	.0224	.0828	.1454	.1279	.0952	.0540	.1123	.1310	.1353	.1437	.1649	.1522
10:11:20	.0160	.0801	.1359	.1273	.0941	.0538	.1124	.1312	.1351	.1436	.1656	.1523
10:12:00	.0174	.0756	.1220	.1264	.0909	.0533	.1124	.1315	.1354	.1437	.1653	.1521
10:12:40	.0187	.0814	.1346	.1271	.0931	.0532	.1121	.1312	.1352	.1432	.1654	.1524
10:13:20	.0174	.0769	.1356	.1278	.0935	.0533	.1123	.1305	.1344	.1427	.1646	.1517
10:14:00	.0165	.0799	.1352	.1281	.0949	.0552	.1129	.1320	.1352	.1433	.1648	.1519
10:14:40	.0153	.0753	.1283	.1210	.0850	.0463	.1081	.1238	.1274	.1356	.1614	.1477
10:15:20	.0317	.2025	.1380	.1252	.0910	.0513	.1104	.1286	.1328	.1411	.1636	.1505
10:16:00	.0209	.0808	.1353	.1265	.0921	.0531	.1119	.1291	.1342	.1420	.1641	.1518
10:16:40	.0165	.0797	.1350	.1233	.0861	.0482	.1089	.1250	.1291	.1367	.1593	.1479
10:17:20	.0210	.0844	.1485	.1310	.0991	.0565	.1138	.1323	.1375	.1466	.1667	.1542
10:18:00	.0154	.0826	.1402	.1232	.0891	.0494	.1093	.1255	.1300	.1378	.1629	.1487
10:19:40	.0147	.0768	.1213	.1223	.0862	.0494	.1103	.1267	.1313	.1392	.1622	.1497
10:19:20	.0195	.0830	.1434	.1273	.0953	.0535	.1119	.1307	.1354	.1434	.1657	.1513
10:20:00	.0142	.0777	.1306	.1267	.0927	.0534	.1119	.1308	.1354	.1429	.1651	.1519
10:20:40	.0153	.0795	.1270	.1257	.0908	.0527	.1118	.1305	.1348	.1429	.1646	.1514
10:21:20	.0240	.0819	.1381	.1242	.0892	.0496	.1100	.1242	.1309	.1377	.1622	.1497
10:22:00	.0152	.0794	.1356	.1258	.0923	.0525	.1114	.1294	.1335	.1412	.1633	.1503
10:22:40	.0129	.0756	.1212	.1251	.0918	.0523	.1117	.1302	.1354	.1442	.1658	.1511
10:23:20	.0190	.0834	.1434	.1209	.0935	.0528	.1114	.1295	.1332	.1413	.1634	.1513
10:24:00	.0119	.0786	.1324	.1287	.0952	.0546	.1133	.1323	.1361	.1442	.1656	.1528
10:24:40	.0110	.0739	.1198	.1237	.0882	.0508	.1108	.1283	.1320	.1391	.1619	.1497
10:25:20	.0230	.0835	.1443	.1200	.0911	.0504	.1104	.1267	.1309	.1379	.1591	.1498
10:26:33	.0137	.0796	.1310	.1260	.0904	.0513	.1113	.1294	.1330	.1413	.1642	.1515
10:28:33	.0115	.0791	.1372	.1266	.0934	.0527	.1114	.1293	.1330	.1418	.1633	.1511
10:30:33	.0154	.0784	.1278	.1209	.0851	.0469	.1081	.1233	.1279	.1355	.1592	.1476
10:32:33	.0169	.0765	.1251	.1258	.0907	.0524	.1116	.1303	.1341	.1423	.1639	.1518
10:34:33	.0192	.0799	.1313	.1260	.0911	.0527	.1118	.1307	.1346	.1426	.1648	.1516
10:36:33	.0200	.0782	.1306	.1199	.0837	.0457	.1076	.1229	.1286	.1358	.1588	.1465
10:39:33	-.0019	.0663	.0995	.1211	.0817	.0477	.1101	.1253	.1290	.1363	.1599	.1489
10:40:33	.0140	.0783	.1317	.1256	.0928	.0540	.1114	.1286	.1332	.1409	.1637	.1499
10:42:33	.0250	.0867	.1598	.1263	.0934	.0518	.1109	.1289	.1331	.1407	.1631	.1524
10:47:00	.0177	.0812	.1381	.1272	.0937	.0533	.1123	.1315	.1349	.1428	.1646	.1523
10:47:40	.0131	.0753	.1231	.1262	.0909	.0534	.1122	.1311	.1352	.1428	.1656	.1521
10:48:20	.0161	.0785	.1281	.1261	.0912	.0522	.1119	.1303	.1347	.1429	.1652	.1521
10:49:00	.0136	.0778	.1438	.1281	.0946	.0561	.1128	.1324	.1358	.1433	.1647	.1522

UGR File #C073/A77, part 2
SAND-77-1992
Oct. 1976-Sept. 1977

TABLE I (Continued)

CONOCO HYDROFRACTURE-CASPER,WYO

FRACTURE-MARCH 22,1977

TIME		0°	20°	40°	Well 39	60°	80°	Well 55	100°	120°	140°	160°	Well 68
10:49:40		.0090	.0751	.1295	.1278	.0942	.0554	.1133	.1324	.1353	.1435	.1638	.1520
10:50:20		.0159	.0788	.1436	.1287	.0966	.0544	.1123	.1313	.1346	.1423	.1644	.1511
10:51:00		.0076	.0735	.1194	.1262	.0896	.0520	.1123	.1307	.1346	.1431	.1645	.1518
10:51:40		.0131	.0766	.1300	.1275	.0937	.0540	.1131	.1311	.1361	.1432	.1655	.1519
10:52:20		.0060	.0779	.1330	.1275	.0941	.0537	.1124	.1308	.1349	.1426	.1643	.1517
10:53:00		.0054	.0771	.1269	.1269	.0926	.0542	.1130	.1312	.1353	.1434	.1651	.1522
10:53:40		.0198	.0757	.1213	.1254	.0891	.0516	.1116	.1294	.1347	.1431	.1646	.1521
10:54:20		.0178	.0815	.1392	.1269	.0932	.0533	.1119	.1308	.1358	.1435	.1662	.1523
10:55:00		.0250	.0819	.1420	.1273	.0948	.0542	.1119	.1318	.1353	.1431	.1654	.1518
10:55:40		.0283	.0744	.1155	.1258	.0889	.0517	.1116	.1302	.1344	.1454	.1657	.1509
10:56:20		.0268	.0837	.1496	.1268	.0941	.0524	.1109	.1294	.1337	.1408	.1634	.1507
10:57:00		.0111	.0799	.1318	.1243	.0896	.0508	.1106	.1289	.1330	.1411	.1632	.1501
10:57:40		.0167	.0756	.1188	.1271	.0897	.0517	.1136	.1327	.1369	.1446	.1674	.1544
10:58:20		.0207	.0836	.1516	.1294	.0973	.0550	.1124	.1324	.1363	.1436	.1664	.1526
10:59:00		.0264	.0847	.1481	.1285	.0908	.0555	.1126	.1334	.1375	.1450	.1677	.1537
10:59:40		.0194	.0760	.1254	.1283	.0940	.0556	.1140	.1345	.1387	.1457	.1652	.1539
11:00:20		.0151	.0831	.1351	.1301	.0973	.0577	.1149	.1375	.1423	.1493	.1724	.1566
11:01:00		.0232	.0881	.1519	.1329	.1022	.0614	.1158	.1406	.1452	.1523	.1739	.1585
11:01:40		.0207	.0875	.1458	.1316	.1013	.0615	.1161	.1415	.1455	.1517	.1731	.1578
11:02:20		.0300	.0904	.1536	.1337	.1049	.0631	.1168	.1428	.1470	.1538	.1756	.1590
11:03:00		.0366	.0924	.1649	.1333	.1038	.0607	.1153	.1395	.1451	.1520	.1747	.1592
11:03:40		.0205	.0859	.1422	.1325	.1021	.0624	.1166	.1425	.1459	.1518	.1735	.1579
11:04:20		.0237	.0848	.1336	.1293	.0958	.0574	.1149	.1382	.1422	.1469	.1715	.1563
11:05:00		.0292	.0889	.1474	.1317	.1005	.0592	.1158	.1402	.1454	.1519	.1747	.1592
11:05:40		.0273	.0941	.1539	.1363	.1065	.0656	.1191	.1453	.1515	.1581	.1787	.1615
11:06:20		.0265	.0815	.1378	.1327	.1016	.0621	.1171	.1421	.1465	.1524	.1738	.1586
11:07:00		.0154	.0883	.1482	.1329	.1015	.0606	.1165	.1403	.1455	.1525	.1746	.1586
11:07:40		.0238	.0862	.1413	.1325	.1012	.0606	.1164	.1408	.1452	.1519	.1735	.1582
11:08:20		.0219	.0874	.1522	.1335	.1034	.0616	.1163	.1405	.1453	.1516	.1732	.1581
11:09:00		.0176	.0858	.1474	.1335	.1036	.0615	.1168	.1417	.1453	.1516	.1732	.1580
11:09:40		.0247	.0871	.1469	.1325	.1014	.0602	.1160	.1414	.1456	.1529	.1756	.1593
11:10:20		.0303	.0902	.1505	.1335	.1045	.0643	.1172	.1440	.1473	.1534	.1739	.1583
11:11:00		.0292	.0925	.1546	.1336	.1035	.0615	.1168	.1419	.1462	.1531	.1747	.1583
11:11:40		.0275	.0905	.1554	.1324	.1019	.0604	.1159	.1405	.1446	.1520	.1728	.1537
11:12:20		.0261	.0853	.1357	.1312	.0985	.0597	.1160	.1396	.1451	.1520	.1741	.1587
11:13:00	Start pumping	.0296	.0918	.1532	.1319	.1003	.0594	.1151	.1390	.1436	.1524	.1722	.1576
11:13:40		.0219	.0816	.1354	.1303	.0976	.0586	.1147	.1372	.1412	.1488	.1735	.1559
11:14:20		.0212	.0844	.1405	.1298	.0974	.0576	.1141	.1314	.1402	.1473	.1689	.1552
11:15:00		.0224	.0824	.1420	.1288	.0965	.0562	.1133	.1342	.1381	.1459	.1675	.1540
11:15:40		.0149	.0778	.1307	.1280	.0946	.0547	.1130	.1336	.1373	.1451	.1664	.1535
11:16:20		.0149	.0763	.1280	.1286	.0968	.0561	.1139	.1334	.1383	.1480	.1685	.1535
11:17:00		.0195	.0793	.1369	.1283	.0959	.0555	.1132	.1339	.1372	.1452	.1668	.1537
11:17:40		.0196	.0851	.1515	.1282	.0953	.0526	.1117	.1315	.1359	.1445	.1668	.1532

TABLE I (Continued)

CONOCO HYDROFRACTURE-CASPER,WYO

FRACTURE-MARCH 22,1977

TIME		0°	20°	40°	Well 39	60°	80°	Well 55	100°	120°	140°	160°	Well 68
11:18:20		.0196	.0818	.1339	.1279	.0943	.0550	.1129	.1343	.1378	.1455	.1672	.1535
11:19:00		.0119	.0818	.1309	.1278	.0947	.0560	.1130	.1344	.1384	.1462	.1673	.1541
11:19:40		.0235	.0823	.1322	.1270	.0913	.0525	.1121	.1320	.1365	.1447	.1682	.1544
11:20:20		.0104	.0764	.1207	.1280	.0944	.0563	.1137	.1354	.1382	.1456	.1680	.1541
11:21:00		.0239	.0863	.1385	.1281	.0948	.0552	.1131	.1346	.1381	.1463	.1681	.1536
11:21:40		.0160	.0824	.1330	.1275	.0931	.0535	.1128	.1333	.1369	.1452	.1673	.1536
11:22:20		.0168	.0835	.1319	.1284	.0935	.0535	.1134	.1342	.1384	.1459	.1671	.1536
11:23:00		.0200	.0815	.1313	.1276	.0939	.0550	.1129	.1337	.1376	.1455	.1676	.1535
11:23:40		.0211	.0873	.1458	.1284	.0964	.0558	.1127	.1328	.1383	.1458	.1673	.1538
11:24:20		.0295	.0844	.1443	.1295	.0974	.0571	.1137	.1347	.1396	.1467	.1685	.1541
11:25:00		.0051	.0759	.1281	.1274	.0940	.0554	.1131	.1334	.1379	.1455	.1663	.1536
11:25:40		.0134	.0784	.1406	.1292	.0967	.0545	.1129	.1326	.1359	.1441	.1669	.1535
11:26:20		.0192	.0840	.1414	.1293	.0971	.0562	.1132	.1348	.1379	.1460	.1669	.1533
11:27:00		.0165	.0848	.1439	.1292	.0976	.0574	.1137	.1357	.1390	.1473	.1671	.1536
11:27:40		.0210	.0868	.1484	.1293	.0969	.0535	.1119	.1331	.1371	.1451	.1675	.1528
11:28:20		.0135	.0811	.1398	.1287	.0964	.0556	.1128	.1344	.1381	.1459	.1680	.1530
11:29:00		.0143	.0840	.1326	.1275	.0948	.0568	.1132	.1348	.1390	.1459	.1693	.1531
11:29:40		.0229	[illegible]	.1400	.1280	.0955	.0550	.1129	.1342	.1385	.1461	.1669	.1537
11:30:20		.0170	.0812	[illegible]	.1285	.0950	.0552	.1130	.1342	.1379	.1457	.1684	.1536
11:31:00		.0225	.0795	.1356	.1277	[illegible]	.0552	.1128	.1347	.1389	.1465	.1676	.1532
11:31:40		.0239	.0818	.1369	[illegible]	[illegible]	.0550	.1128	.1340	.1381	.1458	.1678	.1536
11:32:20		.0151	.0781	.1298	.1282	.0948	.0548	.1132	.1345	.1385	.1458	.1682	.1539
11:33:00		.0117	.0793	.1313	.1284	.0947	.0549	.1127	.1344	.1373	.1455	.1676	.1535
11:33:40		.0290	.0893	.1567	.1297	.0988	.0566	.1123	.1347	.1386	.1463	.1674	.1533
11:34:20		.0187	.0845	.1377	.1280	.0948	.0550	.1128	.1345	.1379	.1457	.1673	.1536
11:35:00		.0139	.0788	.1271	.1268	.0954	.0571	.1140	.1363	.1393	.1463	.1700	.1537
11:35:40		.0144	.0831	.1357	.1282	.0946	.0544	.1128	.1338	.1377	.1456	.1676	.1534
11:36:20		.0219	.0850	.1376	.1284	.0962	.0563	.1131	.1347	.1385	.1460	.1677	.1535
11:37:00		.0185	.0903	.1309	.1277	.0940	.0543	.1130	.1340	.1373	.1454	.1676	.1535
11:37:40		.0228	.0852	.1395	.1284	.0953	.0558	.1128	.1348	.1396	.1466	.1689	.1544
11:38:20		.0169	.0828	.1440	.1292	.0964	.0551	.1130	.1331	.1362	.1445	.1651	.1529
11:39:00		.0191	.0815	.1359	.1287	.0963	.0555	.1133	.1340	.1376	.1449	.1674	.1529
11:39:40		.0249	.0890	.1525	.1285	.0975	.0552	.1126	.1329	.1377	.1460	.1685	.1538
11:40:20		.0161	.0775	.1377	.1289	.0962	.0554	.1131	.1326	.1368	.1450	.1665	.1537
11:41:00		.0098	.0793	.1295	.1282	.0935	.0542	.1128	.1330	.1369	.1452	.1670	.1534
11:41:40		.0263	.0827	.1367	.1284	.0955	.0571	.1135	.1354	.1390	.1465	.1675	.1536
11:42:20	Stop pumping	.0156	.0832	.1471	.1303	.0988	.0583	.1144	.1373	.1390	.1494	.1707	.1552
11:43:00	Total Vol. - 12,000 gal.	.0258	.0851	.1457	.1297	.0980	.0583	.1140	.1371	.1411	.1480	.1701	.1554
11:43:40		.0246	.0838	.1482	.1301	.0987	.0565	.1142	.1359	.1408	.1474	.1697	.1552
11:44:20		.0227	.0883	.1543	.1311	.1007	.0593	.1147	.1371	.1406	.1482	.1701	.1554
11:45:00		.0115	.0780	.1220	.1283	.0939	.0559	.1141	.1376	.1409	.1482	.1700	.1557
11:45:40		.0196	.0863	.1418	.1299	.0972	.0568	.1138	.1363	.1399	.1475	.1699	.1549
11:46:20		.0254	.0849	.1440	.1295	.0972	.0564	.1136	.1358	.1400	.1478	.1699	.1551

SAND-77-1992
Oct. 1976-Sept. 1977

TABLE I (Continued)

CONOCO HYDROFRACTURE-CASPER-WYO

FRACTURE-MARCH 22,1977

TIME	0°	20°	40°	Well 39	60°	80°	Well 55	100°	120°	140°	160°	Well 68
11:47:00	.0175	.0841	.1427	.1304	.0985	.0580	.1145	.1348	.1401	.1474	.1726	.1557
11:47:40	.0193	.0839	.1443	.1303	.0952	.0569	.1133	.1359	.1405	.1479	.1704	.1552
11:48:20	.0147	.0839	.1353	.1295	.0968	.0586	.1146	.1363	.1412	.1482	.1699	.1555
11:49:00	.0238	.0873	.1451	.1301	.0978	.0570	.1140	.1359	.1402	.1482	.1705	.1557
11:49:40	.0150	.0818	.1370	.1299	.0974	.0574	.1146	.1372	.1400	.1476	.1692	.1552
11:50:20	.0273	.0921	.1715	.1313	.1010	.0593	.1144	.1393	.1416	.1486	.1694	.1555
11:51:00	.0169	.0752	.1213	.1282	.0946	.0566	.1141	.1373	.1406	.1479	.1684	.1557
11:51:40	.0193	.0847	.1382	.1293	.0969	.0557	.1140	.1366	.1404	.1482	.1707	.1559
11:52:20	.0194	.0869	.1509	.1309	.1007	.0587	.1142	.1367	.1406	.1477	.1694	.1551
11:53:00	.0136	.0774	.1277	.1302	.0969	.0597	.1154	.1379	.1419	.1436	.1691	.155.
11:53:40	.0291	.0909	.1521	.1302	.0988	.0577	.1142	.1370	.1407	.1462	.1697	.1552
11:54:20	.0196	.0861	.1425	.1297	.0967	.0556	.1137	.1350	.1394	.1469	.1696	.1551
11:55:00	.0282	.0884	.1583	.1321	.1028	.0612	.1145	.1381	.1419	.1482	.1706	.1553
11:55:40	.0264	.0845	.1455	.1298	.0973	.0565	.1134	.1353	.1402	.1477	.1691	.1557
11:56:20	.0189	.0861	.1447	.1297	.0976	.0571	.1138	.1359	.1397	.1471	.1697	.1554
11:57:00	.0225	.0833	.1515	.1314	.1014	.0586	.1148	.1375	.1405	.1491	.1689	.1554
11:57:40	.0156	.0815	.1288	.1286	.0948	.0564	.1140	.1361	.1399	.1483	.1682	.1549
11:58:20	.0223	.0836	.1420	.1294	.0967	.0571	.1143	.1364	.1401	.1482	.1713	.1546
11:59:00	.0193	.0850	.1440	.1302	.0993	.0593	.1149	.1382	.1420	.1491	.1708	.1555
11:59:40	.0211	.0854	.1427	.1299	.0972	.0563	.1136	.1358	.1396	.1472	.1708	.1548
12:00:20	.0136	.0795	.1246	.1288	.0938	.0563	.1144	.1361	.1411	.1485	.1693	.1557
12:01:00	.0186	.0838	.1366	.1294	.0967	.0567	.1138	.1357	.1396	.1472	.1687	.1553
12:01:40	.0255	.0860	.1438	.1305	.0993	.0586	.1147	.1375	.1410	.1484	.1687	.1559
12:02:20	.0152	.0839	.1400	.1296	.0964	.0564	.1139	.1351	.1387	.1467	.1679	.1552

SAND-77-1992
Oct. 1976-Sept. 1977

TABLE I (Continued)

CONOCO HYDROFRACTURE-CASPER,WYO

FRACTURE-MARCH 22,1977

TIME	180°	200°	Well 59	220°	240°	Well 74	260°	280°	300°	320°	Well 53	340°
12:03:00	.2103	.2715	.1907	.3237	.3410	.2290	.3525	.3143	.1428	.0783	.1570	-.1195
12:03:40	.2106	.2694	.1906	.3232	.3401	.2284	.3519	.3101	.1424	.0837	.1565	-.0834
12:04:20	.2113	.2707	.1909	.3238	.3409	.2291	.3520	.3117	.1429	.0820	.1566	-.0972
12:05:00	.2116	.2716	.1914	.3250	.3424	.2293	.3534	.3159	.1437	.0867	.1564	-.0791
12:05:40	.2102	.2694	.1902	.3224	.3386	.2278	.3501	.3078	.1432	.0885	.1569	-.0645
12:06:20	.2106	.2697	.1908	.3234	.3406	.2287	.3518	.3117	.1442	.0856	.1567	-.0824
12:10:00	.2116	.2701	.1907	.3234	.3397	.2283	.3513	.3118	.1414	.0793	.1564	-.1131
12:10:40	.2115	.2706	.1907	.3247	.3412	.2289	.3528	.3128	.1447	.0865	.1573	-.0322
12:11:20	.2115	.2725	.1909	.3240	.3413	.2287	.3527	.3142	.1435	.0821	.1575	-.0999
12:12:00	.2111	.2700	.1907	.3236	.3405	.2287	.3521	.3142	.1422	.0766	.1565	-.1172
12:12:40	.2121	.2714	.1910	.3241	.3414	.2289	.3524	.3127	.1432	.0832	.1577	-.0915
12:13:20	.2112	.2704	.1908	.3234	.3408	.2288	.3522	.3131	.1437	.0826	.1570	-.0980
12:14:00	.2124	.2698	.1906	.3228	.3400	.2284	.3513	.3122	.1423	.0799	.1563	-.0973
12:14:40	.2015	.2642	.1877	.3185	.3359	.2249	.3475	.3043	.1393	.0803	.1527	-.1358
12:15:20	.2055	.2689	.1893	.3225	.3388	.2273	.3504	.3099	.1698	.2302	.1671	.1435
12:16:00	.2068	.2698	.1906	.3235	.3404	.2285	.3517	.3124	.1431	.0832	.1568	-.0923
12:16:40	.2014	.2643	.1878	.3173	.3348	.2243	.3460	.3073	.1389	.0825	.1527	-.1029
12:17:20	.2094	.2723	.1920	.3256	.3424	.2303	.3509	.3135	.1459	.0873	.1590	-.0809
12:18:00	.2026	.2648	.1884	.3196	.3369	.2254	.3478	.3075	.1410	.0844	.1535	-.0867
12:18:40	.2046	.2673	.1891	.3208	.3380	.2264	.3487	.3105	.1401	.0800	.1539	-.1098
12:19:20	.2062	.2692	.1904	.3230	.3400	.2283	.3515	.3102	.1433	.0842	.1556	-.0792
12:20:00	.2068	.2697	.1905	.3232	.3401	.2283	.3517	.3124	.1436	.0817	.1570	-.1036
12:20:40	.2063	.2687	.1903	.3227	.3394	.2279	.3507	.3109	.1423	.0801	.1561	-.0993
12:21:20	.2055	.2679	.1894	.3213	.3376	.2264	.3435	.3072	.1413	.0847	.1544	-.0326
12:22:00	.2050	.2674	.1895	.3213	.3378	.2271	.3494	.3094	.1412	.0810	.1553	-.0973
12:22:40	.2052	.2692	.1902	.3232	.3404	.2283	.3516	.3123	.1420	.0788	.1555	-.1097
12:23:20	.2061	.2686	.1901	.3224	.3393	.2277	.3507	.3098	.1423	.0850	.1562	-.0819
12:24:00	.2062	.2709	.1910	.3242	.3411	.2293	.3527	.3143	.1417	.0772	.1578	-.1153
12:24:40	.2037	.2664	.1889	.3200	.3372	.2262	.3443	.3102	.1392	.0748	.1538	-.1222
12:25:20	.2006	.2638	.1892	.3184	.3356	.2266	.3471	.3044	.1413	0.0000	.1557	0.0000
12:26:33	.2061	.2684	.1903	.3233	.3399	.2283	.3518	.3123	.1432	.0830	.1557	-.0963
12:28:33	.2052	.2670	.1897	.3207	.3377	.2272	.3491	.3090	.1396	.0789	.1552	-.1152
12:30:33	.2002	.2617	.1872	.3171	.3339	.2239	.3450	.3060	.1393	.0793	.1522	-.1034
12:32:33	.2066	.2688	.1905	.3232	.3401	.2284	.3514	.3127	.1423	.0793	.1559	-.1185
12:34:33	.2071	.2690	.1903	.3229	.3396	.2283	.3512	.3121	.1415	.0821	.1569	-.0942
12:36:33	.2004	.2625	.1864	.3155	.3277	.2228	.3364	.3029	.1377	.0838	.1506	-.0958
12:38:33	.2029	.2644	.1880	.3187	.3335	.2240	.3465	.3132	.1370	.0662	.1532	-.1066
12:40:33	.2033	.2649	.1885	.3187	.3362	.2256	.3474	.3084	.1362	.0770	.1545	-.1171
12:42:33	.2047	.2665	.1891	.3197	.3316	.2245	.3467	.3053	.1437	.0860	.1555	-.0677
12:47:03	.2071	.2681	.1904	.3222	.3368	.2271	.3501	.3110	.1412	.0806	.1561	-.0998
12:47:43	.2069	.2678	.1903	.3228	.3393	.2278	.3510	.3126	.1423	.0770	.1565	-.1144
12:48:23	.2072	.2687	.1906	.3241	.3419	.2293	.3533	.3134	.1439	.0811	.1559	-.1087
12:49:03	.2073	.2676	.1903	.3226	.3395	.2283	.3507	.3120	.1415	.0768	.1565	-.1119

UGR File #c073/A77, part 2
SAND-77-1992
Oct. 1976-Sept. 1977

TABLE I (Continued)

CONOCO HYDROFRACTURE-CASPER,WYO

FRACTURE-MARCH 22,1977

TIME		180°	200°	Well 59	220°	240°	Well 74	260°	280°	300°	320°	Well 53	340°
12:49:40		.2072	.2678	.1905	.3227	.3396	.2282	.3513	.3141	.1435	.0761	.1571	-.1289
12:50:20		.2065	.2679	.1905	.3233	.3405	.2286	.3513	.3125	.1421	.0784	.1566	-.1287
12:51:00		.2066	.2681	.1905	.3234	.3399	.2289	.3523	.3150	.1436	.0762	.1565	-.1319
12:51:40		.2074	.2680	.1903	.3226	.3400	.2279	.3505	.3117	.1405	.0749	.1565	-.1142
12:52:20		.2072	.2675	.1904	.3229	.3397	.2284	.3513	.3123	.1432	.0779	.1567	-.1211
12:53:00		.2071	.2680	.1905	.3232	.3402	.2280	.3506	.3129	.1428	.0774	.1556	-.1188
12:53:40		.2083	.2697	.1909	.3239	.3410	.2290	.3532	.3161	.1438	.0772	.1551	-.1167
12:54:20		.2073	.2687	.1906	.3229	.3396	.2277	.3509	.3109	.1430	.0870	.1563	-.0925
12:55:00		.2066	.2673	.1900	.3218	.3367	.2272	.3496	.3097	.1435	.0862	.1562	-.0935
12:55:40		.2054	.2660	.1892	.3205	.3364	.2262	.3491	.3139	.1405	.0735	.1565	-.1343
12:56:20		.2049	.2666	.1893	.3213	.3373	.2268	.3478	.3066	.1413	.0845	.1556	-.0722
12:57:00		.2050	.2657	.1891	.3200	.3339	.2255	.3484	.3082	.1406	.0819	.1542	-.0953
12:57:40		.2104	.2724	.1939	.3280	.3419	.2303	.3560	.3185	.1443	.0753	.1531	-.1332
12:58:20		.2086	.2697	.1910	.3235	.3370	.2274	.3503	.3113	.1427	.0876	.1562	-.0856
12:59:00		.2033	.2702	.1909	.3241	.3369	.2280	.3517	.3127	.1438	.0893	.1565	-.0596
12:59:40		.2093	.2708	.1915	.3259	.3388	.2295	.3543	.3200	.1437	.0753	.1595	-.1415
13:00:20		.2139	.2754	.1941	.3300	.3433	.2333	.3587	.3226	.1485	.0842	.1610	-.1124
13:01:00		.2165	.2779	.1954	.3321	.3467	.2354	.3611	.3240	.1515	.0900	.1631	-.0935
13:01:40		.2152	.2754	.1945	.3308	.3444	.2341	.3592	.3250	.1507	.0892	.1615	-.1392
13:02:20		.2170	.2773	.1949	.3320	.3466	.2346	.3602	.3231	.1516	.0895	.1629	-.0923
13:03:00		.2166	.2784	.1950	.3326	.3471	.2347	.3601	.3208	.1515	.0949	.1619	-.0621
13:03:40		.2152	.2768	.1945	.3314	.3459	.2344	.3605	.3241	.1495	.0837	.1618	-.1182
13:04:20		.2151	.2742	.1932	.3283	.3440	.2327	.3574	.3216	.1470	-.0860	.1588	-.0997
13:05:00		.2164	.2782	.1956	.3332	.3489	.2360	.3620	.3241	.1507	.0934	.1632	-.0327
13:05:40		.2204	.2810	.1970	.3355	.3501	.2378	.3639	.3268	.1544	.0912	.1653	-.0764
13:06:20		.2158	.2768	.1948	.3316	.3469	.2350	.3601	.3254	.1497	.0819	.1628	-.1257
13:07:00		.2167	.2779	.1952	.3335	.3477	.2353	.3620	.3254	.1516	.0872	.1625	-.0957
13:07:40		.2163	.2778	.1954	.3331	.3492	.2360	.3623	.3264	.1513	.0861	.1632	-.1109
13:08:20		.2159	.2776	.1955	.3326	.3478	.2357	.3613	.3245	.1505	.0863	.1632	-.1134
13:09:00		.2149	.2771	.1943	.3314	.3481	.2354	.3606	.3266	.1513	.0830	.1635	-.1123
13:09:40		.2183	.2794	.1957	.3342	.3448	.2362	.3628	.3265	.1509	.0861	.1627	-.0947
13:10:20		.2160	.2762	.1943	.3307	.3459	.2342	.3594	.3213	.1490	.0871	.1632	-.0911
13:11:00		.2163	.2777	.1951	.3324	.3490	.2355	.3603	.3230	.1503	.0916	.1628	-.0942
13:11:40		.2165	.2781	.1955	.3334	.3499	.2362	.3622	.3235	.1529	.0947	.1630	-.0779
13:12:20		.2160	.2779	.1949	.3334	.3500	.2364	.3626	.3262	.1524	.0869	.1624	-.0372
13:13:00	Start pumping	.2146	.2768	.1942	.3312	.3476	.2349	.3602	.3213	.1512	.0963	.1617	-.0723
13:13:40		.2126	.2739	.1930	.3290	.3449	.2327	.3577	.3212	.1469	.0796	.1603	-.1146
13:14:20		.2110	.2722	.1921	.3268	.3437	.2311	.3553	.3181	.1461	.0841	.1582	-.1775
13:15:00		.2126	.2716	.1912	.3265	.3431	.2301	.3555	.3171	.1458	.0855	.1578	-.0870
13:15:40		.2295	.2735	.1914	.3253	.3420	.2299	.3542	.3160	.1443	.0768	.1579	-.1161
13:16:20		.2295	.2706	.1911	.3253	.3410	.2298	.3530	.3175	.1415	.0725	.1563	-.1416
13:17:00		.2091	.2710	.1911	.3255	.3424	.2300	.3545	.3175	.1465	.0812	.1572	-.1182
13:17:40		.2108	.2720	.1924	.3282	.3448	.2314	.3569	.3170	.1482	.0889	.1544	-.3767

TABLE I (Continued)

CONOCO HYDROFRACTURE-CASPER,WYO

FRACTURE-MARCH 22,1977

TIME		180°	200°	Well 59	220°	240°	Well 74	260°	280°	300°	320°	Well 53	340°
11:18:20		.2097	.2702	.1916	.3262	.3432	.2303	.3546	.3173	.1461	.0833	.1577	-.0390
11:19:00		.2097	.2712	.1916	.3262	.3422	.2300	.3531	.3171	.1451	.0788	.1587	-.1074
11:19:40		.2107	.2729	.1925	.3280	.3451	.2316	.3574	.3189	.1480	.0886	.1563	-.0936
11:20:20		.2096	.2708	.1915	.3252	.3420	.2300	.3537	.3187	.1439	.0740	.1574	-.1167
11:21:00		.2095	.2711	.1914	.3254	.3409	.2300	.3535	.3143	.1460	.0859	.1579	-.0821
11:21:40		.2092	.2703	.1917	.3259	.3427	.2306	.3551	.3165	.1470	.0852	.1594	-.0965
11:22:20		.2101	.2708	.1912	.3257	.3425	.2302	.3537	.3162	.1467	.0815	.1573	-.1067
11:23:00		.2100	.2712	.1920	.3268	.3438	.2307	.3551	.3181	.1458	.0833	.1579	-.0882
11:23:40		.2101	.2714	.1914	.3265	.3436	.2308	.3550	.3173	.1487	.0877	.1569	-.0782
11:24:20		.2106	.2713	.1913	.3261	.3425	.2305	.3539	.3159	.1447	.0834	.1577	-.0927
11:25:00		.2099	.2717	.1918	.3271	.3439	.2313	.3560	.3204	.1461	.0803	.1591	-.1238
11:25:40		.2095	.2705	.1917	.3265	.3436	.2311	.3559	.3194	.1454	.0778	.1586	-.1192
11:26:20		.2092	.2706	.1911	.3253	.3428	.2304	.3529	.3165	.1467	.0831	.1560	-.0922
11:27:00		.2098	.2698	.1911	.3238	.3411	.2297	.3526	.3146	.1431	.0839	.1572	-.0897
11:27:40		.2107	.2715	.1917	.3275	.3443	.2309	.3554	.3166	.1496	.0897	.1581	-.0930
11:28:20		.2092	.2709	.1918	.3261	.3434	.2309	.3553	.3174	.1459	.0816	.1582	-.0897
11:29:00		.2100	.2714	.1914	.3253	.3427	.2300	.3535	.3166	.1448	.0827	.1569	-.1044
11:29:40		.2104	.2713	.1916	.3265	.3437	.2306	.3553	.3174	.1475	.0846	.1585	-.0948
11:30:20		.2102	.2714	.1913	.3267	.3439	.2309	.3555	.3202	.1495	.0842	.1576	-.0972
11:31:00		.2095	.2713	.1914	.3262	.3431	.2308	.3550	.3181	.1460	.0828	.1541	-.1042
11:31:40		.2104	.2713	.1917	.3263	.3440	.2310	.3549	.3168	.1461	.0842	.1577	-.0930
11:32:20		.2103	.2717	.1917	.3272	.3435	.2306	.3552	.3178	.1460	.0776	.1573	-.1128
11:33:00		.2107	.2721	.1918	.3268	.3445	.2311	.3559	.3202	.1451	.0768	.1582	-.1168
11:33:40		.2100	.2708	.1915	.3261	.3434	.2306	.3542	.3148	.1466	.0915	.1564	-.0688
11:34:20		.2102	.2715	.1916	.3269	.3443	.2308	.3554	.3167	.1466	.0850	.1583	-.0892
11:35:00		.2094	.2702	.1911	.3253	.3423	.2302	.3546	.3180	.1439	.0763	.1572	-.1330
11:35:40		.2099	.2722	.1920	.3273	.3448	.2314	.3563	.3181	.1456	.0832	.1576	-.1010
11:36:20		.2094	.2701	.1912	.3257	.3429	.2303	.3537	.3158	.1444	.0832	.1576	-.0958
11:37:00		.2095	.2713	.1912	.3257	.3432	.2309	.3545	.3173	.1456	.0824	.1578	-.0971
11:37:40		.2102	.2712	.1915	.3252	.3425	.2303	.3525	.3156	.1448	.0844	.1576	-.0975
11:38:20		.2088	.2701	.1916	.3254	.3428	.2303	.3546	.3146	.1457	.0845	.1563	-.0969
11:39:00		.2096	.2714	.1913	.3255	.3431	.2306	.3543	.3174	.1480	.0841	.1585	-.1030
11:39:40		.2096	.2712	.1913	.3260	.3432	.2305	.3543	.3143	.1454	.0932	.1572	-.0816
11:40:20		.2093	.2705	.1913	.3261	.3431	.2310	.3544	.3170	.1440	.0830	.1568	-.1156
11:41:00		.2095	.2712	.1921	.3264	.3446	.2309	.3557	.3188	.1441	.0815	.1580	-.1128
11:41:40		.2101	.2707	.1913	.3258	.3428	.2299	.3535	.3162	.1434	.0848	.1575	-.1013
11:42:20	Stop pumping	.2117	.2727	.1930	.3286	.3455	.2327	.3569	.3182	.1476	.0834	.1583	-.0970
11:43:00	Total Vol. - 12,000 gal.	.2130	.2733	.1926	.3302	.3469	.2333	.3591	.3241	.1494	.0871	.1602	-.0921
11:43:40		.2119	.2733	.1927	.3286	.3465	.2330	.3577	.3199	.1478	.0855	.1593	-.0852
11:44:20		.2121	.2723	.1922	.3275	.3446	.2318	.3558	.3171	.1467	.0886	.1592	-.0933
11:45:00		.2128	.2744	.1932	.3295	.3464	.2328	.3580	.3226	.1474	.0828	.1593	-.1199
11:45:40		.2122	.2737	.1931	.3282	.3469	.2331	.3580	.3213	.1472	.0851	.1601	-.0916
11:46:20		.2123	.2735	.1930	.3288	.3463	.2328	.3571	.3189	.1490	.0897	.1597	-.0795

UGR File #C075/A77, part 2
SAND-77-1992
Oct. 1976-Sept. 1977

TABLE I (Continued)

CONOCO HYDROFRACTURE-CASPER,WYO

FRACTURE-MARCH 22,1977

TIME	180°	200°	Well 59	220°	240°	Well 74	260°	280°	300°	320°	Well 53	340°
11:47:20	.2112	.2727	.1933	.3283	.3462	.2326	.3565	.3175	.1457	.0874	.1616	-.0913
11:47:40	.2130	.2720	.1932	.3293	.3481	.2327	.3572	.3188	.1488	.0891	.1618	-.0998
11:48:00	.2117	.2735	.1931	.3289	.3456	.2329	.3564	.3216	.1464	.0812	.1587	-.1135
11:48:20	.2126	.2744	.1931	.3297	.3475	.2329	.3585	.3220	.1488	.0872	.1594	-.0972
11:49:00	.2117	.2732	.1929	.3287	.3456	.2324	.3571	.3199	.1459	.0825	.1600	-.1033
11:49:40	.2121	.2728	.1926	.3279	.3448	.2323	.3553	.3157	.1460	.0899	.1588	-.0697
11:50:20	.2117	.2736	.1931	.3283	.3463	.2324	.3568	.3220	.1481	.0792	.1593	-.1174
11:51:00	.2125	.2732	.1928	.3283	.3462	.2331	.3574	.3193	.1485	.0889	.1598	-.0925
11:51:40	.2113	.2727	.1923	.3273	.3453	.2326	.3562	.3176	.1479	.0879	.1595	-.0763
11:52:20	.2118	.2731	.1929	.3285	.3447	.2327	.3562	.3200	.1426	.0771	.1603	-.1289
11:53:00	.2133	.2738	.1927	.3285	.3462	.2326	.3565	.3175	.1477	.0859	.1596	-.0821
11:53:40	.2120	.2737	.1933	.3297	.3473	.2337	.3592	.3225	.1496	.0870	.1605	-.0931
11:54:20	.2112	.2726	.1927	.3272	.3449	.2329	.3560	.3181	.1471	.0874	.1588	-.0913
11:55:00	.2124	.2742	.1931	.3294	.3464	.2336	.3573	.3187	.1486	.0902	.1610	-.0786
11:55:40	.2120	.2739	.1931	.3296	.3479	.2333	.3582	.3216	.1491	.0855	.1611	-.0749
11:56:20	.2123	.2730	.1928	.3286	.3458	.2328	.3561	.3193	.1457	.0842	.1592	-.0923
11:57:00	.2118	.2734	.1931	.3292	.3461	.2332	.3580	.3221	.1471	.0837	.1600	-.1122
11:57:40	.2125	.2742	.1931	.3295	.3466	.2332	.3578	.3209	.1475	.0874	.1597	-.0996
11:58:20	.2125	.2732	.1925	.3273	.3445	.2324	.3554	.3187	.1461	.0879	.1605	-.0864
11:59:00	.2122	.2746	.1932	.3302	.3473	.2330	.3585	.3227	.1481	.0858	.1593	-.0987
11:59:40	.2126	.2743	.1934	.3297	.3471	.2333	.3534	.3240	.1472	.0799	.1589	-.1237
12:00:20	.2119	.2732	.1928	.3293	.3470	.2333	.3530	.3211	.1490	.0869	.1597	-.1015
12:01:00	.2120	.2730	.1923	.3286	.3455	.2328	.3557	.3165	.1483	.0854	.1635	-.0916
12:01:40	.2117	.2733	.1932	.3287	.3479	.2333	.3584	.3235	.1475	.0817	.1595	-.1222

APPENDIX D

TABLE I

SHELL OIL COMPANY - RACHAL NO. 1

FRACTURE - AUGUST 25, 1977

TIME		0°	15°	30°	45°	60°	75°	90°	105°	120°	135°	150°	165°
10:25		1.4233	1.3483	1.2798	1.2334	1.2799	1.3263	1.4164	1.4485	1.4789	1.5704	1.6029	1.6132
10:26		1.4212	1.3456	1.2772	1.2315	1.2774	1.3288	1.4126	1.4470	1.4773	1.5675	1.5990	1.6103
10:27		1.4222	1.3462	1.2767	1.2313	1.2781	1.3280	1.4125	1.4462	1.4775	1.5671	1.6014	1.6117
10:28		1.4035	1.3282	1.2589	1.2142	1.2599	1.3100	1.3938	1.4274	1.4585	1.4846	1.5847	1.5946
10:29		1.3982	1.3228	1.2537	1.2081	1.2541	1.3053	1.3892	1.4229	1.4543	1.4828	1.5793	1.5910
10:30		1.4042	1.3289	1.2599	1.2153	1.2605	1.3110	1.3951	1.4293	1.4594	1.4863	1.5854	1.5979
10:31		1.4003	1.3271	1.2579	1.2176	1.2582	1.3093	1.3930	1.4272	1.4579	1.4866	1.5851	1.5949
10:32		1.4051	1.3294	1.2619	1.2165	1.2621	1.3128	1.3954	1.4288	1.4595	1.4859	1.5856	1.5966
10:33		1.4034	1.3283	1.2591	1.2150	1.2606	1.3098	1.3943	1.4285	1.4588	1.4831	1.5832	1.5941
10:34		1.4001	1.3248	1.2560	1.2118	1.2570	1.3069	1.3905	1.4246	1.4557	1.4831	1.5802	1.5917
10:35		1.4205	1.3453	1.2767	1.2322	1.2771	1.3262	1.4120	1.4462	1.4753	1.5663	1.6035	1.6116
10:36		1.4121	1.3359	1.2675	1.2235	1.2692	1.3181	1.4039	1.4387	1.4688	1.5609	1.5958	1.6056
10:37		1.4108	1.3351	1.2653	1.2221	1.2663	1.3183	1.4022	1.4365	1.4639	1.5586	1.5926	1.6037
10:38		1.4171	1.3418	1.2727	1.2281	1.2737	1.3254	1.4086	1.4431	1.4726	1.5648	1.5982	1.6090
10:39		1.4116	1.3359	1.2670	1.2230	1.2683	1.3186	1.4034	1.4373	1.4684	1.5582	1.5947	1.6037
10:40	Start pumping	1.4163	1.3407	1.2716	1.2277	1.2740	1.3225	1.4084	1.4423	1.4733	1.5643	1.5982	1.6073
10:41		1.4099	1.3344	1.2656	1.2214	1.2665	1.3167	1.4018	1.4360	1.4686	1.5590	1.5919	1.6026
10:42		1.4153	1.3403	1.2709	1.2261	1.2726	1.3217	1.4076	1.4413	1.4714	1.5628	1.5968	1.6062
10:43		1.4181	1.3427	1.2732	1.2296	1.2752	1.3238	1.4096	1.4431	1.4739	1.5667	1.5974	1.6078
10:44		1.4167	1.3428	1.2742	1.2284	1.2752	1.3229	1.4093	1.4443	1.474	1.5643	1.5985	1.6089
10:45		1.4152	1.3396	1.2714	1.2270	1.2723	1.3196	1.4064	1.4400	1.4713	1.5627	1.5962	1.6064
10:46		1.4171	1.3414	1.2723	1.2280	1.2734	1.3227	1.4066	1.4424	1.4723	1.5637	1.5988	1.6084
10:47		1.4154	1.3401	1.2705	1.2269	1.2724	1.3229	1.4075	1.4415	1.4717	1.5643	1.5959	1.607
10:48		1.4192	1.3435	1.2744	1.2297	1.2756	1.3252	1.4105	1.4436	1.4727	1,5644	1.5996	1.6089
10:49		1.4209	1.3454	1.2768	1.2335	1.2787	1.3288	1.4141	1.4476	1.4771	1.5678	1.6027	1.6112
10:50		1.4197	1.344	1.2750	1.2313	1.2773	1.3252	1.4120	1.4466	1.4750	1.5662	1.6009	1.6101
10:51		1.4169	1.3410	1.2722	1.2291	1.2740	1.3224	1.4090	1.4429	1.4737	1.5619	1.5974	1.6081
10:52		1.4194	1.3437	1.2752	1.2305	1.2767	1.3250	1.4111	1.4447	1.4759	1.5654	1.5995	1.6095
10:53		1.4131	1.3377	1.2690	1.2249	1.2703	1.3207	1.4048	1.4381	1.4693	1.5587	1.5958	1.6052
10:54		1.4205	1.3447	1.2754	1.2319	1.2766	1.3251	1.4111	1.4452	1.4736	1.5674	1.6012	1.6094
10:55		1.4173	1.3414	1.2730	1.2286	1.2740	1.3225	1.4090	1.4423	1.4734	1.5634	1.5969	1.6084
10:56		1.4176	1.3425	1.2739	1.2294	1.2754	1.3244	1.4087	1.4435	1.4731	1.5655	1.5982	1.6094
10:57		1.4164	1.3410	1.2728	1.2283	1.2733	1.3251	1.4085	1.4418	1.4718	1.5630	1.5968	1.6072
10:58		1.4157	1.3401	1.2717	1.2274	1.2731	1.3224	1.4073	1.4409	1.4704	1.5627	1.5966	1.6074
10:59		1.4217	1.3471	1.2782	1.2339	1.2787	1.3303	1.4134	1.4473	1.4766	1.5678	1.6021	1.6128
11:00		1.4169	1.3417	1.2730	1.2289	1.2753	1.3232	1.4094	1.4430	1.4732	1.5662	1.5976	1.6082
11:01		1.4134	1.3388	1.2689	1.2253	1.2709	1.3196	1.4050	1.4402	1.4696	1.5629	1.5963	1.6054
11:02		1.4181	1.3434	1.2737	1.2298	1.2756	1.3228	1.4108	1.4449	1.4750	1.5649	1.5980	1.6098
11:03		1.4126	1.3372	1.2679	1.2252	1.2708	1.3198	1.4058	1.4399	1.4695	1.5578	1.5951	1.6069
11:04		1.4151	1.3403	1.2719	1.2285	1.2733	1.3240	1.4082	1.4425	1.4731	1.5649	1.5975	1.6083

SAND-77-1992
Oct. 1976-Sept. 1977

TABLE I (Continued)

SHELL OIL COMPANY - RACHAL NO. 1

FRACTURE - AUGUST 20, 1977

TIME	0°	15°	30°	45°	60°	75°	90°	105°	120°	135°	150°	165°
11:05	1.4146	1.3594	1.2706	1.2276	1.2736	1.3230	1.4077	1.4424	1.4734	1.5629	1.5977	1.6084
11:06	1.4152	1.3593	1.2705	1.2276	1.2729	1.3217	1.4076	1.4418	1.4711	1.5630	1.5959	1.6065
11:07	1.4137	1.3585	1.2710	1.2270	1.2733	1.3231	1.4077	1.4429	1.4729	1.5625	1.5990	1.6083
11:08	1.4197	1.3440	1.2753	1.2207	1.2779	1.3255	1.4130	1.4456	1.4768	1.5676	1.5999	1.6117
11:09	1.4132	1.3329	1.2691	1.2273	1.2725	1.3205	1.4070	1.4413	1.4706	1.5639	1.5965	[illegible]
11:10	1.4101	1.3594	1.2676	1.2243	1.2703	1.3188	1.4057	1.4401	1.4697	1.5588	1.5951	[illegible]
11:11	1.4140	1.3581	1.2699	1.2272	1.2727	1.3215	1.4077	1.4425	1.4724	1.5642	1.5983	[illegible]
11:12	1.4135	1.3566	1.2684	1.2265	1.2714	1.3200	1.4063	1.4403	1.4707	1.5613	1.5950	1.6063
11:13	1.4123	1.3567	1.2694	1.2262	1.2715	1.3177	1.4069	1.4396	1.4695	1.5651	1.5939	[illegible]
11:14	1.4119	1.3567	1.2684	1.2260	1.2715	1.3204	1.4066	1.4397	1.4690	1.5617	1.5946	[illegible]
11:15	1.4136	[illegible]	1.2702	1.2270	1.2734	1.3217	1.4083	1.4419	1.4726	1.5635	[illegible]	[illegible]
11:16	1.4130	1.3578	1.2694	1.2260	1.2713	1.3206	1.4071	1.4409	1.4717	1.5625	1.5958	[illegible]
11:17	1.4122	1.3565	1.2689	1.2259	1.2717	1.3210	1.4065	1.4401	1.4702	1.5602	1.5952	[illegible]
11:18	1.4132	1.3568	1.2724	1.2294	1.2745	1.3239	1.4098	1.4435	1.4729	1.5646	1.5981	[illegible]
11:19	1.4117	1.3567	1.2684	1.2250	1.2710	1.3203	1.4050	1.4397	1.4696	1.5612	1.5947	1.6064
11:20	1.4112	1.3566	1.2681	1.2249	1.2704	1.3184	1.4054	1.4391	1.4701	1.5610	1.5949	[illegible]
11:21	1.4080	1.3565	1.2643	1.2226	1.2681	1.3150	1.4031	1.4367	1.4673	1.559	1.5933	[illegible]
11:22	1.4119	1.3568	1.2684	1.2255	1.2713	1.3191	1.4052	1.4398	1.4689	1.5593	1.5945	1.6064
11:23	1.4167	1.3469	1.2756	1.2307	1.2766	1.3238	1.4106	1.4446	1.4742	1.5681	1.5991	[illegible]
11:24	1.4152	1.3579	1.2693	1.2271	1.2729	1.3205	1.4065	1.4408	1.4707	1.5602	1.5949	1.6061
11:25	1.4118	1.3568	1.2678	1.225	1.2704	1.3198	1.405	1.4396	1.4674	1.5605	1.5934	[illegible]
11:26	1.4106	1.3568	1.2684	1.2257	1.2700	1.3185	1.4045	1.4387	1.4701	1.5589	1.5939	[illegible]
11:27	1.4114	1.3562	1.2676	1.2249	1.2704	1.3183	1.4054	1.4387	1.4691	1.5618	1.5941	[illegible]
11:28	1.4076	1.3543	1.2667	1.2236	1.2697	1.3185	1.4035	1.4380	1.4685	1.5590	1.5921	1.6043
11:29	1.4065	1.3565	1.2657	1.2215	1.2683	1.3157	1.4028	1.4362	1.4669	1.5577	1.5924	1.6038
11:30	1.4162	1.3412	1.2723	1.2291	1.2747	1.322	1.409	1.4438	1.4731	1.5636	1.5963	[illegible]
11:31	1.4105	1.3565	1.2675	1.2245	1.2704	1.3190	1.4045	1.4390	1.4701	1.5595	1.595	1.6047
11:32	1.4150	1.3575	1.2696	1.2254	1.2717	1.3197	1.4061	1.4402	1.4707	1.5597	1.5935	[illegible]
11:33	1.4173	1.3574	1.2684	1.2266	1.2720	1.3204	1.4067	1.4394	1.4695	1.5622	1.5941	[illegible]
11:34	1.4123	1.3419	1.2743	1.2305	1.2757	1.3229	1.4099	1.4442	1.4738	1.5646	1.5972	[illegible]
11:35	1.4123	1.3569	1.2674	1.2253	1.2720	1.3198	1.4059	1.4394	1.4704	1.5637	1.5939	1.6051
11:36	1.4094	1.3569	1.2651	1.2233	1.2675	1.3174	1.4039	1.4374	1.4690	1.5598	1.5915	[illegible]
11:37	1.4145	1.3590	1.2710	1.2278	1.2736	1.3204	1.4089	1.443	1.4719	1.5619	1.5960	1.6063
11:38	1.4152	1.3602	1.2721	1.2285	1.2749	1.3227	1.4093	1.4426	1.4727	1.5652	1.5970	1.6071
11:39	1.4115	[illegible]	1.2672	1.2248	1.2712	1.3193	1.4051	1.4396	1.4683	1.5610	1.5937	1.6043
11:40	1.4109	1.3554	1.2672	1.2247	1.2701	1.3178	1.4049	1.4387	1.4675	1.5573	1.5943	1.6034
11:41	1.4133	1.3576	1.2685	1.2259	1.2716	1.3183	1.4061	1.4393	1.4675	1.5596	1.5931	1.6047
11:42	1.4135	1.3583	1.2707	1.2268	1.2728	1.3204	1.4076	1.4406	1.4709	1.5623	1.5952	[illegible]
11:43	1.4124	1.3569	1.2698	1.2269	1.2726	1.3200	1.4073	1.4406	1.4707	1.5624	1.5939	[illegible]
11:44	1.4149	1.3592	1.2706	1.2262	1.2728	1.3219	1.4087	1.4412	1.4711	1.5611	1.5950	1.6063

USR File #c073/A77, part 2
SAND-77-1992
Oct. 1976-Sept. 1977

TABLE I (Continued)

WELL OIL COMPANY - RACHEL NO. 1

FRACTURE - AUGUST 25, 1977

TIME	0°	15°	30°	45°	60°	75°	90°	105°	120°	135°	150°	165°
11:45	1.4119	1.3371	1.2689	1.2254	1.2717	1.3195	1.4053	1.4370	1.4674	1.5597	1.5939	1.6045
11:46	1.4119	1.3356	1.2676	1.2254	1.2707	1.3195	1.4056	1.4383	1.4693	1.5592	1.5932	1.6043
11:47	1.4132	1.3374	1.2693	1.2258	1.2721	1.3202	1.4070	1.4407	1.4711	1.5610	1.5974	1.6055
11:48	1.4137	1.3384	1.2701	1.2265	1.2731	1.3215	1.4080	1.4415	1.4705	1.5616	1.5926	1.6055
11:49	1.4140	1.3385	1.2700	1.2260	1.2735	1.3205	1.4073	1.4402	1.4715	1.5607	1.5929	1.6059
11:50	1.4118	1.3371	1.2687	1.2252	1.2721	1.3207	1.4065	1.4397	1.4698	1.5601	1.5934	1.6056
11:51	1.4132	1.3363	1.2701	1.2269	1.2735	1.3216	1.4089	1.4416	1.4715	1.5622	1.5932	1.6048
11:52	1.4103	1.3349	1.2663	1.2235	1.2696	1.3164	1.4043	1.4368	1.4664	1.5561	1.5872	1.6004
11:53	1.4152	1.3402	1.2722	1.2281	1.2753	1.3216	1.4091	1.4424	1.4725	1.5633	1.5953	1.6071
11:54	1.4111	1.3364	1.2684	1.2232	1.2715	1.3201	1.4058	1.4386	1.4701	1.5591	1.5913	1.6036
11:55	1.4149	1.3405	1.2726	1.2279	1.2751	1.3231	1.4094	1.4429	1.4724	1.5641	1.5945	1.6061
11:56	1.4168	1.3417	1.2733	1.2293	1.2762	1.3242	1.4102	1.4431	1.4731	1.5625	1.5932	1.6076
11:57	1.4109	1.3363	1.2689	1.2242	1.2702	1.3196	1.4064	1.4392	1.4687	1.5587	1.5903	1.6036
11:58	1.4113	1.3369	1.2677	1.2241	1.2705	1.3187	1.4055	1.4372	1.4680	1.5587	1.5898	1.6032
11:59	1.4140	1.3401	1.2715	1.2272	1.2752	1.3230	1.4096	1.4424	1.4727	1.5621	1.5955	1.6064
12:00	1.4132	1.3391	1.2706	1.2272	1.2737	1.3208	1.4082	1.4413	1.4712	1.5599	1.5932	1.6050
12:01	1.4094	1.3348	1.2655	1.2227	1.2694	1.3182	1.4039	1.4361	1.4668	1.5562	1.5909	1.6024
12:02	1.4154	1.3410	1.2728	1.2287	1.2756	1.3262	1.4102	1.4439	1.4735	1.5637	1.5957	1.6076
12:03	1.4140	1.3395	1.2712	1.2272	1.2731	1.3212	1.4076	1.4412	1.4707	1.5610	1.5932	1.6052
12:04	1.4059	1.3366	1.2673	1.2236	1.2719	1.3197	1.4064	1.4398	1.4704	1.5586	1.5925	1.6042
12:05	1.4106	1.3369	1.2706	1.2271	1.2732	1.3204	1.4074	1.4404	1.4697	1.5601	1.5934	1.6055
12:06	1.4097	1.3364	1.2691	1.2247	1.2714	1.3197	1.4066	1.4396	1.4697	1.5580	1.5926	1.6035
12:07	1.4132	1.3397	1.2722	1.2284	1.2749	1.3237	1.4090	1.4428	1.4721	1.5625	1.5968	1.6065
12:08	1.412	1.3391	1.2699	1.2258	1.2731	1.3205	1.4070	1.4407	1.4692	1.5576	1.5934	1.607
12:09	1.4133	1.3395	1.2722	1.2276	1.2741	1.3219	1.4083	1.4414	1.4717	1.5597	1.5944	1.6056
12:10	1.4111	1.3374	1.2687	1.2255	1.2727	1.3201	1.4060	1.4396	1.4683	1.5573	1.5926	1.6032
12:11	1.4159	1.3416	1.2716	1.2281	1.2760	1.3241	1.4102	1.4428	1.4714	1.5631	1.5957	1.6069
12:12	1.4168	1.3425	1.2732	1.2298	1.2766	1.3249	1.4111	1.445	1.4739	1.5638	1.5970	1.6077
12:13	1.4103	1.3367	1.2676	1.2246	1.2709	1.3169	1.4049	1.4381	1.4688	1.5577	1.5921	1.6028
12:14	1.4155	1.3410	1.2721	1.2295	1.2749	1.3238	1.4099	1.4428	1.4719	1.5627	1.5949	1.607
12:15	1.4118	1.3375	1.2693	1.2256	1.2726	1.3203	1.4076	1.4400	1.4699	1.5585	1.5945	1.6045
12:16	1.4051	1.3314	1.2627	1.2203	1.2672	1.3146	1.4023	1.4356	1.4651	1.5576	1.5880	1.5995
12:17	1.4104	1.3365	1.2687	1.2241	1.2715	1.3197	1.4065	1.4399	1.4680	1.5614	1.5915	1.604
12:18	1.4080	1.3341	1.2646	1.2219	1.2678	1.3162	1.4030	1.4373	1.4671	1.5541	1.5900	1.6009
12:19	1.4104	1.3365	1.2699	1.2247	1.2716	1.3202	1.4064	1.4399	1.4695	1.5591	1.5923	1.6040
12:20	1.4175	1.3425	1.2735	1.2307	1.2775	1.3246	1.4115	1.4443	1.4729	1.5644	1.5966	1.6075
12:21	1.4162	1.3419	1.2728	1.2291	1.2759	1.3242	1.4094	1.4428	1.4713	1.5625	1.5939	1.6071
12:22	1.4119	1.3383	1.2694	1.2262	1.2727	1.3224	1.4079	1.4407	1.4706	1.5616	1.5959	1.6048
12:23	1.4054	1.3321	1.2638	1.2204	1.2674	1.315	1.4021	1.4347	1.4649	1.5564	1.5891	1.6005
12:24	1.4031	1.3293	1.2611	1.2180	1.2644	1.3134	1.4000	1.4328	1.4621	1.5556	1.5874	1.5986

SAND-77-1992
Oct. 1976-Sept. 1977

TABLE I (Continued)

[illegible] OIL COMPANY - [illegible] NO. 1

[illegible] - [illegible] 2[illegible], 1977

TIME		0°	15°	30°	45°	60°	75°	90°	105°	120°	135°	150°	165°
12:25		1.4166	[illegible]	1.2669	1.2244	[illegible]	1.3191	1.4054	1.4591	1.4661	1.5557	1.5730	1.6031
12:26		1.4159	[illegible]	1.2699	1.2269	1.2779	1.3213	1.4067	1.4417	1.4706	1.5585	1.5941	1.6047
12:27		1.4069	1.3521	1.2662	1.2240	1.2711	1.3191	1.4048	1.4593	1.4649	1.5569	[illegible]	[illegible]
12:28		1.4077	[illegible]	1.2664	1.2254	1.2761	1.3197	1.4055	1.4537	1.4670	1.5591	1.5913	[illegible]
12:29		1.4152	[illegible]	[illegible]	1.2261	1.2749	1.3257	1.4067	1.4423	1.4713	1.5650	1.5953	[illegible]
12:30		1.4124	1.3569	1.2664	1.2258	1.2729	1.3211	1.4076	1.4407	1.4692	[illegible]	[illegible]	[illegible]
12:31		1.3973	[illegible]	[illegible]	1.2233	[illegible]	1.3161	[illegible]	[illegible]	1.4669	[illegible]	[illegible]	1.6013
12:32		1.4122	[illegible]	1.2665	1.2260	1.2777	1.3212	[illegible]	1.4401	1.4678	1.5608	1.5710	[illegible]
12:33		1.4152	[illegible]	[illegible]	1.2257	1.2724	1.3222	1.4067	1.4357	1.4687	[illegible]	1.5945	[illegible]
12:34		1.4075	[illegible]	1.2641	1.2212	1.2673	1.3180	1.4058	1.4354	1.4654	1.5605	1.5563	[illegible]
12:35		1.4126	[illegible]	1.2667	1.2261	[illegible]	1.3192	1.4072	[illegible]	1.4676	[illegible]	1.5941	[illegible]
12:36		1.4143	1.3491	1.2675	1.2266	1.2741	1.3215	1.4087	1.4425	1.4702	1.5667	1.5938	[illegible]
12:37		1.4144	1.3597	1.2767	1.2261	1.2745	1.322[illegible]	1.4066	1.4418	1.4704	1.5633	1.5949	[illegible]
12:38		1.4131	1.3591	1.2677	1.2262	1.2769	1.3224	1.4056	1.4409	1.4698	1.5604	1.5949	[illegible]
12:39		1.4156	1.3593	1.2718	1.2261	1.2756	1.3250	1.4093	1.4472	1.4706	1.5637	1.5957	[illegible]
12:40		1.4126	1.3577	1.2664	1.2248	1.2723	1.3219	1.4069	1.4392	1.4696	1.5603	1.5940	[illegible]
12:41		1.4129	1.3550	1.2662	1.2247	1.2722	1.3219	1.4064	1.4395	1.4669	1.5585	1.5940	[illegible]
12:42		1.4121	1.3577	1.2677	1.2243	1.2716	1.3207	1.4065	1.4384	1.4665	1.5600	1.5934	1.6032
12:43		1.4129	[illegible]	1.2700	1.2216	1.2726	1.3257	1.4102	1.4412	1.4729	[illegible]	1.5946	[illegible]
12:44		1.4096	[illegible]	1.2655	1.2191	1.2705	1.3208	1.4060	1.4394	1.4685	1.5610	1.5933	[illegible]
12:45		1.4155	1.3562	1.2676	1.233[illegible]	1.2743	1.3246	1.4092	1.4425	1.4707	1.5659	1.5941	[illegible]
12:46		1.4105	1.3574	1.2661	1.2216	1.2711	1.3222	1.4067	1.4383	1.4698	1.5621	[illegible]	[illegible]
12:47		1.4149	1.3595	1.2700	1.2220	1.2757	1.3254	1.4111	1.4438	1.4736	1.5672	[illegible]	[illegible]
12:48		1.4108	1.3561	1.2665	1.2218	1.2715	1.3210	1.4074	1.4404	1.4697	1.5613	1.5929	1.6041
12:49		1.4075	1.3541	1.2643	1.2211	1.2707	1.3203	1.4056	1.4381	1.4685	1.5606	1.5917	[illegible]
12:50		1.4158	1.3564	1.2677	1.2238	1.2755	1.3226	1.4065	1.4414	1.4700	1.5655	1.5926	[illegible]
12:51		1.4069	1.3508	1.2612	1.2196	1.2669	1.3175	1.4037	1.4363	1.4661	1.5625	1.5891	[illegible]
12:52		1.4102	[illegible]	1.2660	1.2237	1.2727	1.3217	1.4072	1.4404	1.4701	1.5675	1.5930	1.6043
12:53		1.4150	[illegible]	1.2658	1.2223	1.2729	1.3212	1.4070	1.4389	1.4689	1.5612	1.5927	[illegible]
12:54		1.4145	1.3567	1.2678	1.2266	1.2752	1.3248	1.4102	1.4425	1.4720	[illegible]	[illegible]	[illegible]
12:55		1.4042	1.3498	1.2612	1.2189	1.2650	1.3166	1.4057	1.4363	1.4683	1.5633	[illegible]	[illegible]
12:56		1.4116	1.3561	1.2674	1.2244	1.2726	1.3224	1.4066	1.4409	1.4706	1.5637	1.5945	[illegible]
12:57		1.4079	[illegible]	1.2651	1.2200	1.2691	1.3166	1.4045	1.4376	1.4669	1.5613	1.5913	[illegible]
12:58		1.4067	1.3517	1.2669	1.2202	1.2695	1.3189	1.4062	1.4375	1.4678	1.5638	1.5929	[illegible]
12:59		1.4102	1.3545	1.2664	1.2217	1.2764	1.3191	1.4057	1.4362	1.4673	1.5651	1.5909	[illegible]
13:00		1.4171	1.3415	1.2711	1.2266	1.2773	1.3273	1.4134	1.4443	1.4730	1.5677	1.5976	[illegible]
13:01	Stop pumping	1.4167	1.3407	1.2710	1.2292	1.2769	1.3271	1.4132	1.4146	1.4739	1.5664	1.5971	[illegible]
13:02	Total Volume	1.4107	1.3546	1.2668	1.2226	1.2708	1.3203	1.4073	1.4385	1.4687	1.5604	1.5918	[illegible]
13:03	80,000 Gal.	1.4069	1.3523	1.2653	1.2210	1.2693	1.3189	1.4056	1.4376	1.4676	1.5589	1.5923	[illegible]
13:04		1.4063	1.3534	1.2643	1.2215	1.2698	1.3199	1.4065	1.4376	1.4690	1.5607	1.5929	[illegible]

UGR File #c075/A77, part 2
SAND-77-1992
Oct. 1976-Sept. 1977

TABLE I (Continued)

SHELL OIL COMPANY - RACHAL [illegible] 1

FRACTURE - AUGUST 25, 1977

TIME	180°	195°	210°	225°	240°	255°	270°	285°	300°	315°	330°	345°
10:25	1.6671	1.6166	1.8082	1.7492	1.8028	1.7418	1.4362	1.5308	1.7413	1.5212	1.4426	1.4114
10:26	1.6634	1.6157	1.8253	1.7468	1.7997	1.7359	1.5039	1.5327	1.7379	1.5683	1.4403	1.4094
10:27	1.6665	1.6126	1.8266	1.7488	1.8017	1.7411	1.4492	1.5351	1.7403	1.5723	1.4416	1.4107
10:28	1.6491	1.6096	1.8064	1.7311	1.7855	1.7227	1.4357	1.5166	1.7195	1.5518	1.4234	1.3924
10:29	1.6443	1.5973	1.8046	1.7262	1.7790	1.7156	1.4431	1.5126	1.7144	1.5461	1.4196	1.3874
10:30	1.6503	1.6032	1.8112	1.7333	1.7858	1.7258	1.4818	1.5203	1.7239	1.5554	1.4241	1.3930
10:31	1.6485	1.6093	1.8088	1.7301	1.7850	1.7224	1.4339	1.5174	1.7201	1.5516	1.4228	1.3918
10:32	1.6496	1.6014	1.8104	1.7326	1.7864	1.7252	1.4761	1.5193	1.7230	1.5543	1.4252	1.3947
10:33	1.6482	1.6093	1.8081	1.7305	1.7850	1.7231	1.4355	1.518	1.7207	1.5526	1.4233	1.3933
10:34	1.6455	1.5944	1.8053	1.7277	1.7806	1.7202	1.5390	1.5151	1.7170	1.5486	1.4205	1.3904
10:35	1.6660	1.6170	1.8276	1.7480	1.8020	1.7407	1.6995	1.5351	1.7478	1.5707	1.439	1.4074
10:36	1.6597	1.6090	1.8198	1.742	1.7948	1.7328	1.5184	1.5282	1.7322	1.5624	1.4317	1.4020
10:37	1.6580	1.6071	1.8196	1.7406	1.7940	1.7329	1.5356	1.5268	1.7307	1.5608	1.4305	1.4005
10:38	1.6620	1.6150	1.8231	1.7453	1.7984	1.7367	1.5497	1.5311	1.7369	1.5673	1.4366	1.4057
10:39	1.6582	1.6060	1.8187	1.7401	1.7941	1.7321	1.4093	1.5270	1.7315	1.5621	1.4307	1.4010
10:40 Start pumping	1.6613	1.6117	1.8224	1.7434	1.7975	1.7360	1.4197	1.5304	1.7356	1.5654	1.4348	1.4045
10:41	1.6563	1.6046	1.8181	1.7384	1.7927	1.7314	1.4796	1.5256	1.7297	1.5596	1.4294	1.3994
10:42	1.6602	1.6118	1.8216	1.7431	1.7966	1.7347	1.4167	1.5298	1.735	1.5644	1.4345	1.4051
10:43	1.6622	1.6137	1.8240	1.7444	1.7999	1.7377	1.4204	1.5326	1.7383	1.5684	1.4370	1.4080
10:44	1.6624	1.6136	1.8241	1.7449	1.7994	1.738	1.4187	1.5333	1.7393	1.5691	1.4369	1.4080
10:45	1.6603	1.6113	1.8223	1.7438	1.7965	1.7356	1.4584	1.5305	1.7356	1.5648	1.4346	1.4051
10:46	1.6616	1.6118	1.8234	1.7440	1.7987	1.7363	1.4843	1.5314	1.7373	1.5665	1.4351	1.4063
10:47	1.6606	1.6108	1.8220	1.7416	1.7961	1.7348	1.4198	1.5297	1.7354	1.5652	1.4346	1.4054
10:48	1.6622	1.6138	1.8242	1.7464	1.8004	1.7383	1.4309	1.5338	1.7396	1.5690	1.4383	1.4096
10:49	1.6642	1.6151	1.8261	1.7464	1.8004	1.7386	1.5117	1.5335	1.7397	1.5686	1.4388	1.4103
10:50	1.6634	1.6148	1.8252	1.7465	1.8004	1.7380	1.5031	1.5339	1.7405	1.5695	1.4376	1.4093
10:51	1.661	1.6129	1.8234	1.7427	1.7981	1.7361	1.4620	1.5311	1.7370	1.5663	1.4354	1.4067
10:52	1.6638	1.6142	1.8251	1.7460	1.8003	1.7376	1.4823	1.5336	1.7379	1.5666	1.4373	1.4086
10:53	1.6591	1.6102	1.8209	1.7415	1.7961	1.7341	1.4724	1.5292	1.7344	1.5635	1.4323	1.4066
10:54	1.6635	1.6139	1.8260	1.7462	1.8017	1.7397	1.4764	1.5356	1.7424	1.5708	1.4391	1.4108
10:55	1.6618	1.6132	1.8253	1.7441	1.7990	1.7368	1.4485	1.5321	1.7379	1.5669	1.4357	1.4075
10:56	1.6619	1.6131	1.8256	1.746	1.7989	1.7371	1.5341	1.5328	1.7387	1.5678	1.4365	1.4082
10:57	1.6605	1.6123	1.8226	1.7431	1.7979	1.7361	1.5152	1.5310	1.7367	1.5657	1.4344	1.4062
10:58	1.6608	1.6120	1.8227	1.7427	1.7978	1.7355	1.4428	1.5311	1.7371	1.5661	1.4355	1.4064
10:59	1.6666	1.6162	1.8291	1.7495	1.8041	1.7427	1.4072	1.5380	1.7444	1.5726	1.4406	1.4124
11:00	1.6620	1.6133	1.8241	1.7443	1.7993	1.7374	1.3922	1.5325	1.7391	1.5672	1.4354	1.4072
11:01	1.6590	1.6110	1.8213	1.7417	1.7963	1.7343	1.4345	1.5298	1.7354	1.5643	1.4327	1.4040
11:02	1.6602	1.6135	1.8256	1.7465	1.8007	1.7383	1.4498	1.5335	1.7405	1.5681	1.4369	1.4058
11:03	1.6598	1.6133	1.8240	1.7436	1.7988	1.7368	1.4256	1.5321	1.7383	1.5672	1.4317	1.4032
11:04	1.6626	1.6132	1.8252	1.7450	1.8005	1.7369	1.4762	1.5348	1.7410	1.5695	1.4330	1.4061

TABLE I (Continued)

SHELL OIL COMPANY - RACHAL NO. 1

FRACTURE - AUGUST 25, 1977

TIME	180°	195°	210°	225°	240°	255°	270°	285°	300°	315°	330°	345°
11:05	1.6612	1.6132	1.8243	1.7448	1.8064	1.7373	1.4351	1.5336	1.7403	1.5692	[illegible]	[illegible]
11:06	1.6615	1.6144	1.8256	1.7456	1.8013	1.7371	1.3378	1.5361	1.7416	1.5705	1.4336	[illegible]
11:07	1.6623	1.6145	1.8260	1.7454	1.7996	1.7401	1.4369	1.5362	1.7392	[illegible]	1.4316	1.4044
11:08	1.6636	1.6163	1.8276	1.7460	1.8053	1.7414	1.4290	1.5375	1.7442	1.5726	1.4363	[illegible]
11:09	1.6596	1.6165	1.8298	1.7476	1.7935	1.7353	1.4359	1.5412	1.7372	1.5695	[illegible]	[illegible]
11:10	1.6593	1.6114	1.8217	1.7421	1.7966	1.7337	1.4394	1.5298	1.7348	1.5637	[illegible]	[illegible]
11:11	1.6613	1.6143	1.8245	1.7454	1.7991	1.7380	1.9792	1.5334	1.7394	1.5669	1.4318	[illegible]
11:12	[illegible]	1.6161	1.8217	1.7405	1.7966	1.7389	1.8470	1.5301	1.7362	1.5642	1.4296	1.40
11:13	1.6583	1.6193	1.8218	1.7413	1.7966	1.7353	1.8424	1.5296	1.7376	1.5663	1.4294	[illegible]
11:14	[illegible]	1.6192	1.8215	1.7415	1.7975	1.7349	1.8421	1.5294	1.7395	1.5650	1.4307	[illegible]
11:15	1.6593	1.6197	1.8223	1.7434	1.7969	1.7352	1.8418	1.5276	1.7392	1.5667	1.4306	[illegible]
11:16	1.6597	1.6115	1.8226	1.7426	1.7988	1.7368	1.8441	1.5325	1.7391	1.5664	1.4313	[illegible]
11:17	1.6583	1.6106	1.8229	1.7425	1.7971	1.7346	1.8416	1.5298	1.7359	1.5641	1.4291	[illegible]
11:18	1.6612	1.6127	1.8246	1.7457	1.8011	1.7379	1.8457	1.5341	1.7416	1.5694	1.4334	[illegible]
11:19	1.6566	1.6099	1.8221	1.7423	1.7973	1.7350	1.8436	1.5367	1.7379	1.5664	1.4298	1.4027
11:20	1.6576	1.6102	1.8205	1.7414	1.7972	1.7345	1.8426	1.5309	1.7375	1.5664	[illegible]	[illegible]
11:21	[illegible]	1.6065	1.8189	1.7395	1.7948	1.7322	[illegible]	1.5276	1.7341	1.5623	[illegible]	[illegible]
11:22	1.6574	1.6092	1.8213	1.7422	1.7971	1.7349	1.8430	1.5307	1.7375	1.5664	1.4296	[illegible]
11:23	1.6613	1.6124	1.8252	1.7453	1.8002	1.7389	1.8473	1.5349	1.7426	1.5703	[illegible]	[illegible]
11:24	1.6588	1.6124	1.8228	1.7431	1.7983	1.7359	1.8450	1.5319	1.7396	1.5675	1.4315	1.4034
11:25	1.6570	1.6071	1.8204	1.7421	1.7973	1.7336	1.8419	1.5299	1.7365	1.5646	1.4303	1.4027
11:26	1.6564	1.6080	1.8203	1.7412	1.7964	1.7342	1.8431	1.5301	1.7378	1.5658	1.4303	1.4021
11:27	1.6574	1.6079	1.8208	1.7419	1.7965	1.7343	1.8435	1.5297	1.7367	1.5649	1.4291	1.4020
11:28	1.6552	1.6071	1.8191	1.7396	1.7952	1.7324	1.8411	1.5279	1.7355	1.5635	1.4279	[illegible]
11:29	1.6572	1.6087	1.8185	1.7379	1.7952	[illegible]	1.8419	1.5261	1.7351	[illegible]	[illegible]	[illegible]
11:30	1.6588	1.6124	1.8249	1.7445	1.8003	1.7364	1.8473	1.5343	1.7429	1.5700	1.4339	[illegible]
11:31	1.6557	1.6086	1.8200	1.7416	1.7963	1.7337	1.8416	1.5289	1.7371	1.5660	[illegible]	[illegible]
11:32	1.6560	1.6084	1.8211	1.7418	1.7949	1.7344	1.8437	1.5297	1.7383	1.5664	[illegible]	[illegible]
11:33	1.6566	[illegible]	1.8210	1.7413	1.7963	1.7347	[illegible]	1.5302	1.7388	1.5667	1.4303	[illegible]
11:34	1.6591	1.6113	1.8246	1.7443	1.8004	1.7394	1.8460	1.5341	1.7435	1.5714	1.4350	1.4074
11:35	1.6564	1.6085	1.8210	1.7425	1.7974	1.7348	1.8447	1.5304	1.7400	1.5672	1.4310	[illegible]
11:36	1.6545	1.6062	1.8191	1.7385	1.7947	1.7322	1.8410	1.5269	1.7361	1.5634	[illegible]	1.4044
11:37	1.6575	1.6084	1.8205	1.7429	1.7966	1.7354	1.8458	1.5311	1.7407	1.5684	1.4334	1.4047
11:38	1.6579	1.6094	1.8264	1.7443	1.7997	1.7370	1.8431	1.5313	1.7413	1.5670	1.4330	1.4050
11:39	1.6544	1.6072	1.8197	1.7407	1.7959	1.7333	1.8438	1.5265	1.7375	1.5652	1.4299	1.4013
11:40	1.6537	1.6075	1.8199	1.7408	1.7959	1.7332	1.8434	1.5275	1.7374	1.5650	1.4290	1.4013
11:41	1.655	1.6075	1.8202	1.7415	1.7960	1.7346	1.8454	1.5288	1.7389	1.5665	1.4300	1.4019
11:42	1.6550	1.6079	1.8221	1.7421	1.7981	1.7352	1.8451	1.5295	1.7398	1.5674	1.4313	1.4038
11:43	1.6565	1.6078	1.8210	1.7416	1.7970	1.7341	1.8450	1.5287	1.7394	1.5669	1.4301	[illegible]
11:44	1.6566	1.6092	1.8219	1.7430	1.7982	1.7356	1.8470	1.5297	1.7409	1.5682	1.4319	1.4045

USR [illegible] SC[illegible], p[illegible] -
SAND-77-1992
Oct. 1976-Sept. 1977

TABLE I (Continued)

SHELL OIL COMPANY - RACHEL NO. 1

FRACTURE - AUGUST 25, 1977

TIME	180°	195°	210°	225°	240°	255°	270°	285°	300°	315°	330°	345°
11:45	1.6549	1.6063	1.8205	1.7409	1.7960	1.7366	1.8441	1.5273	1.7379	1.5697	1.4293	1.4019
11:46	1.6544	1.6076	1.8195	1.7411	1.7957	1.7359	1.8451	1.5266	1.7370	1.5647	1.4296	1.4[illegible]1
11:47	1.6544	1.6063	1.8207	1.7419	1.7965	1.7366	1.8454	1.5271	1.7377	1.5675	1.4301	1.4[illegible]
11:48	1.6552	1.6063	1.8203	1.7413	1.7963	1.7365	1.8434	1.5274	1.7364	1.5667	1.4302	1.40[illegible]6
11:49	1.6561	1.6066	1.8213	1.7426	1.7988	1.7361	1.8439	1.5264	1.7400	1.5673	1.4308	1.4035
11:50	1.6562	1.6077	1.8197	1.7410	1.7971	1.7356	1.8421	1.5262	1.7375	1.5653	1.4.94	1.4014
11:51	1.6563	1.6076	1.8205	1.7415	1.7968	1.7364	1.8434	1.5276	1.7389	1.5666	1.4307	1.4029
11:52	1.6562	1.6011	1.8163	1.7362	1.7926	1.7374	1.8392	1.5232	1.7348	1.5619	1.4267	1.3992
11:53	1.6570	1.6102	1.8221	1.7447	1.7987	1.7354	1.8448	1.5287	1.7403	1.5679	1.4322	1.4043
11:54	1.6525	1.6063	1.6158	1.7395	1.7953	1.7371	1.8399	1.5244	1.7363	1.5634	1.4280	1.4002
11:55	1.6560	1.6093	1.8218	1.7436	1.7973	1.7356	1.8440	1.5278	1.7402	1.5674	1.4326	1.4047
11:56	1.6567	1.6095	1.8235	1.7438	1.7993	1.7362	1.8446	1.5288	1.7413	1.5685	1.4326	1.4055
11:57	1.6557	1.6061	1.8188	1.7390	1.7949	1.7317	1.8392	1.5235	1.7359	1.5630	1.4281	1.4000
11:58	1.6525	1.6065	1.8182	1.7395	1.7949	1.7324	1.8395	1.5248	1.7361	1.5637	1.4291	1.4000
11:59	1.6558	1.6084	1.8207	1.742	1.7976	1.7344	1.8430	1.5264	1.7392	1.5665	1.4309	1.4034
12:00	1.6546	1.6070	1.8197	1.7404	1.7958	1.7322	1.8406	1.5248	1.7365	1.5644	1.4275	1.4019
12:01	1.6525	1.6069	1.8185	1.7384	1.7934	1.7307	1.8385	1.5224	1.7352	1.5623	1.4272	1.3966
12:02	1.6569	1.6074	1.8230	1.7434	1.7991	1.7354	1.8439	1.5267	1.7404	1.5674	1.4316	1.4042
12:03	1.6547	1.6091	1.8213	1.7424	1.7969	1.7351	1.8441	1.5273	1.7403	1.5676	1.4316	1.4037
12:04	1.6528	1.6075	1.8195	1.7400	1.7956	1.7318	1.8396	1.5237	1.7360	1.5637	1.4279	1.4003
12:05	1.6549	1.6095	1.8211	1.742	1.7981	1.7349	1.8423	1.5268	1.7394	1.5666	1.4304	1.4027
12:06	1.6526	1.6061	1.8188	1.7395	1.7958	1.7316	1.8401	1.5234	1.7366	1.5638	1.4283	1.4002
12:07	1.6559	1.6093	1.8217	1.7422	1.7995	1.7349	1.8451	1.5271	1.7417	1.5690	1.4317	1.4047
12:08	1.6538	1.6081	1.8210	1.7411	1.7980	1.7335	1.8424	1.5259	1.7394	1.5665	1.4306	1.4035
12:09	1.6548	1.6076	1.8215	1.7430	1.7989	1.7348	1.8433	1.5263	1.7396	1.5669	1.431	1.4050
12:10	1.6529	1.6054	1.8197	1.7403	1.7961	1.7321	1.8412	1.5245	1.7375	1.5648	1.4291	1.4007
12:11	1.6554	1.609	1.8224	1.7439	1.7968	1.7357	1.8445	1.5273	1.7421	1.5686	1.4323	1.4048
12:12	1.6570	1.6098	1.8241	1.7448	1.8018	1.7373	1.8456	1.5287	1.7433	1.5703	1.4336	1.4056
12:13	1.6516	1.6066	1.8189	1.7394	1.7964	1.7329	1.8394	1.5227	1.7375	1.5635	1.4280	1.4001
12:14	1.6557	1.6095	1.8221	1.7442	1.8002	1.736	1.8443	1.5275	1.7424	1.5688	1.4324	1.4047
12:15	1.6540	1.6072	1.8204	1.7417	1.7972	1.7327	1.8412	1.5240	1.7387	1.5656	1.4285	1.4006
12:16	1.6488	1.6023	1.8151	1.7352	1.7909	1.7272	1.8316	1.5171	1.7299	1.5575	1.4219	1.3937
12:17	1.6533	1.6067	1.8195	1.7391	1.7962	1.7322	1.8393	1.5227	1.7372	1.5636	1.4260	1.3996
12:18	1.6494	1.6025	1.8169	1.7381	1.7936	1.7293	1.8373	1.5207	1.7343	1.5616	1.4253	1.3974
12:19	1.6519	1.6061	1.8190	1.7393	1.7953	1.7311	1.8353	1.5224	1.7368	1.5636	1.4273	1.3998
12:20	1.6567	1.6091	1.8246	1.7443	1.8012	1.7365	1.8404	1.5275	1.7434	1.5700	1.4332	1.4059
12:21	1.6553	1.6104	1.8233	1.7441	1.8008	1.7379	1.8450	1.5278	1.7438	1.5696	1.4331	1.405
12:22	1.6539	1.6081	1.8212	1.7422	1.7973	1.7369	1.8412	1.5239	1.7390	1.5661	1.4288	1.4010
12:23	1.6490	1.6052	1.8158	1.7367	1.7933	1.7382	1.8361	1.5198	1.7339	1.5606	1.4234	1.3950
12:24	1.6473	1.6011	1.8142	1.7350	1.7910	1.7258	1.8325	1.5159	1.7298	1.5568	1.4202	1.3924

SAND-77-1992
Oct. 1976-Sept. 1977

TABLE I (Continued)

[illegible] - [illegible]

[illegible] - [illegible] 1977

Time		180°	195°	210°	225°	240°	255°	270°	285°	300°	315°	330°	345°
12:25		[illegible]	[illegible]	[illegible]	[illegible]	[illegible]	[illegible]	[illegible]	[illegible]	[illegible]	[illegible]	1.4273	1.3994
12:26		[illegible]	[illegible]	[illegible]	[illegible]	[illegible]	[illegible]	[illegible]	[illegible]	[illegible]	[illegible]	[illegible]	[illegible]
12:27		[illegible]	[illegible]	[illegible]	[illegible]	[illegible]	[illegible]	[illegible]	[illegible]	1.7375	[illegible]	[illegible]	[illegible]
12:28		[illegible]	[illegible]	[illegible]	[illegible]	[illegible]	[illegible]	[illegible]	[illegible]	[illegible]	[illegible]	[illegible]	[illegible]
12:29		[illegible]	[illegible]	[illegible]	[illegible]	[illegible]	[illegible]	[illegible]	[illegible]	[illegible]	[illegible]	[illegible]	[illegible]
12:30		[illegible]	[illegible]	[illegible]	[illegible]	[illegible]	[illegible]	[illegible]	[illegible]	[illegible]	[illegible]	[illegible]	[illegible]
12:31		[illegible]	[illegible]	[illegible]	[illegible]	[illegible]	[illegible]	[illegible]	[illegible]	[illegible]	[illegible]	[illegible]	[illegible]
12:32		[illegible]	[illegible]	[illegible]	[illegible]	[illegible]	[illegible]	[illegible]	[illegible]	[illegible]	[illegible]	[illegible]	[illegible]
12:33		[illegible]	[illegible]	[illegible]	[illegible]	[illegible]	[illegible]	[illegible]	[illegible]	[illegible]	[illegible]	[illegible]	[illegible]
12:34		[illegible]	[illegible]	[illegible]	[illegible]	[illegible]	[illegible]	[illegible]	[illegible]	[illegible]	[illegible]	[illegible]	[illegible]
12:35		[illegible]	[illegible]	[illegible]	[illegible]	[illegible]	[illegible]	[illegible]	[illegible]	[illegible]	[illegible]	[illegible]	[illegible]
12:36		[illegible]	[illegible]	[illegible]	[illegible]	[illegible]	[illegible]	[illegible]	[illegible]	[illegible]	[illegible]	[illegible]	[illegible]
12:37		[illegible]	[illegible]	[illegible]	[illegible]	[illegible]	[illegible]	[illegible]	[illegible]	[illegible]	[illegible]	[illegible]	[illegible]
12:38		[illegible]	[illegible]	[illegible]	[illegible]	[illegible]	[illegible]	[illegible]	[illegible]	[illegible]	[illegible]	[illegible]	[illegible]
12:39		[illegible]	[illegible]	[illegible]	[illegible]	[illegible]	[illegible]	[illegible]	[illegible]	[illegible]	[illegible]	[illegible]	[illegible]
12:40		[illegible]	[illegible]	[illegible]	[illegible]	[illegible]	[illegible]	[illegible]	[illegible]	[illegible]	[illegible]	[illegible]	[illegible]
12:41		[illegible]	[illegible]	[illegible]	[illegible]	[illegible]	[illegible]	[illegible]	[illegible]	[illegible]	[illegible]	[illegible]	[illegible]
1.4.		[illegible]	[illegible]	[illegible]	[illegible]	[illegible]	[illegible]	[illegible]	[illegible]	[illegible]	[illegible]	[illegible]	[illegible]
13:07		[illegible]	[illegible]	[illegible]	[illegible]	[illegible]	[illegible]	[illegible]	[illegible]	[illegible]	[illegible]	[illegible]	[illegible]
13:08		[illegible]	[illegible]	[illegible]	[illegible]	[illegible]	[illegible]	[illegible]	[illegible]	[illegible]	[illegible]	[illegible]	[illegible]
13:09		[illegible]	[illegible]	[illegible]	[illegible]	[illegible]	[illegible]	[illegible]	[illegible]	[illegible]	[illegible]	[illegible]	[illegible]
13:10		[illegible]	[illegible]	[illegible]	[illegible]	[illegible]	[illegible]	[illegible]	[illegible]	[illegible]	[illegible]	[illegible]	[illegible]
13:11		[illegible]	[illegible]	[illegible]	[illegible]	[illegible]	[illegible]	[illegible]	[illegible]	[illegible]	[illegible]	[illegible]	[illegible]
13:12		[illegible]	[illegible]	[illegible]	[illegible]	[illegible]	[illegible]	[illegible]	[illegible]	[illegible]	[illegible]	[illegible]	[illegible]
13:13		[illegible]	[illegible]	[illegible]	[illegible]	[illegible]	[illegible]	[illegible]	[illegible]	[illegible]	[illegible]	[illegible]	[illegible]
13:14		[illegible]	[illegible]	[illegible]	[illegible]	[illegible]	[illegible]	[illegible]	[illegible]	[illegible]	[illegible]	[illegible]	[illegible]
13:15		[illegible]	[illegible]	[illegible]	[illegible]	[illegible]	[illegible]	[illegible]	[illegible]	[illegible]	[illegible]	[illegible]	[illegible]
13:16		[illegible]	[illegible]	[illegible]	[illegible]	[illegible]	[illegible]	[illegible]	[illegible]	[illegible]	[illegible]	[illegible]	[illegible]
13:17		[illegible]	[illegible]	[illegible]	[illegible]	[illegible]	[illegible]	[illegible]	[illegible]	[illegible]	[illegible]	[illegible]	[illegible]
13:18		[illegible]	[illegible]	[illegible]	[illegible]	[illegible]	[illegible]	[illegible]	[illegible]	[illegible]	[illegible]	[illegible]	[illegible]
13:19		[illegible]	[illegible]	[illegible]	[illegible]	[illegible]	[illegible]	[illegible]	[illegible]	[illegible]	[illegible]	[illegible]	[illegible]
13:20		[illegible]	[illegible]	[illegible]	[illegible]	[illegible]	[illegible]	[illegible]	[illegible]	[illegible]	[illegible]	[illegible]	[illegible]
13:21		[illegible]	[illegible]	[illegible]	[illegible]	[illegible]	[illegible]	[illegible]	[illegible]	[illegible]	[illegible]	[illegible]	[illegible]
13:22		[illegible]	[illegible]	[illegible]	[illegible]	[illegible]	[illegible]	[illegible]	[illegible]	[illegible]	[illegible]	[illegible]	[illegible]
13:23		[illegible]	[illegible]	[illegible]	[illegible]	[illegible]	[illegible]	[illegible]	[illegible]	[illegible]	[illegible]	[illegible]	[illegible]
13:24		[illegible]	[illegible]	[illegible]	[illegible]	[illegible]	[illegible]	[illegible]	[illegible]	[illegible]	[illegible]	[illegible]	[illegible]
13:25	Stop pumping	[illegible]	[illegible]	[illegible]	[illegible]	[illegible]	[illegible]	[illegible]	[illegible]	[illegible]	[illegible]	[illegible]	[illegible]
13:26	Total volume	[illegible]	[illegible]	[illegible]	[illegible]	[illegible]	[illegible]	[illegible]	[illegible]	[illegible]	[illegible]	[illegible]	[illegible]
13:27	80,000 Gal.	[illegible]	[illegible]	[illegible]	[illegible]	[illegible]	[illegible]	[illegible]	[illegible]	[illegible]	[illegible]	[illegible]	[illegible]
13:28		[illegible]	[illegible]	[illegible]	[illegible]	[illegible]	[illegible]	[illegible]	[illegible]	[illegible]	[illegible]	[illegible]	[illegible]

UGR File #c073/A77, part 2
SAND-77-1992
Oct. 1976-Sept. 1977

APPENDIX D

TABLE II

SHELL OIL COMPANY - RACHAL NO. 1

FRACTURE - AUGUST 26, 1977

TIME	0°	15°	30°	45°	60°	75°	90°	105°	120°	135°	150°	165°
7:50	1.4347	1.3584	1.2909	1.2435	1.2895	1.3414	1.4247	1.4555	1.4896	1.5831	1.6167	1.6297
7:51	1.4277	[illegible]	1.2866	1.2370	1.2841	1.3377	1.4198	1.4[illegible]	1.4[illegible]	1.5763	1.6152	1.6283
7:52	1.4325	1.3565	1.2888	1.2420	1.2871	1.3402	1.4239	1.4535	1.4863	1.5823	1.6151	1.6291
7:53	1.4379	1.3616	1.2945	1.2469	1.2931	1.3459	1.4295	1.4577	1.4950	1.5870	1.6178	1.6319
7:54	1.4317	1.3567	1.2861	1.2414	1.2866	1.3369	1.4223	1.4513	1.4873	1.5793	1.6141	1.6266
7:55	1.4296	1.3539	1.2865	1.2402	1.2852	1.3378	1.4219	1.4518	1.4865	1.5807	1.6149	1.6273
7:56	1.4318	1.3566	1.2891	1.2421	1.2875	1.3404	1.4230	1.4542	1.4889	1.5822	1.6151	1.6286
7:57	1.4343	1.3636	1.2916	1.2437	1.2897	1.3410	1.4248	1.4556	1.4896	1.5828	1.6173	1.6301
7:58	1.4332	1.3577	1.2900	1.2424	1.2885	1.3410	1.4237	1.4546	1.4902	1.5832	1.6154	1.6296
7:59	1.4312	1.3553	1.2876	1.2408	1.2865	1.3393	1.4224	1.4537	1.4877	1.5808	1.6171	1.6275
8:00	1.4334	1.3572	1.2900	1.2431	1.2875	1.3400	1.4246	1.4546	1.4887	1.5808	1.6150	1.6287
8:01	1.4266	1.3511	1.2839	1.2366	1.2827	1.3347	1.4185	1.4497	1.4842	1.5772	1.6108	1.6239
8:02	1.4293	1.3534	1.2860	1.2387	1.2841	1.3365	1.4198	1.4504	1.4853	1.5782	1.613[illegible]	1.6255
8:03	1.4[illegible]	1.3[illegible]	1.3123	1.2645	1.3098	1.3609	1.4447	1.4747	1.5072	1.5997	1.6355	1.6438
8:04	1.4230	1.3476	1.2799	1.2325	1.2788	1.3300	1.4133	1.4444	1.4787	1.5722	1.6066	1.6205
8:05	1.4286	1.3524	1.2862	1.2386	1.2847	1.3364	1.4191	1.4493	1.4854	1.5778	1.6117	1.6250
8:06	1.4256	1.3491	1.2828	1.2353	1.2807	1.3328	1.4163	1.4468	1.4811	1.5739	1.6093	1.6223
8:07	1.4285	1.3526	1.2867	1.2392	1.2837	1.3366	1.4199	1.4506	1.4856	1.5787	1.6102	1.6243
8:08	1.4293	1.3523	1.2863	1.2377	1.2839	1.3345	1.4197	1.4499	1.4843	1.5774	1.6120	1.6251
8:09	1.4397	1.3634	1.2970	1.2487	1.2951	1.3468	1.4307	1.4617	1.4953	1.5885	1.6214	1.6346
8:10	1.4213	1.3452	1.2783	1.2318	1.2770	1.3290	1.4135	1.4445	1.4793	1.5723	1.6065	1.6200
8:11	1.4298	1.3532	1.2874	1.2391	1.2845	1.3364	1.4198	1.4501	1.4856	1.5795	1.6137	1.6257
8:12	1.4271	1.3509	1.2844	1.2376	1.2829	1.3352	1.4193	1.4499	1.4843	1.5778	1.6115	1.6243
8:13	1.4371	1.3610	1.2942	1.2451	1.2918	1.3438	1.4272	1.4575	1.4926	1.5858	1.6190	1.6318
8:14	1.4325	1.3564	1.2896	1.2417	1.2877	1.3366	1.4231	1.4534	1.4885	1.5821	1.6134	1.6273
8:15	1.4328	1.3566	1.2902	1.2423	1.2877	1.3399	1.4231	1.4532	1.4888	1.5808	1.6164	1.6277
8:16	1.4326	1.3571	1.2898	1.2420	1.2870	1.3389	1.4237	1.4531	1.4887	1.5804	1.6157	1.627[illegible]
8:17	1.4349	1.3591	1.2926	1.2445	1.2906	1.3413	1.4268	1.4554	1.4900	1.5819	1.6165	1.6299
8:18	1.432[illegible]	1.3567	1.2904	1.2324	1.2785	1.3398	1.4131	1.4448	1.4793	1.5718	1.6056	1.6193
8:19	1.4315	1.3552	1.2885	1.2407	1.2863	1.3375	1.4212	1.4506	1.4865	1.5792	1.6133	1.6254
8:20	1.4294	1.3533	1.2863	1.2382	1.2845	1.3365	1.4198	1.4506	1.4863	1.5775	1.6118	1.6244
8:21	1.4308	1.3543	1.2868	1.2401	1.2851	1.3367	1.4204	1.4511	1.4856	1.5774	1.6120	1.6269
8:22	1.4217	1.3453	1.2791	1.2319	1.2772	1.3286	1.4131	1.4441	1.4793	1.5711	1.6075	1.6173
8:23	1.4274	1.3501	1.2835	1.2369	1.2825	1.3323	1.4170	1.4477	1.4825	1.5745	1.6110	1.6221
8:24	1.4282	1.3526	1.2861	1.2399	1.2844	1.3361	1.4190	1.4497	1.4858	1.5771	1.6109	1.6232
8:25	1.4314	1.3549	1.2887	1.2409	1.2864	1.3387	1.4224	1.4531	1.4875	1.5793	1.6137	1.6268
8:26	1.4285	1.3520	1.2852	1.2379	1.2835	1.3344	1.4184	1.4497	1.4831	1.5754	1.6106	1.6240
8:27	1.4255	1.3490	1.2828	1.2349	1.2817	1.3310	1.4166	1.4466	1.4823	1.5748	1.6089	1.6221
8:28	1.4343	1.3577	1.2911	1.2436	1.2878	1.3414	1.4235	1.4538	1.4877	1.5801	1.6139	1.6271
8:29	1.4299	1.3532	1.2862	1.2369	1.2851	1.3375	1.4197	1.4506	1.4843	1.5761	1.6120	1.6250

SAND-77-1992
Oct. 1976-Sept. 1977

TABLE II (Continued)

SHELL OIL COMPANY - RACHEL NO. 1

EXECUTION - AUGUST 26, 1977

Time	0°	15°	30°	45°	60°	75°	90°	105°	120°	135°	150°	165°
8:30 Start pumping	1.4[illegible]1	1.3[illegible]	1.2[illegible]	1.2338	1.2837	1.3356	1.4194	1.4592	1.4848	1.5765	1.6116	1.6240
8:31	1.4[illegible]	1.3[illegible]	1.2[illegible]	1.2[illegible]	1.2[illegible]	1.3[illegible]	1.4141	1.4145	1.4[illegible]	1.5[illegible]	1.6[illegible]	1.6194
8:32	1.4[illegible]	1.4[illegible]	1.2[illegible]	1.2[illegible]	1.2[illegible]	1.3[illegible]	1.4140	1.4141	1.4[illegible]	1.5[illegible]	1.6152	1.6[illegible]
8:33	1.4306	1.3[illegible]	1.2[illegible]	1.2404	1.2868	1.3[illegible]	1.4[illegible]	1.4[illegible]	1.4[illegible]	1.5[illegible]	1.6139	1.6[illegible]
8:34	1.4[illegible]	1.3[illegible]	1.2[illegible]	1.2[illegible]	1.2840	1.3395	1.4167	1.4485	1.4[illegible]	1.5[illegible]	1.6113	1.6[illegible]
8:35	1.4[illegible]	1.3[illegible]	1.2[illegible]	1.2[illegible]	1.2[illegible]	1.3[illegible]	1.4[illegible]	1.4[illegible]	1.4[illegible]	1.5761	1.6119	1.6[illegible]
8:36	1.4[illegible]	1.3[illegible]	1.2[illegible]	1.2361	1.2814	1.3[illegible]	1.4163	1.4474	1.4810	1.5757	1.6072	1.6[illegible]
8:37	1.4[illegible]	1.3[illegible]	1.2[illegible]	1.2371	1.2[illegible]	1.3[illegible]	1.4[illegible]	1.4[illegible]	1.4[illegible]	1.5[illegible]	1.6[illegible]	1.6[illegible]
8:38	1.4[illegible]	1.3[illegible]	1.2[illegible]	1.242[illegible]	1.2[illegible]	1.3[illegible]	1.4[illegible]	1.4[illegible]	1.4[illegible]	1.5[illegible]	1.6131	1.6[illegible]
8:39	1.4[illegible]	1.3617	1.2[illegible]	1.2426	1.2[illegible]	1.3[illegible]	1.4[illegible]	1.4[illegible]	1.4[illegible]	1.5[illegible]	1.6173	1.6312
8:40	1.4[illegible]	1.3[illegible]	1.2[illegible]	1.2[illegible]	1.2[illegible]	1.3[illegible]	1.4[illegible]	1.4[illegible]	1.4[illegible]	1.5777	1.6151	1.6[illegible]
8:41	1.4[illegible]	1.3[illegible]	1.2[illegible]	1.2[illegible]	1.2[illegible]	1.3[illegible]	1.4151	1.4460	1.4[illegible]	1.5[illegible]	1.6073	1.6[illegible]
8:42	1.4[illegible]	1.3[illegible]	1.2[illegible]	1.2397	1.2[illegible]	1.3[illegible]	1.4[illegible]	1.4511	1.4843	1.5770	1.6107	1.6[illegible]
8:43	1.4[illegible]	1.3[illegible]	1.2[illegible]	1.2[illegible]	1.2[illegible]	1.3[illegible]	1.4[illegible]	1.4[illegible]	1.4[illegible]	1.5[illegible]	1.6101	1.6[illegible]
8:44	1.4[illegible]	1.3493	1.2[illegible]	1.2359	1.2800	1.3351	1.4166	1.4473	1.4818	1.5769	1.6069	1.6[illegible]
8:45	1.4[illegible]	1.3[illegible]	1.2[illegible]	1.2353	1.2811	1.3316	1.4162	1.4472	1.4811	1.5735	1.6074	1.6[illegible]
8:46	1.4[illegible]	1.3[illegible]	1.2[illegible]	1.2369	1.2827	1.3[illegible]	1.4[illegible]	1.4470	1.4835	1.5763	1.6067	1.6[illegible]
8:47	1.4374	1.3531	1.2[illegible]	1.2373	1.2830	1.3352	1.4170	1.4495	1.4835	1.5[illegible]	1.6100	1.6[illegible]
8:48	1.4364	1.3538	1.2[illegible]	1.2402	1.2847	1.3352	1.4210	1.4[illegible]	1.4849	1.5[illegible]	1.6104	1.6[illegible]
8:49	1.4361	1.3494	1.2[illegible]	1.2397	1.2809	1.3350	1.4171	1.4471	1.4819	1.5755	1.6072	1.6[illegible]
8:50	1.4363	1.3511	1.2[illegible]	1.2403	1.2837	1.3355	1.4155	1.4506	1.4842	1.5763	1.6103	1.6237
8:51	1.4372	1.3[illegible]	1.2[illegible]	1.2404	1.2840	1.3356	1.4203	1.4[illegible]	1.4846	1.5763	1.6105	1.6[illegible]
8:52	1.4376	1.3[illegible]	1.2[illegible]	1.2396	1.2852	1.3357	1.4204	1.4[illegible]	1.4847	1.5774	1.6094	1.6[illegible]
8:53	1.4378	1.3[illegible]	1.2[illegible]	1.2367	1.2[illegible]	1.3354	1.4[illegible]	1.4491	1.4819	1.5744	1.6[illegible]	1.6[illegible]
8:54	1.4[illegible]	1.3[illegible]	1.2[illegible]	1.2403	1.2869	1.3356	1.4204	1.4[illegible]	1.4848	1.5762	1.6110	1.6[illegible]
8:55	1.4377	1.3412	1.2[illegible]	1.2374	1.2820	1.3352	1.4181	1.4476	1.4814	1.5[illegible]	1.6073	1.6[illegible]
8:56	1.4321	1.3458	1.2788	1.2330	1.2772	1.3374	1.4131	1.4450	1.4781	1.5713	1.6037	1.6179
8:57	1.4263	1.3479	1.2824	1.2366	1.2805	1.3319	1.4171	1.4485	1.4812	1.5740	1.6070	1.6[illegible]
8:58	1.4274	1.3410	1.2[illegible]	1.2373	1.2824	1.3[illegible]	1.4181	1.4494	1.4[illegible]	1.5751	1.6089	1.6215
8:59	1.4273	1.3506	1.2852	1.2377	1.2817	1.3321	1.4167	1.4497	1.4823	1.5752	1.6073	1.6266
9:00	1.4253	1.3469	1.2[illegible]	1.2363	1.2810	1.3318	1.4190	1.4486	1.4853	1.5753	1.6060	1.6[illegible]
9:01	1.4337	1.3577	1.2906	1.2427	1.2877	1.3372	1.4225	1.4527	1.4867	1.5773	1.6118	1.6255
9:02	1.4333	1.3467	1.2[illegible]	1.2331	1.2782	1.3300	1.4145	1.4457	1.4785	1.5714	1.6052	1.6190
9:03	1.4372	1.3619	1.2[illegible]	1.2377	1.2827	1.3354	1.4178	1.4494	1.4815	1.5738	1.6077	1.6209
9:04	1.4305	1.3542	1.2840	1.2405	1.2847	1.3371	1.4206	1.4519	1.4850	1.5766	1.6117	1.6232
9:05	1.4257	1.3473	1.2806	1.2335	1.2786	1.3283	1.4146	1.4460	1.4763	1.5709	1.6067	1.6191
9:06	1.4306	1.3537	1.2[illegible]	1.2404	1.2851	1.3367	1.4[illegible]	1.4529	1.4849	1.5772	1.6098	1.6227
9:07	1.4310	1.3547	1.2[illegible]	1.2409	1.2855	1.3361	1.4219	1.4525	1.4853	1.5770	1.6120	1.6241
9:08	1.4242	1.3477	1.2807	1.2345	1.2790	1.3295	1.4149	1.4456	1.4782	1.5714	1.6056	1.6179
9:09	1.4297	1.3537	1.2864	1.2399	1.2841	1.3343	1.4206	1.4509	1.4841	1.5769	1.6107	1.6[illegible]

UGR File FC073/A77, part -
SAND-77-1992
Oct. 1976-Sept. 1977

TABLE II (Continued)

SHELL OIL COMPANY - RACHEL NO. 1

FRACTURES - AUGUST 26, 1977

Time	0°	15°	30°	45°	60°	75°	90°	105°	120°	135°	150°	165°
9:10	1.4[illegible]	1.[illegible]	1.2[illegible]	1.2[illegible]	1.2[illegible]	1.3[illegible]	1.4[illegible]	1.4[illegible]	1.4792	1.5[illegible]	1.6[illegible]	1.6[illegible]
9:11	1.4[illegible]	1.[illegible]	1.2[illegible]	1.2404	1.2849	1.3[illegible]	1.4[illegible]	1.4[illegible]	1.4[illegible]	1.5[illegible]	1.6104	1.6[illegible]
9:12	1.4[illegible]	1.[illegible]	1.2[illegible]	1.2433	1.2[illegible]	1.3[illegible]	1.4[illegible]	1.4544	1.4[illegible]	1.5[illegible]	1.6134	1.6[illegible]
9:13	1.4[illegible]	1.[illegible]	1.2[illegible]	1.2[illegible]	1.2[illegible]	1.3[illegible]	1.4172	1.4464	1.4608	1.5730	1.6056	1.6[illegible]
9:14	1.4[illegible]	1.[illegible]	1.2[illegible]	1.2[illegible]	1.2812	1.3311	1.4179	1.4464	1.4816	1.5734	1.6[illegible]	1.6194
9:15	1.4[illegible]	1.[illegible]	1.2[illegible]	1.2364	1.2806	1.3[illegible]	1.4[illegible]	1.4474	1.4795	1.5[illegible]	1.6[illegible]	1.6153
9:16	1.4[illegible]	1.[illegible]	1.2[illegible]	1.2[illegible]	1.2[illegible]	1.3341	1.4175	1.4[illegible]	1.4816	1.5[illegible]	1.6054	1.6[illegible]
9:17	1.4[illegible]	1.[illegible]	1.2[illegible]	1.2[illegible]	1.2[illegible]	1.3[illegible]	1.4177	1.4477	1.4816	1.5740	1.6064	1.6[illegible]
9:18	1.4[illegible]	1.[illegible]	1.2774	1.2395	1.2787	1.3793	1.4149	1.4456	1.4778	1.5706	1.6061	1.6174
9:19	1.4[illegible]	1.[illegible]	1.2[illegible]	1.2351	1.2793	1.3[illegible]	1.4151	1.4473	1.4787	1.5714	1.6061	1.6170
9:20	1.4341	1.[illegible]	1.2960	1.2440	1.2863	1.3[illegible]	1.4145	1.4[illegible]	1.4869	1.5787	1.6147	1.6[illegible]
9:21	1.4[illegible]	1.[illegible]	1.2[illegible]	1.2388	1.2842	1.3350	1.4203	1.4509	1.4824	1.5751	1.6066	1.6[illegible]
9:22	1.4246	1.[illegible]	1.2809	1.2352	1.2797	1.3799	1.4162	1.4469	1.4785	1.5717	1.6[illegible]	1.6[illegible]
9:23	1.[illegible]	1.[illegible]	1.2[illegible]	1.2361	1.2802	1.3313	1.4177	1.4479	1.4801	1.5727	1.6066	1.6164
9:24	1.4[illegible]	1.[illegible]	1.2829	1.2377	1.2828	1.3311	1.4189	1.4501	1.4820	1.5759	1.6087	1.6[illegible]
9:25	1.4[illegible]	1.[illegible]	1.2[illegible]	1.2364	1.2813	1.3307	1.4173	1.4467	1.4803	1.5725	1.6078	1.6184
9:26	1.4[illegible]	1.[illegible]	1.2[illegible]	1.2364	1.2803	1.3[illegible]	1.4175	1.4465	1.4[illegible]	1.5[illegible]	1.6[illegible]	1.6[illegible]
9:27	1.4246	1.3[illegible]	1.2865	1.2350	1.2792	1.3[illegible]	1.4151	1.4470	1.4781	1.5715	1.6071	1.6157
9:28	1.4172	1.3[illegible]	1.2792	1.2295	1.2743	1.3240	1.4104	1.4473	1.4738	1.5668	1.5963	1.6116
9:29	1.4[illegible]	1.3[illegible]	1.2[illegible]	1.2377	1.2819	1.3312	1.4182	1.4474	1.4818	1.5737	1.6073	1.6[illegible]
9:30	1.4[illegible]	1.3[illegible]	1.2[illegible]	1.2347	1.2803	1.3330	1.4173	1.4[illegible]	1.4[illegible]	1.5[illegible]	1.6111	1.6[illegible]
9:31	1.4243	1.3471	1.2793	1.2352	1.2794	1.3297	1.4151	1.4473	1.4790	1.5713	1.6061	1.6[illegible]
9:32	1.4[illegible]	1.3477	1.2815	1.2365	1.2812	1.3306	1.4150	1.4498	1.4809	1.5735	1.6044	1.6173
9:33	1.4[illegible]	1.3[illegible]	1.2818	1.2363	1.2802	1.3298	1.4174	1.4493	1.4[illegible]	1.5[illegible]	1.6061	1.6[illegible]
9:34	1.4[illegible]	1.3463	1.2773	1.2376	1.2771	1.3[illegible]	1.414[illegible]	1.4463	1.47[illegible]	1.5[illegible]	1.6[illegible]	1.6160
9:35	1.4[illegible]	1.3[illegible]	1.2846	1.2377	1.2837	1.3344	1.4162	1.4517	1.4838	1.5757	1.6106	1.6[illegible]
9:36	1.4[illegible]	1.3484	1.2772	1.2342	1.2786	1.3278	1.4150	1.4472	1.4752	1.5709	1.6043	1.6166
9:37	1.4177	1.3[illegible]	1.2756	1.2291	1.2755	1.3[illegible]	1.4073	1.4410	1.4776	1.5646	1.5965	1.61[illegible]
9:38	1.4[illegible]	1.3[illegible]	1.2773	1.2342	1.2747	1.3[illegible]	1.4150	1.4463	1.4779	1.5709	1.6061	1.6169
9:39	1.4215	1.3466	1.2777	1.2327	1.2774	1.3276	1.4138	1.4456	1.4753	1.5700	1.6041	1.6161
9:40	1.4217	1.3461	1.2776	1.2319	1.2769	1.3265	1.4134	1.4454	1.4763	1.5674	1.6051	1.6154
9:41	1.4[illegible]	1.34[illegible]	1.2768	1.2351	1.2789	1.3260	1.4152	1.4465	1.4[illegible]	1.5[illegible]	1.6053	1.616[illegible]
9:42	1.4[illegible]	1.3[illegible]	1.2816	1.2371	1.2816	1.3307	1.4176	1.4475	1.4799	1.5757	1.6061	1.6162
9:43	1.4247	1.3498	1.2800	1.2360	1.2793	1.3256	1.4153	1.4468	1.4785	1.5709	1.6072	1.6151
9:44	1.4214	1.3464	1.2767	1.2325	1.2765	1.3256	1.4134	1.4453	1.4756	1.5673	1.6036	1.6131
9:45	1.4212	1.3464	1.2764	1.2320	1.2765	1.3255	1.4134	1.4445	1.4757	1.5667	1.6026	1.6142
9:46	1.4211	1.3462	1.2780	1.2326	1.277[illegible]	1.3254	1.4154	1.4431	1.4736	1.5667	1.6012	1.6154
9:47	1.4205	1.3455	1.2767	1.2321	1.2763	1.3265	1.41[illegible]	1.4440	1.4756	1.5677	1.6033	1.6141
9:48	1.4207	1.3458	1.2766	1.2321	1.2762	1.3254	1.4119	1.4440	1.4741	1.5[illegible]	1.6020	1.6139
9:49	1.4217	1.3468	1.2774	1.2326	1.2767	1.3266	1.4128	1.4446	1.4760	1.5683	1.6028	1.6145

UGR File #C073/A77, part 2
SAND-77-1992
Oct. 1976-Sept. 1977

TABLE II (Continued)

Sandia Test Complex - Machine No. 1

Fragment - August 26, 1977

TIME	0°	15°	30°	45°	60°	75°	90°	105°	120°	135°	150°	165°
9:50	1.4175	1.3[illegible]7	1.2729	1.2289	1.2734	1.3[illegible]	1.3[illegible]	1.4[illegible]	1.4[illegible]	1.5[illegible]	1.5604	1.6115
9:51	1.4[illegible]	1.3[illegible]	1.2[illegible]	1.2512	1.2760	1.3247	1.4[illegible]	1.4444	1.4[illegible]	1.5[illegible]	1.6025	1.6145
9:52	1.4217	1.3[illegible]	1.2720	1.2634	1.2733	1.3[illegible]	1.4[illegible]	1.4447	1.4755	1.5[illegible]	1.5[illegible]	1.6139
9:53	1.4184	1.3492	1.2733	1.2366	1.2758	1.3265	1.4100	1.4422	1.4719	1.5646	1.5991	1.6113
9:54	1.4225	1.3477	1.2777	1.2333	1.2728	1.3265	1.4157	1.4403	1.4708	1.5486	1.6045	1.6162
9:55	1.4277	1.3[illegible]	1.2631	1.2397	1.2[illegible]	1.3343	1.4[illegible]	1.4361	1.4653	1.5751	1.6[illegible]	1.6[illegible]
9:56	1.4173	1.3447	1.2752	1.2305	1.2757	1.3246	1.4114	1.4420	1.4732	1.5663	1.6011	1.6137
9:57	1.4177	1.3442	1.2743	1.2318	1.2744	1.3257	1.4[illegible]	1.4426	1.4754	1.5661	1.6028	1.6144
9:58	1.4146	1.3464	1.2703	1.2365	1.2709	1.3211	1.4[illegible]	1.4393	1.4700	1.5634	1.5990	1.6[illegible]
9:59	1.4205	1.3477	1.2755	1.2305	1.2752	1.3247	1.4119	1.4427	1.4739	1.5667	1.6053	1.6172
10:00	1.4211	1.3467	1.2766	1.2317	1.2764	1.3264	1.4142	1.4451	1.4747	1.5680	1.6030	1.6146
10:01	1.4214	1.3468	1.2764	1.2330	1.2769	1.3272	1.4126	1.4453	1.4752	1.5680	1.6034	1.6150
10:02	1.4145	1.3469	1.2684	1.2260	1.2695	1.3200	1.4068	1.4361	1.4688	1.5616	1.5969	1.6096
10:03	1.4217	1.3478	1.2765	1.2332	1.2776	1.3270	1.4141	1.4454	1.4768	1.5676	1.6042	1.6151
10:04	1.4187	1.3440	1.2735	1.2301	1.2748	1.3241	1.4074	1.4429	1.4723	1.5649	1.6002	1.6116
10:05	1.4206	1.3464	1.2751	1.2319	1.2765	1.3266	1.4128	1.4442	1.4748	1.5674	1.6029	1.6144
10:06	1.4199	1.3456	1.2753	1.2313	1.2770	1.3255	1.4119	1.4445	1.4755	1.5675	1.6027	1.6135
10:07	1.4199	1.3456	1.2746	1.2309	1.2768	1.3219	1.4138	1.4432	1.4752	1.5656	1.6013	1.6[illegible]
10:08	1.4214	1.3470	1.2769	1.2327	1.2774	1.3272	1.4141	1.4469	1.4764	1.5689	1.6028	1.6143
10:09	1.4157	1.3417	1.2708	1.2275	1.2723	1.3217	1.4061	1.4412	1.4718	1.565[illegible]	1.5991	1.6112
10:10	1.4165	1.3438	1.2736	1.2302	1.2744	1.3[illegible]	1.4107	1.4432	1.4745	1.5661	1.5993	1.6117
10:11	1.4177	1.3437	1.2746	1.2303	1.2747	1.3235	1.4106	1.4439	1.4738	1.5666	1.5002	1.6122
10:12	1.4168	1.3427	1.2710	1.2286	1.2725	1.3213	1.4073	1.4422	1.4729	1.5644	1.6008	1.6115
10:13	1.4192	1.3443	1.2742	1.2303	1.2744	1.3129	1.4097	1.4418	1.4712	1.5650	1.6009	1.6131
10:14	1.4105	1.3367	1.2667	1.2238	1.2687	1.3174	1.4068	1.4377	1.4692	1.5625	1.5987	1.6090
10:15	1.4146	1.3403	1.2670	1.2260	1.2710	1.3199	1.4067	1.4392	1.4687	1.5631	1.5982	1.6097
10:16	1.4210	1.3467	1.277[illegible]	1.2330	1.2778	1.3269	1.4125	1.4449	1.4757	1.5681	1.6015	1.6145
10:17	1.4168	1.3431	1.2770	1.2331	1.2729	1.3210	1.4086	1.4417	1.4719	1.5654	1.6003	1.6104
10:18	1.4203	1.3463	1.2794	1.2368	1.2814	1.3276	1.4161	1.4499	1.4793	1.5716	1.6053	1.6170
10:19	1.4184	1.3438	1.2765	1.2332	1.2742	1.3243	1.4111	1.4425	1.4733	1.5654	1.5996	1.6117
10:20	1.4156	1.3405	1.2678	1.2264	1.2709	1.3205	1.4061	1.4388	1.4667	1.5617	1.5973	1.6136
10:21	1.4186	1.3432	1.2734	1.2295	1.2743	1.3225	1.4095	1.4420	1.4705	1.5651	1.5973	1.6104
10:22	1.4131	1.3394	1.2670	1.2258	1.2703	1.3196	1.4062	1.4391	1.4678	1.5616	1.5987	1.6093
10:23	1.4158	1.3424	1.2714	1.2285	1.2734	1.3224	1.4085	1.4416	1.4711	1.5653	1.5973	1.6102
10:24	1.4177	1.3437	1.2734	1.2307	1.2760	1.3227	1.4089	1.4411	1.4708	1.5652	1.5986	1.6108
10:25	1.4123	1.3468	1.2763	1.2354	1.2810	1.3292	1.4176	1.4502	1.4832	1.5731	1.6065	1.6125
10:26	1.4215	1.3472	1.2761	1.2358	1.2763	1.3277	1.4144	1.4465	1.4762	1.5694	1.6006	1.6119
10:27	1.4207	1.3471	1.2760	1.2327	1.2[illegible]	1.3282	1.4140	1.4471	1.4753	1.5693	1.6022	1.6126
10:28	1.4200	1.3454	1.2750	1.2314	1.2769	1.3250	1.4134	1.44[illegible]	1.4744	1.5687	1.6017	1.6130
10:29	1.4184	1.3451	1.2731	1.2297	1.2740	1.3227	1.4095	1.4415	1.4712	1.5651	1.5998	1.6105

SAND-77-1992
Oct. 1976-Sept. 1977

TABLE II (Continued)

SOUTH GAS COMPANY - FRACTURE NO. 1

FRACTURE - AUGUST 26, 1977

TIME	0°	15°	30°	45°	60°	75°	90°	105°	120°	135°	150°	165°
10:30	1.4207	1.3[illegible]	1.2767	1.2[illegible]	1.2771	1.3[illegible]	1.4[illegible]	1.4462	1.4741	1.5[illegible]	1.6[illegible]	1.6134
10:31	1.4165	1.3419	1.2723	1.2306	1.2744	1.3260	1.4074	1.4419	1.4722	1.5648	1.5975	1.6100
10:32	1.4196	1.3417	1.2742	1.2315	1.2751	1.3255	1.4119	1.4473	1.4728	1.5657	1.6019	1.6121
10:33	1.4139	1.3[illegible]	1.2[illegible]	1.2[illegible]	1.2762	1.3177	1.4079	1.4[illegible]	1.4[illegible]	1.5[illegible]	1.5[illegible]	1.6[illegible]
10:34	1.4204	1.3402	1.2753	1.2334	1.2769	1.3265	1.4111	1.4451	1.4741	1.5676	1.6025	1.6124
10:35	1.4165	1.34[illegible]	1.2770	1.2[illegible]	1.2741	1.3204	1.4075	1.4417	1.4716	1.5647	1.5986	1.6093
10:36	1.4107	1.33[illegible]	1.2678	1.2244	1.2667	1.3168	1.4047	1.4376	1.4673	1.5[illegible]	1.5944	1.6[illegible]
10:37	1.4156	1.3372	1.2667	1.2261	1.2700	1.3186	1.4054	1.4379	1.4677	1.5[illegible]	1.5987	1.6052
10:38	1.4164	1.3421	1.2714	1.2293	1.2732	1.3221	1.4092	1.4413	1.4718	1.5634	1.5981	1.6074
10:39	1.4143	1.3400	1.2686	1.2269	1.2705	1.3194	1.4060	1.4381	1.4671	1.5605	1.5[illegible]	1.6[illegible]
10:40	1.4153	1.3401	1.2709	1.2276	1.2715	1.3231	1.4075	1.4407	1.4701	1.5671	1.5976	1.6076
10:41	1.4218	1.3473	1.2770	1.2335	1.2782	1.3275	1.4130	1.4462	1.4759	1.5[illegible]	1.6005	1.6119
10:42	1.4129	1.3384	1.2672	1.2255	1.2702	1.3184	1.4060	1.4384	1.4673	1.5613	1.5947	1.6059
10:43	1.4169	1.3426	1.2737	1.2299	1.2746	1.3236	1.4102	1.4422	1.4729	1.5669	1.5977	1.6073
10:44	1.4134	1.3388	1.2693	1.2262	1.2713	1.3188	1.4062	1.4396	1.4687	1.5625	1.5971	1.6069
10:45	1.4148	1.3401	1.2675	1.2286	1.2738	1.3210	1.4075	1.4412	1.4702	1.5635	1.5950	1.6062
10:46	1.4149	1.3376	1.2694	1.2276	1.2716	1.3207	1.4077	1.4405	1.4694	1.5617	1.5965	1.6079
10:47	1.4157	1.3407	1.2713	1.2285	1.2744	1.3215	1.4079	1.4404	1.47	1.5622	1.5972	1.6078
10:48	1.4147	1.3398	1.2692	1.2265	1.2713	1.3158	1.4063	1.4387	1.4679	1.5612	1.5959	1.6066
10:49	1.4166	1.3419	1.2722	1.2300	1.2752	1.3222	1.4086	1.4414	1.4712	1.5628	1.5974	1.6087
10:50	1.4152	1.3405	1.2701	1.2287	1.2730	1.3207	1.4079	1.4405	1.4705	1.5629	1.5964	1.6076
10:51	1.4175	1.3427	1.2723	1.2303	1.2750	1.3237	1.4096	1.4421	1.4715	1.5652	1.5971	1.6079
10:52	1.4128	1.3360	1.2681	1.2260	1.2708	1.3160	1.4060	1.4389	1.4686	1.5621	1.5939	1.6056
10:53	1.4109	1.3362	1.2663	1.2244	1.2688	1.3169	1.4034	1.4366	1.4664	1.5603	1.5923	1.6046
10:54	1.4146	1.3408	1.2689	1.2280	1.2728	1.3203	1.4067	1.4399	1.4697	1.5621	1.5957	1.6062
10:55	1.4145	1.3402	1.2701	1.2270	1.2726	1.3208	1.4074	1.4402	1.4694	1.5617	1.5956	1.6064
10:56	1.4132	1.3389	1.2684	1.2267	1.2714	1.3186	1.4055	1.4390	1.4676	1.5619	1.5942	1.6056
10:57	1.4116	1.3372	1.2673	1.2248	1.2690	1.3154	1.4037	1.4366	1.4666	1.5583	1.5953	1.6047
10:58	1.4123	1.3378	1.2679	1.2262	1.2703	1.3179	1.4052	1.4387	1.4663	1.5598	1.5942	1.6054
10:59	1.4120	1.3373	1.2666	1.2249	1.2695	1.3175	1.4046	1.4378	1.4673	1.5600	1.5936	1.6054
11:00	1.4151	1.3405	1.2702	1.228	1.2727	1.3201	1.4070	1.4396	1.4695	1.5623	1.5943	1.6059
11:01	1.4134	1.3388	1.2686	1.2265	1.2710	1.3199	1.4059	1.4384	1.4671	1.5603	1.5957	1.6057
11:02	1.4166	1.3419	1.2717	1.2293	1.2743	1.3219	1.4087	1.4422	1.4704	1.5623	1.5959	1.6070
11:03	1.4146	1.3397	1.2692	1.2274	1.2721	1.3197	1.4060	1.4375	1.4685	1.5607	1.5950	1.6061
11:04	1.4124	1.3404	1.2683	1.2260	1.2707	1.3178	1.4061	1.4383	1.4671	1.5594	1.5961	1.6046
11:05	1.4124	1.3379	1.2681	1.2258	1.2697	1.3167	1.4049	1.4387	1.4671	1.56	1.5949	1.6048
11:06	1.4060	1.3313	1.2631	1.2224	1.2665	1.3145	1.4004	1.4334	1.4637	1.5556	1.5906	1.6012
11:07	1.4127	1.3380	1.2679	1.2259	1.2702	1.3163	1.4055	1.4386	1.4677	1.5612	1.5947	1.6046
11:08	1.4132	1.3382	1.2679	1.2265	1.2713	1.3193	1.4074	1.4400	1.4684	1.5627	1.5948	1.6056
11:09	1.4125	1.3379	1.2684	1.2267	1.2710	1.3198	1.4064	1.4381	1.4674	1.5616	1.5951	1.6065

SAND-77-1992
Oct. 1976-Sept. 1977

TABLE II (Continued)

SHELL OIL COMPANY - RACHEL NO. 1

FRACTURE - AUGUST 26, 1977

TIME	0°	15°	30°	45°	60°	75°	90°	105°	120°	135°	150°	165°
11:10	1.4105	1.3355	1.2658	1.2242	1.2686	1.3201	1.4022	1.4365	1.4657	1.5568	1.5917	1.6029
11:11	1.4113	1.3367	1.2670	1.2252	1.2696	1.3173	1.4046	1.4371	1.4665	1.5584	1.5933	1.6036
11:12	1.4121	1.3371	1.2662	1.225	1.2696	1.3180	1.4049	1.4381	1.4670	1.5571	1.5929	1.6037
11:13	1.4128	1.3392	1.2692	1.2263	1.2717	1.3214	1.4062	1.4386	1.4658	1.5608	1.5922	1.6048
11:14	1.4136	1.3360	1.2675	1.2266	1.2713	1.3197	1.4061	1.4396	1.4678	1.5616	1.5956	1.6050
11:15	1.4116	1.3374	1.2680	1.2258	1.2709	1.3184	1.4051	1.4360	1.4669	1.5601	1.5941	1.6035
11:16	[illegible]	[illegible]	[illegible]	1.2230	1.2666	1.3147	1.4019	1.4347	1.4631	1.5565	1.5922	1.6012
11:17	1.4110	1.3365	[illegible]	1.2249	1.2708	[illegible]	1.4053	1.4360	1.4667	1.5585	1.5935	1.6041
11:18	1.4119	1.3370	1.2679	1.2247	1.2693	1.3188	1.4042	1.4344	1.4658	1.5555	1.5937	1.6032
11:19	1.4088	1.3349	[illegible]	[illegible]	[illegible]	1.3166	1.4031	1.4359	1.4651	1.5571	1.5915	1.6022
11:20	1.4120	1.3379	1.2682	[illegible]	1.2708	1.3195	1.4059	1.4391	1.4670	1.5613	1.5937	1.6039
11:21	1.4124	1.3382	1.2667	1.2267	1.2713	1.3177	1.4055	1.4383	1.4668	1.5602	1.5937	1.6036
11:22	1.4151	1.3403	1.2703	1.2278	1.2727	1.3207	1.4072	1.4409	1.4689	1.5627	1.5946	1.6049
11:23	1.4095	1.3348	1.2646	1.2235	1.2686	1.3154	1.4036	1.4361	1.4657	1.5564	1.5909	1.6018
11:24	1.4117	1.3365	1.2670	1.2254	1.2694	1.3185	1.4044	1.4365	1.4659	1.5588	1.5929	1.6031
11:25	1.4130	1.3381	1.2678	1.2269	1.2713	1.3204	1.4057	1.4375	1.4667	1.5617	1.5945	1.6044
11:26	1.4167	1.3418	1.2717	1.2304	1.2749	1.3240	1.4096	1.4427	1.4710	1.5642	1.5979	1.6068
11:27	1.4080	1.3332	1.2618	1.2213	1.2661	1.3145	1.4017	1.4343	1.4632	1.5555	1.5916	1.6012
11:28	1.4111	1.3365	1.2664	1.2245	1.2698	1.3179	1.4047	1.4368	1.4656	1.5579	1.5925	1.6032
11:29	1.4109	1.3362	1.2664	1.2245	1.2689	1.3166	1.4037	1.4361	1.4661	1.5555	1.5922	1.6025
11:30	1.4130	1.3380	1.2677	1.2260	1.2705	1.3182	1.4057	1.4375	1.4669	1.5579	1.5944	1.6032
11:31	1.4120	1.3375	1.2663	1.2255	1.2707	1.3175	1.4056	1.4372	1.4655	1.5577	1.5937	1.6025
11:32	1.4090	1.3344	1.2637	1.2223	1.2674	1.3149	1.4023	1.4352	1.4635	1.5554	1.5908	1.6014
11:33	1.4101	1.3351	1.2654	1.2231	1.2672	1.3156	1.4026	1.4351	1.4635	1.5564	1.5910	1.6004
11:34	1.4108	1.3365	1.2679	1.2253	1.2701	1.3176	1.4062	1.4392	1.4669	1.5603	1.5935	1.6025
11:35	1.4118	1.3371	1.2666	1.2251	1.2701	1.3181	1.4042	1.4370	1.4660	1.5589	1.5941	1.6032
11:36	1.41	1.3352	1.2651	1.2233	1.2683	1.3136	1.4019	1.4340	1.4619	1.5589	1.5908	1.5998
11:37	1.4094	1.3347	1.2649	1.2238	1.2692	1.3159	1.4039	1.4357	1.4637	1.5582	1.5912	1.6012
11:38	1.4126	1.3379	1.2683	1.2261	1.2716	1.3188	1.4056	1.4375	1.4667	1.5607	1.5923	1.6021
11:39	1.4115	1.3378	1.2676	1.2259	1.2707	1.3179	1.4044	1.4380	1.4653	1.5586	1.5919	1.6025
11:40	1.4087	1.3345	1.2643	1.2228	1.2678	1.3165	1.4040	1.4362	1.4649	1.5601	1.5922	1.6005
11:41	1.4090	1.3347	1.2640	1.2216	1.2666	1.3153	1.4016	1.4343	1.4634	1.5567	1.5907	1.6008
11:42	1.4104	1.3353	1.2656	1.2241	1.2690	1.3152	1.4036	1.4362	1.4649	1.5585	1.5915	1.6005
11:43	1.4145	1.3389	1.2690	4.2270	1.2724	1.3200	1.4070	1.4388	1.4678	1.5624	1.5934	1.6037
11:44	1.4084	1.3342	1.2640	1.2213	1.2665	1.3152	1.4019	1.4335	1.4644	1.5546	1.5894	1.5993
11:45	1.4142	1.3396	1.2694	1.2280	1.2738	1.3226	1.4081	1.4404	1.4686	1.5616	1.5955	1.6041
11:46	1.4093	1.3338	1.2639	1.2220	1.2673	1.3142	1.4016	1.4342	1.4629	1.5544	1.5927	1.6007
11:47	1.4088	1.3341	1.2642	1.2223	1.2679	1.3156	1.4031	1.4349	1.4641	1.5565	1.5916	1.5996
11:48	1.4071	1.3324	1.2622	1.2208	1.2653	1.3132	1.4003	1.4323	1.4624	1.555	1.5889	1.5982
11:49	1.4107	1.3358	1.2654	1.2237	1.2691	1.3149	1.4043	1.4369	1.4674	1.5592	1.5923	1.6015

TABLE II (Continued)

SHELL OIL COMPANY - FACHAL NO. 1

FORMATION - [illegible]

TIME	0°	15°	30°	45°	60°	75°	90°	105°	120°	135°	150°	165°
11:50	1.4100	[illegible]	1.2653	1.2267	1.2718	1.3165	1.4057	1.4397	1.4687	1.5578	1.5928	1.6039
11:51	[illegible]	[illegible]	[illegible]	[illegible]	[illegible]	[illegible]	[illegible]	[illegible]	1.4645	[illegible]	1.5912	1.6007
11:52	1.4104	1.3395	1.2669	1.2260	1.2692	1.3171	1.4045	1.4366	1.4662	1.5574	1.5913	1.6005
11:53	1.4095	1.3347	1.2659	1.2236	1.2682	1.3160	1.4050	1.4394	1.4635	1.5571	1.5914	1.6000
11:54	1.4100	[illegible]	1.2644	1.2237	1.2694	1.3165	1.4050	1.4368	1.4666	1.5572	1.5915	1.6007
11:55	1.4078	1.3346	1.2629	1.2212	1.2679	1.3154	1.4018	1.4339	1.4629	1.5547	1.5897	1.6001
11:56	1.4079	1.3352	1.2630	1.2210	1.2686	1.3159	1.4022	1.4344	1.4624	1.5563	1.5901	1.5995
11:57	1.4085	1.3341	1.2632	1.2227	1.2687	1.3156	1.4031	1.4344	1.4633	1.5570	1.5895	1.5993
11:58	1.4113	1.3364	1.2655	1.2254	1.2692	1.3174	1.4035	1.4366	1.4663	1.5570	1.5917	1.6011
11:59	1.4137	1.3376	1.2675	1.2268	1.2721	1.3204	1.4057	1.4378	1.4670	1.5592	1.5933	1.6026
12:00	1.4053	1.3304	1.2604	1.2197	1.2644	1.3122	1.3983	1.4306	1.4603	1.5579	1.5876	1.5964
12:01	1.4087	1.3331	1.2621	1.2213	1.2664	1.3168	1.401	1.4325	1.4625	1.5554	1.5907	1.5993
12:02	1.4137	1.3391	1.2692	1.2268	1.2723	1.3175	1.4077	1.4390	1.4704	1.56	1.5956	1.6049
12:03	1.4063	[illegible]	1.2624	1.2223	1.2676	1.3141	1.4015	1.4339	1.4628	1.5584	1.5883	[illegible]
12:04	1.4068	1.3307	1.2601	1.2195	1.2645	1.3129	1.3965	1.4306	1.4595	1.5519	1.5871	[illegible]
12:05	1.4059	1.3313	1.2611	1.2198	1.2658	1.3123	1.4011	1.4329	1.4628	1.5558	1.5876	1.5926
12:06	1.4066	1.3307	1.2633	1.2218	1.2667	1.3156	1.4025	1.4352	1.4650	1.5568	1.5896	[illegible]
12:07	1.4070	1.3302	1.2625	1.2210	1.2663	1.3135	1.4011	1.4333	1.4631	1.5562	1.5879	1.5974
12:08	1.4104	1.3346	1.2634	1.2233	1.2681	1.3150	1.4031	1.4352	1.4654	1.5571	1.5931	1.6009
12:09	1.4079	1.3334	1.2631	1.2211	1.2673	1.3159	1.4028	1.4343	1.4639	1.5562	1.5892	[illegible]
12:10	1.4075	1.3341	1.2638	1.2221	1.2682	1.3153	1.4024	1.4337	1.4631	1.5561	1.5896	1.5984
12:11	1.4081	1.3335	1.2626	1.2208	1.2660	1.3152	1.4008	1.4325	1.4625	1.5566	1.5885	1.5982
12:12	1.4140	1.3366	1.2657	1.2263	1.2723	1.3214	1.4060	1.4383	1.4697	1.5644	1.5957	1.6043
12:13	1.4079	1.3319	1.2612	1.2198	1.2655	1.3147	1.4007	1.4322	1.4618	1.5543	1.5883	1.5961
12:14	1.4081	1.3330	1.2629	1.2217	1.2668	1.3155	1.4018	1.4337	1.4631	1.5585	1.5881	1.5997
12:15	1.4109	1.3341	1.2637	1.2221	1.2682	1.3166	1.4035	1.4352	1.4643	1.5572	1.5901	1.6003
12:16	1.4074	1.3325	1.2627	1.2211	1.2671	1.3154	1.4021	1.4351	1.4641	1.5519	1.5893	1.5991
12:17	1.4093	1.3343	1.2636	1.2222	1.2686	1.3160	1.4027	1.4336	1.4636	1.5568	1.5905	1.6001
12:18	1.4094	1.3343	1.2639	1.2229	1.2675	1.3165	1.4029	1.4333	1.4650	1.5564	1.5892	1.5996
12:19	1.4087	1.3317	1.2610	1.2196	1.2653	1.3139	1.4003	1.4329	1.4608	1.5540	1.5873	1.5970
12:20	1.4067	1.3313	1.2618	1.2203	1.2658	1.3144	1.4018	1.4330	1.4619	1.5554	1.5882	1.5983
12:21	1.4061	1.3306	1.2603	1.2192	1.2653	1.3148	1.4007	1.4318	1.4620	1.5537	1.5855	1.5969
12:22	1.4107	1.3347	1.2641	1.2229	1.2685	1.3177	1.4055	1.4345	1.4645	1.5579	1.5894	1.5996
12:23	1.4075	1.3318	1.2615	1.2202	1.2659	1.3136	1.4014	1.4329	1.4621	1.5540	1.5874	1.5980
12:24	1.4100	1.3346	1.2643	1.2232	1.2687	1.3161	1.4038	1.4345	1.4637	1.5551	1.5914	1.6003
12:25	1.4120	1.3362	1.2657	1.2250	1.2704	1.3180	1.4044	1.4357	1.4647	1.5557	1.5927	1.6010
12:26	1.4076	1.3341	1.2645	1.2237	1.2687	1.3151	1.4032	1.4343	1.4634	1.5557	1.5895	1.5991
12:27	1.4073	1.3322	1.2611	1.2193	1.2651	1.3144	1.4008	1.4324	1.4614	1.5529	1.5870	1.5981
12:28	1.4080	1.3329	1.2622	1.2206	1.2669	1.3148	1.4018	1.4321	1.4616	1.5524	1.5880	1.5986
12:29	1.4080	1.3337	1.2624	1.2225	1.2678	1.3166	1.4027	1.4336	1.4645	1.5565	1.5892	1.5979

UGR File #c073/A77, part 2
SAND-77-1992
Oct. 1976-Sept. 1977

TABLE II (Continued)

SHELL OIL COMPANY - RACHAL NO. 1

FRACTURE - AUGUST 26, 1977

TIME	0°	15°	30°	45°	60°	75°	90°	105°	120°	135°	150°	165°
12:30	1.4074	1.3318	1.2612	1.2201	1.2665	1.3138	1.4013	1.4329	1.4584	1.5539	1.5884	1.5983
12:31	1.4069	1.3308	1.2606	1.2190	1.2647	1.3129	1.4006	1.4301	1.4603	1.5529	1.5857	1.5954
12:32	1.4092	1.3332	1.2634	1.2225	1.2672	1.3149	1.4029	1.4335	1.4621	1.5549	1.5890	1.5991
12:33	1.4077	1.3316	1.2626	1.2212	1.2667	1.3153	1.4032	1.4336	1.4635	1.5560	1.5893	1.5988
12:34	1.4062	1.3313	1.2589	1.2195	1.2652	1.3126	1.4013	1.4328	1.4621	1.5542	1.5865	1.5968
12:35	1.4081	1.3326	1.2672	1.2207	1.2669	1.3151	1.4017	1.4327	1.4618	1.5556	1.5874	1.5979
12:36	1.4082	1.3356	1.2619	1.2211	1.2677	1.3153	1.4023	1.4323	1.4586	1.5558	1.5890	1.5987
12:37	1.4095	1.3342	1.2644	1.2216	1.2686	1.3169	1.4045	1.4343	1.4649	1.5588	1.5908	1.5994
12:38	1.4052	1.3314	1.2621	1.2196	1.2656	1.3139	1.4011	1.4326	1.4617	1.5549	1.5869	1.5968
12:39	1.4094	1.3336	1.2633	1.2221	1.2678	1.3169	1.4036	1.4349	1.4641	1.5529	1.5883	1.5979
12:40	1.4106	1.3350	1.2652	1.2228	1.2689	1.3178	1.4043	1.4346	1.4646	1.5569	1.5905	1.5993
12:41	1.4050	1.3294	1.2583	1.2186	1.2639	1.3116	1.3994	1.4300	1.4595	1.5511	1.5870	1.5949
12:42	1.4115	1.3362	1.2645	1.2237	1.2696	1.3177	1.4054	1.4358	1.4645	1.5565	1.5899	1.6009
12:43	1.4025	1.3325	1.2606	1.2205	1.2662	1.3140	1.4021	1.4327	1.4637	1.5540	1.5881	1.5973
12:44	1.4046	1.3302	1.2593	1.2186	1.2648	1.3137	1.4003	1.4315	1.4605	1.5523	1.5860	1.5963
12:45	1.4029	1.3299	1.2595	1.2175	1.2646	1.3112	1.3993	1.4305	1.4599	1.5548	1.5857	1.5962
12:46	1.4066	1.3301	1.2599	1.2185	1.2650	1.3132	1.4008	1.4321	1.4608	1.5545	1.5874	1.5962
12:47	1.4077	1.3337	1.2630	1.2221	1.2687	1.3160	1.4032	1.4337	1.4629	1.5560	1.5886	1.5984
12:48	1.4086	1.3345	1.2637	1.2219	1.2683	1.3174	1.4035	1.4342	1.4639	1.5541	1.5893	1.5996
12:49	1.4115	1.3368	1.2675	1.2246	1.2714	1.3210	1.4067	1.4376	1.4666	1.5613	1.5933	1.6023
12:50	1.4083	1.3338	1.2624	1.2229	1.2686	1.3175	1.4040	1.4344	1.4635	1.5555	1.5889	1.5992
12:51	1.4073	1.3319	1.2616	1.2200	1.2666	1.3153	1.4031	1.4328	1.4618	1.5533	1.5899	1.5982
12:52	1.4027	1.3287	1.2576	1.2170	1.2632	1.3115	1.3983	1.4294	1.4592	1.5508	1.5845	1.5950
12:53	1.4072	1.3313	1.2608	1.2191	1.2659	1.3152	1.4016	1.4321	1.4623	1.5533	1.5883	1.5974
12:54	1.4097	1.3340	1.2646	1.2228	1.2696	1.3183	1.4049	1.4350	1.4653	1.5564	1.5890	1.5980
12:55	1.4019	1.3267	1.2554	1.2145	1.2608	1.3108	1.3966	1.4272	1.4569	1.5494	1.5846	1.5938
12:56	1.4058	1.3307	1.2606	1.2185	1.2653	1.3139	1.4003	1.4306	1.4611	1.5552	1.5860	1.5965
12:57	1.4127	1.3377	1.2670	1.2249	1.2719	1.3209	1.4076	1.4380	1.4679	1.5621	1.5938	1.6035
12:58	1.4061	1.3317	1.2601	1.2187	1.2649	1.314	1.4016	1.4314	1.4617	1.5504	1.5865	1.5968
12:59	1.4042	1.3293	1.2584	1.2169	1.2640	1.3120	1.3992	1.4302	1.461	1.5534	1.5844	1.5953
13:00	1.4034	1.3281	1.2566	1.2164	1.2617	1.3103	1.3966	1.4260	1.4564	1.5484	1.5826	1.5923
13:01	1.4071	1.3302	1.2604	1.2193	1.2665	1.3152	1.4021	1.4319	1.4626	1.5534	1.5860	1.5979
13:02	1.4019	1.3267	1.2559	1.2154	1.2613	1.3109	1.3979	1.4277	1.4576	1.5496	1.5834	1.5934
13:03	1.4054	1.3298	1.2584	142178	1.2638	1.3138	1.4003	1.43	1.4613	1.5531	1.5868	1.5959
13:04	1.4057	1.3303	1.2596	1.2183	1.2652	1.3133	1.401	1.4312	1.4635	1.5541	1.5859	1.5971
13:05	1.4060	1.3305	1.2603	1.2189	1.2650	1.3136	1.4014	1.4312	1.4615	1.5530	1.5877	1.5978
13:06	1.4012	1.3264	1.2555	1.2145	1.2613	1.3099	1.3958	1.4256	1.4569	1.5472	1.5835	1.5919
13:07	1.4142	1.3379	1.2663	1.2253	1.2719	1.3215	1.4073	1.4373	1.4683	1.5603	1.5953	1.6022
13:08	1.4065	1.3329	1.2613	1.2201	1.2667	1.3145	1.4034	1.4330	1.4620	1.5542	1.5907	1.5986
13:09	1.4092	1.3334	1.2622	1.2210	1.2690	1.3170	1.4041	1.4344	1.4651	1.5561	1.5872	1.5982

TABLE II (Continued)

SHELL OIL COMPANY - RACHAL NO. 1

FRACTURE - AUGUST 26, 1977

Time		0°	15°	30°	45°	60°	75°	90°	105°	120°	135°	150°	165°
13:10		1.4076	1.3314	1.2608	1.2200	1.2662	1.3144	1.4016	1.4324	1.4625	1.5505	1.5964	1.5976
13:11		1.4049	1.3305	1.2574	1.2170	1.2640	1.3125	1.3972	1.4290	1.4697	1.5517	1.5675	1.5954
13:12		1.4102	1.3336	1.2643	1.2217	1.2690	1.3173	1.4049	1.4345	1.4651	1.5567	1.5699	1.5993
13:13		1.4046	1.3321	1.2634	1.2177	1.2640	1.3120	1.3997	1.4284	1.4577	1.5500	1.5659	1.5956
13:14		1.4027	1.3273	1.2572	1.2153	1.2627	1.3105	1.3983	1.4282	1.4577	1.5482	1.5646	1.5936
13:15		1.4050	1.3295	1.2587	1.2187	1.2648	1.312	1.4005	1.4292	1.4599	1.5523	1.5669	1.5950
13:16		1.4055	1.3296	1.2590	1.2176	1.2648	1.3138	1.4014	1.4310	1.4615	1.5533	1.5672	1.5956
13:17		1.4061	1.3307	1.2622	1.2210	1.2672	1.3154	1.4036	1.4332	1.4636	1.5549	1.5685	1.5976
13:18		1.4076	1.3331	1.2626	1.2203	1.2673	1.3154	1.4034	1.4330	1.4632	1.5526	1.5693	1.5979
13:19		1.4070	1.3312	1.2604	1.2192	1.2654	1.3113	1.4015	1.4307	1.4620	1.5546	1.5662	1.5966
13:20		1.4065	1.3324	1.2624	1.2209	1.2673	1.3167	1.4036	1.4325	1.4625	1.5547	1.5671	1.5971
13:21		1.4062	1.3322	1.2623	1.2207	1.2678	1.3176	1.4037	1.4334	1.4634	1.5536	1.5891	1.5986
13:22		1.4065	1.3320	1.2615	1.2184	1.2652	1.3144	1.4028	1.4322	1.4631	1.5559	1.5685	1.5971
13:23		1.4077	1.3312	1.2609	1.2182	1.2653	1.3136	1.4018	1.4307	1.4613	1.5526	1.5676	1.5965
13:24		1.4064	1.3293	1.2574	1.2168	1.2632	1.3124	1.3999	1.4293	1.4585	1.5514	1.5673	1.5953
13:25		1.4074	1.3334	1.2626	1.2202	1.2672	1.3166	1.4034	1.4334	1.4638	1.5567	1.5706	1.5994
13:26		1.4061	1.3311	1.2604	1.2187	1.2653	1.3133	1.4017	1.4315	1.4613	1.5553	1.5701	1.5982
13:27		1.4063	1.3299	1.2591	1.2170	1.2637	1.3121	1.3995	1.4295	1.4578	1.5543	1.5683	1.5957
13:28		1.4090	1.3323	1.2631	1.2211	1.2671	1.3147	1.4036	1.4335	1.4632	1.5534	1.5703	1.5992
13:29		1.4095	1.3333	1.2637	1.2215	1.2672	1.3159	1.4043	1.4336	1.4639	1.5544	1.5703	1.5980
13:30	Stop pumping	1.4045	1.3324	1.2581	1.2145	1.2623	1.3113	1.3995	1.4287	1.4593	1.5519	1.5659	1.5945
13:31	Total volume	1.4070	1.3307	1.2578	1.2161	1.2632	1.3132	1.4006	1.4305	1.4613	1.5515	1.5666	1.5950
13:32	200,000 Gal.	1.4128	1.3339	1.2655	1.2238	1.2695	1.3189	1.4063	1.4351	1.4658	1.5583	1.5912	1.6001
13:33		1.4073	1.3286	1.2576	1.2157	1.2618	1.3109	1.3988	1.4276	1.4582	1.5505	1.5844	1.5944
13:34		1.4141	1.3375	1.2681	1.2258	1.2733	1.3202	1.4106	1.4400	1.4696	1.5623	1.5936	1.6005
13:35		1.4061	1.3275	1.2568	1.2160	1.2622	1.3107	1.3997	1.4270	1.4576	1.5518	1.5828	1.5921
13:36		1.4103	1.3335	1.2636	1.2204	1.2672	1.3158	1.4032	1.4321	1.4570	1.5536	1.5890	1.5978
13:37		1.4070	1.3311	1.2600	1.2176	1.2657	1.3129	1.4017	1.4302	1.4620	1.5535	1.5851	1.5954
13:38		1.4070	1.3302	1.2605	1.2180	1.2651	1.3144	1.4015	1.4301	1.4615	1.5541	1.5869	1.5963
13:39		1.4063	1.3279	1.2585	1.2176	1.2640	1.3131	1.4005	1.4301	1.4612	1.5509	1.5887	1.5964
13:40		1.4075	1.3324	1.2630	1.2197	1.2645	1.3153	1.4033	1.4317	1.4625	1.5562	1.5902	1.5977
13:41		1.4074	1.3291	1.2583	1.2164	1.2638	1.3118	1.4004	1.4291	1.4614	1.5534	1.5866	1.5970
13:42		1.4107	1.3334	1.2633	1.2206	1.2687	1.3170	1.4043	1.4334	1.4629	1.5545	1.5883	1.5983
13:43		1.4077	1.3306	1.2600	1.2144	1.2613	1.3103	1.3987	1.4278	1.4586	1.5477	1.5867	1.5931
13:44		1.4079	1.3303	1.2601	1.2160	1.2642	1.3117	1.4017	1.4299	1.4607	1.5532	1.5854	1.5[illegible]
13:45		1.4147	1.3382	1.2680	1.2251	1.2723	1.3220	1.4096	1.4382	1.4687	1.5590	1.5939	1.6003
13:46		1.4067	1.3297	1.2586	1.2162	1.2630	1.3115	1.4	1.4293	1.4592	1.5566	1.5886	1.5942
13:47		1.4043	1.3276	1.2580	1.2150	1.2620	1.3109	1.3994	1.4277	1.4584	1.5537	1.5847	1.5926
13:48		1.4062	1.3295	1.2591	1.2159	1.2651	1.3123	1.3998	1.4278	1.4593	1.5543	1.5866	1.5949
13:49		1.4077	1.3302	1.2603	1.2177	1.2653	1.3142	1.4020	1.4315	1.4625	1.5495	1.5878	1.5964

DOE File #C073/A77, part 2
SAND-77-1992
Oct. 1976-Sept. 1977

TABLE II (Continued)

SAFE OIL COMPANY - KACHAL No. 1

FRACTURE - AUGUST 26, 1977

TIME	180°	195°	210°	225°	240°	255°	270°	285°	300°	315°	330°	345°
7:50	1.6808	1.6349	1.8473	1.7732	1.8156	1.7619	1.8072	1.5572	1.7542	1.5893	1.4549	1.4175
7:51	1.6787	1.6353	1.8435	1.7709	1.8155	1.7587	1.8035	1.5532	1.7498	1.5875	1.4499	1.4131
7:52	1.6774	1.6333	1.8399	1.7714	1.8166	1.7602	1.8047	1.5549	1.7519	1.5866	1.4522	1.4153
7:53	1.6830	1.6368	1.8405	1.7748	1.8202	1.7649	1.8095	1.5592	1.7564	1.5921	1.4573	1.4206
7:54	1.6775	1.6299	1.8450	1.7697	1.8151	1.7563	1.8038	1.5555	1.7505	1.5858	1.4509	1.4150
7:55	1.6779	1.6321	1.8435	1.7692	1.8147	1.7578	1.8022	1.5523	1.7490	1.5845	1.4504	1.4137
7:56	1.6786	1.6328	1.8444	1.771	1.8163	1.7600	1.8048	1.5547	1.7514	1.5861	1.4517	1.4151
7:57	1.6814	1.6354	1.8469	1.7735	1.8206	1.7676	1.8093	1.5576	1.7547	1.5904	1.4547	1.4185
7:58	1.6796	1.6345	1.8450	1.7712	1.8177	1.7606	1.8045	1.5552	1.7519	1.5873	1.4533	1.4166
7:59	1.6791	1.6337	1.8441	1.7699	1.8164	1.7592	1.8038	1.554	1.7506	1.5859	1.4528	1.4145
8:00	1.6806	1.6341	1.8444	1.7704	1.8166	1.7598	1.8050	1.5546	1.7513	1.5871	1.4528	1.4151
8:01	1.6749	1.6288	1.8396	1.7668	1.8116	1.7551	1.7991	1.5497	1.7455	1.5815	1.4477	1.4102
8:02	1.6762	1.6305	1.8412	1.7684	1.8132	1.7567	1.8014	1.5514	1.7480	1.5835	1.4492	1.4123
8:03	1.6942	1.6465	1.8591	1.7864	1.8328	1.7755	1.8242	1.5722	1.7734	1.6081	1.4717	1.4368
8:04	1.6713	1.6260	1.837	1.7642	1.8088	1.7521	1.7969	1.5473	1.742	1.5763	1.4445	1.4071
8:05	1.6767	1.6307	1.8417	1.7675	1.8139	1.7568	1.8017	1.5517	1.7481	1.5841	1.4495	1.4123
8:06	1.6739	1.6278	1.8376	1.7653	1.8105	1.7535	1.7973	1.5481	1.7438	1.5802	1.4463	1.4089
8:07	1.6755	1.6293	1.8407	1.7668	1.8130	1.7561	1.8007	1.5510	1.7469	1.5837	1.4497	1.4122
8:08	1.6768	1.6307	1.8407	1.7680	1.8127	1.7562	1.8006	1.5511	1.7470	1.5829	1.4484	1.4118
8:09	1.6857	1.6394	1.8510	1.7782	1.8239	1.7668	1.8125	1.5614	1.7583	1.5947	1.4590	1.4227
8:10	1.6705	1.6251	1.8356	1.7614	1.8067	1.7501	1.7937	1.5447	1.7396	1.5760	1.4424	1.4047
8:11	1.6776	1.6315	1.8429	1.7689	1.8146	1.7585	1.8026	1.5526	1.7491	1.5850	1.4512	1.4135
8:12	1.6756	1.6295	1.8401	1.7672	1.8120	1.7559	1.8005	1.5501	1.7461	1.5828	1.4476	1.4110
8:13	1.6841	1.6386	1.8491	1.7754	1.8207	1.7647	1.8072	1.5567	1.7558	1.5915	1.4569	1.4201
8:14	1.6787	1.633	1.8439	1.7707	1.8162	1.7600	1.8051	1.5546	1.7517	1.5873	1.4526	1.4159
8:15	1.6807	1.6341	1.8457	1.7705	1.8174	1.7612	1.8064	1.5562	1.7528	1.5885	1.4535	1.4168
8:16	1.6771	1.6331	1.8439	1.7704	1.8156	1.7592	1.8043	1.5541	1.7505	1.5867	1.4525	1.4162
8:17	1.6807	1.6352	1.8457	1.7730	1.8183	1.7617	1.8066	1.5561	1.7534	1.5894	1.4545	1.4162
8:18	1.6769	1.6260	1.8355	1.7621	1.8077	1.7515	1.7954	1.5459	1.7408	1.5774	1.4434	1.4065
8:19	1.6778	1.6327	1.8435	1.7697	1.8147	1.7590	1.8034	1.5537	1.7497	1.5865	1.4522	1.4149
8:20	1.6762	1.6302	1.8411	1.768	1.8125	1.7567	1.8014	1.5512	1.7474	1.5839	1.4494	1.4128
8:21	1.6781	1.6328	1.8426	1.7689	1.8141	1.7594	1.8036	1.5526	1.7490	1.5852	1.4511	1.4143
8:22	1.6717	1.6259	1.8359	1.7632	1.8075	1.7512	1.7956	1.5457	1.7408	1.5776	1.4430	1.4057
8:23	1.6744	1.6287	1.8387	4.7667	1.8116	1.7557	1.8006	1.5504	1.7461	1.5825	1.448	1.4117
8:24	1.6757	1.6295	1.8398	1.7658	1.8113	1.7557	1.8019	1.5501	1.7461	1.5833	1.4468	1.4118
8:25	1.6785	1.6324	1.8422	1.7695	1.8154	1.7587	1.8047	1.5530	1.7497	1.5866	1.4518	1.4146
8:26	1.6775	1.6307	1.8405	1.7673	1.8119	1.7563	1.8008	1.5505	1.7464	1.5842	1.4500	1.4123
8:27	1.6745	1.6290	1.8391	1.7653	1.8105	1.7541	1.7993	1.5489	1.7440	1.5816	1.4469	1.4099
8:28	1.6793	1.6336	1.8435	1.7708	1.8156	1.7602	1.8057	1.5550	1.7524	1.5893	1.4545	1.4176
8:29	1.6769	1.6309	1.8411	1.7681	1.8129	1.7576	1.8023	1.5518	1.7475	1.5844	1.4497	1.4133

TABLE II (Continued)

SHELL OIL COMPANY - RACHAL NO. 1

FRACTURE - AUGUST 26, 1977

TIME		180°	195°	210°	225°	240°	255°	270°	285°	300°	315°	330°	345°
8:30	Start pumping	1.6775	1.6311	1.8414	1.7674	1.8127	1.7570	1.8020	1.5512	1.7478	1.5842	1.4494	1.4127
8:31		1.6720	1.6276	1.8364	1.7613	1.8054	1.7513	1.7944	1.545	1.7395	1.5790	1.4451	1.4070
8:32		1.6801	1.6335	1.8442	1.7717	1.8163	1.7606	1.8067	1.5558	1.7531	1.5887	1.4528	1.41[illegible]
8:33		1.6708	1.6305	1.8405	1.7685	1.8135	1.7584	1.8035	1.5526	1.7487	1.5858	1.4512	1.4148
8:34		1.6783	1.6303	1.8399	1.7657	1.8103	1.7552	1.8007	1.5498	1.7464	1.5840	1.4481	1.4118
8:35		1.6765	1.6306	1.8409	1.7675	1.8127	1.7568	1.8027	1.5515	1.7477	1.5845	1.4486	1.4139
8:36		1.6740	1.6272	1.8376	1.7644	1.8089	1.7533	1.7991	1.5482	1.7440	1.5817	1.4467	1.4106
8:37		1.6759	1.6279	1.8401	1.7664	1.8117	1.7567	1.8020	1.5513	1.7469	1.5841	1.45[illegible]	1.4139
8:38		1.6790	1.6325	1.8427	1.7686	1.8142	1.7538	1.8046	1.5535	1.7502	1.5829	1.4525	1.4161
8:39		1.6837	1.6325	1.8474	1.7736	1.8191	1.7635	1.8098	1.5585	1.7561	1.5872	1.4581	1.4221
8:40		1.6778	1.6338	1.8458	1.7703	1.8161	1.7615	1.8070	1.5561	1.7527	1.5876	1.4578	1.4187
8:41		1.6752	1.6294	1.8396	1.7642	1.8110	1.7559	1.8018	1.5506	1.7462	1.5833	1.4472	1.4151
8:42		1.6781	1.6305	1.8422	1.7669	1.8134	1.7581	1.8036	1.5517	1.7492	1.5858	1.4504	1.4160
8:43		1.6763	[illegible]	1.8407	1.7667	1.8122	1.7572	1.8027	1.5516	1.7461	[illegible]	1.4496	1.4153
8:44		[illegible]	[illegible]	[illegible]	1.7636	1.8095	1.7542	1.7995	1.5484	1.7446	1.5821	1.4471	1.4107
8:45		1.6754	1.6267	[illegible]	1.7625	1.8065	[illegible]	1.7980	1.5474	1.7432	1.5806	1.4453	1.4096
8:46		1.6757	1.6292	1.8390	1.7641	[illegible]	1.7562	1.8011	1.5495	1.7452	1.5830	1.4466	1.41[illegible]
8:47		1.6767	1.6301	1.8400	[illegible]	[illegible]	1.7568	1.8020	1.5512	1.7483	1.5854	1.4501	1.4139
8:48		1.6769	1.6301	1.8401	1.7654	1.8122	1.7568	1.8033	1.5516	1.7486	1.5858	1.4503	1.4150
8:49		1.6745	1.6277	1.8371	1.7632	1.8093	1.7540	1.8000	1.5480	1.7450	1.5819	1.4460	1.4111
8:50		1.6774	1.6307	1.8412	1.7669	1.8128	1.7584	1.8041	1.5526	1.7503	1.5870	1.4517	1.4153
8:51		1.6763	1.6308	1.8406	1.7657	1.8122	1.7563	1.8029	1.5508	1.7472	1.5850	1.4495	1.4137
8:52		1.6771	1.6297	1.8394	1.7641	1.8116	1.7563	1.8020	1.5503	1.7470	1.5842	1.4492	1.4136
8:53		1.6764	1.6288	1.8384	1.7653	1.8106	1.7552	1.8014	1.5491	1.7470	1.5837	1.4483	1.4131
8:54		1.6762	1.6310	1.8404	1.7655	1.8117	1.7566	1.8026	1.55[illegible]	1.7476	1.5843	1.4500	1.4144
8:55		1.6758	1.6281	1.8381	1.7630	1.8090	1.7547	1.7999	1.5484	1.7457	1.5825	1.4480	1.4122
8:56		1.6726	1.6257	1.8344	1.7598	1.806[illegible]	1.7507	1.7969	1.5444	1.7409	1.5780	1.4430	1.4075
8:57		1.6754	1.6284	1.8381	1.7629	1.8076	1.7540	1.801[illegible]	1.5481	1.7453	1.5826	1.4478	1.4113
8:58		1.6760	1.6285	1.8390	1.7631	1.8107	1.7549	1.8017	1.5493	1.7471	1.5836	1.4480	1.41[illegible]
8:59		1.6753	1.6273	1.8378	1.7621	1.8089	1.7544	1.8011	1.5475	1.7455	1.5827	1.4473	1.4120
9:00		1.6744	1.6264	1.8362	1.7607	1.8075	1.7536	1.7981	1.5458	1.7439	1.5804	1.4451	1.4107
9:01		1.6764	1.6282	1.8451	1.7672	1.8152	1.7605	1.8070	1.5542	1.7533	1.5876	1.4549	1.41[illegible]
9:02		1.6732	1.6243	1.8349	1.7582	1.8062	1.7512	1.7970	1.5445	1.7418	1.57[illegible]	1.4440	1.4063
9:03		1.6752	1.6273	1.8373	1.7615	1.8090	1.7544	1.8006	1.5479	1.7462	1.5829	1.4473	1.4109
9:04		1.6789	1.6304	1.8396	1.7644	1.8118	1.7568	1.8035	1.5499	1.7435	1.5851	1.45[illegible]	1.4153
9:05		1.6742	1.6257	1.8353	1.7589	1.8068	1.7516	1.7976	1.5447	1.7429	1.5794	1.4439	1.4091
9:06		1.6781	1.6299	1.8393	1.7634	1.8115	1.7568	1.8032	1.5493	1.7489	1.5849	1.4485	1.4147
9:07		1.6799	1.6312	1.8406	1.7641	1.8124	1.7575	1.8041	1.5502	1.7500	1.5858	1.4497	1.4155
9:08		1.6745	1.6241	1.8348	1.7583	1.8067	1.7515	1.7976	1.5447	1.7434	1.5791	1.4437	1.4092
9:09		1.6783	1.6302	1.8398	1.7634	1.8121	1.7565	1.8038	1.5497	1.7491	1.5853	1.4490	1.4151

SAND-77-1992
Oct. 1976-Sept. 1977

TABLE II (Continued)

SHELL OIL COMPANY - [illegible] NO. 1

FRACTURE - AUGUST 26, 1977

TIME	180°	195°	210°	225°	240°	255°	270°	285°	300°	315°	330°	345°
9:10	1.6755	[illegible]	1.8368	1.7696	1.8088	1.754	[illegible]	[illegible]	1.7457	[illegible]	1.4464	1.4126
9:11	[illegible]	[illegible]	1.8400	1.7631	[illegible]	[illegible]	[illegible]	1.5500	1.7474	[illegible]	1.4497	1.4154
9:12	[illegible]	[illegible]	1.8421	1.7653	1.8133	1.7590	[illegible]	1.5514	1.7503	[illegible]	1.4526	1.4187
9:13	1.6764	[illegible]	1.8377	1.7666	1.8077	1.7544	1.8016	1.5470	1.7471	1.5523	1.4481	1.4130
9:14	1.6757	1.6771	1.8368	1.7586	1.8079	1.7523	1.7996	[illegible]	1.7453	1.5810	1.4454	1.4116
9:15	1.6752	1.6763	1.8358	1.7591	1.8081	1.7526	1.7955	1.5424	1.7452	1.5815	1.4462	1.4122
1:6771	1.6773	1.6374	1.7612	1.8104	1.7556	[illegible]	1.5473	1.7480	[illegible]	1.4477	1.4137
9:16	1.6767	[illegible]	1.8374	1.7593	1.8094	1.7541	1.8009	1.5461	1.7468	1.5816	1.4464	1.4126
9:17	1.6739	1.6753	1.8341	1.7563	1.8067	1.7510	1.7985	1.5431	1.7431	1.5784	1.4429	1.4095
9:18	1.6743	[illegible]	1.8345	1.7571	1.8074	1.7516	1.7989	1.5440	1.7447	1.5794	1.4449	1.4105
9:19	1.6822	1.6822	1.8413	1.7639	1.8149	1.7577	1.8073	1.5509	1.7534	1.5879	1.4523	1.4193
9:20	1.6768	1.6775	1.8376	1.7595	1.8089	1.7531	1.8017	1.5455	1.7466	1.5822	1.4478	1.4141
9:21	1.674	1.6747	1.8346	1.7559	1.8065	1.7502	1.7979	1.5430	1.7441	1.5788	1.4443	1.4104
9:22	1.6749	[illegible]	1.8349	1.7574	1.8066	1.7512	1.7987	1.5432	1.7445	1.5786	1.4447	1.4112
9:23	1.6768	1.6767	1.8357	1.7581	1.8088	1.7528	1.7997	1.5448	1.7463	1.5811	1.4459	1.4131
9:24	1.6750	1.6757	1.8355	1.7561	1.8081	1.7516	1.7994	1.5446	1.7454	1.5801	1.4457	1.4121
9:25	1.6747	1.6753	1.8357	1.7568	1.8073	1.7505	1.7987	1.5426	1.7447	1.5793	1.4452	1.4119
9:26	1.6758	1.6758	1.8354	1.7568	1.8071	1.7508	1.7988	1.5428	1.7443	1.5785	1.4442	1.4107
9:27	1.6687	1.6148	1.8287	1.7492	1.8015	1.7447	1.7927	1.5375	1.7351	1.5727	1.4390	1.4052
9:28	1.6756	1.6749	1.8356	1.7568	1.8082	1.7515	1.8004	1.5438	1.7460	1.5810	1.4456	1.4128
9:29	1.6795	1.6793	1.8391	1.7604	1.8113	1.7548	[illegible]	1.5468	1.7491	1.5830	1.4484	1.4150
9:30	1.6744	1.6751	1.8341	1.7551	1.8059	1.7476	1.7981	1.5415	1.7439	1.5781	1.4438	1.4106
9:31	1.6736	1.6747	1.8340	1.7548	1.8068	1.7494	1.7986	1.5419	1.7446	1.5787	1.4438	1.4110
9:32	1.6753	1.6757	1.8355	1.7558	1.8060	1.7506	1.7994	1.543	1.7453	1.5784	1.4438	1.4118
9:33	1.6755	[illegible]	1.8317	1.7529	1.8043	1.7470	1.7962	1.5357	1.7407	1.5754	1.4409	1.4060
9:34	1.6793	1.6802	1.8380	1.7592	1.8111	1.7544	[illegible]	1.5459	1.7490	1.5824	1.4483	1.4154
9:35	1.6710	1.6246	1.8329	1.7548	1.8060	1.7492	1.7984	1.5412	1.7441	1.5780	1.4432	1.4104
9:36	1.6687	1.6194	1.8282	1.7496	1.8023	1.7442	1.7926	1.5367	1.7384	1.5722	1.4380	1.4053
9:37	1.6737	[illegible]	1.8333	1.7536	1.8059	1.7490	1.7977	1.5410	1.7453	1.5774	1.4424	1.4105
9:38	1.6722	1.6228	1.8318	1.7529	1.8042	1.7470	1.7961	1.5390	1.7419	1.5758	1.4411	1.4065
9:39	1.6732	1.6220	1.8316	1.7518	1.8042	1.7470	1.7955	1.5391	1.7413	1.5757	1.4408	1.4094
9:40	1.6734	1.6233	1.8323	1.7529	1.8050	1.7478	1.7974	1.5402	1.7432	1.5767	1.4422	1.4101
9:41	1.6747	1.6248	1.8341	1.7546	1.8076	1.7503	1.8003	1.5429	1.7462	1.5798	1.4454	1.4129
9:42	1.6750	1.6253	1.8345	1.7546	1.8071	1.7499	1.7986	1.5417	1.7451	[illegible]	1.4439	1.4113
9:43	1.6724	1.6234	1.8297	1.7510	1.8014	1.7454	1.7939	1.5377	1.7408	1.5741	1.4406	1.4079
9:44	1.6716	1.6229	1.8302	1.7514	1.8029	1.7463	1.7947	1.5386	1.7410	1.5744	1.4408	1.4089
9:45	1.6698	1.6165	1.8292	1.7496	1.8029	1.7450	1.7947	1.5376	1.7412	1.5744	1.4394	1.4076
9:46	1.6712	1.6221	1.8309	1.7506	1.8032	1.7458	1.7948	1.5381	1.7413	1.5743	1.4396	1.4076
9:47	1.6714	1.6199	1.8305	1.7499	1.8032	1.7458	1.7953	1.5380	1.7413	1.5743	1.4404	1.4054
9:48	1.6714	1.6210	1.8296	1.7502	1.8026	1.7456	1.7949	1.5381	1.7414	1.5743	1.4404	1.4087
9:49												

SAND-77-1992
Oct. 1976-Sept. 1977

TABLE II (Continued)

SOHIO OIL COMPANY - FACHAN NO. 1

FRACTURE - AUGUST 26, 1977

TIME	180°	195°	210°	225°	240°	255°	270°	285°	300°	315°	330°	345°
9:50	1.6690	1.6169	1.8275	1.7475	1.7979	1.7416	1.7962	1.5361	1.7360	1.5706	1.4372	1.4[illegible]
9:51	1.6709	1.6215	1.8295	1.7478	1.8015	1.7437	1.7934	1.5360	1.7376	1.5731	1.4387	1.4072
9:52	1.6715	1.6216	1.8306	1.7507	1.8033	1.7439	1.7954	1.5384	1.7423	1.5705	1.4406	1.4091
9:53	1.6688	1.6180	1.8272	1.7471	1.8014	1.7424	1.7916	1.5361	1.7385	1.5711	1.4377	1.4060
9:54	1.6727	1.6217	1.8313	1.7512	1.8043	1.7466	1.7963	1.5391	1.7430	1.5754	1.4413	1.4102
9:55	1.6750	1.6247	1.8336	1.7538	1.8072	1.7494	1.7999	1.542	1.7469	1.5795	1.4456	1.4145
9:56	1.6706	1.6203	1.8284	1.7487	1.8018	1.7443	1.7941	1.5367	1.7401	1.5725	1.4385	1.4072
9:57	1.6710	1.6193	1.8287	1.7469	1.8014	1.7441	1.7944	1.5362	1.7402	1.5722	1.4393	1.4075
9:58	1.6664	1.615	1.8255	1.7435	1.7965	1.7386	1.7882	1.5313	1.7339	1.5668	1.4340	1.4026
9:59	1.6742	1.6230	1.8326	1.7521	1.8053	1.7465	1.7973	1.5384	1.7428	1.5740	1.4406	1.4087
10:00	1.6719	1.6215	1.8302	1.7498	1.8029	1.7457	1.7956	1.5378	1.7416	1.5742	1.4400	1.4083
10:01	1.6721	1.6220	1.8297	1.7495	1.8025	1.7445	1.7952	1.5370	1.7413	1.5732	1.4400	1.4093
10:02	1.6683	1.6187	1.8244	1.7433	1.7970	1.7386	1.7866	1.5311	1.7345	1.5664	1.4328	1.4017
10:03	1.6723	1.6219	1.8307	1.7502	1.8037	1.7457	1.7965	1.5364	1.7429	1.5744	1.4404	1.4074
10:04	1.6694	1.6185	1.8276	1.7468	1.8011	1.7439	1.7929	1.5355	1.7396	1.5714	1.4378	1.4067
10:05	1.6712	1.6202	1.8297	1.7480	1.8026	1.7445	1.7956	1.5370	1.7415	1.5739	1.4394	1.4085
10:06	1.6709	1.6194	1.8284	1.7477	1.8022	1.7434	1.7939	1.5357	1.7401	1.5718	1.4387	1.4080
10:07	1.6704	1.6193	1.8279	1.7482	1.8025	1.7439	1.7949	1.5370	1.7412	1.5728	1.4388	1.4079
10:08	1.6727	1.6212	1.8299	1.7490	1.8037	1.7451	1.7961	1.5381	1.7425	1.5738	1.4401	1.4096
10:09	1.6677	1.6158	1.8250	1.7444	1.7986	1.7403	1.7895	1.5328	1.7357	1.5673	1.4347	1.4037
10:10	1.6683	1.6173	1.8268	1.7461	1.8004	1.7419	1.7931	1.5348	1.7390	1.5703	1.4374	1.4066
10:11	1.6695	1.6184	1.8274	1.7461	1.8005	1.7416	1.7932	1.5351	1.7388	1.5709	1.4370	1.4067
10:12	1.6691	1.6181	1.8264	1.7459	1.8001	1.7415	1.7924	1.5348	1.7383	1.5695	1.4356	1.4058
10:13	1.6706	1.6193	1.828	1.7462	1.8016	1.7429	1.7940	1.5358	1.7404	1.5710	1.4380	1.4074
10:14	1.6656	1.6135	1.8235	1.7407	1.7952	1.7354	1.7861	1.5281	1.7313	1.5628	1.4298	1.3996
10:15	1.6664	1.6146	1.8243	1.7427	1.7974	1.7388	1.7870	1.5318	1.7352	1.5665	1.4334	1.4035
10:16	1.671	1.6204	1.8270	1.7474	1.8022	1.7434	1.7950	1.5368	1.7411	1.5727	1.4395	1.4097
10:17	1.6684	1.6165	1.8259	1.7457	1.7995	1.7405	1.7919	1.5343	1.7382	1.5689	1.4353	1.4066
10:18	1.6735	1.6229	1.8322	1.7509	1.8061	1.7473	1.7990	1.5407	1.7460	1.5762	1.4426	1.4131
10:19	1.6682	1.6172	1.8272	1.7453	1.9004	1.7409	1.7931	1.5352	1.7390	1.5705	1.4373	1.4071
10:20	1.6664	1.6153	1.8246	1.7423	1.7982	1.7394	1.7909	1.5323	1.7366	1.5672	1.4342	1.4040
10:21	1.6677	1.6167	1.8257	1.7451	1.7997	1.7406	1.7929	1.5345	1.739	1.5698	1.4368	1.4071
10:22	1.6665	1.6162	1.8239	1.7429	1.7983	1.7380	1.7897	1.5321	1.7353	1.5659	1.4333	1.4034
10:23	1.6674	1.6163	1.8258	1.7443	1.7992	1.7396	1.7919	1.5336	1.7377	1.5679	1.4352	1.4053
10:24	1.6677	1.6177	1.8259	1.7447	1.8003	1.7412	1.7932	1.5355	1.7395	1.5694	1.4372	1.4074
10:25	1.6690	1.6184	1.8281	1.7468	1.8027	1.7434	1.7963	1.5378	1.7431	1.5739	1.4409	1.4117
10:26	1.6692	1.6184	1.8275	1.7464	1.8014	1.7423	1.7949	1.5372	1.7424	1.5724	1.4397	1.4101
10:27	1.6702	1.6187	1.8280	1.7465	1.8023	1.7430	1.7956	1.5375	1.7423	1.5717	1.4397	1.4101
10:28	1.6696	1.6181	1.8279	1.7464	1.8021	1.7426	1.7956	1.5373	1.7430	1.5726	1.4384	1.4090
10:29	1.6673	1.6160	1.8253	1.7446	1.8000	1.7411	1.7935	1.5355	1.7395	1.5695	1.4369	1.4073

UGR File [illegible], part 2
SAND-77-1992
Oct. 1976-Sept. 1977

TABLE II (Continued)

SHELL OIL COMPANY - RACHAL NO. 1

FRACTURE - AUGUST 26, 1977

TIME	180°	195°	210°	225°	240°	255°	270°	285°	300°	315°	330°	345°
10:30	1.6598	1.6181	1.8264	1.7471	1.8028	1.7454	1.7962	1.5383	1.7426	1.5733	1.4401	1.4108
10:31	1.6653	1.6153	1.8249	1.7453	1.7992	1.7396	1.7954	1.5340	1.7367	1.5656	1.4359	1.4066
10:32	1.6694	1.6177	1.8227	1.7458	1.8017	1.7421	1.7977	1.5371	1.7421	1.5714	1.4384	1.4092
10:33	1.663	1.6127	1.8216	1.7397	1.7948	1.736	1.7881	1.5304	1.7338	1.5639	1.4321	1.4027
10:34	1.6600	1.6143	1.8251	1.7464	1.8017	1.7426	1.7967	1.5375	1.7426	1.5723	1.4334	1.4096
10:35	1.6605	1.6145	1.8248	1.7430	1.7991	1.7375	1.7927	1.5338	1.7388	1.5683	1.4357	1.4066
10:36	1.6608	1.6111	1.8203	1.7379	1.7938	1.7337	1.7869	1.5287	1.7312	1.5615	1.4298	1.4002
10:37	1.6645	1.6140	1.8238	1.7406	1.7969	1.7370	1.7902	1.5323	1.7359	1.5676	1.4329	1.4035
10:38	1.6665	1.6150	1.8244	1.7431	1.7982	1.7383	1.7919	1.5343	1.7381	1.5682	1.4355	1.4065
10:39	1.6643	1.6158	1.8253	1.7408	1.7958	1.7365	1.7903	1.5323	1.7364	1.5661	1.4334	1.4042
10:40	1.6646	1.6151	1.8237	1.7419	1.7984	1.7383	1.7913	1.5346	1.7374	1.5670	1.4341	1.4052
10:41	1.6687	1.6175	1.8276	1.7461	1.8024	1.7426	1.7977	1.5385	1.7436	1.5724	1.4402	1.4114
10:42	1.6623	1.6118	1.8213	1.7396	1.7965	1.7351	1.7889	1.5316	1.7344	1.5649	1.4322	1.4034
10:43	1.6651	1.6147	1.8247	1.7436	1.7996	1.7389	1.7934	1.5352	1.7390	1.5669	1.4361	1.4073
10:44	1.6624	1.6137	1.8224	1.7405	1.7968	1.7369	1.7903	1.5329	1.7362	1.5661	1.4329	1.4039
10:45	1.6624	1.6115	1.8223	1.7414	1.7976	1.7374	1.7910	1.5332	1.7371	1.5665	1.4337	1.4052
10:46	1.6639	1.6127	1.8251	1.7416	1.7975	1.7367	1.7918	1.5332	1.7371	1.5664	1.4337	1.4050
10:47	1.6643	1.6134	1.8229	1.7418	1.7979	1.7371	1.7918	1.5339	1.7386	1.5671	1.4340	1.4051
10:48	1.6635	1.6137	1.8228	1.7421	1.7975	1.7371	1.7909	1.5335	1.7368	1.5665	1.4336	1.4048
10:49	1.6654	1.6150	1.8247	1.7430	1.7993	1.7394	1.7938	1.5361	1.7403	1.5693	1.4369	1.4082
10:50	1.6634	1.6133	1.8230	1.7416	1.7976	1.7371	1.7916	1.5337	1.7375	1.5663	1.4347	1.4055
10:51	1.6647	1.6146	1.8242	1.7428	1.7989	1.7386	1.7939	1.5354	1.7399	1.5683	1.4354	1.4079
10:52	1.6613	1.6111	1.8208	1.7394	1.7954	1.7348	1.7889	1.5313	1.7353	1.5647	1.4317	1.4030
10:53	1.6605	1.6106	1.8202	1.7382	1.7942	1.7337	1.7875	1.5300	1.7328	1.5621	1.4301	1.4012
10:54	1.6629	1.6116	1.8215	1.7399	1.7968	1.7358	1.7903	1.5329	1.7366	1.5659	1.4333	1.4049
10:55	1.6626	1.6125	1.8218	1.7401	1.7968	1.7364	1.7908	1.5331	1.7365	1.566	1.4338	1.4051
10:56	1.6606	1.6105	1.8214	1.7397	1.7961	1.7354	1.7906	1.5320	1.7363	1.5655	1.4326	1.4037
10:57	1.6601	1.6097	1.8200	1.7375	1.7948	1.7340	1.7881	1.5307	1.7335	1.5631	1.4308	1.4021
10:58	1.6608	1.6106	1.8208	1.7388	1.7947	1.7342	1.7880	1.5306	1.7348	1.5637	1.4311	1.4027
10:59	1.6603	1.6110	1.8209	1.7388	1.7954	1.7347	1.7887	1.5309	1.7343	1.5640	1.4312	1.4023
11:00	1.6616	1.6107	1.8219	1.7388	1.7971	1.7366	1.7908	1.5331	1.7369	1.5660	1.4334	1.4053
11:01	1.6613	1.6101	1.8217	1.7387	1.7968	1.7356	1.7909	1.5322	1.7359	1.5647	1.4317	1.4039
11:02	1.6629	1.6117	1.8227	1.7413	1.7981	1.7377	1.7923	1.5347	1.7367	1.5680	1.4350	1.4069
11:03	1.6595	1.6110	1.8218	1.7393	1.7965	1.7362	1.7907	1.5337	1.7367	1.5664	1.4333	1.4051
11:04	1.6597	1.6095	1.821	1.7389	1.7955	1.7343	1.7893	1.5317	1.7349	1.5642	1.4317	1.4039
11:05	1.6594	1.6099	1.8209	1.7390	1.7959	1.7348	1.7898	1.5319	1.7355	1.5644	1.4311	1.4031
11:06	1.6576	1.6066	1.8173	1.7353	1.7923	1.7315	1.7860	1.5288	1.7313	1.5606	1.4276	1.3996
11:07	1.6595	1.6078	1.8198	1.7383	1.7958	1.7341	1.7890	1.5316	1.7349	1.5636	1.4312	1.4030
11:08	1.6601	1.6107	1.8217	1.7395	1.7963	1.7354	1.7904	1.5325	1.7359	1.5647	1.4324	1.4041
11:09	1.6590	1.6096	1.8203	1.7391	1.7959	1.7349	1.7897	1.5316	1.7353	1.5642	1.4320	1.4039

SAND-77-1992
Oct. 1976-Sept. 1977

TABLE II (Continued)

SAFFE OIL COMPANY - [illegible] NO. 1

FRACTURE - AUGUST 26, 1977

TIME	180°	195°	210°	225°	240°	255°	270°	285°	300°	315°	330°	345°
11:10	1.6[illegible]	1.6[illegible]	1.8179	1.7367	1.7957	1.7374	1.7877	1.5293	1.7334	1.5623	1.4[illegible]	1.4015
11:11	1.6[illegible]	1.6060	1.8188	1.738	1.7945	1.7357	1.7869	1.5306	1.7344	1.5[illegible]	1.4[illegible]	1.4022
11:12	1.6[illegible]	1.6074	1.8197	1.7372	1.79[illegible]	1.7367	1.7879	1.5306	1.7359	1.5631	1.4303	1.4023
11:13	1.6572	1.6075	1.8206	1.7382	1.7951	1.7365	1.7864	1.5304	1.7369	1.5629	1.4313	1.4037
11:14	1.6575	1.6102	1.8203	1.7390	1.7966	1.7360	1.7900	1.5323	1.7362	1.5646	1.4318	1.4037
11:15	1.6544	1.6073	1.8212	1.7379	1.7959	1.7347	1.7892	1.5315	1.7357	1.5620	1.4308	1.4031
11:16	1.6564	1.6060	1.8167	1.7351	1.7921	1.7301	1.7856	1.5278	1.7315	1.5603	1.4275	1.4[illegible]
11:17	1.6564	1.6055	1.8205	1.7376	1.7944	1.7334	1.7881	1.53	1.7346	1.5624	1.4298	1.4024
11:18	1.6574	1.6064	1.8169	1.7361	1.7940	1.7328	1.7878	1.5301	1.7341	1.5625	1.4302	1.4029
11:19	1.6567	1.6071	1.8178	1.7361	1.7939	1.7313	1.7865	1.5280	1.7318	1.5611	1.4289	1.4[illegible]
11:20	1.6585	1.6037	1.8201	1.7379	1.7955	1.7344	1.7871	1.5315	1.7356	1.5639	1.4306	1.4032
11:21	1.6584	1.6087	1.8204	1.7379	1.7958	1.7356	1.7876	1.5315	1.7358	1.5639	1.4312	1.4033
11:22	1.6590	1.6077	1.8214	1.7389	1.7968	1.7358	1.7910	1.5326	1.7375	1.5662	1.4331	1.4053
11:23	1.6567	1.6064	1.8177	1.7358	1.7933	1.7312	1.7861	1.5283	1.7326	1.5608	1.4[illegible]	1.4[illegible]
11:24	1.6566	1.6073	1.8195	1.7366	1.7951	1.7353	1.7864	1.5303	1.7350	1.5631	1.4301	1.4024
11:25	1.6586	1.6086	1.6292	1.7381	1.7957	1.7340	1.7894	1.5315	1.7356	1.5636	1.4307	1.4035
11:26	1.6621	1.6111	1.8244	1.7408	1.7990	1.7373	1.7930	1.5338	1.7396	1.5660	1.4345	1.4068
11:27	1.6552	1.6065	1.8177	1.7351	1.7931	1.7306	1.7852	1.5269	1.7316	1.5597	1.4270	1.3985
11:28	1.6566	1.6061	1.8188	1.7368	1.7940	1.7324	1.7879	1.5296	1.7343	1.5625	1.4300	1.4016
11:29	1.6571	1.6075	1.8191	1.7370	1.7942	1.7331	1.7881	1.5295	1.7345	1.5629	1.4299	1.4017
11:30	1.6576	1.6068	1.8199	1.7375	1.7962	1.7343	1.7878	1.5311	1.7364	1.5646	1.4318	1.4041
11:31	1.6562	1.6067	1.8167	1.7373	1.7950	1.7331	1.7879	1.5295	1.7349	1.5631	1.4301	1.4021
11:32	1.6545	1.6054	1.8174	1.7346	1.7917	1.7306	1.7863	1.5267	1.7322	1.5605	1.4277	1.3994
11:33	1.6546	1.6056	1.8169	1.7350	1.7923	1.7305	1.7854	1.5272	1.7325	1.5601	1.4260	1.4031
11:34	1.6560	1.6071	1.8193	1.7366	1.7946	1.7329	1.7876	1.5295	1.7347	1.5626	1.4292	1.4017
11:35	1.6567	1.6063	1.8195	1.7362	1.7943	1.7326	1.7870	1.5297	1.7347	1.5623	1.4300	1.4021
11:36	1.6543	1.6045	1.8166	1.7343	1.7922	1.7311	1.7853	1.5270	1.7330	1.5611	1.4285	1.4002
11:37	1.6549	1.6049	1.8176	1.7344	1.7923	1.7306	1.7850	1.5265	1.7328	1.5602	1.4277	1.3996
11:38	1.6568	1.6068	1.8191	1.7372	1.7950	1.7330	1.7863	1.5288	1.7357	1.5633	1.4307	1.4031
11:39	1.6554	1.6059	1.8191	1.7353	1.7942	1.7321	1.7869	1.5282	1.7346	1.5629	1.4295	1.4023
11:40	1.6543	1.6042	1.8167	1.7338	1.7924	1.7307	1.7851	1.526	1.7329	1.5604	1.4272	1.3993
11:41	1.6540	1.6040	1.8170	1.7341	1.7924	1.7303	1.7855	1.5262	1.7315	1.5602	1.4278	1.3992
11:42	1.6544	1.6047	1.8180	1.7345	1.7928	1.7310	1.7863	1.5267	1.7333	1.5613	1.4286	1.4005
11:43	1.6567	1.6064	1.8204	1.7376	1.796	1.7342	1.7892	1.5306	1.7377	1.5654	1.4316	1.4042
11:44	1.6528	1.6032	1.8163	1.7329	1.7922	1.7302	1.7849	1.5256	1.7322	1.5596	1.4279	1.3989
11:45	1.6541	1.6024	1.8200	1.7372	1.7953	1.7330	1.7860	1.5282	1.7359	1.5638	1.4313	1.4039
11:46	1.6543	1.6042	1.8172	1.7332	1.7926	1.7302	1.7862	1.5253	1.7328	1.5601	1.4269	1.3993
11:47	1.6531	1.6040	1.8158	1.7331	1.7920	1.7297	1.7859	1.5246	1.7326	1.5596	1.4265	1.3987
11:48	1.6518	1.6029	1.8159	1.7328	1.7907	1.7282	1.7828	1.5231	1.7305	1.5580	1.4256	1.3974
11:49	1.6546	1.6044	1.8180	1.7348	1.7939	1.7316	1.7863	1.5263	1.7347	1.5616	1.4287	1.4009

SGR File #0073/A77, part 2
SAND-77-1992
Oct. 1976-Sept. 1977

TABLE II (Continued)

SHELL OIL COMPANY - NUCHAL NO. 1

FRACTURE - [illegible] 1977

TIME	180°	195°	210°	225°	240°	255°	270°	285°	300°	315°	330°	345°
11:50	[illegible]	[illegible]	[illegible]	1.7369	1.7960	[illegible]	[illegible]	[illegible]	1.7364	1.5637	1.4307	1.4030
11:51	[illegible]	[illegible]	[illegible]	[illegible]	[illegible]	[illegible]	[illegible]	[illegible]	1.7351	[illegible]	1.4275	1.3975
11:52	[illegible]	[illegible]	1.8176	1.7343	1.7923	1.7312	[illegible]	[illegible]	1.7343	[illegible]	1.4278	1.4003
11:53	[illegible]	[illegible]	1.8177	1.7343	1.7924	1.7306	[illegible]	[illegible]	1.7332	1.5612	1.4277	1.3999
11:54	1.6541	[illegible]	1.8174	1.7338	[illegible]	[illegible]	[illegible]	[illegible]	1.7329	[illegible]	1.4272	1.3996
11:55	1.6533	[illegible]	1.8177	1.7341	1.7929	1.7313	[illegible]	1.5264	1.7341	1.5609	1.4278	1.4
11:56	1.6535	[illegible]	1.8176	1.7332	1.7920	1.7276	[illegible]	1.5262	1.7316	1.5592	1.4265	1.3992
11:57	[illegible]	[illegible]	1.8169	1.7332	1.7917	[illegible]	[illegible]	[illegible]	[illegible]	1.5601	1.4270	1.3990
11:58	1.6530	1.6047	1.8165	1.7360	1.7949	1.7326	1.7874	1.5262	1.7361	1.5628	1.4265	1.4013
11:59	1.6535	1.6062	1.82	1.7369	1.7955	1.7335	1.7866	1.5268	1.7371	1.5639	1.4296	1.4024
12:00	[illegible]	1.6004	1.8157	[illegible]	[illegible]	[illegible]	[illegible]	[illegible]	[illegible]	1.5568	1.4233	1.3953
12:01	1.6523	1.6036	1.8167	1.7327	1.7920	1.7296	1.7843	1.5231	1.7327	1.5598	1.4265	1.3982
12:02	1.6521	1.6095	1.8218	1.7379	1.7973	1.7350	1.7892	1.5274	1.7381	1.5657	1.4310	1.4031
12:03	1.6502	1.6015	1.8144	1.7313	1.7906	1.7283	1.7826	1.5215	1.7319	1.5593	1.4252	1.3978
12:04	1.6491	[illegible]	1.8133	1.7300	1.7854	1.7264	1.7807	1.5200	1.7292	1.5571	1.4233	1.3954
12:05	1.6502	1.6015	1.8143	1.7317	1.7902	1.7274	1.7868	1.5196	1.7299	1.5576	1.4236	1.3958
12:06	1.6513	[illegible]	1.8161	1.7339	1.7918	1.7292	1.7830	1.5214	1.7321	1.5590	1.4250	1.3961
12:07	1.6500	1.6016	1.8147	1.7323	1.7898	1.7279	1.7815	1.5206	1.7313	1.5584	1.4244	1.3965
12:08	1.6533	1.6044	1.8172	1.7336	1.7933	1.7303	1.7844	1.5233	1.7341	1.5616	1.4273	1.3990
12:09	1.6517	1.6016	1.8157	1.7331	1.7914	1.7289	1.7823	1.5211	1.7315	1.5592	1.4253	1.3973
12:10	1.6516	1.6016	1.8164	1.7328	1.7915	1.7294	1.7835	1.522	1.7334	1.5605	1.4263	1.3982
12:11	1.6506	[illegible]	1.8153	1.7323	1.7906	1.7278	1.7817	1.5206	1.7315	1.5570	1.4252	1.3968
12:12	1.6507	1.6020	1.8204	1.7376	1.7957	1.7338	1.7887	[illegible]	1.7378	1.5647	1.4303	1.4024
12:13	1.6505	1.6018	1.8157	1.7318	1.7917	1.7285	1.7824	1.5204	1.7323	1.5595	1.4246	1.3964
12:14	1.6514	1.6015	1.8154	1.7318	1.7909	1.7289	1.7821	1.5204	1.7316	1.5587	1.4249	1.3970
12:15	1.6509	1.6017	1.8164	1.7330	1.7919	1.7296	1.7835	1.5219	1.7332	1.5604	1.4262	1.3984
12:16	1.6520	1.6023	1.8158	1.7322	1.7909	1.7276	1.7816	1.5196	1.7312	1.5586	1.4243	1.396
12:17	1.6529	[illegible]	1.8163	1.7333	1.7943	1.7299	1.7840	1.5219	1.7335	1.5609	1.4265	1.3982
12:18	1.6514	1.6024	1.8160	1.7334	1.7916	1.7292	1.7825	1.5207	1.7330	1.5600	1.4257	1.3976
12:19	1.6492	1.5998	1.8145	1.7311	1.7902	1.727	1.7814	1.5186	1.7301	1.5575	1.4235	1.3955
12:20	1.6495	1.6005	1.8144	1.7319	1.7898	1.7272	1.7806	1.5187	1.7304	1.5581	1.4236	1.3954
12:21	1.6488	1.5986	1.8131	1.7299	1.7890	1.7262	1.7795	1.5178	1.7298	1.5575	1.4230	1.3947
12:22	1.6513	1.6017	1.8166	1.7322	1.7924	1.7299	1.7835	1.5212	1.7344	1.5616	1.4269	1.3983
12:23	1.6503	1.5992	1.8131	1.7311	1.7905	1.7277	1.7808	1.5191	1.7315	1.5581	1.4240	1.3956
12:24	1.6515	1.6007	1.8168	1.7332	1.7922	1.729	1.7834	1.5211	1.7338	1.5611	1.4266	1.3981
12:25	1.6528	1.6031	1.8136	1.7346	1.7941	1.7316	1.7865	1.5235	1.7376	1.5642	1.4287	1.4001
12:26	1.6507	1.6010	1.8160	1.7333	1.7923	1.7287	1.7836	1.5196	1.7337	1.5605	1.4256	1.3977
12:27	1.6495	1.6001	1.8141	1.7321	1.7899	1.7271	1.7816	1.5177	1.7310	1.5587	1.4243	1.3951
12:28	1.6502	1.6001	1.8149	1.7318	1.7906	1.7282	1.7842	1.5192	1.7326	1.5596	1.4249	1.3961
12:29	1.6495	1.5996	1.8149	1.7324	1.7905	1.7278	1.7816	1.5189	1.7322	1.5596	1.4253	1.3965

SAND-77-1992
Oct. 1976-Sept. 1977

TABLE II (Continued)

SHELL OIL COMPANY - RACHAL NO. 1

FRACTURE - AUGUST 26, 1977

TIME	180°	195°	210°	225°	240°	255°	270°	285°	300°	315°	330°	345°
12:30	1.6497	1.6001	1.8158	1.7324	1.7912	1.7262	1.7808	1.5189	1.7306	1.5539	1.4139	1.3753
12:31	1.6494	[illegible]	[illegible]	1.7273	1.7922	1.7250	1.7778	1.5157	1.7287	[illegible]	1.4127	[illegible]
[illegible]	1.6504	1.6000	1.8150	1.7357	1.7926	1.7291	1.7852	1.5203	1.7349	1.5515	[illegible]	[illegible]
12:33	1.6519	1.5994	1.8149	1.7325	1.7909	1.7257	1.7808	1.5188	1.7324	[illegible]	1.4145	1.3756
12:34	[illegible]	[illegible]	[illegible]	1.7304	[illegible]	[illegible]	[illegible]	[illegible]	[illegible]	[illegible]	[illegible]	[illegible]
12:35	1.6500	[illegible]	1.8115	1.7317	1.7908	1.7276	1.7799	1.5184	1.7321	[illegible]	1.4145	[illegible]
12:36	[illegible]	[illegible]	[illegible]	[illegible]	[illegible]	1.7277	[illegible]	[illegible]	[illegible]	[illegible]	1.4148	[illegible]
12:37	[illegible]	[illegible]	[illegible]	1.7287	[illegible]	[illegible]	[illegible]	[illegible]	[illegible]	[illegible]	[illegible]	[illegible]
12:38	1.6487	[illegible]	1.8136	1.7297	1.7889	[illegible]	1.7785	1.5150	1.7304	[illegible]	[illegible]	1.3735
12:39	1.6496	[illegible]	1.8154	1.7306	1.7907	1.7276	1.7801	1.5181	1.7324	1.5596	1.4152	1.3762
12:40	[illegible]	[illegible]	1.8114	1.7334	1.7910	1.7285	[illegible]	1.5191	1.7340	1.5612	1.4168	1.3771
12:41	1.6488	1.5969	1.8121	1.7278	1.7875	1.7240	1.7761	1.5148	1.7289	1.5564	1.4115	1.3721
12:42	1.6525	[illegible]	1.8181	1.7347	1.7936	1.7307	1.7857	1.5214	1.7364	1.5631	1.4181	1.3787
12:43	1.6487	[illegible]	[illegible]	1.7303	1.7904	[illegible]	1.7787	1.5187	1.7317	[illegible]	1.4139	1.3711
12:44	1.6472	[illegible]	1.8122	1.7297	1.7871	1.7254	1.7770	1.5169	1.7298	1.5571	1.4120	1.3724
12:45	1.6466	[illegible]	1.8134	1.7298	1.7876	1.7245	1.7770	1.5168	1.7296	1.5571	1.4114	1.3719
12:46	1.6479	[illegible]	1.8127	1.7299	1.7886	1.7252	1.7769	1.5184	1.7300	1.5570	[illegible]	1.3731
12:47	1.6491	1.5996	1.8147	1.7309	1.7911	1.7269	1.7799	1.5176	1.7329	1.5598	1.4155	1.3757
12:48	1.6498	[illegible]	1.8161	1.7326	1.7915	1.7281	1.7800	1.5184	1.7342	1.5606	1.4164	[illegible]
12:49	1.6542	[illegible]	1.8190	1.7366	1.7947	1.7311	1.7835	1.5213	1.7368	1.5639	1.4182	1.3786
12:50	1.6505	1.6014	1.8154	1.7324	1.7911	1.7275	1.7805	1.5176	1.7333	1.5601	1.4151	1.3753
12:51	1.6485	1.6007	1.8130	1.7320	1.7905	1.7269	1.7786	1.5169	1.7325	1.5593	1.4134	1.3738
12:52	1.6459	1.5969	1.8070	1.7278	1.7869	1.7251	1.7751	1.5135	1.7285	1.5558	1.4104	1.3702
12:53	1.6486	1.5975	1.813	1.7301	1.7899	1.7271	1.7784	1.5170	1.7325	1.5590	1.4136	1.3725
12:54	1.6494	1.6010	1.8149	1.7317	1.7912	1.7277	1.7793	1.5176	1.7336	1.5601	1.4156	1.3754
12:55	1.6444	1.5956	1.8095	1.7250	1.7846	1.7209	1.7729	1.5114	1.7263	1.5533	1.4104	1.3719
12:56	1.6470	1.5968	1.8130	1.7303	1.7890	1.7257	1.7772	1.5156	1.7306	1.5579	1.4129	1.3724
12:57	1.6545	1.6005	1.8199	1.7370	1.7941	1.7321	1.7840	1.5215	1.7384	1.5646	1.4189	1.3788
12:58	1.6476	[illegible]	[illegible]	1.7320	1.7900	[illegible]	1.7805	1.5168	1.7331	1.5595	1.4140	[illegible]
12:59	1.6465	1.5983	1.8115	1.7274	1.7869	1.7237	1.7746	1.5132	1.7285	1.5555	1.4114	1.3707
13:00	1.6441	1.5961	1.8096	1.7270	1.7856	1.7232	1.7737	1.5129	1.7286	1.5546	1.4100	1.3693
13:01	1.6483	[illegible]	1.8149	1.7315	1.7899	[illegible]	1.7777	1.5165	1.7327	1.5594	1.4141	[illegible]
13:02	1.6441	1.5953	1.8095	1.7262	1.7846	1.7211	1.7718	1.5111	1.7260	1.5531	1.4184	1.3674
13:03	1.6473	1.5980	1.8123	1.7298	1.7883	1.7246	1.7757	1.5144	1.7299	1.5574	1.4121	1.3708
13:04	1.6477	1.5983	1.8125	1.7292	1.7883	1.7246	1.7752	1.5145	1.7298	1.5568	1.4118	1.3712
13:05	1.6486	1.5993	1.8138	1.7303	1.7893	1.7251	1.7760	1.5153	1.7306	1.5578	1.4125	1.3715
13:06	1.6462	1.5949	1.8096	1.7257	1.7841	1.7210	1.7707	1.5111	1.7260	1.5532	1.4186	1.3673
13:07	1.6545	1.6063	1.8210	1.7373	1.7964	1.7328	1.7849	1.5220	1.7390	1.5656	1.4295	1.3786
13:08	1.6517	1.6022	1.8164	1.7333	1.7922	1.7285	1.7795	1.5180	1.7349	1.5613	1.4249	1.3737
13:09	1.6492	1.6004	1.8143	1.7322	1.7909	1.7269	1.7777	1.5166	1.7327	1.5603	1.4231	1.3734

UGR File #c073/A77, part 2
SAND-77-1992
Oct. 1976-Sept. 1977

TABLE II (Continued)

SHELL OIL COMPANY - RACHEL No. 1

FRACTURE - AUGUST 26, 1977

TIME		180°	195°	210°	225°	240°	255°	270°	285°	300°	315°	330°	345°
13:10		1.6492	1.6005	1.8137	1.7311	1.7901	1.7264	1.7765	1.5160	1.7324	1.5606	1.4235	1.3920
13:11		1.6473	1.5953	1.8124	1.7299	1.7898	1.7257	1.7762	1.5156	1.7322	1.5606	1.4226	1.3907
13:12		1.6503	1.6013	1.8167	1.7334	1.7917	1.7295	1.7807	1.5190	1.7362	1.5626	1.4264	1.3951
13:13		1.6466	1.5973	1.8118	1.7288	1.7877	1.7257	1.7733	1.5138	1.7295	1.5571	1.4213	1.3894
13:14		1.6449	1.5965	1.8099	1.7279	1.7862	1.7228	1.7722	1.5126	1.7288	1.5562	1.4202	1.3885
13:15		1.6469	1.5972	1.8111	1.7281	1.7875	1.7240	1.7718	1.5133	1.7298	1.5566	1.4213	1.3896
13:16		1.6472	1.5989	1.8136	1.7300	1.7896	1.7254	1.7751	1.5150	1.7313	1.5578	1.4229	1.3905
13:17		1.6492	1.6006	1.8145	1.7321	1.7911	1.7276	1.7772	1.5174	1.7337	1.5601	1.4242	1.3926
13:18		1.6490	1.6004	1.8149	1.7319	1.7901	1.7272	1.7768	1.5173	1.7338	1.5612	1.4251	1.3930
13:19		1.6476	1.5991	1.8139	1.7312	1.7901	1.7259	1.7755	1.5159	1.7326	1.5595	1.4235	1.3913
13:20		1.6496	1.5992	1.8149	1.7317	1.7913	1.7264	1.7762	1.5163	1.7363	1.5598	1.4246	1.3926
13:21		1.6497	1.6006	1.8146	1.7321	1.7905	1.7266	1.7757	1.5158	1.7324	1.5584	1.4240	1.3920
13:22		1.6477	1.5992	1.8129	1.7301	1.7892	1.7242	1.7744	1.5148	1.731	1.5577	1.4227	1.3905
13:23		1.6482	1.5984	1.8139	1.7303	1.7902	1.7258	1.7759	1.5160	1.7328	1.5591	1.4236	1.3917
13:24		1.6474	1.5976	1.8133	1.7313	1.7904	1.7255	1.7753	1.5160	1.7317	1.5583	1.4237	1.3900
13:25		1.6507	1.6024	1.8165	1.7331	1.7926	1.7268	1.7784	1.5183	1.7351	1.5617	1.4253	1.3927
13:26		1.6501	1.6006	1.8159	1.7340	1.7918	1.7274	1.7768	1.5168	1.7335	1.5600	1.4241	1.3915
13:27		1.6478	1.5995	1.8130	1.7311	1.7898	1.7255	1.7754	1.5155	1.7326	1.5587	1.4226	1.3905
13:28		1.6507	1.6005	1.8164	1.734	1.7926	1.7284	1.7777	1.5182	1.7350	1.5613	1.4251	1.3921
13:29		1.6501	1.5994	1.8156	1.7321	1.7919	1.7277	1.7775	1.5170	1.7346	1.5606	1.4244	1.3929
13:30	Stop pumping	1.6469	1.5951	1.8113	1.7285	1.7877	1.7238	1.7723	1.5131	1.7298	1.5563	1.4202	1.3880
13:31	Total volume	1.6471	1.5964	1.8127	1.7303	1.7901	1.7253	1.7746	1.5152	1.7321	1.5587	1.4232	1.3900
13:32	200,000 Gal.	1.6511	1.6006	1.8178	1.7354	1.7946	1.7305	1.7804	1.5202	1.7384	1.5640	1.4281	1.3954
13:33		1.6458	1.5967	1.8117	1.7295	1.7886	1.7244	1.7729	1.5138	1.7305	1.5565	1.4215	1.3884
13:34		1.6514	1.6021	1.8178	1.7354	1.7949	1.7304	1.7796	1.5195	1.7378	1.5645	1.4278	1.3959
13:35		1.6482	1.5998	1.8094	1.7262	1.7871	1.7226	1.7768	1.5114	1.7284	1.5539	1.4189	1.3863
13:36		1.6482	1.5997	1.8151	1.7329	1.7921	1.7275	1.7770	1.5169	1.7349	1.5606	1.4241	1.3922
13:37		1.6468	1.5971	1.8134	1.7302	1.7898	1.7252	1.7742	1.5148	1.7318	1.5587	1.4226	1.3896
13:38		1.6487	1.5967	1.8129	1.7309	1.7903	1.7251	1.7735	1.5147	1.7321	1.5584	1.4222	1.3895
13:39		1.6477	1.5968	1.8134	1.7302	1.7906	1.7256	1.7745	1.5144	1.7322	1.5583	1.4218	1.3885
13:40		1.6494	1.5981	1.8152	1.7334	1.7927	1.7277	1.7769	1.5170	1.7356	1.5614	1.4248	1.3918
13:41		1.6466	1.5962	1.8115	1.7291	1.7872	1.7238	1.7724	1.5141	1.7307	1.5573	1.4209	1.3876
13:42		1.6496	1.5995	1.8159	1.7331	1.7927	1.7280	1.7778	1.5180	1.7360	1.5624	1.4257	1.3926
13:43		1.6442	1.5956	1.80954	1.7265	1.7852	1.7218	1.7694	1.5102	1.7274	1.5535	1.4178	1.3847
13:44		1.6490	1.5994	1.8141	1.7324	1.7910	1.7267	1.7748	1.5157	1.7327	1.5591	1.4239	1.3895
13:45		1.6524	1.601	1.8174	1.7365	1.7941	1.7310	1.7815	1.5208	1.7401	1.5662	1.4284	1.3941
13:46		1.6436	1.5945	1.8108	1.7289	1.7884	1.7236	1.7716	1.5130	1.7301	1.5587	1.4207	1.3874
13:47		1.6445	1.5937	1.8106	1.7277	1.7875	1.7227	1.7707	1.5124	1.7290	1.5557	1.4194	1.3863
13:48		1.6458	1.5961	1.8114	1.7295	1.7891	1.7247	1.7732	1.5137	1.7311	1.5569	1.4218	1.3882
13:49		1.6475	1.5970	1.8129	1.7299	1.7896	1.7250	1.7737	1.5144	1.7321	1.5587	1.4219	1.3887

DISTRIBUTION:

G. Fumich
Acting Program Manager
Fossil Energy
U. S. Department of Energy
Washington, DC 20545

H. D. Guthrie, Director
J. W. Watkins, Deputy Director
J. D. Ham, Assistant Director
D. C. Ward
J. B. Smith
A. B. Crawley
Division of Oil, Gas, Shale
and In Situ Technology
U. S. Department of Energy
400 First St. NW
Washington, DC 20545

E. Lievens, Acting Director
Office of Program Planning
and Analysis
U. S. Department of Energy
20 Massachusetts Ave. NW
Washington, DC 20545

A. A. Pitrolo, Director
L. A. Schrider
W. K. Overbey, Jr.
U. S. Department of Energy
Morgantown Energy Research Center
P. O. Box 880
Morgantown, WV 26505

C. H. Atkinson
U. S. Department of Energy
Nevada Operations Office
P. O. Box 14100
Las Vegas, NV 89114

G. R. Leutkenhans
R. L. Mann
CER Corporation
P. O. Box 15090
Las Vegas, NV 89114

J. S. Ball, Director
R. T. Johansen
U. S. Department of Energy
Bartlesville Energy Research Center
Bartlesville, OK 74003

D. K. Nowlin, Director
Special Programs Division
U. S. Department of Energy
Albuquerque Operations Office
Albuquerque, NM 87185

M. E. Hanson
Lawrence Livermore Laboratory
Livermore, CA 94550

R. Brownlee G-Division
W. G. Davey Q-Division
Los Alamos Scientific Laboratory
Los Alamos, NM 87545

A. B. Waters
A. A. Daneshy
Halliburton Services
Research Center
Duncan, OK 73533

W. B. Bradley
Shell Development Co.
3737 Bellaire Boulevard
Houston, TX 77001

J. Fitch
W. L. Medlin
Mobil Research and
Development Corporation
Field Research Laboratory
P. O. Box 900
Dallas, TX 75211

H. C. Walther
H. Wahl
Production Research Division
Continental Oil Company
Ponca City, OK 74601

L. S. Cook
Columbia Gas System Service Corp.
1600 Dublin Road
Columbus, OH 43215

J. Short
Gas Producing Enterprises, Inc.
2100 Prudential Plaza
P. O. Box 749
Denver, CO 80201

Distribution, continued

T. Nyquist
Dowell
P. O. Box 21
Tulsa, OK 74102

J. P. Pavlich
Dowell
Division of Dow Chemical
220 W. Loop S
Houston, TX 77027

R. L. Huggins
R. W. Veatch
M. B. Smith
Amoco Production Co.
P. O. Box 591
Tulsa, OK 74102

M. D. Woods
131 Mimosa Way
Portola Valley, CA 94025

R. P. Trump
Gulf Research and
Development Company
P. O. Drawer 2038
Pittsburgh, PA 15230

1 M. Sparks
1000 G. A. Fowler
1100 C. D. Broyles
1110 J. D. Kennedy
Attn: C. R. Mehl, 1111
C. W. Smith, 1111

1120 G. E. Hansche
1130 H. E. Viney
Attn: W. D. Statler, 1133
W. C. Vollendorf, 1133

5100 J. K. Galt
Attn: W. Herrmann, 5160

5163 D. E. Munson
5200 E. H. Beckner
5337 L. D. Tyler
5400 A. W. Snyder
5700 J. H. Scott
5710 G. E. Brandvold
5730 H. M. Stoller
5731 R. K. Traeger
5732 D. A. Northrop (6)
5733 C. L. Schuster
5734 A. L. Stevens
5735 S. G. Varnado
5736 A. F. Veneruso
5740 V. L. Dugan
5800 R. S. Claassen
8266 E. A. Aas (1)
9420 T. L. Pace
3141 C. A. Pepmueller (5)
3151 W. L. Garner (3)
for DOE/TIC (25)
Attn: R. P. Campbell, 3173-2

UGR File #C073/A78
Oct. 1978-Sept. 1979
Sandia Labs.

SAND79-2428
UNLIMITED RELEASE

ENHANCED GAS RECOVERY PROGRAM
FOURTH ANNUAL REPORT

UGR FILE #C073/A78

OCTOBER 1978 THROUGH SEPTEMBER 1979

D. A. NORTHROP AND C. L. SCHUSTER, EDITORS

NOVEMBER 1979

Sandia Laboratories
energy report

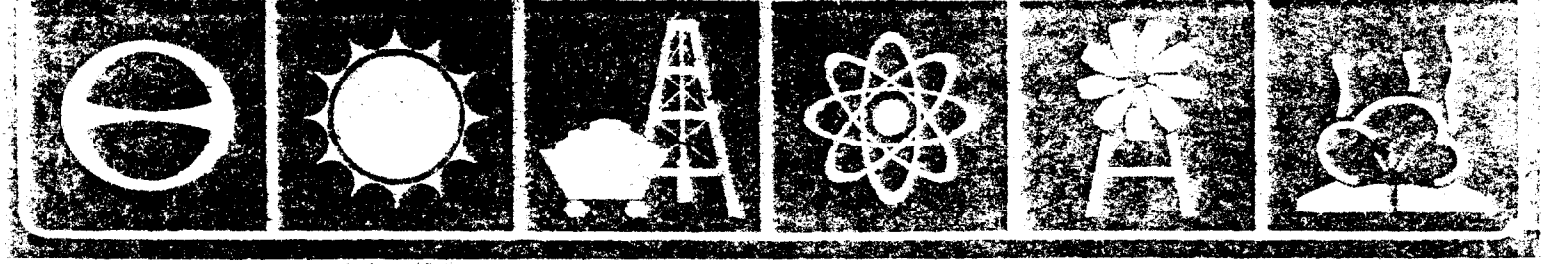

SF 2900 Q(8) 3-74

UGR File #C073/A78
Oct. 1978-Sept. 1979
Sandia Labs.

SAND79-2428
Unlimited Release

ENHANCED GAS RECOVERY PROGRAM

FOURTH ANNUAL REPORT

October 1978 through September 1979

ABSTRACT

Massive hydraulic fracture diagnostic experiments continued in FY 79 with the major activity being focused on the development of wireline tool instrumentation. The development of the Borehole Seismic System and Borehole Hydrophone System should lead to a more direct method of obtaining fracture orientations and fracture heights than presently exists. These systems can be deployed in the well to be stimulated and can monitor seismic activities before and after nonproppant fluid pumping periods. This seismic activity should occur along the induced fractures, and the location of the seismic sources will be indicative of the fracture locations. The experiments conducted at DOE's Nevada Test Site with known signal locations substantiate field data obtained in two experiments with Amoco in their Wattenberg field where fracture orientation was detected.

A high resolution, three-dimensional seismic survey program was initiated this year in an attempt to delineate lenticular sand formations from the surface. The program will start with some experiments at shallow depths where the sand lenses outcrop and then move into greater depths to evaluate this technique. In addition, a logging program has also been established to evaluate formation properties. This program hopes to evaluate the dispersive electrical parameters of the formation and relate these parameters to the formation permeability and porosity.

Hydraulic and dynamic fracturing experiments have been conducted adjacent to a tunnel complex at the Nevada Test Site and which are then directly observed by mining through the experiment area. Emphasis has been placed on the study of the factors which influence the containment, and hence the overall geometry, of hydraulic fractures at a formation interface. Evaluation of

full-scale fracturing tests at an interface between geologic formations with significantly different properties, most notably an order of magnitude difference in elastic modulus, showed that the interface did not contain the fractures. Numerous smaller scale experiments at the same interface have confirmed these results. Thus, it has been shown that material property differences alone are insufficient for containment, and that the in situ stress is the dominant parameter. Fracture growth and terminations have been shown to coincide with variations in in situ stress even within the same formation. Rock mechanics and fluid mechanics studies have supported these conclusions. In particular, a microcrack model has been formulated which downplays the importance of material properties and emphasizes the role of in-situ stresses for processes occurring at a crack tip.

Multiple fracturing from a wellbore has been demonstrated for a High Energy Gas Frac concept. In this concept, the gas pressure pulse due to the deflagration of a propellant is designed to give pressure loading rates sufficient to initiate multiple fractures, peak pressures below the flow stress of the formation to avoid rock compaction, and a duration of burn sufficient to allow gas penetration and fracture extention. An expanded test series has been initiated to quantify several techniques for multiple fracturing based on this concept.

Finally, a Multi-Well Experiment has been defined whose objectives are to characterize in detail a lenticular gas reservoir of the Western United States and to evaluate state-of-the-art and developing technology for the recovery of gas from them. This research-oriented field experiment will be initiated in 1980.

UGR File #C073/A78
Oct. 1978-Sept. 1979
Sandia Labs.

TABLE OF CONTENTS

		PAGE
I.	Introduction and Summary	5
II.	Massive Hydraulic Fracture Mapping and Characterization Program	10
	A. Borehole Seismic System	10
	1. System Description.	10
	2. NTS Minifrac	14
	3. Amoco Experiments	16
	4. NTS Borehole Tests.	20
	B. Borehole Hydrophone System	24
	1. System Applications	24
	2. System Description.	25
	3. Prototype Testing	26
	C. Surface Electrical Potential System (SEPS)	29
	1. System Description.	29
	2. Amoco Wattenberg Field Fracture Experiment.	32
	3. Design Changes to SEPS	35
III.	Advanced Logging Technology and Formation Evaluation	37
	A. Seismic Formation Mapping Program.	37
	1. Introduction	37
	2. Task Description	38
	3. Site Descriptions.	39
	4. Program Progress	40
	B. Nuclear Magnetism Logging.	40
	C. Advanced Electromagnetic Logging	42
	1. Logging Techniques Based on Dispersive Electrical Parameters	42
	2. An Inverse Process for Evaluating Constitutive Parameters.	46
IV.	Stimulation Research for Unconventional Gas Recovery	61
	A. Hydraulic Fracturing	61
	1. Hydraulic Fracturing Containment Experiments.	61
	2. Modeling and Analysis.	81
	B. Dynamic Wellbore Fracturing	100
	1. Background	100
	2. Multi-Frac Test Series	101
	3. Modeling & Analysis	106

C. Multi-Well Experiment 111

V. Publications, Presentations, and Other Communications 113

A. Publications and Presentations 113

B. Other Communications. 115

I. Introduction and Summary

A. Introduction

Sandia Laboratories conducts several projects which are part of the United States Department of Energy's (DOE) Unconventional Gas Recovery Program. One is the Massive Hydraulic Fracture Characterization Project whose objective is to develop instrumentation systems for characterizing fracture systems, formations, and other parameters contributing to enhanced gas recovery. Another is the Stimulation Research Project whose objective is to understand, and thus improve, fracturing processes for stimulation of natural gas production from low permeability formations which contain a high potential resource. Another is the Advanced Logging for Formation Evaluation Program being conducted for the Bartlesville Energy Technology Center in support of the Western Gas Sands Project. A fourth is the in situ testing of well shooting concepts being conducted for the Morgantown Energy Technology Center in support of the Eastern Gas Shales Project. Finally, a Multi-Well Experiment was initiated which will be the major field test conducted under the Western Gas Sands Project in future years. This report summarizes activities conducted under these projects during Fiscal Year 1979; October 1, 1978, through September 30, 1979.

The Massive Hydraulic Fracture (MHF) Characterization Project began in 1974 with the initial application of Sandia's instrumentation capability in a joint experiment with El Paso Natural Gas in the Pinedale Field, Green River Basin, Wyoming. The initial effort was an attempt to measure the orientation and growth of a massive hydraulic fracture using both surface seismic recording and electrical potential mapping techniques. In the ensuing years, the surface seismic program has been discontinued because of its inability to map fractures from the surface. The surface electrical potential technique has been developed and fielded on several experiments over the past five years. This instrumentation system has demonstrated the capability to determine fracture orientation induced by massive hydraulic fracturing, provide a measure of the asymmetry of fracture wings created, and provide some insight into the stimulation processes occurring within the reservoir.

The original surface seismic program has been redirected and now is concentrating on a borehole seismic system that can be utilized in the fracture well. This system records seismic signals before and after nonproppant fluid injections that can determine the orientation of the hydraulic fracture by knowing the orientation of the system within the borehole. Utilization of borehole tools for fracture mapping should greatly enhance the obtaining of these data by substantially reducing the costs. A second system utilizing hydrophones is under development for determination of fracture heights. In addition to fracture diagnostics, there has been a broadening of the project scope to develop other instrumentation systems and techniques for characterizing and evaluating the formation. These include defining the boundaries of lenticular sand lenses and evaluating the formation parameters involved in hydrocarbon production. For example, a logging program hopes to evaluate the dispersive electrical parameters of the formation and relate these parameters to the formation permeability and porosity.

The Stimulation Research Project was initiated in FY 77. However, the program has built upon fracturing and mineback activities which have been conducted since 1974 in G-tunnel at DOE's Nevada Test Site as part of a nuclear containment program sponsored by the Division of Military Applications of DOE. The commonality of objectives between the nuclear containment program and enhanced gas recovery activities are striking, and the close relationship between the two programs has been mutually beneficial.

A major activity has been in situ fracturing experiments in an environment which allows for direct examination and evaluation. The mineback capability provided at the Nevada Test Site provides this opportunity. A detailed physical description can be obtained directly and can be correlated with measured geologic material properties, in situ stress distributions, fluid behavior, and the operational parameters of the test. Rock mechanics and fluid mechanics laboratory and modeling work support the design and analysis of the field experiments

and are producing new insight into fracturing behavior. The experiments also provide the opportunities to calibrate instrumentation techniques under known conditions and to examine innovative fracturing techniques. Thus, such mine-back experiments provides considerably more information than the evaluation of a commercial frac job which is based primarily upon gas production alone. Industry and service company representatives participate in the planning and analysis of the experiments. This project is providing a unique opportunity to quantify and understand fracture behavior.

Sandia's projects are supported by DOE's Unconventional Gas Recovery Program through the Eastern Gas Shales Project, Western Gas Sands Project, and the Morgantown and Bartlesville Energy Technology Centers. Sandia's projects provide a broad supporting research and development capability. Activities are planned, conducted, and reported with the aim of contributing to the objectives of both the Eastern and Western Projects and to the overall development of Unconventional Gas Recovery technology.

B. Summary

Two field experiments and two NTS experiments were conducted in FY 79 utilizing the borehole seismic system. The second experiment at NTS utilized the seismic system as it would be used in a regular borehole experiment and located seismic sources in the vicinity of a wellbore. This data analysis was similar to and provided a basis for the analysis of the full scale fracture experiments. These two field experiments were conducted with Amoco in their Wattenberg field and produced excellent fracture orientation results.

The other borehole tool is the stacked hydrophone system which has been a prototype design. Preliminary testing in the laboratory and in a shallow borehole indicates this system is operational, and it will be evaluated in FY 80. It will be utilized in two diagnostic modes; one for determining fracture heights and another for determining formation interval velocities.

The formation evaluation portion of the program has had two efforts this

year; the first effort being the initiation of a program utilizing high resolution seismic surveys for determining the boundaries of lenticular sand formations. The other program is the electromagnetic logging program which is directed at understanding the relationships between dispersive electrical parameters and formation parameters. The formation parameters of interest include both permeability and porosities. The program is in the feasibility study area this year and should move into a prototype system design in FY 80.

The Stimulation Research Project activities have focused upon the study of the containment of hydraulic fractures by geologic formation interfaces, material properties and in situ stresses. Coring operations are delineating the extent of the full-scale Hole #6 experiment conducted and mined out last year. It was observed that the fractures broke through the interface between ash fall tuff and welded tuff formations having significantly different properties, most notably an order of magnitude difference in modulus. Coring has confirmed that the fracture geometry was not affected by the presence of the interface; in fact, fracture growth was predominantly upwards and downwards instead of lateral resulting in a fracture length of 150 ft as compared with a 600-ft "design". An Interface Test Series was conducted this year to further examine the behavior at the interface; 31 small volume (150 gal) hydraulic fractures were created from horizontal wellbores located just below the same geologic interface used in the Hole #6 experiment. Fractures propagated upwards through the interface into the higher modulus formation but only limited downwards growth was observed in the same lower modulus formation where the fractures were initiated. In situ stresses were calculated from the fracturing pressure records, and fracture growth was observed to be limited by increases in the in situ stress measured in the same formation. Thus, in situ stresses are the predominant factor affecting hydraulic fracture growth; the character of the interface (bonded or nonbonded) and material property differences play a subordinate role.

A microcrack rock mechanics model has been formulated which confirms these field results. Essentially, it shows that the zone of influence at a crack tip decreases rapidly with increased stress and is not affected significantly by material properties. The model has been extended to include the effects of an anisotropic in situ stress state. Laboratory experiments with materials with smeared interfaces, where the properties change smoothly over a short distance, are being conducted to further test the fracture propagation at such an interface.

In a series of three experiments conducted last year, it was demonstrated that multiple fracturing from a wellbore was possible for a gas pressure pulse produced by the deflagration of a propellant. The pulse must be designed to give: 1) pressure loading rates sufficient to initiate multiple fractures, 2) peak pressures below the flow stress of the formation to avoid rock compaction and wellbore enlargement, and 3) a duration of burn sufficient to allow gas penetration and fracture extension. An expanded test series - the Multi-frac Test Series - has been initiated to investigate several techniques based upon this tailored-pulse concept. The test design is complete and assembly for five different experiments is underway; the tests will be conducted in the second quarter of FY 80. These tests will be extensively instrumented and evaluated to provide data for the modeling and development of such a dynamic wellbore fracturing technique for unconventional gas stimulation.

A Multi-Well Experiment has been defined. This is a research-oriented field experiment where two (or more) wells will be drilled at close spacings on a given site and will be used to characterize in detail one of the lenticular, tight gas reservoirs of the Western United States and to evaluate state-of-the-art and developing technology for the recovery of gas from them. Program planning is underway and an industry advisory group has been formed and is active. The experiment consists of six major activities (analysis and evaluation, laboratory testing, field drilling, stimulation, production testing, and field diagnostics). Field activities will be initiated in the spring of 1980, most likely at a site in the Piceance Basin, Colorado.

II. Massive Hydraulic Fracture Mapping and Characterization Program

A. Borehole Seismic System (R. W. Seavey, 4733)

1. System Description

The determination of fracture orientation is possible with the use of one triaxial geophone package. If two horizontal and one vertical geophones are clamped in the treatment well at or near the zone to be fractured, seismic signals can be detected and recorded which can be analyzed to determine the direction to the seismic source. Since the geophone response is a function of the angle of incidence of the compression component of the seismic signal, direction to the source can be determined. If a seismic source in space produces a response on geophones aligned with the X-Y-Z axes (Fig. II-1), the output of the horizontal geophones will be $Y=C \sin A$ and $X=C \cos A$. The ratio of the horizontal amplitude is then $Y/X= \tan A$ from which the horizontal direction may be obtained if one knows the orientation of the geophones. The vertical angle of incidence, β, can be determined as the angle whose tangent is the ratio of the vertical response to the vector sum of the horizontal responses.

The borehole seismic system was fabricated using commercially available components where possible. These components were integrated into an overall system that would allow operation on a single conductor wire line. The single conductor wire line provides power to the electronics, control to the clamping arm, monitoring circuitry for the clamping arm, and the return path for the multiplexed output from the geophones. The lower section of the system (Fig. II-2) is the orientation package which contains its own power supply package, camera, and orientation unit. Either of two orientation units can be used: 1) a compass unit for operation in an open hole, and 2) a gyroscopic unit for operation in a cased hole. The entire system is 3-5/8" diameter and up to 16 ft long and is capable of being clamped into boreholes from 4-1/2" up to 15" diameter. Figure II-3 shows this borehole seismic system with the cases removed to show interior parts.

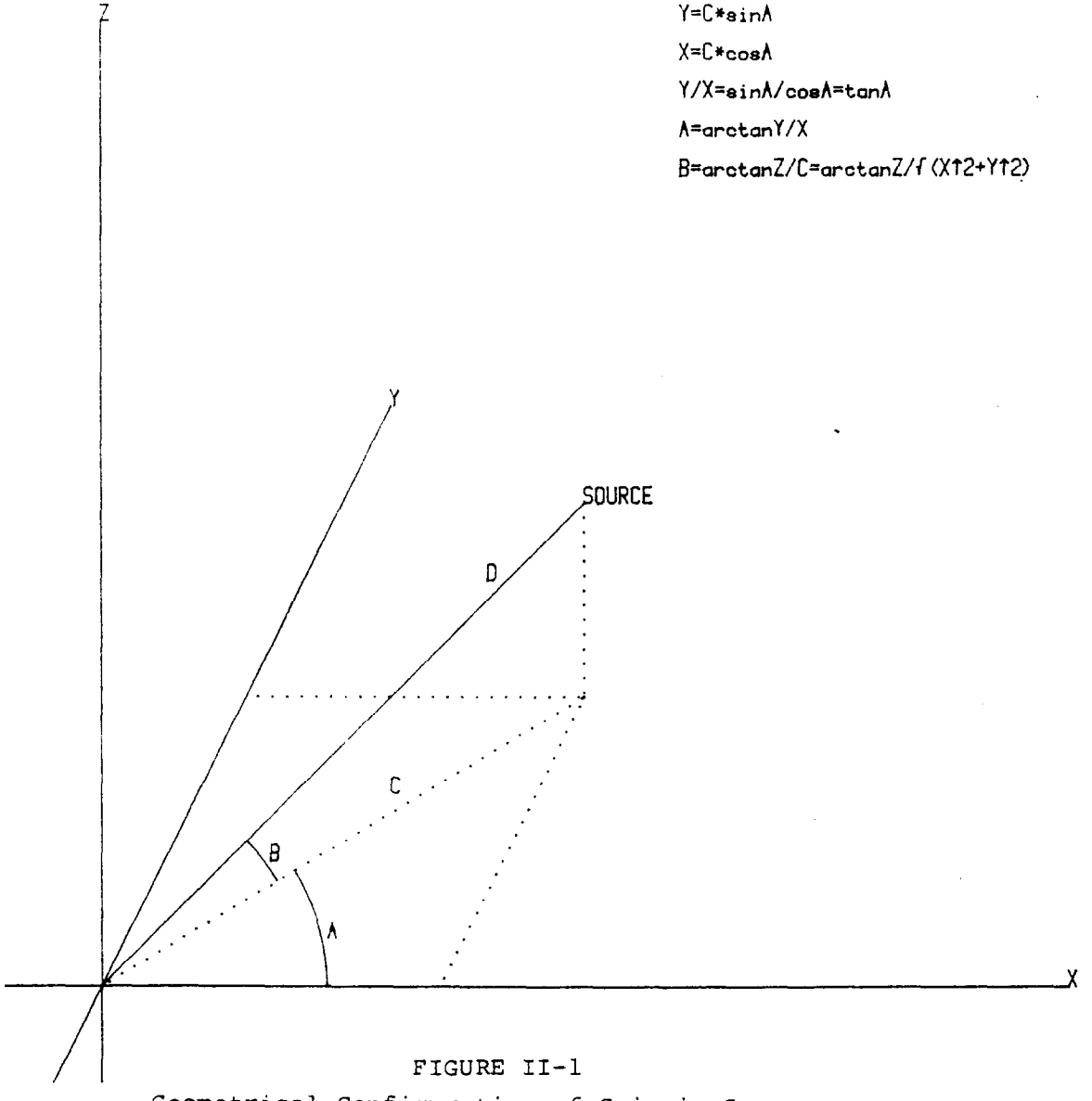

FIGURE II-1
Geometrical Configuration of Seismic Source and Geophones

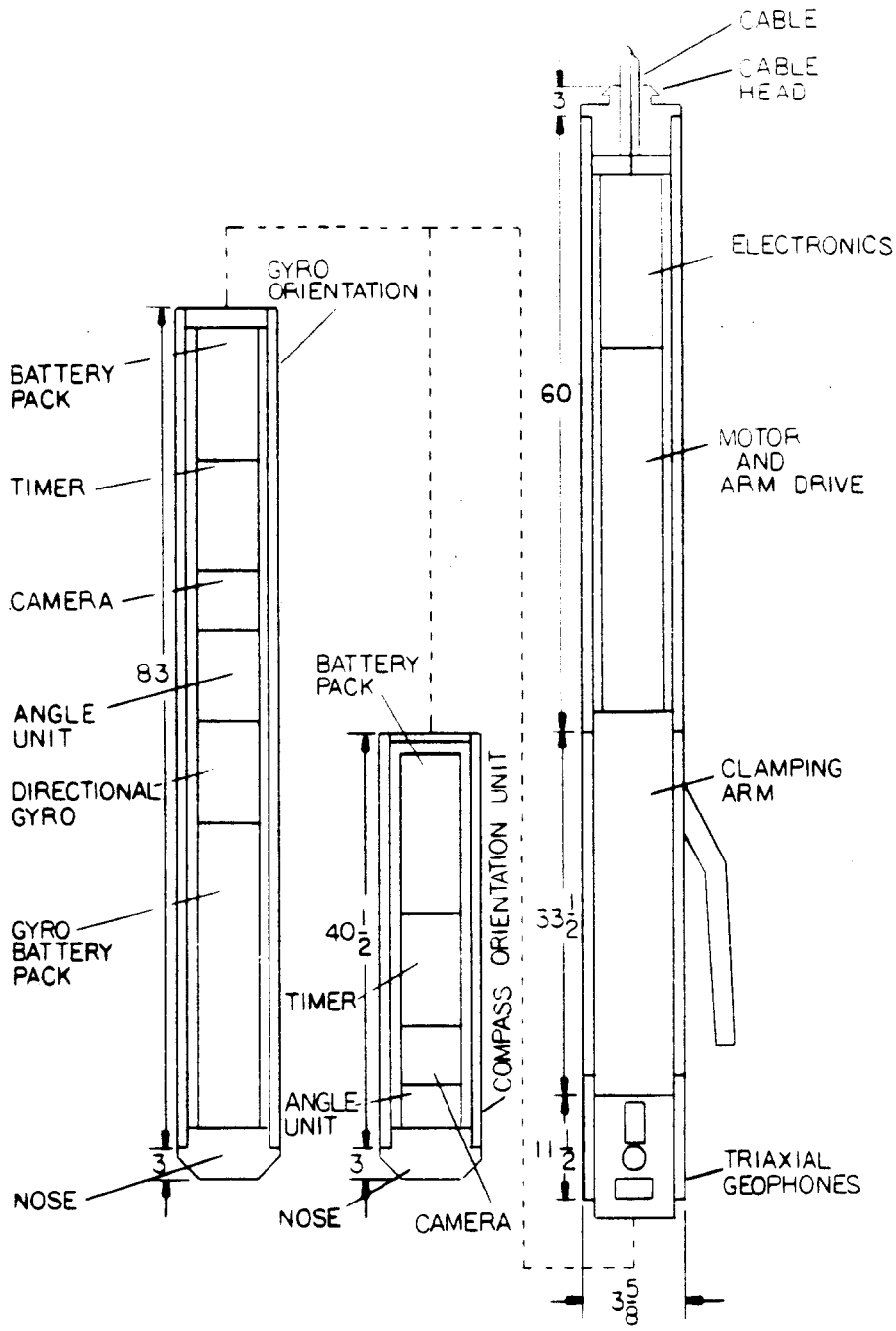

FIGURE II-2

Borehole Seismic System Configuration and Dimensions (inches

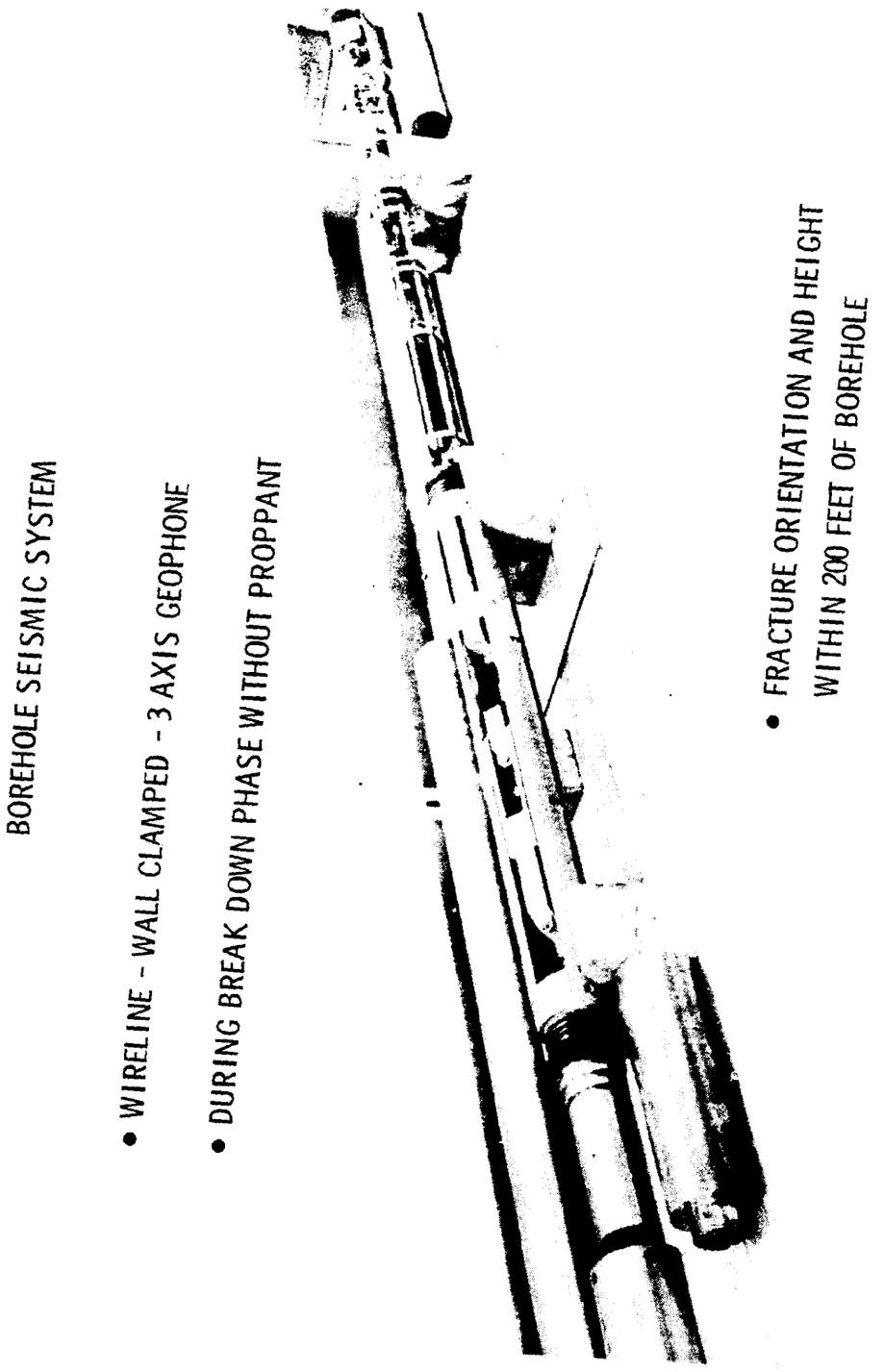

FIGURE II-3
Borehole Seismic System

Two horizontal and one vertical geophones produced by Mark Products (Model L-25A) were selected for use in this system. The output of each geophone is amplified by a specially designed amplifier, each of which then feeds a voltage controlled oscillator (VCO). The three geophone VCO signals are multiplexed with a VCO signal that monitors the clamp arm operation and then transmits to the surface. Figure II-4 is a block diagram of the downhole system. The geophone VCO's are standard IRIG frequencies and allow a 2 kHz bandwidth signal to be transmitted to the surface from each geophone. Magnetic tape recordings at the surface are made to allow for future data analysis. The entire system has been pressure tested and found to operate satisfactorily up to pressures of 12,000 psi.

2. NTS Minifrac

In October of 1978, two very small fractures were performed in the HF20 drift of G-Tunnel at the Nevada Test Site. Three triaxial geophone packages were grouted into the drift and the borehole seismic unit was placed in a horizontal position within another, horizontal borehole. All four sets of geophones were placed such that the larger of the two fractures would be expected to intersect their positions.

The purpose of this experiment was: 1) to compare the signals from grouted units with the clamped unit, 2) to examine near field seismic signals, 3) and to examine the tail of the seismic signal (coda) because of peculiarities observed in data collected in testing during the previous year (Ref. 1).

The first fracture was performed with 20 gallons of clear water and the second fracture with 80 gallons of clear water. During the first fracture, no signals were observed on the borehole seismic unit. Insufficient amplitude of the few signals observed on the other units prevented any significant evaluation of signal characteristics or source location. The second fracture produced more signals but all of a very low amplitude. These were further

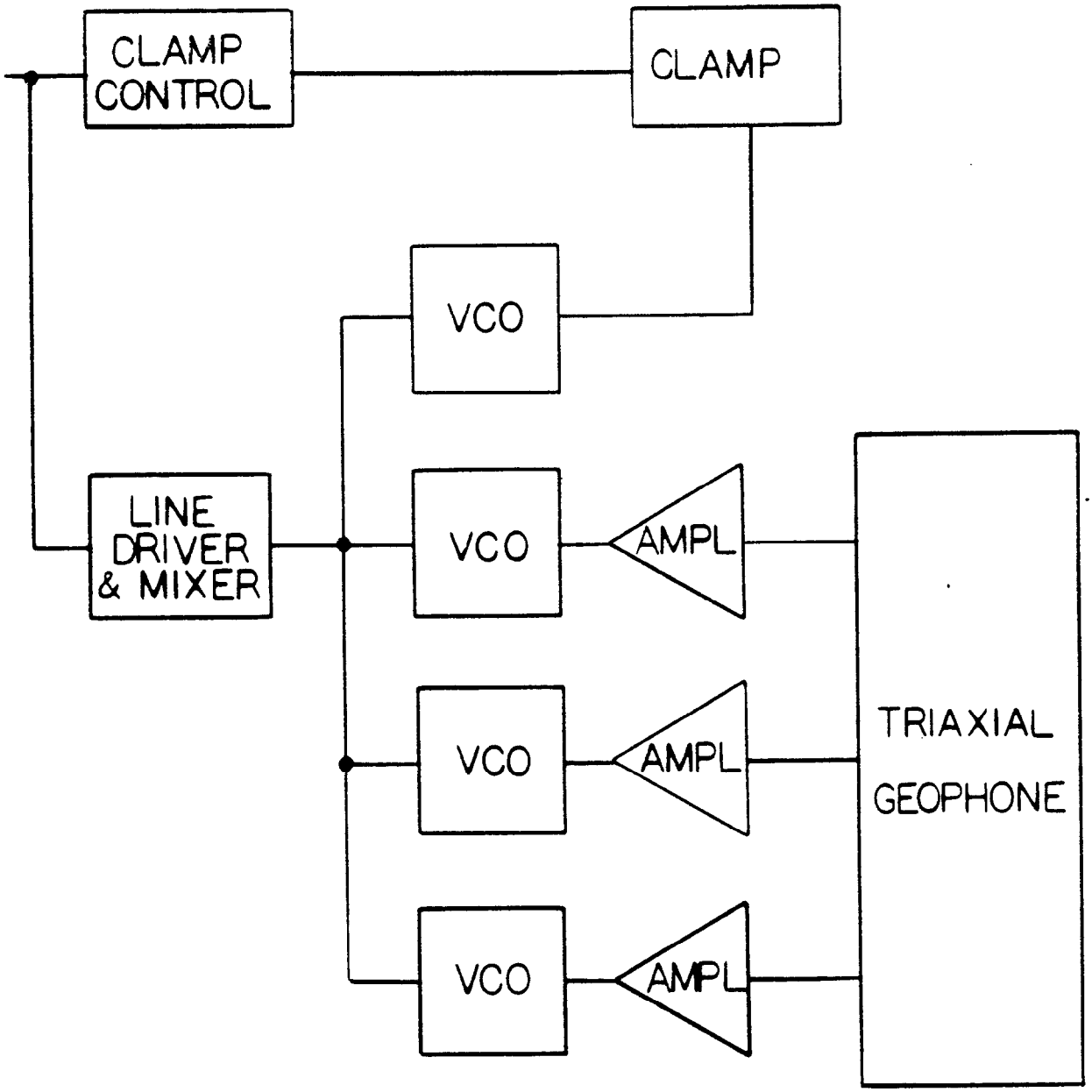

FIGURE II-4
Block Diagram of the Borehole Seismic System

complicated by intermittant tape recorder malfunctions to the extent that no signal characterization or source location could be determined. The borehole seismic unit because of its horizontal position, went into large mechanical resonance. One horizontal geophone had extremely large resonant characteristics indicating that in all likelihood it had been damaged in a previous test.

As a result of the low signal levels and malfunctions, no useful conclusion could be made from these tests and additional NTS tests were planned.

3. Amoco Experiments

Sandia participated in two experiments in November, 1978 with Amoco in the Wattenberg field, north of Denver, CO. These experiments were conducted in the Muddy J gas sand at approximately 8,000 feet.

The breakdown pumping schedules were designed to study seismic signals generated from fractures and hopefully to determine the direction of the fracture.

a) Experiment #1

The well was cased to a depth of 7,965 ft and open for approximately another 100 ft. Sandia's triaxial geophone package was clamped at 7,945 ft, and the well was fractured with 15,000 gallons of KCl water in small stages. An initial breakdown was performed with 100 gallons at five barrels-per-minute (BPM) followed with an additional 100 gallons at 1/4 to 1/2 BPM to determine closure stress. Following these two stages, the well was shut in and seismic activity was monitored and recorded for several minutes. Subsequent pumping stages were of 100, 200, 500, 1,000, 2,000, 4,000 and 7,000 gallons at 5 BPM, and each stage was followed by a 3 to 10 minute shut-in period in order to monitor seismic activity.

More than 65 signals were observed during these quiet periods. Of these signals, seventeen appeared to have sufficient amplitude to be examined. Five of these signals saturated this system and three were too low in amplitude to be usable leaving nine signals that could be analyzed.

The signals were bandpass filtered from 10 Hz to 400 Hz and digitized at

a 1 kHz rate. The signals were then further processed by using an adaptive filter to help eliminate periodic background noise. Hodograms of the horizontal geophones were then examined to predict fracture orientation. Bearings were obtained that ranged from 290° to 320° with an average of 305° indicating a fracture direction of N55°W to S55°E. A typical hodogram is shown in Fig. II-5.

b) Experiment #2

On 11/30/78, a breakdown fracture was conducted on Experiment #2. This well was completely cased and perforated from 7,910 to 7,940 ft. The Sandia seismic package was placed at 7,926 ft. The pumping schedule was the same as on Experiment #1, except that the breakdown and closure stress determination was a total of 100 gallons and the 2,000-gallon stage was increased to 2,100 gallons for a total of 15,000 gallons.

More than 10 seismic signals were observed but of lower amplitudes than those on the first test. Only five signals were large enough to obtain source direction. Bearings on these signals were from 105° to 147° with an average of 130° indicating a fracture direction of N50°W to S50°E. A typical hodogram is shown in Fig. II-6.

Shear wave arrivals could be observed in most of the signals for both tests as shown in Figs. II-5 and II-6 and ranged from a few milliseconds to as much as perhaps 15 ms following the compressional wave.

Distance to seismic sources can be determined as follows if the p and s wave velocities are known.

$$D = V_p(t_p - t_o) \qquad (1)$$

where D = distance to the seismic source

V_p = p-wave velocity

t_p = the time at which the p-wave arrives

t_o = the time at which the seismic wave was produced

also

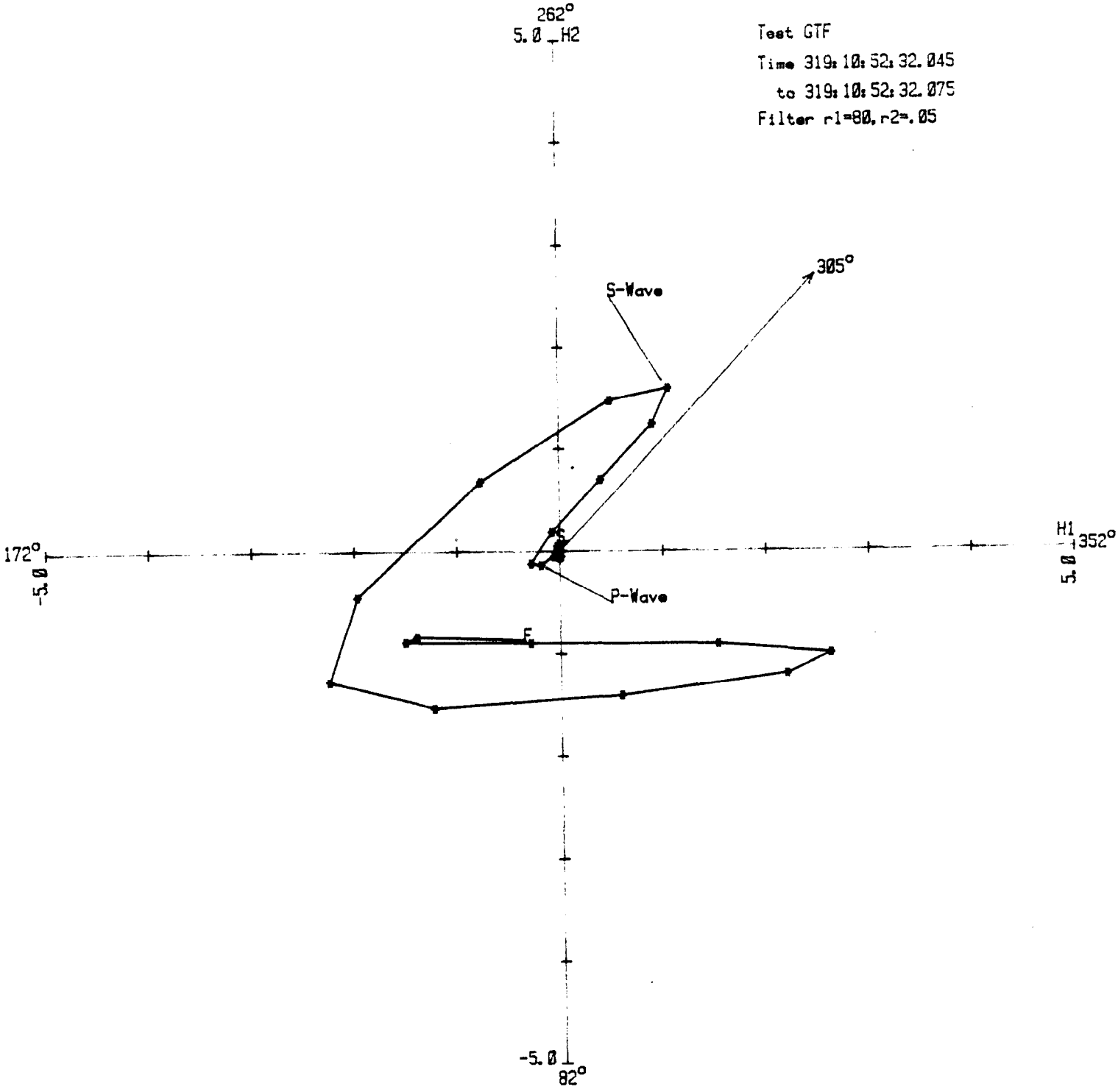

FIGURE II-5

Typical Hodogram for Experiment #1

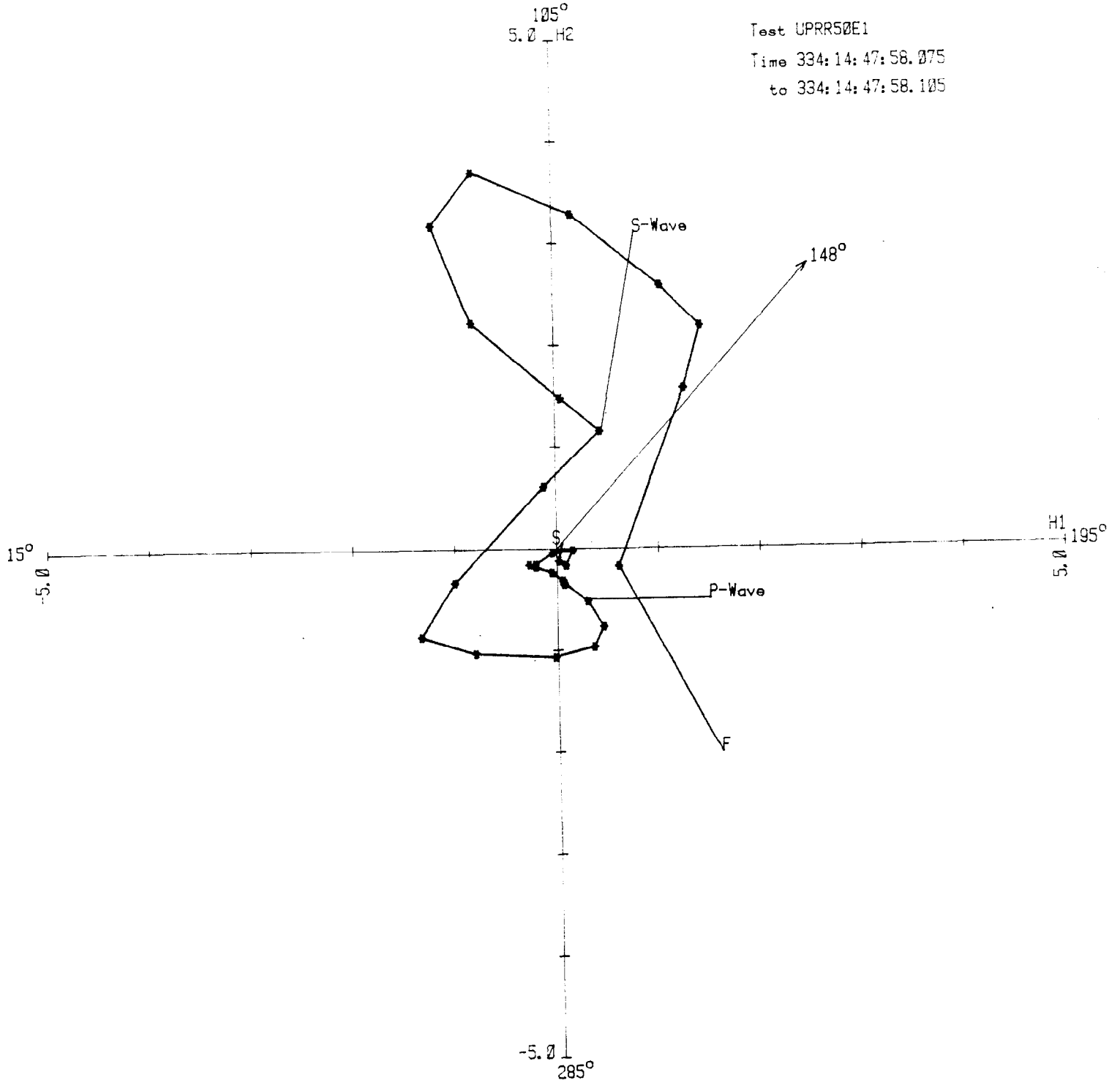

FIGURE II-6
Typical Hodogram for Experiment #2

$$D = V_s(t_s - t_o) \quad (2)$$

where V_s = s-wave velocity

t_s = the time at which the s-wave arrives

rearranging eqs. 1 and 2 we have

$$D/V_p = t_p - t_o \quad (3)$$

$$D/V_s = t_s - t_o \quad (4)$$

subtracting 3 from 4

$$\frac{D}{V_s} - \frac{D}{V_p} = t_s - t_p$$

rearranging 5 produces

$$D = \frac{V_s V_p \Delta t}{(V_p - V_s)}$$

where Δt = the time difference of the p-wave and s-wave arrival.

If one uses a p-wave velocity of 10,000 feet-per-second and an s-wave velocity of 5,000, which could be typical for sandstone formations, the seismic sources producing the signal shown in Figures 5 and 6 would be approximately 20 and 150 ft from the wellbore.

4. NTS Borehole Tests

In order to determine the origin of known seismic sources and study the oscillatory signals, an evaluation test of the borehole seismic unit was designed and performed at the Nevada Test Site. The clamp package was installed in the floor of G-Tunnel and adjacent to it, a triaxial geophone package using the same type of geophones was grouted in a borehole. Seismic signals were then induced, and the received signals analyzed for determining the source locations. In addition to the induced seismic signals, a triaxial geophone was attached to the clamp unit and driven from a sine wave source at various frequencies to see if resonances did exist in the clamp package.

Seven holes were drilled in the floor of the Madison drift in G-Tunnel. The relative locations of these holes are shown in Fig. II-7 as R, C, and W3

through W7. A triaxial geophone unit was placed in Hole R at a depth of 18 ft with the horizontal geophones oriented as indicated by H1 and H2 in Fig. II-7. The hole was then filled with acoustic matching grout. The borehole seismic unit was placed in Hole C at a depth of 18 feet with the horizontal geophones oriented as shown by H1 and H2 and clamped to the sidewall.

The shaker geophones attached to the borehole seismic unit were driven from 20 Hz to 2 kHz and resonances were observed at a number of different frequencies. At a later time, the borehole seismic unit was coupled to the wall through sand (i.e., the hole was filled with sand) and the resonant frequencies changed. The resonances were large enough to prohibit extraction of any useful information from the seismic tail.

A number of methods of inducing seismic signals were attempted both on the floor of the tunnel and in the bottom of the holes. The only sources that produced adequate signals were hammer blows on the floor and a spark plug fired in water at the bottom of the holes. The results of these tests are tabulated in Table II-1

In tests 1 through 3 (Table II-1) the seismic source was from firing a spark plug in the bottom of the hole. By recording the ignition times, the p-wave and s-wave travel times could be obtained and velocities calculated. The average velocities were then used to obtain distances in the other tests.

In each test, the borehole seismic system determination of the source was at least as good as the grouted reference package. Some of the source locations are rather poor, but this is to be expected whenever the signal levels are too low or too large. The reference unit has a decided shift in location in the clockwise direction. It is expected that the unit had been rotated during grouting from its original position.

Based on the tests and experiments performed with the borehole seismic system, it is reasonable to conclude that fracture orientation can be determined in most cases. With knowledge of p-wave and s-wave velocities, fracture distances could be estimated. Any additional information that may have been

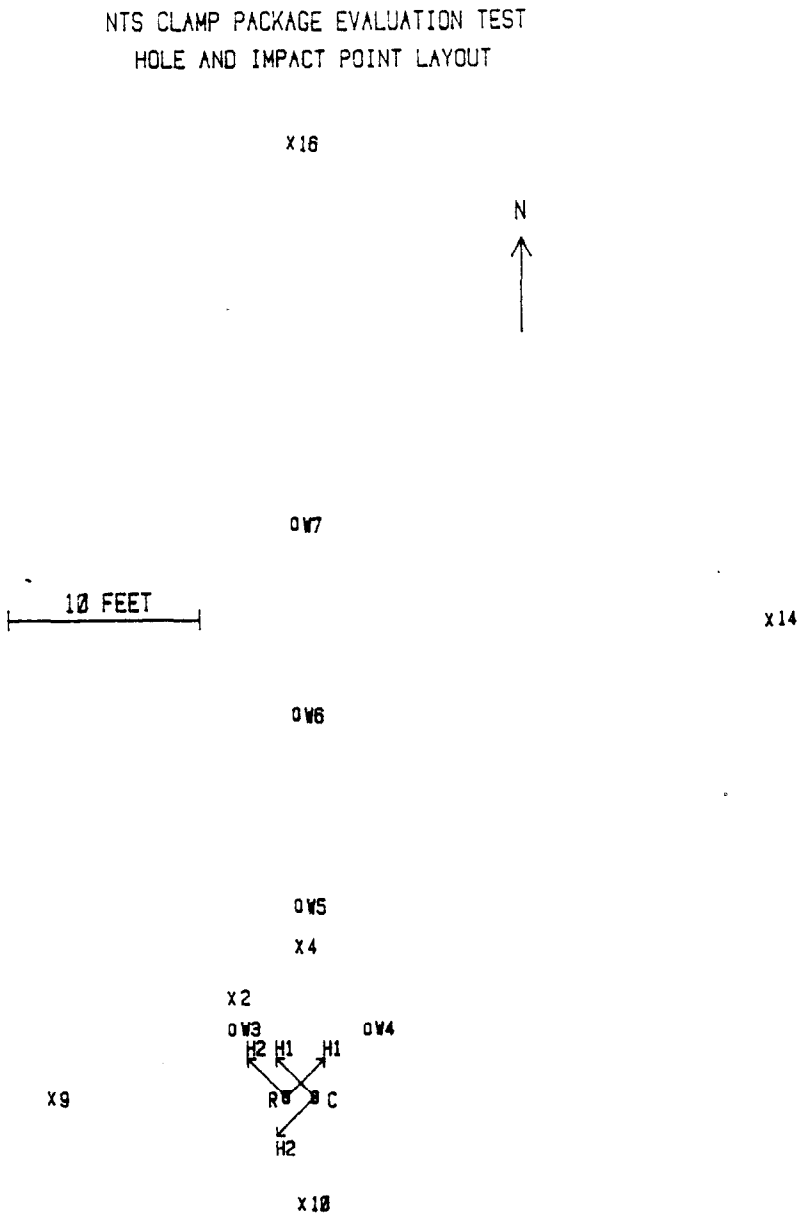

FIGURE II-7

NTS Clamp Package Evaluation Test
Hole and Impact Point Layout

Test	Source	Source Location (Note 1)	Unit	Actual Source Position (Note 2)					Measured Source Position (Note 2)					Arrival Time (MS)		Velocity (Ft/Sec)		S-P Time (MS)
				Direction (Deg.)	Elevation (Ft)	Vertical Angle (Deg.)	Distance (Ft)	Horizontal Distance (Ft.)	Direction (Deg.)	Elevation (Ft.)	Verticle Angle (Deg.)	Distance (Ft)	Horizontal Distance (Ft)	P-Wave	S-Wave	P-Wave	S-Wave	
1	Spark Plug	W7	Clamp	N1.4W	0	0	30.0	30.0	N14W	0	0	29.3	29.3	4.6	8.4	6526	3575	3.8
			Reference	N1.4E	0	0	30.0	30.0	N32E	0	0	33.9	33.9	4.4	8.8	6825	3412	4.4
2	Spark Plug	W7	Clamp	N1.4W	0	0	30.0	30.0	N20W	0	0	30.8	30.8	4.6	8.6	6528	3492	4.0
			Reference	N1.4E	0	0	30.0	30.0	N16E	0	0	30.8	30.8	4.4	8.4	6825	3575	4.0
3	Spark Plug	W6	Clamp	N2.2W	0	0	20.0	20.0	N15W	0	0	21.6	21.6	3.4	6.0	5885	3335	2.8
			Reference	N2.2E	0	0	20.0	20.0	N34E	0	0	17.0	17.0	3.0	5.2	6670	3848	2.2
4	Hammer	2	Clamp	N39.5W	18	70.6	19.2	6.8	N45W	14.9	75	15.4	4.0					2.0
			Reference	N28.2W	18	72.7	19.0	5.9	N53W	15.4	87	15.4	0.8					2.0
5	Hammer	4	Clamp	N5.4W	18	68.0	19.7	8.0	N64W (Note 3) (Note 4)	33.4	70	35.5	12.1					4.6
			Reference	N5.4E	18	68.0	19.7	8.0										
6	Hammer	W7	Clamp	N1.4W	18	30.9	35.0	30.0	N12W	17.0	30	33.9	29.4					4.4
			Reference	N1.4E	18	30.9	35.0	30.0	N20E	18.0	32	33.9	28.8					4.4
7	Hammer	9	Clamp	N90W	18	52.6	22.6	13.8	N81W	12.4	53	15.4	9.2					2.0
			Reference	N90W	18	55.8	21.8	12.2	N76W	10.8	61	12.3	6.0					1.6
8	Hammer	10	Clamp	S7.7W	18	72.6	18.9	5.6	S19W		83							Note 5
			Reference	S7.7E	18	72.6	18.9	5.6	S45W		62							Note 5
9	Hammer	W3	Clamp	N50.5W	18	72.8	18.8	5.6	W78W		69							Note 5
			Reference	N38.2W	18	75.9	18.6	4.5	N5W		83							Note 5
10	Hammer	W4	Clamp	N38.2E	18	75.9	18.6	4.5	W27E		85 (Note 5)							Note 5
			Reference	N50.5E	18	72.8	18.8	5.6	W88E	17.6	65-80 (Note 5)	18.5	5.6					2.4
11	Sledge	14	Clamp	N44.1E	18	27.4	38.9	34.5	N45E		9-32 (Note 5)							Note 5
			Reference	N45.9E	18	26.9	39.8	35.5	N88E	11.2	27	24.7	22.0					3.2
12	Sledge	16	Clamp	N0.9W	18	19.4	53.2	50.0	N4W	12.8	28	27.8	24.7					3.6
	Hammer		Reference	N0.9E	18	19.4	53.2	50.0	N9E	5.1	10	29.3	28.8					3.8

1 - Refer to Figure 5
2 - With respect to each geophone package
3 - P-wave very low - difficult to obtain direction
4 - P-wave amplitude too low to estimate direction
5 - P-wave saturated - cannot obtain S-wave arrival
6 - S-wave saturated - SP time can be in error

TABLE II-1

Results of NTS Borehole Tests

contained in the seismic tail could not be extracted due to the system resonances which generally occurred after the s-wave arrival.

3. Borehole Hydrophone System (R. P. McCann, 4733)

1. System Applications

The downhole hydrophone system under development by Sandia Laboratories is to be used in two distinct areas. The first considered is in the measurement of formation velocities to aid in the investigation of oil and gas formations; the second is for the downhole detection of passive acoustic signals for the purpose of hydraulic fracture diagnostics.

a) Formation velocity. The idea of using compressional waves as an aid in the assessment of oil and gas formations is not new. It was established early that the compressional wave propagation velocity depends on the lithology and porosity of a formation[2]. One of the basic tools used as an aid in determining formation porosity and helpful in interpreting seismic records has been the acoustic velocity log. The log is a recording, as a function of depth, of the time required for an acoustic wave to travel a unit distance of formation. The basic logging tool includes an acoustic projector and two receivers which are incorporated in the logging tool. In general, the acoustic wave velocity is higher in the formation than in the drilling mud, and in measuring first arrival times, the propagation velocity in the formation can be determined. Because the acoustic wave penetration of the formation is a function of projector to receiver spacing, the prime velocity measurement is often of the invaded zone of the formation, and measurements in the past have indicated that the velocity in the invaded zone around the well can be substantially different from the true velocity in the deeper uncontaminated zone. Therefore, it is desirable to extend the spacing between the acoustic projector and receivers to the maximum possible length[3]. An acoustic velocity system making use of this principle has been designed and is now available for evaluation and test.

b) Source locator. Early experiments in techniques to detect and map hydraulic fractures have shown that acoustic signals in the 100 Hz to 2,000 Hz frequency range are detected by a downhole hydrophone immediately following a hydraulic fracturing operation[4]. At the conclusion of pumping, these signals continue at about a constant rate throughout a 30-minute period while the well is shut-in. Because only one acoustic detector was employed, it was not possible to obtain information on source locations. Attempts have been made to measure at the earth's suface fracture oriented seismic or acoustic signals. The very poor signal-to-noise ratio encountered with such distances involved makes detection of the signal highly improbable[5]. Signal detection from fractures thus require that multiple sensor receivers be deployed near the fracture source.

2. System Description

The borehole hydrophone system makes use of commercially available components where possible. The electronic system circuitry and components are designed to allow operation on a single conductor wireline. In both intended uses of the hydrophone system, the single conductor wireline provides power to the electronics and transmits the received hydrophone signal via multiplexed voltage-controlled oscillators to the surface for recording and analysis.

The downhole hydrophone package consists of a stainless steel rod approximately 30 ft in length and 1.5 in diameter. The frequency response of the system to $\pm$ 3 db is approximately 30 Hz to 4 kHz. The maximum operating temperature is 250°F, and the specified maximum operating pressure is 10,000 psi.

The rod contains four hydroacoustic transducers spaced at 10-ft intervals. The electronics package is contained in the section of rod between the top two transducers. This packlage includes four high-gain acoustic amplifiers, four constant-bandwidth voltage-controlled oscillators, a mixer-line driving amplifier, and a $\pm$ 15 Vdc power supply.

Although the design and fabrication of the acoustic transducer unit in itself is well within the state-of-the-art, the mechanical housing and its design is a task which has not been attempted in the past. Because of the unique mechanical and environmental requirement, two sets of transducer units have been received from two different manufacturers. One set of hydrophones (6 each) has been received from Edo Western Corporation, Salt Lake City, Utah and the other from International Transducer Corporation (ITC), Goleta, California.

3. Prototype Testing

A system was designed at Sandia Laboratories for electrical testing of the acoustic hydrophones to 10,000 psi. Although the testing performed was of a rudimentary nature, the data collected clearly indicated that all the Edo hydrophones operated to 10,000 psi and, as expected, the signal sensitivity is reduced at the higher pressures. Some testing has been completed on the six hydrophone units received from International Transducer Corporation. Pressure tests were made to 10,000 psi. As with the Edo Western the high pressure seal system of the hydrophones functioned satisfactorily on all of the units, however several of the units failed to operate electrically above 9,000 psi. Because the electrical test performed was a very simple go-no-go type, the failure could be anywhere in the testing system and further tests will be required to determine if an electrical operational problem with the transducer unit does exist at high pressures. The required electronics and mechanical hardware is on hand for the assembly of a 30-ft ITC system. The system tool will be assembled and tested in the near future.

The complete 30-ft system containing the hydrophones fabricated by Edo Western has undergone some testing in the Sandia borehole located at the laboratory. The bottom of the 6-in diameter hole is at a depth of 245 ft. The casing is to a depth of 200 feet. The water level in the borehole was detected at a depth of 142 feet. Two types of tests were made on the hydrophone system. One consisted of a series of hammer blows on the ground

surface at various distances from the borehole. The second included a small vibrator placed at a distance of approximately 40 feet from the borehole which was driven at CW frequencies of 30 Hz to 500 Hz. A driving frequency of 100 Hz was chosen in recording the hydrophone output signals. In addition to recording the output on a paper recorder and a magnetic tape recorder, the differences in phase between all hydrophone output signals were measured on an oscilloscope. These measurements were made with the top of the hydrophone tool varying from a depth of 150 ft to 170 ft in 2-ft increments. Analysis of the data indicates that the measured formation velocity is in the range of 1,000 ft-per-second to 2,000 ft-per-second. The actual formation velocity is believed to be more in the order of 5,000 ft-per-second. Because the vibrator output is small, distances greater than approximately 40 ft from the borehole lead to small signals of an eratic nature and phase measurements became very difficult to measure. It is believed that surface waves from the vibrator were coupled into the borehole and a borehole wave was created which interfered with the direct wave. Consequently, erroneous formation-velocities were measured. A series of tests are to be scheduled in an area where deeper boreholes and a more powerful vibrator are available.

The hammer blow testing was done only to determine that differences in the time of arrival at the downhole hydrophones could be detected. A sophisticated measurement attempt was not made. The test was successful and differences in arrival time could be detected. Fig. II-8 shows the output from a hammer blow struck 100 ft from the borehole. The differences in arrival time are not readily apparent in this time scale, however when expanded in time the differences are quite discernable.

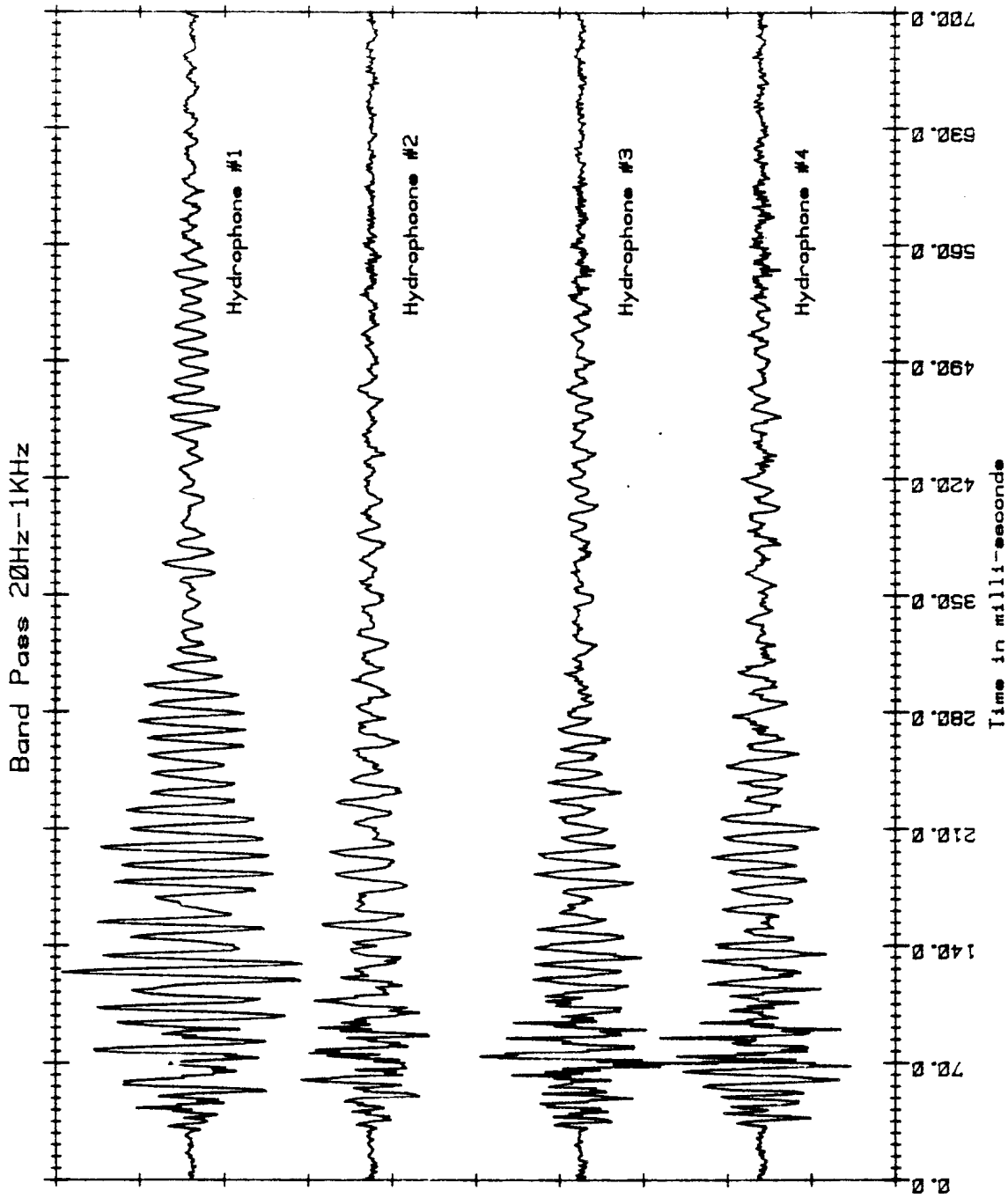

Fig. II-8 Surface Hammer Blow 100 feet from Borehole

FIGURE II-8
Surface Hammer Blow 100 Feet From Borehole

C. Surface Electrical Potential System (SEPS) (L. J. Keck, 4733)

1. System Description

Electrical prospecting is a well-known technique that is used in the investigation of geological structures beneath the surface of the earth. The approach taken is to determine the variation of the electrical constants of the earth's crust, and variation in resistivity is by far the greatest. The induced surface electrical potential method used in MHF characterization uses the variation in the resistivity contrast and is associated with the science (or art) of electrical prospecting. A current injection probe is placed at the fracture formation depth in the fracture well. A remote well casing serves as the return current probe. The resulting potential distribution is measured at the surface of the earth on circumferences around the fracture well.

Theoretically, before the fracture, equipotential ellipsoids form concentrically around the well casing as their center. These ellipsoids form concentric circles around the fracture well at the surface. During fracture, the fracture zone, along with the well casing (both filled with conducting fluid) acts as a changing current injection electrode. As the fracture progresses, the changes in electrode geometry cause a predictable distortion in the concentric equipotential circles around the fracture well.

The surface electrical potential data are taken by periodically recording the induced potential differences at the earth's surface between data probes (in concentric circles) placed every 15° circumferentially around the fracture well, and a data reference probe (stake). The injected current is of a bipolar pulse form to minimize the effects of electrode polarization. Prior to fracture initiation, background data are taken to establish the baseline potential levels around the fracture well at the data probes. These then become the reference data for detecting the changes when the conductive fracture fluid alters the electrical geometry of the fracture

zone. This change in the fracture zone current distribution, caused by fracture growth, alters the induced surface electrical potential around the fracture well. If the electrical potential measurements before, during and after the fracturing are compared, diagnostic information about the fracture is obtained.

SEPS is capable of acquiring 48 electrical potentials around the fracture well. These potential points are arranged in two concentric circles (Fig. II-9) around the well, each circle consisting of 24 stainless steel stakes (data probes) approximately 2 ft long.

Each of the 48 data sources exist between a data probe and the reference probe. This data acquisition arrangement will provide a confidence factor if the data from each data radius flags the same fracture direction. The data probe array radii range from 1000 to 4000 ft and are determined from a mathematical model which considers such parameters as fracture depth and expected fracture length(s). The potential measurement boxes (PMB) are connected to the reference probe via the instrumentation van. This enables the PMB signal common to be used as a common tie for both the fracture data acquisition and for calibration.

Each (PMB) includes a radius 1-radius 2 select capability, a 1 Hz passive bandpass filter in front of an isolation amplifier, and a 4-pole active linear phase low-pass filter. The active filter has a cutoff of 1.75 Hz which gives a data bandwidth from approximately .25 to 1.75 Hz. The 1 Hz bandpass filter helps eliminate probe-to-reference probe current flow via the isolation amplifier input impedance. The combined filter effects reduce that portion of the telluric spectrum outside the pulse's fundamental frequency of 1/2 Hz.

The reference probe is located a distance five to ten times the radius 1 from the fracture well, and this common is one of the conductors within the interconnecting six conductor cables. These cables are also used to interconnect the 24 PMB's to the instrumentation van. The cables supply power, control and calibrate inputs to the PMB's and carry the subcarrier VCO outputs back to the instrumentation van. Test control in the instrumentation van interrelates all

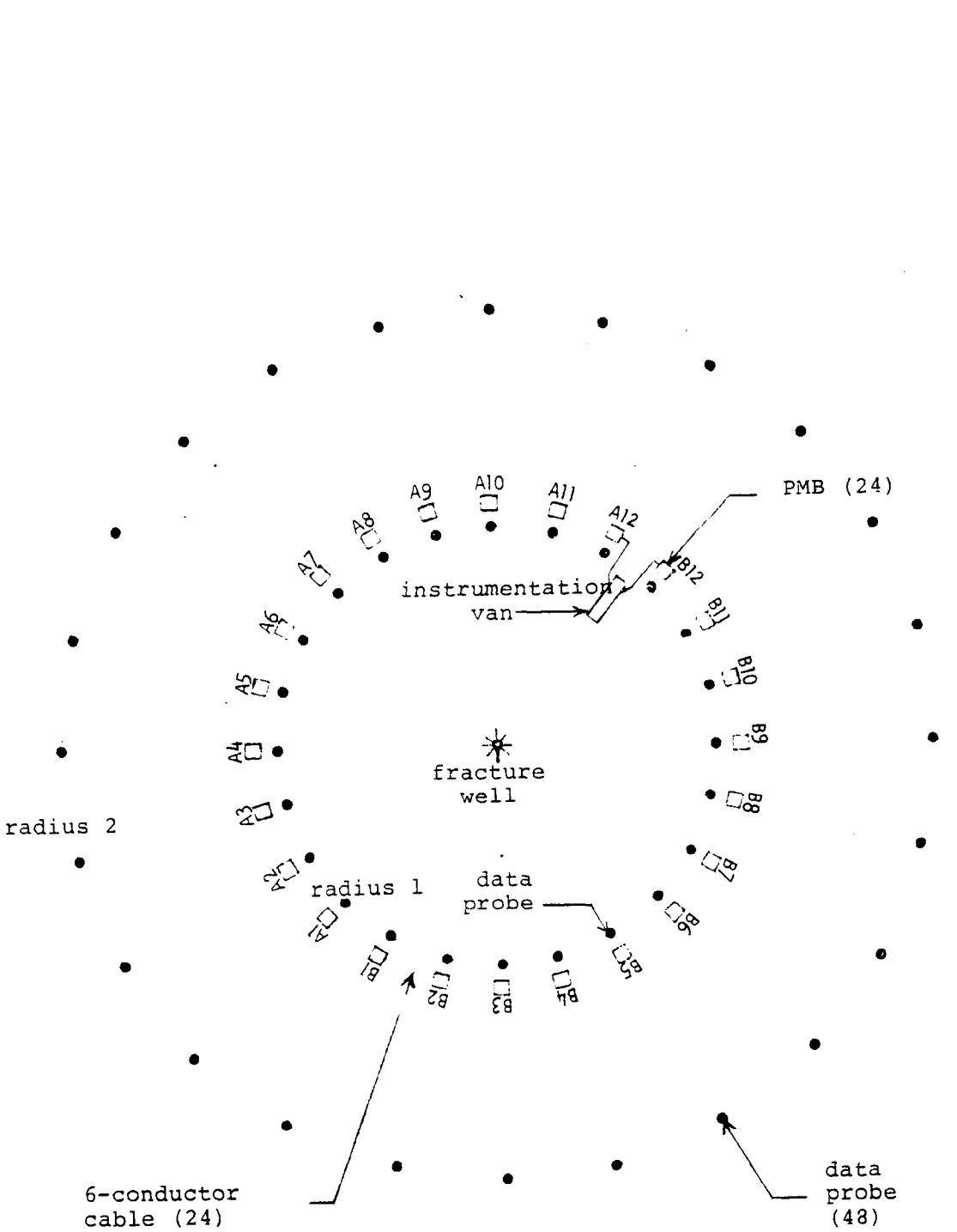

FIGURE II-9

Surface Electrical Potential System - Fracture Well Layout

functional aspects of SEPS. The computer is a DEC PDP 11/34 and includes dual soft and hard discs for data storage and handling. Digital outputs from the computer control a programmable supply for the bipolar calibration source. The computer, via the test control, also controls the radius 1-radius 2 selection. The A and B sets of twelve subcarriers from the PMB's, containing either calibrate or radius-1 and radius-2 data, are extracted from the six conductor cables in the test control and input to the A and B subcarrier discriminators. The outputs of these 24 data sources are digitized in the computer. When SEPS is stored in the instrumentation vans, the test control can simulate radius 1-radius 2 operations from the calibrate source and makes them available as inputs to the PMB's. The SEPS has undergone many hours of testing in this configuration.

2. AMOCO Wattenberg Field Fracture Experiment

Sandia participated in only one hydraulic fracture experiment using the SEPS system in FY 79 not being in the Amoco Wattenberg field, in FY 79. The well was fractured using 8,000 barrels of fluid with 2% KCL in the Muddy J gas sands at a depth of 7,972 ft. The Surface Electrical Potential System (SEPS) recorded data at radii of 1,200 and 2,400 ft (Fig. II-10) for the main fracture. Five data points on radius 2 were less than 2,400 ft due to lack of land use permission. The data reference probe was located approximately 1.6 miles east of the D-1 well. Current from the SEPS was injected via the current injection probe located at a depth of 7,964 ft via a wireline hung inside the casing. Two current sink wells were used and a set of data was obtained for each sink well and potential radius. Loop 1 had a resistance of 64.4 ohms and used the West sink well. Loop 2 had a resistance of 71 ohms and used the North sink well. Figure II-11 illustrates the data reference stake and sink well layout.

Fracture pressure and flow were recorded by SEPS using the Dowell transducer. Fracture fluid pumping stopped temporarily at 9:33 am and resumed at 10:00 am. Several such pumping interruptions occurred throughout the fracture treatment.

The induced surface potential data collected during the MHF experiment has been analyzed and no positive indication of fracture direction was obtained.

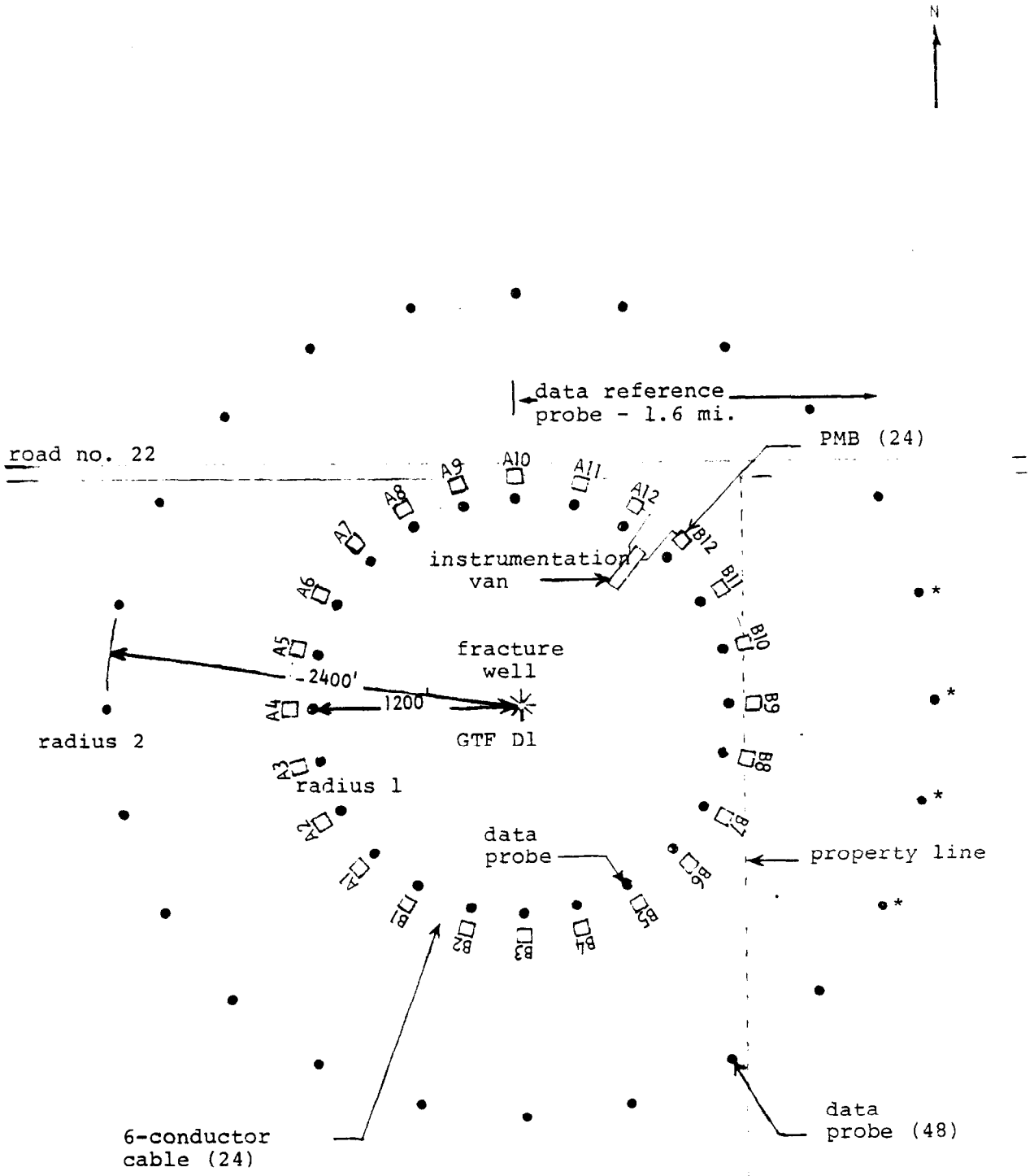

FIGURE II-10
Experimental Layout

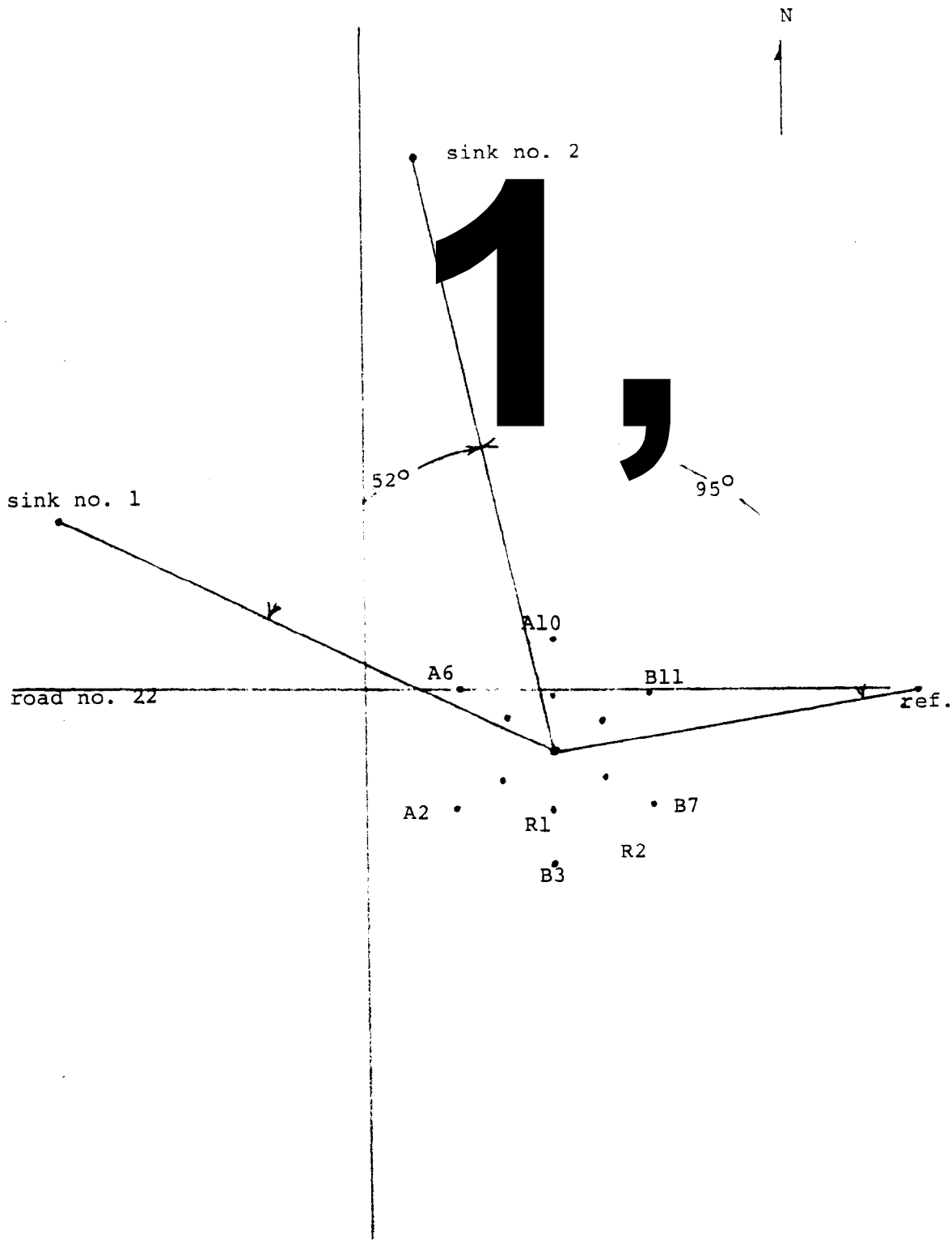

FIGURE II-11

Data Reference and Sink Well Layout

Two factors prevented these data from being useful for determining the fracture orientation. First, transient voltage spikes in excess of 1 volt were present on the leading and trailing edges of the millivolt level potentials. These transients saturated the instrumentation amplifiers and prevented an accurate measurement of the desired signals. These high-voltage spikes were evidently caused by the high rate of charge on the leading and trailing edges of the current pulse. Second, the injected current level from the pulse generator increased abruptly from 4 amps to 12 amps, approximately half way through the experiment, with no corresponding increase in potential voltages. Turbulence and/or fluid flow in the tubing could have caused a change in the character of the conductive fluid. Changes in the injected current of this magnitude hinder the comparison of induced surface potential signals occurring before and immediately after pumping commenced with those potentials occurring during the latter stages of the experiment.

3. Design Changes To SEPS

This experiment prompted several design changes to SEPS. First, the risetime of the current injection pulse has been significantly increased. This has reduced the pulse upper frequency content to approximately 10 Hz. The intent is to reduce the frequency content that is assumed to produce the high amplitude leading and trailing edge spikes. Second, the Potential Measurement Boxes (PMB) have been modified to increase the speed of recovery from such a high amplitude spike. Finally, consideration is being given to methods whereby the unintended surface current injection due to test layout can be reduced. One approach considered is that of using shielded current wire from the pulses to the frac well wireline and sink well.

REFERENCES

1. Third Annual Report-EGR, 10/77-9/78, D. Northrup and C. L. Schuster, (1978).

2. Pirson, S. J., "Handbook of Well Log Analysis", Prentice-Hall, Inc. Englewood Cliffs, NJ, (1963).

3. Gretener, P. E. F., "An Analysis of the Observed Time Discrepancies Between Continuous and Conventional Well Velocity Surveys", Geophysics, Vol. 26, No. 1, February (1961).

4. Power, D. V., C. L. Schuster, R. G. Hay, and J. Twombly, "Detection of Hydraulic Fracture Orientation and Dimensions in Cased Wells", SPE5626, presented at the SPE 50th Annual Fall Meeting, Dallas, TX, September 25 - October 1 (1975).

5. McCann, R. P., R. G. Hay, and L. C. Bartel, "Massive Hydraulic Fracture Mapping and Characterization Program, First Annual Report: August 1975-July 1976", Sandia Laboratories Report SAND77-0286, June (1977).

III. Advanced Logging Technology and Formation Evaluation

A. Seismic Formation Mapping Program (T. L. Dobecki, 4733)

1. Introduction

Gas production from formations of interest to the U. S. DOE Western Gas Sand Project (WGSP) is from tight, lenticular sand intervals typical of the upper Cretaceous Mesa Verde group and the Tertiary Wasatch formation. The lenticularity and the meandering nature of the reservoirs is a direct consequence of their being laid down in a fluvial environment. Characterization and separation of such reservoirs, prior to field development, are important to the efficient exploitation of the contained gas resource through proper well placement, understanding of geometry of individual traps, and the proper design of fracture treatments which are required to increase permeability in these tight reservoirs. It is the objective of this program to evaluate state-of-the-art seismic reflection techniques as a means of mapping the three-dimensional geometry of channel sands utilizing surface-derived data.

This new program is an outgrowth of discussions held at the Borehole Logging Program meeting convened at CER Corporation in October 1978, wherein concern was raised over the present inability to delineate and map individual sand channel reservoirs typical of the Mesa Verde Group. Sandia proposed at this meeting that state-of-the-art seismic reflection concepts (seismic stratigraphy, 3-D seismic) might be a means of delineating sand channels from surface derived data. Applicable case histories have been compiled and interviews conducted with experts in the fields of seismic reflection surveying and Cretaceous stratigraphy in the Utah, Colorado, Wyoming areas. The results of this preliminary investigation were presented in a briefing for CER and DOE personnel held at CER, Las Vegas, in February, 1979. It was decided that a limited seismic program should be performed and that a coordinated effort with C. K. Geoenergy Corporation, which is performing statistical analyses of primary sedimentary structures in channel sands in outcrop, would be mutually beneficial.

A site (Fig. III-1) in the southern Uinta Basin in Utah, approximately 45

miles northwest of Grand Junction, CO was chosen for this combined seismic and stratigraphic program.

The prime criteria to be met by a satisfactory site were: a) relatively flat ground on top of a mesa or ridge, b) exposed Mesa Verde group in the cliff walls, and c) adequate existing well control for stratigraphic information and for access for the proposed drilling operation. Such a site was found in the general area of Sections 4, 5, 8, 9, 16, and 17, T17S, R24E. This area is on a ridge just west of East Canyon with approximately 1,000 ft of Mesa Verde group exposed in the cliff faces.

An additional site was located a few miles to the northwest on top of the highest ridge in the area. The same Mesa Verde interval is found at 1,800 ft subsurface with outcropping Green River formation. This site has a large flat area and at least one gas well for subsurface control. This site will be a seismic site only (i.e. no corehole study) with the intent of determining the ability of seismic to map unknown structures at a greater depth than at Site #1.

The U.S.G.S. Phoenix (seismic) computer has a substantial seismic modeling capability which would be useful in modeling the synthetic seismic response of channel sands embedded in a sand-shale sequence. This is an important aspect in evaluating seismic techniques for mapping sand lenses. The computing facility has been made available to Sandia and a preliminary model study has been completed.

2. Task Description

Phase I of the program includes a seismic reflection survey at a specific site (see "Site No. 1" description below) in the Southern Uinta Basin, Utah. This site has shallow (0-1,500 ft) Mesa Verde group of which the upper 1,200 ft is exposed in adjacent cliff walls. This site is also undergoing geologic and corehole scrutiny by C. K. Geoenergy Corporation as part of the WGSP, while the U.S.G.S. has been involved in mapping throughout this area. By analysis of outcrop mapping, detailed core analysis, and analysis of

available well log data at this site, an evaluation of the seismic mapping capability may be made directly. Although this site presents depths substantially less than expected production depths, it presents a unique opportunity to assess seismic ability by comparison to both visual (outcrop) and geologic data.

Phase II of the program will investigate deeper sand bodies. At a site some seven miles northwest of Site No. 1 (see "Site No. 2" description below), a seismic survey is to be performed to map channel sands in the Mesa Verde group and in overlying formations. At this site, the top of the Mesa Verde is some 1,800 ft subsurface. Overlying rock includes sand channels of the Tertiary Wasatch fm. and the relatively channel-free Green River fm. No corresponding outcrop and dense well control is available at this site. The intent of this phase is to compare seismic ability with that at Site No. 1. Here, the objective bed is (a) at a greater depth and (b) is complicated by stratigraphic variation in overlying beds.

3. Site Descriptions

Site No. 1 is situated on the top of a ridge within the Bryson Canyon Gas Field (Sections 8, 9, 16; T17S; R24E; Grand County, Utah). The general elevation of the ridge top is 7,000 ft, while the adjacent canyon bottom is approximately 5,600 ft. The sides of the ridges are very steep, while the tops are relatively flat and are traversed by well service roads.

Exposed on the canyon walls are the Upper Cretaceous Farrer Fm. and overlying Tuscher Fm. (both in Mesa Verde group), although the higher elevations in the area are capped with Tertiary formations. The upper 1,000-1,400 ft beneath the ridge top, seismic line area consists, then, of numerous sandstones of variable thickness (up to approximately 60 ft), some of which are continuous over the area while others are lenticular and of limited cross-sectional extent. Softer, shaley layers make up the remaining section observed in the canyon walls. Numerous wells are available in this area for

subsurface control.

Site No. 2 is situated on the highest ridge in the area within the Horse Point Gas Field (Sections 11, 13, 14; T16S; R23E; Grand County, Utah). The general elevation of the ridge top is 8,200 ft; the ridge top is quite flat, over 1/2 mile wide, and is traversed by service roads. As with Site No. 1, the bounding canyon walls are quite precipitous.

Site No. 2 is situated on Eocene Green River Fm. The depth to the Upper Cretaceous bed outcropping at Site No. 1 is believed to be approximately 1,800 ft through the Green River, Wasatch, and other Tertiary formations. A single well is available in this area for subsurface control.

4. Program Progress

Drilling has begun on the corehole located at Site No. 1 of the proposed seismic survey. This corehole, together with outcrop mapping of sand lenses, will provide important input to the interpretive phase of the proposed seismic survey.

The contract for performance of this three-dimensional seismic reflection program has been awarded to Seismic Research International (SRI) of Denver, CO. In early July, patterns of areal seismic coverage for each site were designed. In addition, specific "target" sand lenses cropping out in the cliff faces at Site No. 1 were noted for use in preliminary transmission/reflection tests to determine frequency content of wavelets transmitted from the top of the cliff (survey location) as well as travel times to these specific units.

SRI has secured Bureau of Land Management (BLM) approval for survey operations. This task was compounded by the fact that the two sites, although less than 12 miles apart, fall under the jurisdiction of two separate BLM offices. Topographic survey activity began the latter half of August, and the reflection work is now in progress.

B. Nuclear Magnetism Logging (T. L. Dobecki, 4733)

A constant complication in field development involving tight, Western gas sand reservoirs is an effective means of determining in-situ formation

permeability. Typical pumping tests require several weeks of testing before reliable, usable data are acquired. Several reports[1,2,3,4,5,6] in petroleum literature have noted the theoretical effects of pore size, permeability, and fluid saturation on the observed nuclear magnetic resonance (NMR) behavior of formation samples. Further, empirical relationships have been developed to relate free-fluid index, FFI (a quantity derivable from a nuclear magnetism log, NML) thermal relaxation time, T_1, of the fluid bearing rock, and the bulk relaxation time, T_B, of the saturating liquid to the permeability of the formation. The relationship has been based primarily upon the Kozeny-Carman equation which links permeability to porosity, specific surface area, and pore space tortuosity. What has been observed is that NML measurements can provide a measure of permeability which is both rapid and reliable within a given producing field. What is lacking, however, is a test of the reliability and accuracy of NMR measurements in low permeability (~10-50 μd), shaley sandstones, typical of the western gas sands. Emphasized is "NMR" as opposed to "NML" because currently available NML tools have intrinsic operational time lags which do not allow T_1 determinations in such low permeability rocks. Sandia's program is to evaluate the applicability of NMR measurements to permeability analysis for low permeability formations. If valid, empirical relationships can be observed for typical, tight western gas sands, then a concerted hardware effort to develop a "fast" NML tool would be warranted.

To accomplish this task, Sandia has formed a cooperative research program with Chevron Oil Field Research Company (COFRC) with support from the U.S.G.S. (Denver) to analyze samples from a western gas sands project well and evaluate the NMR methods which have been applied to higher permeability reservoirs. The well, CIGE #21, is in the Natural Buttes Field, Uinta Basin, Northeast Utah. This well has been logged extensively and cored. Eleven core samples were secured by Sandia from zones of interest as determined from log analyses and by advice from the well operator.

A 20 mm end section from each sample was given to the U.S.G.S. for their

analyses, to include thin sectioning, scanning electron microscopy, x-ray diffraction, and electron microprobe analyses. Core sampling and testing, including permeability, porosity, and cation exchange capacity measurements is being performed by Petroleum Testing Service (PTS) of Santa Fe Springs, CA. Finally, laboratory NMR measurements on these samples will be performed by COFRC at their facility in La Habra, CA. To date, the U.S.G.S. analysis is complete and awaiting the results of standard core analysis which are underway at PTS.

C. Advanced Electromagnetic Logging (P. C. Lysne, 2353)

1. Logging Techniques Based on Dispersive Electrical Parameters

Electromagnetic techniques have often been successful for the production evaluation of oil and gas reservoirs. For example, direct current resistivity measurements yield production parameters such as the porosity through ancillary relations like Archie's Law. In another class of measurements, pulsed or sinusoidal electromagnetic fields are introduced into the formation. Then, the measured quantity is the electrical impedance which is dependent upon the dielectric constant and the magnetic permeability as well as the resistivity. Furthermore, these latter three independent electric parameters are often dispersive, that is they are frequency or time dependent. This fact has proven useful in "induced polarization" logging for sulfide mineralization and "nuclear magnetic" logging for fluid flow permeabilities.

The purpose of this study is to delve into hopes and difficulties associated with the usage of dispersive electrical parameters as production indicators in hydrocarbon reservoirs. In particular, logging techniques based on the dielectric and resistive properties of formation materials are considered. A simple (perhaps too simple) model for a dispersive dielectric is developed which may be fit in an approximate manner to the data of Poley, Nooteboom and de Wall[7] and which can yield ancillary relations directed toward water saturations and fluid flow permeabilities. It is emphasized that this work is preliminary; directions for future studies are discussed.

To solve electromagnetic problems it is necessary to have a set of constitutive equations that describe the properties of the media in question. A common set using standard notation is

$$D = \varepsilon E, \tag{1a}$$

$$B = \mu H, \tag{1b}$$

and Ohm's Law

$$J = \sigma E. \tag{1c}$$

These equations describe a linear media since only first powers of the variables are present. In a simple medium, ε, μ and σ are constants. This means that no matter how fast local changes in E and H occur, corresponding changes in D, B and J can keep pace; that is the medium is not dispersive.

Inhomogeneous materials such as rocks saturated with conducting fluids are dispersive. The case where B cannot follow fast changes in H is the basis for "nuclear magnetic" logging. Dispersive effects in Ohm's Law may be caused by many phenomena including the kinetics of oxidation-reduction reactions at ionic-electronic conductor interfaces and viscous drag on ions in solution. Dispersion in the dielectric permittivity can occur when semiconducting inclusions are present in a nonconducting matrix. This Maxwell-Wagner-Sillars Effect will be discussed following a short digression into dispersive modeling in general.

Measurements of dispersive effects can be made either by using pulsed techniques or by continuous wave techniques conducted at many frequencies; the ultimate description of the material dispersion must be the same in either case. However, experimental considerations often enter into the choice of measurement mode. For compatibility with existing data, the continuous wave description is chosen herein. Then dispersion in ε, μ and σ results in these parameters being complex and functions of frequency, that is

$$\varepsilon(\omega) = \varepsilon'(\omega) + i\,\varepsilon''(\omega), \tag{2a}$$

$$\mu(\omega) = \mu'(\omega) + i\,\mu''(\omega), \tag{2b}$$

and $$\sigma(\omega) = \sigma'(\omega) + i\,\sigma''(\omega), \tag{2c}$$

where $i = \sqrt{-1}$.

The theory of dispersive systems has been under investigation for a long time. This theory is difficult and beyond the scope of this report. However, an important consequence of this theory is cited, that is the real and imaginary components of each parameter in Eqs. (2) are related. Thus, if $\varepsilon'(\omega)$ is known for all frequencies, then $\varepsilon''(\omega)$ is also known, etc. The constraint between the real and imaginary components is a manifestation of the linearity of Eqs. (1) and causality, that is cause must precede effect. It is noted that some constitutive relations used in the past did not satisfy these Kramers-Kronig relations. In this study, which is directed toward modeling the experiments of Poley, et al, $\mu(\omega)$ is of no consequence, σ' is a constant given by Archie's Law, and σ'' is zero.

To exactly model the dielectric properties of inhomogeneous materials such as saturated rocks is very difficult, if not impossible. Such an effort would require the geometric description of each grain and void constitutent along with their individual electrical properties. Perhaps a statistical theory could be developed. For the present, an available model is used which yields, qualitatively, the dielectric constitutive relation of formation material. While imperfect, the model does point out the hopes of logging techniques based on dispersive dielectric properties.

Maxwell was the first to model the electrical properties of an inhomogeneous material, and he demonstrated that the dielectric properties of a layered medium were dispersive. Wagner extended the model to semiconducting spheres imbedded in a nonconducting matrix. For the same volume ratio of constitutents, Wagner's model is more dispersive than Maxwell's. Sillars[8] extended Wagner's model by considering imbedded spheroids. Sillars' model can be made very dispersive, and, hence, is suggestive of some of the observed dielectric properties of saturated rocks. In all of the above models,

Maxwell's Equations are satisfied at material interfaces, i.e., matrix-inclusion boundaries. This is why these models are geometry-dependent, a point which is lacking from constitutive relations based on simple mixture laws.

Historically, conduction currents are governed by Ohm's Law, Eq. (2c) and are treated as being unconstrained in that a given charged body such as an ion in a liquid can migrate an indefinite distance under the influence of a constant electric field. On the other hand, charge motion governed by dielectric laws is limited to some characteristic length such as the effective length of a dipole associated with a polar molecule or a ferroelectric domain. Consequently, dielectric currents (displacement currents) cannot flow indefinitely when influenced only by a constant electric field. In Sillars' model, the characteristic length is the unique dimension a of a spheroidal inclusion aligned with the electric field. The dimension b is the radius of the circle at the meridian of the spheroid and is perpendicular to a. If the ratio a/b is small, the inclusions are penny-shaped. Large a/b ratios mean needleshaped inclusions and this leads to large dispersive effects. Collectively, the Maxwell-Wganer-Sillars models describe the pinning of conduction charge carriers at material boundaries after they have migrated some characteristic length. The time required for this migration and pinning leads to the dispersive properties of the models.

A number of important observations follow from the work of Sillars. First of all, the dielectric response is strongly dependent upon the a-to-b ratio. Thus composite materials with the same volume fraction of constituent materials may have appreciably different dielectric properties. An illustration of this phenomenon is given in Figure III-2. Another observation is that, if, for the same rock specimen, the pore fluid salinity (conductivity) is changed, then the dielectric response is simply shifted along the frequency axis. This means that the right-hand-curve of Figure III-3 (upper) should be congruent with the other curve if it is shifted two frequency decades to the left. Likewise, for the lower curves, the offsets $\varepsilon''/\varepsilon_o$ should be equal. While the model has

some defects, it appears to be qualitatively reasonable.

In conclusion, a model based on a constant conductivity and a dispersive dielectric has been proposed to explain the frequency dependent impedance of sandstones saturated with waters of different salinities. The present model qualitatively represents the available data. A quantitative model will require a distribution function describing the pore shapes. With such a function in hand, the rock matrix is much better described than if only the porosity is known. For example, a continuum of pore-volume pore-surface areas may be modeled thereby paving the way for fluid permeability determinations through the use of a generalized Kozeny Equation. Furthermore, the extensions of the model to a three-component system could yield hydrocarbon-water ratios for pore fluids.

(J. S. Yu, 2353)

2. An Inverse Process for Evaluating Constitutive Parameters

The electromagnetic (EM) constitutive parameters of a medium are known to vary with the composition and structure of its substances. In gas/oil exploration and production, many of the "production parameters" are also known to be relatable to the constitutive parameters of borehole formations. Thus, techniques for evaluating the EM constitutive parameters using EM probes in a borehole are of interest to supplement or complement other useful techniques. EM logging has taken an added significance for areas where tight-gas sands are prevalent and "production parameters" are more difficult to discern.

In the process of analyzing EM-probe responses, there are instances where explicit functional dependences on the constitutive parameters can be formulated. One example is the open circuit voltage of a receiving coil aligned coaxially to a transmitting coil. Open-circuit voltages can be determined from a set of constitutive parameters, together with geometric and EM-source parameters; an inverse process is to determine constitutive parameters from voltage responses. The project efforts that have been directed toward such an inverse process are the subject of this progress report. Technical results to date are summarized as follows:

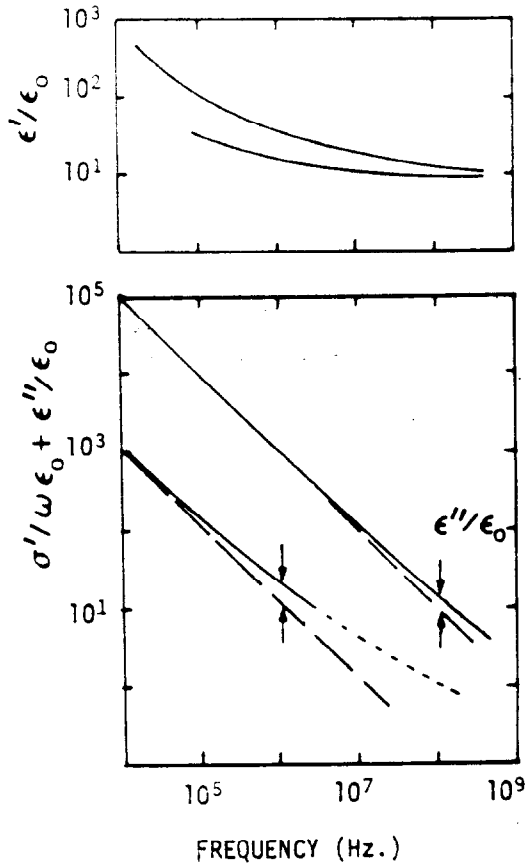

Figure III-3 illustrating data from Ref. 2. (solid and dotted). The dashed lines were obtained from Archie's Law and the conductivity of the pore fluids. The porosity of the specimen was 15 percent. In each figure, the upper curve is for saline pore water (15 kg./m^3 NaCl) and the lower curve is for fresh water. If the proposed model were exactly correct, the upper curves would overlap if the right hand curve were transposed two frequency decades to the left and the offsets, $\varepsilon''/\varepsilon_o$ of the lower plot would be equal.

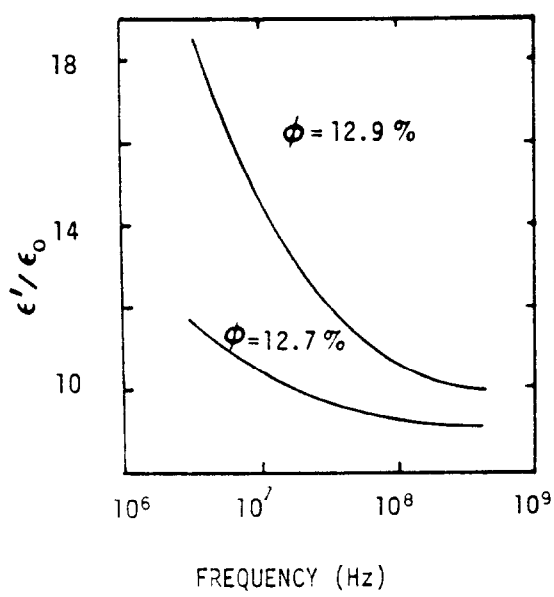

Figure III-2. illustrating $\varepsilon'/\varepsilon_o$ for two freshwater saturated sandstones. The data are from Ref. 2. Note the appreciable differences in $\varepsilon'/\varepsilon_o$ for specimens of nearly the same porosity.

a. A rigorous solution has been obtained for a 2-coil coupling in a homogeneous formation with complex constitutive parameters and has been compared with the common solution assuming point-like coils.

b. Universal curves are plotted for coupling sensitivities in empty space with variable geometric and source parameters to facilitate probe designs, and to provide references for earth formations.

c. Complex magnetic permeability of a formation has been evaluated from the ratio of transfer impedances, and the attendent errors are estimated by universal curves varying with formation properties.

d. Universal curves are plotted for fixed coil separations to determine the complex refractive index of a formation whose properties may vary from being a lossy dielectric to a lossy conductor.

e. A comprehensive data base is obtained for 2-coil couplings in a homogeneous, isotropic formation to serve as a reference for coil designs and for coil responses inside a more complicated earth formation.

Following the convention that the displacement and conduction currents are separated in the Maxwell's equations, three constitutive parameters are defined as functions of (the angular frequency of variation for time-harmonics) for a homogeneous, isotropic medium: the magnetic permeability μ (henry/m), the electric permittivity (farad/m), and the electric conductivity σ (mho/m). Also by the convention of using the empty space as reference ($\mu_o = 4\pi \times 10^{-7}$, $\varepsilon_o \approx 10^{-9}/36\pi$, and $\sigma = 0$), a set of relative parameters is defined as

$\mu_r = \mu/\mu_o$, the relative magnetic permeability; and

$\varepsilon_r = \varepsilon/\varepsilon_o$, the relative electric permittivity or dielectric "constant".

A related set of parameters is found to be more convenient for describing EM-wave propagations and interactions in a medium. Using the time-harmonic convention exp($j\omega t$), this set is

$$\nu_r = c/v = [\mu_r (\varepsilon_r - j\sigma/\omega\varepsilon_o]$$, the refractive index; and

$$\eta_r = \eta/\eta_o = [\mu_r/(\varepsilon_r - j\sigma/\omega\varepsilon_o)]$$, the relative intrinsic impedance

The values of c and v are respectively the phase velocities of a uniform plane wave in empty space and in the medium of interest. In general, the relative parameters are complex in that they have real and imaginary parts both of which are functions of ω. A point of caution is in order for the above definitions. While a complex ε_r is associated with charges bound to material points such as inclusions, and a complex σ is associated with mobile charges, the inverse process discussed in this report does not imply that these two parameters are separable through measurements of EM-probe responses.

A rigorous solution has been obtained for the boundary-value problem of a 2-coil coaxial-coupling in a homogeneous, isotropic medium. Since the constitutive parameters are conventionally referenced to those of the empty space, the coupling sensitivities between two coils in the empty space are also desired for reference purposes. Results, in the form of parametric curves, are plotted in Figures III-4. Geometrically the transmitting coil is centered at the origin of circular-cylindrical coordinates. The receiving coil is coaxially placed z (meter) from the transmitter. Both coils have the same diameter d (meter) which is restricted to less than 0.1 of empty-space wavelength λ_o so that the coupling between the two coils is through a nearly pure magnetic-dipole mode. The abscissas in Figures III-4 and III-5 are the same. Their values are dimensionless when d/λ_o is used. When the diameter d is fixed in coil designs the abscissas can be converted into the transmitter frequencies. For example, should the diameter d be fixed at 10 cm, the transmitter frequencies would have to be less than 300 MHz to assure that the coupling is accurately accounted for by using only a magnetic-dipole mode. The open-circuit voltage V_{oc} at the receiving

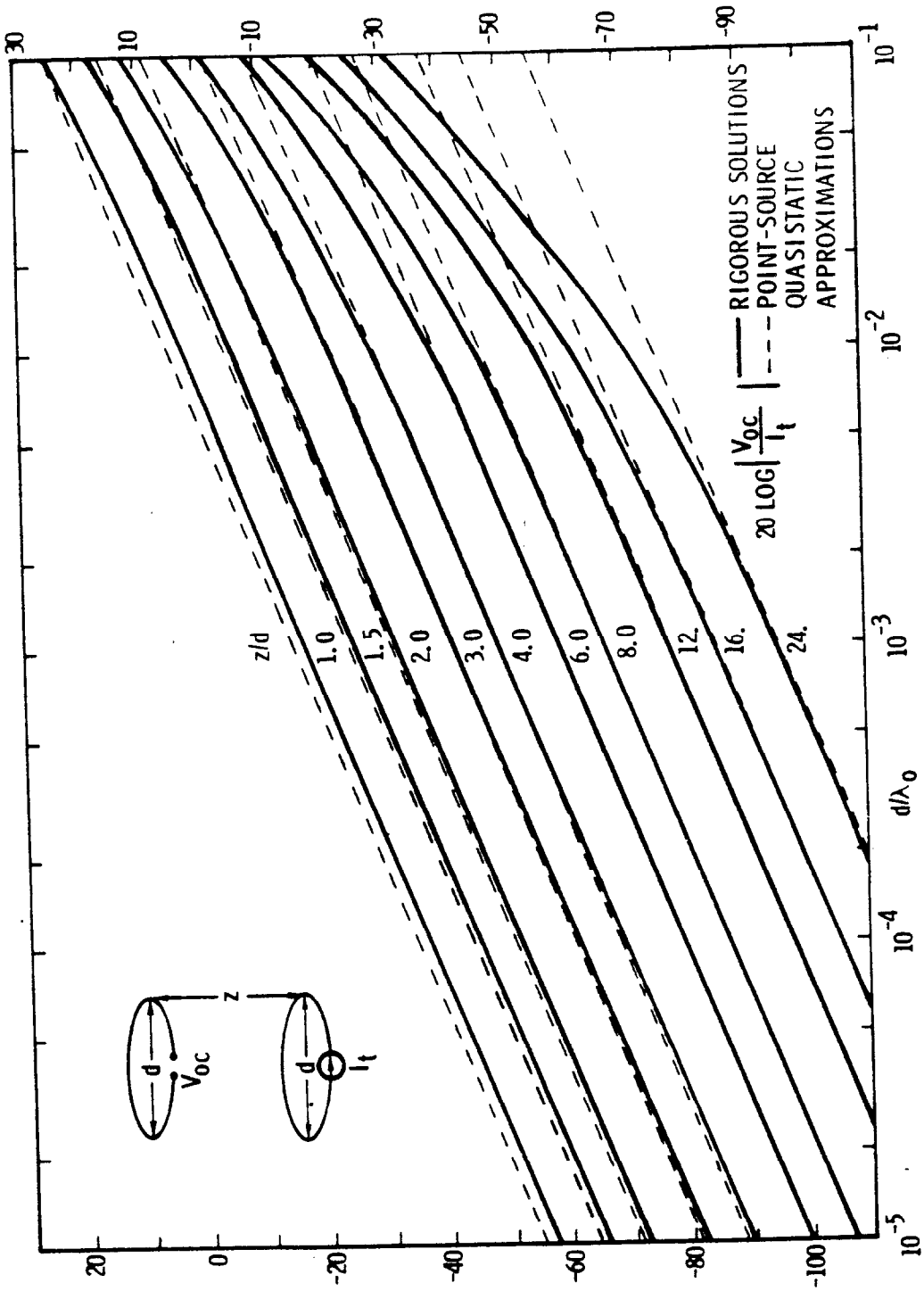

FIGURE III-4

Magnitude-Sensitivity Curves of Transfer Impedance $Z_{11} = V_{oc}/I_t$ between two coils through Magnetic-Dipole Coupling in the Empty Space. (The abscissa is for coil diameter d over empty-space wavelength λ_o, the ordinates are for 20 $\log|V_{oc}/I_t|$, and the curves are parameterized for coil separation z over d.)

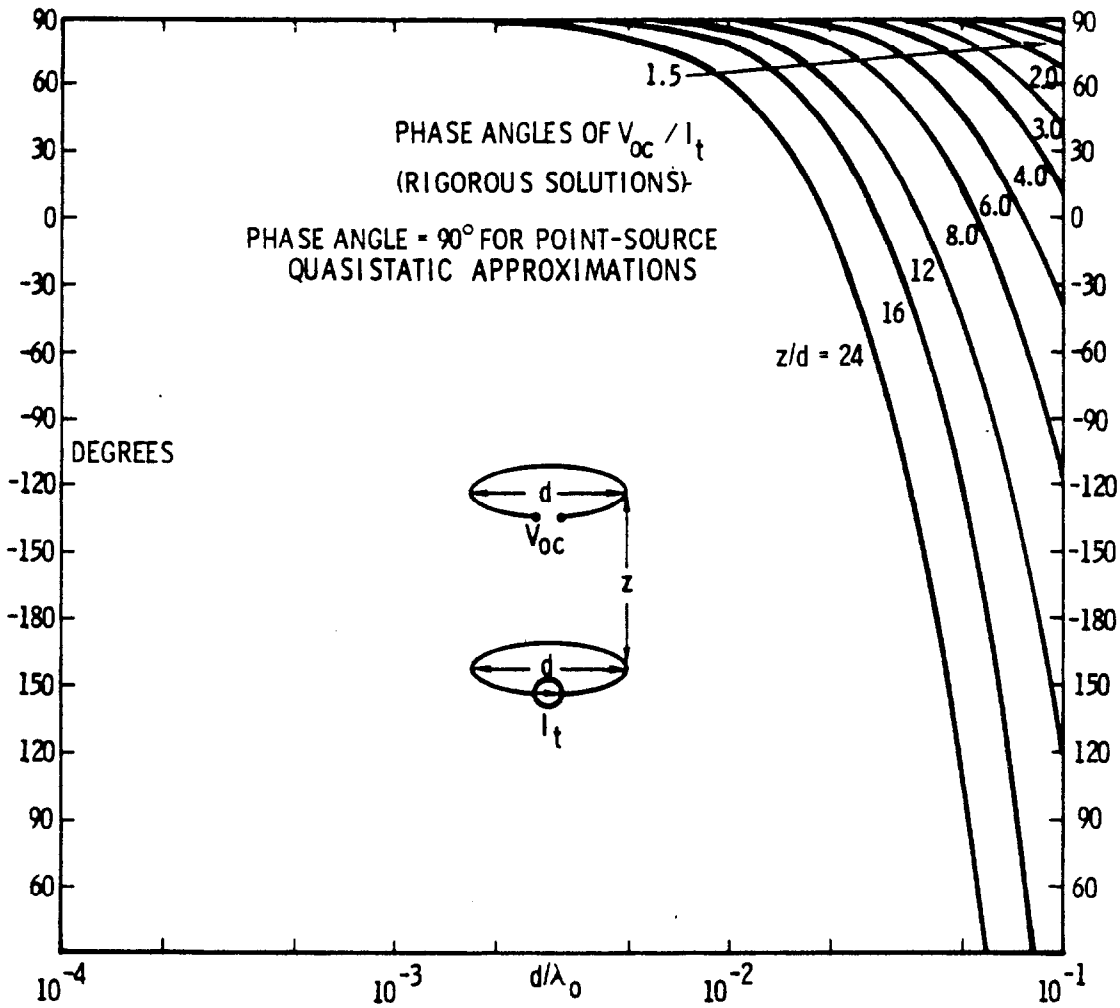

FIGURE III-5

Phase Angles of Transfer Impedance $Z_{12} = V_{oc}/I_t$ between two coils through Magnetic-Dipole Coupling in the Empty Space. (The abscissa is for coil diameter d over empty-space wavelength λ_o, the ordinate is for phase angles in degrees, and the curves are parameterized for coil separation z over d.)

coil is directly proportional to the transmitting-coil current I_t. Their ratio is known as the transfer impedance with magnitudes spanning more than seven decades for various coil spacings z/d and coil diameters d/λ_o. To make a more compact presentation, the magnitudes of transfer impedance are transformed into a familiar form 20 log (V_{oc}/I_t) as marked along the ordinate of Figure III-4. The solid curves are the results of the analytically rigorous solutions. The dashed lines represent the point-source quasistatic solutions under two simplifying assumptions that the coils are point-like $(d/\lambda_o \to 0)$ and the separation is vanishingly small $(z/\lambda_o \to 0)$. The corresponding phase angles of the transfer impedance are plotted in Figure III-5 indicating the extents of phase shifts for various combinations of d/λ_o and z/d. An example will serve to illustrate how the coupling sensitivities can be estimated from the curves as shown. Let a set of geometrical and source parameters be specified:

Diameter of coils	$d = 0.1$ meter
Spacing of coils	$z = 2.4$ meters
Transmitter frequency	$f = 6 \times 10^7$ Hz
Amplitude of current	$I_t = 10^{-1}$ ampere

The open-circuit voltage V_{oc} can be estimated to have an amplitude about 10^{-4} volt from Figure III-4 and a relative phase angle about -3° from Figure III-5. For the purpose of estimating coupling sensitivities for design considerations, adequate results may be obtained through graphic interpolations for other specifications.

The main object in this report is an inverse process to evaluate the constitutive parameters when the coils are placed in an earth formation assumed to be homogeneous and isotropic. The transfer impedance between the coils in a formation is solved rigorously by assigning a set of constitutive parameters ν_r and η_r (or equivalently a set of μ_r, ε_r, and σ) to the formation, and by imposing $(d/\lambda_o)\ R_e(\nu_r)<0.1$ to maintain a strictly magnetic-dipole coupling. For the inverse process under consideration, it is convenient to designate explicity two transfer impedances assuming that d, z, and f are fixed:

$\mu z_{12}(\mu_o, \varepsilon_o) = V_{oc}/I_t)$ in the empty space; and

$Z_{12}(\mu_r, \nu_r) = (V_{oc}/I_t)$ in an undetermined formation.

Inherent in the 2-coil coupling is the quasistatic property that the relative magnetic permeability can be evaluated as

$$\mu_r = z_{12}(\mu_r, \nu_r)/z_{12}(\mu_o, \varepsilon_o)$$

Should the quasistatic conditions not be met, the μ_r estimated by the ratio of transfer impedances would have certain errors depending on the other parameters involved. The rigorous solutions for the transfer impedances have been used to evaluate the normalized errors as shown in the parametric curves of Figure III-6 with the coil separation set equal to one coil diameter. As an illustration, for d =10 cm and f = 30 MHz the ratio d/λ_o is 0.01. To assure the magnetic-dipole coupling condition, the first condition to be satisfied is $(d/\lambda_o)R_e(\nu_r)<0.1$. This means the real part of refractive index may not exceed 10 in order to use the rigorous solution and its inverse process. The second step in evaluating the normalized errors for μ_r-estimation is to divide all the number assigned to the solid curves by the factor $(200d/\lambda_o)^2 = 4$, and to obtain $Re(\nu_r^2) = Re[\mu_r(\varepsilon_r - j\sigma/\omega\varepsilon_o)] =$ 45, 40, 35, 30 . . . . Allowing that there are other data sources to estimate ν_r^2 as a complex value, a desired estimate on errors can be made using Figure III-6. For $\nu_r^2 = 30-j24$ and $d/\lambda_o = 0.01$, the normalized error associated with estimating μ_r (by the ratio of transfer impedances) is about $-0.055 + j0.08$ falling within a 10% error circle centered at the true value of μ_r. If d/λ_o is reduced to 0.005 and 0.0025 while ν_r^2 remains the same, the normalized errors according to Figure III-6 are within a 2.5% - error circle and a 0.7% - error circle, respectively. Thus, a mean of determining μ_r using the 2-coil coupling is established with error estimates.

To complete the inverse process requires another complex number from the 2-coil coupling mechanisms to determine the refractive index ν_r. Although most earth formations are known to have μ_r near unity, the general form of $\nu_r = [\mu_r(\varepsilon_r - j\sigma/\omega\varepsilon_o)]$ is retained for possibilities when the assumption

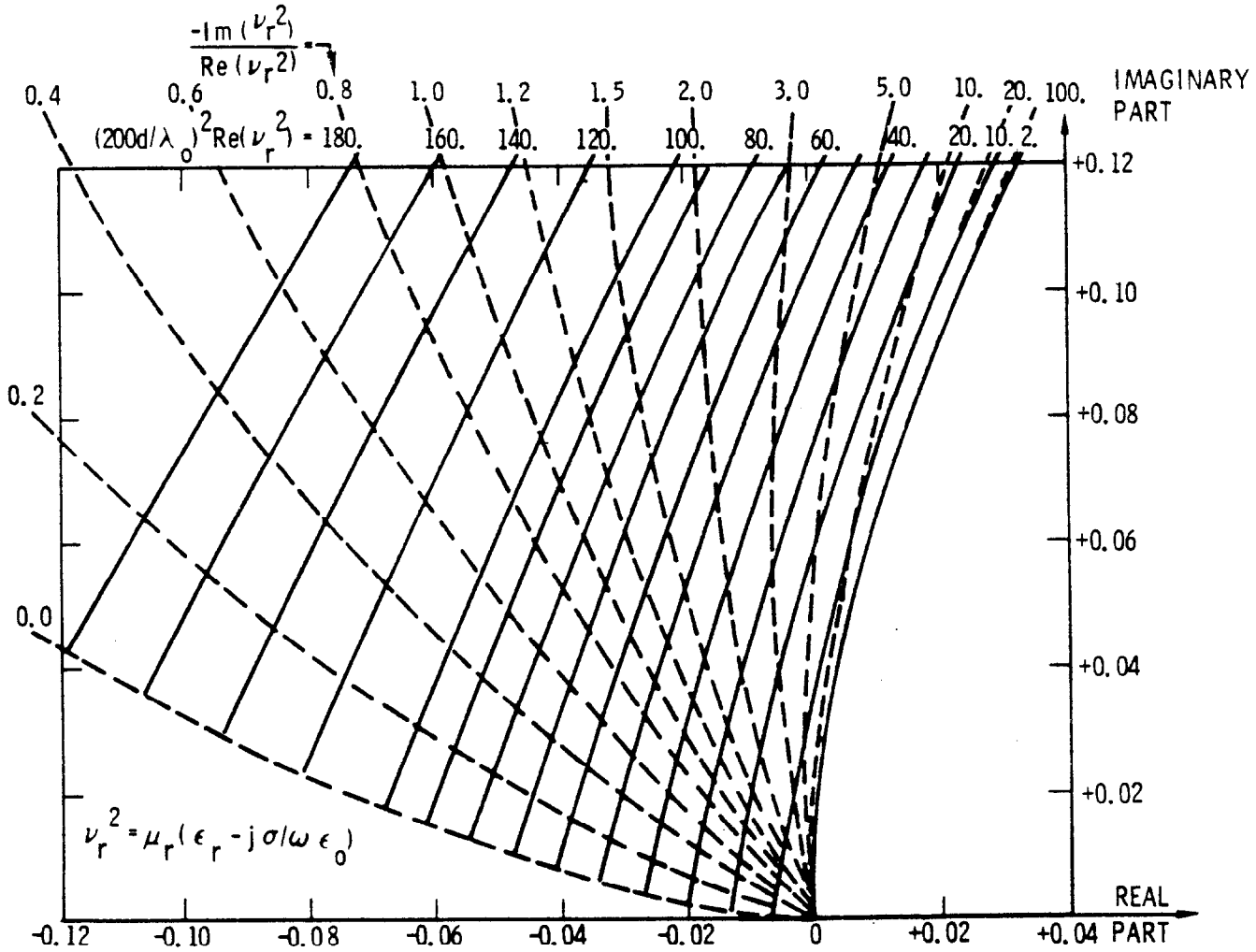

FIGURE III-6

Normalized Errors (1. - Estimated μ_r/True μ_r) in Real (Abscissa) and Imaginary (Ordinate) Parts for Estimating the Relative Magnetic Permeability μ_r from $z_{12}(\mu_r, \nu_r)/z_{12}(\mu_0, \varepsilon_0)$ with the Coil Separation z/d = 1. [The $z_{12}(\mu_r, \nu_r)$ is the transfer impedance measured in an undetermined medium characterized by μ_r and refractive index ν_r which in general depends also on conductivitiy σ and relative electric permittivity ε_r. The $z_{12}(\mu_0, \varepsilon_0)$ is measured in the empty space. The curves are parameterized for the real and imaginary parts of ν_r^2 with the restriction that $d/\lambda_0 R_e(\nu_r)<0.1$].

$\mu_r = 1$ is in doubt prior to an in-situ EM logging. The solution for 2-coil coupling has the inherent property that the induced voltage is more sensitive to ν_r variations when z/d is increased. Figures III-7 and III-8 are parametric curves for the ratio

$$z_{12}(\mu_r, \nu_r)/\mu_r\, z_{12}(\mu_o, \varepsilon_o)$$

with z/d values set to 10 and 20, respectively. The transfer impedance $z_{12}(\mu_o, \varepsilon_o)$ in empty space is multiplied by μ_r and used as the normalization factor for $z_{12}(\mu_r, \nu_r)$ when the coils are in the formation under evaluation. The magnitudes of ratio are seen to vary from 1 to 3 for $(200d/\lambda_o)^2 R_e(\nu_r^2)$ ranging from 2 to 100 if z/d = 10. The phase angles of the ratio vary in the fourth quadrant depending on the values of d/λ_o and the ν_r^2. Better sensitivities in Figure III-8 indicate that the corresponding magnitudes vary from 1.2 to 4.3 and the corresponding phase angles span three quadrants when z/d is set to 20. Consider an example with $d/\lambda_o = 0.005$ and z/d = 20. If the ratio $z_{12}(\mu_r, \nu_r)/z_{12}(\mu_o, \varepsilon_o)$ is measured to be $-2 + j2$ and if μ_r is known to be unity, the value of ν_r^2 is about $70 - j14$ according to Figure III-8. Using the definition $\nu_r^2 = \mu_r(\varepsilon_r - j\sigma/\omega\varepsilon_o) = \varepsilon_r$ with the assumptions $\mu_r = 1$ and $\sigma = 0$, the complex ε_r would be $70 - j14$. Thus one can quickly estimate ε_r using Figure III-7 or 8, or other selections of z/d. Granted, the number of parametric curves appears to be too sparse to perform graphic interpolations with high accuracies. Refinement and enlargement would be warranted should these theoretical curves prove to be optimal for practical applications. The results presented thus far are intended to demonstrate that universal curves can be parametrized to perform the inverse process of determining two constitutive parameters. All theoretical assumptions and restrictions are considered to have been fully formalized in this inverse process. Practical limitations in an actual implementation will ultimately set the ranges of its applicability. Thus the feasibility of EM logging using 2-coil couplings has at least been theoretically established for an earth formation that is assumed homogeneous and isotropic. Specific limits of this feasibility can now be quantified through the rigorous solution or its

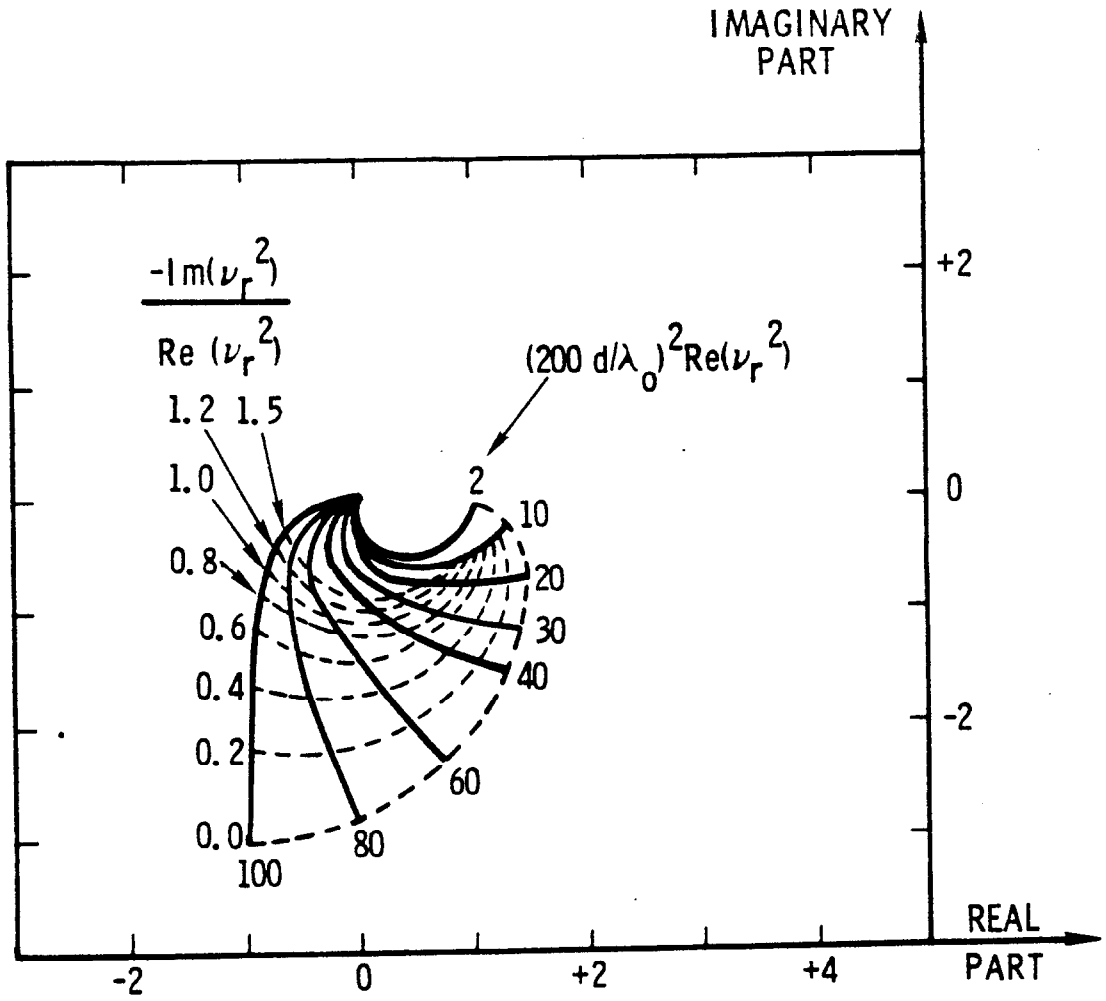

FIGURE III-7

The Real (Abscissa) and Imaginary (Ordinate) Parts of $z_{12}(\mu_r, \nu_r)/\mu_r z_{12}(\mu_0, \varepsilon_0)$ with Coil Separation $z/\lambda_0 = 10$ for Evaluating the $\nu_r^2 = \mu_r(\varepsilon_r - j\sigma/\omega\varepsilon_0)$ of an Undetermined Medium. [The real part of ν_r^2 is first evaluated from the solid curves and the imaginary part of ν_r^2 is then evaluated from the dashed curves. End results are valid if $d/\lambda_0 R_e(\nu_r) < 0.1$, otherwise the coil diameter needs to be reduced and measurements of transfer impedances need to be repeated for reusing the curves.]

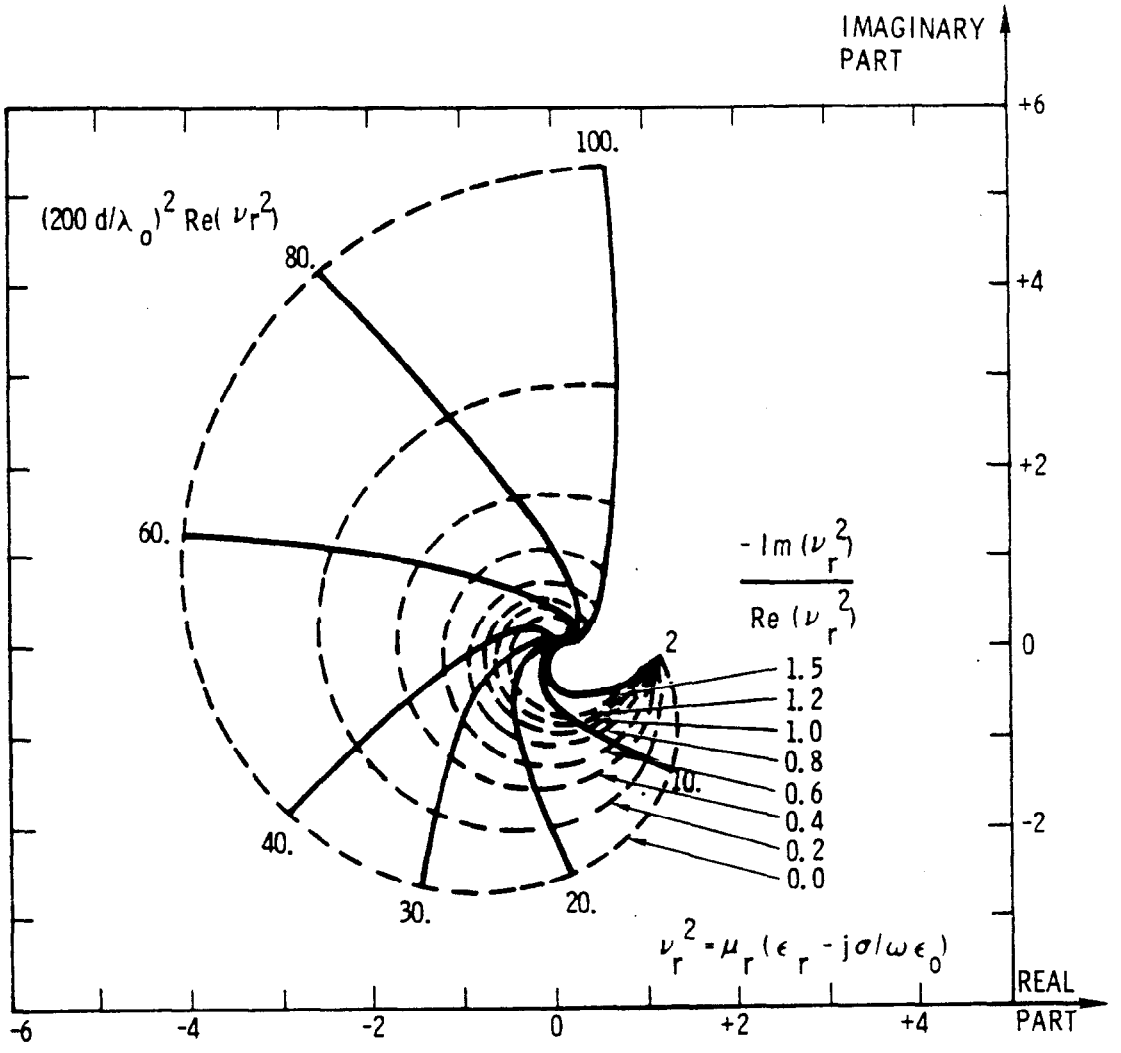

FIGURE III-8

The Real (Abscissa) and Imaginary (Ordinate) Parts of $z_{12}(\mu_r, \nu_r)/\mu_r z_{12}(\mu_0, \varepsilon_0)$ with Coil Separation $z/d = 20$ for Evaluating the $\nu_r^2 = \mu_r(\varepsilon_r - j\sigma/\omega\varepsilon_0)$ of an Undetermined Medium. [The real part of ν_r^2 is first evaluated from the solid curves and the imaginary part of ν_r^2 is then evaluated from the dashed curves. End results are valid if $d/\lambda_0 R_e(\nu_r) < 0.1$, otherwise the coil diameter needs to be reduced and measurements of transfer impedances need to be repeated for reusing the curves.]

parametric curves. Refinements on the curves are anticipated if better accuracies are needed from graphic interpolations. Perhaps the most significant aspect of the progress to date is a solid data base, both theoretically and graphically, upon which all responses measurable in a more realistic borehole can be referred to. While solutions for more realistic boreholes are in progress, several issues remain unresolved even for the 2-coil coupling in a homogeneous, isotropic media. Three outstanding issues are briefly outlined next.

First, the rigorous solution has been obtained assuming a uniform transmitting current whose amplitude and phase are used to nominalize the induced voltage at receiving coil. This is comfortable analytically, because two difficult questions are being suppressed. They are: What would be the theoretical values of I_t when a wire loop of finite radius is driven across a finite gap, and how well the theoretical values would agree with actual values when the wire loop is driven by a real feeder. Field values in the presence of actual feeders may deviate significantly from the theoretically assumed conditions. Recognizing that empirical "fixes" are commonly employed in practice, it is recommended that further theoretical understanding should be developed to reduce the need and to improve the effectiveness of these "fixes". Perhaps a more significant point is to establish the self impedance of transmitting coil that is consistent with theory and measurement. The inverse process for a realistic borehole could be uniquely improved by this new capability.

Secondly, the rigorous solution is strictly applicable to single-turn coils only. Solutions for multiturn coils in general are not available for assessing the degree of purity in magnetic-dipole-mode couplings. Although a significant amount of effort may be needed to develop this capability, it is considered an essential part of EM logging studies based on magnetic-dipole-mode couplings.

Thirdly, there is the most basic issue regarding whether coil couplings are the most suitable EM logging techniques. One may argue that the issue has been squarely resolved by the past history of EM loggings. On the other hand,

there are many other types of EM logging that have not received adequate investigations. An obvious example is the complementary case of using linear current elements instead of the circular ones in coil couplings. Less obvious ones are transmission and reflection types that are potentially capable of exploiting more fully the three basic modes of EM-wave propagation and interactions with linear or circular polarizations.

In summary, the rigorous solution is considered to have provided a comprehensive data base for 2-coil couplings and to have established the inverse process using universal curves. These results are considered to be valuable in that they serve as the baselines to which the results for more complicated formations can be referred. However, despite its wide use in the past, it is not immediately clear that coil-couplings are the EM loggings best suited for gas/oil explorations. There are theoretical foundations indicating that other modes of EM coupling may be more advantageous, especially when μ_r of earth formation is assumed unity and carrying no useful information. Strong recommendations for studying other types of EM coupling can be justified by the theoretical results obtained to date.

REFERENCES

1. Brown, R. J. S. and B. W. Gamson, Nuclear magnetism logging: Petroleum Transactions, A.I.M.E., Vol. 219, pp. 199-207 (1970).

2. Seevers, D. O., A nuclear magnetic method for determining the permeability of sandstones: SPWLA logging symposium transactions, paper L. (1966).

3. Timur, A. Effective porosity and permeability of sandstones investigated through nuclear magnetic resonance principles: SPWLA logging symposium transactions, paper K (1968).

4. Timur, A., Pulsed nuclear magnetic resonance studies of porosity, movable fluid, and permeability of sandstones: Jour. Pet. Tech., June, pp. 773-786 (1969).

5. Loren, J. D. and J. D. Robinson, Relations between pore size, fluid and matrix properties and NML measurements: Paper No. SPE2529, Soc. of Pet. Engineers of AIME (1969).

6. Loren, J. D., Permeability estimates from NML measurements: Jour. Pet. Tech., August, pp. 923-928 (1972).

7. J. Ph. Poley, J. J. Nooteboom, and P. J. de Waal, Use of V.H.F. Dielectric Measurements for Borehole Formation Analysis, The Log Analyst, MayJune, (1978).

8. R. W. Sillars, The properties of a Dielectric Containing Semiconducting Particles of Various Shapes, J. Inst. Elec. Eng. (London) 80, 37 (1937).

IV. Stimulation Research for Unconventional Gas Recovery

A. Hydraulic Fracturing

In the tight, gas-sands basins of the Western United States there exists a large resource of natural gas that cannot be produced economically at today's prices with today's technology. Massive hydraulic fracturing appears to be the most favorable technique for exploiting this resource; however, the results to date have been less than expected, and the reasons for this are unclear. Sandia Laboratories is conducting both basic and applied research to aid in the evolution of this technique as a practical method for producing a large portion of these resources. Types of research being performed include in situ testing of hydraulic fracturing theory and technology, modeling of hydraulic fracturing behavior, and laboratory testing.

The in situ testing is being performed at DOE's Nevada Test Site (NTS) in a tunnel complex driven through volcanic ash-fall tuff under 1400 ft of overburden. This complex provides the facilities and equipment for mineback of the created hydraulic fractures for direct observation, a capability for determining in situ stresses and obtaining rock samples for testing in regions of interest, and a direct knowledge of the "reservoir" parameters and structure (i.e., permeability, porosity, location of faults, fractures, etc.). Modeling efforts include the range from details of the processes occurring at the fracture tip to numerical codes describing the coupled fluid mechanics and rock mechanics of the entire fracture. Laboratory testing includes the determination of rock properties and the conducting of small-scale experiments.

1. Hydraulic Fracturing Containment Experiments (N. R. Warpinski, 4732)

Sandia Laboratories has been actively studying the problem of containment of hydraulic fractures by conducting in situ experiments at the Nevada Test Site. Knowledge of the parameters which affect hydraulic fracture growth is very important if hydraulic fracturing is to be used successfully on tight gas reservoirs. In these low permeability reservoirs, it is necessary to create

fractures of up to 4000 ft length in order to obtain sufficient drainage for the well to be "economic" at today's prices. To achieve this fracture length, it is imperative that the fracture be contained largely to the pay zone or the volume of fluid and sand necessary will be prohibitively expensive. It is equally important that the fracture not intersect an underlying or overlying water-bearing zone.

The study of the containment of hydraulic fractures is directed towards determining the parameters and conditions which will limit the height of a fracture and control its direction of propagation so that the necessary fracture lengths will be obtained. Implicit in these studies is the presumption that sufficient understanding of these conditions will allow operators to alter treatment parameters to help control containment, at least in those formations where there is already some propensity for containing the fractures. If this is not possible, then it still may be possible to define a priori those zones that will most likely provide economic production due to favorable fracture growth (or containment) conditions.

There are several parameters which are considered to have some effect on the containment of hydraulic fractures. Simonson, et al.[1*] and Rogers, et al. calculated that a hydraulic fracture attempting to propagate from a low modulus material into a high modulus material would be arrested at the interface between the two materials because the stress intensity factor at the crack tip approaches zero as the interface is approached. This, however, has not been born out by laboratory experiments.[3,4,5] They[1,2] also showed that a bounding layer of higher minimum principal in situ stress should restrict fracture growth. Daneshy[3] performed experiments that suggested that fracture containment may be more a result of the nature of the interface rather than any difference in material properties, but this would be most often the case at shallow depths where the bonding is likely to be weaker. None of these phenomena have been verified in the field, however, except for the near-wellbore data that can be obtained from temperature logs or emplacement of radioactive sand.

*References for Section IV-A are given at the end of the section on p. 99.

The purpose of the hydraulic fracturing containment experiments is to examine the effect of these parameters under realistic in situ conditions. Two experiments have been conducted at the Nevada Test Site to study this problem: the Hole #6 Formation Interface Fracture Experiment and an Interface Test Series.

a) Hole #6 Formation Interface Fracture Experiment

The objective of the Hole #6 Formation Interface Fracture Experiment[6] was to examine the effect of a formation or material property interface on hydraulic fracture growth. Hydraulic fracture treatments were conducted above and below a welded tuff/ash-fall tuff interface and were mined back for direct observation and for determination of material properties and in situ stresses. This experiment was initiated in FY77, and the fractures were created in August and October 1977. The fracture initiated in the ash-fall tuff (low modulus) below the interface was treated with 5000 gal of green cement followed by 4000 gal of black cement at 6 bbl/min. In the upper welded tuff (high modulus), 5000 gal of blue grout was injected at 6 bbl/min. Mineback of the fractures was completed in FY78.

The entire length of the fractures at the interface was mined back, and it was found that the lower fracture (initiated in the low modulus ash-fall tuff) broke through the interface everywhere it contacted it even though the modulus of the overlying welded tuff is an order of magnitude greater than the modulus of the ash-fall tuff. Unfortunately, the upper fracture broke out along side the lower fracture which was initiated first so that little information was gained from this second test. However, the results of these experiments do show that a significant difference in material properties is insufficient to contain the fracture.

Since it is impossible to mine out more than a small fraction of these fractures due to tunnel size and economic constraints, an exploratory coring program was initiated to delineate the overall shape of the fractures. This program's aim is to determine whether the high modulus bounding layer has

an effect on fracture growth or shape (i.e., restricts growth) even though the interface itself does not terminate the fracture. Determination of the shape of the fracture may also indicate the effect of in situ stress variations, if any exist in this area. Nine holes were completed in FY78, and 14 more were cored in FY79.

Figure IV-1 shows the location where these coreholes intersected the fracture plane relative to the borehole, the mined back region, and the interface. It can be seen that fracture growth was predominantly vertical: fracture length at the interface is 150 ft, and total height is at least 200 ft. The injected volumes were sufficient to create fractures 50 ft high by 600 ft in length according to conventional fracture calculations. Estimates show that approximately 45% of the grout has been located. There appears to be no effect of the interface on fracture shape as it passed through the interface. The coring program is continuing at present with several more cores planned in early FY80 to determine the upper limit of the fractures and thus see if the welded tuff layer restricted fracture growth in any way.

b) Interface Test Series

The Interface Test Series is a set of small scale hydraulic fracture experiments which were conducted at NTS to further examine the factors that affect containment of hydraulic fractures. The basic procedure of these experiments was to create small hydraulic fractures in horizontal boreholes drilled from the tunnel at various distances below the same welded tuff/ash-fall tuff interface using a dyed-water frac fluid injected at low flow rates. Mineback of these fractures would thus provide detailed evidence of the behavior of many fractures under different conditions. These tests would also confirm the results of the Hole #6 experiment, but under different conditions, i.e., different fluid, different flow rates and a horizontal borehole entirely under the interface versus a vertical borehole through the interface.

Since these were only small volume fractures, the actual interface that was "seen" by the fractures was the contact between the ash-fall tuff and the

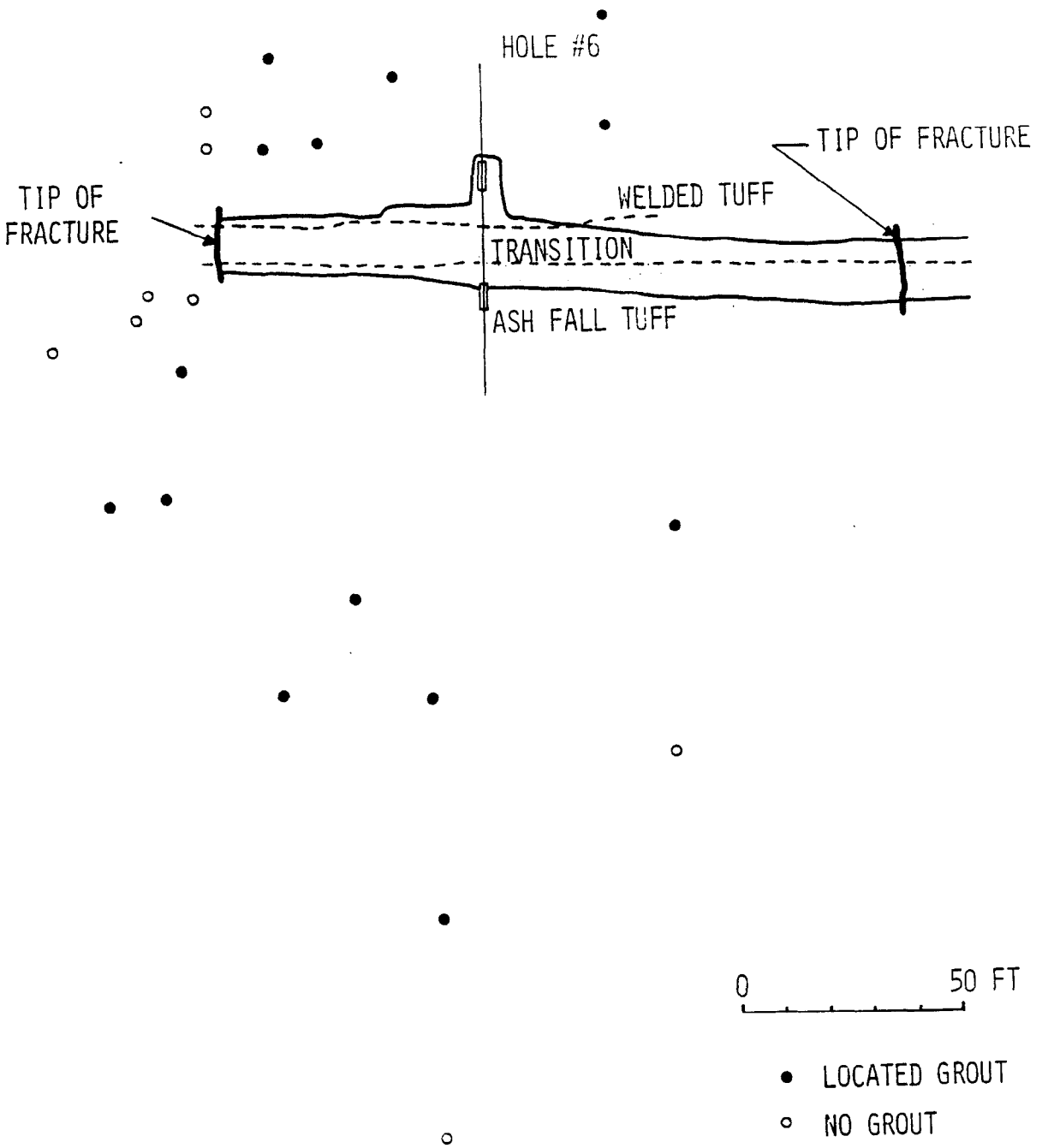

FIGURE IV-1
Results of Exploratory Coring, Hole #6
Experiment at the End of FY 79

lower transition of the ash-flow tuff. This interface is shown schematically in Figure IV-2 with the elastic modulus of the various layers given. At the contact between the ash-fall tuff and the lowest layer of the transition zone there is still a factor of 4-5 difference in modulus.

Three sets of experiments in this series were completed in FY79. These were designated CFE (Crack 'r Frac Experiment) - 1, CFE-2, and a combination experiment, CFE-3 and CFE-4. Their location relative to Hole #6 and the grout filled fractures of Hole #6 are shown in Figure IV-3. Essentially, these tests were conducted from the side of the Hole #6 mineback drift.

CFE-1 was a preliminary test of the concept and a confirmation of the Hole #6 results. The borehole was drilled so that at total depth (TD) the hole was 3 in below the interface and at the collar it was ~4 ft below the interface. Six different zones in this hole were fractured in three stages with 150 gal of dyed water at 8 gal/min. First, a small breakdown pump (3-8 gal) was conducted to determine the instantaneous shut-in pressure (ISIP), which is equivalent to the minimum principal in situ stress, for a small region around the borehole. After the pressure decayed, a second small volume (3-8 gal) was pumped to determine the ISIP again. Finally, the remainder of the 150 gal was pumped into the zone.

Figure IV-4 shows the pressure data for the six zones in CFE-1 and Table IV-I lists the important pressure data points such as the breakdown pressure (P_c) and the ISIP. As can be seen in Figure IV-4, only two zones (66' and 78') exhibited definite breakdowns and possibly the zone at 19' did also. There was no anomalous behavior to indicate that the fractures broke through the interface or otherwise behaved unexpectedly. The zones at 11' and 45' had shut downs in the middle of the main pump because of leaks around the packer.

Three tiltmeters were employed in this experiment in a vertical line ~6 ft apart at the location shown in Figure IV-3 to test the feasibility of such instruments for more accurately measuring fracturing parameters. The tilts[7]

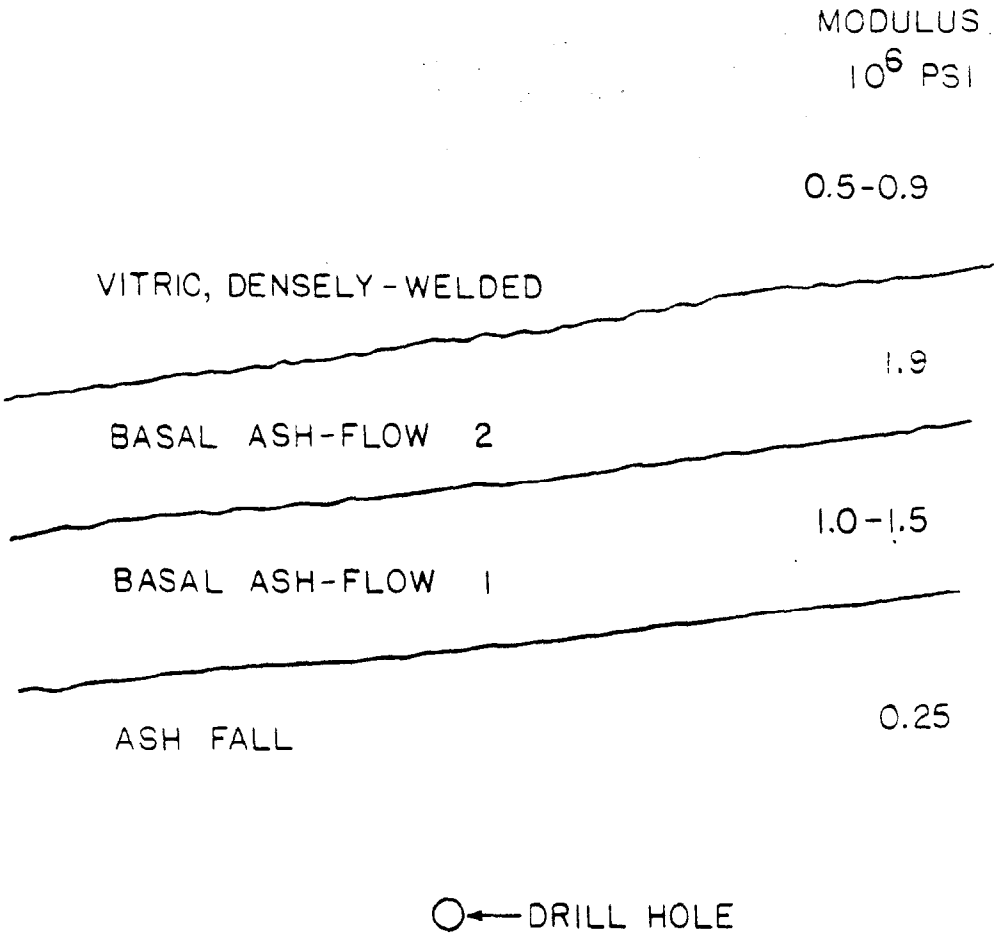

FIGURE IV-2
Interface Test Series Experimental Configuration

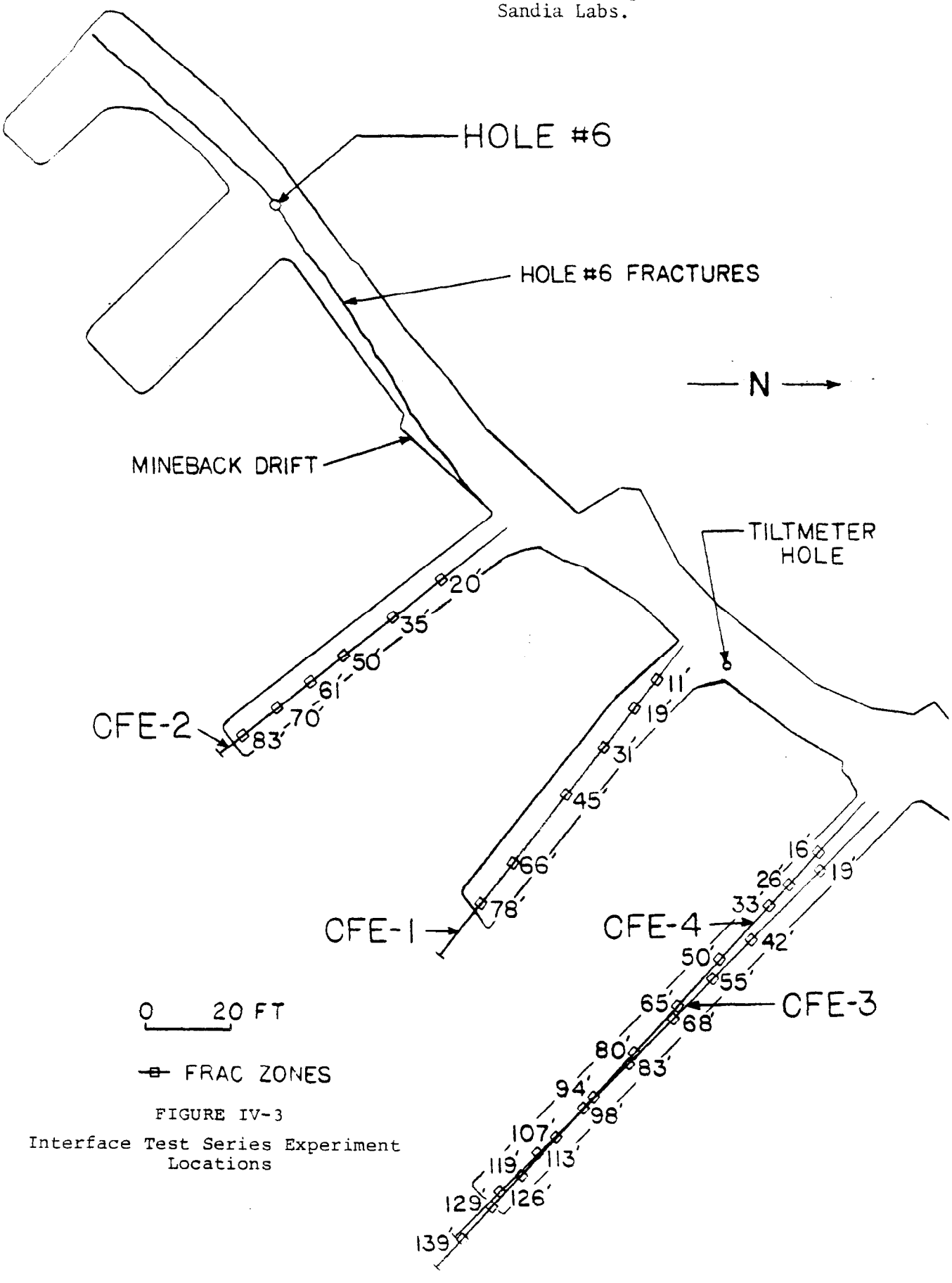

FIGURE IV-3
Interface Test Series Experiment Locations

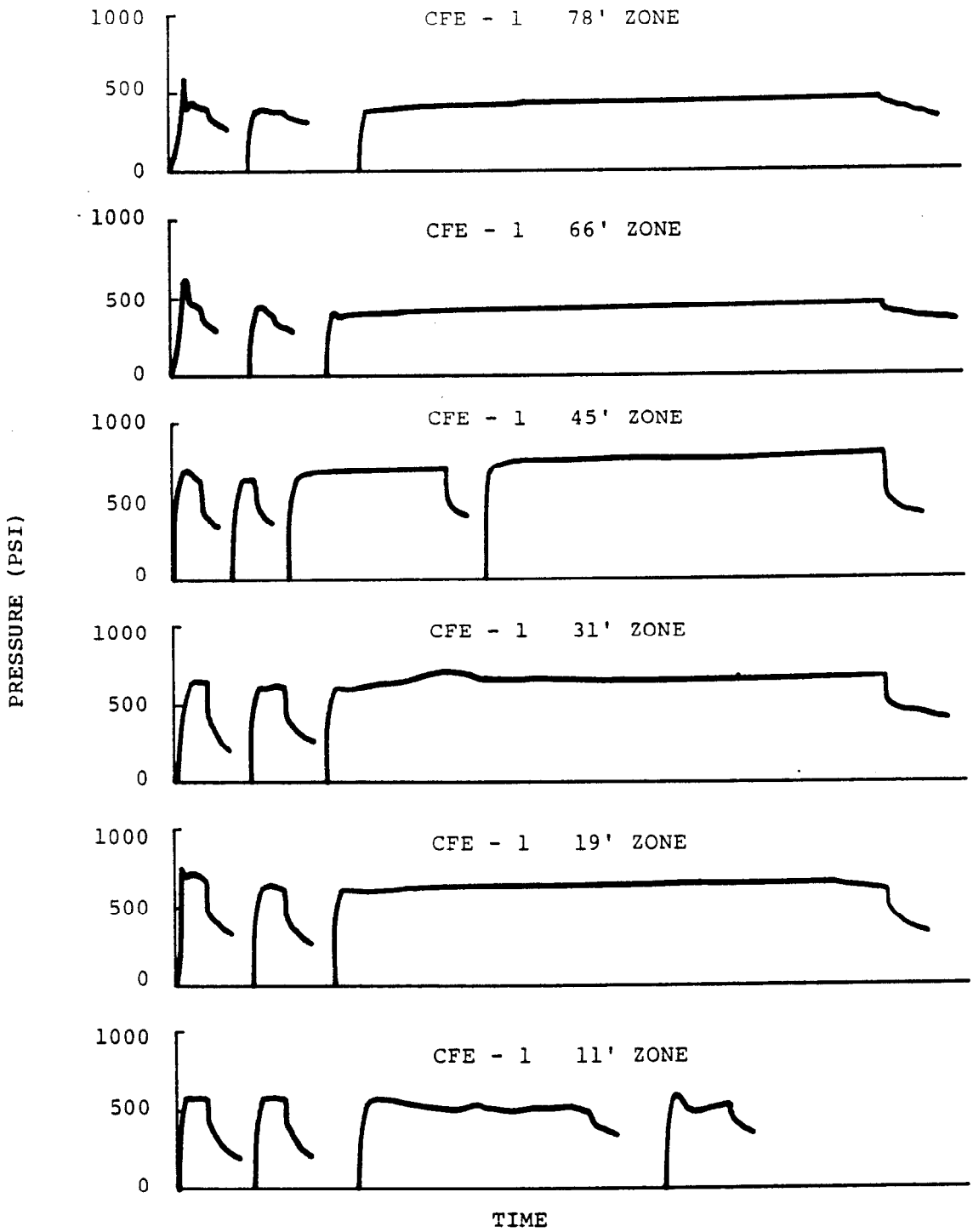

FIGURE IV-4

CFE-1 Pressure Data

TABLE IV-I. CFE Fracturing Data

ZONE*	BREAKDOWN				RECYCLE			MAIN PUMP		
(ft)	P_c (psi)	P_f (psi)	P_{isi} (psi)	Vol. (gal)	P_f (psi)	P_{isi} (psi)	Vol. (gal)	P_f (psi)	P_{isi} (psi)	Vol. (gal)
11	---	585	435	8.3	585	435	6.9	530-570	435	134.8
19	735	680	480	5.5	630	440	7.8	615	500	138.7
31	---	655	420	7.6	600	400	6.0	610-655	510	136.4
45	---	630	450	6.6	630	450	3.9	630-780	540	139.5
66	625	440	355	6.0	390	315	5.1	380-447	410	138.9
78	600	390	325	3.7	400	350	7.0	370-447	430	139.3
20	---	700	575	6.8	640	580	2.5	840	810	40.7
35	---	1060	855	7.6	1000	840	3.9	980	870	38.5
50	---	1200	1160	9.7	1150	---	3.1	1275	---	37.2
61	---	1070	950	8.4	1070	970	7.6	1100	1025	36.0
70	---	1010	930	7.9	1120	1050	5.8	1120	1050	36.3
83	---	1000	740	8.1	900	720	5.1	750	700	137.0
19	750	665	510	7.0	670	510	4.7	685-1015	665	138.3
42	1075	700	535	6.7	675	535	3.0	670	540	140.3
55	1050	835	600	10.5	790	570	3.6	815-1190	800	135.9
68	1150	680	520	7.6	625	515	4.6	600-700	600	90.0
83	1090	850	550	5.7	750	585	2.8	700	600	90.2
98	1365	725	585	5.6	700	585	3.7	680-1420	1140	140.7
113	1290	790	610	9.0	735	585	3.2	770-1230	850	137.8
126	900	710	635	7.7	750	640	4.5	650	600	137.8
16	948	532	470	3.6	539	470	1.9	545	475	2.0
26	1193	832	600	4.6	920	670	2.0	950	700	2.4
33	1193	1118	780	4.2	1300	1010	2.0	982	765	2.1
50	873	702	505	5.1	668	485	2.1	675	520	2.1
65	954	614	480	5.4	580	505	1.9	580	490	2.1
80	1125	627	480	5.2	586	475	2.1	580	485	2.2
94	1132	614	450	5.3	597	425	2.3	600	425	2.1
107	1173	1077	700	6.0	838	585	2.1	850	600	2.2
119	1028	676	470	6.4	600	440	2.3	545	435	2.6
129	580	470	310	3.8	464	300	2.6	456	295	2.3
139	---	---	---	8.0	470	380	4.2	416	360	3.0

*Flow rate was 8 gal/min for main pump on all tests except for CFE-2, Zones 20 and 50 at 2 gal/min, and CFE-2, Zones 35, 70, and 83 at 4 gal/min.

were clearly discernible for all six fractures and increased with decreasing distance between insturments and the fracture plane. Also, the form of tilt-time curves followed theoretical expectations. Tiltmeters were shown to be an effective way of observing fracture growth in real time.

All six zones of the CFE-1 fractures were then mined back, mapped, and photographed. It was found that all six fractures propagated upwards through the interface into the higher modulus material. This confirmed the results of the Hole #6 experiment. Figures IV-5 and 6 show photographs taken during mineback. It can be seen that the fractures crossed the interface, which occurs at the first brown oxide layer above the hole, but it should also be noted that the fractures only propagated 1-3 ft below the hole. Sufficient volume (150 gal) was injected into each zone to create a penny-shaped crack of 20-30 ft radius, yet, in all six zones the fracture terminated 2-4 ft below the interface. The only mechanism capable of limiting fracture propagation to such an extent is a sharp increase in the magnitude of the minimum principal in situ stress a few feet below the hole. This would be further investigated in the following tests.

CFE-2 was the second series of tests and was conducted in a borehole ~40 ft away from CFE-1, as shown in Figure IV-3. The purpose of these tests was to create the fractures at very low flow rates to determine if the pumping rate was an important factor in the containment of the fractures at a material property interface. Four zones were originally chosen; the 20' and 50' zones were fraced at 2 gal/min and the 35' and 70' zones were fraced at 4 gal/min. Only 50 gal of fluid were utilized in each test, but this should have still been sufficient to create at least 15 ft radius fractures. The hole was drilled such that it was 5 ft below the interface at the collar and 8 ft below at TD to further investigate the in situ stress variations below the interface.

When mineback was initiated, it was found that the fractures in the first two zones (20' and 35') were extremely small (3 ft x 8 ft); this is typically the size of 5-10 gal fractures in the tuffs. To make certain that there was

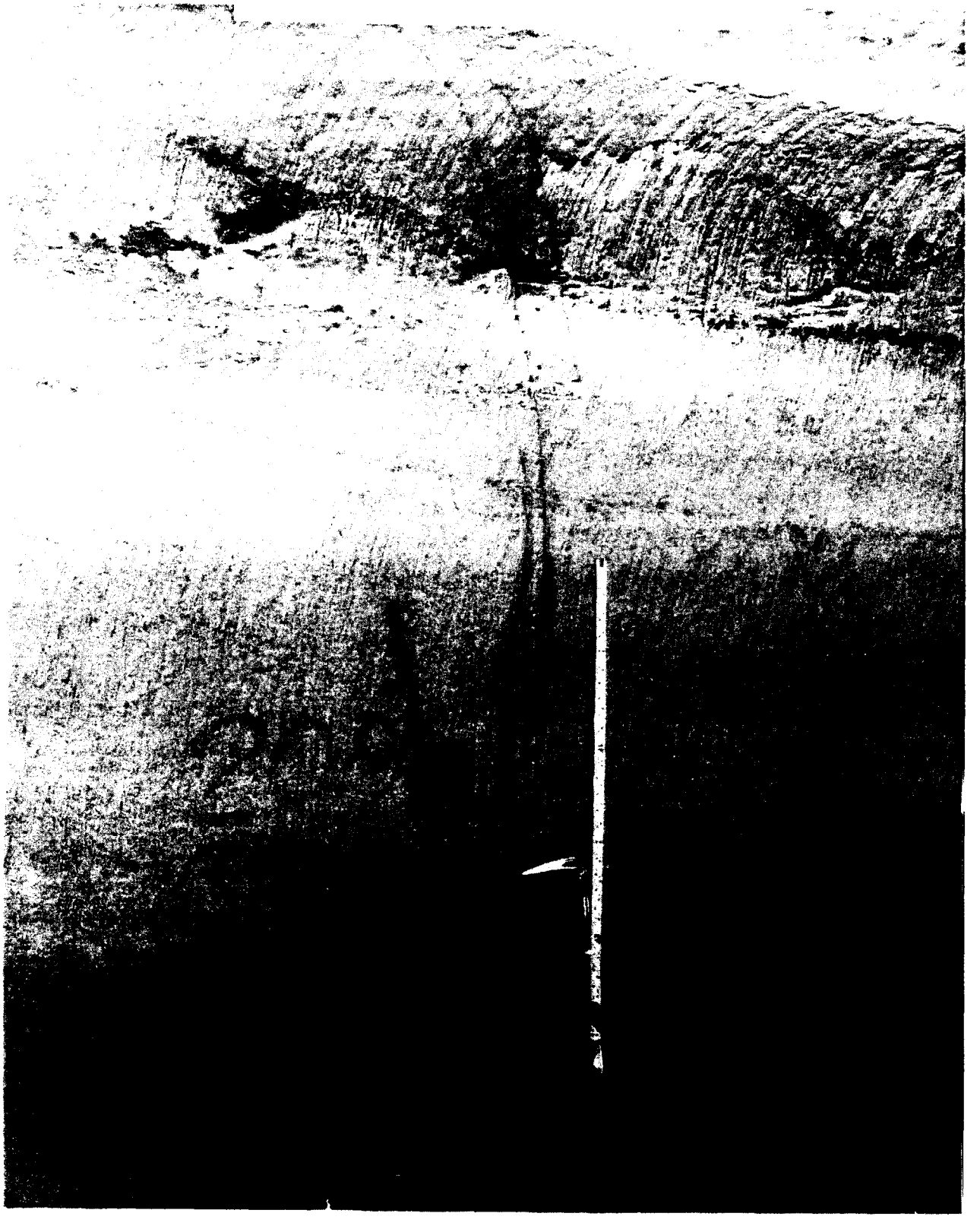

FIGURE IV-5
Hydraulic Fracture at 19 ft Zone of CFE-1

FIGURE IV-6

Hydraulic Fracture at 66 ft Zone of CFE-1 (Surrounding rock has been chipped away to show the fracture plane.)

not a mechanical problem that resulted in pumping a much smaller volume into the zones than expected - such as packer leakage or flow rate transducer malfunction, mineback was temporarily halted at 43 ft in the hole and two extra zones at 61' and 83' were fractured as controls. The total volume pumped was measured carefully and care was taken not to allow fluid to leak around the packer. The pressure data from all six of these zones is shown in Figure IV-7, and the important data points are given in Table IV-I. It can be seen that the variations in the fracturing pressure and the in situ stresses are considerable in this region.

When mineback resumed, it was found that all six fractures were very small. The first three (20', 35', 50') were essentially rectangular fractures, confined to a vertical zone from about 2 ft to 7 ft below the interface. The other three fractures (61', 70', 83') were also arrested about 2 ft below the interface; however, they propagated 3-6 ft further down than the other zones.

In order to explain the behavior of these fractures, it is necessary to understand the in situ stress distribution in the region below the interface. Figure IV-8 shows a graph of the ISIP (or minimum principal in situ stress) from both CFE-1 and CFE-2 as a function of distance below the interface. In CFE-1 the magnitude of the stress is increasing with depth below the interface, and this stress increase is probably responsible for crack termination 2-4 ft below the interface. In CFE-2, a peak in the vertical stress distribution is observed. The fractures in the three zones above the peak propagated in a layer between 2 and 7 ft below the interface, locations that characterize the stress increases seen in CFE-1 (2-4' below) and CFE-2 (6-7' below). The fractures in the three zones on or below the peak propagated both upward to about the 2 ft level and also downward. The exact location of the stress peak cannot be determined from the pressure data alone since the hydraulic fracture has a finite area over which the stresses act. However, it is clear that these stress peaks do exist and that they are the controlling influence on hydraulic fracture propagation.

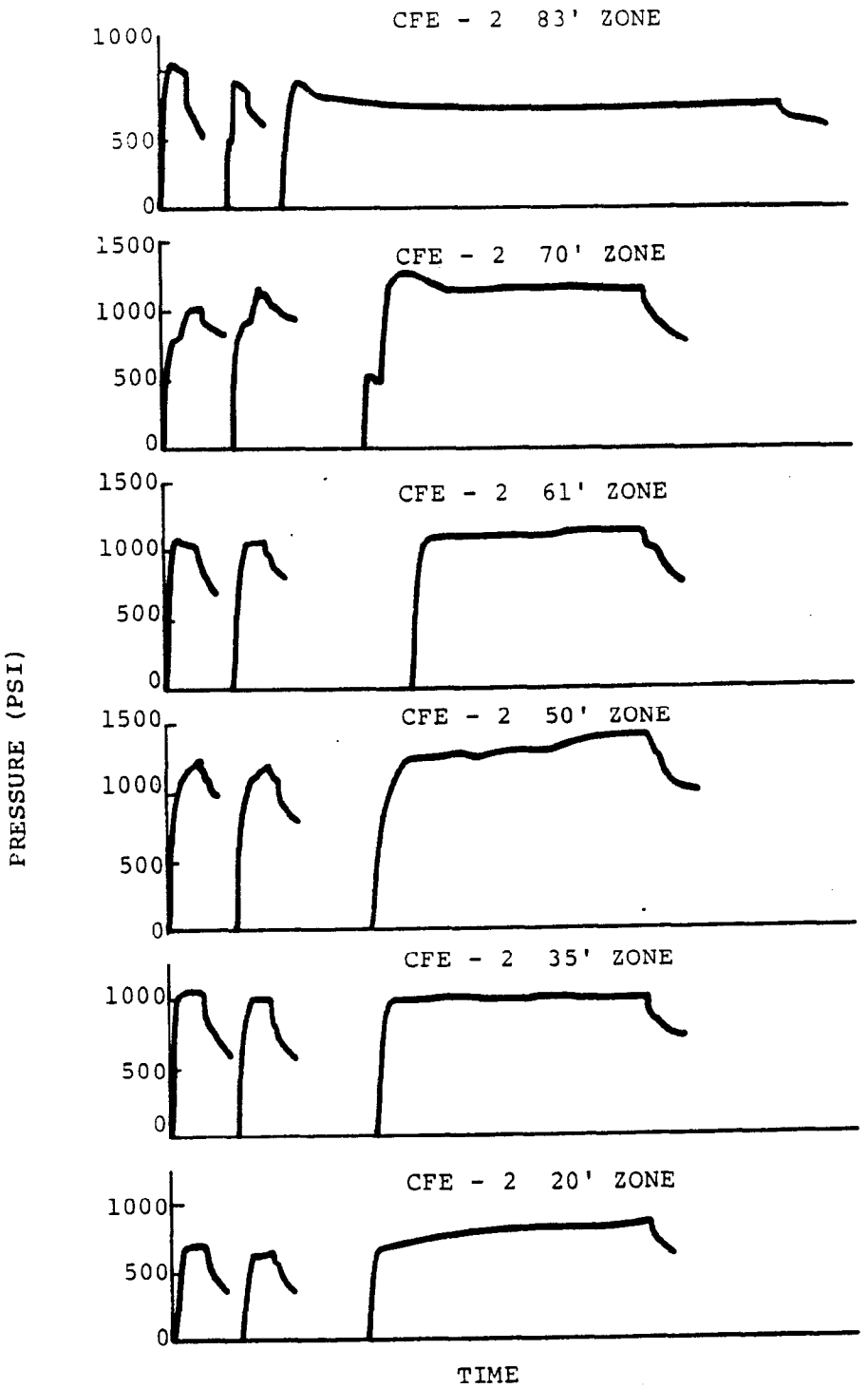

FIGURE IV-7
CFE-2 Pressure Data

FIGURE IV-8

Vertical Distribution of the Minimum Principal In Situ Stress Below the Interface - CFE-1 and CFE-2

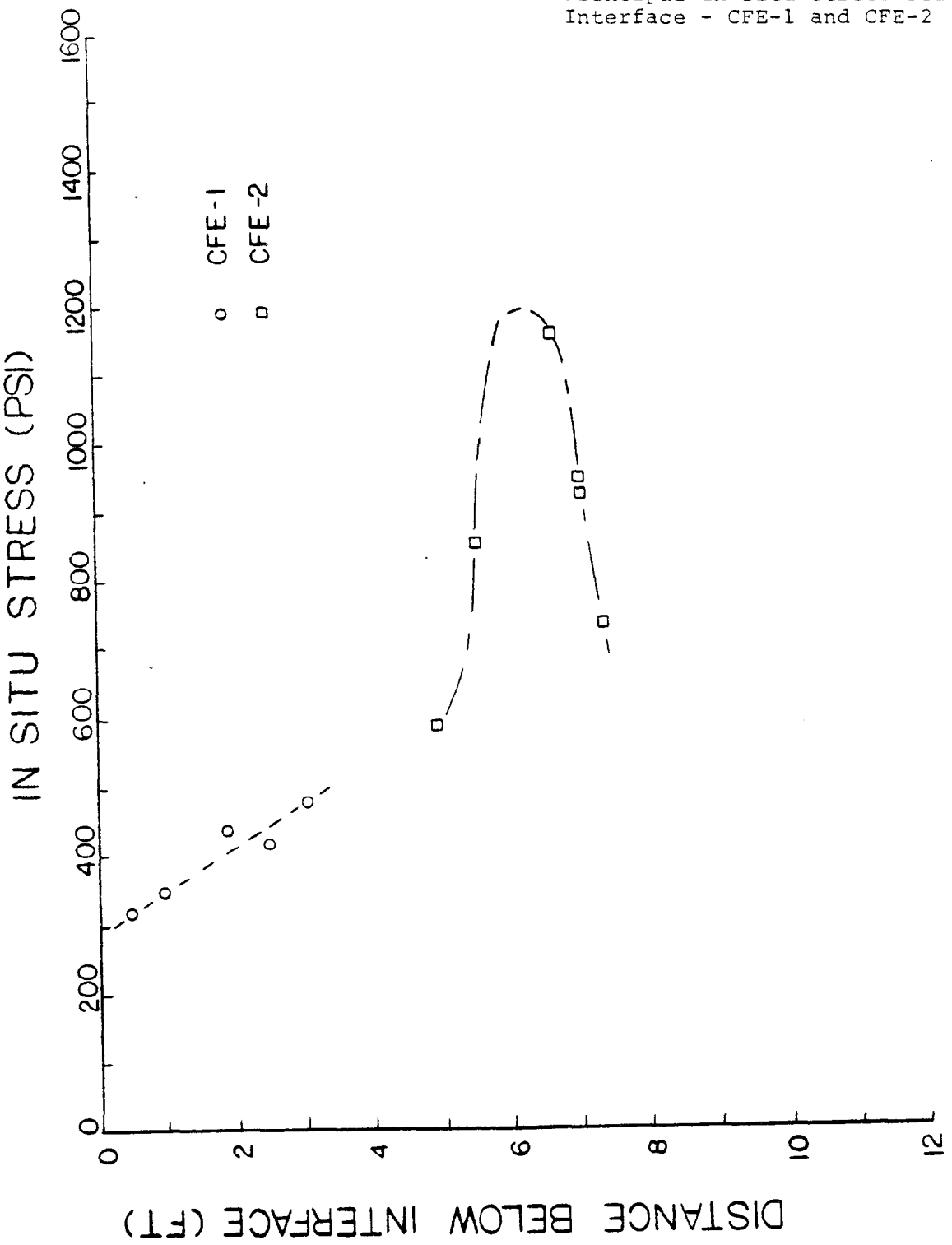

This may also help explain why the fractures in CFE-2 were very small. The fractures were contained in a region of high in situ stresses resulting in fracturing pressures that were twice those expected and resulted in greater leakoff. Leakoff is also aided by indications of increased permeability in this region.

CFE-3 and CFE-4 were two experiments conducted together to thoroughly define the nature of the stress irregularities below the interface and demonstrate its significance to hydraulic fracture propagation. As shown in Figure 3, CFE-3 and CFE-4 were conducted in nearby parallel holes which were drilled at different angles with respect to the interface. Eight zones in CFE-3 were fractured at 8 gal/min with 150 gal of dyed water in three stages similar to CFE-1. These were the "test" fractures which would be mined back and their behavior observed. Figure IV-9 show the pressure data from CFE-3, and the important data points are given in Table IV-I. There are considerable variations in the magnitude of the fracturing pressure from zone to zone; this is apparently due to variations in the in situ stresses in this region. In CFE-4, small volume hydraulic fractures (minifracs) were conducted in eleven zones to provide better resolution of the vertical stress distribution below the interface. The data from these tests are shown in Table IV-I.

The minimum principal in situ stress variations below the interface, as determined from CFE-3 and CFE-4, are shown in Figure IV-10. The stresses in this region apparently also have a double peak in the vertical distribution. It is believed that the stress peaks are actually larger than is shown because the fracturing pressure in some of these zones was much higher than the stress values indicate. Mineback of CFE-3 revealed the same phenomena as seen in CFE-1 and CFE-2.

Figure IV-11 shows a representation of the different fracture behavior observed in all the tests; the direction of fracture growth is clearly a function of the location of fracture initiation with respect to the stress peaks. Fractures which were initiated above the upper stress peak, either in the ash

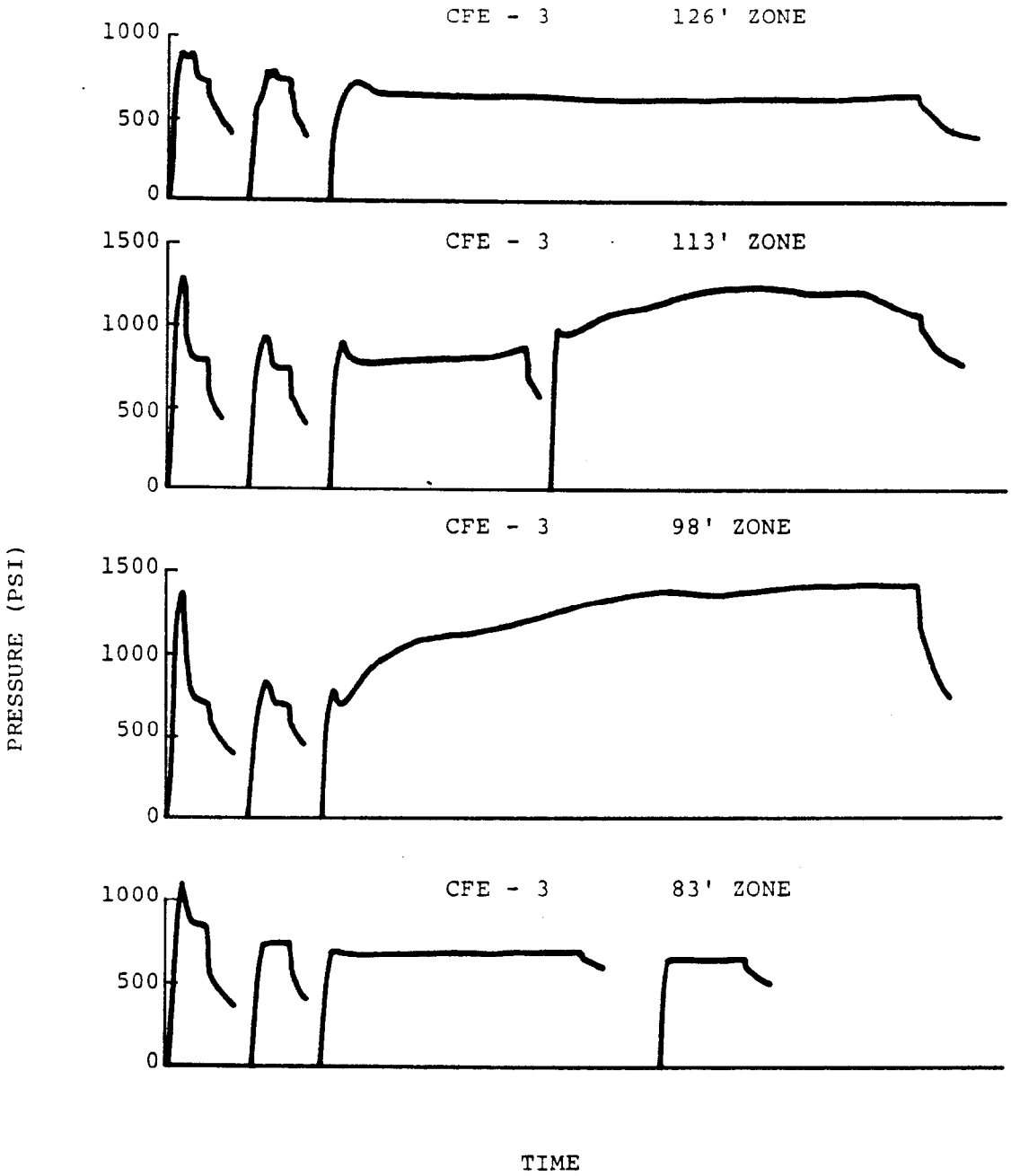

FIGURE IV-9

CFE-3 Pressure Data - 126, 113, 98 and 83 ft Zones

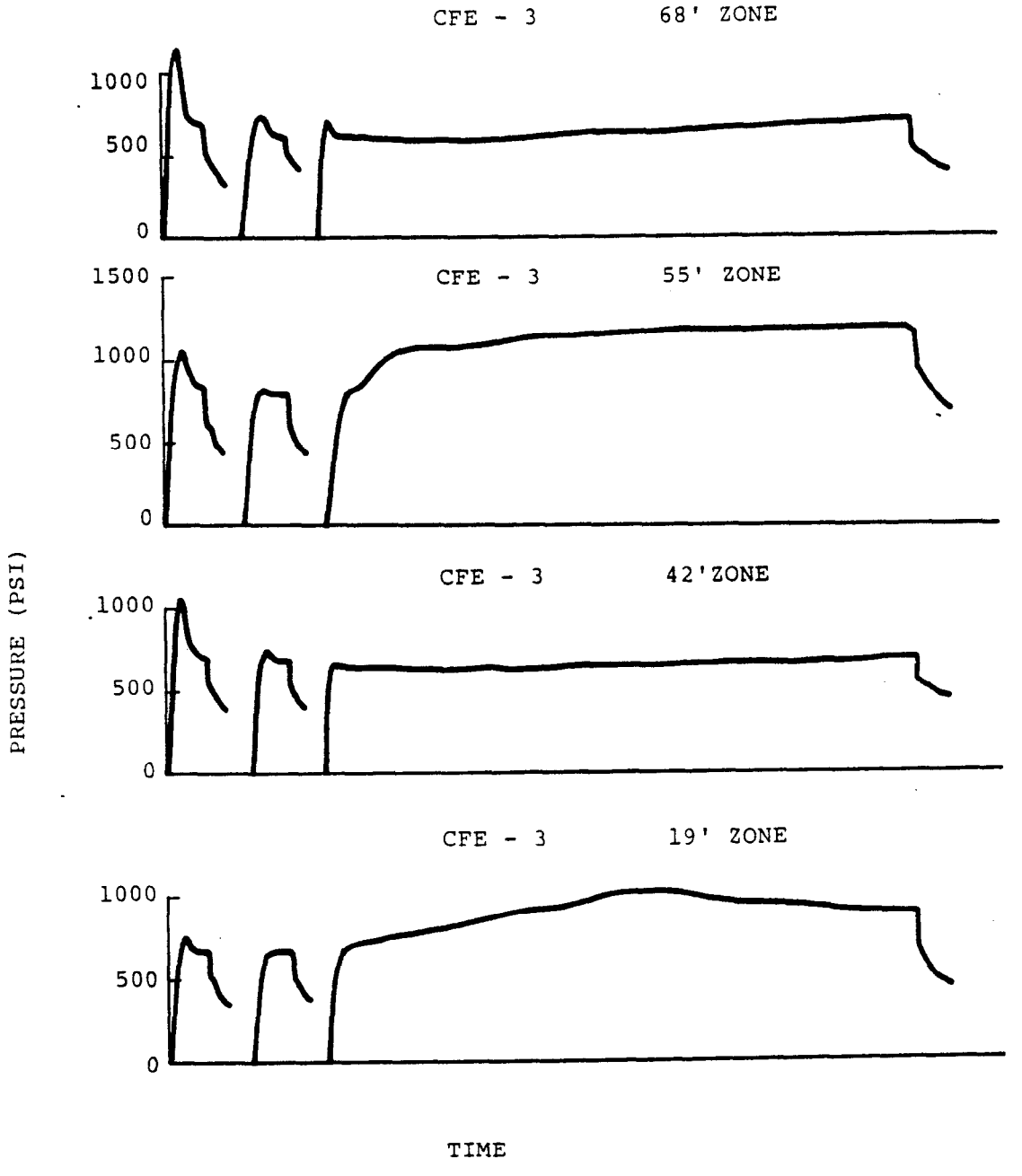

FIGURE IV-9, Cont.
CFE-3 Pressure Data - 68, 55, 42 and 19 ft Zones

FIGURE IV - 10

Vertical Distribution of the Minimum Principal in situ Stress Principal Below the Interface - CFE-3 and CFE-4.

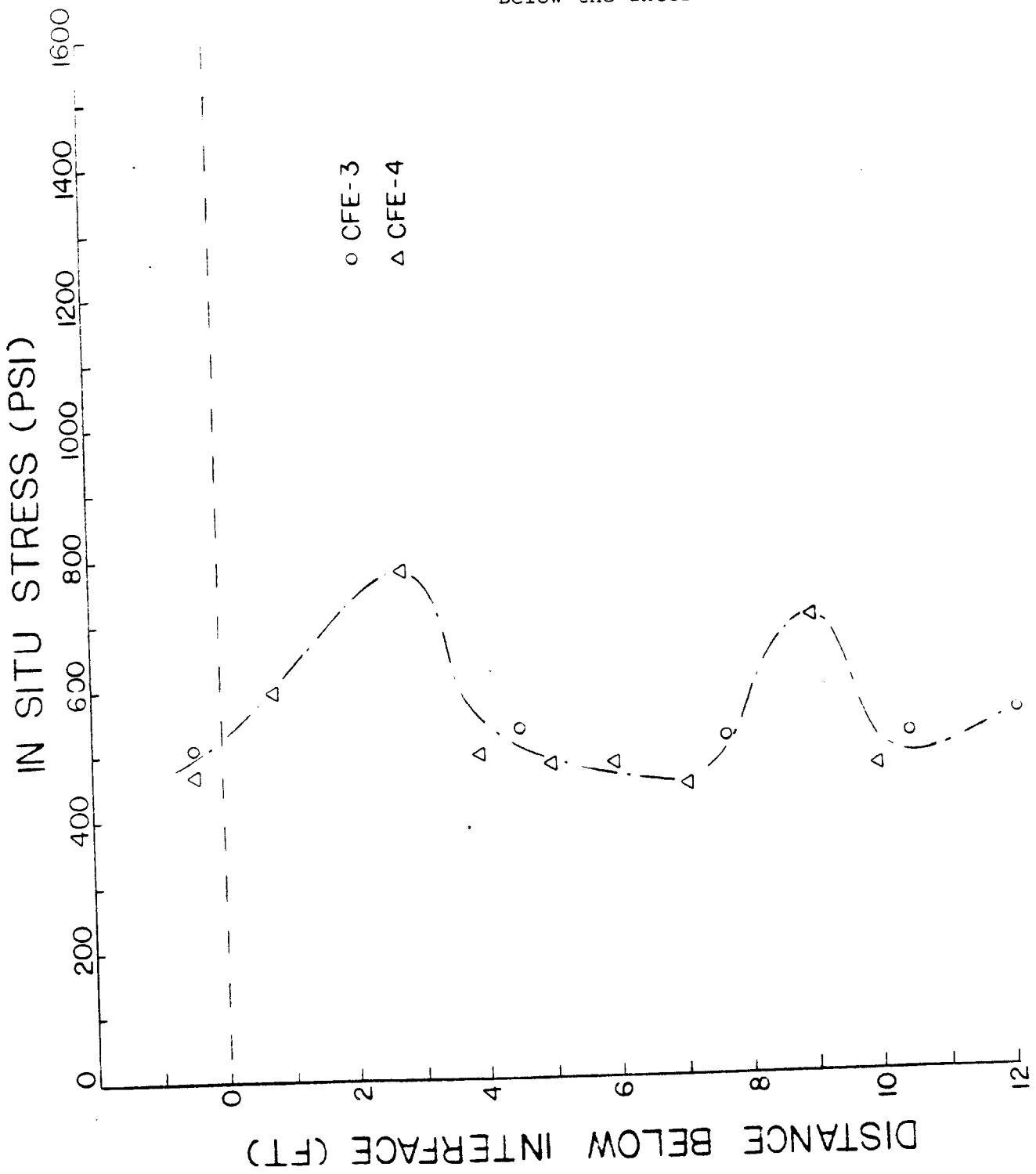

fall or welded tuff, had their downward growth terminated by the unfavorable stress gradient; they preferred to propagate into the higher modulus material. Fractures which were initiated between the stress peaks were often confined to that region, as seen in CFE-2. Fractures which were initiated below the lower stress peak for the most part remained below the peak and primarily propagated downward; however, the fractures in CFE-2 which were initiated in zones near or on the peak did propagate upward as well.

These experiments have shown that material property interfaces have little effect on the containment of hydraulic fractures. It has been demonstrated, however, that the in situ stresses have an overwhelming influence on fracture behavior and direction of fracture growth. In particular, it is the in situ stress variations which are most likely to contain a hydraulic fracture. It thus becomes imperative to determine the in situ stresses in regions where containment is desired and, therefore, development of an in situ stress measuring tool or technique should be a priority for future research.

2. Modeling and Analysis

a) Rock Mechanics and Microcrack Model (R. A. Schmidt, 4732)

A rock mechanics/fracture mechanics model was formulated that describes the probable character of the microcrack zone at a crack tip in rock. Knowledge of the crack tip process zone is an important step in the general understanding of fracture propagation in rock. In particular, it may prove useful in descriptions and models of hydraulic fracture propagation near formation interfaces to be described in the next section. Such a microcrack model is also needed in order to understand rock fracture testing on the laboratory scale and to help set standards for fracture toughness testing. Initial calculations and results with this model have, in fact, revealed several explanations for "anomalous" behavior in hydraulic fracturing and in fracture toughness testing. Other, less obvious, benefits may result from this model in understanding the permeability changes that occur to the rock material near a hydraulic fracture surface. For example, a propagating fracture leaves a damaged zone

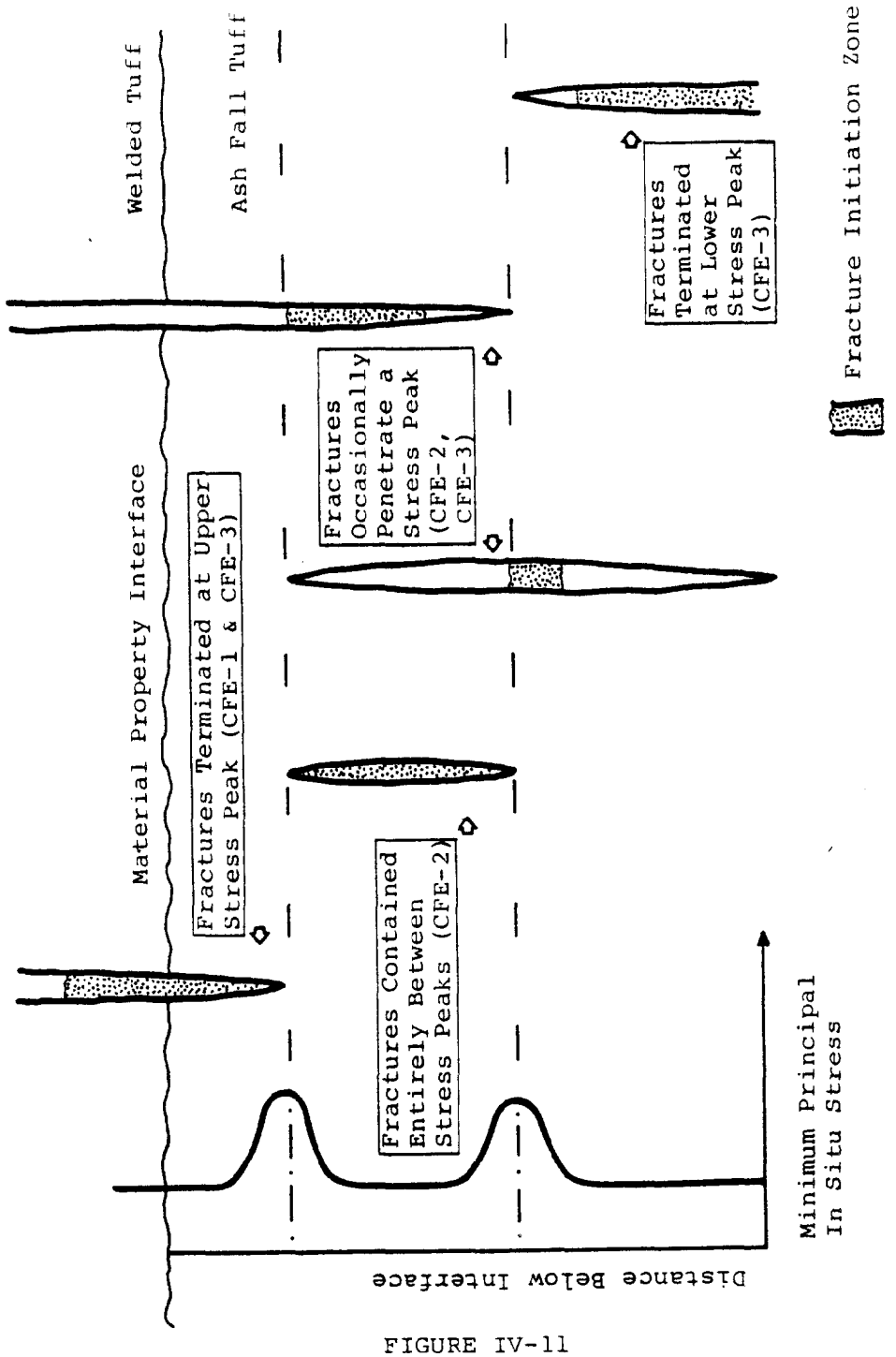

FIGURE IV-11

Representation of the Various Types of Fracture Behavior Observed in Interface Test Series Experiments

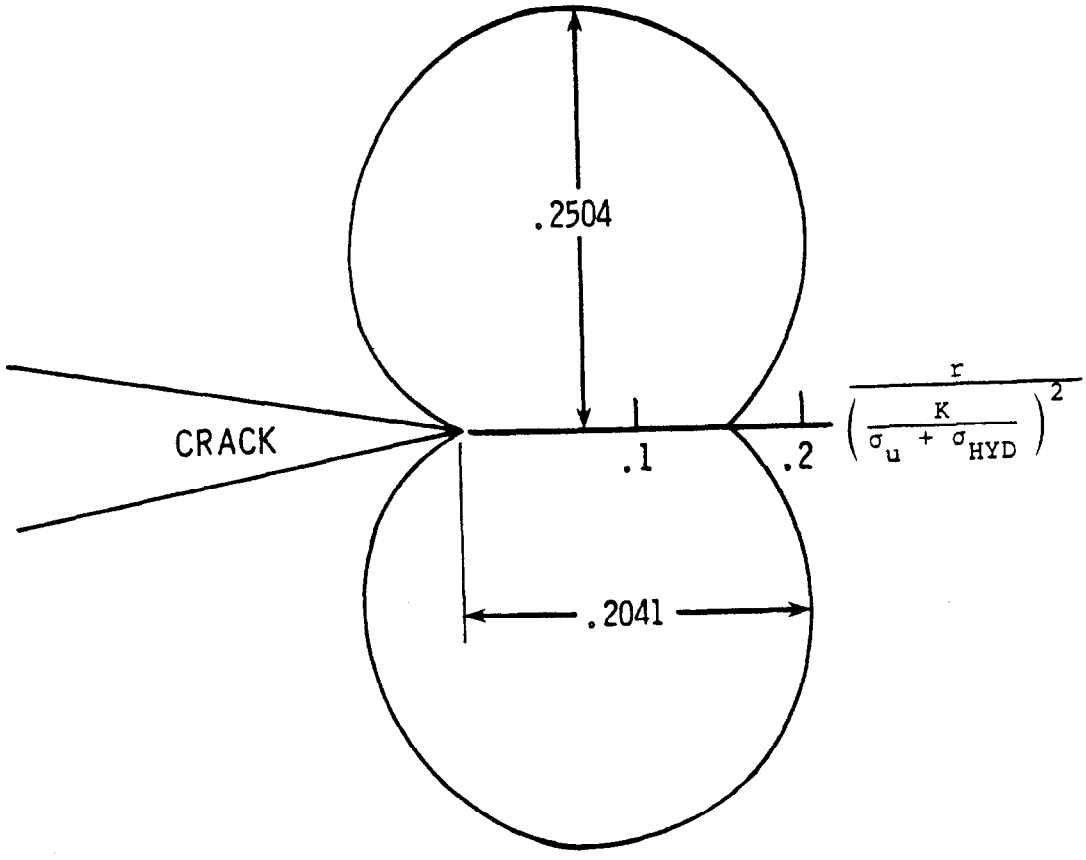

FIGURE IV-12

Damage Zone at a Crack Tip in Rock Based on Maximum Tensile Stress

in its wake as a result of the microcracking that occurs at the crack tip.

A straightforward modification of existing theories for metals was made which uses a failure theory more appropriate for rock. Some kind of process zone occurs at any crack tip regardless of the material, and much has been written in particular about the character of the "plastic zone" that occurs in metals. Most metals obey a von Mises yield condition while rocks tend to fail due to the maximum tensile stress. With this in mind, the classic equations for crack tip stresses were used to determine the contour for which the maximum tensile stress is equal to the ultimate stress. With the addition of hydrostatic in situ stresses, the equation for this contour becomes

$$r = \frac{1}{2\pi} \left(\frac{K_{Ic}}{\sigma_u + \bar{\sigma}} \right)^2 \cos\frac{\theta}{2} \left(1 + \sin\frac{\theta}{2}\right)^2 \qquad (1)$$

where

r, θ are polar coordinates from the crack tip

K_{Ic} is fracture toughness

σ_u is ultimate stress

$\bar{\sigma}$ is hydrostatic stress

This equation can be made nondimensional and is plotted in Figure IV-12.

The size of the microcrack zone decreases rapidly with in increase in hydrostatic stress. This is contrary to the behavior of metals where plastic zone sizes are unaffected by hydrostatic stress. For example, calculations from Nevada ash-fall tuff indicated that the zone size decreases from 0.4 in for an unconfined laboratory experiment to 0.03 in for the in situ stress conditions near the Hole #6 experiment. This dramatic effect of hydrostatic stress leads to two main conclusions:

1) Results from unconfined laboratory experiments that attempt to model hydraulic fracture behavior may not be applicable to field results, particularly those at considerable depths. The unconfined specimen may have a crack tip process zone that is larger, by several orders

of magnitude, than its in situ counterpart. This fact will tend to be exaggerated by the already greatly-reduced scale of the laboratory simulation.

2) Fracture toughness, K_{Ic}, of rock has been observed to increase with an increase of hydrostatic stress, and this effect is probably a direct result of the decreased microcrack zone size. This behavior for rock has been considered anomalous by some since K_{Ic} of metals is generally unaffected by hydrostatic stress. Unlike the plastic zone size in metals, the size of the microcrack zone is unaffected by out-of-plane stresses (i.e., plane stress versus plane strain). This is amost certainly the reason that K_{Ic} of rock and concrete are known not to depend on specimen thickness while K_{Ic} of metals exhibit a strong dependence on thickness. The fact that this result fits observed behavior so well lends strong support to the model itself.

The model was then extended to include: 1) a description of the orientation of the microcracks within the zone and 2) effects of an anistropic in situ stress state. Referring to Equation 1, the stress state at each point within the zone of microcracking can be transformed to principal stress to determine the orientation of the maximum tensile stress which then gives the most probable orientation of microcracks at each point. The equation that defines these orientations, α, is simply

$$\alpha = \frac{1}{2}\left(\frac{3\theta}{2} + \frac{\pi}{2}\right) \qquad (2)$$

This equation is depicted in Figure IV-13 by short lines within the microcrack zone which represent microcrack orientation.

The description of this microcrack zone becomes considerably more complicated when the in situ stress state is not hydrostatic. The solution process is similar to that followed for Equation 1 and, after considerable algebra, the equation becomes

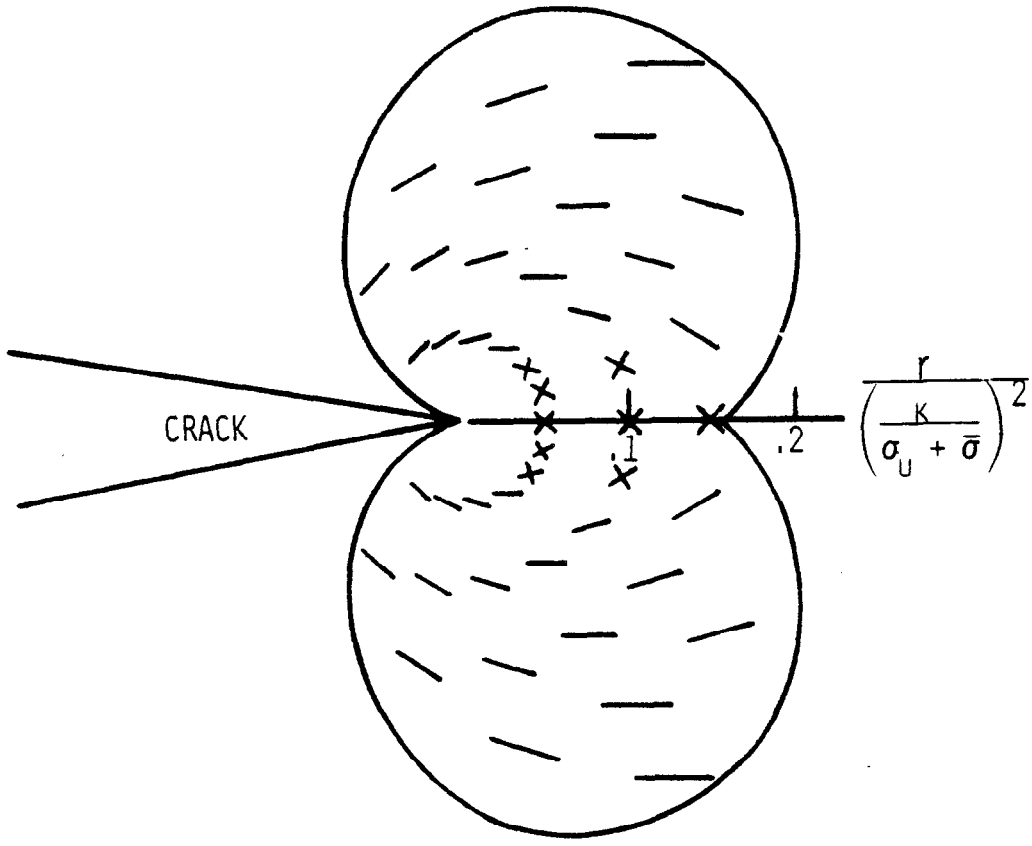

FIGURE IV-13

Damage zone at a crack tip in rock based on maximum tensile stress. Short lines are perpendicular to tensile stress and indicate probable orientation of microcracks.

$$r = \frac{1}{2\pi}\left(\frac{K_{Ic}}{\sigma_u + \bar{\sigma}}\right)^2\left(\cos\frac{\Theta}{2}\,\frac{1 + \beta\sin\frac{\Theta}{2}\sin\frac{3\Theta}{2} + \sqrt{\left(1 + \beta\sin\frac{\Theta}{2}\sin\frac{3\Theta}{2}\right)^2 - (1 - \beta^2)\cos^2\frac{\Theta}{2}}}{1 - \beta^2}\right)^2 \tag{3}$$

and

$$\beta = \frac{\sigma_{\parallel} - \sigma_{\perp}}{2(\sigma_u + \bar{\sigma})}$$

where

$\sigma_{\parallel}$ is in situ stress parallel to the crack

$\sigma_{\perp}$ is in situ stress perpendicular to the crack

σ is mean stress

β is degree of insitu stress anisotropy, $0 \leq \beta < 1$.

Note that, since hydraulic fractures are generally perpendicular to the least principal stress, $\sigma_{\perp}$ is considered a principal stress and $\sigma_{\perp} < \sigma_{\parallel}$. Observe that Equation 3 reduces to Equation 1 for $\beta = 0$. Equation 3 can be nondimensionalized and is plotted in Figure IV-14 for various values of β.

Although several well known rock fracture characteristics correlate well with this microcrack model, verification by direct observation would be highly desirable. An activity is presently being considered that involves microscopic studies on rock samples fractured in the laboratory under various confining pressures. The rock type selected (probably Solenhofen limestone) needs to be fine-grained and easily polished, with a low porosity, and a relatively low ratio of tensile strength to fracture toughness. This last condition should result in a relatively large microcrack zone.

b) Rock Mechanics of Fracture Propagation Near an Interface

(R. A. Schmidt, 4732)

The main purpose of the Hole #6 experiment was to examine the containment aspects of a hydraulic fracture near a formation interface. Simplified analytical models[1,8] and laboratory experiments[3,4,5] have suggested that a discontinuous increase in Young's modulus in advance of a propagating hydraulic fracture would

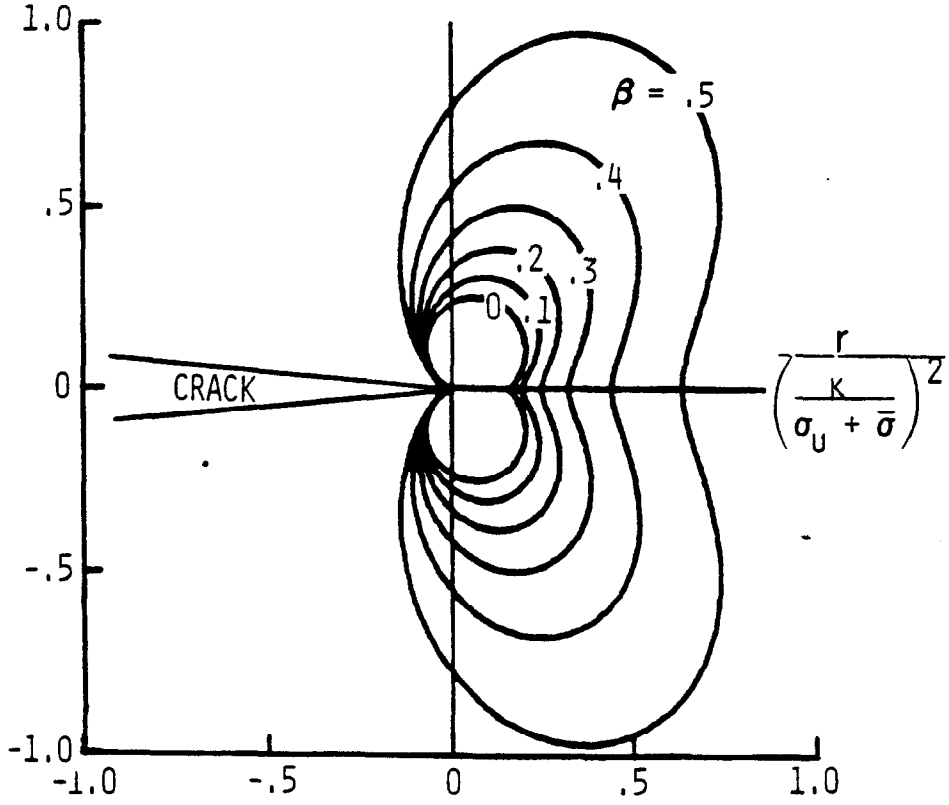

FIGURE IV-14

Microcrack Zone as a Function of in situ Stress Anisotropy, β.

cause crack arrest and thus effectively contain the fracture in the lower modulus material. The formation interface for the Hole #6 experiment had a Young's modulus increase of at least a factor of 10 and yet mineback of the fracture showed that containment did not occur; this behavior was confirmed by the Interface Test Series results. This suggests that the existing models either do not accurately represent fracture behavior in a layered medium or that the actual conditions existing in the formation do not suit the model description.

The actual interface is not a single discontinuous surface and involves an increase in modulus over the distance of several feet. With this in mind, the first step was made to measure the important material properties in this region. (A Rock Properties Laboratory was established this year for the purpose, among other reasons, of preparing rock samples which could then be tested in existing facilities.) Several cores were obtained along each of five stratigraphic layers for the purpose of obtaining values of tensile strength, elastic moduli, and fracture toughness. Tensile strength and Young's modulus were obtained from direct-pull tension tests; fracture toughness was measured using the "short rod" specimen configuration.[10] Table IV-2 summarizes the results of these tests.

The various layers are listed in order of their occurrence with the ash-fall tuff being the deepest layer. While these data are still sparce, a distinct change of Young's modulus does occur between the ash-fall tuff and the basal ash-flow tuff. With this in mind, the analytical models were reexamined, and two shortcomings are apparent:

1) While material properties may change abruptly, the crack-tip microcrack zone has the effect of averaging the properties over some distance and the mathematical idealization of a discrete interface probably leads to erroneous results.

2) The fracture criterion used in these models is one based on a critical stress intensity factor. This may have little or no meaning at a

TABLE IV-2. Material Property Data Near Hole #6 Experiment

Zone	Specimen Diameter (inches)	Fracture Toughness (psi $\sqrt{in}$)	Tensile Strength (psi)	Initial Young's Modulus (x 10^6 psi)
Welded*	---	---	---	-----
Vitric Ash-Flow	4.0	518	119	0.492
Ash-Flow With Abundant Lithics	6.0	649	89	1.868
Basal Ash-Flow	4.1	198	422	1.512
		530	>140**	0.963
Ash Fall	3.9	254	>28**	0.236
		151	18	0.271

*Data from two sets suspect due to fractured samples.
**Failed at endcap, but failure was imminent.

discrete interface when the character of the stress field can no longer be described by this parameter.

Initially it was hoped that the model inadequacies could be alleviated by replacing the discrete interface with a "smeared interface" in which property changes were gradual. A direct analytical approach to the problem was addressed on contract, but excessive mathematical difficulties were encountered and this attempt was abandoned. Numerical simulations of a "smeared interface" were made using a finite element code known as APES.[1] Results from these numerical calclulations and several interfaces can be treated in this way, but two shortcomings still exist:

1) Each interface is still discrete and needs to be "smeared" to account for the averaging effect of the microcrack zone.
2) While this code is very powerful, the number of elements used is very limited, and the external boundaries are not far enough from the crack to accurately simulate infinite boundaries.

The best approach for handling the actual question of fracture growth at the interface appears to be in using a more realistic fracture criterion than is used in the existing models. Since the stress field for a crack near an interface is known analytically, the most direct approach is to average the stresses ahead of the crack tip over a region as predicted by the microcrack model discussed earlier. One can then assume that crack propagation will occur when this average stress reaches some critical value as determined experimentally. This criterion is consistent with the well-tested fracture criterion for crack growth in homogenous materials as based on linear-elastic fracture mechanics.

Calculations based on this approach are needed, followed by verification with experiments. In addition to the mineback experiments at NTS (Hole #6 and Interface Test Series) and published laboratory investigations, experiments are being conducted on contract to Sandia on concrete and rock samples by Dr. A. Ingraffea at Cornell University. These latter tests are designed to examine fracture behavior near a material interface. Several three-point-bend

samples of layered concrete and rock such as shown in Figure IV-15 will be tested.

Progress to date on this investigation is as follows:

1) Five different mixes of Portland cement concrete have been designed, mixed, cured, and tested for Young's modulus in compression, Poisson ratio, and uniaxial compressive strength. The moduli range from a low of 2.5×10^6 psi to a high of 6×10^6 psi.
2) Eighteen Westerly granite ($E = 9 \times 10^6$ psi) beam-segments were purchased and prepared (honing, roughening, chevron notch-sawing) for casting in layers with the concrete. Cores and three-point-bend samples of the granite were prepared for properties determination.
3) All necessary formwork was constructed and loading system modified to test these samples. Single-composition concrete beams were tested as dry runs and controlled crack growth was achieved using crack-mouth-displacement as the feedback parameter.
4) Two methods for crack tip location monitoring using flourescent dyes and crack propagation gages were developed and tested.

All of these analytical, numerical, and experimental efforts must, however, be put in perspective with regard to recent findings from the NTS mineback experiments. An overwhelming amount of evidence indicates that the minimum principal in situ stress is the dominant parameter that dictates the geometry of a hydraulic fracture. The fact that a hydraulic fracture generally orients itself perpendicular to the least principal stress has been widely accepted, but it now appears that the direction of fracture growth, including the question of fracture containment at an interface, is primarily governed by the spatial variation in the least principal stress.

This does not, however, resolve the problem of why existing models predict containment where containment is not achieved. This dilemma still needs to be resolved and the approach described above still seems appropriate, but the emphasis needs to shift somewhat. Calculations and laboratory experiments

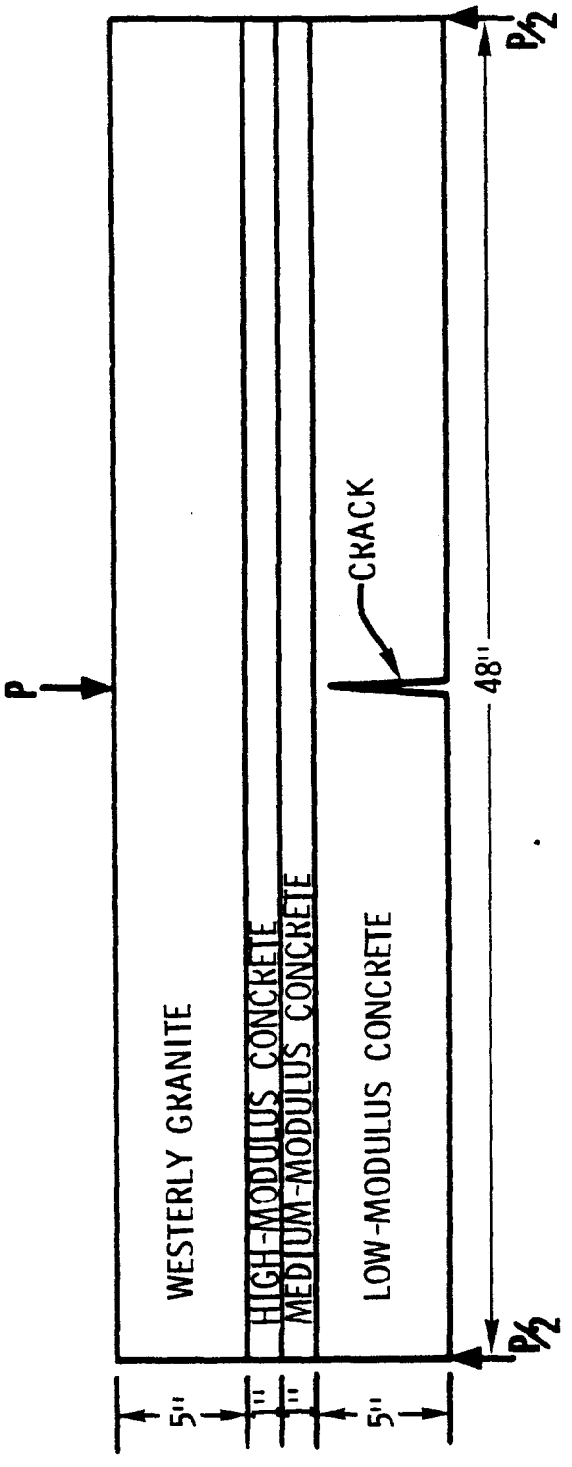

FIGURE IV-15

Laboratory Simulation of Fracture Propagation Near a Material Interface

need to address the important effects that changes in the minimum principal stress have on containment of hydraulic fractures.

c) Fluid Mechanics (N. R. Warpinski, 4732)

An effort to assemble a realistic model of the fluid mechanics of fracturing was initiated in FY79. The purposes of this modeling effort are: 1) to obtain a better understanding of the interplaying mechanisms that control the fracturing process, 2) to aid in the interpretation of previous in situ experiments and the design of new ones, and 3) to provide realistic conditions (e.g., pressure loading in the crack) upon which to apply rock mechanics considerations for the study of the effect of interfaces, in situ stresses, etc. on fracture propagation.

The type of model being developed is for a rectangular, two-dimensional fracture; this is probably a poor representation of a typical hydraulic fracture but a necessary geometric restriction to avoid a much more complicated three-dimensional calculation at this time. A model for a penny-shaped fracture, which may or may not be more realistic than a rectangular fracture, will be developed along the same lines as the rectangular fracture if the model proves suitable. Any 2-D, rectangular model automatically suffers another restriction since it is necessary to choose whether the width is a function of fracture length or fracture height whereas the actual situation is probably a combination of the two. This present model uses the length criterion since it will, for the most part, be used to analyze the short fractures typically conducted in the mineback experiments.

The width of a fracture for a given pressure distribution, P(x), where x is the distance along the fracture as measured from the wellbore, is given by England and Green[12] as

$$w = \frac{8(1-\nu^2)L}{\pi E}\left\{\int_{\varepsilon}^{1}\frac{\eta\, d\eta}{\sqrt{\eta^2-\varepsilon^2}}\left[\int_{0}^{\eta}\frac{P(\xi)\,d\xi}{\sqrt{\eta^2-\xi^2}}\right]-\frac{\pi}{2}\,S\,\sqrt{1-\varepsilon^2}\right\} \qquad (4)$$

where

w is the width of the fracture

ν is Poisson's ratio,

E is Young's modulus

L is the length of the fracture,

$\varepsilon = x/L$ is a dimensionless location in the fracture,

S is the minimum principal in situ stress, and

η & ζ are dummy variables

If $P(x)$ is known, the width of the fracture can be determined by performing the double integration. In reality, $P(x)$ depends on $w(x)$ and neither are known a priori. Thus a solution of this coupled rock mechanics/fluid mechanics problem can only be determined by solving the fluid mechanics of the flow through the fracture in conjunction with Equation 4. Notice that Barenblatt's condition[13] is not incorporated into Equation 4; it felt that it is overzealous to impose the smooth closure condition on a macroscopic scale when this feature probably occurs on the microscopic level.

The fluid mchanics of this problem are incorporated by applying the conservation laws to flow through a segment of the fracture. Time-dependent terms are not discarded (as is usually the case in hydraulic fracture models) because they may be significant for short times (small fractures) which is the particular situation which this model is designed for. For one-dimensional fluid flow in the fracture, the conservation of mass principle yields the continuity equation

$$\frac{\partial w}{\partial t} + \frac{\partial (Uw)}{\partial x} + 2U_L = 0 \ , \tag{5}$$

where

t is time,

U is the velocity, and

U_L is the leakoff velocity

Application of the conservation of momentum law results in

$$\frac{\partial(Uw)}{\partial t} + \frac{\partial(U^2w)}{2x} = \frac{-w}{\rho}\frac{\partial p}{\partial x} - \frac{2\tau_w}{\rho}, \tag{6}$$

where

ρ is the density and

τ_w is the shear stress

Although the model is being developed using a Newtonian fluid in the laminar flow regime, non-Newtonian fluids and turbulent flow conditions can also be included by correct calculation of τ_w in Equation 6. The leakoff velocity in Equation 5 is calculated using Howard and Fast's equations.[14] The boundary conditions for the fluid flow are:

i) at $x = 0$ $\mu = q/(2wH)$

where

q is the pump rate and

H is the zone height; (7)

ii) at $x = L$ $\mu = dL/dt$; and

iii) at $x = L$ $P = S$.

Equations 5 and 6 are finite differenced using a Crank-Nicholson technique. Two of the boundary conditions of Equation 7 are needed to obtain solutions of these equations. The final boundary condition determines the correct value of all the parameters such that a correct solution of Equations 4, 5, and 6 is obtained which is consistent with the solution from the previous time step. In practice the calculations occur in the following manner. A pressure distribution is assumed (usually the pressure distribution from the previous step or an initial guess if it is the first step) and the width distribution is obtained from numerical integration of Equation 4. The velocity distribution in the fracture is calculated from the differenced version of Equation 5 with the appropriate value of U_L calculated for each segment at that time period. Using the calculated width and velocity distributions and the appropriate value of the shear stress for each segment, Equation 6 in finite difference form can

be solved for a corrected pressure distribution in the fracture. This distribution is then inserted into Equation 4 and the process is repeated. Iterations continue until the third boundary condition of Equation 7 is satisfied to a sufficiently accurate degree. It has been found, however, that this iteration does not readily converge to the solution point, and it is necessary to use some technique to force it to converge.

Although solutions have been obtained with this model, work is being performed to test various transformations, differencing techniques and convergence methods to optimize solution of the equations. This is important since one convergence technique may work with one set of fracture parameters but not with somewhat different ones. Efforts are directed towards developing a general model which will obtain solutions for any case.

Results obtained to date do illustrate the importance of the transient terms in the fluid flow equations as well as the use of the complete width equation. Figure IV-16 shows calculated pressure distributions in a hydraulic fracture having the same parameters as found in the Hole #6 Formation Interface Experiment. The steady-state curve is the calculated pressure distribution if the transient terms are discarded. This is not far from the constant pressure condition that is employed by most hydraulic fracture models and is probably the situation that would occur at large times when the transient terms decrease in importance (i.e., for a given time step, the fracture width and length increase less with increasing time). However, the transient curve shows the calculated pressure distribution with the transient terms retained, and it can be seen that this is considerably different from the usually assumed constant pressure. This pressure distribution was obtained at a time about midway through the Hole #6 fracturing treatment (after 100 bbls) so it can be seen that the transient terms are important for a considerable time span. When the model is operating efficiently, calculations will be made to see how severely this affects present design models.

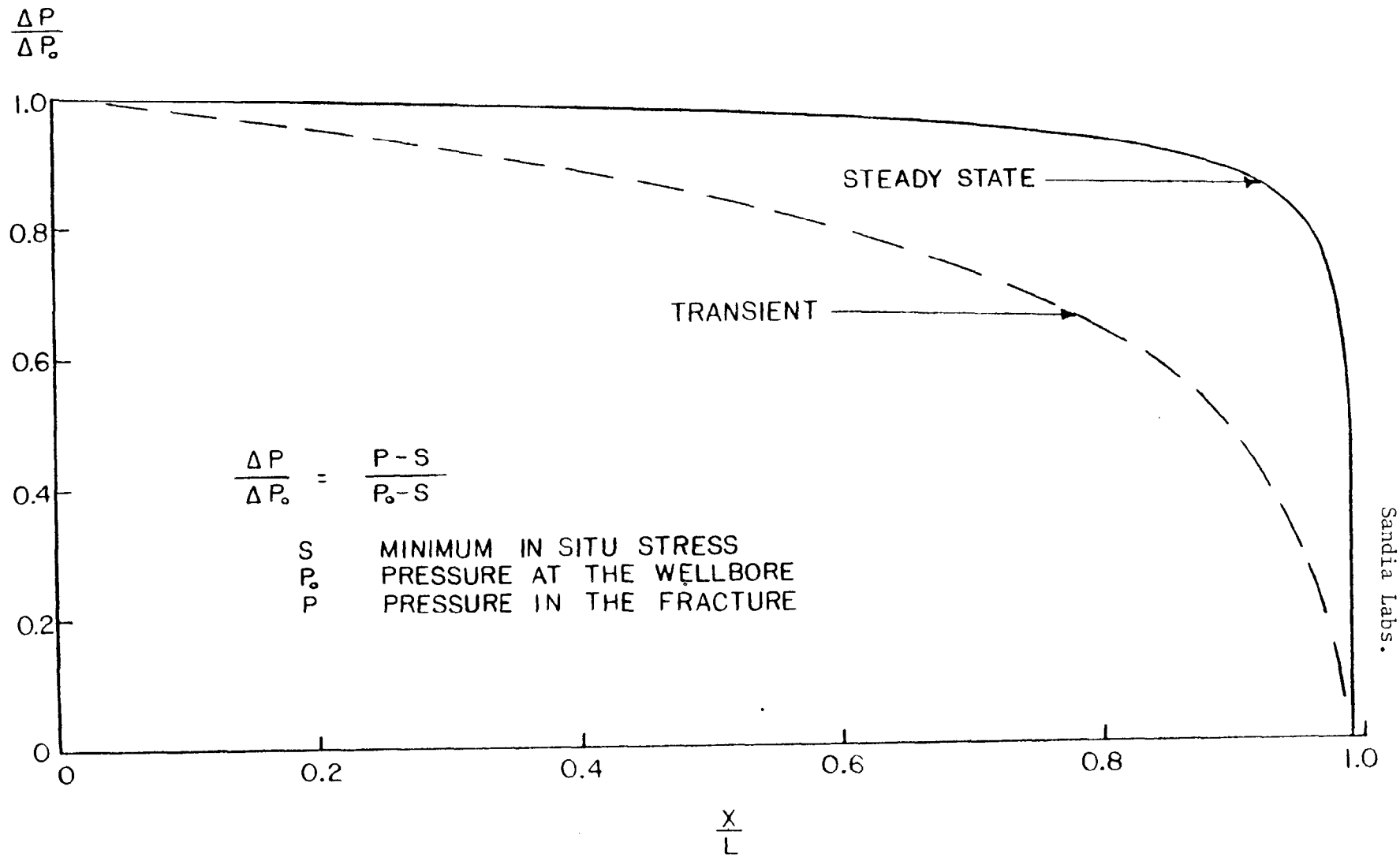

UGR File #C073/A78
Oct. 1978-Sept. 1979
Sandia Labs.

FIGURE IV-16

Calculated Pressure Distribution in a Hydraulic Fracture

References for Section IV-A

1. Simonson, E. R., et al., "Containment of Massive Hydraulic Fractures," Soc. of Petroleum Engineers Journal, p. 27-32, Feb. (1978).

2. Rogers, L. A., et al., "Massive Hydraulic Fracture Containment Analysis Utilizing Rock Mechanics Considerations," Proceedings of the Massive Hydraulic Fracturing Symposium, U. Of Oklahoma, Norman, OK, (1977).

3. Daneshy, A. A., "Hydraulic Fracture Propagation in Layered Formations," Society of Petroleum Engineers Journal, p. 33-41, Feb. (1978).

4. Hanson, M. E., et al., "LLL Gas Stimulation Program, Quarterly Progress Report, April through June 1978," Lawrence Livermore Laboratory Report UCRL-50036-78-2, July (1978).

5. Hanson, M. E., et al., "Theoretical and Experimental Research on Hydraulic Fracturing," Proceedings, Fourth Annual DOE Symposium on Enhanced Oil and Gas Recovery and Improved Drilling Methods, Tulsa, OK, (1978).

6. Warpinski, N. R., et al, "Direct Observation of Hydraulic Fractures: Behavior at a Formation Interface," Sandia Laboratories Report, SAND78-1935, Oct. (1978).

7. Holzhausen, G. R., "Analysis of Earth Tilts Resulting From Formation of Six Hydraulic Fractures, Crack 'r Frac Experiment #1, March 27 and 28, 1979, G-Tunnel, Nevada Test Site, Nye County, Nevada," M. D. Wood, Inc., Contractor Report for Sandia Laboratores, Jan. 19, (1978).

8. Cook, T. S. and Erdogan, F., "Stresses in Bonded Materials with a Crack Perpendicular to the Interface," Inter. J. of Eng. Sci., Vol. 10, p. 677-697, (1973).

9. Teufel, L. W., "An Experimental Study of Hydraulic Fracture Propagation in Layered Rock," PhD dissertation, Texas A&M University, Aug. (1979).

10. Barker, L. M., "K_{Ic} Measurements Using Short Rod Specimens--The Elastic-Plastic Case," Terra Tek Report, TR77-91R, (1977).

11. Gifford, L. N., and Hilton, P. D., "Stress Intensity Factors by Enriched Finite Elements," Engineering Fracture Mechanics, Vol. 10, p. 485-496, (1978).

12. England, A. H. and Green, A. E., "Some Two-Dimensional Punch and Crack Problems in Classical Elasticity," Proceedings of the Cambridge Philosophical Society, Vol. 59, p. 489, (1963).

13. Barenblatt, G. I., "The Mathematical Theory of Equilibrium Cracks in Brittle Fracture," Advances in Applied Mechanics, Vol. 7, p. 56 (1962).

14. Howard, G. C. and Fast, C. R., "Optimum Fluid Characteristics for Fracture Extension," API Drilling and Production Practices, p. 261, (1957).

B. Dynamic Wellbore Fracturing

1. Background

Oil and gas wells hve been stimulated with high-energy explosives since the late 1800's. Well shooting techniques are usually applied for the purpose of introducing random multiple fractures rather than a single large fracture as is created by hydraulic fracturing. Multiple fracturing is desired for eleminating "skin damage" caused during drilling and for effectively connecting the wellbore to an existing fracture system as might occur, for example, in a gas-bearing Devonian shale. Connecting a well to a fracture network is often not possible by hydraulic fracturing since there is little or no control over fracture orientation and the created fracture will often run parallel to existing fractures.

Studies have repeatedly demonstrated the effect that contained explosions have on the surrounding rock formations. These studies, which include field experiments[1-3]* laboratory experiments[4] and code calculations[1,5] demonstrate the existence of residual stresses and compaction that can cause deleterious effects in a wellbore. In essence, the high pressures of a detonation in a wellbore are known to be sufficient to cause the nearby rock to yield and compact by plastic flow. When the stress wave passes, the rock unloads elastically leaving an increased borehole diameter and a residual stress field which is compressive near the wellbore. The creation of this residual stress field is closely analogous to the process of autofrettage or the "gun barrel problem" in which pressure vessels are often over-pressurized sufficiently to yield the inside wall and develop residual compressive stresses that help prevent crack growth during service. The zone of highly compacted rock with its associated residual compressive stresses is sometimes referred to as a stress cage, and the phenomenon is sometimes called the bladder effect. Fracturing caused by high pressure gas may also be inhibited in this situation since fines are created during the compaction process that can plug newly formed cracks and prevent gas penetration.

*References for Section IV-B are given at the end of the section on p 111.

Some or all of these effects may actually cause decreased permeablity near the wellbore and are probably responsible for many well-shooting failures.

Several alternatives to explosive well shooting hve been considered and tested in recent years that show promise of substantial improvement[3,6-8] An approach that has received considerable attention is to tailor the pressure-time behavior of the explosive or a suitable propellant so as to keep the maximum pressure below the yield stress of the rock and thereby avoid forming the stress cage. Several of these concepts rely on the use of propellants which deflagrate rather than detonate. Unlike explosives, the burn front in these materials travels slower than the sound speed, and the burning rate can be varied over a wide range. Pressure-time behavior of propellants differ from explosives in that peak pressures are lower, and burn times are longer. Total energy available, however, is similar in both materials (typically 1000 cal/g).

2. Multi-Frac Test Series (R. A. Schmidt, 4732)

Last year three propellant shots known as the Gas Frac[3] Experiment were conducted at the Nevada Test Site and included mineback of the in situ experiment for direct observation. These shots demonstrated both the ability of a tailored pulse to create multiple fractures in a borehole and the feasibility and usefulness of testing such concepts in a realistic in situ environment with mineback. As a result, another series of five in situ experiments are presently being conducted at the Nevada Test Site in a similar ash-fall tuff formation. This series, known as the Multi-Frac Test Series, is supported by the Morgantown Energy Technology Center's Eastern Gas Shales Project. The objectives of this series are: 1) to evaluate the characteristics of five tailored-pulse fracturing concepts--Dynafrac,[6] Augmented Dynafrac,[6] Kinefrac[7] multiple firings of Kinefrac, and Gas Frac[3] and 2) to provide inputs for modeling efforts which are necessary for design if such concepts are to be applied effectively to particular reservoirs such as the Devonian shales.

These five tests are being extensively instrumented and analyzed. The instrumentation includes several cavity-pressure transducers as well as stress

gages and accelerometers grouted in the surrounding rock to measure formation response. Caliper logs will be performed before and after each shot to determine if any permanent borehole enlargement occurred, which would give indications of the existence of a stress cage. A permeability measurement will be made to give an indication of the conductivity of a particular fracture network. Televiewer logs are also planned.

In general, the setup for all five tests will be similar and a schematic of the Augmented Dynafrac shot is depicted in Figure IV-17. The shots will be performed in horizontal boreholes that are 6 in diameter and 40 ft deep. There will be a 10 or 20 ft open-hole test section, depending on the test, with the remainder being grouted casing. All tests except Gas Frac will be shot in water; the water will be dyed to enhance the visibility of the fracture patterns observed during mineback. Figure IV-18 shows the experiment layout of the five shots with the planned mineback route. Note that the mineback will cut through half of each test section leaving the fracture pattern at the midpoint of each experiment preserved in the tunnel rib (sidewall) for later inspection. Figure IV-18 also includes in situ stress data which are the averages of several small volume hydraulic fractures conducted in this region.

The planned layout for the instrumentation holes containing the accelerometers and stress gages is displayed in Figure IV-19. The holes are staggered rather than in a line to maximize the chances of obtaining transverse accelerations from a nearby propagating fracture and to minimize the chances of a single crack intersecting all three holes. Transverse accelerometers will be used even though a symmetric displacement field would produce no transverse displacement or accelerations. Rather, these gages will hopefully detect motions due to the dynamic propagation of a nearby crack.

At the end of FY79, the design of the test series was complete, including instrumentation, hardware, firing circuits, operating procedure, and test evaluation plans. All necessary equipment and transducers were ordered and

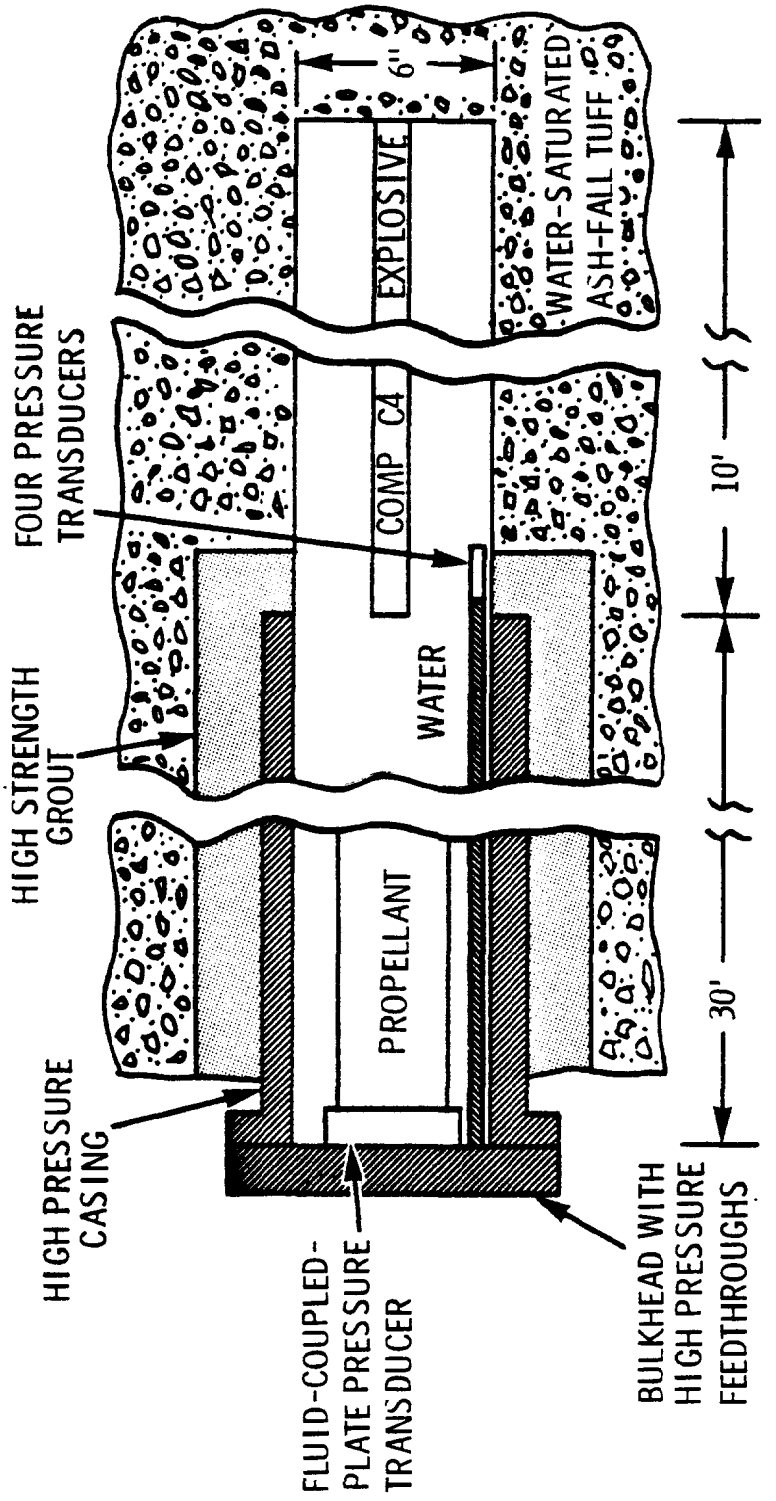

TEST SETUP FOR AUGMENTED DYNAFRAC

FIGURE IV-17

Test Configuration for Augmented Dynafrac. Stress and Acceleration Transducers in Surrounding Rock not Shown.

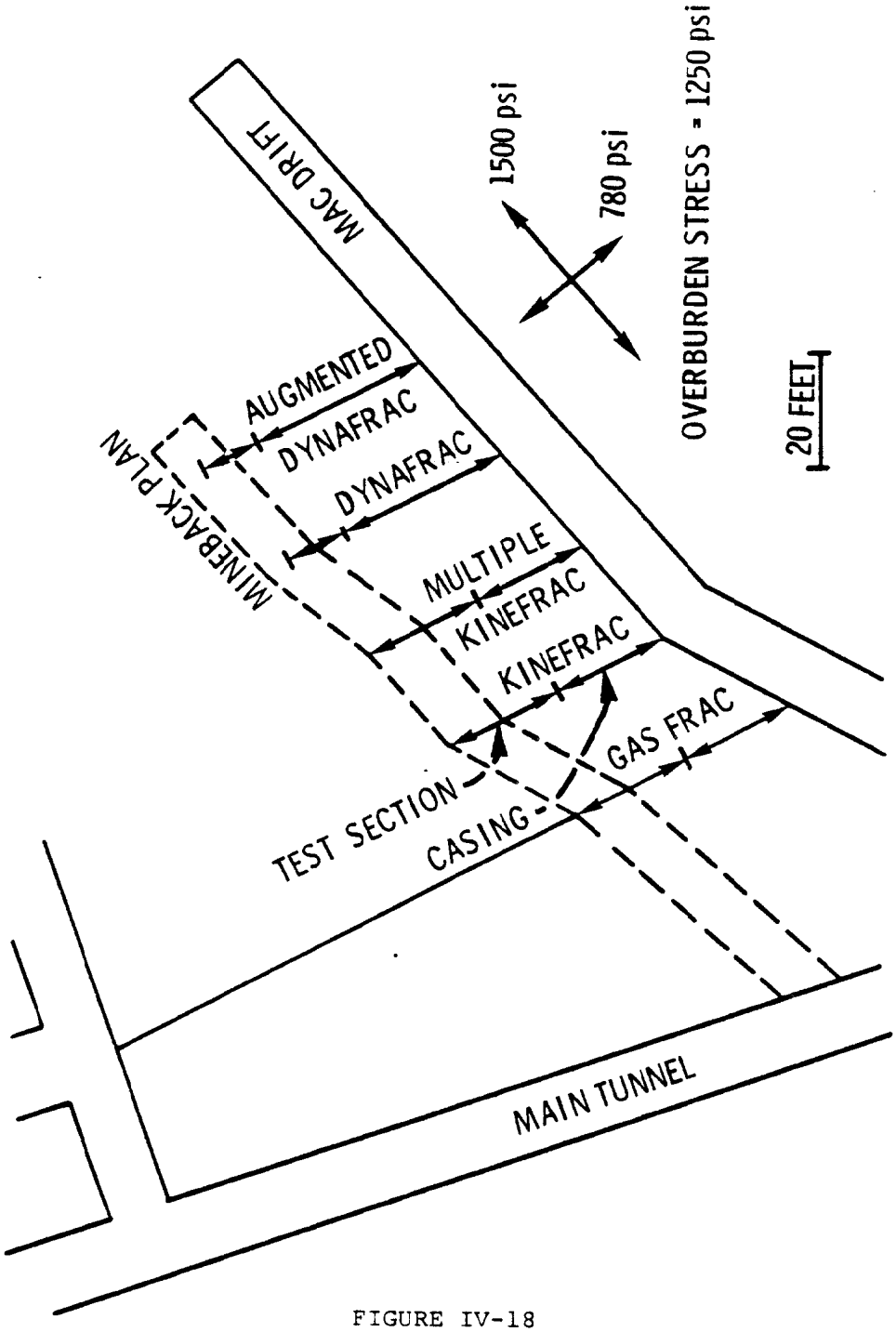

FIGURE IV-18

Tunnel plan for Multi-Frac Test Series with proposed mineback route.

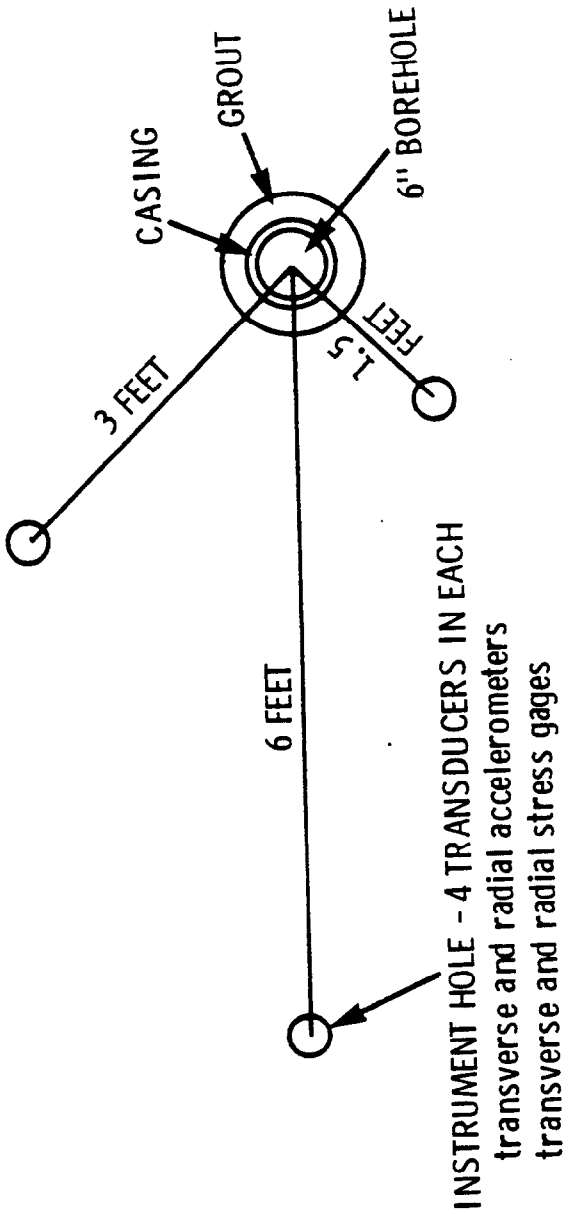

FIGURE IV-19

Typical test setup viewed along the axis of the borehole with satellite holes for instrumentation.

outside contracts placed. Fabrication of hardware and installation in G-tunnel were nearing completion. The shots are scheduled to be fired in January 1980, with post-test analysis and mineback immediately following.

3. Modeling and Analysis (R. A. Schmidt and N. R. Warpinski, 4732)

The modeling and analysis efforts that are being conducted in conjunction with these tests are being performed cooperatively by Sandia Laboratories, Stanford Research Institute, University of Maryland, Science Applications Incorporated, and Los Alamos Scientific Laboratory. These efforts have two primary goals: 1) to provide design criteria for the optimization of stimulation efforts for a particular, site-specific well and 2) to provide a predictive capability for determining, *a priori*, the number, length, and conductivity of fractures created by any particular pulse in any given well. Achieving the second goal automatically includes the first, but developing a design optimization scheme may not require the complete solution necessary in a predictive capability.

This cooperative effort has the form of a "modeling committee" that meets every month or so. Both the test series and the modeling efforts have benefited by this association: calculations have been made to determine transducer locations and ranges, and the modelers have suggested changes in the tests that will maximize the useful output.

Sandia's modeling efforts have focused on two areas: 1) specific calculations for the test series itself to provide for the best means of data analysis and evaluation (especially with regard to measurements of in situ permeability) and 2) development of design criteria that define the conditions that cause compaction and the creation of residual stresses so as to optimize a tailored-pulse stimulation of specific gas reservoirs.

In the first area, calculations were conducted to identify the requirements for pre- and post-test permeability evaluations. Although stressmeter and accelerometer gages will be installed around the wellbore to determine the effect of the pulse on the rock, and mineback will provide qualitative evidence

of the induced fractures, the only method of determining the result of these tests regarding stimulation of the "reservoir" is to perform flow or pressure tests.

In order to examine the feasibility of utilizing such tests to quantify the results, a number of calculations have been performed for Darcy flow in the ash-fall tuff with water as the test fluid. Two cases are considered: 1) constant flow rate injection while recording pressure and 2) constant pressure injection while recording the flow rate. Analytic solutions can be obtained for both cases. It is assumed that the reservoir has a matrix permeability (k) of 0.01 md and a porosity (ϕ) of 40%. Calculations show that the preferred case is constant pressure injection if the low flow rates can be measured. This avoids the problem of the pressures rising too high and possibly fracturing the rock.

Assuming that the created multiple fracture systems of these tests can be modeled as an "enlarged borehole," Figure IV-20 shows the calculated results for four different wellbore radii with a wellbore pressure (P_o) of 200 psi, and a pretest wellbore radius of 3 in. As can be seen, fairly small changes in the apparent borehole radius result in significant differences in flow rate. Thus, if the low flow rates can be adequately measured, useful measurements should be obtained.

In the second area, that of design criteria for avoiding stress cage formation, a closed-form analysis was conducted to determine elastic stresses in a dynamically pressurized cavity. In particular, this analysis determines the stress wave propagation behavior in an elastic medium from a given pressure pulse for a deeply-buried spherical charge. Complete stress histories were calculated for the three previous Gas Frac experiments[3] assuming that the cavity pressure in each case could be adequately simulated with the following:

$$P(t) = P_o t e^{-\alpha t} = \frac{P_{max}}{t_{max}} t \exp\left(1 - \frac{t}{t_{max}}\right)$$

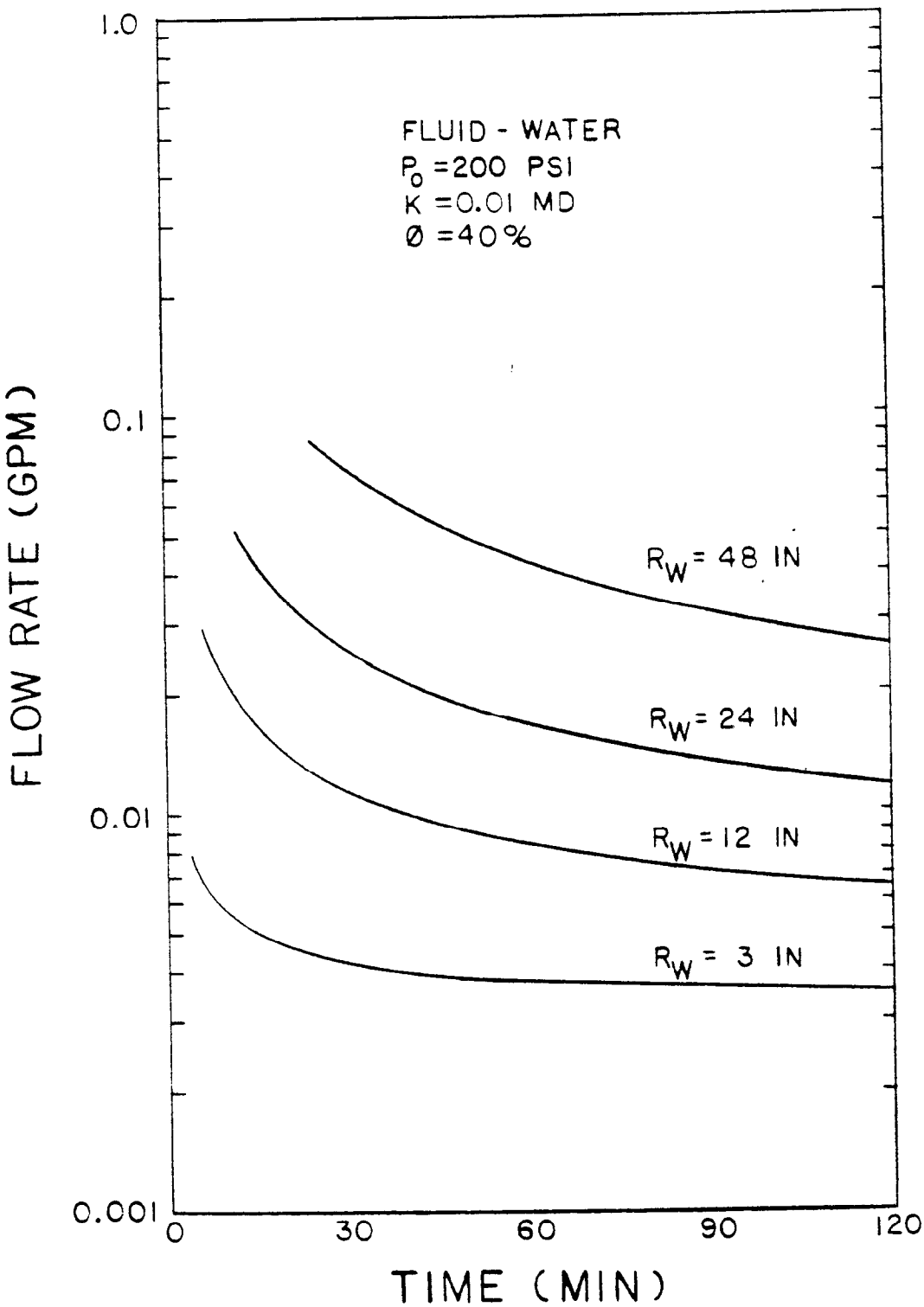

FIGURE IV-20

Injection Flow Rates for Constant Borehole Pressure as a Function of Effective Wellbore Radius

where P_o and α are constants adjusted to fit the actual input pulse. P_{max} is the maximum pressure and t_{max} is the time corresponding to P_{max}.

Results indicate that the loading rates for the intermediate and slow burning propellant tests (GF#2 and GF#1, respectively[3]) gave peak stresses equivalent with the static solution. Of particular interest is the fact that the calculation for the fast burning test (GF#3)[3] shows not only substantially different behavior from the static solution but that the tangential stresses begin as compressive and later become tensile. Recalling that mineback of GF#3 showed many incipient cracks that did not propagate, a new criteria is suggested for gas penetrating fracture growth. Rather than only requiring peak cavity pressure to remain below a level that would cause plastic flow or crushing, it may also be important to keep the loading rate below a level that produces initial compressive stresses in the tangential direction on the cavity wall. This loading rate criterion is affected by cavity size, elastic constants, and wave speed; it is not affected by rock strength.

The actual value of the peak pressure, P_{max}, does not affect this critical time, t_c. While this may seem obvious, the implication is that the actual value of the pressure loading rate does not affect the results. Wellbore diameter, on the other hand, does have a small effect. Using typical material properties for ash-fall tuff, t_c was evaluated by iteration and found to be 108 μsec for an 8 in diameter wellbore and 200 μsec for a 16 in diameter wellbore. The next step is to determine the effect of material properties (elastic constants and wave speed) on t_c. Further computer programming is needed to make the iterative process more efficient. Additional analytic work to place the suggested criterion in closed form would also be useful.

Finally, material property measurements are needed in conjunction with the Multi-Frac Test Series as inputs to the various modeling efforts. Several core samples were taken from the test bed area. Some samples were sent to Stanford Research Institute for small-scale explosive shots that will determine input parameters for calculations with the NAG-FRAG model.[8] Other samples

were sent to Science Applications, Inc., where high rate compressive properties were measured and triaxial compression tests will be run to determine the material's yield surface; these data help define the loading conditions that result in compaction. Still other samples were used by Sandia to measure tensile strength, Young's modulus, Poisson's ratio, and fracture toughness are being conducted. Preliminary results from these tests have shown a tensile strength of 100 psi, and Young's modulus of 1.0×10^6 psi. The degree of saturation seems to have some effect on the results, but more tests will be conducted to define these parameters further.

References for Section IV-B

1. Smith, C. W., Bass, R. C., and Tyler, L. D., "Puff 'n Tuff, a Residual Stress - Gas Fracturing Experiment," Proceedings of 19th U. S. Symposium on Rock Mechanics, Stateline, NV (1978).

2. Boade, R. R., Stevens, A. L., Harak, A. E., and Long, A., "Bed Preparation Concepts for True In Situ Oil Shale Processing: An Evaluation of Current Technology," Proceedings of the 1979 Society of Petroleum Engineers Annual Technical Conference and Exhibition, SPE 8447 (1979).

3. Warpinski, N. R., Schmidt, R. A., Cooper, P. W., Walling, H. C., and Northrop, D. A., "High-Energy Gas Frac: Multiple Fracturing in a Wellbore," Proceedings of 20th U. S. Symposium on Rock Mechanics, Austin, TX (1979).

4. Florence, A. L., and Gates, R. W., "Explosive Cavity Residual Stress Experiment," 76-3702-2, Stanford Research Institute, Menlo Park, CA (1976).

5. Schmidt, R. A., Boade, R. R., and Bass, R. C., "A New Perspective on Well Shooting - The Behavior of Contained Explosions and Deflagrations," Proceedings of 1979 Society of Petroleum Engineers Annual Technical Conference and Exhibition, SPE 8346 (1979).

6. Moore, E. T., Mumma, D. M., and Seifert, K. D., "Dynafrac - Application of a Novel Rock Fracturing Method to Oil and Gas Recovery," Physics International Final Report 827, April 1977.

7. Fitzgerald, R., and Anderson, R., "Kine-Frac: A New Approach to Well Stimulation," ASME Paper 78-PET-25, ASME Energy Technology Conference and Exhibition, Houston, TX (1978).

8. Shockey, D. A., Curran, D. R., Seamon, L., Rosenberg, J. T., and Petersen, C. F., "Fragmentation of Rock Under Dynamic Loads," Int. J. Rock Mech. & Min. Sc., 11, 303-317 (1974).

C. Multi-Well Experiment (D. A. Northrop, 4732)

The Western Gas Sands Project has initiated a major field experiment which will provide an unprecedented opportunity for R&D in the tight gas reservoirs in the Western United States. The Experiment's overall objectives are (1) to obtain a comprehensive geologic characterization of low-permeability, lenticular gas sands and (2) to evaluate state-of-the-art and developing technology for gas recovery from these reservoirs.

The Experiment consists of three phases: Phase 1 - drilling and testing of the first well; Phase 2 - drilling and testing of one (or more) offset well(s); and Phase 3 - a series of stimulation programs and the associated analyses and evaluation. Experiment planning and site selection are underway. The first well, and possibly the second well, will be completed in 1980. The first of several stimulation programs to be conducted over the following three years will be performed in 1981.

Features of the Experiment include: (1) research-oriented activities, schedules, and budgets; (2) a site with a variety of lenticular and continuous gas sands; (3) close-spaced wells (100-500 ft) for detailed reservoir characterization, well-to-well flow testing and downhole geophysical techniques, and placement of diagnostic instrumentation adjacent to fracture treatments; (4) complete core, much of it oriented, taken through the Mesaverde sequence with both conventional and pressure coring techniques; (5) a comprehensive core analysis program with prioritized analyses for data required for well location, interval selection, and data interpretation; (6) an extensive logging program featuring conventional and experimental logs and repetitive logs with different operators and borehole fluids; (7) a detailed well testing program with both pre- and post-stimulation interval testing and pulse and interference testing between wells; (8) in situ stress determinations as a function of depth; (9) wide application of geophysical and fracture diagnostic techniques, and (10) varied stimulation programs to examine fluids, proppants, treatment conditions, fracture growth, fracture conductivity, etc.

The Experiment has six tasks: field drilling, laboratory testing, stimulation, production testing, field diagnostics, and analysis and evaluation. An industry advisory group is providing guidance in the selection and planning of Experiment activities. A wide variety of contractors and agencies will be involved in the acquisition and analysis of the experiment data. These analyses are expected to yield a geologic characterization of lenticular reservoirs, a reservoir model, hydraulic fracture stimulation model with resultant fracture geometries, core-log-well test correlations, technology assessments, economic evaluations, and recommendations for gas recovery from these reservoirs.

Active planning of the Experiment was initiated in May 1979, when the concept for a DOE-conducted, research-oriented experiment in the tight gas sands was endorsed. The initial experiment plan was prepared by Sandia and CER Corporation and was then presented to an industry advisory group formed for this Experiment. Meetings of this group with key DOE, national laboratory and contractor personnel were held on July 19, August 23, and September 24, 1979. The Experiment's activities and plans continue to evolve at the end of FY79.

A site is being sought in the Piceance Basin east of Collbran, CO, at an elevation of 7000 ft where the Mesaverde sequence lies at depths between 4000-8000 ft. It was hoped initially that the site would be acquired and first well drilled prior to winter, but this was not accomplished. The prime site could not be satisfactorily acquired, and others are being pursued. The additional time for planning and coordination will be useful prior to initial field activities in the Spring of 1980.

V. Publications, Presentations, and Other Communications

A. Publications and Presentations

1. C. L. Schuster presented the paper "Detection Within the Wellbore of Seismic Signals Created by Hydraulic Fracturing" (SPE 7448) at the 53rd Annual SPE Technical Conference and Exhibition, Houston, TX, October 1-4, 1978.

2. Sandia Laboratories participated in the Second Annual Eastern Gas Shales Symposium, held at the Lakeview Inn, Morgantown, WV, on October 16-18, 1978, by presenting one paper and displaying two poster papers. C. L. Schuster presented "Gas Simulation Mapping and Characterization Program." Poster displays were "Tools for Wireline Fracture Mapping" by R. P. McCann and C. L. Schuster and "Direct Observation of Hydraulic Fractures" by N. R. Warpinski and D. A. Northrop.

3. C. L. Schuster presented the paper "An Overview of the Electrical Potential Method for Determining Fracture Orientation" at the 1978 Annual ASCE Meeting, Chicago, IL, October 19, 1978.

4. T. L. Dobecki presented the paper "Resistivity Mapping of Expanding Spheroids as Measured in Nearby Boreholes," at the 48th International Meeting of the Society of Exploration Geophysicists in San Francisco, CA, October 29 - November 2, 1978.

5. N. R. Warpinski, R. A. Schmidt, D. A. Northrop, and L. D. Tyler, "Hydraulic Fracture Behavior at a Geologic Formation Interface: Pre-Mineback Report," Sandia Laboratories Report, SAND78-1578, October 1978.

6. R. A. Schmidt presented the paper "Direct Observation of Hydraulic Fractures: Behavior at a Formation Interface," by N. R. Warpinski, D. A. Northrop, and R. A. Schmidt, at the Energy Technology Conference and Exhibition in Houston, TX, on November 5-9, 1978. A Sandia Report, SAND78-1935, covering this work was made available to attendees.

7. N. R. Warpinski, R. A. Schmidt, H. C. Welling, P. W. Cooper, and S. J. Finley, "High Energy Gas Frac," Sandia Laboratories Report, SAND78-2342, December 1978.

8. D. A. Northrop presented aspects of the mineback fracturing experiments at the bimonthly noon meeting of the Albuquerque Section of the American Society of Civil Engineers on January 10, 1979, in Albuquerque, NM.

9. D. A. Northrop and C. L. Schuster (Editors), "Enhanced Gas Recovery Program, Third Annual Report, October 1977 through September 1978," Sandia Laboratories Report, SAND79-0056, March 1979.

10. R. A. Schmidt gave a presentation entitled "A Microcrack Model and Its Significance to Fracture Toughness Testing of Rock," at a committee meeting of the American Society for Testing and Materials held in Cincinnati, OH, on April 29, 1979.

11. R. A. Schmidt presented two invited seminars at Lehigh University, Bethelehem, PA, and Cornell University, Ithaca, NY, on May 1 and May 3, 1979, entitled "Fracture Mechanics of Rock with Applications to Fossil Energy Research."

12. Two presentations were made at the 20th United States Symposium on Rock Mechanics held in Austin, TX, on June 4-6, 1979: R. A. Schmidt presented "Hydraulic Fracturing Near an Interface: Observations and Calculations Regarding Geometry and Containment," by R. A. Schmidt, D. A. Northrop, and N. R. Warpinski, and N. R. Warpinski presented "High Energy Gas Frac - Multiple Fracturing in a Wellbore," by N. R. Warpinski, R. A. Schmidt, P. W. Cooper, H. C. Walling, and D. A. Northrop.

13. Two papers were presented at the 5th Annual DOE Symposium on Enhanced Oil and Gas Recovery and Improved Drilling Technology, held in Tulsa, OK, on August 22-24, 1979: C. L. Schuster, "Fracture Mapping has Become a Viable Technology," and D. A. Northrop, N. R. Warpinski, and R. A. Schmidt, "EGR Stimulation Project - Direct Observation of Hydraulic and Dynamic Fracturing."

14. R. A. Schmidt presented a paper SPE 8346, "A New Perspective on Well Shooting - The Behavior of Contained Explosions and Deflagrations" by R. A. Schmidt, R. R. Boade, and R. C. Bass at the 54th Annual Meeting of the Society of Petroleum Engineers held in Las Vegas, NV, on September 24-26, 1979,

B. Other Communications

1. D. A. Northrop met with Dr. P. L. Randolph and R. L. Rogers of the Institute of Gas Technology in Chicago on October 19, 1978 to discuss data on in situ stress variations.

2. R. A. Schmidt co-chaired a meeting of ASTM Committee E-24.07, Fracture Testing of Brittle Non-Metallic Materials, in Philadelphia, PA, November 7, 1978.

3. C. L. Schuster and P. C. Lysne met with H. B. Carroll and BETC staff members at Bartlesville on November 14, 1978, to present a seminar on electrical impedance measurements in reservoir rock and to discuss Sandia's scope of work in this area.

4. P. C. Lysne and T. L. Dobecki met with Dr. J. H. Moran of the New Mexico Institute of Technology in Socorro, NM, on November 21, 1978, to discuss Sandia's planned electromagnetic logging studies.

5. D. A. Northrop, R. A. Schmidt, and N. R. Warpinski participated in another of a series of Stimulation Modeling Workshops for the Eastern Gas Shales Project, held in Golden, CO, on December 12 and 13, 1978.

6. R. Trump and P. Winchell from Gulf Research visited Sandia on January 8, 1979, to discuss the borehole seismic system and its application to fracture mapping.

7. R. A. Schmidt briefed J. B. Smith, DOE/FEE on the High Energy Gas Frac and related containment activities on February 8, 1979, in Albuquerque, NM.

8. C. L. Schuster and D. A. Northrop briefed C. W. Draffin and A. B. Crawley, DOE/FEE, on the status of Sandia's EGR Program Activities in Washington, DC, on February 13, 1979.

9. T. L. Dobecki visited Mr. S. D. Brasel, Seismic International Research, in Denver, CO, on February 13, 1979, to discuss problems involved with seismic mapping of relatively shallow, discontinuous sandstone bodies.

10. T. L. Dobecki visited Dr. R. Weimer, Colorado School of Mines, Golden, CO, on February 15, 1979, to discuss general stratigraphic relationships which exist in the upper Cretaceous rocks of the Unita, Piceance, and Green River basins.

11. N. R. Warpinski briefed T. McLaughlin of Battelle Northwest on Sandia's hydraulic fracture activities at the Nevada Test Site and gave him a tour of G tunnel on February 14, 1979.

12. N. R. Warpinski attended the Natural Gas Reservoirs Symposium on Analytical Techniques and Applications for Natural Gas Reservoirs sponsored by the Stanford University Department of Petroleum Engineering and the American Gas Association in Palo Alto, CA, on February 15-16, 1979.

13. C. L. Schuster visited M. D. Wood, Inc., in Palo Alto, CA, with Dr. M. Smith from AMOCO, to exchange data collected from the fracture-orientation experiments; excellent agreement was obtained from all methods.

14. C. L. Schuster and T. L. Dobecki provided a briefing of possibilities of mapping sand channels using surface seismic methods to CER, Inc., and DOE personnel in Las Vegas, NV, on February 20 and 21, 1979.

15. A summary and discussion of Sandia's Enhanced Gas Recovery Program was given to Mr. J. Sharer, Gas Research Institute, and the GRI Advisory Board for Unconventional Gas Recovery in Albuquerque, NM, on April 26, 1979. C. L. Schuster (instrumentation), D. A. Northrop (mineback testing), R. A. Schmidt (high energy gas fracturing), and A. L. McFall (drilling) gave presentations. L. Keck, R. McCann and R. Seavey discussed various instrumentation techniques during a tour of a field instrumentation trailer.

16. H. B. Carroll and J. B. Jennings, Bartlesville Energy Technology Center, visited Sandia on May 2, 1979, and received an updated briefing by P. C. Lysne on the status of the advanced logging program.

17. At the request of A. B. Crawley, DOE's Manager of its Unconventional Gas Recovery Program (UGR), Sandia arranged a meeting in Tulsa, OK, on May 7 and 8, 1979, to obtain industry's review and comments on a preliminary draft of the Tight Gas Sands portion of the overall UGR program plan.

18. C. L. Schuster and T. L. Dobecki attended a meeting with CER and C. K. Geoenergy in Las Vegas, NV, on May 10, 1979, to discuss program plans for the seismic measurement program to delineate lenticular lenses.

19. D. A. Northrop and C. L. Schuster attended a meeting at CER, Las Vegas, NV, on May 18, 1979, to discuss ideas for a Multi-Well Experiment to be initiated in FY 79.

20. C. L. Schuster attended the SPE meeting on Low Permeability Reservoirs in Denver, CO, on May 21-22, 1979.

21. D. A. Northrop and C. L. Schuster met with A. B. Crawley, DOE/FFE, in Denver, CO, on May 22, 1979, to discuss the status of DOE's UGR Program planning and an update on the Multi-Well Expeiment plans.

22. D. A. Northrop met with R. L. Mann, CER, to prepare further a program statement of work for the proposed Multi-Well Experiment, in Las Vegas, NV, on JUne 5-6, 1979.

23. D. A. Northrop and C. L. Schuster attended DOE's Unconventional Gas Recovery Project Review at Morgantown, WV, on June 12-14, 1979, where they presented reviews of current Sandia program activities, were involved in the UGR program planning exercises for the Tight Gas Sands section, and participated in a detailed review of FY 80 plans.

24. D. A. Northrop attended a working meeting at CER, Las Vegas, NV, on June 21-22, 1979, to finalize the draft of the Tight Gas Sands section of the UGR program plan.

25. C. L. Schuster, T. L. Dobecki, and P. C. Lysne met with the U.S.G.S Western Gas Sands Project Staff in Denver, CO, on July 12, 1979, to discuss current activities of interest to the project.

26. Dr. P. L. Randolph, Institute of Gas Technology, visited Sandia on July 20, 1979, to discuss his current core analysis work and the application of this work to the new Multi-Well Experiment.

27. R. A. Schmidt and N. R. Warpinski briefed Mr. J. Edl, Carbondale Mining and Technology Center, on Stimulation Research Project activities on July 27, 1979, at Sandia, Albuquerque, NM.

28. R. A. Schmidt attended an Eastern Gas Shales Modeling meeting at Los Alamos Scientific Laboratory, Los Alamos, NM, on July 30, 1979.

29. T. L. Dobecki, and P. C. Lysne attended the Society of Petroleum Engineers Forum "Properties of Saturated Rocks of Interest to Petrophysicists and Geophysicists," July 29 - August 3, 1979, at Colorado Mountain College, Glenwood Springs, CO.

30. R. A. Schmidt attended a working meeting for the Eastern Gas Shales Project at the Denver Project Office, Lakewood, CO, on August 30, 1979.

31. Sandia conducted a tour of the Nevada Test Site for the project advisors group of the Gas Research Institute, on August 28, 1979.

32. D. A. Northrop and T. Gerlach attended an Unconventional/Non-Conventional Gas Recovery Workshop held at Los Alamos Scientific Laboratory, Los Alamos, NM, on September 5 and 6, 1979.

33. D. A. Northrop and C. L. Stein visited with C. W. Spencer, T. D. Fouch, and their co-workers involved with WGSP activities at the U. S. Geological Survey in Denver, CO, on September 20, 1979.

34. Sandia Laboratories co-sponsored a tour for over 80 people at the Nevada Test Site on September 28, 1979, held in conjunction with the 54th Annual Technical Conference and Exhibition of the Society of Petroleum Engineers, Las Vegas, NV, September 23-26, 1979. In-tunnel presentations focused on hydraulic fractures experiments at formation interfaces and the effects of in situ stress (N. R. Warpinski) and effects of explosive and tailored propellant fracturing (R. A. Schmidt).

SAND79-2428
UNLIMITED RELEASE

ENHANCED GAS RECOVERY PROGRAM
FOURTH ANNUAL REPORT

OCTOBER 1978 THROUGH SEPTEMBER 1979

D. A. NORTHROP AND C. L. SCHUSTER, EDITORS

FILE #C073/A79

Issued by Sandia Laboratories, operated for the United States Department of Energy by Sandia Corporation.

NOTICE

This report was prepared as an account of work sponsored by the United States Government. Neither the United States nor the Department of Energy, nor any of their employees, nor any of their contractors, subcontractors, or their employees, makes any warranty, express or implied, or assumes any legal liability or responsibility for the accuracy, completeness or usefulness of any information, apparatus, product or process disclosed, or represents that its use would not infringe privately owned rights.

SF 1004-DF(11-77)

Printed in the United States of America

Available from National Technical Information Service
U.S. Dept. of Commerce
5285 Port Royal Road
Springfield, VA 22161

Price: Printed Copy: $5.50
Microfiche: $3.00

SAND79-2428
Unlimited Release

ENHANCED GAS RECOVERY PROGRAM

FOURTH ANNUAL REPORT

October 1978 through September 1979

ABSTRACT

Massive hydraulic fracture diagnostic experiments continued in FY 79 with the major activity being focused on the development of wireline tool instrumentation. The development of the Borehole Seismic System and Borehole Hydrophone System should lead to a more direct method of obtaining fracture orientations and fracture heights than presently exists. These systems can be deployed in the well to be stimulated and can monitor seismic activities before and after nonproppant fluid pumping periods. This seismic activity should occur along the induced fractures, and the location of the seismic sources will be indicative of the fracture locations. The experiments conducted at DOE's Nevada Test Site with known signal locations substantiate field data obtained in two experiments with Amoco in their Wattenberg field where fracture orientation was detected.

A high resolution, three-dimensional seismic survey program was initiated this year in an attempt to delineate lenticular sand formations from the surface. The program will start with some experiments at shallow depths where the sand lenses outcrop and then move into greater depths to evaluate this technique. In addition, a logging program has also been established to evaluate formation properties. This program hopes to evaluate the dispersive electrical parameters of the formation and relate these parameters to the formation permeability and porosity.

Hydraulic and dynamic fracturing experiments have been conducted adjacent to a tunnel complex at the Nevada Test Site and which are then directly observed by mining through the experiment area. Emphasis has been placed on the study of the factors which influence the containment, and hence the overall geometry, of hydraulic fractures at a formation interface. Evaluation of

full-scale fracturing tests at an interface between geologic formations with significantly different properties, most notably an order of magnitude difference in elastic modulus, showed that the interface did not contain the fractures. Numerous smaller scale experiments at the same interface have confirmed these results. Thus, it has been shown that material property differences alone are insufficient for containment, and that the in situ stress is the dominant parameter. Fracture growth and terminations have been shown to coincide with variations in in situ stress even within the same formation. Rock mechanics and fluid mechanics studies have supported these conclusions. In particular, a microcrack model has been formulated which downplays the importance of material properties and emphasizes the role of in-situ stresses for processes occurring at a crack tip.

Multiple fracturing from a wellbore has been demonstrated for a High Energy Gas Frac concept. In this concept, the gas pressure pulse due to the deflagration of a propellant is designed to give pressure loading rates sufficient to initiate multiple fractures, peak pressures below the flow stress of the formation to avoid rock compaction, and a duration of burn sufficient to allow gas penetration and fracture extention. An expanded test series has been initiated to quantify several techniques for multiple fracturing based on this concept.

Finally, a Multi-Well Experiment has been defined whose objectives are to characterize in detail a lenticular gas reservoir of the Western United States and to evaluate state-of-the-art and developing technology for the recovery of gas from them. This research-oriented field experiment will be initiated in 1980.

TABLE OF CONTENTS

		PAGE
I.	Introduction and Summary	5
II.	Massive Hydraulic Fracture Mapping and Characterization Program	10
	A. Borehole Seismic System	10
	1. System Description.	10
	2. NTS Minifrac	14
	3. Amoco Experiments	16
	4. NTS Borehole Tests.	20
	B. Borehole Hydrophone System	24
	1. System Applications	24
	2. System Description.	25
	3. Prototype Testing	26
	C. Surface Electrical Potential System (SEPS)	29
	1. System Description.	29
	2. Amoco Wattenberg Field Fracture Experiment.	32
	3. Design Changes to SEPS	35
III.	Advanced Logging Technology and Formation Evaluation	37
	A. Seismic Formation Mapping Program.	37
	1. Introduction	37
	2. Task Description	38
	3. Site Descriptions.	39
	4. Program Progress	40
	B. Nuclear Magnetism Logging.	40
	C. Advanced Electromagnetic Logging	42
	1. Logging Techniques Based on Dispersive Electrical Parameters	42
	2. An Inverse Process for Evaluating Constitutive Parameters.	46
IV.	Stimulation Research for Unconventional Gas Recovery	61
	A. Hydraulic Fracturing	61
	1. Hydraulic Fracturing Containment Experiments.	61
	2. Modeling and Analysis.	81
	B. Dynamic Wellbore Fracturing	100
	1. Background	100
	2. Multi-Frac Test Series	101
	3. Modeling & Analysis	106

C. Multi-Well Experiment 111

V. Publications, Presentations, and Other Communications 113

A. Publications and Presentations 113

B. Other Communications. 115

I. Introduction and Summary

A. Introduction

Sandia Laboratories conducts several projects which are part of the United States Department of Energy's (DOE) Unconventional Gas Recovery Program. One is the Massive Hydraulic Fracture Characterization Project whose objective is to develop instrumentation systems for characterizing fracture systems, formations, and other parameters contributing to enhanced gas recovery. Another is the Stimulation Research Project whose objective is to understand, and thus improve, fracturing processes for stimulation of natural gas production from low permeability formations which contain a high potential resource. Another is the Advanced Logging for Formation Evaluation Program being conducted for the Bartlesville Energy Technology Center in support of the Western Gas Sands Project. A fourth is the in situ testing of well shooting concepts being conducted for the Morgantown Energy Technology Center in support of the Eastern Gas Shales Project. Finally, a Multi-Well Experiment was initiated which will be the major field test conducted under the Western Gas Sands Project in future years. This report summarizes activities conducted under these projects during Fiscal Year 1979; October 1, 1978, through September 30, 1979.

The Massive Hydraulic Fracture (MHF) Characterization Project began in 1974 with the initial application of Sandia's instrumentation capability in a joint experiment with El Paso Natural Gas in the Pinedale Field, Green River Basin, Wyoming. The initial effort was an attempt to measure the orientation and growth of a massive hydraulic fracture using both surface seismic recording and electrical potential mapping techniques. In the ensuing years, the surface seismic program has been discontinued because of its inability to map fractures from the surface. The surface electrical potential technique has been developed and fielded on several experiments over the past five years. This instrumentation system has demonstrated the capability to determine fracture orientation induced by massive hydraulic fracturing, provide a measure of the asymmetry of fracture wings created, and provide some insight into the stimulation processes occurring within the reservoir.

The original surface seismic program has been redirected and now is concentrating on a borehole seismic system that can be utilized in the fracture well. This system records seismic signals before and after nonproppant fluid injections that can determine the orientation of the hydraulic fracture by knowing the orientation of the system within the borehole. Utilization of borehole tools for fracture mapping should greatly enhance the obtaining of these data by substantially reducing the costs. A second system utilizing hydrophones is under development for determination of fracture heights. In addition to fracture diagnostics, there has been a broadening of the project scope to develop other instrumentation systems and techniques for characterizing and evaluating the formation. These include defining the boundaries of lenticular sand lenses and evaluating the formation parameters involved in hydrocarbon production. For example, a logging program hopes to evaluate the dispersive electrical parameters of the formation and relate these parameters to the formation permeability and porosity.

The Stimulation Research Project was initiated in FY 77. However, the program has built upon fracturing and mineback activities which have been conducted since 1974 in G-tunnel at DOE's Nevada Test Site as part of a nuclear containment program sponsored by the Division of Military Applications of DOE. The commonality of objectives between the nuclear containment program and enhanced gas recovery activities are striking, and the close relationship between the two programs has been mutually beneficial.

A major activity has been in situ fracturing experiments in an environment which allows for direct examination and evaluation. The mineback capability provided at the Nevada Test Site provides this opportunity. A detailed physical description can be obtained directly and can be correlated with measured geologic material properties, in situ stress distributions, fluid behavior, and the operational parameters of the test. Rock mechanics and fluid mechanics laboratory and modeling work support the design and analysis of the field experiments

and are producing new insight into fracturing behavior. The experiments also provide the opportunities to calibrate instrumentation techniques under known conditions and to examine innovative fracturing techniques. Thus, such mine-back experiments provides considerably more information than the evaluation of a commercial frac job which is based primarily upon gas production alone. Industry and service company representatives participate in the planning and analysis of the experiments. This project is providing a unique opportunity to quantify and understand fracture behavior.

Sandia's projects are supported by DOE's Unconventional Gas Recovery Program through the Eastern Gas Shales Project, Western Gas Sands Project, and the Morgantown and Bartlesville Energy Technology Centers. Sandia's projects provide a broad supporting research and development capability. Activities are planned, conducted, and reported with the aim of contributing to the objectives of both the Eastern and Western Projects and to the overall development of Unconventional Gas Recovery technology.

B. Summary

Two field experiments and two NTS experiments were conducted in FY 79 utilizing the borehole seismic system. The second experiment at NTS utilized the seismic system as it would be used in a regular borehole experiment and located seismic sources in the vicinity of a wellbore. This data analysis was similar to and provided a basis for the analysis of the full scale fracture experiments. These two field experiments were conducted with Amoco in their Wattenberg field and produced excellent fracture orientation results.

The other borehole tool is the stacked hydrophone system which has been a prototype design. Preliminary testing in the laboratory and in a shallow borehole indicates this system is operational, and it will be evaluated in FY 80. It will be utilized in two diagnostic modes; one for determining fracture heights and another for determining formation interval velocities.

The formation evaluation portion of the program has had two efforts this

year; the first effort being the initiation of a program utilizing high resolution seismic surveys for determining the boundaries of lenticular sand formations. The other program is the electromagnetic logging program which is directed at understanding the relationships between dispersive electrical parameters and formation parameters. The formation parameters of interest include both permeability and porosities. The program is in the feasibility study area this year and should move into a prototype system design in FY 80.

The Stimulation Research Project activities have focused upon the study of the containment of hydraulic fractures by geologic formation interfaces, material properties and in situ stresses. Coring operations are delineating the extent of the full-scale Hole #6 experiment conducted and mined out last year. It was observed that the fractures broke through the interface between ash fall tuff and welded tuff formations having significantly different properties, most notably an order of magnitude difference in modulus. Coring has confirmed that the fracture geometry was not affected by the presence of the interface; in fact, fracture growth was predominantly upwards and downwards instead of lateral resulting in a fracture length of 150 ft as compared with a 600-ft "design". An Interface Test Series was conducted this year to further examine the behavior at the interface; 31 small volume (150 gal) hydraulic fractures were created from horizontal wellbores located just below the same geologic interface used in the Hole #6 experiment. Fractures propagated upwards through the interface into the higher modulus formation but only limited downwards growth was observed in the same lower modulus formation where the fractures were initiated. In situ stresses were calculated from the fracturing pressure records, and fracture growth was observed to be limited by increases in the in situ stress measured in the same formation. Thus, in situ stresses are the predominant factor affecting hydraulic fracture growth; the character of the interface (bonded or nonbonded) and material property differences play a subordinate role.

A microcrack rock mechanics model has been formulated which confirms these field results. Essentially, it shows that the zone of influence at a crack tip decreases rapidly with increased stress and is not affected significantly by material properties. The model has been extended to include the effects of an anisotropic in situ stress state. Laboratory experiments with materials with smeared interfaces, where the properties change smoothly over a short distance, are being conducted to further test the fracture propagation at such an interface.

In a series of three experiments conducted last year, it was demonstrated that multiple fracturing from a wellbore was possible for a gas pressure pulse produced by the deflagration of a propellant. The pulse must be designed to give: 1) pressure loading rates sufficient to initiate multiple fractures, 2) peak pressures below the flow stress of the formation to avoid rock compaction and wellbore enlargement, and 3) a duration of burn sufficient to allow gas penetration and fracture extension. An expanded test series - the Multi-frac Test Series - has been initiated to investigate several techniques based upon this tailored-pulse concept. The test design is complete and assembly for five different experiments is underway; the tests will be conducted in the second quarter of FY 80. These tests will be extensively instrumented and evaluated to provide data for the modeling and development of such a dynamic wellbore fracturing technique for unconventional gas stimulation.

A Multi-Well Experiment has been defined. This is a research-oriented field experiment where two (or more) wells will be drilled at close spacings on a given site and will be used to characterize in detail one of the lenticular, tight gas reservoirs of the Western United States and to evaluate state-of-the-art and developing technology for the recovery of gas from them. Program planning is underway and an industry advisory group has been formed and is active. The experiment consists of six major activities (analysis and evaluation, laboratory testing, field drilling, stimulation, production testing, and field diagnostics). Field activities will be initiated in the spring of 1980, most likely at a site in the Piceance Basin, Colorado.

II. Massive Hydraulic Fracture Mapping and Characterization Program

A. Borehole Seismic System (R. W. Seavey, 4733)

1. System Description

The determination of fracture orientation is possible with the use of one triaxial geophone package. If two horizontal and one vertical geophones are clamped in the treatment well at or near the zone to be fractured, seismic signals can be detected and recorded which can be analyzed to determine the direction to the seismic source. Since the geophone response is a function of the angle of incidence of the compression component of the seismic signal, direction to the source can be determined. If a seismic source in space produces a response on geophones aligned with the X-Y-Z axes (Fig. II-1), the output of the horizontal geophones will be Y=C sin A and X=C cos A. The ratio of the horizontal amplitude is then Y/X= tan A from which the horizontal direction may be obtained if one knows the orientation of the geophones. The vertical angle of incidence, β, can be determined as the angle whose tangent is the ratio of the vertical response to the vector sum of the horizontal responses.

The borehole seismic system was fabricated using commercially available components where possible. These components were integrated into an overall system that would allow operation on a single conductor wire line. The single conductor wire line provides power to the electronics, control to the clamping arm, monitoring circuitry for the clamping arm, and the return path for the multiplexed output from the geophones. The lower section of the system (Fig. II-2) is the orientation package which contains its own power supply package, camera, and orientation unit. Either of two orientation units can be used: 1) a compass unit for operation in an open hole, and 2) a gyroscopic unit for operation in a cased hole. The entire system is 3-5/8" diameter and up to 16 ft long and is capable of being clamped into boreholes from 4-1/2" up to 15" diameter. Figure II-3 shows this borehole seismic system with the cases removed to show interior parts.

$Y=C*\sin A$

$X=C*\cos A$

$Y/X=\sin A/\cos A=\tan A$

$A=\arctan Y/X$

$B=\arctan Z/C=\arctan Z/\sqrt{(X^2+Y^2)}$

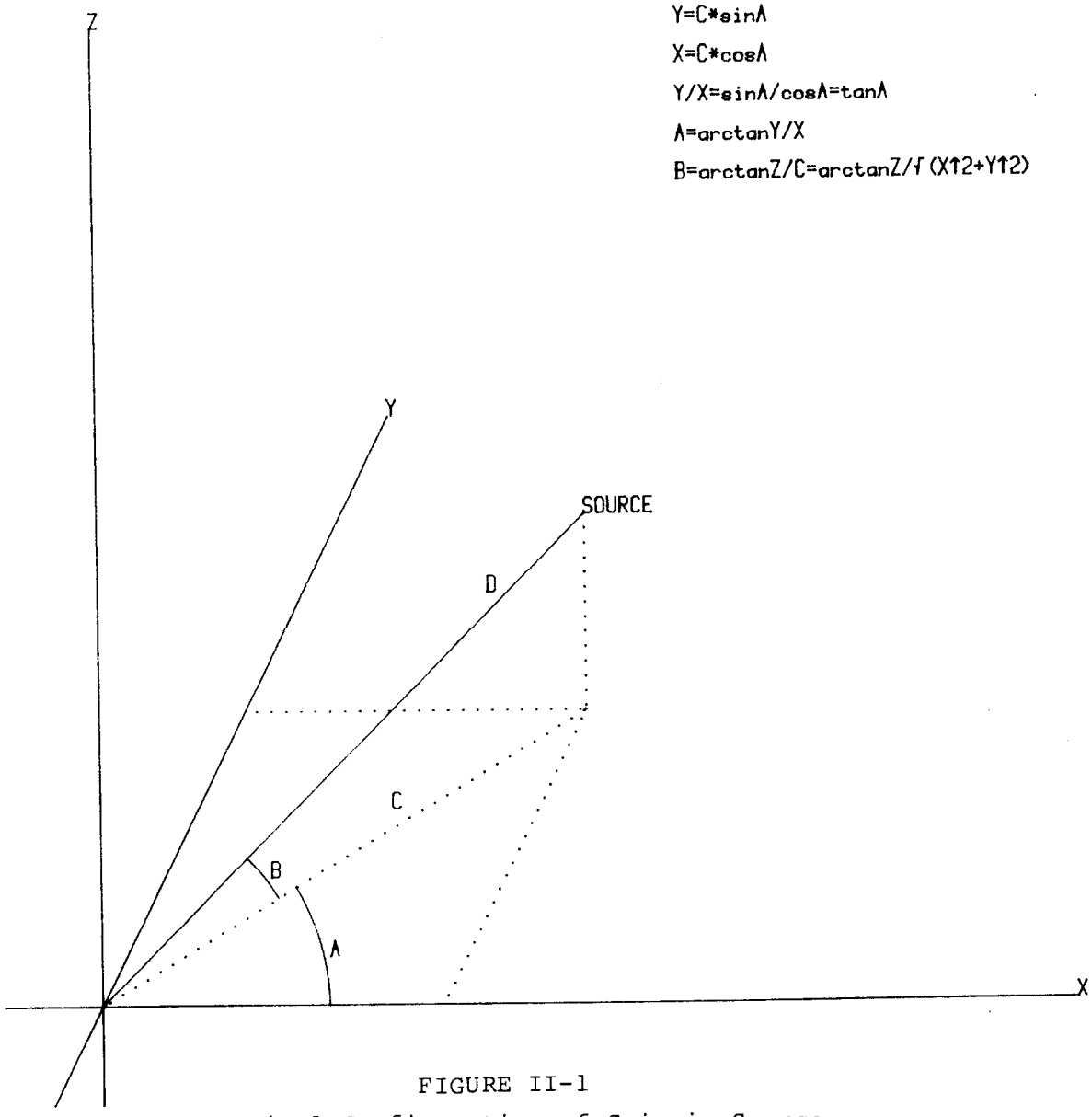

FIGURE II-1

Geometrical Configuration of Seismic Source and Geophones

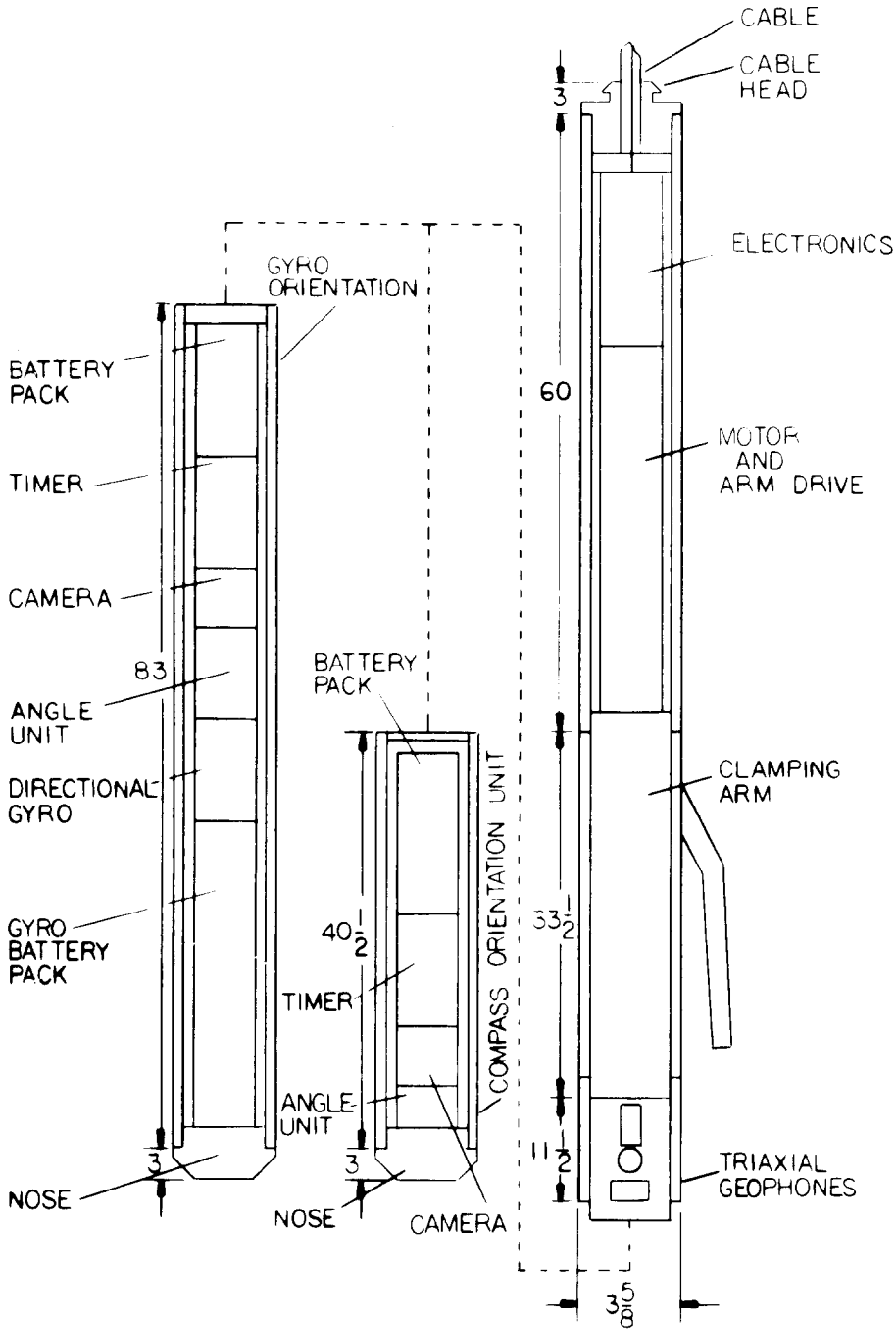

FIGURE II-2

Borehole Seismic System Configuration and Dimensions (inches

BOREHOLE SEISMIC SYSTEM

- WIRELINE - WALL CLAMPED - 3 AXIS GEOPHONE
- DURING BREAK DOWN PHASE WITHOUT PROPPANT

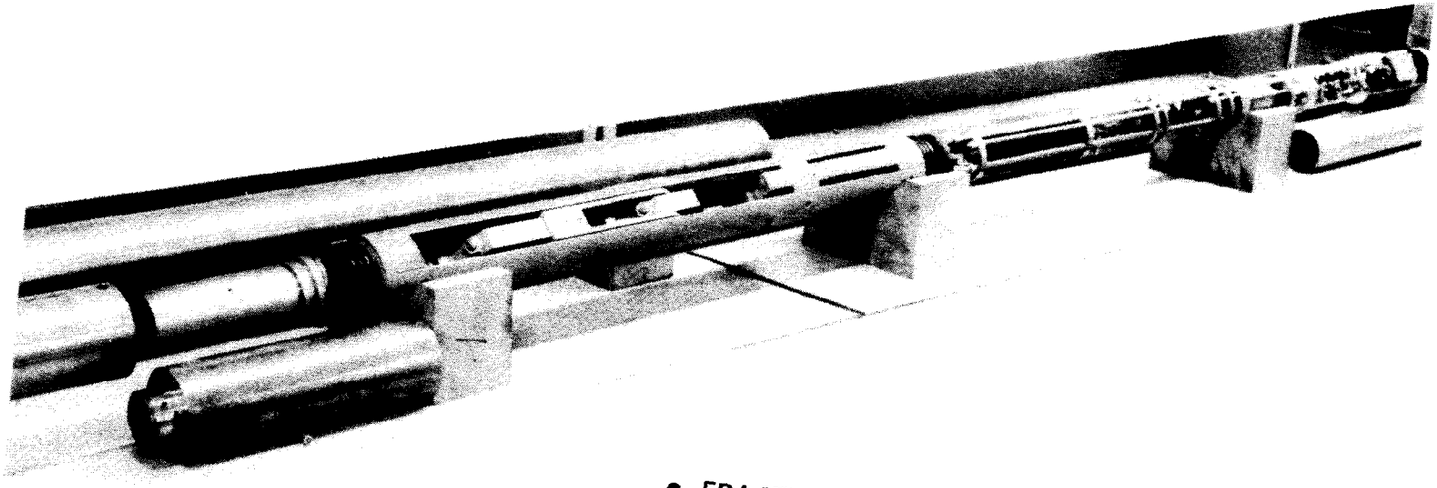

- FRACTURE ORIENTATION AND HEIGHT WITHIN 200 FEET OF BOREHOLE

FIGURE II-3
Borehole Seismic System

Two horizontal and one vertical geophones produced by Mark Products (Model L-25A) were selected for use in this system. The output of each geophone is amplified by a specially designed amplifier, each of which then feeds a voltage controlled oscillator (VCO). The three geophone VCO signals are multiplexed with a VCO signal that monitors the clamp arm operation and then transmits to the surface. Figure II-4 is a block diagram of the downhole system. The geophone VCO's are standard IRIG frequencies and allow a 2 kHz bandwidth signal to be transmitted to the surface from each geophone. Magnetic tape recordings at the surface are made to allow for future data analysis. The entire system has been pressure tested and found to operate satisfactorily up to pressures of 12,000 psi.

2. NTS Minifrac

In October of 1978, two very small fractures were performed in the HF20 drift of G-Tunnel at the Nevada Test Site. Three triaxial geophone packages were grouted into the drift and the borehole seismic unit was placed in a horizontal position within another, horizontal borehole. All four sets of geophones were placed such that the larger of the two fractures would be expected to intersect their positions.

The purpose of this experiment was: 1) to compare the signals from grouted units with the clamped unit, 2) to examine near field seismic signals, 3) and to examine the tail of the seismic signal (coda) because of peculiarities observed in data collected in testing during the previous year (Ref. 1).

The first fracture was performed with 20 gallons of clear water and the second fracture with 80 gallons of clear water. During the first fracture, no signals were observed on the borehole seismic unit. Insufficient amplitude of the few signals observed on the other units prevented any significant evaluation of signal characteristics or source location. The second fracture produced more signals but all of a very low amplitude. These were further

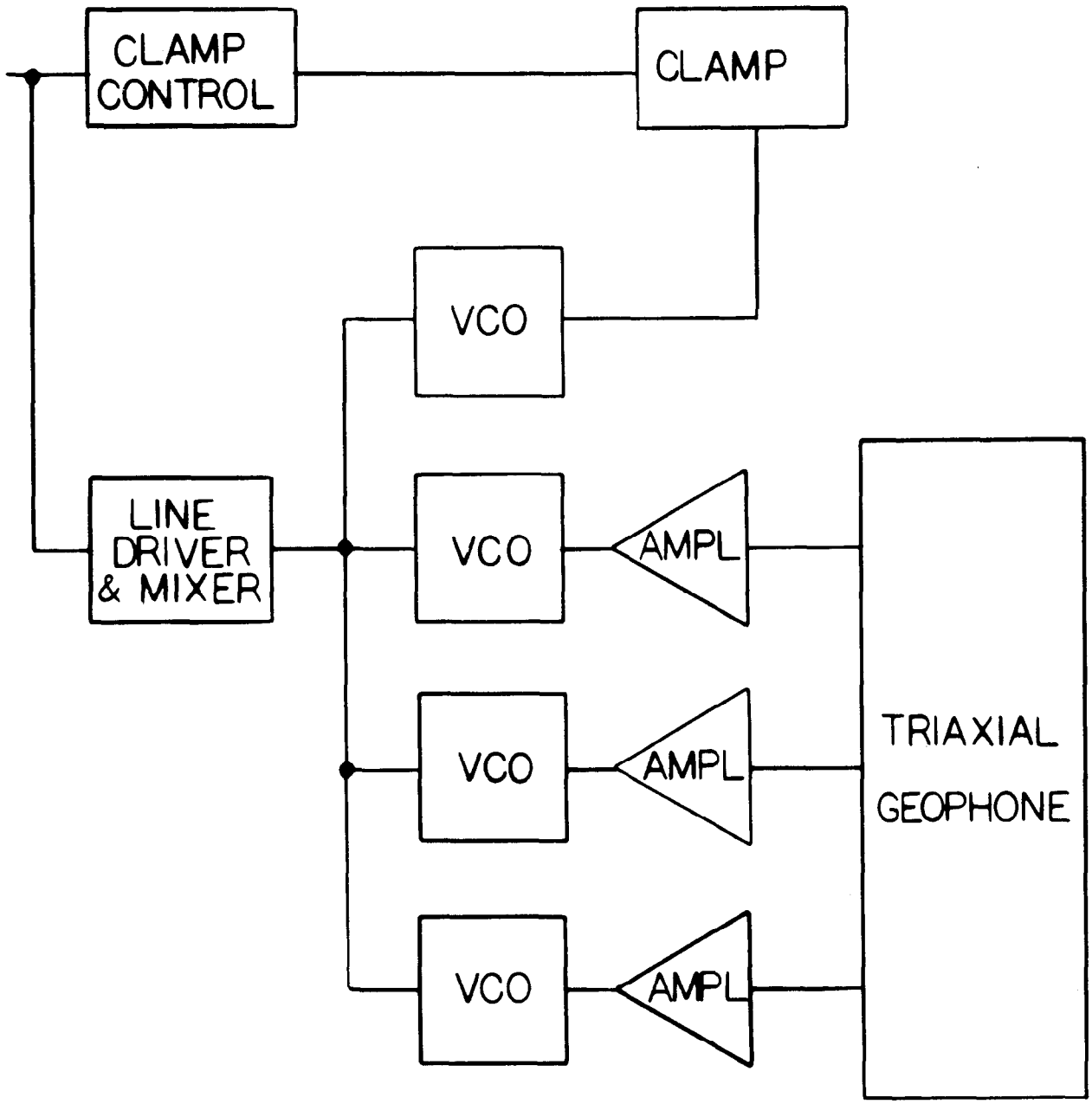

FIGURE II-4
Block Diagram of the Borehole Seismic System

complicated by intermittant tape recorder malfunctions to the extent that no signal characterization or source location could be determined. The borehole seismic unit because of its horizontal position, went into large mechanical resonance. One horizontal geophone had extremely large resonant characteristics indicating that in all likelihood it had been damaged in a previous test.

As a result of the low signal levels and malfunctions, no useful conclusion could be made from these tests and additional NTS tests were planned.

3. Amoco Experiments

Sandia participated in two experiments in November, 1978 with Amoco in the Wattenberg field, north of Denver, CO. These experiments were conducted in the Muddy J gas sand at approximately 8,000 feet.

The breakdown pumping schedules were designed to study seismic signals generated from fractures and hopefully to determine the direction of the fracture.

a) Experiment #1

The well was cased to a depth of 7,965 ft and open for approximately another 100 ft. Sandia's triaxial geophone package was clamped at 7,945 ft, and the well was fractured with 15,000 gallons of KCl water in small stages. An initial breakdown was performed with 100 gallons at five barrels-per-minute (BPM) followed with an additional 100 gallons at 1/4 to 1/2 BPM to determine closure stress. Following these two stages, the well was shut in and seismic activity was monitored and recorded for several minutes. Subsequent pumping stages were of 100, 200, 500, 1,000, 2,000, 4,000 and 7,000 gallons at 5 BPM, and each stage was followed by a 3 to 10 minute shut-in period in order to monitor seismic activity.

More than 65 signals were observed during these quiet periods. Of these signals, seventeen appeared to have sufficient amplitude to be examined. Five of these signals saturated this system and three were too low in amplitude to be usable leaving nine signals that could be analyzed.

The signals were bandpass filtered from 10 Hz to 400 Hz and digitized at

a 1 kHz rate. The signals were then further processed by using an adaptive filter to help eliminate periodic background noise. Hodograms of the horizontal geophones were then examined to predict fracture orientation. Bearings were obtained that ranged from 290° to 320° with an average of 305° indicating a fracture direction of N55°W to S55°E. A typical hodogram is shown in Fig. II-5.

b) Experiment #2

On 11/30/78, a breakdown fracture was conducted on Experiment #2. This well was completely cased and perforated from 7,910 to 7,940 ft. The Sandia seismic package was placed at 7,926 ft. The pumping schedule was the same as on Experiment #1, except that the breakdown and closure stress determination was a total of 100 gallons and the 2,000-gallon stage was increased to 2,100 gallons for a total of 15,000 gallons.

More than 10 seismic signals were observed but of lower amplitudes than those on the first test. Only five signals were large enough to obtain source direction. Bearings on these signals were from 105° to 147° with an average of 130° indicating a fracture direction of N50°W to S50°E. A typical hodogram is shown in Fig. II-6.

Shear wave arrivals could be observed in most of the signals for both tests as shown in Figs. II-5 and II-6 and ranged from a few milliseconds to as much as perhaps 15 ms following the compressional wave.

Distance to seismic sources can be determined as follows if the p and s wave velocities are known.

$$D = V_p(t_p - t_o) \qquad (1)$$

where D = distance to the seismic source

V_p = p-wave velocity

t_p = the time at which the p-wave arrives

t_o = the time at which the seismic wave was produced

also

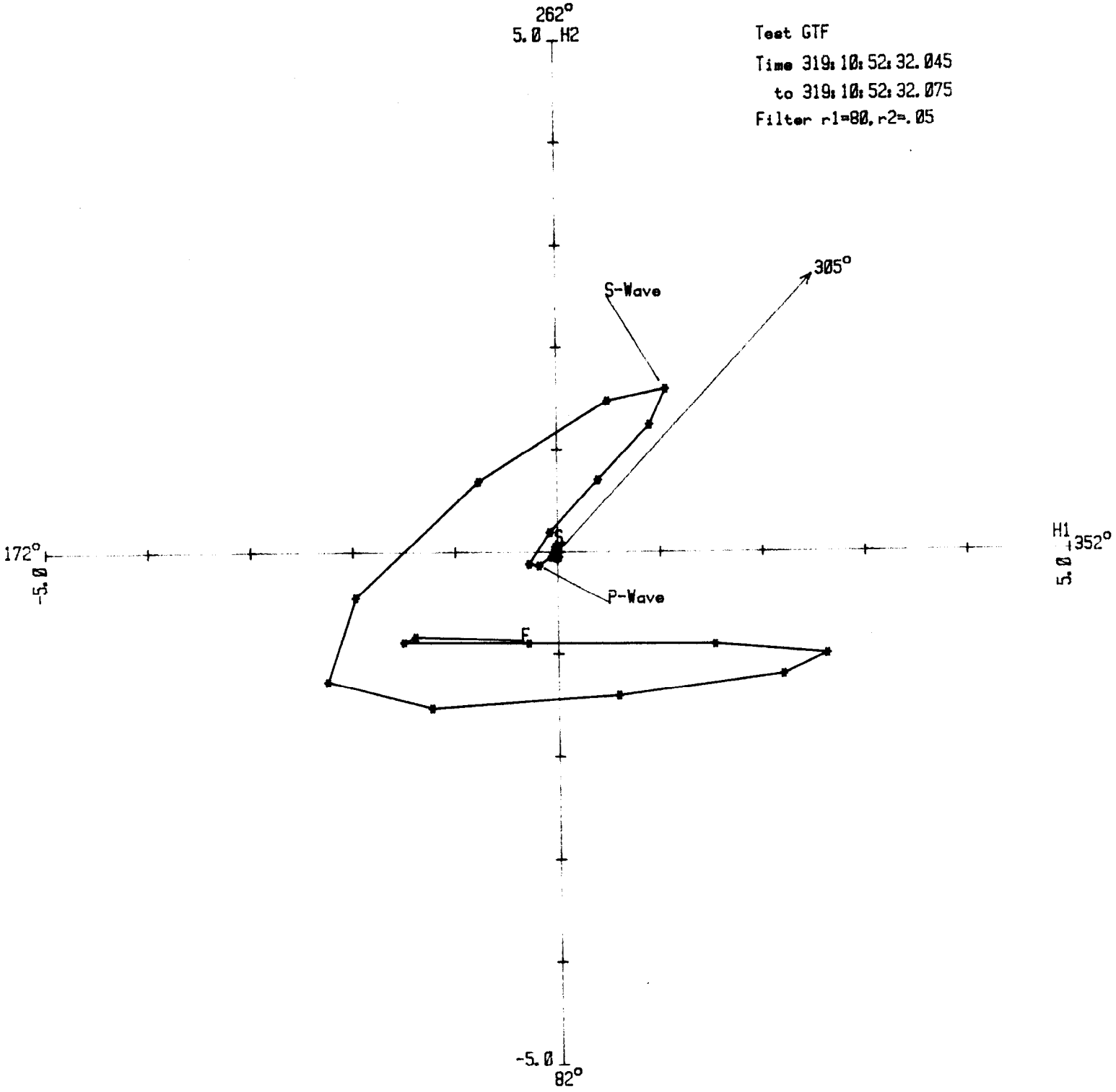

FIGURE II-5

Typical Hodogram for Experiment #1

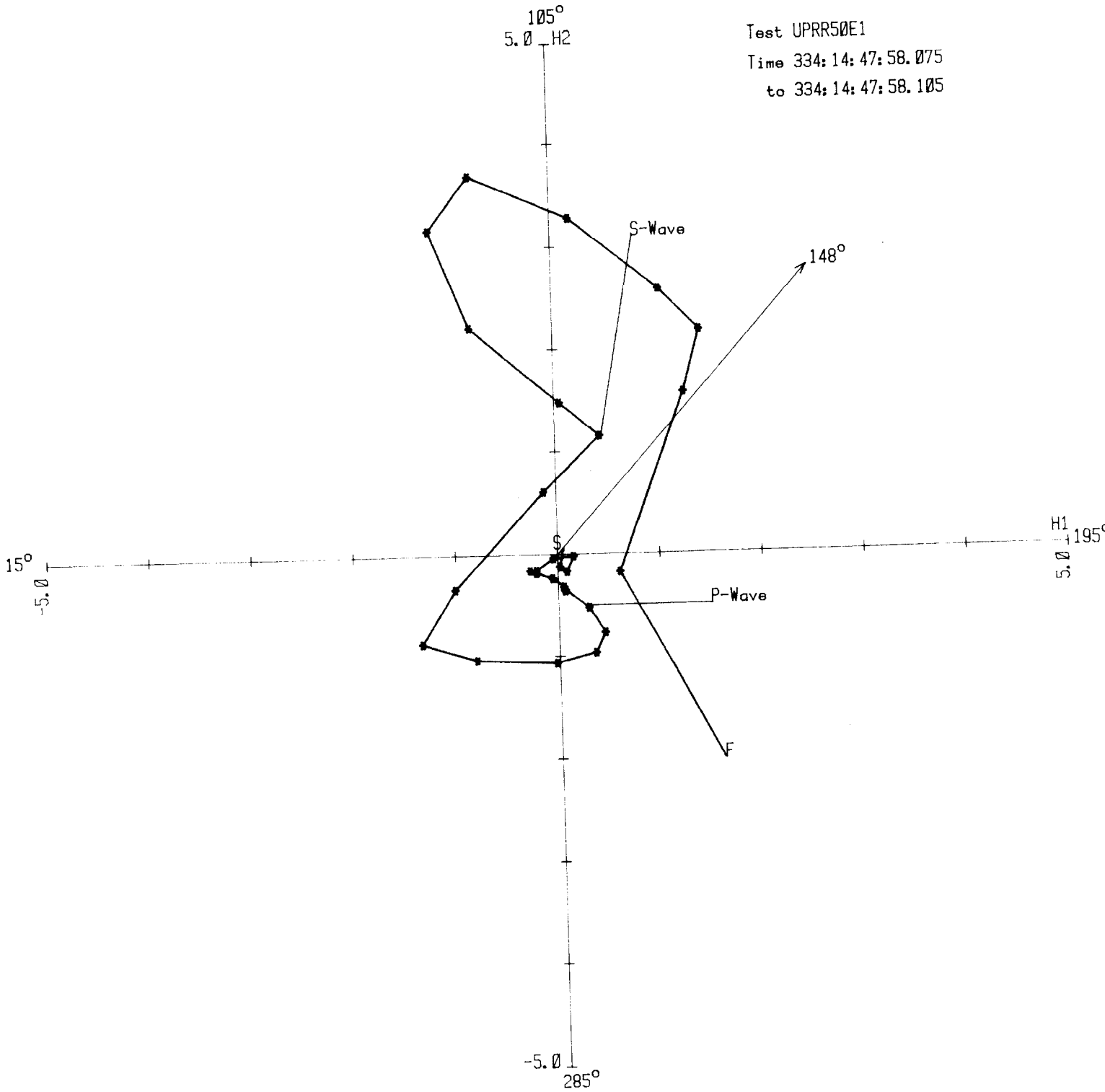

FIGURE II-6
Typical Hodogram for Experiment #2

$$D = V_s(t_s - t_o) \quad (2)$$

where V_s = s-wave velocity

t_s = the time at which the s-wave arrives

rearranging eqs. 1 and 2 we have

$$D/V_p = t_p - t_o \quad (3)$$

$$D/V_s = t_s - t_o \quad (4)$$

subtracting 3 from 4

$$\frac{D}{V_s} - \frac{D}{V_p} = t_s - t_p$$

rearranging 5 produces

$$D = \frac{V_s V_p \Delta t}{(V_p - V_s)}$$

where Δt = the time difference of the p-wave and s-wave arrival.

If one uses a p-wave velocity of 10,000 feet-per-second and an s-wave velocity of 5,000, which could be typical for sandstone formations, the seismic sources producing the signal shown in Figures 5 and 6 would be approximately 20 and 150 ft from the wellbore.

4. NTS Borehole Tests

In order to determine the origin of known seismic sources and study the oscillatory signals, an evaluation test of the borehole seismic unit was designed and performed at the Nevada Test Site. The clamp package was installed in the floor of G-Tunnel and adjacent to it, a triaxial geophone package using the same type of geophones was grouted in a borehole. Seismic signals were then induced, and the received signals analyzed for determining the source locations. In addition to the induced seismic signals, a triaxial geophone was attached to the clamp unit and driven from a sine wave source at various frequencies to see if resonances did exist in the clamp package.

Seven holes were drilled in the floor of the Madison drift in G-Tunnel. The relative locations of these holes are shown in Fig. II-7 as R, C, and W3

through W7. A triaxial geophone unit was placed in Hole R at a depth of 18 ft with the horizontal geophones oriented as indicated by H1 and H2 in Fig. II-7. The hole was then filled with acoustic matching grout. The borehole seismic unit was placed in Hole C at a depth of 18 feet with the horizontal geophones oriented as shown by H1 and H2 and clamped to the sidewall.

The shaker geophones attached to the borehole seismic unit were driven from 20 Hz to 2 kHz and resonances were observed at a number of different frequencies. At a later time, the borehole seismic unit was coupled to the wall through sand (i.e., the hole was filled with sand) and the resonant frequencies changed. The resonances were large enough to prohibit extraction of any useful information from the seismic tail.

A number of methods of inducing seismic signals were attempted both on the floor of the tunnel and in the bottom of the holes. The only sources that produced adequate signals were hammer blows on the floor and a spark plug fired in water at the bottom of the holes. The results of these tests are tabulated in Table II-1

In tests 1 through 3 (Table II-1) the seismic source was from firing a spark plug in the bottom of the hole. By recording the ignition times, the p-wave and s-wave travel times could be obtained and velocities calculated. The average velocities were then used to obtain distances in the other tests.

In each test, the borehole seismic system determination of the source was at least as good as the grouted reference package. Some of the source locations are rather poor, but this is to be expected whenever the signal levels are too low or too large. The reference unit has a decided shift in location in the clockwise direction. It is expected that the unit had been rotated during grouting from its original position.

Based on the tests and experiments performed with the borehole seismic system, it is reasonable to conclude that fracture orientation can be determined in most cases. With knowledge of p-wave and s-wave velocities, fracture distances could be estimated. Any additional information that may have been

NTS CLAMP PACKAGE EVALUATION TEST
HOLE AND IMPACT POINT LAYOUT

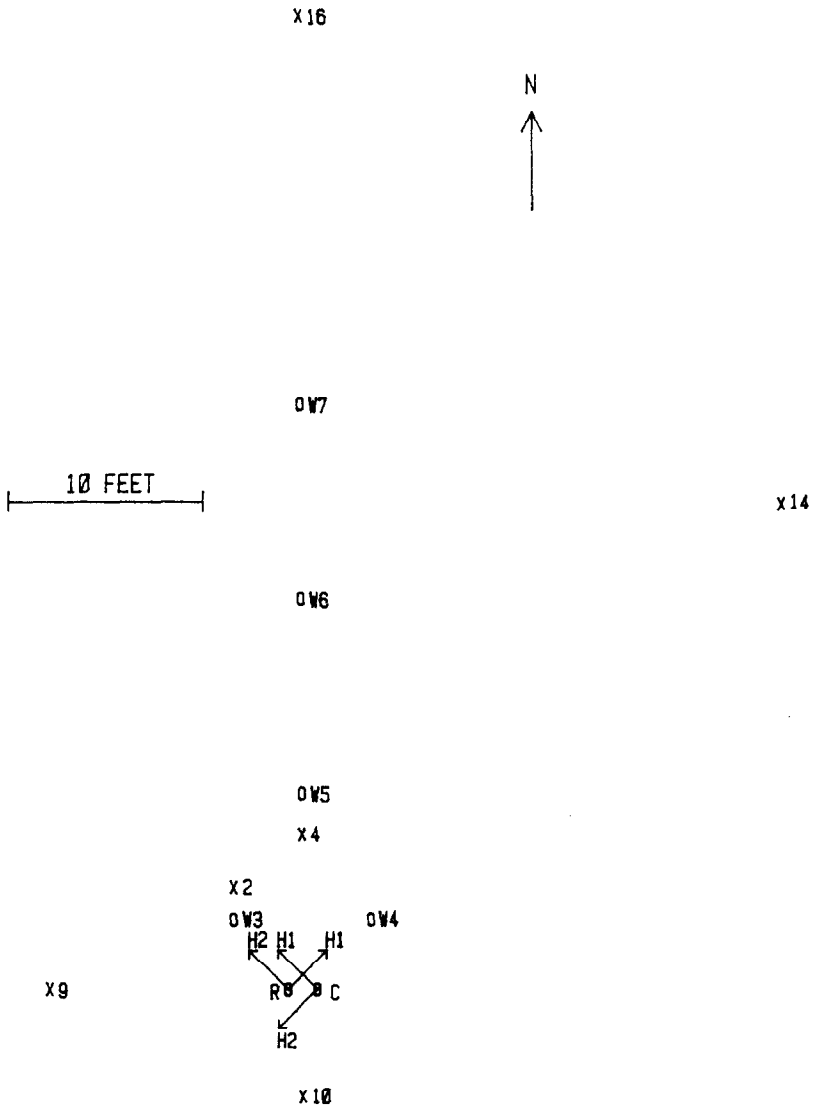

FIGURE II-7

NTS Clamp Package Evaluation Test
Hole and Impact Point Layout

Test	Source	Source Location (Note 1)	Unit	Actual Source Position (Note 2)					Measured Source Position (Note 2)					Arrival Time (MS)		Velocity (Ft/Sec)		S-P time (MS)
				Direction (Deg.)	Elevation (Ft)	Vertical Angle (Deg.)	Distance (Ft)	Horizontal Distance (Ft.)	Direction (Deg.)	Elevation (Ft.)	Verticle Angle (Deg.)	Distance (Ft)	Horizontal Distance (Ft)	P-Wave	S-Wave	P-Wave	S-Wave	
1	Spark Plug	W7	Clamp	N1.4W	0	0	30.0	30.0	N14W	0	0	29.3	29.3	4.6	8.4	6528	3575	3.8
			Reference	N1.4E	0	0	30.0	30.0	N32E	0	0	33.9	33.9	4.4	8.8	6825	3412	4.4
2	Spark Plug	W7	Clamp	N1.4W	0	0	30.0	30.0	N20W	0	0	30.8	30.8	4.6	8.6	6528	3492	4.0
			Reference	N1.4E	0	0	30.0	30.0	N16E	0	0	30.8	30.8	4.4	8.4	6825	3575	4.0
3	Spark Plug	W6	Clamp	N2.2W	0	0	20.0	20.0	N15W	0	0	21.6	21.6	3.4	6.0	5885	3335	2.8
			Reference	N2.2E	0	0	20.0	20.0	N34E	0	0	17.0	17.0	3.0	5.2	6670	3848	2.2
4	Hammer	2	Clamp	N39.5W	18	70.6	19.2	6.8	N45W	14.9	75	15.4	4.0					2.0
			Reference	N28.2W	18	72.7	19.0	5.9	N53W	15.4	87	15.4	0.8					2.0
5	Hammer	4	Clamp	N5.4W	18	68.0	19.7	8.0	N64W (Note 3) (Note 4)	33.4	70	35.5	12.1					4.6
			Reference	N5.4E	18	68.0	19.7	8.0										
6	Hammer	W7	Clamp	N1.4W	18	30.9	35.0	30.0	N12W	17.0	30	33.9	29.4					4.4
			Reference	N1.4E	18	30.9	35.0	30.0	N20E	18.0	32	33.9	28.8					4.4
7	Hammer	9	Clamp	N90W	18	52.6	22.6	13.8	N01W	12.4	53	15.4	9.2					2.0
			Reference	N90W	18	55.8	21.8	12.2	N76W	10.8	61	12.3	6.0					1.6
8	Hammer	10	Clamp	S7.7W	18	72.6	18.9	5.6	S19W		83							Note 5
			Reference	S7.7E	18	72.6	18.9	5.6	S45W		62							Note 5
9	Hammer	W3	Clamp	N50.5W	18	72.8	18.8	5.6	W70W		69							Note 5
			Reference	N38.2W	18	75.9	18.6	4.5	N5W		83							Note 5
10	Hammer	W4	Clamp	N38.2E	18	75.9	18.6	4.5	W27E		85 (Note 5)							Note 5
			Reference	N50.5E	18	72.8	18.8	5.6	W88E	17.6	65-80 (Note 5)	18.5	5.6					2.4
11	Sledge	14	Clamp	N44.1E	18	27.6	38.9	34.5	N45E		9-32 (Note 5)							Note 5
			Reference	N45.9E	18	26.9	39.8	35.5	W88E	11.2	27	24.7	22.0					Note 5 3.2
12	Sledge	16	Clamp	W0.9W	18	19.8	53.2	50.0	N4W	12.8	28	27.8	24.7					3.6
	Hammer		Reference	W0.9E	18	19.8	53.2	50.0	N9E	5.1	10	29.3	28.8					Note 6 3.8

1 - Refer to Figure 5
2 - With respect to each geophone package
3 - P-wave very low - difficult to obtain direction
4 - P-wave amplitude too low to estimate direction
5 - P-wave saturated - cannot obtain S-wave arrival
6 - S-wave saturated - SP time can be in error

TABLE II-1

Results of NTS Borehole Tests

contained in the seismic tail could not be extracted due to the system resonances which generally occurred after the s-wave arrival.

B. Borehole Hydrophone System (R. P. McCann, 4733)

1. System Applications

The downhole hydrophone system under development by Sandia Laboratories is to be used in two distinct areas. The first considered is in the measurement of formation velocities to aid in the investigation of oil and gas formations; the second is for the downhole detection of passive acoustic signals for the purpose of hydraulic fracture diagnostics.

a) Formation velocity. The idea of using compressional waves as an aid in the assessment of oil and gas formations is not new. It was established early that the compressional wave propagation velocity depends on the lithology and porosity of a formation[2]. One of the basic tools used as an aid in determining formation porosity and helpful in interpreting seismic records has been the acoustic velocity log. The log is a recording, as a function of depth, of the time required for an acoustic wave to travel a unit distance of formation. The basic logging tool includes an acoustic projector and two receivers which are incorporated in the logging tool. In general, the acoustic wave velocity is higher in the formation than in the drilling mud, and in measuring first arrival times, the propagation velocity in the formation can be determined. Because the acoustic wave penetration of the formation is a function of projector to receiver spacing, the prime velocity measurement is often of the invaded zone of the formation, and measurements in the past have indicated that the velocity in the invaded zone around the well can be substantially different from the true velocity in the deeper uncontaminated zone. Therefore, it is desirable to extend the spacing between the acoustic projector and receivers to the maximum possible length[3]. An acoustic velocity system making use of this principle has been designed and is now available for evaluation and test.

b) Source locator. Early experiments in techniques to detect and map hydraulic fractures have shown that acoustic signals in the 100 Hz to 2,000 Hz frequency range are detected by a downhole hydrophone immediately following a hydraulic fracturing operation[4]. At the conclusion of pumping, these signals continue at about a constant rate throughout a 30-minute period while the well is shut-in. Because only one acoustic detector was employed, it was not possible to obtain information on source locations. Attempts have been made to measure at the earth's suface fracture oriented seismic or acoustic signals. The very poor signal-to-noise ratio encountered with such distances involved makes detection of the signal highly improbable[5]. Signal detection from fractures thus require that multiple sensor receivers be deployed near the fracture source.

2. System Description

The borehole hydrophone system makes use of commercially available components where possible. The electronic system circuitry and components are designed to allow operation on a single conductor wireline. In both intended uses of the hydrophone system, the single conductor wireline provides power to the electronics and transmits the received hydrophone signal via multiplexed voltage-controlled oscillators to the surface for recording and analysis.

The downhole hydrophone package consists of a stainless steel rod approximately 30 ft in length and 1.5 in diameter. The frequency response of the system to $\pm$ 3 db is approximately 30 Hz to 4 kHz. The maximum operating temperature is 250°F, and the specified maximum operating pressure is 10,000 psi.

The rod contains four hydroacoustic transducers spaced at 10-ft intervals. The electronics package is contained in the section of rod between the top two transducers. This packlage includes four high-gain acoustic amplifiers, four constant-bandwidth voltage-controlled oscillators, a mixer-line driving amplifier, and a $\pm$ 15 Vdc power supply.

Although the design and fabrication of the acoustic transducer unit in itself is well within the state-of-the-art, the mechanical housing and its design is a task which has not been attempted in the past. Because of the unique mechanical and environmental requirement, two sets of transducer units have been received from two different manufacturers. One set of hydrophones (6 each) has been received from Edo Western Corporation, Salt Lake City, Utah and the other from International Transducer Corporation (ITC), Goleta, California.

3. Prototype Testing

A system was designed at Sandia Laboratories for electrical testing of the acoustic hydrophones to 10,000 psi. Although the testing performed was of a rudimentary nature, the data collected clearly indicated that all the Edo hydrophones operated to 10,000 psi and, as expected, the signal sensitivity is reduced at the higher pressures. Some testing has been completed on the six hydrophone units received from International Transducer Corporation. Pressure tests were made to 10,000 psi. As with the Edo Western the high pressure seal system of the hydrophones functioned satisfactorily on all of the units, however several of the units failed to operate electrically above 9,000 psi. Because the electrical test performed was a very simple go-no-go type, the failure could be anywhere in the testing system and further tests will be required to determine if an electrical operational problem with the transducer unit does exist at high pressures. The required electronics and mechanical hardware is on hand for the assembly of a 30-ft ITC system. The system tool will be assembled and tested in the near future.

The complete 30-ft system containing the hydrophones fabricated by Edo Western has undergone some testing in the Sandia borehole located at the laboratory. The bottom of the 6-in diameter hole is at a depth of 245 ft. The casing is to a depth of 200 feet. The water level in the borehole was detected at a depth of 142 feet. Two types of tests were made on the hydrophone system. One consisted of a series of hammer blows on the ground

surface at various distances from the borehole. The second included a small vibrator placed at a distance of approximately 40 feet from the borehole which was driven at CW frequencies of 30 Hz to 500 Hz. A driving frequency of 100 Hz was chosen in recording the hydrophone output signals. In addition to recording the output on a paper recorder and a magnetic tape recorder, the differences in phase between all hydrophone output signals were measured on an oscilloscope. These measurements were made with the top of the hydrophone tool varying from a depth of 150 ft to 170 ft in 2-ft increments. Analysis of the data indicates that the measured formation velocity is in the range of 1,000 ft-per-second to 2,000 ft-per-second. The actual formation velocity is believed to be more in the order of 5,000 ft-per-second. Because the vibrator output is small, distances greater than approximately 40 ft from the borehole lead to small signals of an eratic nature and phase measurements became very difficult to measure. It is believed that surface waves from the vibrator were coupled into the borehole and a borehole wave was created which interfered with the direct wave. Consequently, erroneous formation-velocities were measured. A series of tests are to be scheduled in an area where deeper boreholes and a more powerful vibrator are available.

The hammer blow testing was done only to determine that differences in the time of arrival at the downhole hydrophones could be detected. A sophisticated measurement attempt was not made. The test was successful and differences in arrival time could be detected. Fig. II-8 shows the output from a hammer blow struck 100 ft from the borehole. The differences in arrival time are not readily apparent in this time scale, however when expanded in time the differences are quite discernable.

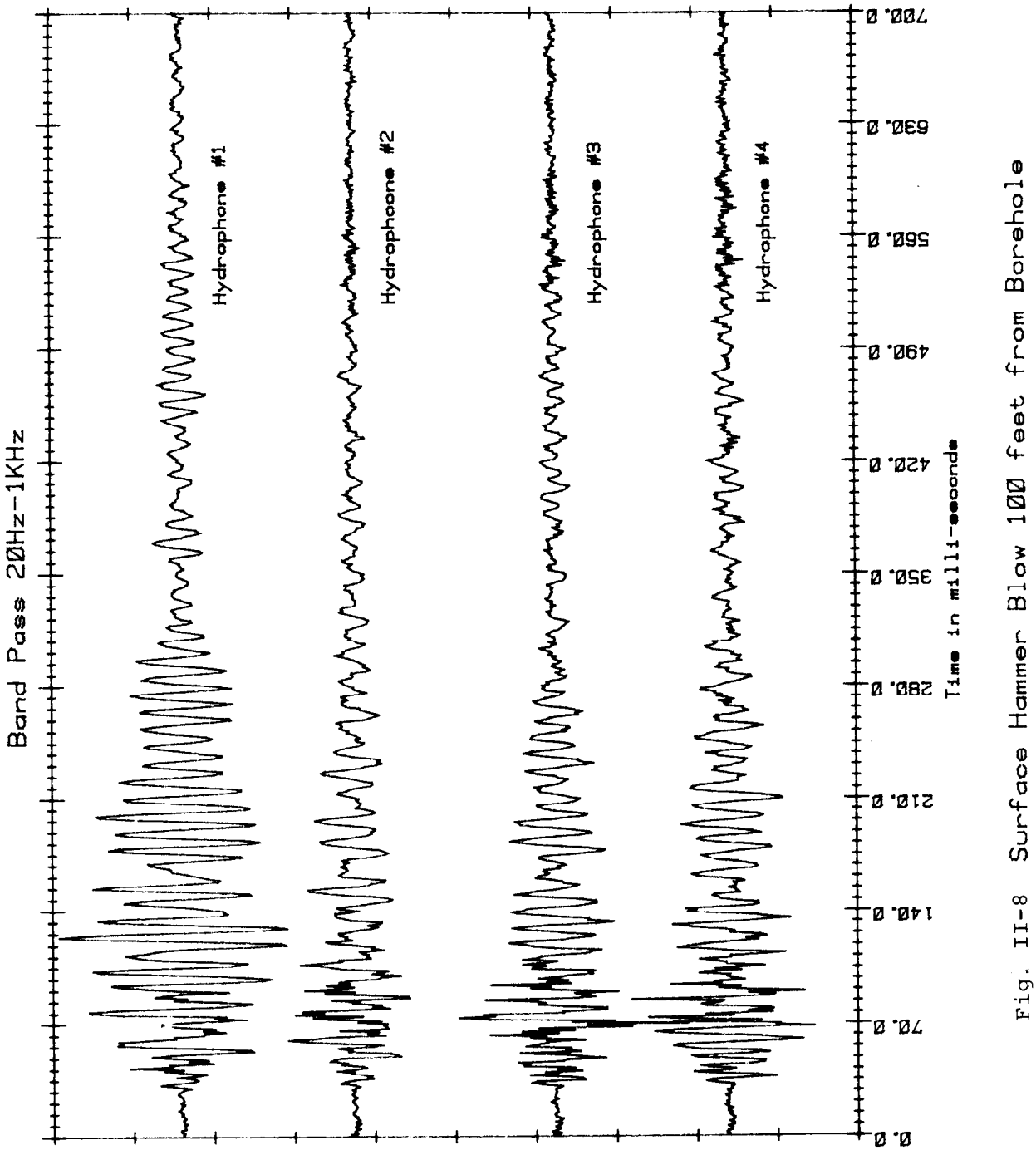

FIGURE II-8

Surface Hammer Blow 100 Feet From Borehole

C. Surface Electrical Potential System (SEPS) (L. J. Keck, 4733)

1. System Description

Electrical prospecting is a well-known technique that is used in the investigation of geological structures beneath the surface of the earth. The approach taken is to determine the variation of the electrical constants of the earth's crust, and variation in resistivity is by far the greatest. The induced surface electrical potential method used in MHF characterization uses the variation in the resistivity contrast and is associated with the science (or art) of electrical prospecting. A current injection probe is placed at the fracture formation depth in the fracture well. A remote well casing serves as the return current probe. The resulting potential distribution is measured at the surface of the earth on circumferences around the fracture well.

Theoretically, before the fracture, equipotential ellipsoids form concentrically around the well casing as their center. These ellipsoids form concentric circles around the fracture well at the surface. During fracture, the fracture zone, along with the well casing (both filled with conducting fluid) acts as a changing current injection electrode. As the fracture progresses, the changes in electrode geometry cause a predictable distortion in the concentric equipotential circles around the fracture well.

The surface electrical potential data are taken by periodically recording the induced potential differences at the earth's surface between data probes (in concentric circles) placed every 15° circumferentially around the fracture well, and a data reference probe (stake). The injected current is of a bipolar pulse form to minimize the effects of electrode polarization. Prior to fracture initiation, background data are taken to establish the baseline potential levels around the fracture well at the data probes. These then become the reference data for detecting the changes when the conductive fracture fluid alters the electrical geometry of the fracture

zone. This change in the fracture zone current distribution, caused by fracture growth, alters the induced surface electrical potential around the fracture well. If the electrical potential measurements before, during and after the fracturing are compared, diagnostic information about the fracture is obtained.

SEPS is capable of acquiring 48 electrical potentials around the fracture well. These potential points are arranged in two concentric circles (Fig. II-9) around the well, each circle consisting of 24 stainless steel stakes (data probes) approximately 2 ft long.

Each of the 48 data sources exist between a data probe and the reference probe. This data acquisition arrangement will provide a confidence factor if the data from each data radius flags the same fracture direction. The data probe array radii range from 1000 to 4000 ft and are determined from a mathematical model which considers such parameters as fracture depth and expected fracture length(s). The potential measurement boxes (PMB) are connected to the reference probe via the instrumentation van. This enables the PMB signal common to be used as a common tie for both the fracture data acquisition and for calibration.

Each (PMB) includes a radius 1-radius 2 select capability, a 1 Hz passive bandpass filter in front of an isolation amplifier, and a 4-pole active linear phase low-pass filter. The active filter has a cutoff of 1.75 Hz which gives a data bandwidth from approximately .25 to 1.75 Hz. The 1 Hz bandpass filter helps eliminate probe-to-reference probe current flow via the isolation amplifier input impedance. The combined filter effects reduce that portion of the telluric spectrum outside the pulse's fundamental frequency of 1/2 Hz.

The reference probe is located a distance five to ten times the radius 1 from the fracture well, and this common is one of the conductors within the interconnecting six conductor cables. These cables are also used to interconnect the 24 PMB's to the instrumentation van. The cables supply power, control and calibrate inputs to the PMB's and carry the subcarrier VCO outputs back to the instrumentation van. Test control in the instrumentation van interrelates all

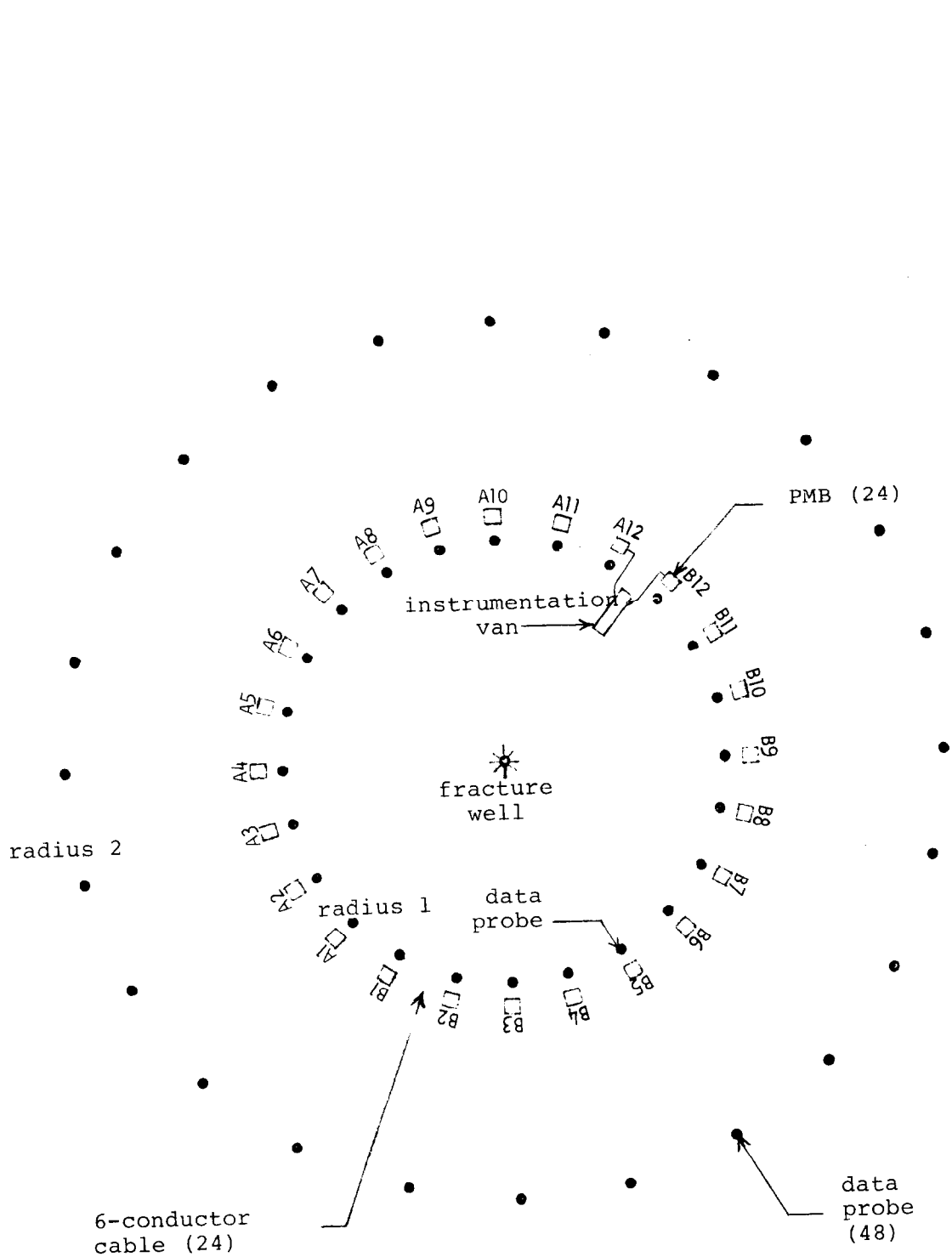

FIGURE II-9

Surface Electrical Potential System - Fracture Well Layout

functional aspects of SEPS. The computer is a DEC PDP 11/34 and includes dual soft and hard discs for data storage and handling. Digital outputs from the computer control a programmable supply for the bipolar calibration source. The computer, via the test control, also controls the radius 1-radius 2 selection. The A and B sets of twelve subcarriers from the PMB's, containing either calibrate or radius-1 and radius-2 data, are extracted from the six conductor cables in the test control and input to the A and B subcarrier discriminators. The outputs of these 24 data sources are digitized in the computer. When SEPS is stored in the instrumentation vans, the test control can simulate radius 1-radius 2 operations from the calibrate source and makes them available as inputs to the PMB's. The SEPS has undergone many hours of testing in this configuration.

2. AMOCO Wattenberg Field Fracture Experiment

Sandia participated in only one hydraulic fracture experiment using the SEPS system in FY 79 not being in the Amoco Wattenberg field, in FY 79. The well was fractured using 8,000 barrels of fluid with 2% KCL in the Muddy J gas sands at a depth of 7,972 ft. The Surface Electrical Potential System (SEPS) recorded data at radii of 1,200 and 2,400 ft (Fig. II-10) for the main fracture. Five data points on radius 2 were less than 2,400 ft due to lack of land use permission. The data reference probe was located approximately 1.6 miles east of the D-1 well. Current from the SEPS was injected via the current injection probe located at a depth of 7,964 ft via a wireline hung inside the casing. Two current sink wells were used and a set of data was obtained for each sink well and potential radius. Loop 1 had a resistance of 64.4 ohms and used the West sink well Loop 2 had a resistance of 71 ohms and used the North sink well. Figure II-11 illustrates the data reference stake and sink well layout.

Fracture pressure and flow were recorded by SEPS using the Dowell transducer. Fracture fluid pumping stopped temporarily at 9:33 am and resumed at 10:00 am. Several such pumping interruptions occurred throughout the fracture treatment.

The induced surface potential data collected during the MHF experiment has been analyzed and no positive indication of fracture direction was obtained.

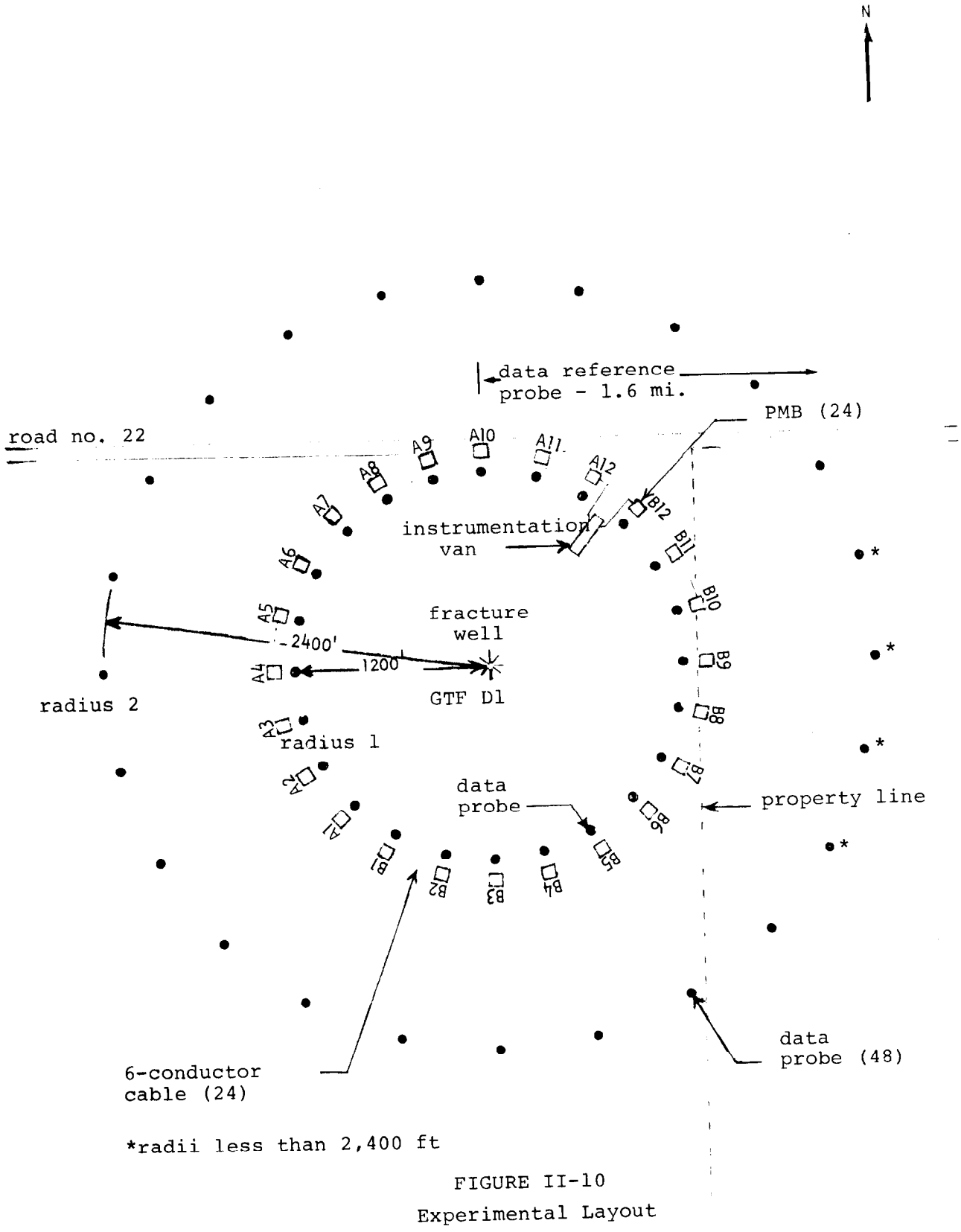

FIGURE II-10

Experimental Layout

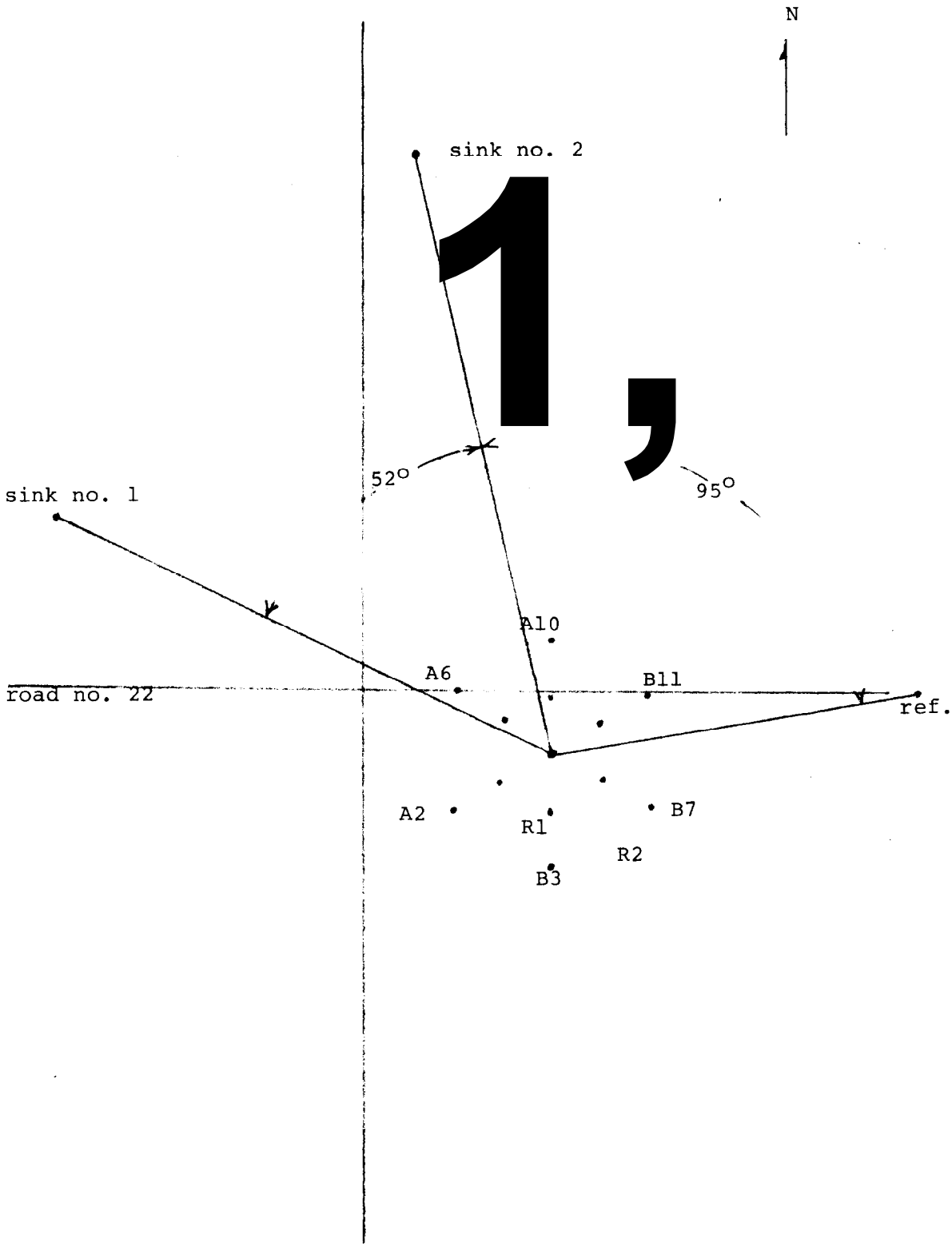

FIGURE II-11

Data Reference and Sink Well Layout

Two factors prevented these data from being useful for determining the fracture orientation. First, transient voltage spikes in excess of 1 volt were present on the leading and trailing edges of the millivolt level potentials. These transients saturated the instrumentation amplifiers and prevented an accurate measurement of the desired signals. These high-voltage spikes were evidently caused by the high rate of charge on the leading and trailing edges of the current pulse. Second, the injected current level from the pulse generator increased abruptly from 4 amps to 12 amps, approximately half way through the experiment, with no corresponding increase in potential voltages. Turbulence and/or fluid flow in the tubing could have caused a change in the character of the conductive fluid. Changes in the injected current of this magnitude hinder the comparison of induced surface potential signals occurring before and immediately after pumping commenced with those potentials occurring during the latter stages of the experiment.

3. Design Changes To SEPS

This experiment prompted several design changes to SEPS. First, the risetime of the current injection pulse has been significantly increased. This has reduced the pulse upper frequency content to approximately 10 Hz. The intent is to reduce the frequency content that is assumed to produce the high amplitude leading and trailing edge spikes. Second, the Potential Measurement Boxes (PMB) have been modified to increase the speed of recovery from such a high amplitude spike. Finally, consideration is being given to methods whereby the unintended surface current injection due to test layout can be reduced. One approach considered is that of using shielded current wire from the pulses to the frac well wireline and sink well.

REFERENCES

1. Third Annual Report-EGR, 10/77-9/78, D. Northrup and C. L. Schuster, (1978).

2. Pirson, S. J., "Handbook of Well Log Analysis", Prentice-Hall, Inc. Englewood Cliffs, NJ, (1963).

3. Gretener, P. E. F., "An Analysis of the Observed Time Discrepancies Between Continuous and Conventional Well Velocity Surveys", Geophysics, Vol. 26, No. 1, February (1961).

4. Power, D. V., C. L. Schuster, R. G. Hay, and J. Twombly, "Detection of Hydraulic Fracture Orientation and Dimensions in Cased Wells", SPE5626, presented at the SPE 50th Annual Fall Meeting, Dallas, TX, September 25 - October 1 (1975).

5. McCann, R. P., R. G. Hay, and L. C. Bartel, "Massive Hydraulic Fracture Mapping and Characterization Program, First Annual Report: August 1975-July 1976", Sandia Laboratories Report SAND77-0286, June (1977).

III. Advanced Logging Technology and Formation Evaluation

A. Seismic Formation Mapping Program (T. L. Dobecki, 4733)

1. Introduction

Gas production from formations of interest to the U. S. DOE Western Gas Sand Project (WGSP) is from tight, lenticular sand intervals typical of the upper Cretaceous Mesa Verde group and the Tertiary Wasatch formation. The lenticularity and the meandering nature of the reservoirs is a direct consequence of their being laid down in a fluvial environment. Characterization and separation of such reservoirs, prior to field development, are important to the efficient exploitation of the contained gas resource through proper well placement, understanding of geometry of individual traps, and the proper design of fracture treatments which are required to increase permeability in these tight reservoirs. It is the objective of this program to evaluate state-of-the-art seismic reflection techniques as a means of mapping the three-dimensional geometry of channel sands utilizing surface-derived data.

This new program is an outgrowth of discussions held at the Borehole Logging Program meeting convened at CER Corporation in October 1978, wherein concern was raised over the present inability to delineate and map individual sand channel reservoirs typical of the Mesa Verde Group. Sandia proposed at this meeting that state-of-the-art seismic reflection concepts (seismic stratigraphy, 3-D seismic) might be a means of delineating sand channels from surface derived data. Applicable case histories have been compiled and interviews conducted with experts in the fields of seismic reflection surveying and Cretaceous stratigraphy in the Utah, Colorado, Wyoming areas. The results of this preliminary investigation were presented in a briefing for CER and DOE personnel held at CER, Las Vegas, in February, 1979. It was decided that a limited seismic program should be performed and that a coordinated effort with C. K. Geoenergy Corporation, which is performing statistical analyses of primary sedimentary structures in channel sands in outcrop, would be mutually beneficial.

A site (Fig. III-1) in the southern Uinta Basin in Utah, approximately 45

miles northwest of Grand Junction, CO was chosen for this combined seismic and stratigraphic program.

The prime criteria to be met by a satisfactory site were: a) relatively flat ground on top of a mesa or ridge, b) exposed Mesa Verde group in the cliff walls, and c) adequate existing well control for stratigraphic information and for access for the proposed drilling operation. Such a site was found in the general area of Sections 4, 5, 8, 9, 16, and 17, T17S, R24E. This area is on a ridge just west of East Canyon with approximately 1,000 ft of Mesa Verde group exposed in the cliff faces.

An additional site was located a few miles to the northwest on top of the highest ridge in the area. The same Mesa Verde interval is found at 1,800 ft subsurface with outcropping Green River formation. This site has a large flat area and at least one gas well for subsurface control. This site will be a seismic site only (i.e. no corehole study) with the intent of determining the ability of seismic to map unknown structures at a greater depth than at Site #1.

The U.S.G.S. Phoenix (seismic) computer has a substantial seismic modeling capability which would be useful in modeling the synthetic seismic response of channel sands embedded in a sand-shale sequence. This is an important aspect in evaluating seismic techniques for mapping sand lenses. The computing facility has been made available to Sandia and a preliminary model study has been completed.

2. Task Description

Phase I of the program includes a seismic reflection survey at a specific site (see "Site No. 1" description below) in the Southern Uinta Basin, Utah. This site has shallow (0-1,500 ft) Mesa Verde group of which the upper 1,200 ft is exposed in adjacent cliff walls. This site is also undergoing geologic and corehole scrutiny by C. K. Geoenergy Corporation as part of the WGSP, while the U.S.G.S. has been involved in mapping throughout this area. By analysis of outcrop mapping, detailed core analysis, and analysis of

available well log data at this site, an evaluation of the seismic mapping capability may be made directly. Although this site presents depths substantially less than expected production depths, it presents a unique opportunity to assess seismic ability by comparison to both visual (outcrop) and geologic data.

Phase II of the program will investigate deeper sand bodies. At a site some seven miles northwest of Site No. 1 (see "Site No. 2" description below), a seismic survey is to be performed to map channel sands in the Mesa Verde group and in overlying formations. At this site, the top of the Mesa Verde is some 1,800 ft subsurface. Overlying rock includes sand channels of the Tertiary Wasatch fm. and the relatively channel-free Green River fm. No corresponding outcrop and dense well control is available at this site. The intent of this phase is to compare seismic ability with that at Site No. 1. Here, the objective bed is (a) at a greater depth and (b) is complicated by stratigraphic variation in overlying beds.

3. Site Descriptions

Site No. 1 is situated on the top of a ridge within the Bryson Canyon Gas Field (Sections 8, 9, 16; T17S; R24E; Grand County, Utah). The general elevation of the ridge top is 7,000 ft, while the adjacent canyon bottom is approximately 5,600 ft. The sides of the ridges are very steep, while the tops are relatively flat and are traversed by well service roads.

Exposed on the canyon walls are the Upper Cretaceous Farrer Fm. and overlying Tuscher Fm. (both in Mesa Verde group), although the higher elevations in the area are capped with Tertiary formations. The upper 1,000-1,400 ft beneath the ridge top, seismic line area consists, then, of numerous sandstones of variable thickness (up to approximately 60 ft), some of which are continuous over the area while others are lenticular and of limited cross-sectional extent. Softer, shaley layers make up the remaining section observed in the canyon walls. Numerous wells are available in this area for

subsurface control.

Site No. 2 is situated on the highest ridge in the area within the Horse Point Gas Field (Sections 11, 13, 14; T16S; R23E; Grand County, Utah). The general elevation of the ridge top is 8,200 ft; the ridge top is quite flat, over 1/2 mile wide, and is traversed by service roads. As with Site No. 1, the bounding canyon walls are quite precipitous.

Site No. 2 is situated on Eocene Green River Fm. The depth to the Upper Cretaceous bed outcropping at Site No. 1 is believed to be approximately 1,800 ft through the Green River, Wasatch, and other Tertiary formations. A single well is available in this area for subsurface control.

4. Program Progress

Drilling has begun on the corehole located at Site No. 1 of the proposed seismic survey. This corehole, together with outcrop mapping of sand lenses, will provide important input to the interpretive phase of the proposed seismic survey.

The contract for performance of this three-dimensional seismic reflection program has been awarded to Seismic Research International (SRI) of Denver, CO. In early July, patterns of areal seismic coverage for each site were designed. In addition, specific "target" sand lenses cropping out in the cliff faces at Site No. 1 were noted for use in preliminary transmission/reflection tests to determine frequency content of wavelets transmitted from the top of the cliff (survey location) as well as travel times to these specific units.

SRI has secured Bureau of Land Management (BLM) approval for survey operations. This task was compounded by the fact that the two sites, although less than 12 miles apart, fall under the jurisdiction of two separate BLM offices. Topographic survey activity began the latter half of August, and the reflection work is now in progress.

B. Nuclear Magnetism Logging (T. L. Dobecki, 4733)

A constant complication in field development involving tight, Western gas sand reservoirs is an effective means of determining in-situ formation

permeability. Typical pumping tests require several weeks of testing before reliable, usable data are acquired. Several reports[1,2,3,4,5,6] in petroleum literature have noted the theoretical effects of pore size, permeability, and fluid saturation on the observed nuclear magnetic resonance (NMR) behavior of formation samples. Further, empirical relationships have been developed to relate free-fluid index, FFI (a quantity derivable from a nuclear magnetism log, NML) thermal relaxation time, T_1, of the fluid bearing rock, and the bulk relaxation time, T_B, of the saturating liquid to the permeability of the formation. The relationship has been based primarily upon the Kozeny-Carman equation which links permeability to porosity, specific surface area, and pore space tortuosity. What has been observed is that NML measurements can provide a measure of permeability which is both rapid and reliable within a given producing field. What is lacking, however, is a test of the reliability and accuracy of NMR measurements in low permeability (~10-50 μd), shaley sandstones, typical of the western gas sands. Emphasized is "NMR" as opposed to "NML" because currently available NML tools have intrinsic operational time lags which do not allow T_1 determinations in such low permeability rocks. Sandia's program is to evaluate the applicability of NMR measurements to permeability analysis for low permeability formations. If valid, empirical relationships can be observed for typical, tight western gas sands, then a concerted hardware effort to develop a "fast" NML tool would be warranted.

To accomplish this task, Sandia has formed a cooperative research program with Chevron Oil Field Research Company (COFRC) with support from the U.S.G.S. (Denver) to analyze samples from a western gas sands project well and evaluate the NMR methods which have been applied to higher permeability reservoirs. The well, CIGE #21, is in the Natural Buttes Field, Uinta Basin, Northeast Utah. This well has been logged extensively and cored. Eleven core samples were secured by Sandia from zones of interest as determined from log analyses and by advice from the well operator.

A 20 mm end section from each sample was given to the U.S.G.S. for their

analyses, to include thin sectioning, scanning electron microscopy, x-ray diffraction, and electron microprobe analyses. Core sampling and testing, including permeability, porosity, and cation exchange capacity measurements is being performed by Petroleum Testing Service (PTS) of Santa Fe Springs, CA. Finally, laboratory NMR measurements on these samples will be performed by COFRC at their facility in La Habra, CA. To date, the U.S.G.S. analysis is complete and awaiting the results of standard core analysis which are underway at PTS.

C. Advanced Electromagnetic Logging (P. C. Lysne, 2353)

1. Logging Techniques Based on Dispersive Electrical Parameters

Electromagnetic techniques have often been successful for the production evaluation of oil and gas reservoirs. For example, direct current resistivity measurements yield production parameters such as the porosity through ancillary relations like Archie's Law. In another class of measurements, pulsed or sinusoidal electromagnetic fields are introduced into the formation. Then, the measured quantity is the electrical impedance which is dependent upon the dielectric constant and the magnetic permeability as well as the resistivity. Furthermore, these latter three independent electric parameters are often dispersive, that is they are frequency or time dependent. This fact has proven useful in "induced polarization" logging for sulfide mineralization and "nuclear magnetic" logging for fluid flow permeabilities.

The purpose of this study is to delve into hopes and difficulties associated with the usage of dispersive electrical parameters as production indicators in hydrocarbon reservoirs. In particular, logging techniques based on the dielectric and resistive properties of formation materials are considered. A simple (perhaps too simple) model for a dispersive dielectric is developed which may be fit in an approximate manner to the data of Poley, Nooteboom and de Wall[7] and which can yield ancillary relations directed toward water saturations and fluid flow permeabilities. It is emphasized that this work is preliminary; directions for future studies are discussed.

To solve electromagnetic problems it is necessary to have a set of constitutive equations that describe the properties of the media in question. A common set using standard notation is

$$D = \varepsilon E, \tag{1a}$$

$$B = \mu H, \tag{1b}$$

and Ohm's Law

$$J = \sigma E. \tag{1c}$$

These equations describe a linear media since only first powers of the variables are present. In a simple medium, ε, μ and σ are constants. This means that no matter how fast local changes in E and H occur, corresponding changes in D, B and J can keep pace; that is the medium is not dispersive.

Inhomogeneous materials such as rocks saturated with conducting fluids are dispersive. The case where B cannot follow fast changes in H is the basis for "nuclear magnetic" logging. Dispersive effects in Ohm's Law may be caused by many phenomena including the kinetics of oxidation-reduction reactions at ionic-electronic conductor interfaces and viscous drag on ions in solution. Dispersion in the dielectric permittivity can occur when semiconducting inclusions are present in a nonconducting matrix. This Maxwell-Wagner-Sillars Effect will be discussed following a short digression into dispersive modeling in general.

Measurements of dispersive effects can be made either by using pulsed techniques or by continuous wave techniques conducted at many frequencies; the ultimate description of the material dispersion must be the same in either case. However, experimental considerations often enter into the choice of measurement mode. For compatibility with existing data, the continuous wave description is chosen herein. Then dispersion in ε, μ and σ results in these parameters being complex and functions of frequency, that is

$$\varepsilon(\omega) = \varepsilon'(\omega) + i\,\varepsilon''(\omega), \tag{2a}$$

$$\mu(\omega) = \mu'(\omega) + i\,\mu''(\omega), \tag{2b}$$

and $$\sigma(\omega) = \sigma'(\omega) + i\,\sigma''(\omega), \tag{2c}$$

where $i = \sqrt{-1}$.

The theory of dispersive systems has been under investigation for a long time. This theory is difficult and beyond the scope of this report. However, an important consequence of this theory is cited, that is the real and imaginary components of each parameter in Eqs. (2) are related. Thus, if $\varepsilon'(\omega)$ is known for all frequencies, then $\varepsilon''(\omega)$ is also known, etc. The constraint between the real and imaginary components is a manifestation of the linearity of Eqs. (1) and causality, that is cause must precede effect. It is noted that some constitutive relations used in the past did not satisfy these Kramers-Kronig relations. In this study, which is directed toward modeling the experiments of Poley, et al, $\mu(\omega)$ is of no consequence, σ' is a constant given by Archie's Law, and σ'' is zero.

To exactly model the dielectric properties of inhomogeneous materials such as saturated rocks is very difficult, if not impossible. Such an effort would require the geometric description of each grain and void constitutent along with their individual electrical properties. Perhaps a statistical theory could be developed. For the present, an available model is used which yields, qualitatively, the dielectric constitutive relation of formation material. While imperfect, the model does point out the hopes of logging techniques based on dispersive dielectric properties.

Maxwell was the first to model the electrical properties of an inhomogeneous material, and he demonstrated that the dielectric properties of a layered medium were dispersive. Wagner extended the model to semiconducting spheres imbedded in a nonconducting matrix. For the same volume ratio of constitutents, Wagner's model is more dispersive than Maxwell's. Sillars[8] extended Wagner's model by considering imbedded spheroids. Sillars' model can be made very dispersive, and, hence, is suggestive of some of the observed dielectric properties of saturated rocks. In all of the above models,

Maxwell's Equations are satisfied at material interfaces, i.e., matrix-inclusion boundaries. This is why these models are geometry-dependent, a point which is lacking from constitutive relations based on simple mixture laws.

Historically, conduction currents are governed by Ohm's Law, Eq. (2c) and are treated as being unconstrained in that a given charged body such as an ion in a liquid can migrate an indefinite distance under the influence of a constant electric field. On the other hand, charge motion governed by dielectric laws is limited to some characteristic length such as the effective length of a dipole associated with a polar molecule or a ferroelectric domain. Consequently, dielectric currents (displacement currents) cannot flow indefinitely when influenced only by a constant electric field. In Sillars' model, the characteristic length is the unique dimension a of a spheroidal inclusion aligned with the electric field. The dimension b is the radius of the circle at the meridian of the spheroid and is perpendicular to a. If the ratio a/b is small, the inclusions are penny-shaped. Large a/b ratios mean needleshaped inclusions and this leads to large dispersive effects. Collectively, the Maxwell-Wganer-Sillars models describe the pinning of conduction charge carriers at material boundaries after they have migrated some characteristic length. The time required for this migration and pinning leads to the dispersive properties of the models.

A number of important observations follow from the work of Sillars. First of all, the dielectric response is strongly dependent upon the a-to-b ratio. Thus composite materials with the same volume fraction of constituent materials may have appreciably different dielectric properties. An illustration of this phenomenon is given in Figure III-2. Another observation is that, if, for the same rock specimen, the pore fluid salinity (conductivity) is changed, then the dielectric response is simply shifted along the frequency axis. This means that the right-hand-curve of Figure III-3 (upper) should be congruent with the other curve if it is shifted two frequency decades to the left. Likewise, for the lower curves, the offsets $\varepsilon''/\varepsilon_o$ should be equal. While the model has

some defects, it appears to be qualitatively reasonable.

In conclusion, a model based on a constant conductivity and a dispersive dielectric has been proposed to explain the frequency dependent impedance of sandstones saturated with waters of different salinities. The present model qualitatively represents the available data. A quantitative model will require a distribution function describing the pore shapes. With such a function in hand, the rock matrix is much better described than if only the porosity is known. For example, a continuum of pore-volume pore-surface areas may be modeled thereby paving the way for fluid permeability determinations through the use of a generalized Kozeny Equation. Furthermore, the extensions of the model to a three-component system could yield hydrocarbon-water ratios for pore fluids.

(J. S. Yu, 2353)

2. An Inverse Process for Evaluating Constitutive Parameters

The electromagnetic (EM) constitutive parameters of a medium are known to vary with the composition and structure of its substances. In gas/oil exploration and production, many of the "production parameters" are also known to be relatable to the constitutive parameters of borehole formations. Thus, techniques for evaluating the EM constitutive parameters using EM probes in a borehole are of interest to supplement or complement other useful techniques. EM logging has taken an added significance for areas where tight-gas sands are prevalent and "production parameters" are more difficult to discern.

In the process of analyzing EM-probe responses, there are instances where explicit functional dependences on the constitutive parameters can be formulated. One example is the open circuit voltage of a receiving coil aligned coaxially to a transmitting coil. Open-circuit voltages can be determined from a set of constitutive parameters, together with geometric and EM-source parameters; an inverse process is to determine constitutive parameters from voltage responses. The project efforts that have been directed toward such an inverse process are the subject of this progress report. Technical results to date are summarized as follows:

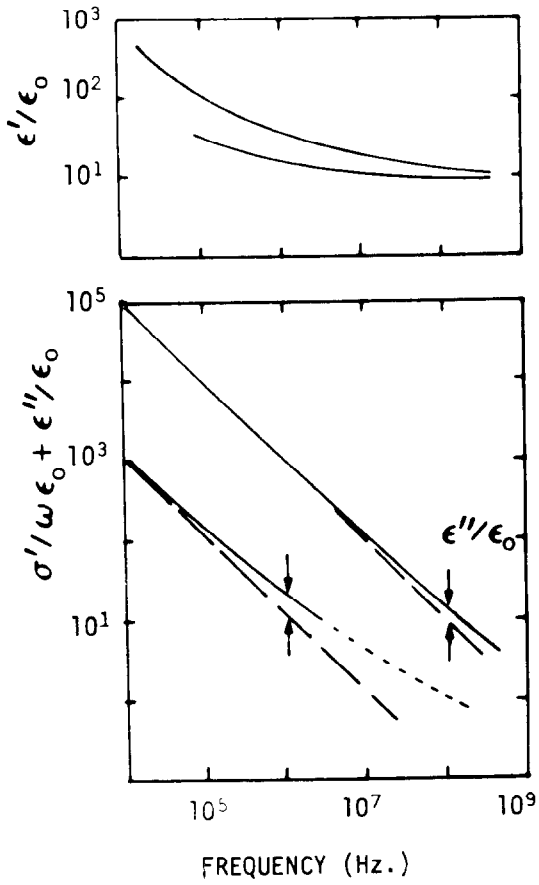

Figure III-3 illustrating data from Ref. 2. (solid and dotted). The dashed lines were obtained from Archie's Law and the conductivity of the pore fluids. The porosity of the specimen was 15 percent. In each figure, the upper curve is for saline pore water (15 kg./m^3 NaCl) and the lower curve is for fresh water. If the proposed model were exactly correct, the upper curves would overlap if the right hand curve were transposed two frequency decades to the left and the offsets, $\varepsilon''/\varepsilon_o$ of the lower plot would be equal.

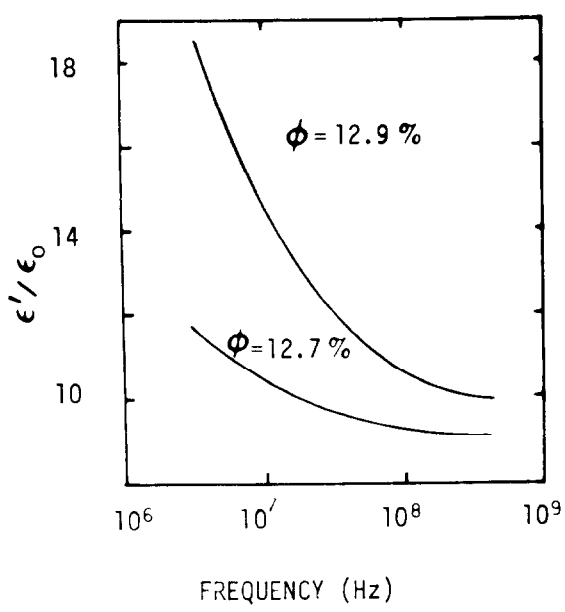

Figure III-2. illustrating $\varepsilon'/\varepsilon_o$ for two freshwater saturated sandstones. The data are from Ref. 2. Note the appreciable differences in $\varepsilon'/\varepsilon_o$ for specimens of nearly the same porosity.

a. A rigorous solution has been obtained for a 2-coil coupling in a homogeneous formation with complex constitutive parameters and has been compared with the common solution assuming point-like coils.

b. Universal curves are plotted for coupling sensitivities in empty space with variable geometric and source parameters to facilitate probe designs, and to provide references for earth formations.

c. Complex magnetic permeability of a formation has been evaluated from the ratio of transfer impedances, and the attendent errors are estimated by universal curves varying with formation properties.

d. Universal curves are plotted for fixed coil separations to determine the complex refractive index of a formation whose properties may vary from being a lossy dielectric to a lossy conductor.

e. A comprehensive data base is obtained for 2-coil couplings in a homogeneous, isotropic formation to serve as a reference for coil designs and for coil responses inside a more complicated earth formation.

Following the convention that the displacement and conduction currents are separated in the Maxwell's equations, three constitutive parameters are defined as functions of (the angular frequency of variation for time-harmonics) for a homogeneous, isotropic medium: the magnetic permeability μ (henry/m), the electric permittivity (farad/m), and the electric conductivity σ (mho/m). Also by the convention of using the empty space as reference ($\mu_o = 4\ \pi \times 10^{-7}$, $\varepsilon_o \approx 10^{-9}/36\pi$, and $\sigma = 0$), a set of relative parameters is defined as

$\mu_r = \mu/\mu_o$, the relative magnetic permeability; and

$\varepsilon_r = \varepsilon/\varepsilon_o$, the relative electric permittivity or dielectric "constant".

A related set of parameters is found to be more convenient for describing EM-wave propagations and interactions in a medium. Using the time-harmonic convention exp($j\omega t$), this set is

$$\nu_r = c/v = [\mu_r (\varepsilon_r - j\sigma/\omega\varepsilon_o)] \quad \text{, the refractive index; and}$$

$$\eta_r = \eta/\eta_o = [\mu_r/(\varepsilon_r - j\sigma/\omega\varepsilon_o)] \quad \text{, the relative intrinsic impedance}$$

The values of c and v are respectively the phase velocities of a uniform plane wave in empty space and in the medium of interest. In general, the relative parameters are complex in that they have real and imaginary parts both of which are functions of ω. A point of caution is in order for the above definitions. While a complex ε_r is associated with charges bound to material points such as inclusions, and a complex σ is associated with mobile charges, the inverse process discussed in this report does not imply that these two parameters are separable through measurements of EM-probe responses.

A rigorous solution has been obtained for the boundary-value problem of a 2-coil coaxial-coupling in a homogeneous, isotropic medium. Since the constitutive parameters are conventionally referenced to those of the empty space, the coupling sensitivities between two coils in the empty space are also desired for reference purposes. Results,in the form of parametric curves, are plotted in Figures III-4. Geometrically the transmitting coil is centered at the origin of circular-cylindrical coordinates. The receiving coil is coaxially placed z (meter) from the transmitter. Both coils have the same diameter d (meter) which is restricted to less than 0.1 of empty-space wavelength λ_o so that the coupling between the two coils is through a nearly pure magnetic-dipole mode. The abscissas in Figures III-4 and III-5 are the same. Their values are dimensionless when d/λ_o is used. When the diameter d is fixed in coil designs the abscissas can be converted into the transmitter frequencies. For example, should the diameter d be fixed at 10 cm, the transmitter frequencies would have to be less than 300 MHz to assure that the coupling is accurately accounted for by using only a magnetic-dipole mode. The open-circuit voltage V_{oc} at the receiving

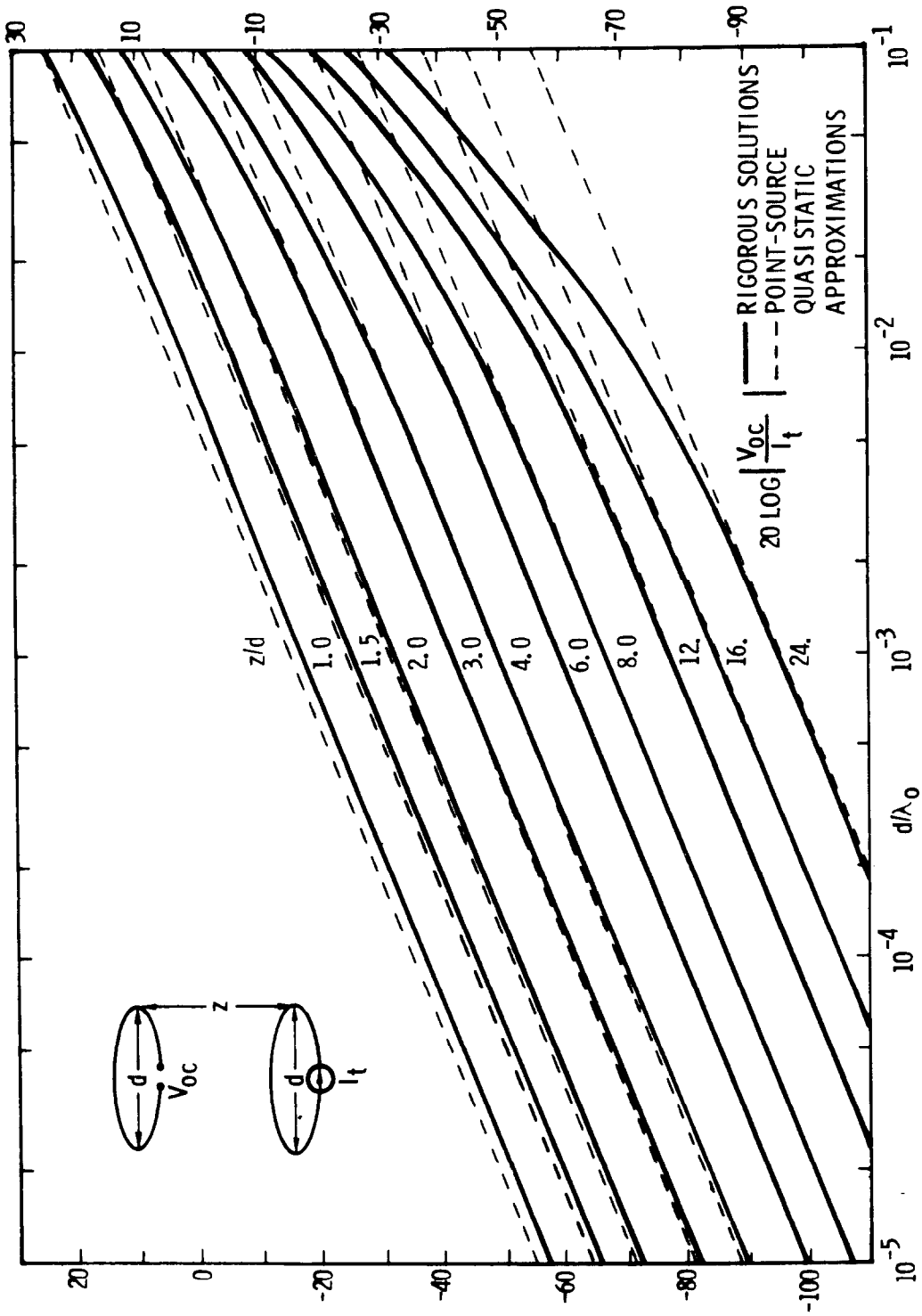

FIGURE III-4

Magnitude-Sensitivity Curves of Transfer Impedance $Z_{11} = V_{oc}/I_t$ between two coils through Magnetic-Dipole Coupling in the Empty Space. (The abscissa is for coil diameter d over empty-space wavelength λ_o, the ordinates are for 20 $\log|V_{oc}/I_t|$, and the curves are parameterized for coil separation z over d.)

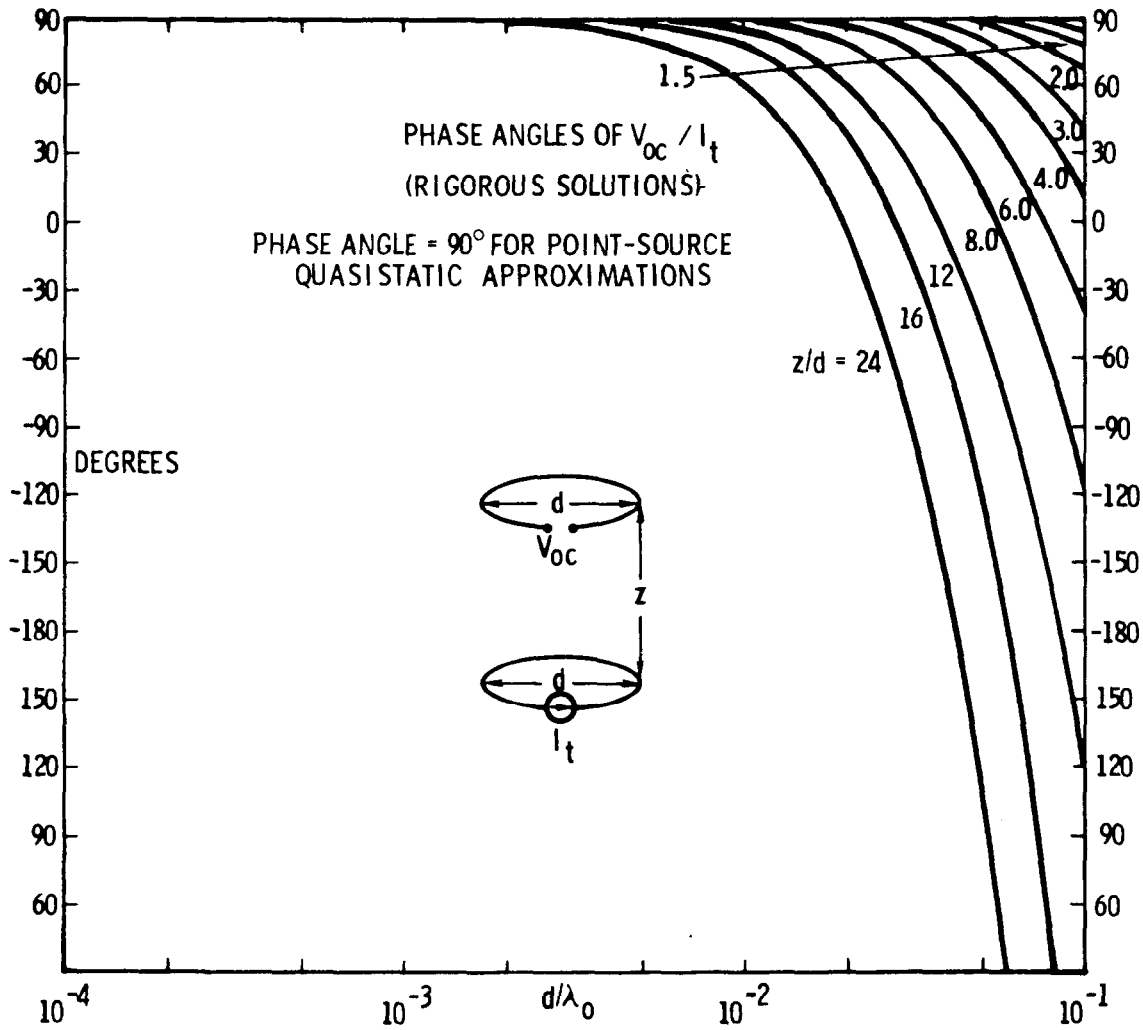

FIGURE III-5

Phase Angles of Transfer Impedance $Z_{12} = V_{oc}/I_t$ between two coils through Magnetic-Dipole Coupling in the Empty Space. (The abscissa is for coil diameter d over empty-space wavelength λ_o, the ordinate is for phase angles in degrees, and the curves are parameterized for coil separation z over d.)

coil is directly proportional to the transmitting-coil current I_t. Their ratio is known as the transfer impedance with magnitudes spanning more than seven decades for various coil spacings z/d and coil diameters d/λ_o. To make a more compact presentation, the magnitudes of transfer impedance are transformed into a familiar form 20 log (V_{oc}/I_t) as marked along the ordinate of Figure III-4. The solid curves are the results of the analytically rigorous solutions. The dashed lines represent the point-source quasistatic solutions under two simplifying assumptions that the coils are point-like $(d/\lambda_o \rightarrow 0)$ and the separation is vanishingly small $(z/\lambda_o \rightarrow 0)$. The corresponding phase angles of the transfer impedance are plotted in Figure III-5 indicating the extents of phase shifts for various combinations of d/λ_o and z/d. An example will serve to illustrate how the coupling sensitivities can be estimated from the curves as shown. Let a set of geometrical and source parameters be specified:

Diameter of coils	$d = 0.1$ meter
Spacing of coils	$z = 2.4$ meters
Transmitter frequency	$f = 6 \times 10^7$ Hz
Amplitude of current	$I_t = 10^{-1}$ ampere

The open-circuit voltage V_{oc} can be estimated to have an amplitude about 10^{-4} volt from Figure III-4 and a relative phase angle about -3° from Figure III-5. For the purpose of estimating coupling sensitivities for design considerations, adequate results may be obtained through graphic interpolations for other specifications.

The main object in this report is an inverse process to evaluate the constitutive parameters when the coils are placed in an earth formation assumed to be homogeneous and isotropic. The transfer impedance between the coils in a formation is solved rigorously by assigning a set of constitutive parameters ν_r and η_r (or equivalently a set of μ_r, ε_r, and σ) to the formation, and by imposing $(d/\lambda_o)\ R_e(\nu_r) < 0.1$ to maintain a strictly magnetic-dipole coupling. For the inverse process under consideration, it is convenient to designate explicity two transfer impedances assuming that d, z, and f are fixed:

$$\mu z_{12}(\mu_o, \varepsilon_o) = V_{oc}/I_t) \text{ in the empty space; and}$$

$$Z_{12}(\mu_r, \nu_r) = (V_{oc}/I_t) \text{ in an undetermined formation.}$$

Inherent in the 2-coil coupling is the quasistatic property that the relative magnetic permeability can be evaluated as

$$\mu_r = z_{12}(\mu_r, \nu_r)/z_{12}(\mu_o, \varepsilon_o)$$

Should the quasistatic conditions not be met, the μ_r estimated by the ratio of transfer impedances would have certain errors depending on the other parameters involved. The rigorous solutions for the transfer impedances have been used to evaluate the normalized errors as shown in the parametric curves of Figure III-6 with the coil separation set equal to one coil diameter. As an illustration, for d =10 cm and f = 30 MHz the ratio d/λ_o is 0.01. To assure the magnetic-dipole coupling condition, the first condition to be satisfied is $(d/\lambda_o)R_e(\nu_r)<0.1$. This means the real part of refractive index may not exceed 10 in order to use the rigorous solution and its inverse process. The second step in evaluating the normalized errors for μ_r-estimation is to divide all the number assigned to the solid curves by the factor $(200d/\lambda_o)^2 = 4$, and to obtain $Re(\nu_r^2) = Re[\mu_r(\varepsilon_r - j\sigma/\omega\varepsilon_o)] =$ 45, 40, 35, 30 . . . . Allowing that there are other data sources to estimate ν_r^2 as a complex value, a desired estimate on errors can be made using Figure III-6. For $\nu_r^2 = 30-j24$ and $d/\lambda_o = 0.01$, the normalized error associated with estimating μ_r (by the ratio of transfer impedances) is about $-0.055 + j0.08$ falling within a 10% error circle centered at the true value of μ_r. If d/λ_o is reduced to 0.005 and 0.0025 while ν_r^2 remains the same, the normalized errors according to Figure III-6 are within a 2.5% - error circle and a 0.7% - error circle, respectively. Thus, a mean of determining μ_r using the 2-coil coupling is established with error estimates.

To complete the inverse process requires another complex number from the 2-coil coupling mechanisms to determine the refractive index ν_r. Although most earth formations are known to have μ_r near unity, the general form of $\nu_r = [\mu_r(\varepsilon_r - j\sigma/\omega\varepsilon_o)]$ is retained for possibilities when the assumption

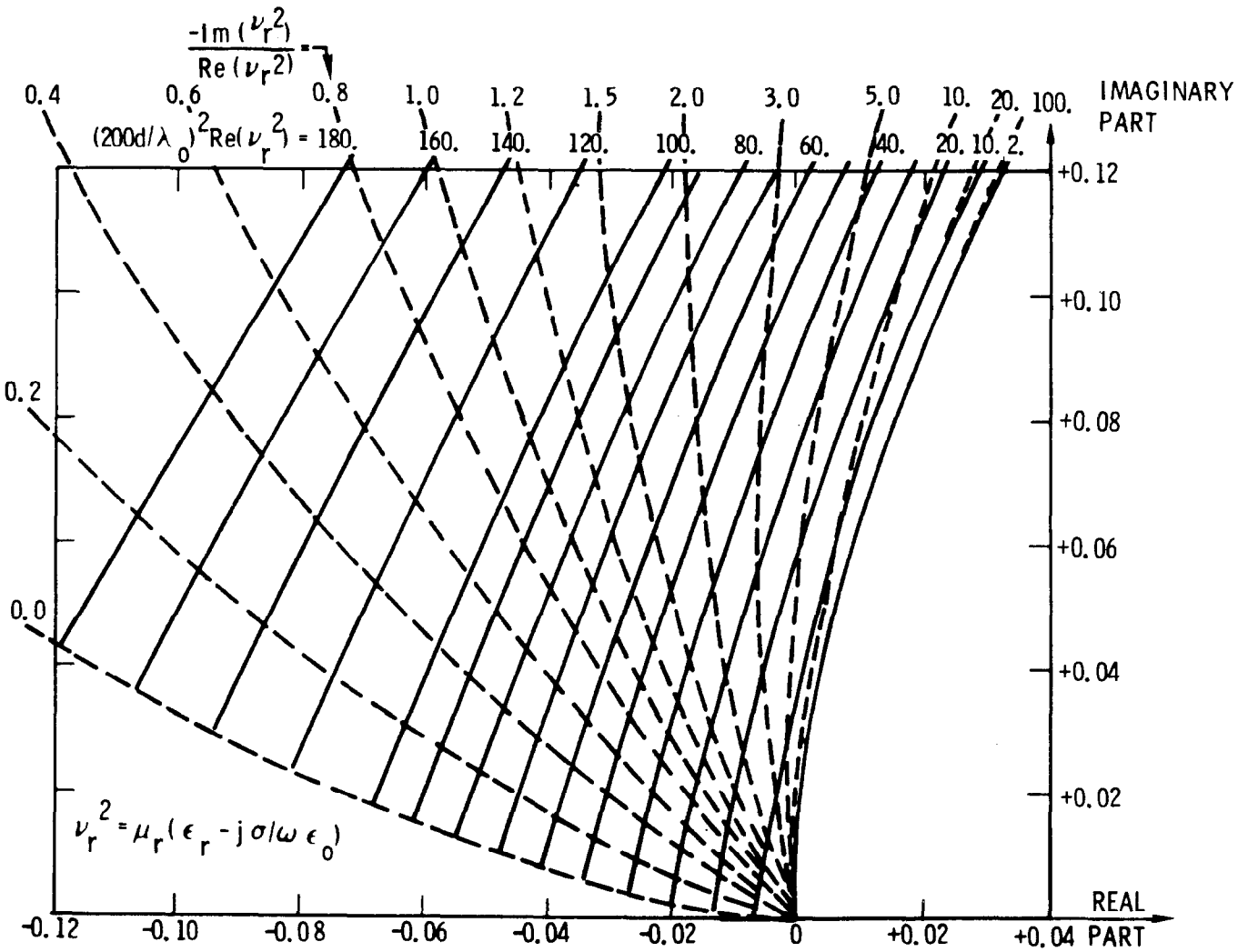

FIGURE III-6

Normalized Errors (1. - Estimated μ_r/True μ_r) in Real (Abscissa) and Imaginary (Ordinate) Parts for Estimating the Relative Magnetic Permeability μ_r from $z_{12}(\mu_r, \nu_r)/z_{12}(\mu_0, \varepsilon_0)$ with the Coil Separation z/d = 1. [The $z_{12}(\mu_r, \nu_r)$ is the transfer impedance measured in an undetermined medium characterized by μ_r and refractive index ν_r which in general depends also on conductivitiy σ and relative electric permittivity ε_r. The $z_{12}(\mu_0, \varepsilon_0)$ is measured in the empty space. The curves are parameterized for the real and imaginary parts of ν_r^2 with the restriction that $d/\lambda_0 R_e(\nu_r) < 0.1$].

$\mu_r = 1$ is in doubt prior to an in-situ EM logging. The solution for 2-coil coupling has the inherent property that the induced voltage is more sensitive to ν_r variations when z/d is increased. Figures III-7 and III-8 are parametric curves for the ratio

$$z_{12}(\mu_r, \nu_r)/\mu_r\ z_{12}(\mu_o, \varepsilon_o)$$

with z/d values set to 10 and 20, respectively. The transfer impedance $z_{12}(\mu_o, \varepsilon_o)$ in empty space is multiplied by μ_r and used as the normalization factor for $z_{12}(\mu_r, \nu_r)$ when the coils are in the formation under evaluation. The magnitudes of ratio are seen to vary from 1 to 3 for $(200d/\lambda_o)^2 R_e(\nu_r^2)$ ranging from 2 to 100 if z/d = 10. The phase angles of the ratio vary in the fourth quadrant depending on the values of d/λ_o and the ν_r^2. Better sensitivities in Figure III-8 indicate that the corresponding magnitudes vary from 1.2 to 4.3 and the corresponding phase angles span three quadrants when z/d is set to 20. Consider an example with $d/\lambda_o = 0.005$ and z/d = 20. If the ratio $z_{12}(\mu_r, \nu_r)/z_{12}(\mu_o, \varepsilon_o)$ is measured to be -2 + j2 and if μ_r is known to be unity, the value of ν_r^2 is about 70 - j14 according to Figure III-8. Using the definition $\nu_r^2 = \mu_r(\varepsilon_r - j\sigma/\omega\varepsilon_o) = \varepsilon_r$ with the assumptions $\mu_r = 1$ and $\sigma = 0$, the complex ε_r would be 70 - j14. Thus one can quickly estimate ε_r using Figure III-7 or 8, or other selections of z/d. Granted, the number of parametric curves appears to be too sparse to perform graphic interpolations with high accuracies. Refinement and enlargement would be warranted should these theoretical curves prove to be optimal for practical applications. The results presented thus far are intended to demonstrate that universal curves can be parametrized to perform the inverse process of determining two constitutive parameters. All theoretical assumptions and restrictions are considered to have been fully formalized in this inverse process. Practical limitations in an actual implementation will ultimately set the ranges of its applicability. Thus the feasibility of EM logging using 2-coil couplings has at least been theoretically established for an earth formation that is assumed homogeneous and isotropic. Specific limits of this feasibility can now be quantified through the rigorous solution or its

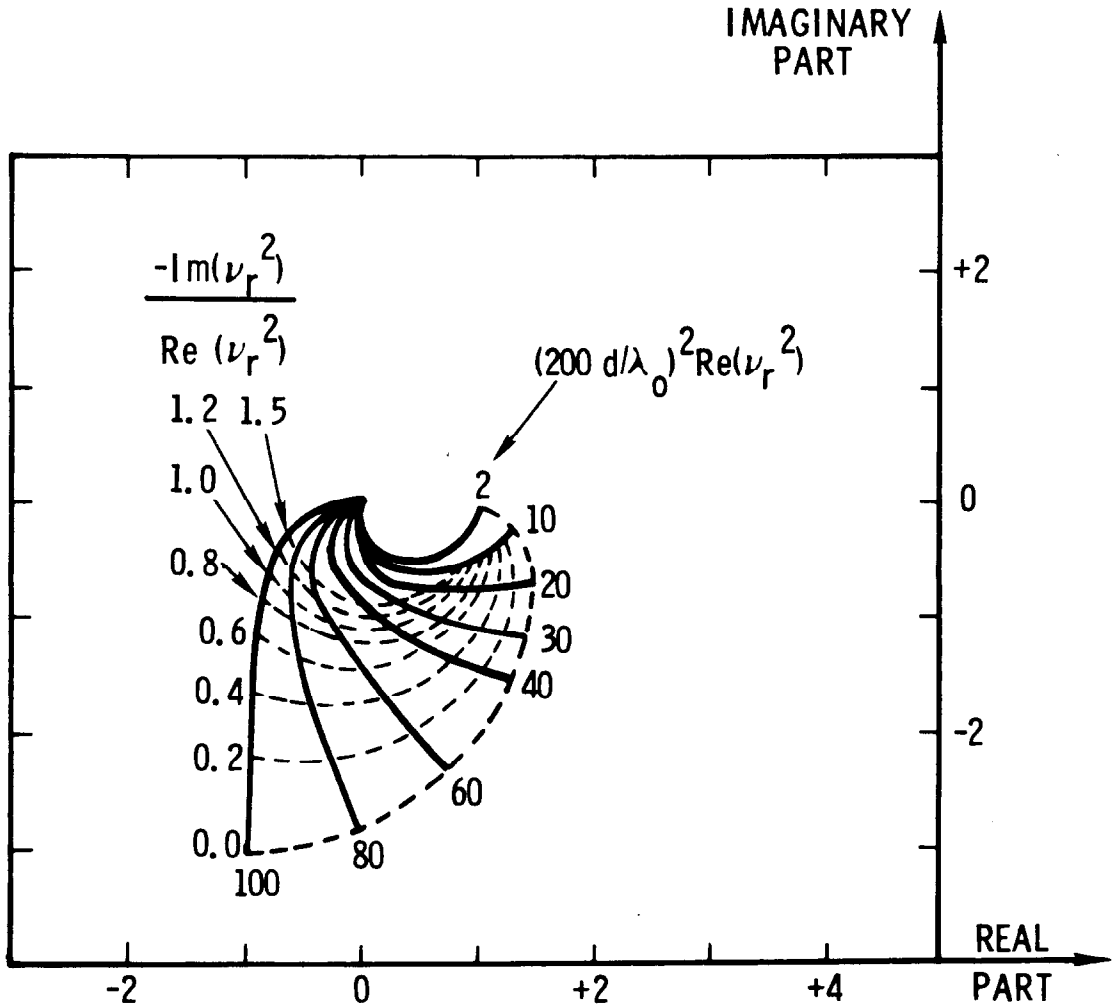

FIGURE III-7

The Real (Abscissa) and Imaginary (Ordinate) Parts of $z_{12}(\mu_r, \nu_r)/\mu_r z_{12}(\mu_0, \varepsilon_0)$ with Coil Separation $z/\lambda_0 = 10$ for Evaluating the $\nu_r^2 = \mu_r(\varepsilon_r - j\sigma/\omega\varepsilon_0)$ of an Undetermined Medium. [The real part of ν_r^2 is first evaluated from the solid curves and the imaginary part of ν_r^2 is then evaluated from the dashed curves. End results are valid if $d/\lambda_0 R_e(\nu_r) < 0.1$, otherwise the coil diameter needs to be reduced and measurements of transfer impedances need to be repeated for reusing the curves.]

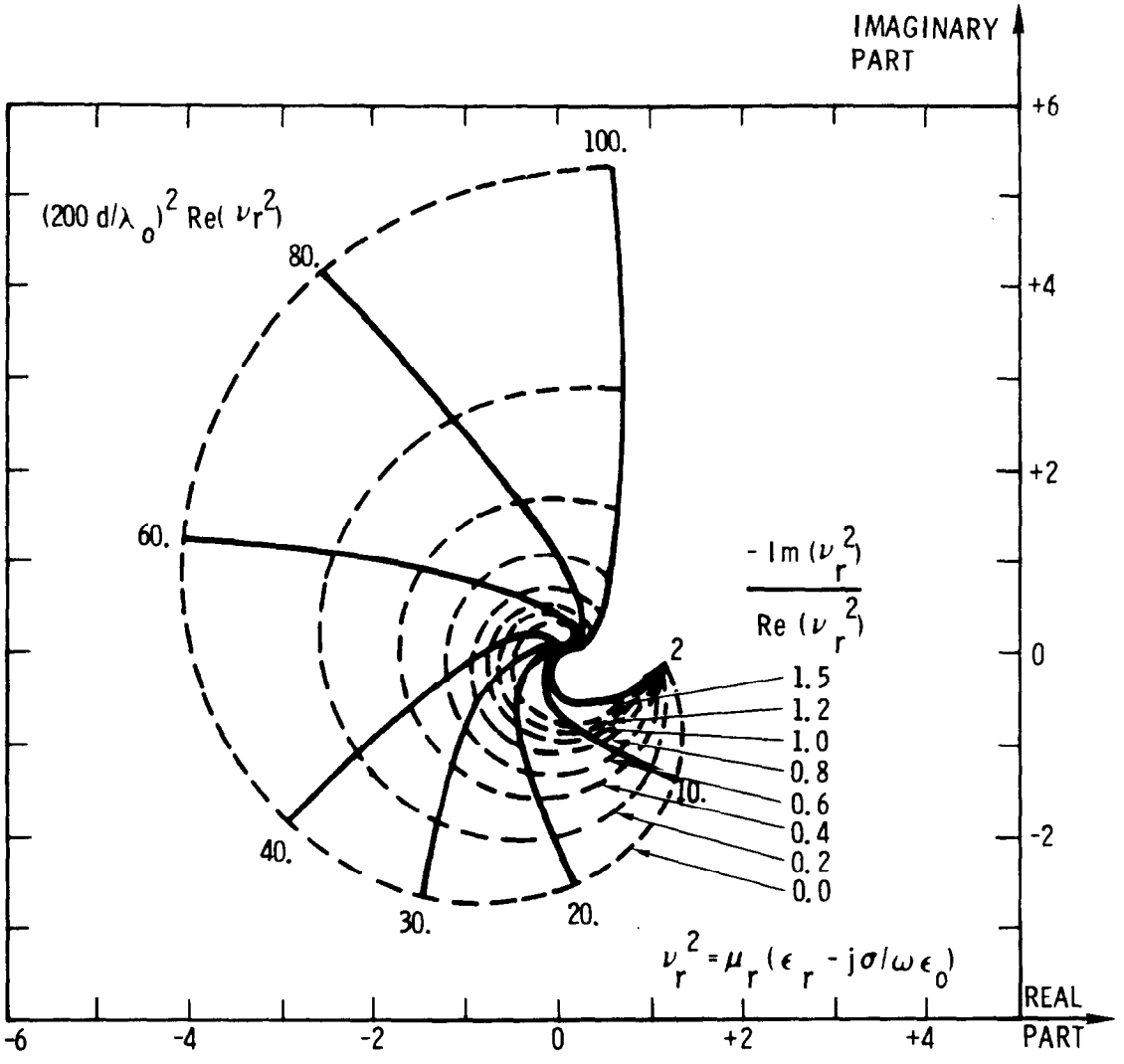

FIGURE III-8

The Real (Abscissa) and Imaginary (Ordinate) Parts of $z_{12}(\mu_r, \nu_r)/\mu_r z_{12}(\mu_0, \varepsilon_0)$ with Coil Separation $z/d = 20$ for Evaluating the $\nu_r^2 = \mu_r(\varepsilon_r - j\sigma/\omega\varepsilon_0)$ of an Undetermined Medium. [The real part of ν_r^2 is first evaluated from the solid curves and the imaginary part of ν_r^2 is then evaluated from the dashed curves. End results are valid if $d/\lambda_o R_e(\nu_r) < 0.1$, otherwise the coil diameter needs to be reduced and measurements of transfer impedances need to be repeated for reusing the curves.]

parametric curves. Refinements on the curves are anticipated if better accuracies are needed from graphic interpolations. Perhaps the most significant aspect of the progress to date is a solid data base, both theoretically and graphically, upon which all responses measurable in a more realistic borehole can be referred to. While solutions for more realistic boreholes are in progress, several issues remain unresolved even for the 2-coil coupling in a homogeneous, isotropic media. Three outstanding issues are briefly outlined next.

First, the rigorous solution has been obtained assuming a uniform transmitting current whose amplitude and phase are used to nominalize the induced voltage at receiving coil. This is comfortable analytically, because two difficult questions are being suppressed. They are: What would be the theoretical values of I_t when a wire loop of finite radius is driven across a finite gap, and how well the theoretical values would agree with actual values when the wire loop is driven by a real feeder. Field values in the presence of actual feeders may deviate significantly from the theoretically assumed conditions. Recognizing that empirical "fixes" are commonly employed in practice, it is recommended that further theoretical understanding should be developed to reduce the need and to improve the effectiveness of these "fixes". Perhaps a more significant point is to establish the self impedance of transmitting coil that is consistent with theory and measurement. The inverse process for a realistic borehole could be uniquely improved by this new capability.

Secondly, the rigorous solution is strictly applicable to single-turn coils only. Solutions for multiturn coils in general are not available for assessing the degree of purity in magnetic-dipole-mode couplings. Although a significant amount of effort may be needed to develop this capability, it is considered an essential part of EM logging studies based on magnetic-dipole-mode couplings.

Thirdly, there is the most basic issue regarding whether coil couplings are the most suitable EM logging techniques. One may argue that the issue has been squarely resolved by the past history of EM loggings. On the other hand,

there are many other types of EM logging that have not received adequate investigations. An obvious example is the complementary case of using linear current elements instead of the circular ones in coil couplings. Less obvious ones are transmission and reflection types that are potentially capable of exploiting more fully the three basic modes of EM-wave propagation and interactions with linear or circular polarizations.

In summary, the rigorous solution is considered to have provided a comprehensive data base for 2-coil couplings and to have established the inverse process using universal curves. These results are considered to be valuable in that they serve as the baselines to which the results for more complicated formations can be referred. However, despite its wide use in the past, it is not immediately clear that coil-couplings are the EM loggings best suited for gas/oil explorations. There are theoretical foundations indicating that other modes of EM coupling may be more advantageous, especially when μ_r of earth formation is assumed unity and carrying no useful information. Strong recommendations for studying other types of EM coupling can be justified by the theoretical results obtained to date.

REFERENCES

1. Brown, R. J. S. and B. W. Gamson, Nuclear magnetism logging: Petroleum Transactions, A.I.M.E., Vol. 219, pp. 199-207 (1970).

2. Seevers, D. O., A nuclear magnetic method for determining the permeability of sandstones: SPWLA logging symposium transactions, paper L. (1966).

3. Timur, A. Effective porosity and permeability of sandstones investigated through nuclear magnetic resonance principles: SPWLA logging symposium transactions, paper K (1968).

4. Timur, A., Pulsed nuclear magnetic resonance studies of porosity, movable fluid, and permeability of sandstones: Jour. Pet. Tech., June, pp. 773-786 (1969).

5. Loren, J. D. and J. D. Robinson, Relations between pore size, fluid and matrix properties and NML measurements: Paper No. SPE2529, Soc. of Pet. Engineers of AIME (1969).

6. Loren, J. D., Permeability estimates from NML measurements: Jour. Pet. Tech., August, pp. 923-928 (1972).

7. J. Ph. Poley, J. J. Nooteboom, and P. J. de Waal, Use of V.H.F. Dielectric Measurements for Borehole Formation Analysis, The Log Analyst, MayJune, (1978).

8. R. W. Sillars, The properties of a Dielectric Containing Semiconducting Particles of Various Shapes, J. Inst. Elec. Eng. (London) 80, 37 (1937).

IV. Stimulation Research for Unconventional Gas Recovery

A. Hydraulic Fracturing

In the tight, gas-sands basins of the Western United States there exists a large resource of natural gas that cannot be produced economically at today's prices with today's technology. Massive hydraulic fracturing appears to be the most favorable technique for exploiting this resource; however, the results to date have been less than expected, and the reasons for this are unclear. Sandia Laboratories is conducting both basic and applied research to aid in the evolution of this technique as a practical method for producing a large portion of these resources. Types of research being performed include in situ testing of hydraulic fracturing theory and technology, modeling of hydraulic fracturing behavior, and laboratory testing.

The in situ testing is being performed at DOE's Nevada Test Site (NTS) in a tunnel complex driven through volcanic ash-fall tuff under 1400 ft of overburden. This complex provides the facilities and equipment for mineback of the created hydraulic fractures for direct observation, a capability for determining in situ stresses and obtaining rock samples for testing in regions of interest, and a direct knowledge of the "reservoir" parameters and structure (i.e., permeability, porosity, location of faults, fractures, etc.). Modeling efforts include the range from details of the processes occurring at the fracture tip to numerical codes describing the coupled fluid mechanics and rock mechanics of the entire fracture. Laboratory testing includes the determination of rock properties and the conducting of small-scale experiments.

1. Hydraulic Fracturing Containment Experiments (N. R. Warpinski, 4732)

Sandia Laboratories has been actively studying the problem of containment of hydraulic fractures by conducting in situ experiments at the Nevada Test Site. Knowledge of the parameters which affect hydraulic fracture growth is very important if hydraulic fracturing is to be used successfully on tight gas reservoirs. In these low permeability reservoirs, it is necessary to create

fractures of up to 4000 ft length in order to obtain sufficient drainage for the well to be "economic" at today's prices. To achieve this fracture length, it is imperative that the fracture be contained largely to the pay zone or the volume of fluid and sand necessary will be prohibitively expensive. It is equally important that the fracture not intersect an underlying or overlying water-bearing zone.

The study of the containment of hydraulic fractures is directed towards determining the parameters and conditions which will limit the height of a fracture and control its direction of propagation so that the necessary fracture lengths will be obtained. Implicit in these studies is the presumption that sufficient understanding of these conditions will allow operators to alter treatment parameters to help control containment, at least in those formations where there is already some propensity for containing the fractures. If this is not possible, then it still may be possible to define a priori those zones that will most likely provide economic production due to favorable fracture growth (or containment) conditions.

There are several parameters which are considered to have some effect on the containment of hydraulic fractures. Simonson, et al.[1*] and Rogers, et al. calculated that a hydraulic fracture attempting to propagate from a low modulus material into a high modulus material would be arrested at the interface between the two materials because the stress intensity factor at the crack tip approaches zero as the interface is approached. This, however, has not been born out by laboratory experiments.[3,4,5] They[1,2] also showed that a bounding layer of higher minimum principal in situ stress should restrict fracture growth. Daneshy[3] performed experiments that suggested that fracture containment may be more a result of the nature of the interface rather than any difference in material properties, but this would be most often the case at shallow depths where the bonding is likely to be weaker. None of these phenomena have been verified in the field, however, except for the near-wellbore data that can be obtained from temperature logs or emplacement of radioactive sand.

*References for Section IV-A are given at the end of the section on p. 99.

The purpose of the hydraulic fracturing containment experiments is to examine the effect of these parameters under realistic in situ conditions. Two experiments have been conducted at the Nevada Test Site to study this problem: the Hole #6 Formation Interface Fracture Experiment and an Interface Test Series.

a) Hole #6 Formation Interface Fracture Experiment

The objective of the Hole #6 Formation Interface Fracture Experiment[6] was to examine the effect of a formation or material property interface on hydraulic fracture growth. Hydraulic fracture treatments were conducted above and below a welded tuff/ash-fall tuff interface and were mined back for direct observation and for determination of material properties and in situ stresses. This experiment was initiated in FY77, and the fractures were created in August and October 1977. The fracture initiated in the ash-fall tuff (low modulus) below the interface was treated with 5000 gal of green cement followed by 4000 gal of black cement at 6 bbl/min. In the upper welded tuff (high modulus), 5000 gal of blue grout was injected at 6 bbl/min. Mineback of the fractures was completed in FY78.

The entire length of the fractures at the interface was mined back, and it was found that the lower fracture (initiated in the low modulus ash-fall tuff) broke through the interface everywhere it contacted it even though the modulus of the overlying welded tuff is an order of magnitude greater than the modulus of the ash-fall tuff. Unfortunately, the upper fracture broke out along side the lower fracture which was initiated first so that little information was gained from this second test. However, the results of these experiments do show that a significant difference in material properties is insufficient to contain the fracture.

Since it is impossible to mine out more than a small fraction of these fractures due to tunnel size and economic constraints, an exploratory coring program was initiated to delineate the overall shape of the fractures. This program's aim is to determine whether the high modulus bounding layer has

an effect on fracture growth or shape (i.e., restricts growth) even though the interface itself does not terminate the fracture. Determination of the shape of the fracture may also indicate the effect of in situ stress variations, if any exist in this area. Nine holes were completed in FY78, and 14 more were cored in FY79.

Figure IV-1 shows the location where these coreholes intersected the fracture plane relative to the borehole, the mined back region, and the interface. It can be seen that fracture growth was predominantly vertical: fracture length at the interface is 150 ft, and total height is at least 200 ft. The injected volumes were sufficient to create fractures 50 ft high by 600 ft in length according to conventional fracture calculations. Estimates show that approximately 45% of the grout has been located. There appears to be no effect of the interface on fracture shape as it passed through the interface. The coring program is continuing at present with several more cores planned in early FY80 to determine the upper limit of the fractures and thus see if the welded tuff layer restricted fracture growth in any way.

b) Interface Test Series

The Interface Test Series is a set of small scale hydraulic fracture experiments which were conducted at NTS to further examine the factors that affect containment of hydraulic fractures. The basic procedure of these experiments was to create small hydraulic fractures in horizontal boreholes drilled from the tunnel at various distances below the same welded tuff/ash-fall tuff interface using a dyed-water frac fluid injected at low flow rates. Mineback of these fractures would thus provide detailed evidence of the behavior of many fractures under different conditions. These tests would also confirm the results of the Hole #6 experiment, but under different conditions, i.e., different fluid, different flow rates and a horizontal borehole entirely under the interface versus a vertical borehole through the interface.

Since these were only small volume fractures, the actual interface that was "seen" by the fractures was the contact between the ash-fall tuff and the

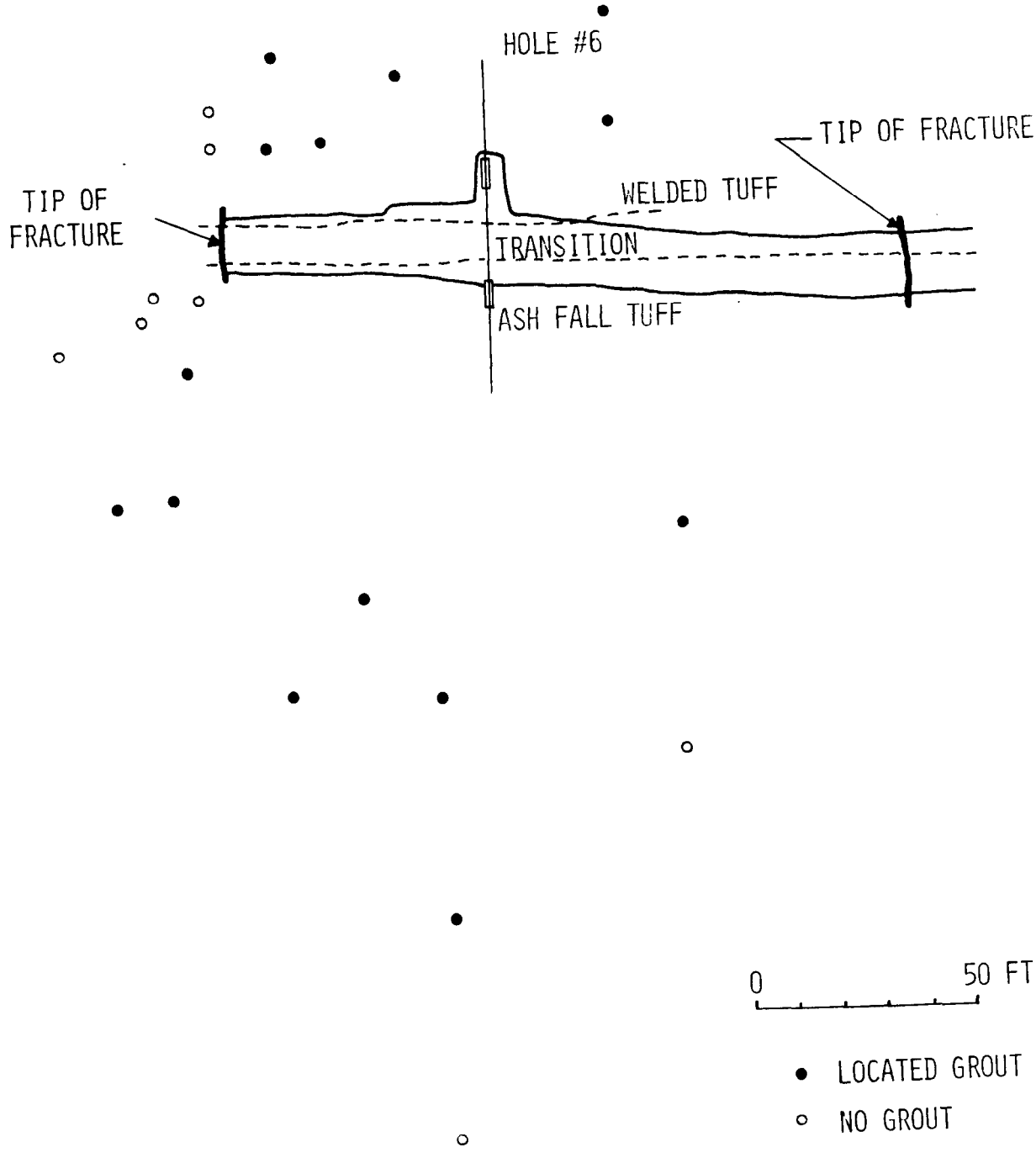

FIGURE IV-1
Results of Exploratory Coring, Hole #6
Experiment at the End of FY 79

lower transition of the ash-flow tuff. This interface is shown schematically in Figure IV-2 with the elastic modulus of the various layers given. At the contact between the ash-fall tuff and the lowest layer of the transition zone there is still a factor of 4-5 difference in modulus.

Three sets of experiments in this series were completed in FY79. These were designated CFE (Crack 'r Frac Experiment) - 1, CFE-2, and a combination experiment, CFE-3 and CFE-4. Their location relative to Hole #6 and the grout filled fractures of Hole #6 are shown in Figure IV-3. Essentially, these tests were conducted from the side of the Hole #6 mineback drift.

CFE-1 was a preliminary test of the concept and a confirmation of the Hole #6 results. The borehole was drilled so that at total depth (TD) the hole was 3 in below the interface and at the collar it was ~4 ft below the interface. Six different zones in this hole were fractured in three stages with 150 gal of dyed water at 8 gal/min. First, a small breakdown pump (3-8 gal) was conducted to determine the instantaneous shut-in pressure (ISIP), which is equivalent to the minimum principal in situ stress, for a small region around the borehole. After the pressure decayed, a second small volume (3-8 gal) was pumped to determine the ISIP again. Finally, the remainder of the 150 gal was pumped into the zone.

Figure IV-4 shows the pressure data for the six zones in CFE-1 and Table IV-I lists the important pressure data points such as the breakdown pressure (P_c) and the ISIP. As can be seen in Figure IV-4, only two zones (66' and 78') exhibited definite breakdowns and possibly the zone at 19' did also. There was no anomalous behavior to indicate that the fractures broke through the interface or otherwise behaved unexpectedly. The zones at 11' and 45' had shut downs in the middle of the main pump because of leaks around the packer.

Three tiltmeters were employed in this experiment in a vertical line ~6 ft apart at the location shown in Figure IV-3 to test the feasibility of such instruments for more accurately measuring fracturing parameters. The tilts[7]

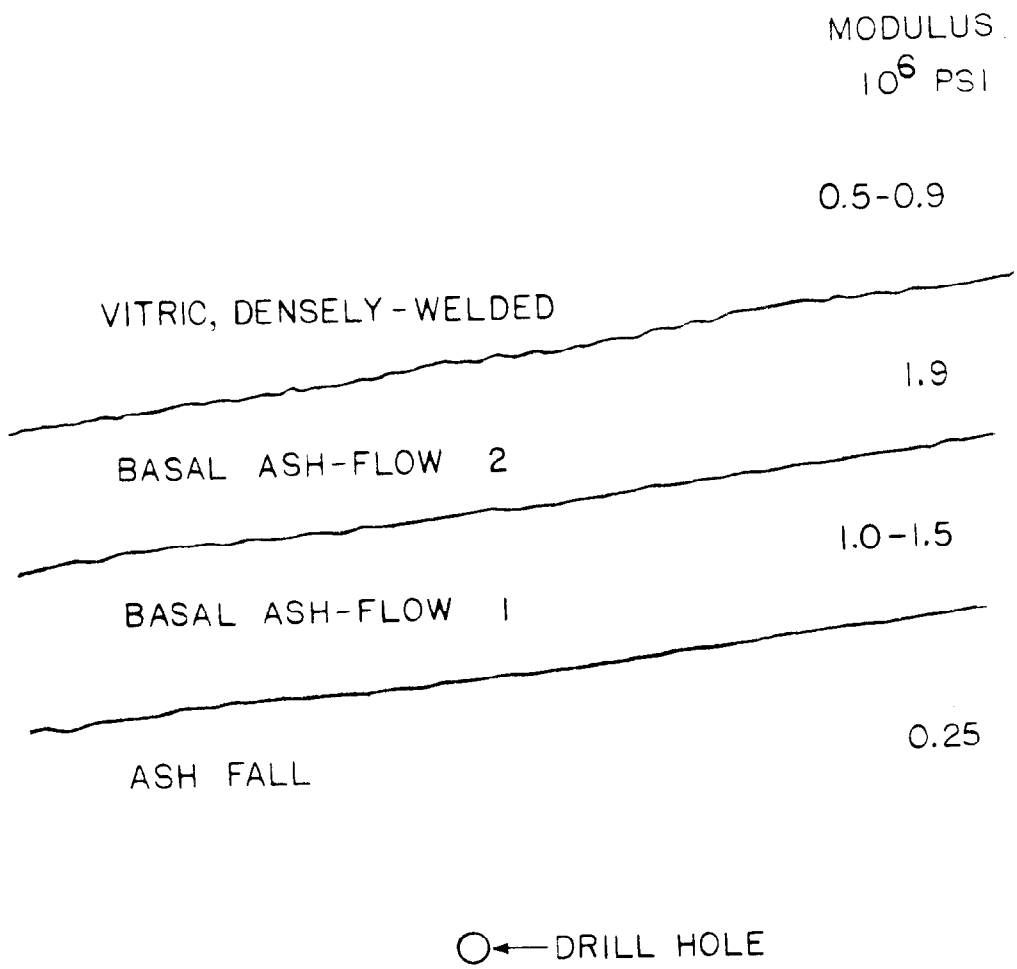

FIGURE IV-2

Interface Test Series Experimental Configuration

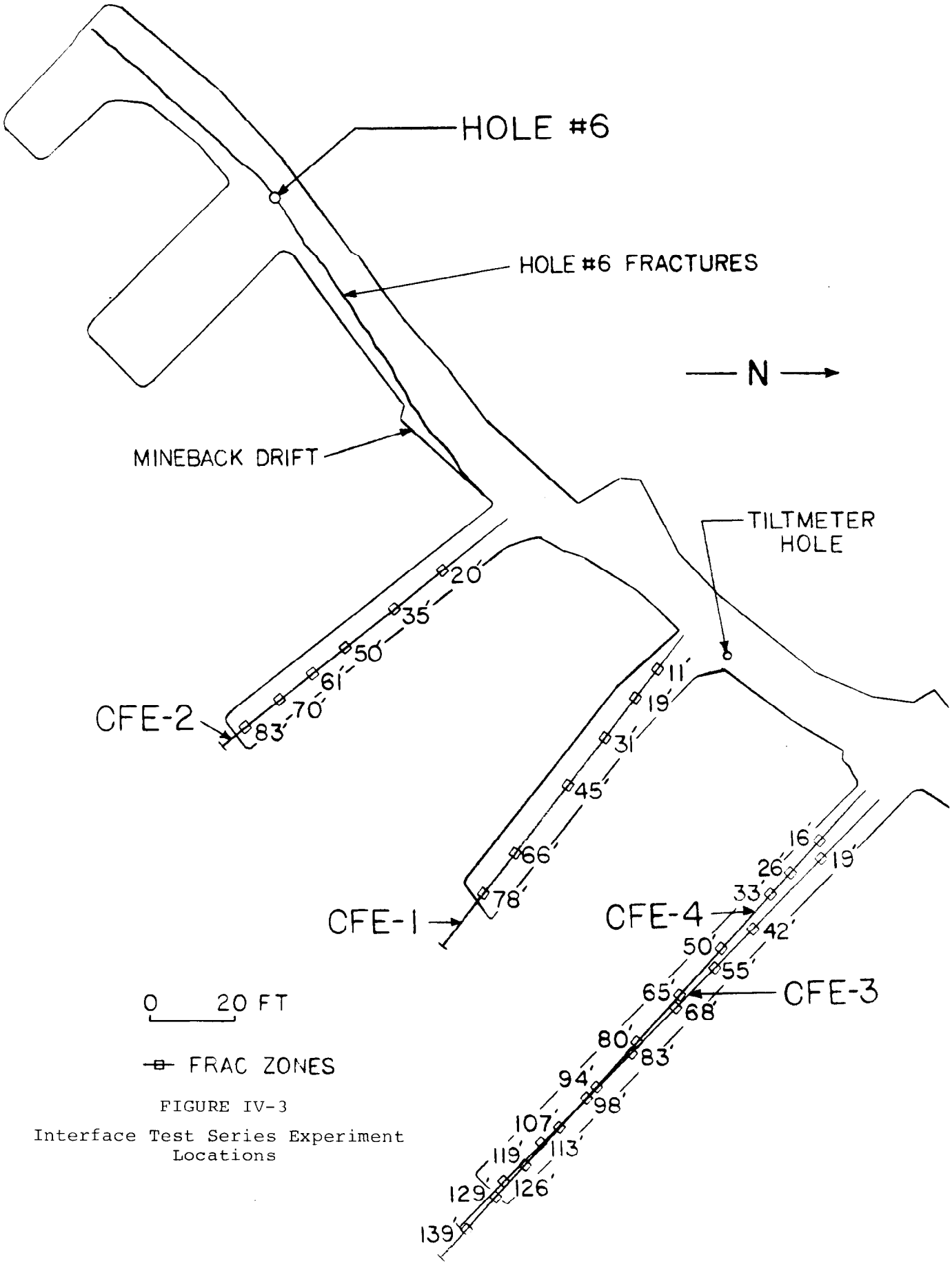

FIGURE IV-3

Interface Test Series Experiment Locations

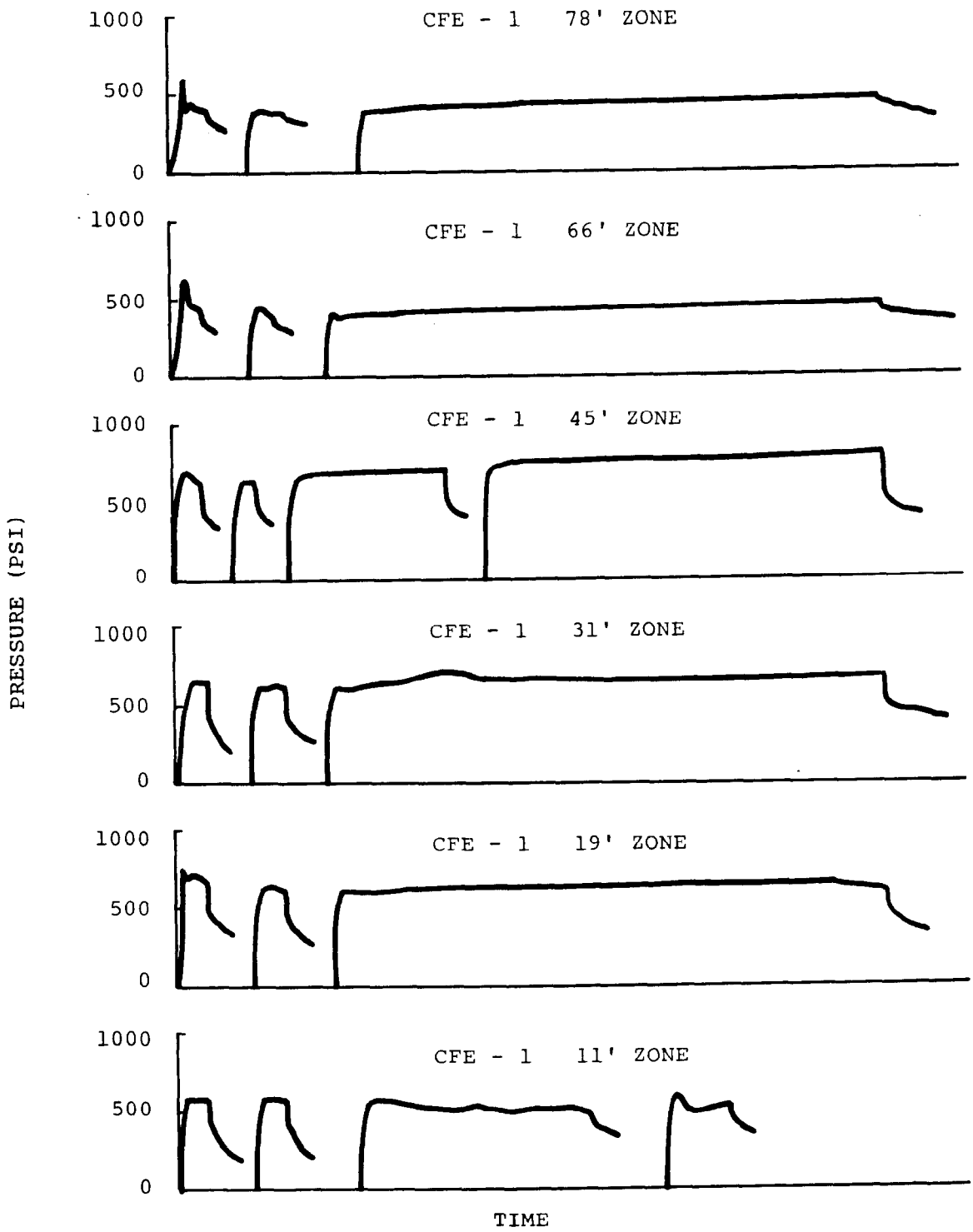

FIGURE IV-4

CFE-1 Pressure Data

TABLE IV-I. CFE Fracturing Data

ZONE*	BREAKDOWN				RECYCLE			MAIN PUMP		
(ft)	P_c (psi)	P_f (psi)	P_{isi} (psi)	Vol. (gal)	P_f (psi)	P_{isi} (psi)	Vol. (gal)	P_f (psi)	P_{isi} (psi)	Vol. (gal)
11	---	585	435	8.3	585	435	6.9	530-570	435	134.8
19	735	680	480	5.5	630	440	7.8	615	500	138.7
31	---	655	420	7.6	600	400	6.0	610-655	510	136.4
45	---	630	450	6.6	630	450	3.9	630-780	540	139.5
66	625	440	355	6.0	390	315	5.1	380-447	410	138.9
78	600	390	325	3.7	400	350	7.0	370-447	430	139.3
20	---	700	575	6.8	640	580	2.5	840	810	40.7
35	---	1060	855	7.6	1000	840	3.9	980	870	38.5
50	---	1200	1160	9.7	1150	---	3.1	1275	---	37.2
61	---	1070	950	8.4	1070	970	7.6	1100	1025	36.0
70	---	1010	930	7.9	1120	1050	5.8	1120	1050	36.3
83	---	1000	740	8.1	900	720	5.1	750	700	137.0
19	750	665	510	7.0	670	510	4.7	685-1015	665	138.3
42	1075	700	535	6.7	675	535	3.0	670	540	140.3
55	1050	835	600	10.5	790	570	3.6	815-1190	800	135.9
68	1150	680	520	7.6	625	515	4.6	600-700	600	90.0
83	1090	850	550	5.7	750	585	2.8	700	600	90.2
98	1365	725	585	5.6	700	585	3.7	680-1420	1140	140.7
113	1290	790	610	9.0	735	585	3.2	770-1230	850	137.8
126	900	710	635	7.7	750	640	4.5	650	600	137.8
16	948	532	470	3.6	539	470	1.9	545	475	2.0
26	1193	832	600	4.6	920	670	2.0	950	700	2.4
33	1193	1118	780	4.2	1300	1010	2.0	982	765	2.1
50	873	702	505	5.1	668	485	2.1	675	520	2.1
65	954	614	480	5.4	580	505	1.9	580	490	2.1
80	1125	627	480	5.2	586	475	2.1	580	485	2.2
94	1132	614	450	5.3	597	425	2.3	600	425	2.1
107	1173	1077	700	6.0	838	585	2.1	850	600	2.2
119	1028	676	470	6.4	600	440	2.3	545	435	2.6
129	580	470	310	3.8	464	300	2.6	456	295	2.3
139	---	---	---	8.0	470	380	4.2	416	360	3.0

*Flow rate was 8 gal/min for main pump on all tests except for CFE-2, Zones 20 and 50 at 2 gal/min, and CFE-2, Zones 35, 70, and 83 at 4 gal/min.

were clearly discernible for all six fractures and increased with decreasing distance between insturments and the fracture plane. Also, the form of tilt-time curves followed theoretical expectations. Tiltmeters were shown to be an effective way of observing fracture growth in real time.

All six zones of the CFE-1 fractures were then mined back, mapped, and photographed. It was found that all six fractures propagated upwards through the interface into the higher modulus material. This confirmed the results of the Hole #6 experiment. Figures IV-5 and 6 show photographs taken during mineback. It can be seen that the fractures crossed the interface, which occurs at the first brown oxide layer above the hole, but it should also be noted that the fractures only propagated 1-3 ft below the hole. Sufficient volume (150 gal) was injected into each zone to create a penny-shaped crack of 20-30 ft radius, yet, in all six zones the fracture terminated 2-4 ft below the interface. The only mechanism capable of limiting fracture propagation to such an extent is a sharp increase in the magnitude of the minimum principal in situ stress a few feet below the hole. This would be further investigated in the following tests.

CFE-2 was the second series of tests and was conducted in a borehole ~40 ft away from CFE-1, as shown in Figure IV-3. The purpose of these tests was to create the fractures at very low flow rates to determine if the pumping rate was an important factor in the containment of the fractures at a material property interface. Four zones were originally chosen; the 20' and 50' zones were fraced at 2 gal/min and the 35' and 70' zones were fraced at 4 gal/min. Only 50 gal of fluid were utilized in each test, but this should have still been sufficient to create at least 15 ft radius fractures. The hole was drilled such that it was 5 ft below the interface at the collar and 8 ft below at TD to further investigate the in situ stress variations below the interface.

When mineback was initiated, it was found that the fractures in the first two zones (20' and 35') were extremely small (3 ft x 8 ft); this is typically the size of 5-10 gal fractures in the tuffs. To make certain that there was

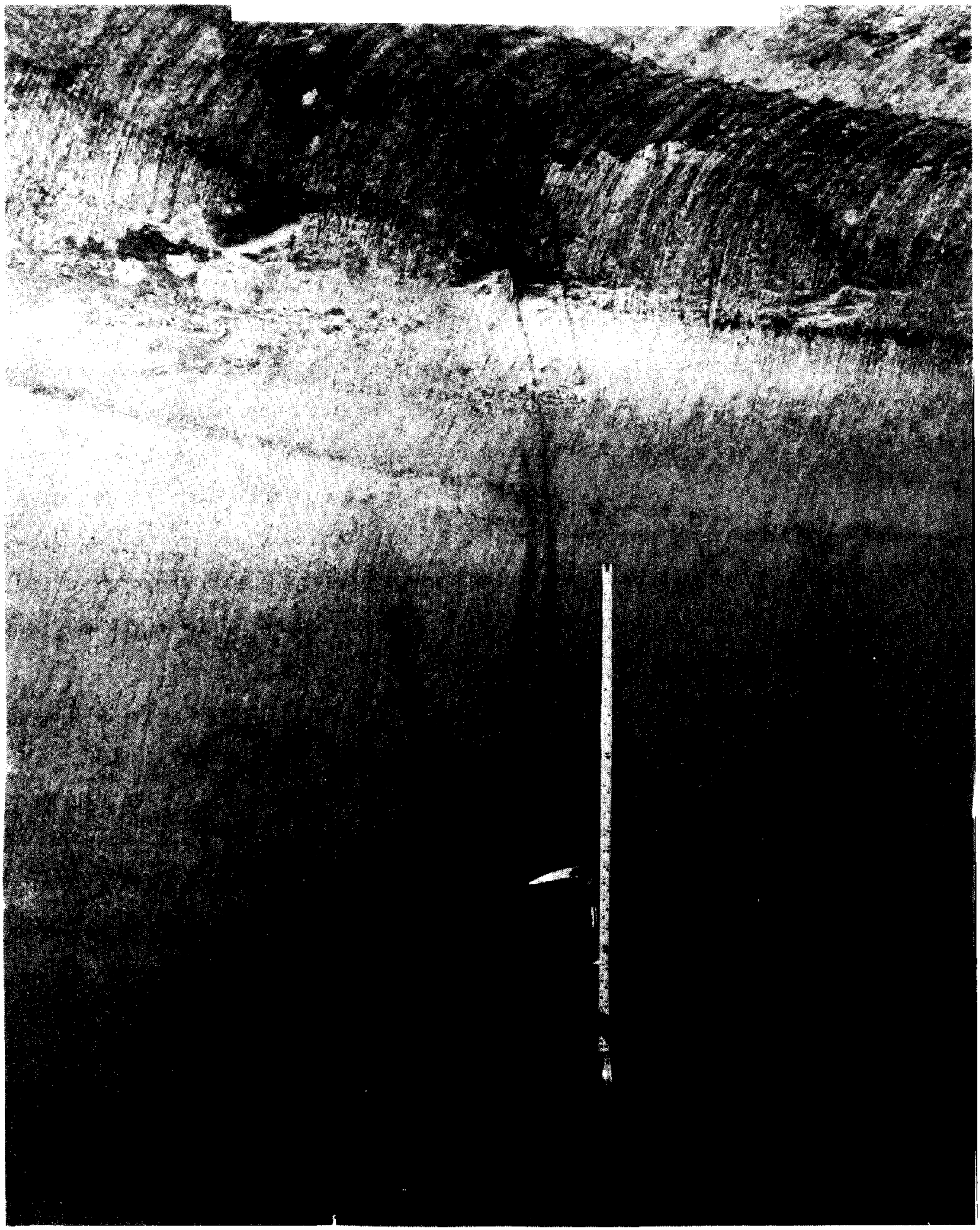

FIGURE IV-5

Hydraulic Fracture at 19 ft Zone of CFE-1

FIGURE IV-6

Hydraulic Fracture at 66 ft Zone of CFE-1 (Surrounding rock has been chipped away to show the fracture plane.)

not a mechanical problem that resulted in pumping a much smaller volume into the zones than expected - such as packer leakage or flow rate transducer malfunction, mineback was temporarily halted at 43 ft in the hole and two extra zones at 61' and 83' were fractured as controls. The total volume pumped was measured carefully and care was taken not to allow fluid to leak around the packer. The pressure data from all six of these zones is shown in Figure IV-7, and the important data points are given in Table IV-I. It can be seen that the variations in the fracturing pressure and the in situ stresses are considerable in this region.

When mineback resumed, it was found that all six fractures were very small. The first three (20', 35', 50') were essentially rectangular fractures, confined to a vertical zone from about 2 ft to 7 ft below the interface. The other three fractures (61', 70', 83') were also arrested about 2 ft below the interface; however, they propagated 3-6 ft further down than the other zones.

In order to explain the behavior of these fractures, it is necessary to understand the in situ stress distribution in the region below the interface. Figure IV-8 shows a graph of the ISIP (or minimum principal in situ stress) from both CFE-1 and CFE-2 as a function of distance below the interface. In CFE-1 the magnitude of the stress is increasing with depth below the interface, and this stress increase is probably responsible for crack termination 2-4 ft below the interface. In CFE-2, a peak in the vertical stress distribution is observed. The fractures in the three zones above the peak propagated in a layer between 2 and 7 ft below the interface, locations that characterize the stress increases seen in CFE-1 (2-4' below) and CFE-2 (6-7' below). The fractures in the three zones on or below the peak propagated both upward to about the 2 ft level and also downward. The exact location of the stress peak cannot be determined from the pressure data alone since the hydraulic fracture has a finite area over which the stresses act. However, it is clear that these stress peaks do exist and that they are the controlling influence on hydraulic fracture propagation.

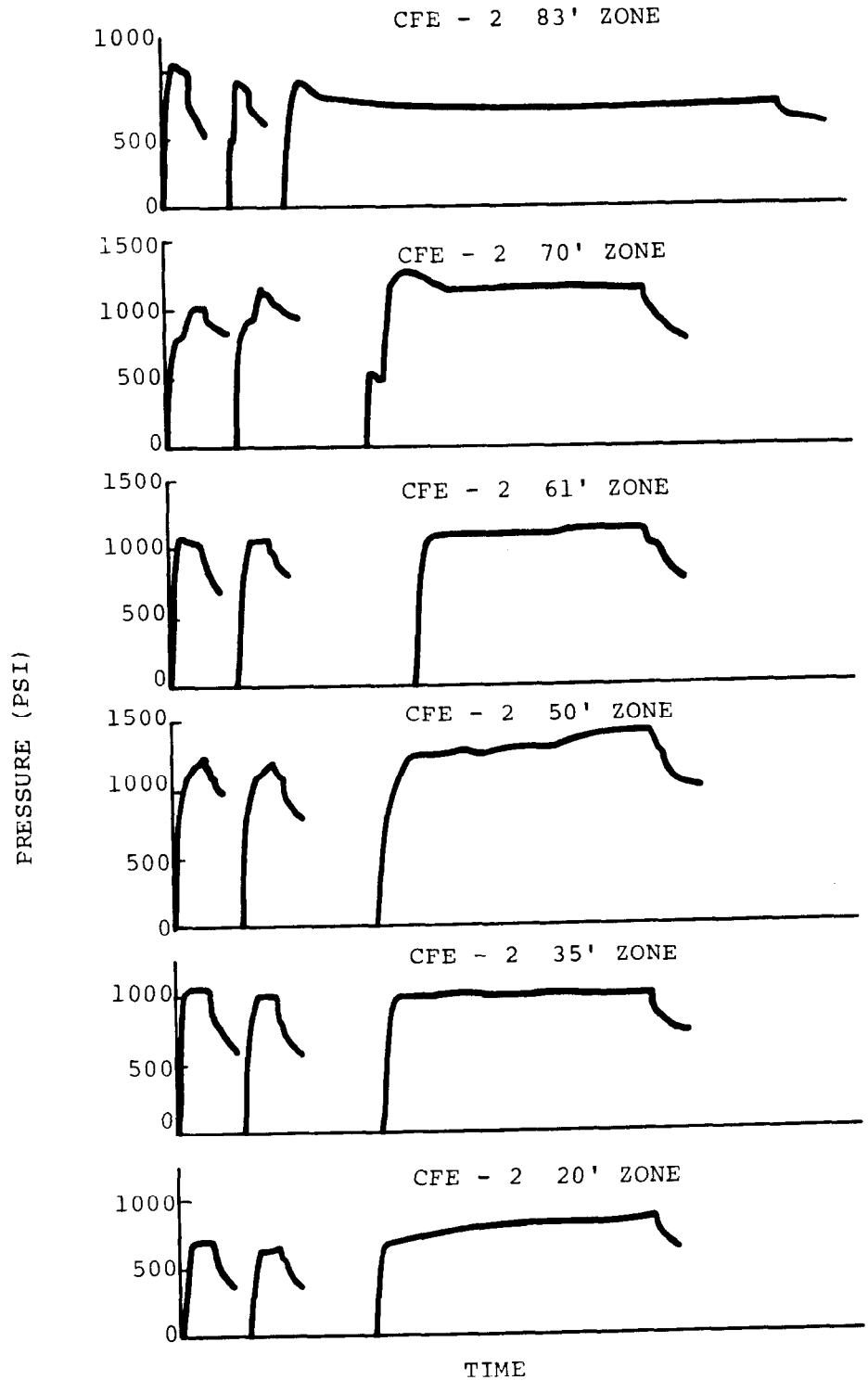

FIGURE IV-7

CFE-2 Pressure Data

FIGURE IV-8

Vertical Distribution of the Minimum Principal In Situ Stress Below the Interface - CFE-1 and CFE-2

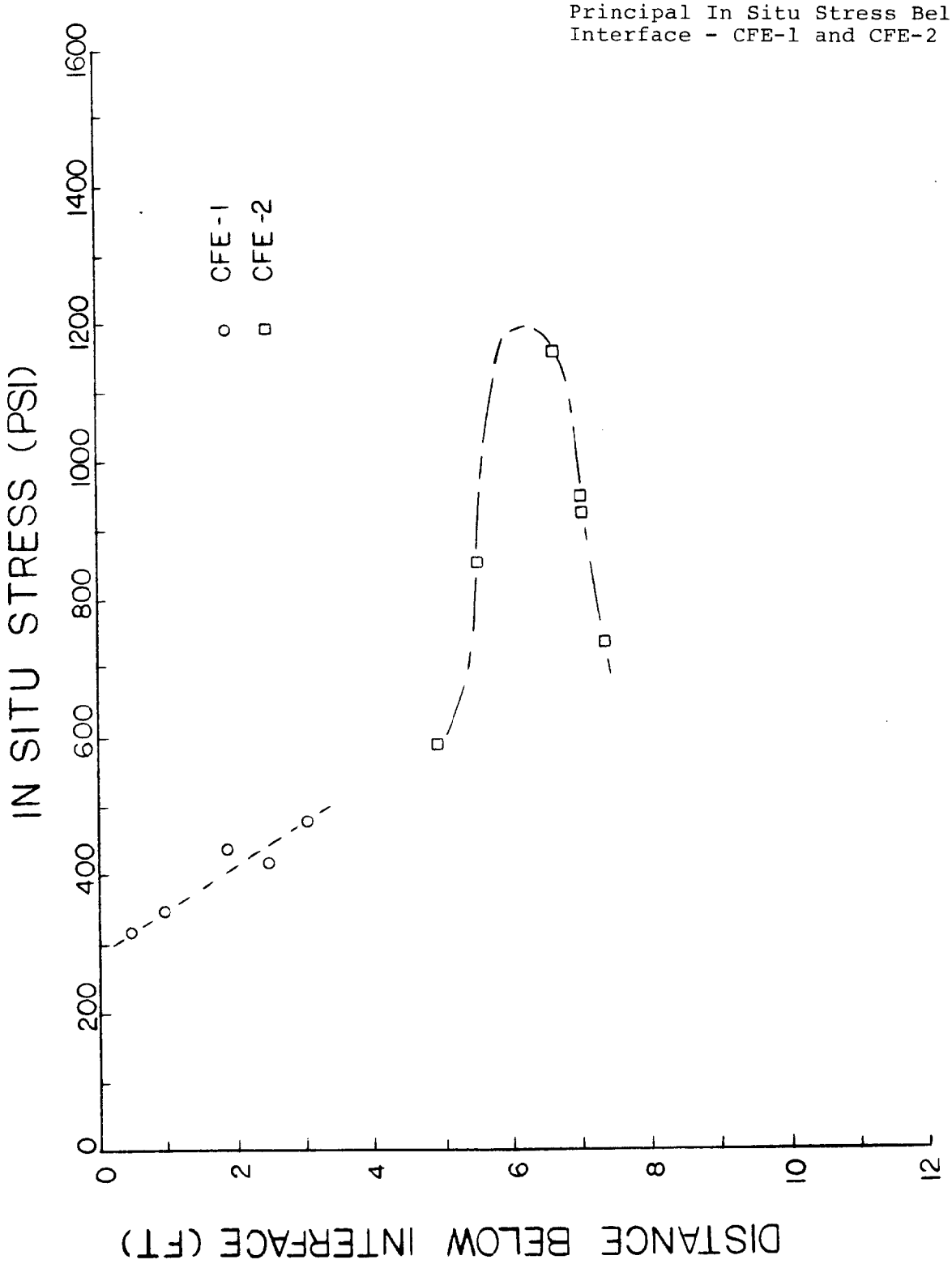

This may also help explain why the fractures in CFE-2 were very small. The fractures were contained in a region of high in situ stresses resulting in fracturing pressures that were twice those expected and resulted in greater leakoff. Leakoff is also aided by indications of increased permeability in this region.

CFE-3 and CFE-4 were two experiments conducted together to thoroughly define the nature of the stress irregularities below the interface and demonstrate its significance to hydraulic fracture propagation. As shown in Figure 3, CFE-3 and CFE-4 were conducted in nearby parallel holes which were drilled at different angles with respect to the interface. Eight zones in CFE-3 were fractured at 8 gal/min with 150 gal of dyed water in three stages similar to CFE-1. These were the "test" fractures which would be mined back and their behavior observed. Figure IV-9 show the pressure data from CFE-3, and the important data points are given in Table IV-I. There are considerable variations in the magnitude of the fracturing pressure from zone to zone; this is apparently due to variations in the in situ stresses in this region. In CFE-4, small volume hydraulic fractures (minifracs) were conducted in eleven zones to provide better resolution of the vertical stress distribution below the interface. The data from these tests are shown in Table IV-I.

The minimum principal in situ stress variations below the interface, as determined from CFE-3 and CFE-4, are shown in Figure IV-10. The stresses in this region apparently also have a double peak in the vertical distribution. It is believed that the stress peaks are actually larger than is shown because the fracturing pressure in some of these zones was much higher than the stress values indicate. Mineback of CFE-3 revealed the same phenomena as seen in CFE-1 and CFE-2.

Figure IV-11 shows a representation of the different fracture behavior observed in all the tests; the direction of fracture growth is clearly a function of the location of fracture initiation with respect to the stress peaks. Fractures which were initiated above the upper stress peak, either in the ash

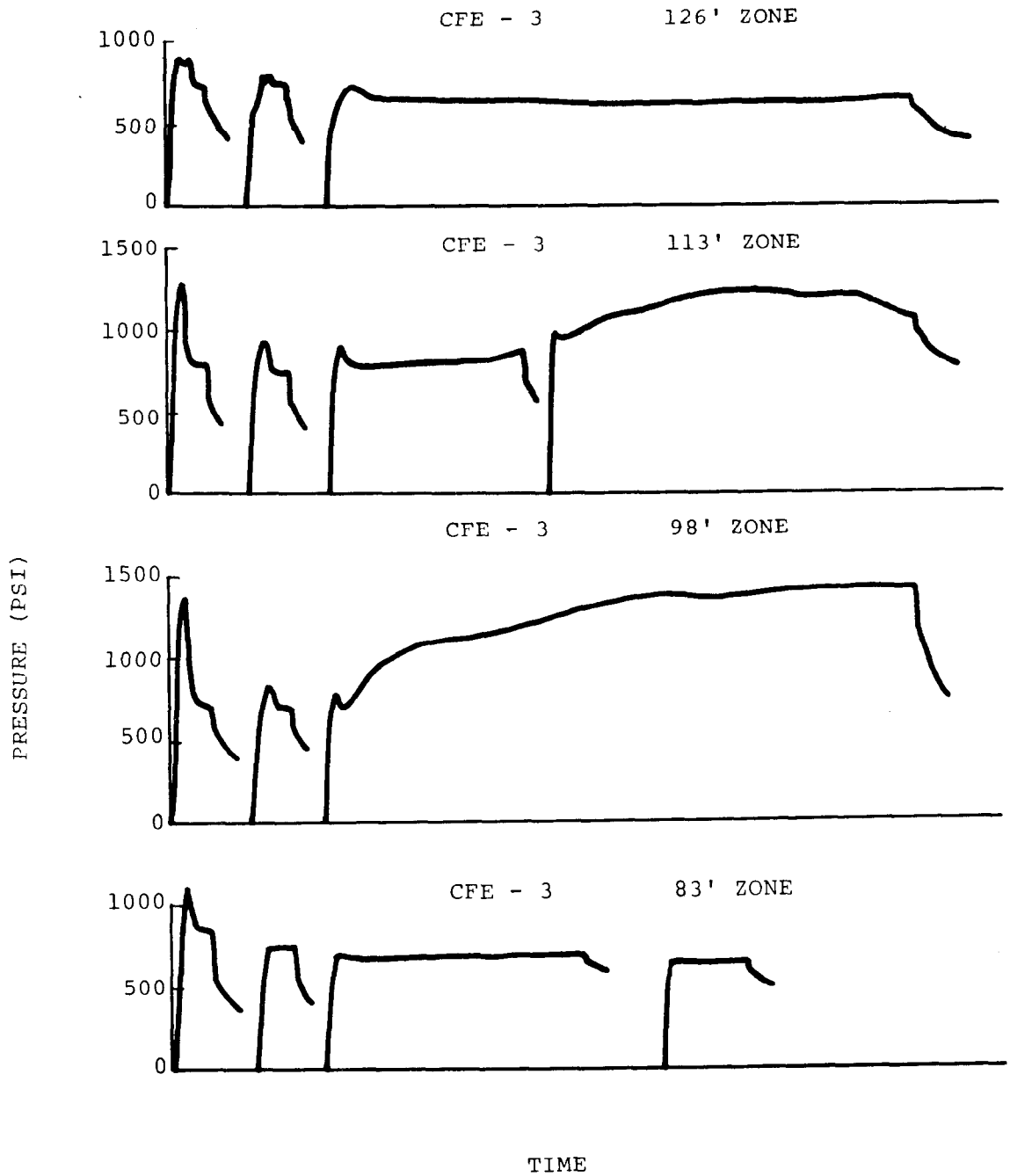

FIGURE IV-9

CFE-3 Pressure Data - 126, 113, 98 and 83 ft Zones

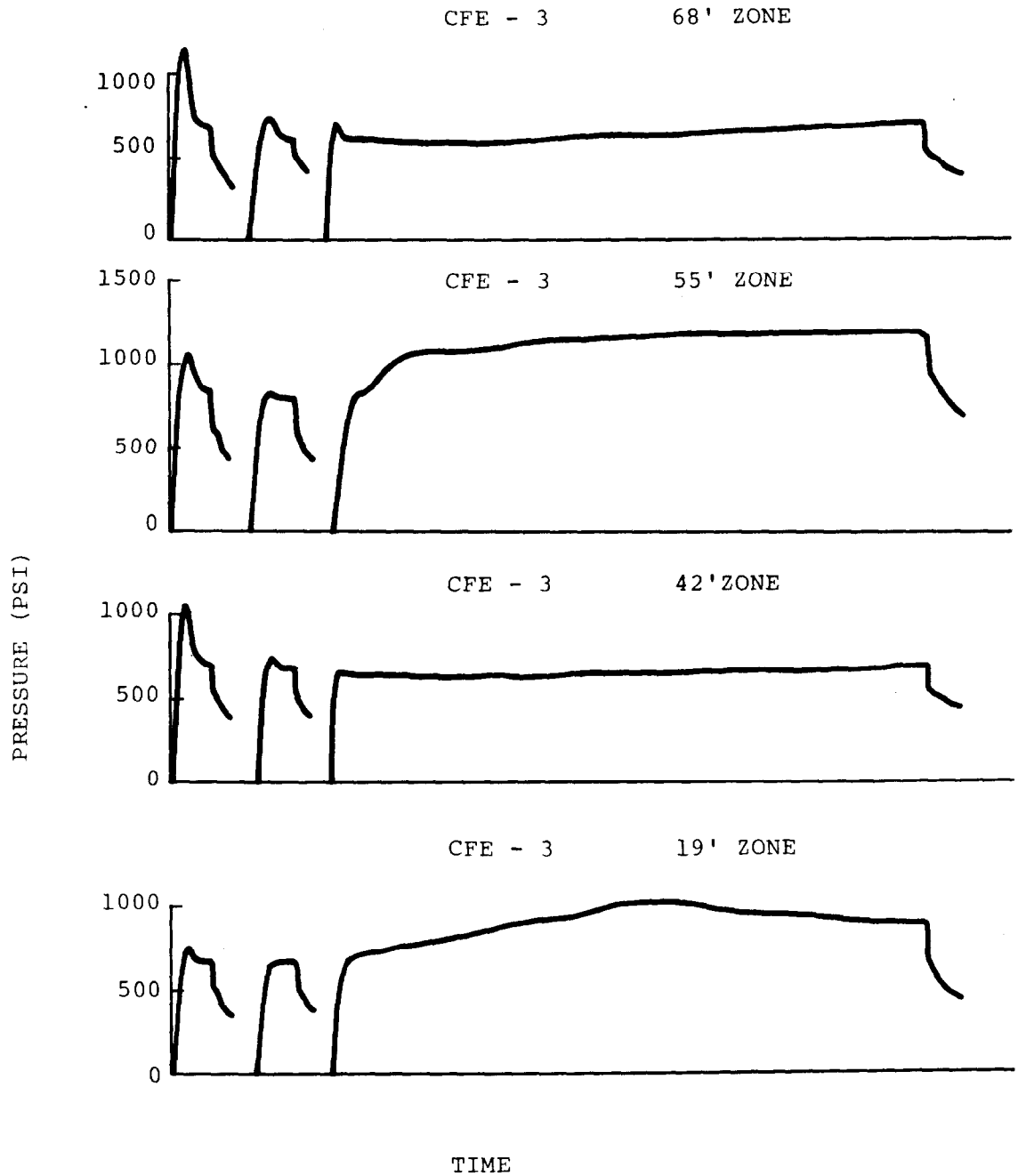

FIGURE IV-9, Cont.
CFE-3 Pressure Data - 68, 55, 42 and 19 ft Zones

FIGURE IV - 10

Vertical Distribution of the Minimum Principal in situ Stress Principal Below the Interface - CFE-3 and CFE-4.

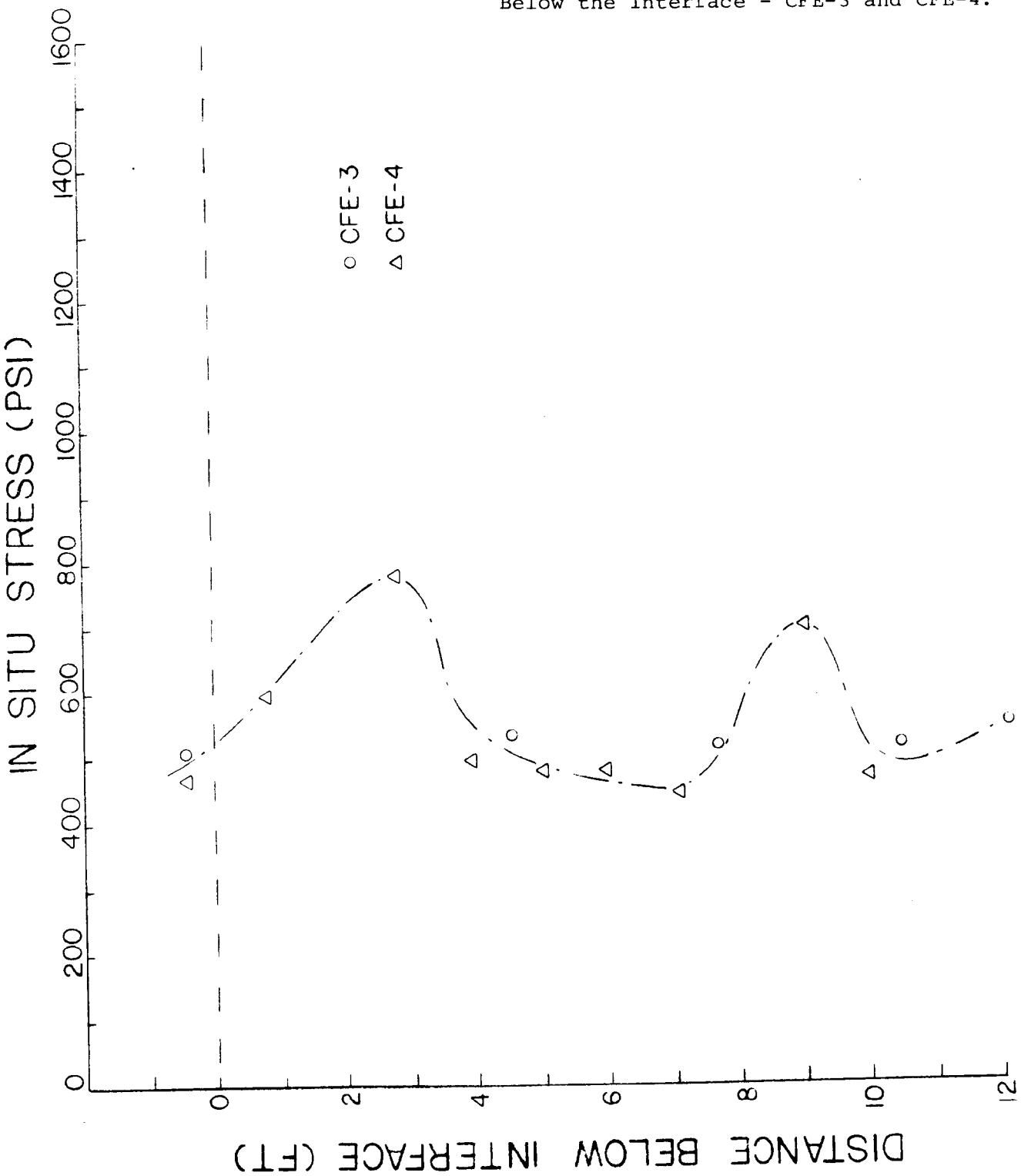

fall or welded tuff, had their downward growth terminated by the unfavorable stress gradient; they preferred to propagate into the higher modulus material. Fractures which were initiated between the stress peaks were often confined to that region, as seen in CFE-2. Fractures which were initiated below the lower stress peak for the most part remained below the peak and primarily propagated downward; however, the fractures in CFE-2 which were initiated in zones near or on the peak did propagate upward as well.

These experiments have shown that material property interfaces have little effect on the containment of hydraulic fractures. It has been demonstrated, however, that the in situ stresses have an overwhelming influence on fracture behavior and direction of fracture growth. In particular, it is the in situ stress variations which are most likely to contain a hydraulic fracture. It thus becomes imperative to determine the in situ stresses in regions where containment is desired and, therefore, development of an in situ stress measuring tool or technique should be a priority for future research.

2. Modeling and Analysis

a) Rock Mechanics and Microcrack Model (R. A. Schmidt, 4732)

A rock mechanics/fracture mechanics model was formulated that describes the probable character of the microcrack zone at a crack tip in rock. Knowledge of the crack tip process zone is an important step in the general understanding of fracture propagation in rock. In particular, it may prove useful in descriptions and models of hydraulic fracture propagation near formation interfaces to be described in the next section. Such a microcrack model is also needed in order to understand rock fracture testing on the laboratory scale and to help set standards for fracture toughness testing. Initial calculations and results with this model have, in fact, revealed several explanations for "anomalous" behavior in hydraulic fracturing and in fracture toughness testing. Other, less obvious, benefits may result from this model in understanding the permeability changes that occur to the rock material near a hydraulic fracture surface. For example, a propagating fracture leaves a damaged zone

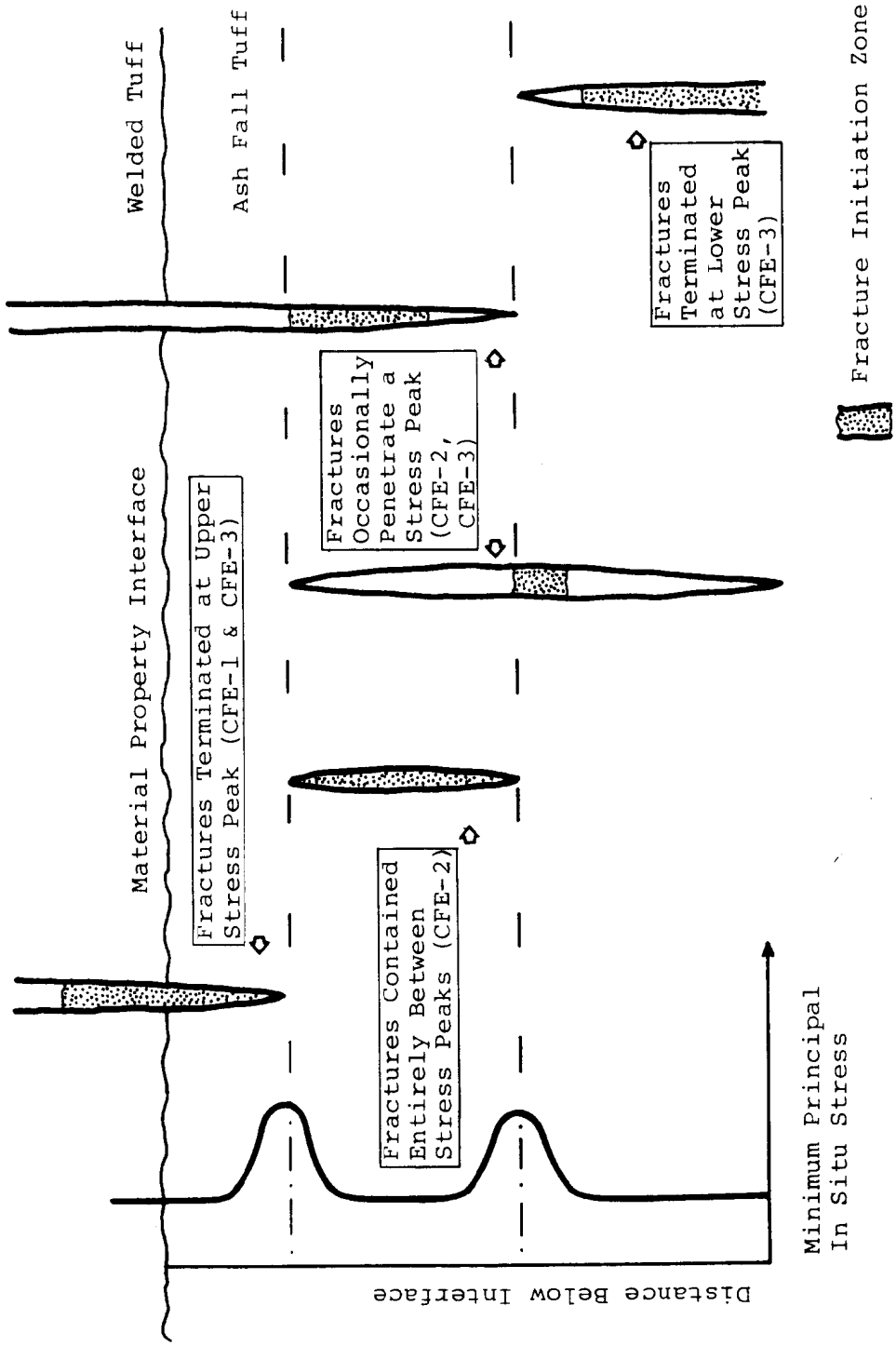

FIGURE IV-11

Representation of the Various Types of Fracture Behavior Observed in Interface Test Series Experiments

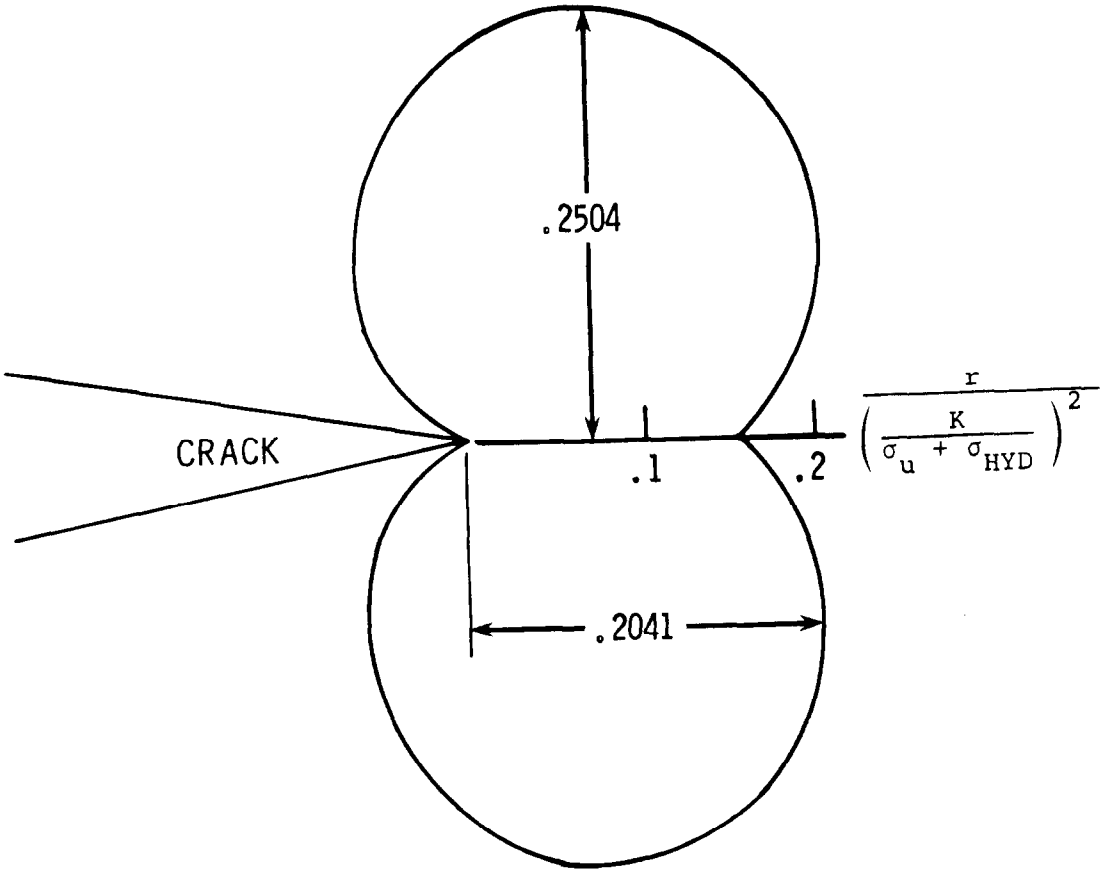

FIGURE IV-12

Damage Zone at a Crack Tip in Rock Based on Maximum Tensile Stress

in its wake as a result of the microcracking that occurs at the crack tip.

A straightforward modification of existing theories for metals was made which uses a failure theory more appropriate for rock. Some kind of process zone occurs at any crack tip regardless of the material, and much has been written in particular about the character of the "plastic zone" that occurs in metals. Most metals obey a von Mises yield condition while rocks tend to fail due to the maximum tensile stress. With this in mind, the classic equations for crack tip stresses were used to determine the contour for which the maximum tensile stress is equal to the ultimate stress. With the addition of hydrostatic in situ stresses, the equation for this contour becomes

$$r = \frac{1}{2\pi} \left(\frac{K_{Ic}}{\sigma_u + \bar{\sigma}} \right)^2 \cos \frac{\Theta}{2} \left(1 + \sin \frac{\Theta}{2}\right)^2 \qquad (1)$$

where

r, Θ are polar coordinates from the crack tip

K_{Ic} is fracture toughness

σ_u is ultimate stress

$\bar{\sigma}$ is hydrostatic stress

This equation can be made nondimensional and is plotted in Figure IV-12.

The size of the microcrack zone decreases rapidly with in increase in hydrostatic stress. This is contrary to the behavior of metals where plastic zone sizes are unaffected by hydrostatic stress. For example, calculations from Nevada ash-fall tuff indicated that the zone size decreases from 0.4 in for an unconfined laboratory experiment to 0.03 in for the in situ stress conditions near the Hole #6 experiment. This dramatic effect of hydrostatic stress leads to two main conclusions:

1) Results from unconfined laboratory experiments that attempt to model hydraulic fracture behavior may not be applicable to field results, particularly those at considerable depths. The unconfined specimen may have a crack tip process zone that is larger, by several orders

of magnitude, than its in situ counterpart. This fact will tend to be exaggerated by the already greatly-reduced scale of the laboratory simulation.

2) Fracture toughness, K_{Ic}, of rock has been observed to increase with an increase of hydrostatic stress, and this effect is probably a direct result of the decreased microcrack zone size. This behavior for rock has been considered anomalous by some since K_{Ic} of metals is generally unaffected by hydrostatic stress. Unlike the plastic zone size in metals, the size of the microcrack zone is unaffected by out-of-plane stresses (i.e., plane stress versus plane strain). This is amost certainly the reason that K_{Ic} of rock and concrete are known not to depend on specimen thickness while K_{Ic} of metals exhibit a strong dependence on thickness. The fact that this result fits observed behavior so well lends strong support to the model itself.

The model was then extended to include: 1) a description of the orientation of the microcracks within the zone and 2) effects of an anistropic in situ stress state. Referring to Equation 1, the stress state at each point within the zone of microcracking can be transformed to principal stress to determine the orientation of the maximum tensile stress which then gives the most probable orientation of microcracks at each point. The equation that defines these orientations, α, is simply

$$\alpha = \frac{1}{2}\left(\frac{3\Theta}{2} + \frac{\pi}{2}\right) \qquad (2)$$

This equation is depicted in Figure IV-13 by short lines within the microcrack zone which represent microcrack orientation.

The description of this microcrack zone becomes considerably more complicated when the in situ stress state is not hydrostatic. The solution process is similar to that followed for Equation 1 and, after considerable algebra, the equation becomes

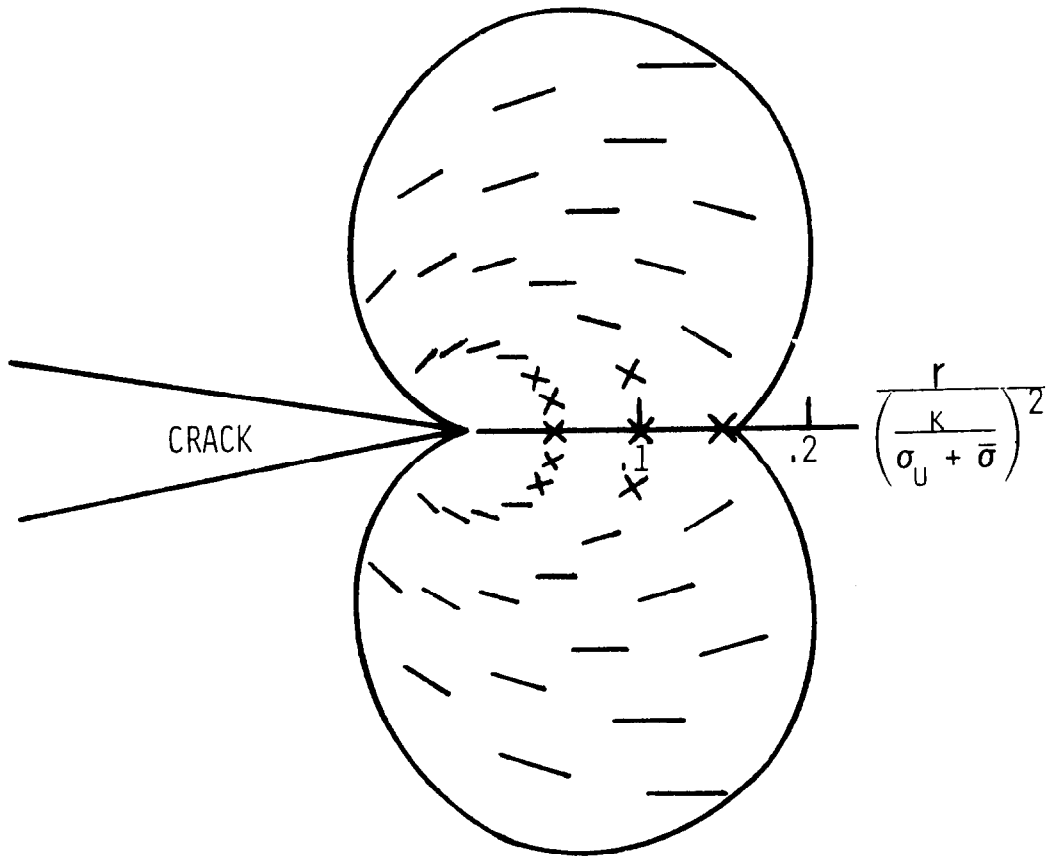

FIGURE IV-13

Damage zone at a crack tip in rock based on maximum tensile stress. Short lines are perpendicular to tensile stress and indicate probable orientation of microcracks.

$$r = \frac{1}{2\pi}\left(\frac{K_{Ic}}{\sigma_u + \bar{\sigma}}\right)^2\left(\cos\frac{\Theta}{2}\,\frac{1 + \beta\sin\frac{\Theta}{2}\sin\frac{3\Theta}{2} + \sqrt{\left(1 + \beta\sin\frac{\Theta}{2}\sin\frac{3\Theta}{2}\right)^2 - (1 - \beta^2)\cos^2\frac{\Theta}{2}}}{1 - \beta^2}\right)^2 \tag{3}$$

and

$$\beta = \frac{\sigma_{\parallel} - \sigma_{\perp}}{2(\sigma_u + \bar{\sigma})}$$

where

$\sigma_{\parallel}$ is in situ stress parallel to the crack

$\sigma_{\perp}$ is in situ stress perpendicular to the crack

$\bar{\sigma}$ is mean stress

β is degree of insitu stress anisotropy, $0 \leq \beta < 1$.

Note that, since hydraulic fractures are generally perpendicular to the least principal stress, $\sigma_{\perp}$ is considered a principal stress and $\sigma_{\perp} < \sigma_{\parallel}$. Observe that Equation 3 reduces to Equation 1 for $\beta = 0$. Equation 3 can be nondimensionalized and is plotted in Figure IV-14 for various values of β.

Although several well known rock fracture characteristics correlate well with this microcrack model, verification by direct observation would be highly desirable. An activity is presently being considered that involves microscopic studies on rock samples fractured in the laboratory under various confining pressures. The rock type selected (probably Solenhofen limestone) needs to be fine-grained and easily polished, with a low porosity, and a relatively low ratio of tensile strength to fracture toughness. This last condition should result in a relatively large microcrack zone.

b) Rock Mechanics of Fracture Propagation Near an Interface

(R. A. Schmidt, 4732)

The main purpose of the Hole #6 experiment was to examine the containment aspects of a hydraulic fracture near a formation interface. Simplified analytical models[1,8] and laboratory experiments[3,4,5] have suggested that a discontinuous increase in Young's modulus in advance of a propagating hydraulic fracture would

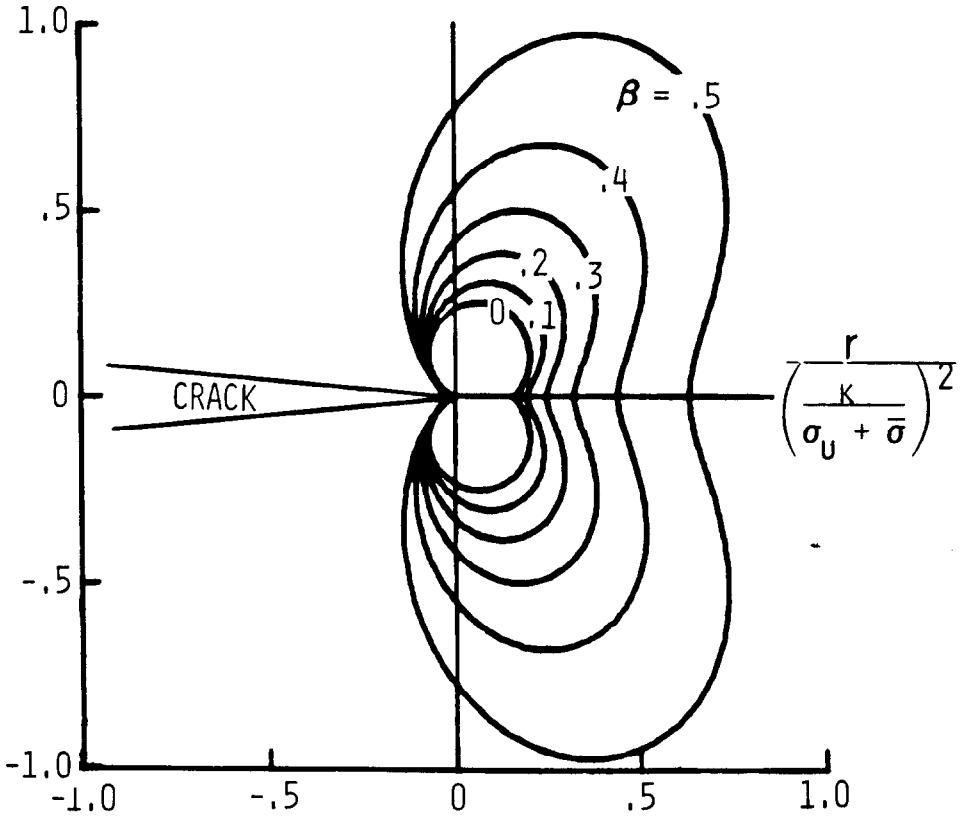

FIGURE IV-14

Microcrack Zone as a Function of in situ Stress Anisotropy, β.

cause crack arrest and thus effectively contain the fracture in the lower modulus material. The formation interface for the Hole #6 experiment had a Young's modulus increase of at least a factor of 10 and yet mineback of the fracture showed that containment did not occur; this behavior was confirmed by the Interface Test Series results. This suggests that the existing models either do not accurately represent fracture behavior in a layered medium or that the actual conditions existing in the formation do not suit the model description.

The actual interface is not a single discontinuous surface and involves an increase in modulus over the distance of several feet. With this in mind, the first step was made to measure the important material properties in this region. (A Rock Properties Laboratory was established this year for the purpose, among other reasons, of preparing rock samples which could then be tested in existing facilities.) Several cores were obtained along each of five stratigraphic layers for the purpose of obtaining values of tensile strength, elastic moduli, and fracture toughness. Tensile strength and Young's modulus were obtained from direct-pull tension tests; fracture toughness was measured using the "short rod" specimen configuration.[10] Table IV-2 summarizes the results of these tests.

The various layers are listed in order of their occurrence with the ash-fall tuff being the deepest layer. While these data are still sparce, a distinct change of Young's modulus does occur between the ash-fall tuff and the basal ash-flow tuff. With this in mind, the analytical models were reexamined, and two shortcomings are apparent:

1) While material properties may change abruptly, the crack-tip microcrack zone has the effect of averaging the properties over some distance and the mathematical idealization of a discrete interface probably leads to erroneous results.
2) The fracture criterion used in these models is one based on a critical stress intensity factor. This may have little or no meaning at a

TABLE IV-2. Material Property Data Near Hole #6 Experiment

Zone	Specimen Diameter (inches)	Fracture Toughness (psi $\sqrt{in}$)	Tensile Strength (psi)	Initial Young's Modulus (x 10^6 psi)
Welded*	---	---	---	-----
Vitric Ash-Flow	4.0	518	119	0.492
Ash-Flow With Abundant Lithics	6.0	649	89	1.868
Basal Ash-Flow	4.1	198	422	1.512
		530	>140**	0.963
Ash Fall	3.9	254	>28**	0.236
		151	18	0.271

*Data from two sets suspect due to fractured samples.
**Failed at endcap, but failure was imminent.

discrete interface when the character of the stress field can no longer be described by this parameter.

Initially it was hoped that the model inadequacies could be alleviated by replacing the discrete interface with a "smeared interface" in which property changes were gradual. A direct analytical approach to the problem was addressed on contract, but excessive mathematical difficulties were encountered and this attempt was abandoned. Numerical simulations of a "smeared interface" were made using a finite element code known as APES.[1] Results from these numerical calclulations and several interfaces can be treated in this way, but two shortcomings still exist:

1) Each interface is still discrete and needs to be "smeared" to account for the averaging effect of the microcrack zone.
2) While this code is very powerful, the number of elements used is very limited, and the external boundaries are not far enough from the crack to accurately simulate infinite boundaries.

The best approach for handling the actual question of fracture growth at the interface appears to be in using a more realistic fracture criterion than is used in the existing models. Since the stress field for a crack near an interface is known analytically, the most direct approach is to average the stresses ahead of the crack tip over a region as predicted by the microcrack model discussed earlier. One can then assume that crack propagation will occur when this average stress reaches some critical value as determined experimentally. This criterion is consistent with the well-tested fracture criterion for crack growth in homogenous materials as based on linear-elastic fracture mechanics.

Calculations based on this approach are needed, followed by verification with experiments. In addition to the mineback experiments at NTS (Hole #6 and Interface Test Series) and published laboratory investigations, experiments are being conducted on contract to Sandia on concrete and rock samples by Dr. A. Ingraffea at Cornell University. These latter tests are designed to examine fracture behavior near a material interface. Several three-point-bend

samples of layered concrete and rock such as shown in Figure IV-15 will be tested.

Progress to date on this investigation is as follows:

1) Five different mixes of Portland cement concrete have been designed, mixed, cured, and tested for Young's modulus in compression, Poisson ratio, and uniaxial compressive strength. The moduli range from a low of 2.5×10^6 psi to a high of 6×10^6 psi.
2) Eighteen Westerly granite ($E = 9 \times 10^6$ psi) beam-segments were purchased and prepared (honing, roughening, chevron notch-sawing) for casting in layers with the concrete. Cores and three-point-bend samples of the granite were prepared for properties determination.
3) All necessary formwork was constructed and loading system modified to test these samples. Single-composition concrete beams were tested as dry runs and controlled crack growth was achieved using crack-mouth-displacement as the feedback parameter.
4) Two methods for crack tip location monitoring using flourescent dyes and crack propagation gages were developed and tested.

All of these analytical, numerical, and experimental efforts must, however, be put in perspective with regard to recent findings from the NTS mineback experiments. An overwhelming amount of evidence indicates that the minimum principal in situ stress is the dominant parameter that dictates the geometry of a hydraulic fracture. The fact that a hydraulic fracture generally orients itself perpendicular to the least principal stress has been widely accepted, but it now appears that the direction of fracture growth, including the question of fracture containment at an interface, is primarily governed by the spatial variation in the least principal stress.

This does not, however, resolve the problem of why existing models predict containment where containment is not achieved. This dilemma still needs to be resolved and the approach described above still seems appropriate, but the emphasis needs to shift somewhat. Calculations and laboratory experiments

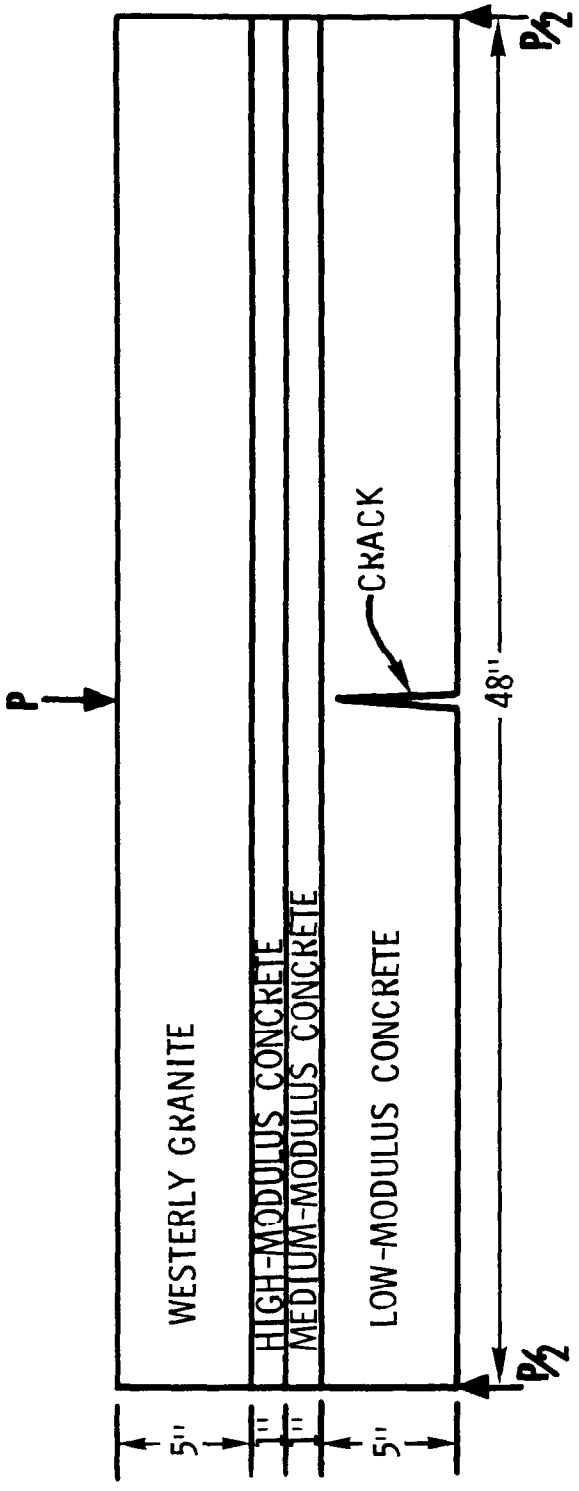

FIGURE IV-15

Laboratory Simulation of Fracture Propagation Near a Material Interface

need to address the important effects that changes in the minimum principal stress have on containment of hydraulic fractures.

c) Fluid Mechanics (N. R. Warpinski, 4732)

An effort to assemble a realistic model of the fluid mechanics of fracturing was initiated in FY79. The purposes of this modeling effort are: 1) to obtain a better understanding of the interplaying mechanisms that control the fracturing process, 2) to aid in the interpretation of previous in situ experiments and the design of new ones, and 3) to provide realistic conditions (e.g., pressure loading in the crack) upon which to apply rock mechanics considerations for the study of the effect of interfaces, in situ stresses, etc. on fracture propagation.

The type of model being developed is for a rectangular, two-dimensional fracture; this is probably a poor representation of a typical hydraulic fracture but a necessary geometric restriction to avoid a much more complicated three-dimensional calculation at this time. A model for a penny-shaped fracture, which may or may not be more realistic than a rectangular fracture, will be developed along the same lines as the rectangular fracture if the model proves suitable. Any 2-D, rectangular model automatically suffers another restriction since it is necessary to choose whether the width is a function of fracture length or fracture height whereas the actual situation is probably a combination of the two. This present model uses the length criterion since it will, for the most part, be used to analyze the short fractures typically conducted in the mineback experiments.

The width of a fracture for a given pressure distribution, P(x), where x is the distance along the fracture as measured from the wellbore, is given by England and Green[12] as

$$w = \frac{8(1 - \nu^2)L}{\pi E} \left\{ \int_{\varepsilon}^{1} \frac{\eta d\eta}{\sqrt{\eta^2 - \varepsilon^2}} \left[\int_{0}^{\eta} \frac{P(\xi)d\xi}{\sqrt{\eta^2 - \xi^2}} \right] - \frac{\pi}{2} S \sqrt{1 - \varepsilon^2} \right\} \qquad (4)$$

where

w is the width of the fracture

ν is Poisson's ratio,

E is Young's modulus

L is the length of the fracture,

$\varepsilon = x/L$ is a dimensionless location in the fracture,

S is the minimum principal in situ stress, and

η & ζ are dummy variables

If $P(x)$ is known, the width of the fracture can be determined by performing the double integration. In reality, $P(x)$ depends on $w(x)$ and neither are known a priori. Thus a solution of this coupled rock mechanics/fluid mechanics problem can only be determined by solving the fluid mechanics of the flow through the fracture in conjunction with Equation 4. Notice that Barenblatt's condition[13] is not incorporated into Equation 4; it felt that it is overzealous to impose the smooth closure condition on a macroscopic scale when this feature probably occurs on the microscopic level.

The fluid mchanics of this problem are incorporated by applying the conservation laws to flow through a segment of the fracture. Time-dependent terms are not discarded (as is usually the case in hydraulic fracture models) because they may be significant for short times (small fractures) which is the particular situation which this model is designed for. For one-dimensional fluid flow in the fracture, the conservation of mass principle yields the continuity equation

$$\frac{\partial w}{\partial t} + \frac{\partial (Uw)}{\partial x} + 2U_L = 0 \ , \tag{5}$$

where

t is time,

U is the velocity, and

U_L is the leakoff velocity

Application of the conservation of momentum law results in

$$\frac{\partial(Uw)}{\partial t} + \frac{\partial(U^2w)}{2x} = \frac{-w}{\rho}\frac{\partial p}{\partial x} - \frac{2\tau_w}{\rho}, \tag{6}$$

where

ρ is the density and

τ_w is the shear stress

Although the model is being developed using a Newtonian fluid in the laminar flow regime, non-Newtonian fluids and turbulent flow conditions can also be included by correct calculation of τ_w in Equation 6. The leakoff velocity in Equation 5 is calculated using Howard and Fast's equations.[14] The boundary conditions for the fluid flow are:

i) at $x = 0$ $\mu = q/(2wH)$

where

q is the pump rate and

H is the zone height; (7)

ii) at $x = L$ $\mu = dL/dt$; and

iii) at $x = L$ $P = S$.

Equations 5 and 6 are finite differenced using a Crank-Nicholson technique. Two of the boundary conditions of Equation 7 are needed to obtain solutions of these equations. The final boundary condition determines the correct value of all the parameters such that a correct solution of Equations 4, 5, and 6 is obtained which is consistent with the solution from the previous time step. In practice the calculations occur in the following manner. A pressure distribution is assumed (usually the pressure distribution from the previous step or an initial guess if it is the first step) and the width distribution is obtained from numerical integration of Equation 4. The velocity distribution in the fracture is calculated from the differenced version of Equation 5 with the appropriate value of U_L calculated for each segment at that time period. Using the calculated width and velocity distributions and the appropriate value of the shear stress for each segment, Equation 6 in finite difference form can

be solved for a corrected pressure distribution in the fracture. This distribution is then inserted into Equation 4 and the process is repeated. Iterations continue until the third boundary condition of Equation 7 is satisfied to a sufficiently accurate degree. It has been found, however, that this iteration does not readily converge to the solution point, and it is necessary to use some technique to force it to converge.

Although solutions have been obtained with this model, work is being performed to test various transformations, differencing techniques and convergence methods to optimize solution of the equations. This is important since one convergence technique may work with one set of fracture parameters but not with somewhat different ones. Efforts are directed towards developing a general model which will obtain solutions for any case.

Results obtained to date do illustrate the importance of the transient terms in the fluid flow equations as well as the use of the complete width equation. Figure IV-16 shows calculated pressure distributions in a hydraulic fracture having the same parameters as found in the Hole #6 Formation Interface Experiment. The steady-state curve is the calculated pressure distribution if the transient terms are discarded. This is not far from the constant pressure condition that is employed by most hydraulic fracture models and is probably the situation that would occur at large times when the transient terms decrease in importance (i.e., for a given time step, the fracture width and length increase less with increasing time). However, the transient curve shows the calculated pressure distribution with the transient terms retained, and it can be seen that this is considerably different from the usually assumed constant pressure. This pressure distribution was obtained at a time about midway through the Hole #6 fracturing treatment (after 100 bbls) so it can be seen that the transient terms are important for a considerable time span. When the model is operating efficiently, calculations will be made to see how severely this affects present design models.

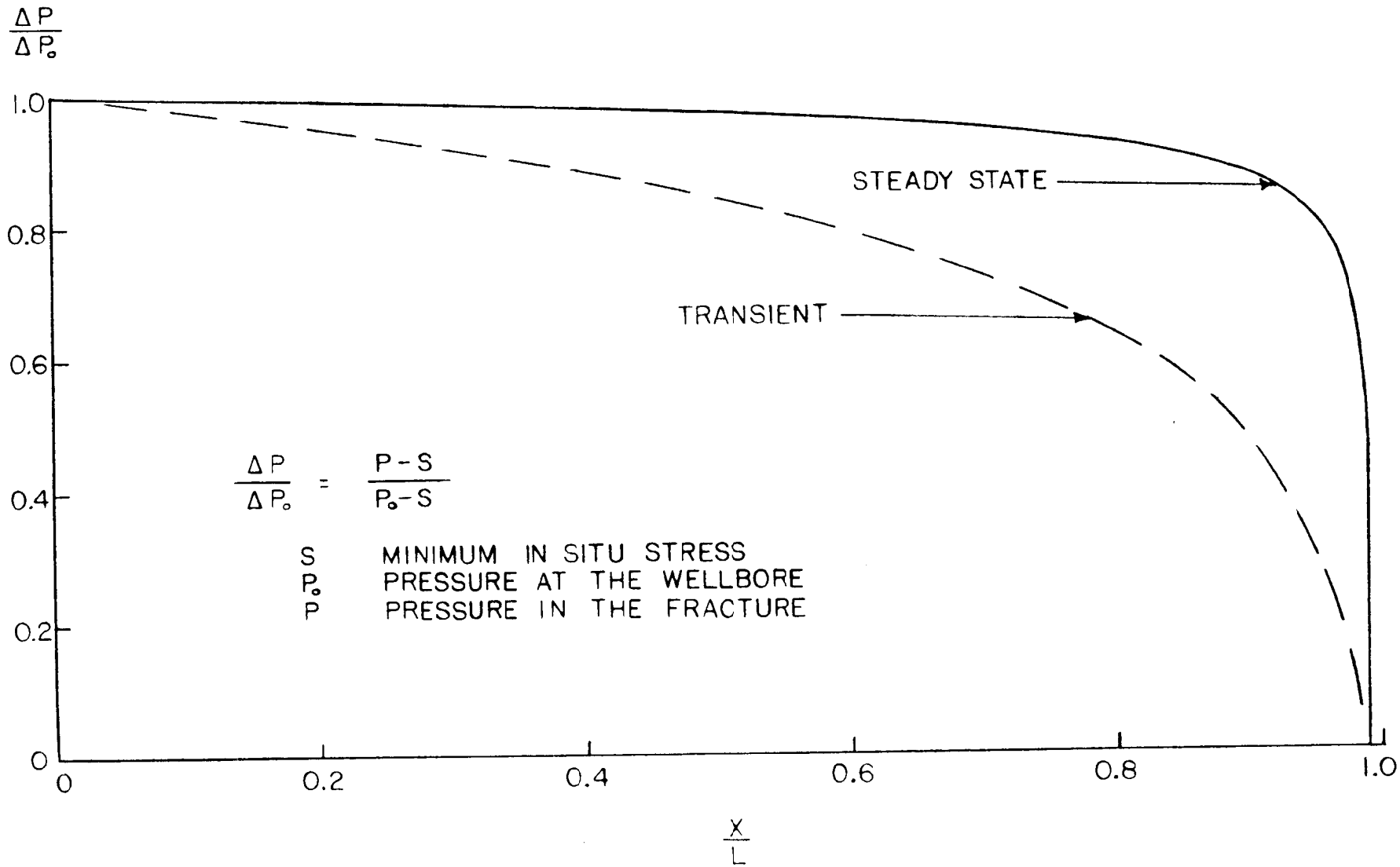

FIGURE IV-16

Calculated Pressure Distribution in a Hydraulic Fracture

References for Section IV-A

1. Simonson, E. R., et al., "Containment of Massive Hydraulic Fractures," Soc. of Petroleum Engineers Journal, p. 27-32, Feb. (1978).

2. Rogers, L. A., et al., "Massive Hydraulic Fracture Containment Analysis Utilizing Rock Mechanics Considerations," Proceedings of the Massive Hydraulic Fracturing Symposium, U. Of Oklahoma, Norman, OK, (1977).

3. Daneshy, A. A., "Hydraulic Fracture Propagation in Layered Formations," Society of Petroleum Engineers Journal, p. 33-41, Feb. (1978).

4. Hanson, M. E., et al., "LLL Gas Stimulation Program, Quarterly Progress Report, April through June 1978," Lawrence Livermore Laboratory Report UCRL-50036-78-2, July (1978).

5. Hanson, M. E., et al., "Theoretical and Experimental Research on Hydraulic Fracturing," Proceedings, Fourth Annual DOE Symposium on Enhanced Oil and Gas Recovery and Improved Drilling Methods, Tulsa, OK, (1978).

6. Warpinski, N. R., et al, "Direct Observation of Hydraulic Fractures: Behavior at a Formation Interface," Sandia Laboratories Report, SAND78-1935, Oct. (1978).

7. Holzhausen, G. R., "Analysis of Earth Tilts Resulting From Formation of Six Hydraulic Fractures, Crack 'r Frac Experiment #1, March 27 and 28, 1979, G-Tunnel, Nevada Test Site, Nye County, Nevada," M. D. Wood, Inc., Contractor Report for Sandia Laboratores, Jan. 19, (1978).

8. Cook, T. S. and Erdogan, F., "Stresses in Bonded Materials with a Crack Perpendicular to the Interface," Inter. J. of Eng. Sci., Vol. 10, p. 677-697, (1973).

9. Teufel, L. W., "An Experimental Study of Hydraulic Fracture Propagation in Layered Rock," PhD dissertation, Texas A&M University, Aug. (1979).

10. Barker, L. M., "K_{Ic} Measurements Using Short Rod Specimens--The Elastic-Plastic Case," Terra Tek Report, TR77-91R, (1977).

11. Gifford, L. N., and Hilton, P. D., "Stress Intensity Factors by Enriched Finite Elements," Engineering Fracture Mechanics, Vol. 10, p. 485-496, (1978).

12. England, A. H. and Green, A. E., "Some Two-Dimensional Punch and Crack Problems in Classical Elasticity," Proceedings of the Cambridge Philosophical Society, Vol. 59, p. 489, (1963).

13. Barenblatt, G. I., "The Mathematical Theory of Equilibrium Cracks in Brittle Fracture," Advances in Applied Mechanics, Vol. 7, p. 56 (1962).

14. Howard, G. C. and Fast, C. R., "Optimum Fluid Characteristics for Fracture Extension," API Drilling and Production Practices, p. 261, (1957).

B. Dynamic Wellbore Fracturing

1. Background

Oil and gas wells hve been stimulated with high-energy explosives since the late 1800's. Well shooting techniques are usually applied for the purpose of introducing random multiple fractures rather than a single large fracture as is created by hydraulic fracturing. Multiple fracturing is desired for eleminating "skin damage" caused during drilling and for effectively connecting the wellbore to an existing fracture system as might occur, for example, in a gas-bearing Devonian shale. Connecting a well to a fracture network is often not possible by hydraulic fracturing since there is little or no control over fracture orientation and the created fracture will often run parallel to existing fractures.

Studies have repeatedly demonstrated the effect that contained explosions have on the surrounding rock formations. These studies, which include field experiments[1-3]* laboratory experiments[4] and code calculations[1,5] demonstrate the existence of residual stresses and compaction that can cause deleterious effects in a wellbore. In essence, the high pressures of a detonation in a wellbore are known to be sufficient to cause the nearby rock to yield and compact by plastic flow. When the stress wave passes, the rock unloads elastically leaving an increased borehole diameter and a residual stress field which is compressive near the wellbore. The creation of this residual stress field is closely analogous to the process of autofrettage or the "gun barrel problem" in which pressure vessels are often over-pressurized sufficiently to yield the inside wall and develop residual compressive stresses that help prevent crack growth during service. The zone of highly compacted rock with its associated residual compressive stresses is sometimes referred to as a stress cage, and the phenomenon is sometimes called the bladder effect. Fracturing caused by high pressure gas may also be inhibited in this situation since fines are created during the compaction process that can plug newly formed cracks and prevent gas penetration.

*References for Section IV-B are given at the end of the section on p 111.

Some or all of these effects may actually cause decreased permeablity near the wellbore and are probably responsible for many well-shooting failures.

Several alternatives to explosive well shooting hve been considered and tested in recent years that show promise of substantial improvement[3,6-8] An approach that has received considerable attention is to tailor the pressure-time behavior of the explosive or a suitable propellant so as to keep the maximum pressure below the yield stress of the rock and thereby avoid forming the stress cage. Several of these concepts rely on the use of propellants which deflagrate rather than detonate. Unlike explosives, the burn front in these materials travels slower than the sound speed, and the burning rate can be varied over a wide range. Pressure-time behavior of propellants differ from explosives in that peak pressures are lower, and burn times are longer. Total energy available, however, is similar in both materials (typically 1000 cal/g).

2. Multi-Frac Test Series (R. A. Schmidt, 4732)

Last year three propellant shots known as the Gas Frac[3] Experiment were conducted at the Nevada Test Site and included mineback of the in situ experiment for direct observation. These shots demonstrated both the ability of a tailored pulse to create multiple fractures in a borehole and the feasibility and usefulness of testing such concepts in a realistic in situ environment with mineback. As a result, another series of five in situ experiments are presently being conducted at the Nevada Test Site in a similar ash-fall tuff formation. This series, known as the Multi-Frac Test Series, is supported by the Morgantown Energy Technology Center's Eastern Gas Shales Project. The objectives of this series are: 1) to evaluate the characteristics of five tailored-pulse fracturing concepts--Dynafrac,[6] Augmented Dynafrac,[6] Kinefrac[7] multiple firings of Kinefrac, and Gas Frac[3] and 2) to provide inputs for modeling efforts which are necessary for design if such concepts are to be applied effectively to particular reservoirs such as the Devonian shales.

These five tests are being extensively instrumented and analyzed. The instrumentation includes several cavity-pressure transducers as well as stress

gages and accelerometers grouted in the surrounding rock to measure formation response. Caliper logs will be performed before and after each shot to determine if any permanent borehole enlargement occurred, which would give indications of the existence of a stress cage. A permeability measurement will be made to give an indication of the conductivity of a particular fracture network. Televiewer logs are also planned.

In general, the setup for all five tests will be similar and a schematic of the Augmented Dynafrac shot is depicted in Figure IV-17. The shots will be performed in horizontal boreholes that are 6 in diameter and 40 ft deep. There will be a 10 or 20 ft open-hole test section, depending on the test, with the remainder being grouted casing. All tests except Gas Frac will be shot in water; the water will be dyed to enhance the visibility of the fracture patterns observed during mineback. Figure IV-18 shows the experiment layout of the five shots with the planned mineback route. Note that the mineback will cut through half of each test section leaving the fracture pattern at the midpoint of each experiment preserved in the tunnel rib (sidewall) for later inspection. Figure IV-18 also includes in situ stress data which are the averages of several small volume hydraulic fractures conducted in this region.

The planned layout for the instrumentation holes containing the accelerometers and stress gages is displayed in Figure IV-19. The holes are staggered rather than in a line to maximize the chances of obtaining transverse accelerations from a nearby propagating fracture and to minimize the chances of a single crack intersecting all three holes. Transverse accelerometers will be used even though a symmetric displacement field would produce no transverse displacement or accelerations. Rather, these gages will hopefully detect motions due to the dynamic propagation of a nearby crack.

At the end of FY79, the design of the test series was complete, including instrumentation, hardware, firing circuits, operating procedure, and test evaluation plans. All necessary equipment and transducers were ordered and

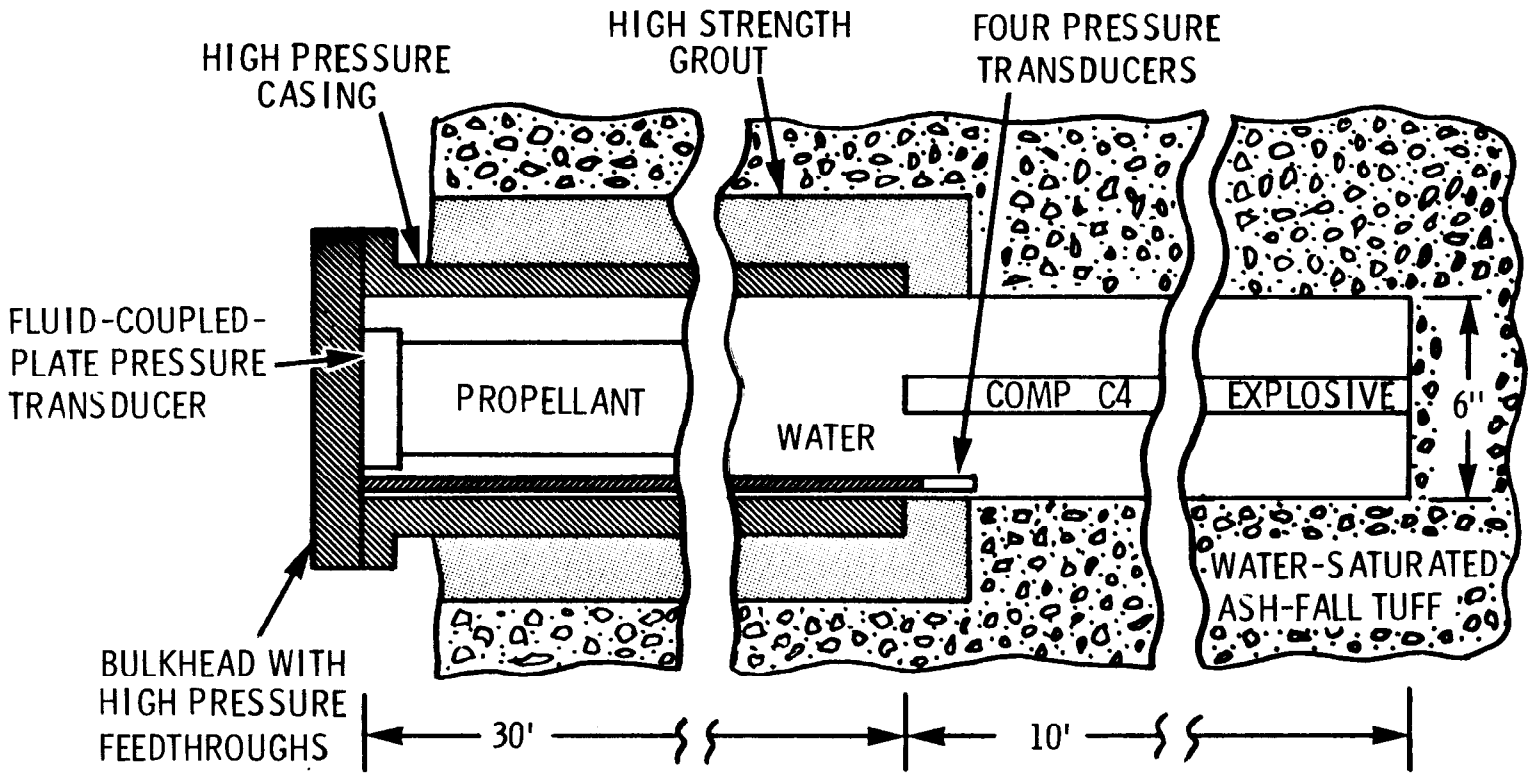

TEST SETUP FOR AUGMENTED DYNAFRAC

FIGURE IV-17

Test Configuration for Augmented Dynafrac. Stress and Acceleration Transducers in Surrounding Rock not Shown.

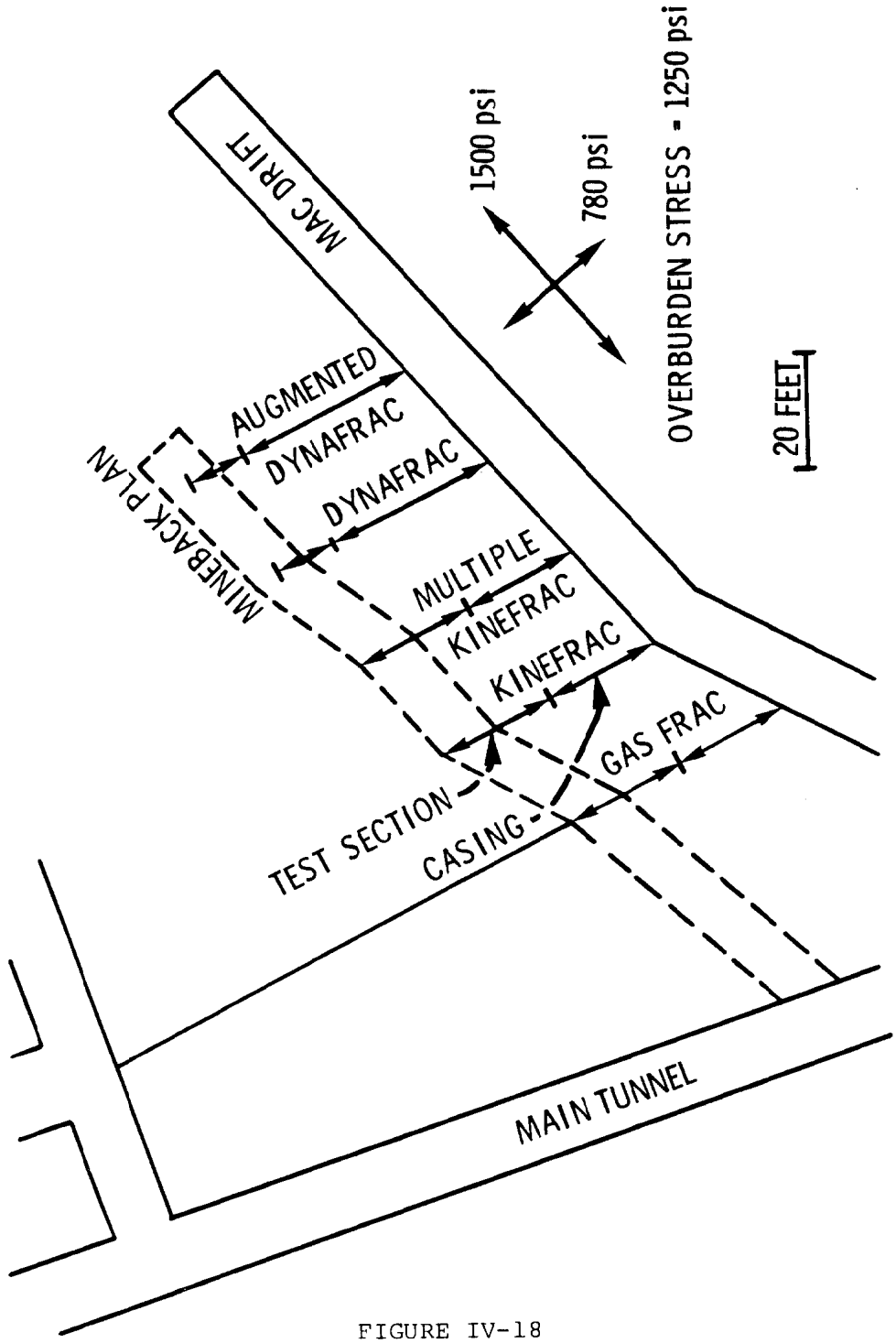

FIGURE IV-18

Tunnel plan for Multi-Frac Test Series with proposed mineback route.

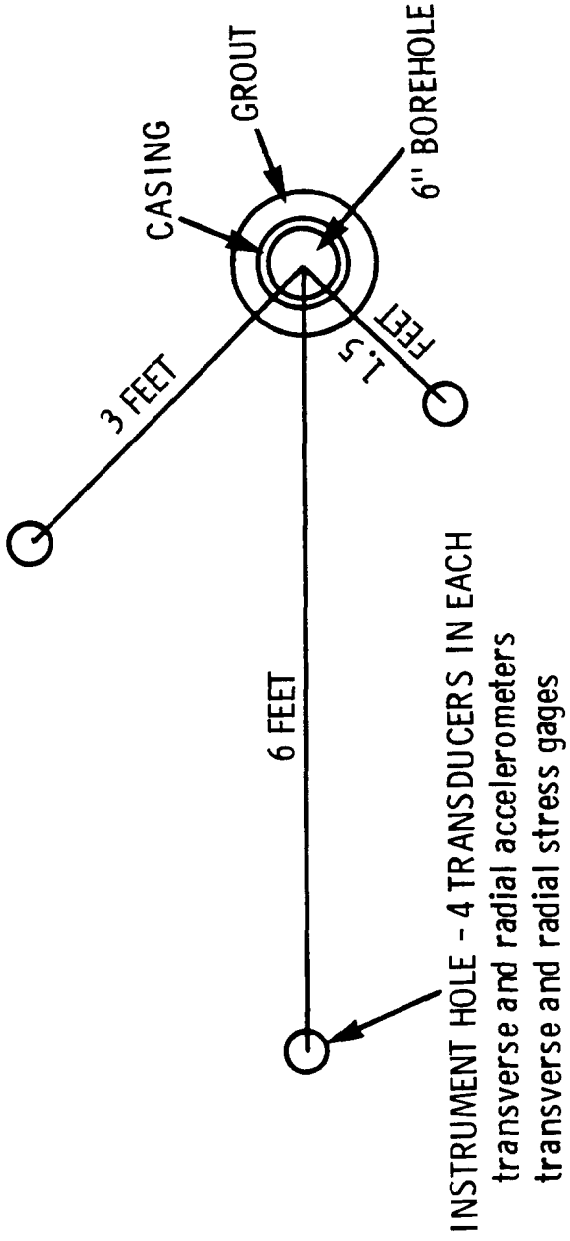

FIGURE IV-19

Typical test setup viewed along the axis of the borehole with satellite holes for instrumentation.

outside contracts placed. Fabrication of hardware and installation in G-tunnel were nearing completion. The shots are scheduled to be fired in January 1980, with post-test analysis and mineback immediately following.

3. Modeling and Analysis (R. A. Schmidt and N. R. Warpinski, 4732)

The modeling and analysis efforts that are being conducted in conjunction with these tests are being performed cooperatively by Sandia Laboratories, Stanford Research Institute, University of Maryland, Science Applications Incorporated, and Los Alamos Scientific Laboratory. These efforts have two primary goals: 1) to provide design criteria for the optimization of stimulation efforts for a particular, site-specific well and 2) to provide a predictive capability for determining, *a priori*, the number, length, and conductivity of fractures created by any particular pulse in any given well. Achieving the second goal automatically includes the first, but developing a design optimization scheme may not require the complete solution necessary in a predictive capability.

This cooperative effort has the form of a "modeling committee" that meets every month or so. Both the test series and the modeling efforts have benefited by this association: calculations have been made to determine transducer locations and ranges, and the modelers have suggested changes in the tests that will maximize the useful output.

Sandia's modeling efforts have focused on two areas: 1) specific calculations for the test series itself to provide for the best means of data analysis and evaluation (especially with regard to measurements of in situ permeability) and 2) development of design criteria that define the conditions that cause compaction and the creation of residual stresses so as to optimize a tailored-pulse stimulation of specific gas reservoirs.

In the first area, calculations were conducted to identify the requirements for pre- and post-test permeability evaluations. Although stressmeter and accelerometer gages will be installed around the wellbore to determine the effect of the pulse on the rock, and mineback will provide qualitative evidence

of the induced fractures, the only method of determining the result of these tests regarding stimulation of the "reservoir" is to perform flow or pressure tests.

In order to examine the feasibility of utilizing such tests to quantify the results, a number of calculations have been performed for Darcy flow in the ash-fall tuff with water as the test fluid. Two cases are considered: 1) constant flow rate injection while recording pressure and 2) constant pressure injection while recording the flow rate. Analytic solutions can be obtained for both cases. It is assumed that the reservoir has a matrix permeability (k) of 0.01 md and a porosity (ϕ) of 40%. Calculations show that the preferred case is constant pressure injection if the low flow rates can be measured. This avoids the problem of the pressures rising too high and possibly fracturing the rock.

Assuming that the created multiple fracture systems of these tests can be modeled as an "enlarged borehole," Figure IV-20 shows the calculated results for four different wellbore radii with a wellbore pressure (P_o) of 200 psi, and a pretest wellbore radius of 3 in. As can be seen, fairly small changes in the apparent borehole radius result in significant differences in flow rate. Thus, if the low flow rates can be adequately measured, useful measurements should be obtained.

In the second area, that of design criteria for avoiding stress cage formation, a closed-form analysis was conducted to determine elastic stresses in a dynamically pressurized cavity. In particular, this analysis determines the stress wave propagation behavior in an elastic medium from a given pressure pulse for a deeply-buried spherical charge. Complete stress histories were calculated for the three previous Gas Frac experiments[3] assuming that the cavity pressure in each case could be adequately simulated with the following:

$$P(t) = P_o t e^{-\alpha t} = \frac{P_{max}}{t_{max}} t \exp\left(1 - \frac{t}{t_{max}}\right)$$

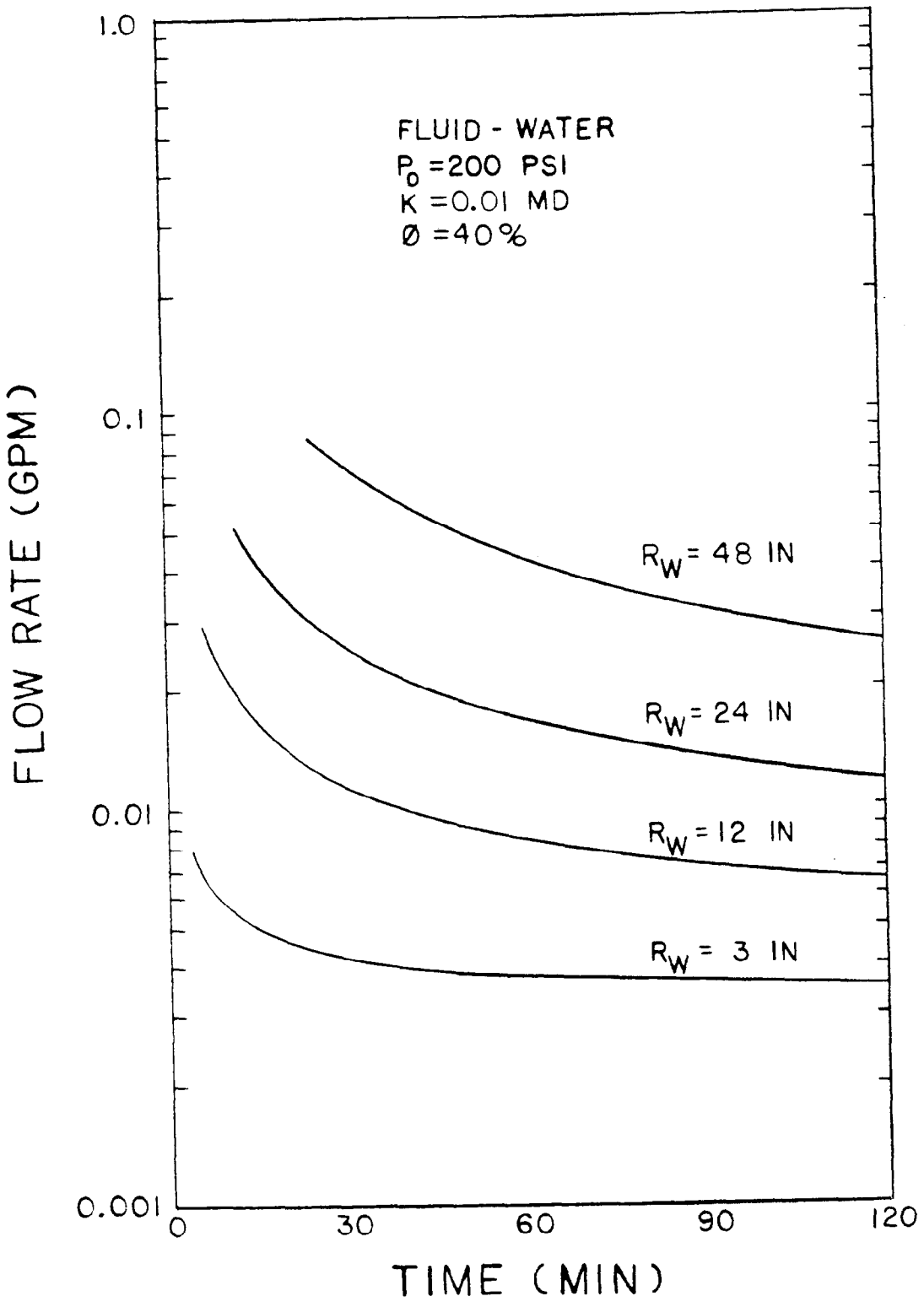

FIGURE IV-20

Injection Flow Rates for Constant Borehole Pressure as a Function of Effective Wellbore Radius

where P_o and α are constants adjusted to fit the actual input pulse. P_{max} is the maximum pressure and t_{max} is the time corresponding to P_{max}.

Results indicate that the loading rates for the intermediate and slow burning propellant tests (GF#2 and GF#1, respectively[3]) gave peak stresses equivalent with the static solution. Of particular interest is the fact that the calculation for the fast burning test (GF#3)[3] shows not only substantially different behavior from the static solution but that the tangential stresses begin as compressive and later become tensile. Recalling that mineback of GF#3 showed many incipient cracks that did not propagate, a new criteria is suggested for gas penetrating fracture growth. Rather than only requiring peak cavity pressure to remain below a level that would cause plastic flow or crushing, it may also be important to keep the loading rate below a level that produces initial compressive stresses in the tangential direction on the cavity wall. This loading rate criterion is affected by cavity size, elastic constants, and wave speed; it is not affected by rock strength.

The actual value of the peak pressure, P_{max}, does not affect this critical time, t_c. While this may seem obvious, the implication is that the actual value of the pressure loading rate does not affect the results. Wellbore diameter, on the other hand, does have a small effect. Using typical material properties for ash-fall tuff, t_c was evaluated by iteration and found to be 108 μsec for an 8 in diameter wellbore and 200 μsec for a 16 in diameter wellbore. The next step is to determine the effect of material properties (elastic constants and wave speed) on t_c. Further computer programming is needed to make the iterative process more efficient. Additional analytic work to place the suggested criterion in closed form would also be useful.

Finally, material property measurements are needed in conjunction with the Multi-Frac Test Series as inputs to the various modeling efforts. Several core samples were taken from the test bed area. Some samples were sent to Stanford Research Institute for small-scale explosive shots that will determine input parameters for calculations with the NAG-FRAG model.[8] Other samples

were sent to Science Applications, Inc., where high rate compressive properties were measured and triaxial compression tests will be run to determine the material's yield surface; these data help define the loading conditions that result in compaction. Still other samples were used by Sandia to measure tensile strength, Young's modulus, Poisson's ratio, and fracture toughness are being conducted. Preliminary results from these tests have shown a tensile strength of 100 psi, and Young's modulus of 1.0×10^6 psi. The degree of saturation seems to have some effect on the results, but more tests will be conducted to define these parameters further.

References for Section IV-B

1. Smith, C. W., Bass, R. C., and Tyler, L. D., "Puff 'n Tuff, a Residual Stress - Gas Fracturing Experiment," Proceedings of 19th U. S. Symposium on Rock Mechanics, Stateline, NV (1978).

2. Boade, R. R., Stevens, A. L., Harak, A. E., and Long, A., "Bed Preparation Concepts for True In Situ Oil Shale Processing: An Evaluation of Current Technology," Proceedings of the 1979 Society of Petroleum Engineers Annual Technical Conference and Exhibition, SPE 8447 (1979).

3. Warpinski, N. R., Schmidt, R. A., Cooper, P. W., Walling, H. C., and Northrop, D. A., "High-Energy Gas Frac: Multiple Fracturing in a Wellbore," Proceedings of 20th U. S. Symposium on Rock Mechanics, Austin, TX (1979).

4. Florence, A. L., and Gates, R. W., "Explosive Cavity Residual Stress Experiment," 76-3702-2, Stanford Research Institute, Menlo Park, CA (1976).

5. Schmidt, R. A., Boade, R. R., and Bass, R. C., "A New Perspective on Well Shooting - The Behavior of Contained Explosions and Deflagrations," Proceedings of 1979 Society of Petroleum Engineers Annual Technical Conference and Exhibition, SPE 8346 (1979).

6. Moore, E. T., Mumma, D. M., and Seifert, K. D., "Dynafrac - Application of a Novel Rock Fracturing Method to Oil and Gas Recovery," Physics International Final Report 827, April 1977.

7. Fitzgerald, R., and Anderson, R., "Kine-Frac: A New Approach to Well Stimulation," ASME Paper 78-PET-25, ASME Energy Technology Conference and Exhibition, Houston, TX (1978).

8. Shockey, D. A., Curran, D. R., Seamon, L., Rosenberg, J. T., and Petersen, C. F., "Fragmentation of Rock Under Dynamic Loads," Int. J. Rock Mech. & Min. Sc., 11, 303-317 (1974).

C. Multi-Well Experiment (D. A. Northrop, 4732)

The Western Gas Sands Project has initiated a major field experiment which will provide an unprecedented opportunity for R&D in the tight gas reservoirs in the Western United States. The Experiment's overall objectives are (1) to obtain a comprehensive geologic characterization of low-permeability, lenticular gas sands and (2) to evaluate state-of-the-art and developing technology for gas recovery from these reservoirs.

The Experiment consists of three phases: Phase 1 - drilling and testing of the first well; Phase 2 - drilling and testing of one (or more) offset well(s); and Phase 3 - a series of stimulation programs and the associated analyses and evaluation. Experiment planning and site selection are underway. The first well, and possibly the second well, will be completed in 1980. The first of several stimulation programs to be conducted over the following three years will be performed in 1981.

Features of the Experiment include: (1) research-oriented activities, schedules, and budgets; (2) a site with a variety of lenticular and continuous gas sands; (3) close-spaced wells (100-500 ft) for detailed reservoir characterization, well-to-well flow testing and downhole geophysical techniques, and placement of diagnostic instrumentation adjacent to fracture treatments; (4) complete core, much of it oriented, taken through the Mesaverde sequence with both conventional and pressure coring techniques; (5) a comprehensive core analysis program with prioritized analyses for data required for well location, interval selection, and data interpretation; (6) an extensive logging program featuring conventional and experimental logs and repetitive logs with different operators and borehole fluids; (7) a detailed well testing program with both pre- and post-stimulation interval testing and pulse and interference testing between wells; (8) in situ stress determinations as a function of depth; (9) wide application of geophysical and fracture diagnostic techniques, and (10) varied stimulation programs to examine fluids, proppants, treatment conditions, fracture growth, fracture conductivity, etc.

The Experiment has six tasks: field drilling, laboratory testing, stimulation, production testing, field diagnostics, and analysis and evaluation. An industry advisory group is providing guidance in the selection and planning of Experiment activities. A wide variety of contractors and agencies will be involved in the acquisition and analysis of the experiment data. These analyses are expected to yield a geologic characterization of lenticular reservoirs, a reservoir model, hydraulic fracture stimulation model with resultant fracture geometries, core-log-well test correlations, technology assessments, economic evaluations, and recommendations for gas recovery from these reservoirs.

Active planning of the Experiment was initiated in May 1979, when the concept for a DOE-conducted, research-oriented experiment in the tight gas sands was endorsed. The initial experiment plan was prepared by Sandia and CER Corporation and was then presented to an industry advisory group formed for this Experiment. Meetings of this group with key DOE, national laboratory and contractor personnel were held on July 19, August 23, and September 24, 1979. The Experiment's activities and plans continue to evolve at the end of FY79.

A site is being sought in the Piceance Basin east of Collbran, CO, at an elevation of 7000 ft where the Mesaverde sequence lies at depths between 4000-8000 ft. It was hoped initially that the site would be acquired and first well drilled prior to winter, but this was not accomplished. The prime site could not be satisfactorily acquired, and others are being pursued. The additional time for planning and coordination will be useful prior to initial field activities in the Spring of 1980.

V. Publications, Presentations, and Other Communications

A. Publications and Presentations

1. C. L. Schuster presented the paper "Detection Within the Wellbore of Seismic Signals Created by Hydraulic Fracturing" (SPE 7448) at the 53rd Annual SPE Technical Conference and Exhibition, Houston, TX, October 1-4, 1978.

2. Sandia Laboratories participated in the Second Annual Eastern Gas Shales Symposium, held at the Lakeview Inn, Morgantown, WV, on October 16-18, 1978, by presenting one paper and displaying two poster papers. C. L. Schuster presented "Gas Simulation Mapping and Characterization Program." Poster displays were "Tools for Wireline Fracture Mapping" by R. P. McCann and C. L. Schuster and "Direct Observation of Hydraulic Fractures" by N. R. Warpinski and D. A. Northrop.

3. C. L. Schuster presented the paper "An Overview of the Electrical Potential Method for Determining Fracture Orientation" at the 1978 Annual ASCE Meeting, Chicago, IL, October 19, 1978.

4. T. L. Dobecki presented the paper "Resistivity Mapping of Expanding Spheroids as Measured in Nearby Boreholes," at the 48th International Meeting of the Society of Exploration Geophysicists in San Francisco, CA, October 29 - November 2, 1978.

5. N. R. Warpinski, R. A. Schmidt, D. A. Northrop, and L. D. Tyler, "Hydraulic Fracture Behavior at a Geologic Formation Interface: Pre-Mineback Report," Sandia Laboratories Report, SAND78-1578, October 1978.

6. R. A. Schmidt presented the paper "Direct Observation of Hydraulic Fractures: Behavior at a Formation Interface," by N. R. Warpinski, D. A. Northrop, and R. A. Schmidt, at the Energy Technology Conference and Exhibition in Houston, TX, on November 5-9, 1978. A Sandia Report, SAND78-1935, covering this work was made available to attendees.

7. N. R. Warpinski, R. A. Schmidt, H. C. Welling, P. W. Cooper, and S. J. Finley, "High Energy Gas Frac," Sandia Laboratories Report, SAND78-2342, December 1978.

8. D. A. Northrop presented aspects of the mineback fracturing experiments at the bimonthly noon meeting of the Albuquerque Section of the American Society of Civil Engineers on January 10, 1979, in Albuquerque, NM.

9. D. A. Northrop and C. L. Schuster (Editors), "Enhanced Gas Recovery Program, Third Annual Report, October 1977 through September 1978," Sandia Laboratories Report, SAND79-0056, March 1979.

10. R. A. Schmidt gave a presentation entitled "A Microcrack Model and Its Significance to Fracture Toughness Testing of Rock," at a committee meeting of the American Society for Testing and Materials held in Cincinnati, OH, on April 29, 1979.

11. R. A. Schmidt presented two invited seminars at Lehigh University, Bethelehem, PA, and Cornell University, Ithaca, NY, on May 1 and May 3, 1979, entitled "Fracture Mechanics of Rock with Applications to Fossil Energy Research."

12. Two presentations were made at the 20th United States Symposium on Rock Mechanics held in Austin, TX, on June 4-6, 1979: R. A. Schmidt presented "Hydraulic Fracturing Near an Interface: Observations and Calculations Regarding Geometry and Containment," by R. A. Schmidt, D. A. Northrop, and N. R. Warpinski, and N. R. Warpinski presented "High Energy Gas Frac - Multiple Fracturing in a Wellbore," by N. R. Warpinski, R. A. Schmidt, P. W. Cooper, H. C. Walling, and D. A. Northrop.

13. Two papers were presented at the 5th Annual DOE Symposium on Enhanced Oil and Gas Recovery and Improved Drilling Technology, held in Tulsa, OK, on August 22-24, 1979: C. L. Schuster, "Fracture Mapping has Become a Viable Technology," and D. A. Northrop, N. R. Warpinski, and R. A. Schmidt, "EGR Stimulation Project - Direct Observation of Hydraulic and Dynamic Fracturing."

14. R. A. Schmidt presented a paper SPE 8346, "A New Perspective on Well Shooting - The Behavior of Contained Explosions and Deflagrations" by R. A. Schmidt, R. R. Boade, and R. C. Bass at the 54th Annual Meeting of the Society of Petroleum Engineers held in Las Vegas, NV, on September 24-26, 1979,

B. Other Communications

1. D. A. Northrop met with Dr. P. L. Randolph and R. L. Rogers of the Institute of Gas Technology in Chicago on October 19, 1978 to discuss data on in situ stress variations.

2. R. A. Schmidt co-chaired a meeting of ASTM Committee E-24.07, Fracture Testing of Brittle Non-Metallic Materials, in Philadelphia, PA, November 7, 1978.

3. C. L. Schuster and P. C. Lysne met with H. B. Carroll and BETC staff members at Bartlesville on November 14, 1978, to present a seminar on electrical impedance measurements in reservoir rock and to discuss Sandia's scope of work in this area.

4. P. C. Lysne and T. L. Dobecki met with Dr. J. H. Moran of the New Mexico Institute of Technology in Socorro, NM, on November 21, 1978, to discuss Sandia's planned electromagnetic logging studies.

5. D. A. Northrop, R. A. Schmidt, and N. R. Warpinski participated in another of a series of Stimulation Modeling Workshops for the Eastern Gas Shales Project, held in Golden, CO, on December 12 and 13, 1978.

6. R. Trump and P. Winchell from Gulf Research visited Sandia on January 8, 1979, to discuss the borehole seismic system and its application to fracture mapping.

7. R. A. Schmidt briefed J. B. Smith, DOE/FEE on the High Energy Gas Frac and related containment activities on February 8, 1979, in Albuquerque, NM.

8. C. L. Schuster and D. A. Northrop briefed C. W. Draffin and A. B. Crawley, DOE/FEE, on the status of Sandia's EGR Program Activities in Washington, DC, on February 13, 1979.

9. T. L. Dobecki visited Mr. S. D. Brasel, Seismic International Research, in Denver, CO, on February 13, 1979, to discuss problems involved with seismic mapping of relatively shallow, discontinuous sandstone bodies.

10. T. L. Dobecki visited Dr. R. Weimer, Colorado School of Mines, Golden, CO, on February 15, 1979, to discuss general stratigraphic relationships which exist in the upper Cretaceous rocks of the Unita, Piceance, and Green River basins.

11. N. R. Warpinski briefed T. McLaughlin of Battelle Northwest on Sandia's hydraulic fracture activities at the Nevada Test Site and gave him a tour of G tunnel on February 14, 1979.

12. N. R. Warpinski attended the Natural Gas Reservoirs Symposium on Analytical Techniques and Applications for Natural Gas Reservoirs sponsored by the Stanford University Department of Petroleum Engineering and the American Gas Association in Palo Alto, CA, on February 15-16, 1979.

13. C. L. Schuster visited M. D. Wood, Inc., in Palo Alto, CA, with Dr. M. Smith from AMOCO, to exchange data collected from the fracture-orientation experiments; excellent agreement was obtained from all methods.

14. C. L. Schuster and T. L. Dobecki provided a briefing of possibilities of mapping sand channels using surface seismic methods to CER, Inc., and DOE personnel in Las Vegas, NV, on February 20 and 21, 1979.

15. A summary and discussion of Sandia's Enhanced Gas Recovery Program was given to Mr. J. Sharer, Gas Research Institute, and the GRI Advisory Board for Unconventional Gas Recovery in Albuquerque, NM, on April 26, 1979. C. L. Schuster (instrumentation), D. A. Northrop (mineback testing), R. A. Schmidt (high energy gas fracturing), and A. L. McFall (drilling) gave presentations. L. Keck, R. McCann and R. Seavey discussed various instrumentation techniques during a tour of a field instrumentation trailer.

16. H. B. Carroll and J. B. Jennings, Bartlesville Energy Technology Center, visited Sandia on May 2, 1979, and received an updated briefing by P. C. Lysne on the status of the advanced logging program.

17. At the request of A. B. Crawley, DOE's Manager of its Unconventional Gas Recovery Program (UGR), Sandia arranged a meeting in Tulsa, OK, on May 7 and 8, 1979, to obtain industry's review and comments on a preliminary draft of the Tight Gas Sands portion of the overall UGR program plan.

18. C. L. Schuster and T. L. Dobecki attended a meeting with CER and C. K. Geoenergy in Las Vegas, NV, on May 10, 1979, to discuss program plans for the seismic measurement program to delineate lenticular lenses.

19. D. A. Northrop and C. L. Schuster attended a meeting at CER, Las Vegas, NV, on May 18, 1979, to discuss ideas for a Multi-Well Experiment to be initiated in FY 79.

20. C. L. Schuster attended the SPE meeting on Low Permeability Reservoirs in Denver, CO, on May 21-22, 1979.

21. D. A. Northrop and C. L. Schuster met with A. B. Crawley, DOE/FFE, in Denver, CO, on May 22, 1979, to discuss the status of DOE's UGR Program planning and an update on the Multi-Well Expeiment plans.

22. D. A. Northrop met with R. L. Mann, CER, to prepare further a program statement of work for the proposed Multi-Well Experiment, in Las Vegas, NV, on JUne 5-6, 1979.

23. D. A. Northrop and C. L. Schuster attended DOE's Unconventional Gas Recovery Project Review at Morgantown, WV, on June 12-14, 1979, where they presented reviews of current Sandia program activities, were involved in the UGR program planning exercises for the Tight Gas Sands section, and participated in a detailed review of FY 80 plans.

24. D. A. Northrop attended a working meeting at CER, Las Vegas, NV, on June 21-22, 1979, to finalize the draft of the Tight Gas Sands section of the UGR program plan.

25. C. L. Schuster, T. L. Dobecki, and P. C. Lysne met with the U.S.G.S Western Gas Sands Project Staff in Denver, CO, on July 12, 1979, to discuss current activities of interest to the project.

26. Dr. P. L. Randolph, Institute of Gas Technology, visited Sandia on July 20, 1979, to discuss his current core analysis work and the application of this work to the new Multi-Well Experiment.

27. R. A. Schmidt and N. R. Warpinski briefed Mr. J. Edl, Carbondale Mining and Technology Center, on Stimulation Research Project activities on July 27, 1979, at Sandia, Albuquerque, NM.

28. R. A. Schmidt attended an Eastern Gas Shales Modeling meeting at Los Alamos Scientific Laboratory, Los Alamos, NM, on July 30, 1979.

29. T. L. Dobecki, and P. C. Lysne attended the Society of Petroleum Engineers Forum "Properties of Saturated Rocks of Interest to Petrophysicists and Geophysicists," July 29 - August 3, 1979, at Colorado Mountain College, Glenwood Springs, CO.

30. R. A. Schmidt attended a working meeting for the Eastern Gas Shales Project at the Denver Project Office, Lakewood, CO, on August 30, 1979.

31. Sandia conducted a tour of the Nevada Test Site for the project advisors group of the Gas Research Institute, on August 28, 1979.

32. D. A. Northrop and T. Gerlach attended an Unconventional/Non-Conventional Gas Recovery Workshop held at Los Alamos Scientific Laboratory, Los Alamos, NM, on September 5 and 6, 1979.

33. D. A. Northrop and C. L. Stein visited with C. W. Spencer, T. D. Fouch, and their co-workers involved with WGSP activities at the U. S. Geological Survey in Denver, CO, on September 20, 1979.

34. Sandia Laboratories co-sponsored a tour for over 80 people at the Nevada Test Site on September 28, 1979, held in conjunction with the 54th Annual Technical Conference and Exhibition of the Society of Petroleum Engineers, Las Vegas, NV, September 23-26, 1979. In-tunnel presentations focused on hydraulic fractures experiments at formation interfaces and the effects of in situ stress (N. R. Warpinski) and effects of explosive and tailored propellant fracturing (R. A. Schmidt).

DISTRIBUTION:

U. S. Dept. of Energy
MS D-107
Fossil Energy
Washington, DC 20545
Attn: G. Fumich
Assist. Secretary for
Fossil Energy

U. S. Dept. of Energy (4)
Office of Oil and Gas Technology
MS D-107
Washington, DC 20545
Attn: M. Adams
J. W. Watkins
P. R. Wieber
J. B. Smith

U. S. Dept. of Energy
Office of Fossil Energy
Rm. A-117
Washington, DC 20545
Attn: C. W. Guidice
Acting Deputy, Assist.
Secretary for Management

U. S. Dept. of Energy (9)
Morgantown Energy Technology Center
P. O. Box 880
Morgantown, WV 26505
Attn: A. A. Pitrolo, Director
L. A. Schrider
A. E. Hunt
R. L. Wise (5)
C. A. Komar

U. S. Dept. of Energy
Nevada Operations Office
P. O. Box 14100
Las Vegas, NV 89114
Attn: C. H. Atkinson

CER Corporation (2)
P. O. Box 15090
Las Vegas, NV 89114
Attn: G. R. Leutkenhans
R. L. Mann

U. S. Dept. of Energy (8)
Bartlesville Energy Tech. Center
Bartlesville, OK 74003
Attn: R. T. Johansen
D. C. Ward
A. B. Crawley (5)
H. B. Carroll

U. S. Dept. of Energy
Special Programs Division
Albuquerque Operations Office
Albuquerque, NM 87185
Attn: D. L. Krenz, Director

Lawrence Livermore Laboratory
Livermore, CA 94550
Attn: M. E. Hanson

Los Alamos Scientific (3)
Laboratory
Los Alamos, NM 87545
Attn: R. Brownlee, G-Division
W. G. Davey, Q-Division
W. J. Carter, G-7

Halliburton Services (2)
Research Center
Duncan, OK 73533
Attn: A. B. Waters
A. A. Daneshy

Shell Development Company
3737 Bellaire Boulevard
Houston, TX 77001
Attn: R. Saucier

Mobil Research and Development
Corporation
Field Research Laboratory
P. O. Box 900
Dallas, TX 75211
Attn: J. L. Fitch

Continental Oil Company (2)
Production Research Division
Ponca City, OK 74601
Attn: H. C. Walther
H. Wahl

Columbia Gas System Service (2)
Corporation
1600 Dublin Road
Columbus, OH 43215
Attn: R. Forrest
S. McKetta

DISTRIBUTION Cont'd.

Gas Producing Enterprises, Inc.
2100 Prudential Plaza
P. O. Box 749
Denver, CO 80201
Attn: R. Merrill

Dowell
P. O. Box 21
Tulsa, OK 74102
Attn: R. Steanson

Institute of Gas Technology
3424 S. State St.
Chicago, IL 60616
Attn: P. Randolph

Amoco Production Co. (3)
P. O. Box 591
Tulsa, OK 74102
Attn: R. L. Huggins
R. W. Veatch
M. B. Smith

M. D. Wood, Inc.
1000 Elwell Court
Suite 218
Palo Alto, CA 94303
Attn: M. D. Wood

Gulf Research and Development Company
P. O. Drawer 2038
Pittsburgh, PA 15230
Attn: R. P. Trump

Terratek
University Research Park
420 Wakara Way
Salta Lake City, UT 84108
Attn: A. S. Abou-Sayed

Dept. of Engineering Mechanics
Ohio State University
Boyd Laboratory
155 West Woodruff Avenue
Columbus, OH 43210
Attn: Prof. S. H. Advani, Chairman

University of Minnesota
Dept. of Civil and Mineral Eng.
Minneapolis, MN 55455
Attn: Dr. Charles Fairhurst

School of Civil and Environmental Engineering
Hollister Hall
Cornell University
Ithaca, NY 14853
Attn: Dr. A. R. Ingraffea

U. S. Geological Survey
345 Middlefield Road
Menlo Park, CA 94025
Attn: Dr. D. D. Pollard

Fracturing Technology Inc.
10301 N.W. Freeway
Suite 202
Houston, TX 77092
Attn: A. R. Sinclair, President

1 M. Sparks
1000 G. A. Fowler
1100 C. D. Broyles
1110 J. D. Kennedy
Attn: C. R. Mehl, 1111
C. W. Smith, 1111
1120 T. L. Pace
1130 H. E. Viney
Attn: B. G. Edwards, 1131
W. C. Vollendorf, 1131
4400 A. W. Snyder
4500 E. H. Beckner
4537 L. D. Tyler
4700 J. H. Scott
4710 G. E. Brandvold
4720 V. L. Dugan
4730 H. M. Stoller
4731 B. Granoff
4732 D. A. Northrop (25)
4733 C. L. Schuster (15)
4734 A. L. Stevens
4737 B. E. Bader
4738 R. L. Fox
4740 R. K. Traeger
5500 O. E. Jones
Attn: W. Herrmann, 5530
5800 R. S. Claassen
8266 E. A. Aas
3141 T. Werner (5)
3151 W. L. Garner (3)
3154-3 R. P. Campbell for DOE/TIC (25)

Org.	Bldg.	Name	Rec'd by *	Org.	Bldg.	Name	Rec'd by *

* Recipient must initial on classified documents.

UGR File #C073/76Q2
February 1976-April 1976
Sandia Laboratories

SAND-76-0317
Specified Distribution Only

MASSIVE HYDRAULIC FRACTURE MAPPING AND CHARACTERIZATION PROGRAM

Third Quarterly Report: February 1976 through April 1976

Edited by:
C. L. Schuster, Supervisor
Sensors Systems Division 5733

Prepared by Sandia Laboratories, Albuquerque, New Mexico 87115 and Livermore, California 94550 for the United States Atomic Energy Commission under Contract AT (29-1)-789

July 1976

EGSP
OPEN FILE # 073/76Q2

Sandia Laboratories

UGR File #C073/76Q2
February 1976-April 1976
Sandia Laboratories

Issued by Sandia Laboratories, operated for the United States Energy Research and Development Administration by Sandia Corporation.

NOTICE

This report was prepared as an account of work sponsored by the United States Government. Neither the United States nor the United States Energy Research and Development Administration, nor any of their employees, nor any of their contractors, subcontractors, or their employees, makes any warranty, express or implied, or assumes any legal liability or responsibility for the accuracy, completeness or usefulness of any information, apparatus, product or process disclosed, or represents that its use would not infringe privately owned rights.

SAND-76-0317

Specified Distribution

MASSIVE HYDRAULIC FRACTURE MAPPING AND CHARACTERIZATION PROGRAM

Third Quarterly Report: February 1976 through April 1976

Edited by: C. L. Schuster, Supervisor
Sensor Systems Division
Sandia Laboratories
Albuquerque, New Mexico 87115

July 1976

ABSTRACT

The electrical potential data for UPRR-22 was further analyzed and showed changes as a function of the volume pumped. An upgrading of the potential system has been completed and this should allow improved data to be collected in future experiments. Additional seismic data analysis has been completed and has indicated marginal results. These results will however guide the future seismic programs.

TABLE OF CONTENTS

		Page
I.	INTRODUCTION	7
II.	ELECTRICAL POTENTIAL SYSTEM	8
III.	SEISMIC DATA REDUCTION	9
	A. Pinedale #7, Sept. 1974	9
	B. Pinedale #5, July 1975	14
	C. Wattenberg	24
	D. Other Seismic Activities	25

I. INTRODUCTION

This is the third quarterly report for the Sandia Laboratories Program on Massive Hydraulic Fracture (MHF) Mapping and Characterization Program funded by the Division of Oil, Gas and Shale Technology of ERDA. This report summarizes the activities from February 1, 1976, through April 30, 1976.

Following the third experiment for Amoco in the Wattenberg field, all test equipment and instrumentation vans were returned to Albuquerque. Several pieces of test equipment had been on loan and were returned, and planning has been initiated for future testing. New, improved and modified equipment, based upon the results to-date, has been developed and will be tested on a Devonian shale MHF experiment in FY'76T. Further analysis of the Wattenberg UPRR-22 data has indicated potential changes versus growth of the fracture.

Seismic data analysis efforts have continued to be focused on the July 1975 Pinedale experiments. Softwave development is complete and has been verified by several methods. The six hours of breakdown data has been digitized and run through the routines and several hundred solutions calculated. Obviously these contain a large number of noise sources and perhaps some fracture-related source. The time intervals that resulted in plausible solutions, that is, solutions with the correct depth, velocity of propagation, and located in the vicinity of the well bore, have been further examined.

II. ELECTRICAL POTENTIAL SYSTEM (C. L. Schuster, Div. 5733)

Surface potential data from the January UPRR-22 experiment have been further analyzed and indicates a progressive growth along the southeast to northwest line during the pumping. This growth is shown in Figure 1 where each increment is approximately 75,000 gallons of fluid. The growth away from the southeast quadrant is clearly shown and this represents the major frac length being in the northwest direction. The reversal in the northwest quadrant is not clearly understood, but could be caused by the total length being increased while the fracture was also remaining asymmetrical.

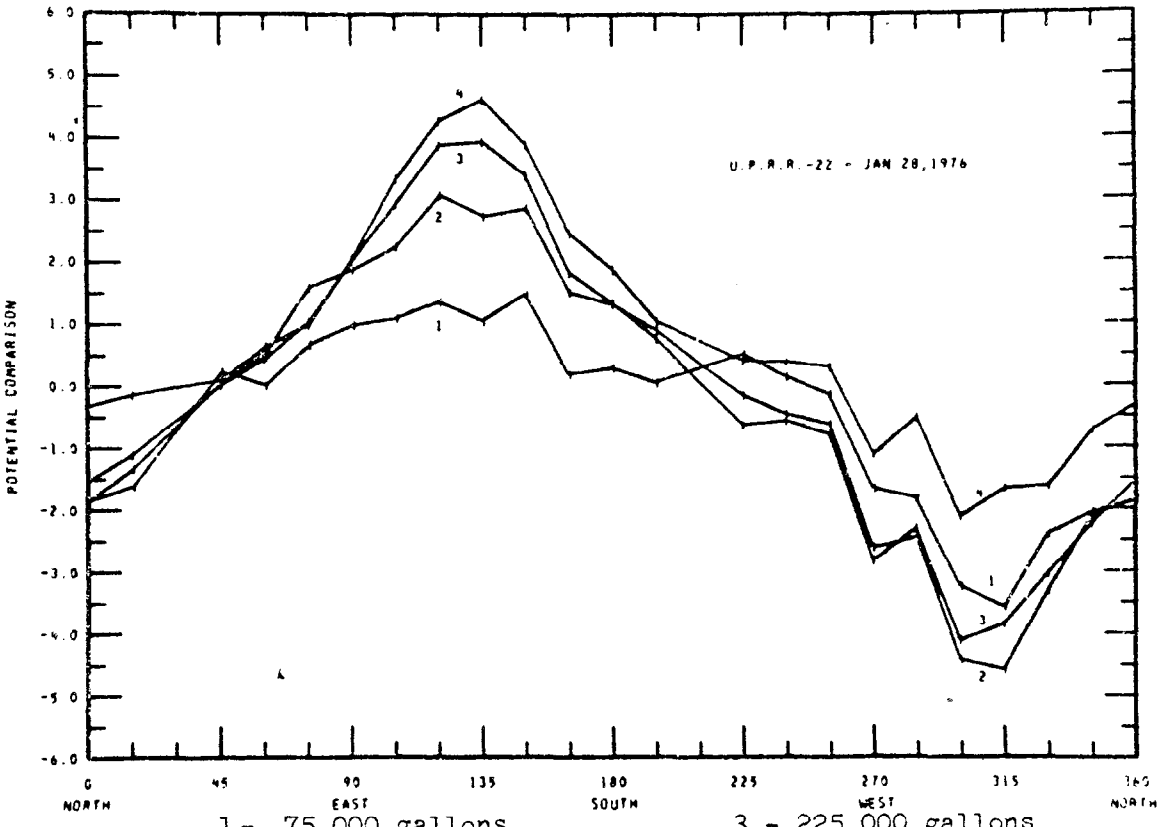

1 - 75,000 gallons
2 - 150,000 gallons
3 - 225,000 gallons
4 - 300,000 gallons

Figure 1. Potential Change

The electrical surface potential system has been up-graded and modified into a configuration that should allow for its dissemination and use by the service companies. Present signal levels are probably too marginal to readily allow data interpretation. System redesign has been completed, and all components have been placed on order. This redesign did not change the basic system as it was deployed at Wattenberg. The potential measurement system modifications include the following:

1. Voltage gain or sensitivity will be field adjustable by switch setting.
2. Increased filtering for both R.F. noise and 60 cycle pick up.
3. Voltage controlled oscillators will be replaced with constant bandwidth oscillators to give all channels identical data responses.
4. Individual battery power supplies will be eliminated, and all systems will be powered from a central supply.

Current pulsing system has also been upgraded to 600 volts along with the necessary safety and interlock systems. The control circuitry is to be replaced and will be completely computer controlled. A complete technical description of the system design and specifications will be published in a separate development report.

III. SEISMIC DATA REDUCTION (R. G. Hay, Div. 5733)

A. Pinedale #7, Sept. 1974

The thrust of the reduction efforts during the current quarter has been an attempt to identify the seismic signature of fracture related signals. Assuming that the time of a seismic event can be determined,

then the problem is to characterize that seismic activity. The times of events can be determined directly by detecting a rapid increase in energy at the sensor or by cross correlation techniques or by measuring some other phenomenon such as a well pressure fluctuation which might indicate a fracture occurrence. An indirect approach would be to assume that the cross correlation technique would contain the fracture signals and by examining the intervals which produced the known result, study the fracture signals.

Both a direct and indirect approach were tried during the current quarter and neither produced striking positive results.

For the indirect approach, the known property is the tendency of the fracture to occur perpendicular to the least principal stress in the formation. This property has been postulated and confirmed in field mine-back experiments at NTS.[1] If such a fracture is plotted in a plan view for deep fracture, the result will be a straight line through the well bore for a symmetrical fracture (i.e., wings of equal length from the well bore). If a plot of seismic signal locations were generated for all time intervals and a clear line were found through the well bore, then the assumption could be made that time intervals which plotted points on the line contained fracture related signals.

[1]Tyler & Vollendorf. Physical Observations and Mapping of Cracks Resulting from Hydraulic Fracturing In Situ Stress Measurements. SPE paper #5542, 1975.

That this process may indeed produce the required signals was supported by early hand computer plots for very limited quantities of data from the September 1974 Pinedale hydrofracture experiment. A plan view plot of that data is shown in Figure 2. Forty-four ten-second intervals were processed to generate the plot. These intervals were selected from careful screening of analog records as possibly containing information which correlated across three of the seismic sensing stations. The grouping of points to the N.E. is in general agreement with other

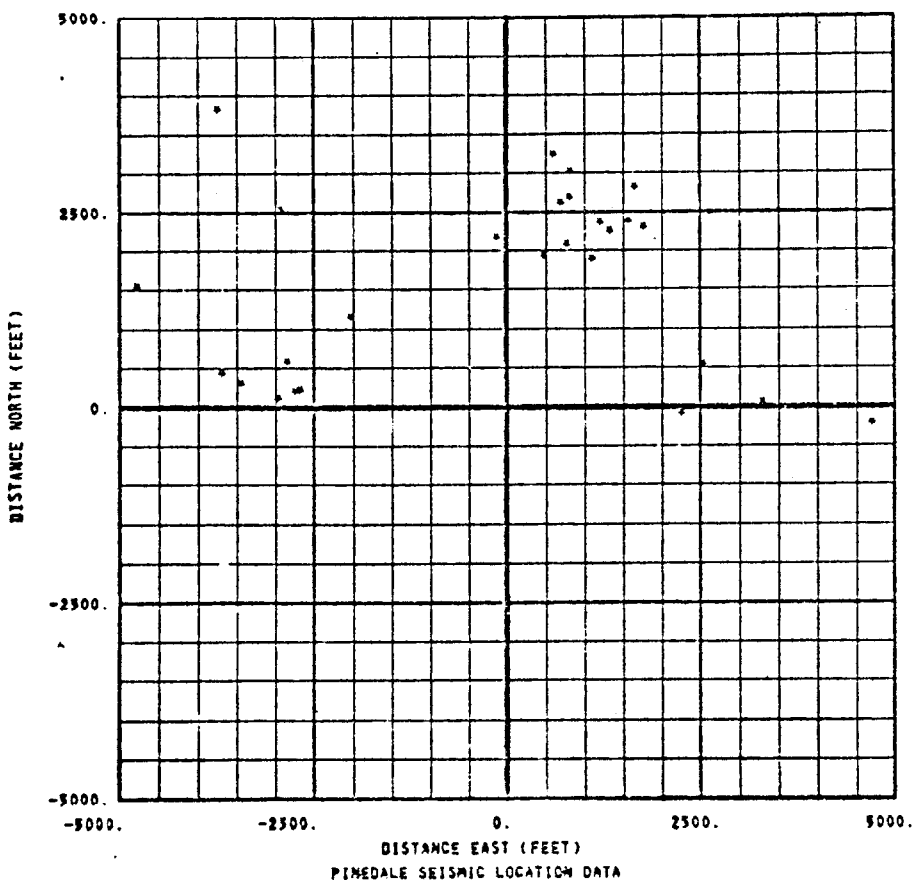

Figure 2. Pinedale Sept. 74 Fracture Experiment

fracture diagnostic techniques used to attempt mapping of the experiment.[2] At that time, the lack of a line was not particularly disturbing due to the very limited quantity of data processed. Even with only the few intervals the data handling task was immense. Obviously the magnitude of this task increases directly with the number of time intervals considered and geometrically is related to the number of monitor stations. For this reason, the software procedure outlined in the previous quarterly report was developed to automate the data analysis process.

In the current quarter the remainder of the Pinedale #7 breakdown data was processed utilizing the data analysis techniques. The resultant hypocenter locations are shown in Figures 3 and 4. For these two plots over 1300 intervals are processed. The plots were derived for three monitor stations--each one approximately 3000 ft. from the well and spaced at 120° increments around the well. The "three spoke" pattern does not appear to show a line through the well.*

The seismic data tended to be periodic which in each interval created several peaks in each of the correlation functions. This resulted in a single time interval plotting several points. By examining the plots

*Note that the "electrical potential mapping technique" appears to indicate the formation of an asymmetrical fracture. Consequently, a seismic "line" through the well bore may not be the hypocenter location result to be expected.

[2]Power, Schuster, Hay and Twonbly. Detection of Hydraulic Fracture Orientation and Dimensions in Cased Wells. SPE paper #5626.

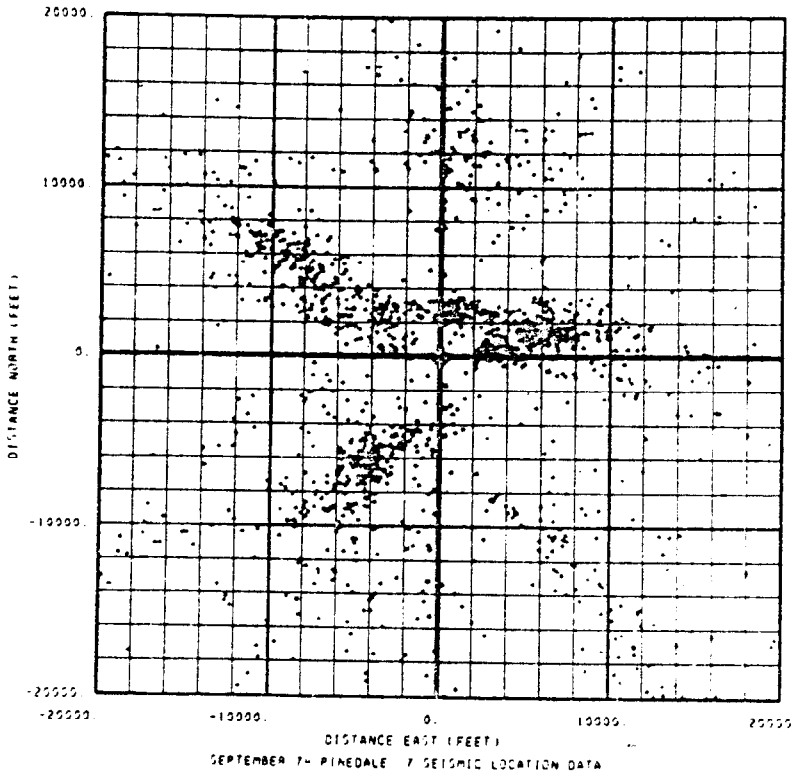

Figure 3. First Hour Pumping

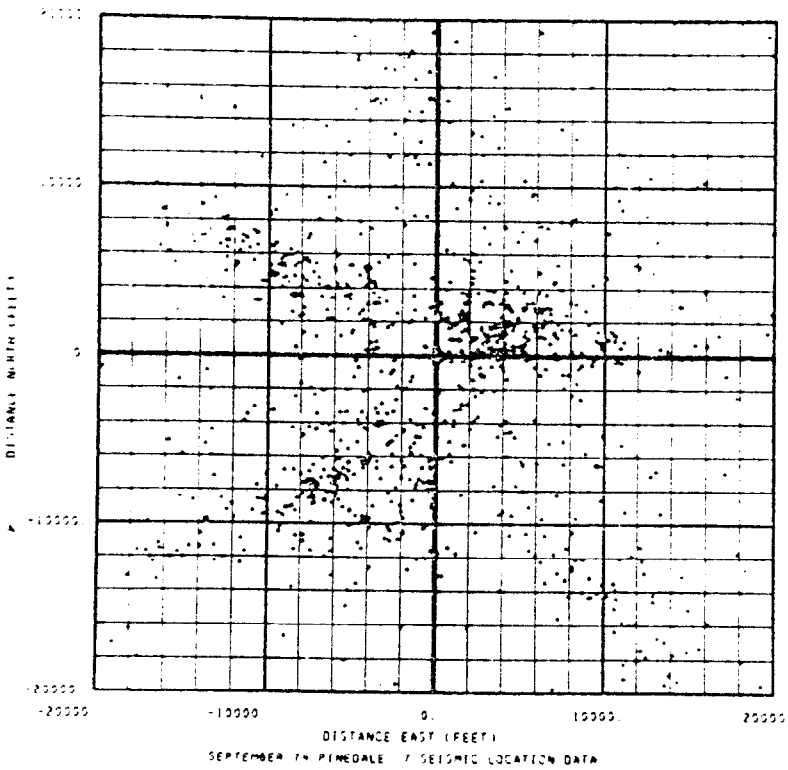

Figure 4. Second Hour Pumping

for individual intervals it was found that if a point occurred in one spoke then its images, due to periodicity, would occur in the other spokes. Clearly, if one spoke were indeed fracture related then the obtained pattern would result.

The question immediately arises about the relation between the three spoke patterns and the three station array. Perhaps the pattern is more related to the array geometry than it is to the seismic signals.

To test this theory, random numbers were inputed to the location routine rather than measured time differences. If the array determined the location pattern then the pattern should be apparent in the random data plot. The plot in Figure 5 shows no spoked pattern which indicates that some sort of systematic signal must have been present at Pinedale #7.

B. Pinedale #5, July 1975

Because of the limited number of monitor stations at Pinedale #7 and the complication of logrithmic amplifiers, attention was shifted to the July Pinedale #5 data. The data plots for the six-hour breakdown period for this experiment are shown in Figures 6 through 11. For these plots approximately 3500 intervals were processed for six monitor stations and fifteen correlation functions being calculated in each interval. The sequence of events in the plots are that pumping began at the start of the period for Figure 6 and proceeded through

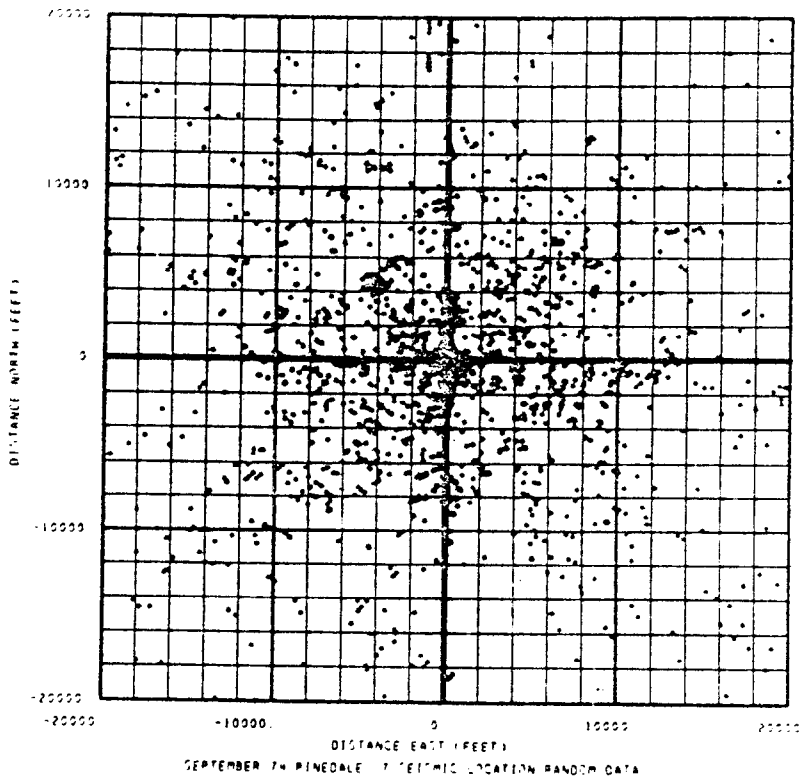

Figure 5.

Figure 7. Pumping stopped at the beginning of the data for Figure 8; however, the well was capped off and the pressure held during Figure 9 and until pumping resumed in Figure 10 and was finally terminated in Figure 11.

There is a definite trend in this data to line up in a northwesterly/southeasterly direction during times when fracturing should be taking place. This line passes to the south of the well through a region which is approximately the geometric mean for the monitor station array.

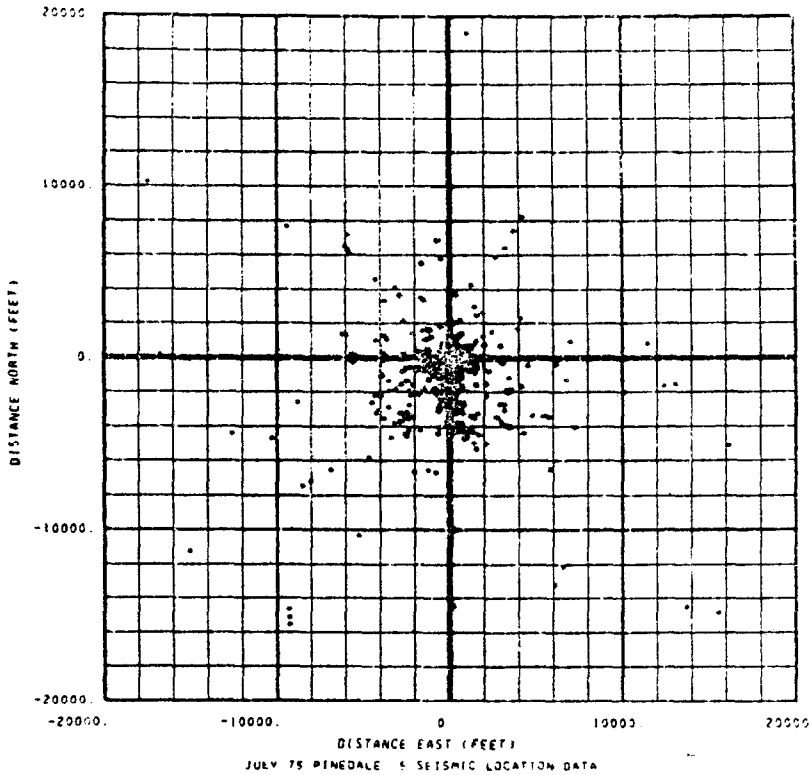

Figure 6. First Hour Breakdown

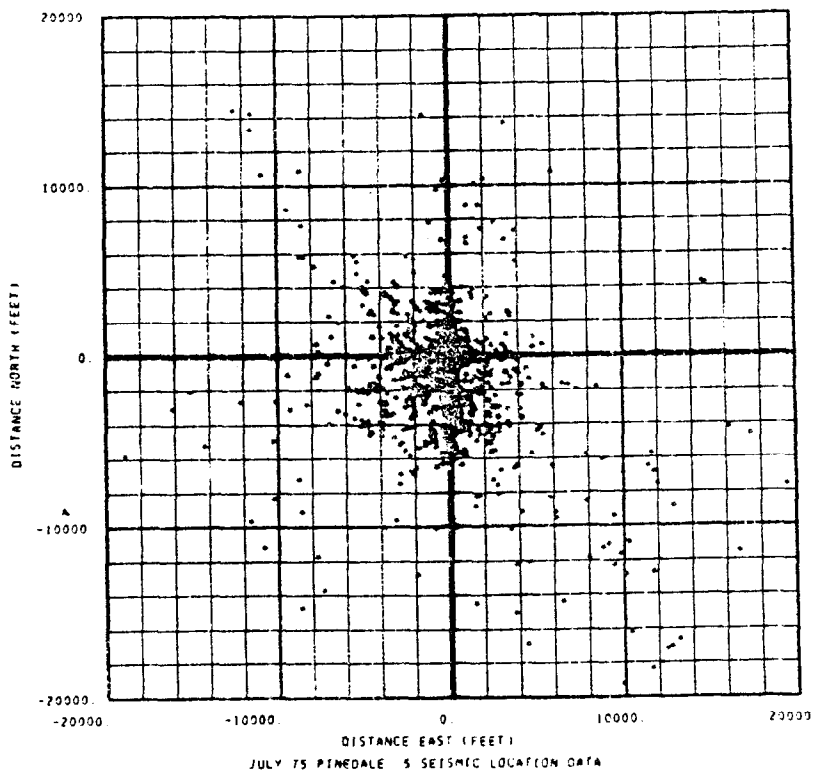

Figure 7. Second Hour Breakdown

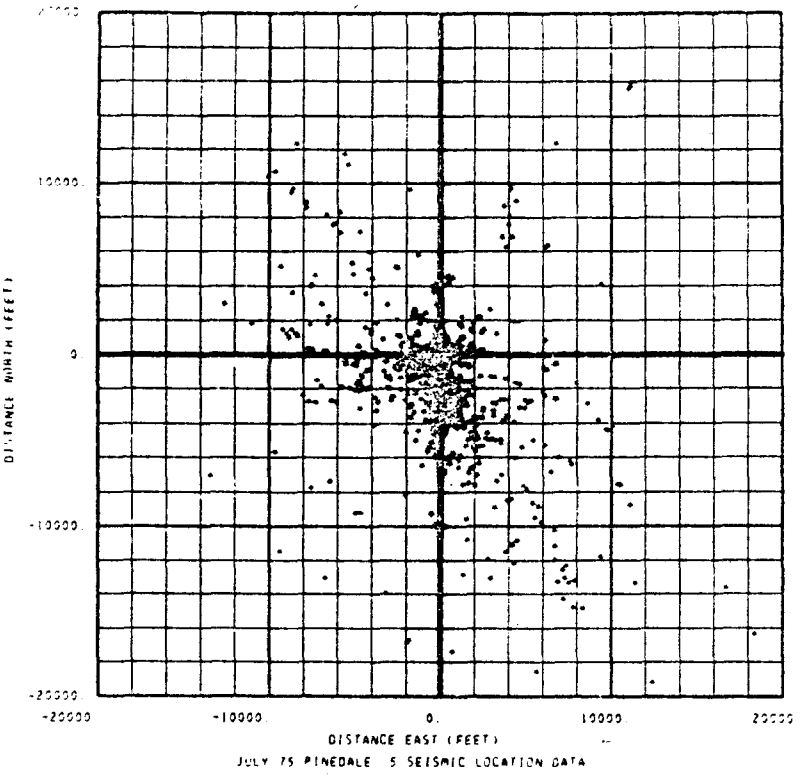

Figure 8. Third Hour Breakdown

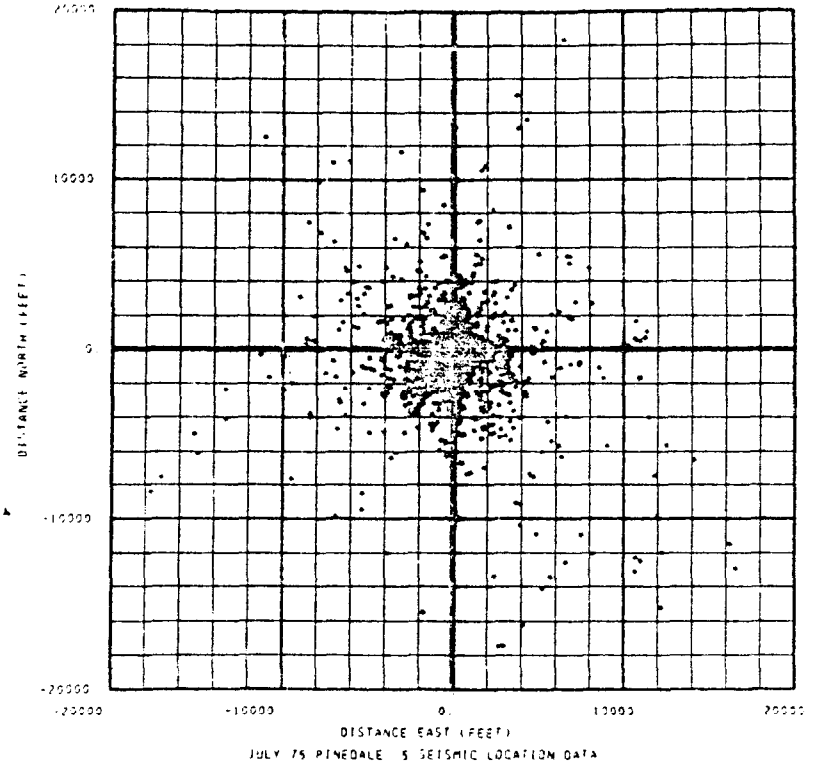

Figure 9. Fourth Hour Breakdown

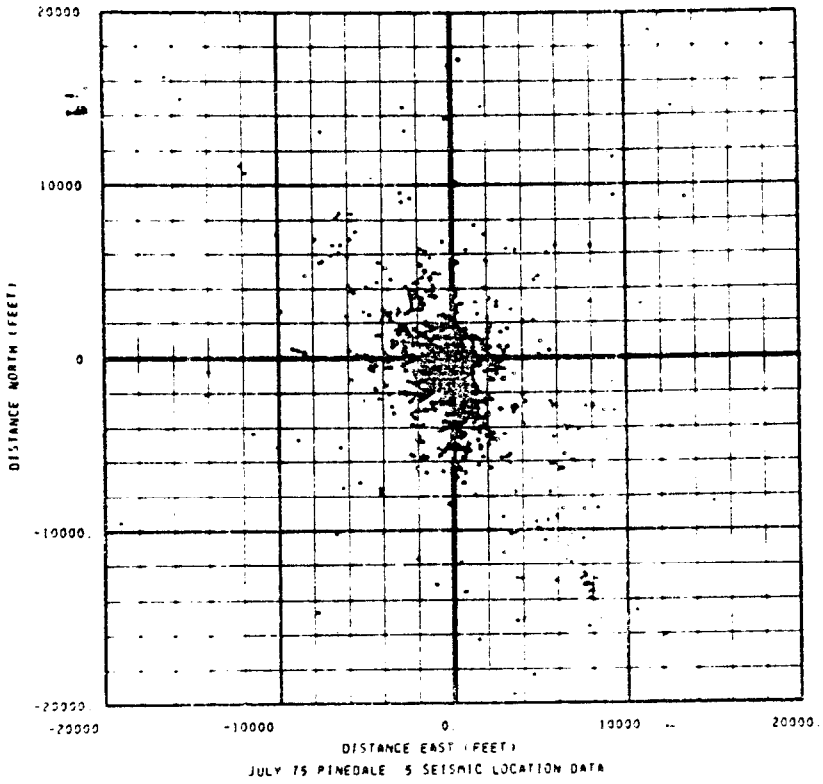

Figure 10. Fifth Hour Breakdown

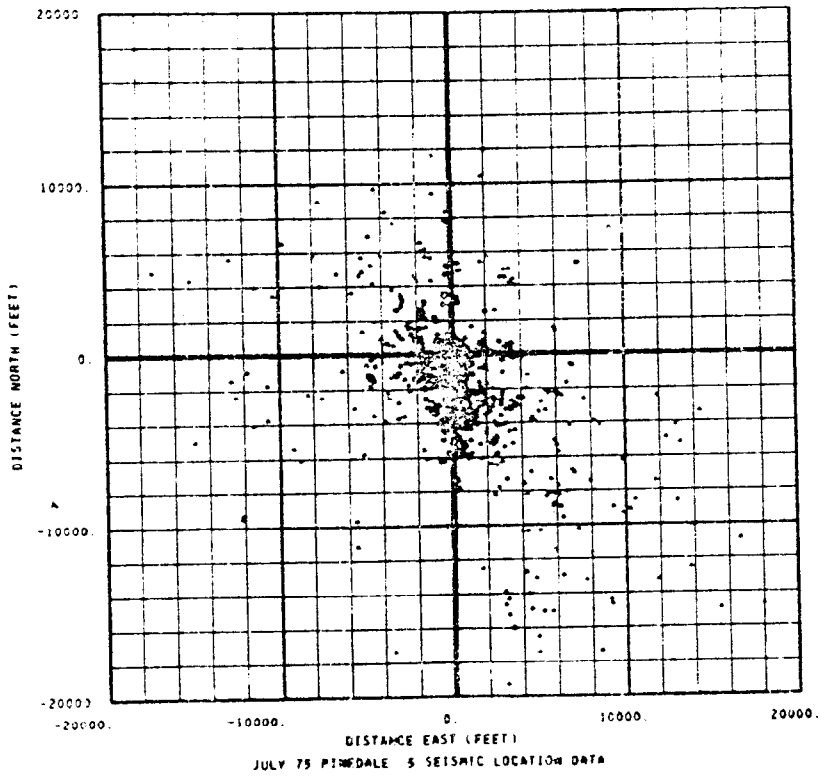

Figure 11. Sixth Hour Breakdown

As in the case with the Pinedale #7 data, the extreme dimensions of the line are inconsistent with the quantity of fluid pumped. It is possible however that the extremes are merely images due to periodicity or uncertainties in velocity and depth and are therefore only indications of what is happening closer to the well. To check what close-in effects are in the data, a second set of plots on an expanded scale are shown in Figures 12 through 17. Here, again, the line tendency is present during suspected fracture times.

Three other plots are of interest and are shown in Figures 18, 19 and 20. Figures 18 and 19 show the locations for two, one-hour periods recorded prior to the fracture operation. Clearly, the line trend is not present. Also, the data is centered about the geometric mean noted earlier. The plot in Figure 20 shows the random data and indicates no line effect due to array geometry.

The results for the Pinedale #5 plots may be summarized as follows: It is encouraging that a line structure occurs in the data. The discouraging aspect is that the extreme length of the line is not consistent with the quantity of fluid pumped. The times of occurrence of the line, the shape of the line and the indications that the line shape is not related to array geometry are encouraging.

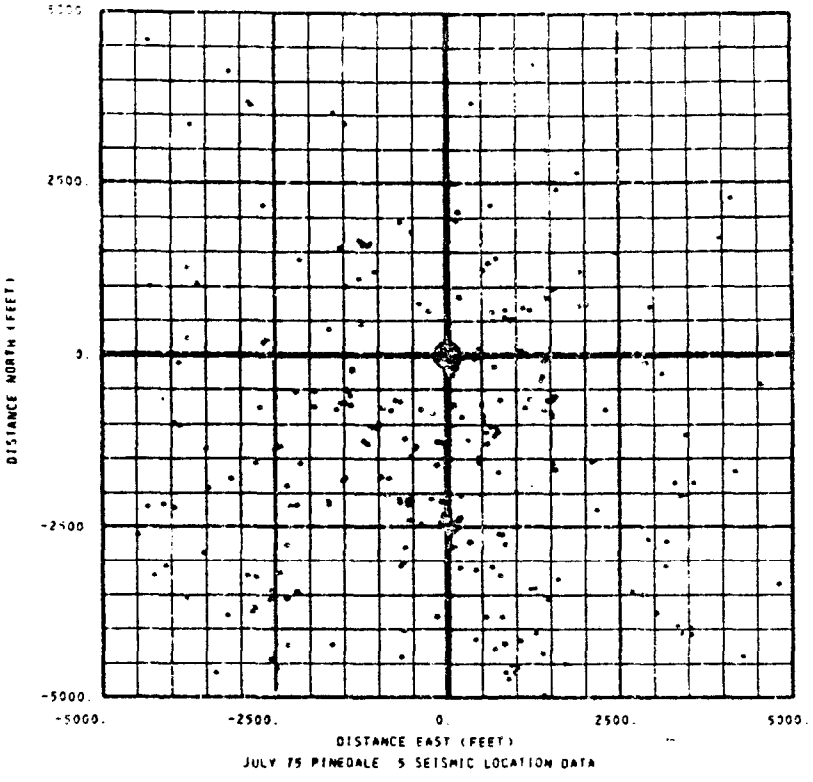

Figure 12. First Hour Breakdown

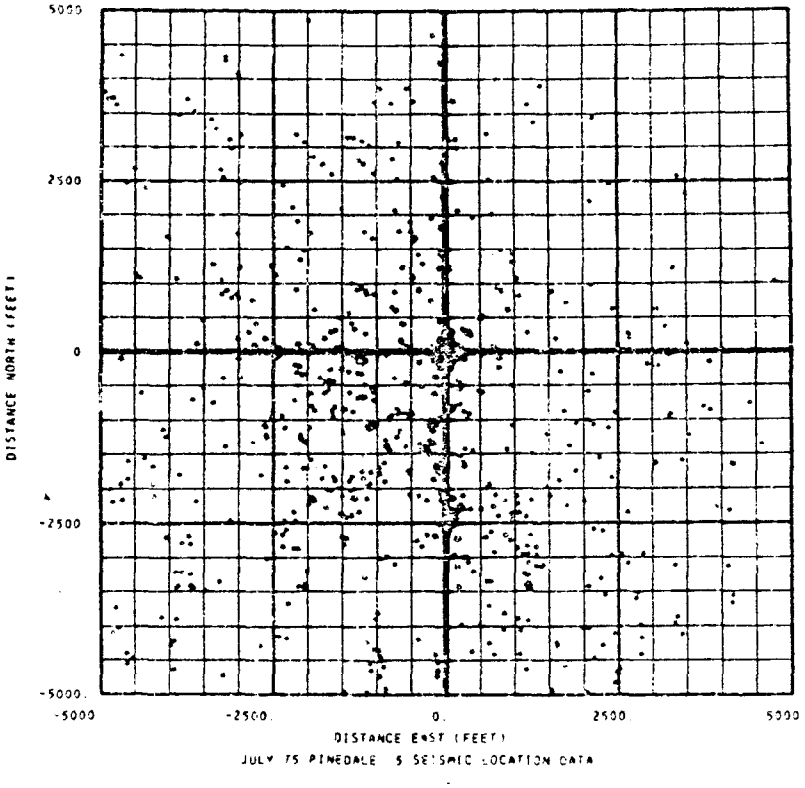

Figure 13. Second Hour Breakdown

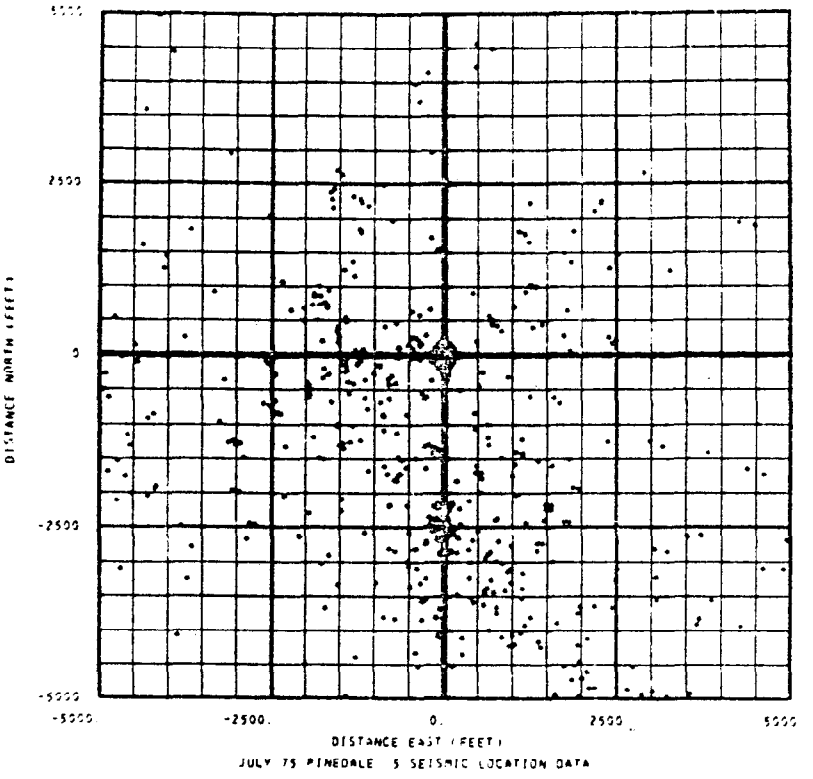

Figure 14. Third Hour Breakdown

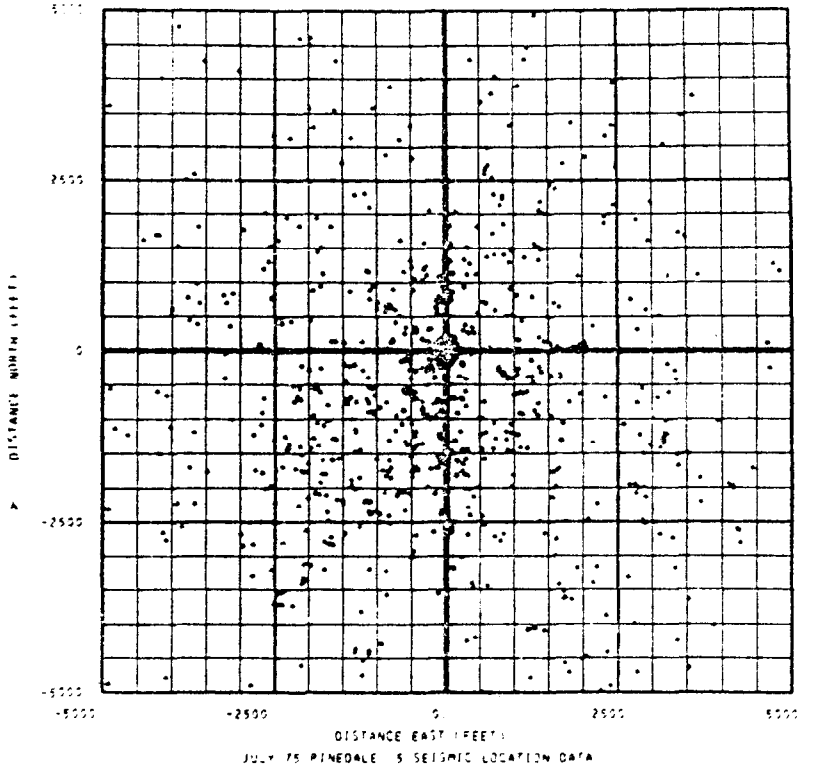

Figure 15. Fourth Hour Breakdown

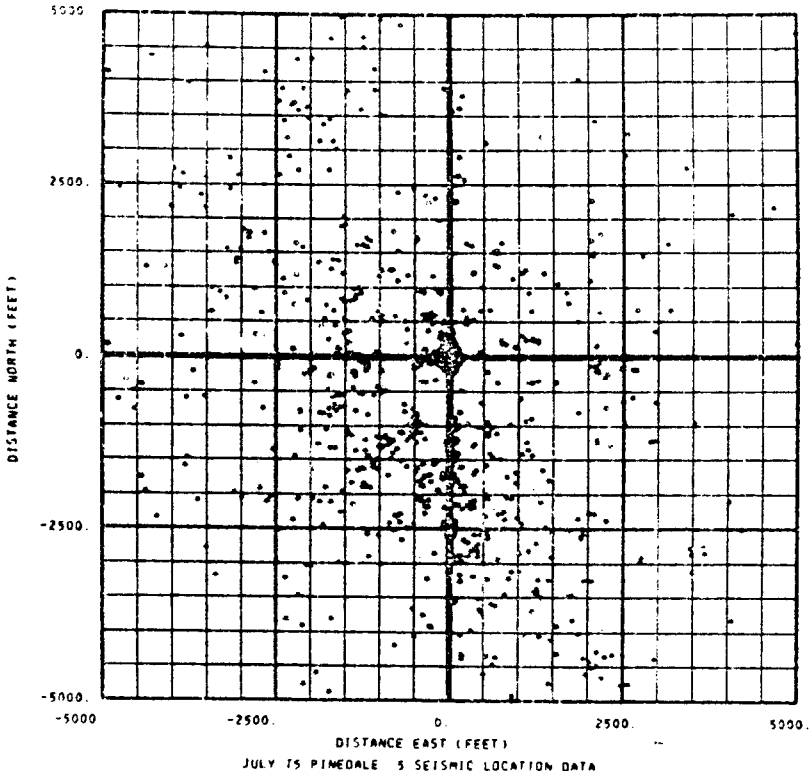

Figure 16. Fifth Hour Breakdown

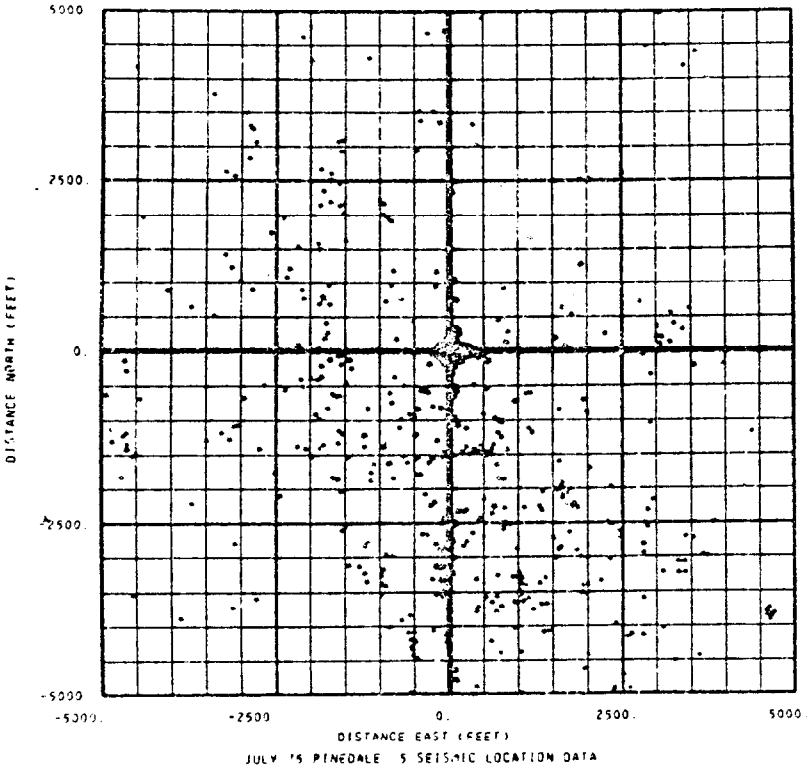

Figure 17. Sixth Hour Breakdown

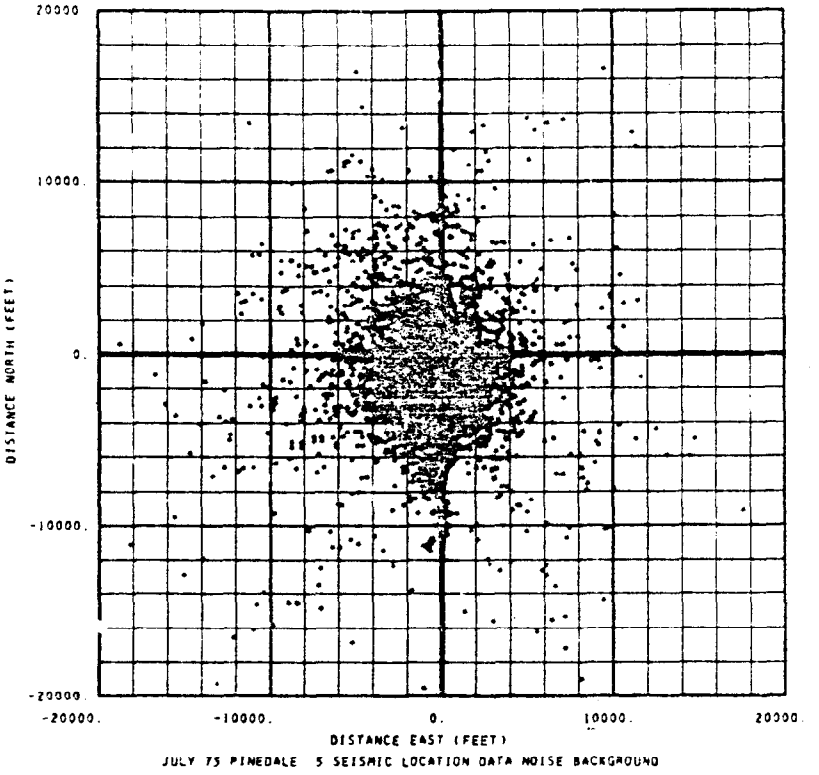

Figure 18.

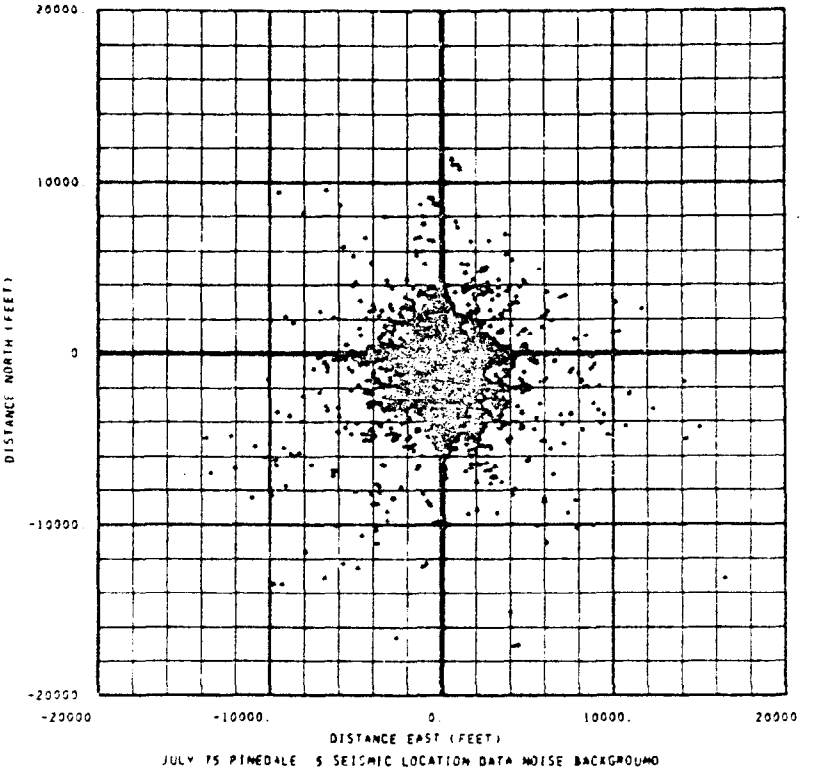

Figure 19.

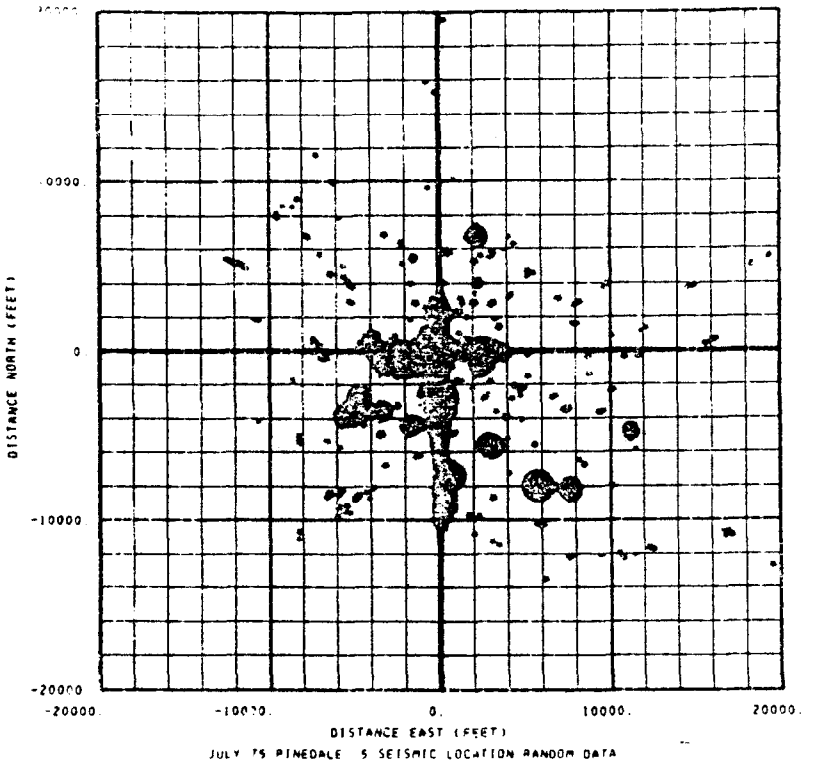

Figure 20.

In an attempt to identify the signals giving rise to the line, the seismic analog signals for several intervals plotting points near the well and on the line were examined. No obvious differences were found between these intervals and the surrounding intervals.

C. Wattenberg

In a direct attempt at finding fracture signals during the current quarter, attention was shifted to the Wattenberg data. A down-hole pressure measurement was made through a tubing with a static column of fluid during the fracture of the UPRR-22P well in January 1976. This pressure record was compared with seismic data during a six-hour

period to see if any relation could be noted between changes of downhole pressure and fluctuations in the seismic data. No relation was noted during the entire six hours of examination. Future plans are to digitize and cross correlate this data also.

D. Other Seismic Activities

The other activities of interest during the quarter included the beginning of long lead preparations for seismically monitoring during an NTS mineback hydrofracture exercise to be conducted next quarter and the opening of discussions with various rock mechanic experts to try and formulate an analytic support modeling program. Both of these items are designed to better understand the fracture and the seismic phenomenon.

DISTRIBUTION:

D. K. Nowlin, Director
Special Programs Division
U. S. ERDA
Albuquerque, New Mexico 87115

Alex Crawley (10)
20 Massachusetts Ave., N.W.
Fossil Energy U. S. ERDA
Washington, D. C. 20545

Don Ward, Chief
Natural Gas Branch
20 Massachusetts Ave. N.W.
Fossil Energy U. S. ERDA
Washington, D. C. 20545

Dr. P. C. White, Asst. Admin.
Fossil Energy, U. S. ERDA
20 Massachusetts Ave. N.W.
Washington, D. C. 20545

Dr. J. D. Ham
Asst. Div. Dir. for Petroleum
and Natural Gas
Fossil Energy, U. S. ERDA
Washington, D. C. 20545

Hugh D. Guthrie, Director
Div. of Oil, Gas and Shale Tech.
Fossil Energy, U. S. ERDA
20 Massachusetts Ave. N.W.
Washington, D. C. 20240

Charles H. Atkinson
Bartlesville Energy Research
Center, U. S. ERDA
Bartlesville, Oklahoma 74003

J. S. Ball
Bartlesville Energy Research Center
U. S. ERDA
Bartlesville, Oklahoma 74003

C. R. Fast
Amoco Production Company
P. O. Box 591
Tulsa, Oklahoma 74102

A. A. Pitrolo, Director
Morgantown Energy Research Center
U. S. ERDA
Morgantown, West Virginia 26505

Dr. L. Z. Shuck
Morgantown Energy Research Center
U. S. ERDA
Morgantown, West Virginia 26505

Dr. P. L. Randolph, Director
Research, Energy Resource Dev.
El Paso Natural Gas Co.
El Paso, Texas 79978

Dr. M. C. Smith, Q22
Los Alamos Scientific Labs.
Los Alamos, New Mexico

Dr. Merle Hanson
Lawrence Livermore Laboratory
Livermore, California 94550

1100 C. D. Broyles
1110 J. D. Kennedy
1120 G. E. Hansche
Attn: B. C. Benjamin, 1123
1130 H. E. Viney
Attn: R. D. Statler, 1133
5163 D. E. Munson
5700 J. H. Scott
5710 G. E. Brandvold
5730 H. M. Stoller
5732 D. A. Northrop
5733 C. L. Schuster (15)
9420 T. L. Pace
9415 J. L. Rogers
3151 W. L. Garner (3)
for ERDA/TIC (SDO)
8266 E. A. Aas (2)
3141 C. A. Pepmueller (Actg) (5)

SAND77-1132
UNLIMITED RELEASE

UGR File # C073/77Q2
Sandia Laboratories
February 1977-April 1977

NATURAL GAS MASSIVE HYDRAULIC FRACTURE RESEARCH AND ADVANCED TECHNOLOGY PROJECT

QUARTERLY REPORT: FEBRUARY 1977 THROUGH APRIL 1977

CARL L. SCHUSTER AND DAVID A. NORTHROP

Prepared by Sandia Laboratories, Albuquerque, New Mexico 87115 and Livermore, California 94550 for the United States Energy Research and Development Administration under Contract AT (29-1)-789

PRINTED JULY 1977

EGSP
OPEN FILE # 073/77Q2

Sandia Laboratories
energy report

SF 2900-Q0813-74

UGR File # C073/77Q2
Sandia Laboratories
February 1977–April 1977

Issued by Sandia Laboratories, operated for the United States Energy Research & Development Administration by Sandia Corporation.

NOTICE

This report was prepared as an account of work sponsored by the United States Government. Neither the United States nor the United States Energy Research & Development Administration, nor any of their employees, nor any of their contractors, subcontractors, or their employees, makes any warranty, express or implied, or assumes any legal liability or responsibility for the accuracy, completeness or usefulness of any information, apparatus, product or process disclosed, or represents that its use would not infringe privately owned rights.

Printed in the United States of America
Available from:
National Technical Information Service
U.S. Department of Commerce
5285 Port Royal Road
Springfield, VA 22151
Price: Printed Copy $3.50; Microfiche $3.00

*Add $2.50 per copy for foreign price.

UGR File # C073/77Q2
Sandia Laboratories
February 1977-April 1977

SAND77-1132
Unlimited Release
Printed July 1977

NATURAL GAS MASSIVE HYDRAULIC FRACTURE RESEARCH AND ADVANCED TECHNOLOGY PROJECT

Quarterly Report: February 1977 through April 1977

Edited by: C. L. Schuster and D. A. Northrop
Geo Energy Technology Department
Sandia Laboratories
Albuquerque, New Mexico 87115

TABLE OF CONTENTS

		Page
I.	SUMMARY	5
II.	G.P.E. UTAH MHF EXPERIMENT	6
III.	CONOCO EOR EXPERIMENT	7
IV.	ELECTROLYTIC MODEL TANK	8
V.	BOREHOLE SEISMIC LOCATOR	14
VI.	DEEP WELL INSTRUMENTATION SYSTEM	15
VII.	MINEBACK EXPERIMENTS AT THE NEVADA TEST SITE	15
VIII.	TECHNICAL MEETINGS, SYMPOSIUMS AND REPORTS	22

I. SUMMARY

This is the third quarterly report of the second reporting year for the Sandia Laboratories Program titled, "Natural Gas Massive Hydraulic Fracture Research and Advanced Technology Project." The program is funded by the Division of Oil, Gas and Shale Technology of ERDA. This report summarizes the activities from February 1, 1977 through April 30, 1977.

During this quarter two field experiments were conducted with the surface electrical potential measurement system. The first was an MHF experiment with G.P.E. (Gas Producing Enterprises) on March 15 south of Vernal, Utah. This fracture was a joint ERDA-industry funded experiment. Approximately 640,000 gallons of fluid and 1.1 million pounds of proppant was injected into multilayered gas pay zones from a depth of 6500 feet to 8000 feet. This analysis of the data has produced several new and different concepts related to fracture design and growth.

The G.P.E. experiment design called for eight stages of pad, proppant and balls to fracture 15 zones. The thinking was that each stage would treat two zones and the balls would seal the perforations taking fluid and new zones would then be treated. Surface electrical potential data was collected every two minutes and was smoothed using digital filtering techniques in the PDP-11. The potential changes that occurred did not agree with the preconceived conceptual plan of eight stages of fracturing operation. The potential changes and their interpretations do shed a completely different light on the fracturing events. The significant interpretations are listed below:

1) Fracture initiation and termination is not associated with ball action.
2) Fracture growth termination is possibly associated with formation properties rather than pressures, fluid density or pumping rate.
3) Only four substantial fractures were created; three in the first stage and one in the fourth stage.
4) The balance of the pumping evidently resulted in these fractures being inflated and receiving the proppant.

The second experiment conducted during this quarter was the CONOCO hydrofracture that was performed as a part of their tertiary oil recovery experiment in the Big Muddy Field east of Casper, Wyoming. It was a small fracture (300 bbl) initiated at a depth of approximately 3500 feet. Eighteen pairs of potential probes were placed at 20° intervals around the fracture well at spacings of 1000 feet and 2000 feet. In addition, the relative potential was measured on six wells adjacent (< 1000 feet) to the fracture

well. These wells contained the CONOCO pressure gages to monitor formation pressure during the fracture and subsequent recovery operations. Potential measurements were made at twenty second intervals on alternate current probes: one a downhole sinker bar at formation depth and the other the casing of the fracture well. The downhole data analysis indicates an asymmetric fracture in the easterly direction.

Electrical modeling effort has continued and has been centered on the design and fabrication of the model facility. This facility should be completed next quarter and allow several configurations of fracture to be studied.

Seismic work has been completely shifted to the downhole, wall clamped system. Fabrication has been completed and testing will begin during the next quarter.

Mineback to a multistaged, proppant distribution experiment has been completed at the Nevada Test Site. The mineback has revealed a complex fracture system in which no consistent proppant transport pattern was obtained. The complexity of the fracture is in contrast to previous fracture experiments conducted elsewhere in the tunnel. Further mapping, in situ stress determinations, and material property measurements are underway to examine the phenomena. Planning has been initiated for a formation-interface hydraulic fracture experiment to be conducted later this year.

II. G.P.E. UTAH MHF EXPERIMENT

On March 15, 1977, Sandia participated in G.P.E.'s MHF experiment in their Natural Buttes #14 well is located approximately 40 miles south of Vernal, Utah; the fracture was performed by Dowell. The electrical potential measurement system consisted of 24 pairs of potential probes placed around the well with an inner probe radius of 1800 feet and an outer probe radius of 3800 feet. Field data were collected at intervals of two minutes starting at 0650 hours and continued through 1815 hours. Pumping started at 0715 hours and continued through 1800 hours at a near constant rate of 25 barrels per minute. Approximately 640,000 gallons of pumping fluid and 1.1 million pounds of proppant were injected in a multilayered gas pay zone at depths of 6500 to 8000 feet.

The surface electrical potential system was the only fracture mapping system deployed for the experiment. The G.P.E. well is an old well that was being refractured and where 4-1/2 inch casing was already installed. Hence, a downhole current probe couldn't be utilized and the current was injected at the well head.

G.P.E.'s fracture design called for eight stages of pad, proppant and balls to fracture 15 zones. The thinking was that each stage would treat two zones and the balls would seal the perforations taking fluid and new zones would then be treated. Surface electrical potential data was collected every two minutes and was smoothed using digital filtering techniques in the PDP-11. The potential changes that occurred did not agree with the preconceived conceptual plan of eight stages of fracturing operation. The potential changes and their interpretations do shed a completely different light on the fracturing events. The significant interpretations are listed below:

1) Fracture initiation and termination is not associated with ball action.

2) Fracture growth termination is possibly associated with formation properties rather than pressures, fluid density or pumping rate.

3) Only four substantial fractures were created; three in the first stage and one in the fourth stage.

4) The balance of the pumping evidently resulted in these fractures being inflated and receiving the proppant.

These interpretations are speculative in nature and will certainly require further verifications. If true, the surface electrical potential system would provide considerably more insight into fracturing operations than just the orientation. These concepts will be discussed with the producing company, service companies and all interested ERDA contractors in the coming months. Undoubtedly, several fracturing experiments will have to be analyzed before the significance of this data can truly be understood.

An experiment data report containing all the data and its analysis will be prepared and disseminated to all interested organizations in the near future.

III. CONOCO EOR EXPERIMENT

The CONOCO hydrofracture was performed on March 22 as a part of a tertiary oil recovery experiment in the Big Muddy Field east of Casper, Wyoming. It was a small fracture (300 bbl) initiated at a depth of approximately 3500 feet. Sandia Laboratories' objective in this experiment was to test the effectiveness of the surface potential measurement system on a small open hole hydrofracture. In addition to the Sandia array, CONOCO had installed several pressure gages in surrounding wells as a diagnostic tool to assist in determining fracture orientation. The well had been completed, open hole, and a downhole current probe was emplaced. Software modifications to the PDP-11 allowed for two sets of potential data to be collected. One set used the well head, the other the

downhole current probe for injecting the current. Post-data analysis will allow these two configurations to be compared.

Measurements were taken by recording the potentials at 24 locations around the well before, during, and after the fracture. Eighteen pairs of potential probes were placed at 20° intervals around the fracture well at spacings of 1000 feet and 2000 feet. In addition, the relative potential was measured on six wells adjacent (< 1000 feet) to the fracture well. These were the wells containing the pressure gages to monitor formation pressure during the fracture and subsequent recovery operations.

Potential measurements were made at twenty second intervals on alternate current probes. Approximately 12,000 gallons of fluid containing 4% potassium chloride were pumped which was calculated to produce a fracture length of approximately 500 feet. This conductive fluid which results in a changing geometry for the current electrode creates the potential changes that are seen at the surface.

As discussed previously, changes in the surface potential indicate the direction and asymmetry of the fracture. The measurement just prior to breakdown is used as the reference and percentage changes in potential from this reference are plotted versus azimuth. These plots are shown in Fig. 1. Based on the computer modeling calculations, the plots indicate an asymmetrical east-west fracture with the major length of the fracture going primarily east from the fractured well.

Figure 2 is a plot of the data taken on radial A1 located 10° south of East, after being filtered by a 0.004 Hz low pass filter. Fracture growth can be recognized by a decreasing potential. Figure 2 then suggests that the primary time of fracture growth then occurred from 11:12:20 to 11:14:20. Thus, during the first four minutes of pumping, the majority of the electrical length of the fracture was created and during the balance of the pumping this fracture was only made wider.

An experiment data report will also be prepared for this fracture experiment and disseminated.

IV. ELECTROLYTIC MODEL TANK

To date, the primary technique employed for monitoring the effectiveness of massive hydraulic fracture (MHF) programs has been the surface measurement of induced electrical potentials when the fracture, or fracture plus well casing, are charged with electrical current. Mathematical modeling of this boundary value problem has been performed for the case of an homogeneous earth with an uniform casing/fracture source electrode. However,

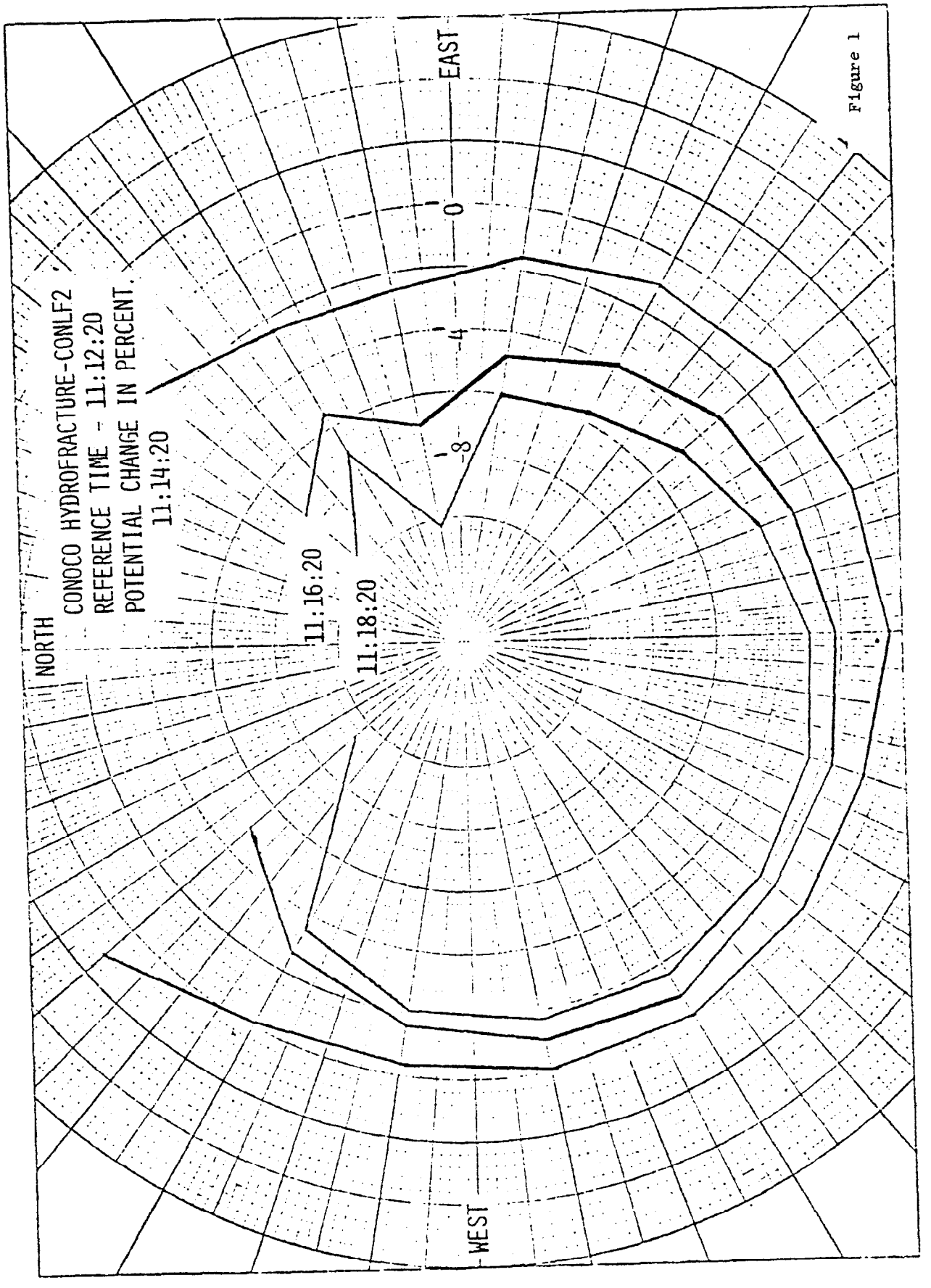
NORTH
CONOCO HYDROFRACTURE-CONLF2
REFERENCE TIME - 11:12:20
POTENTIAL CHANGE IN PERCENT
11:14:20
11:16:20
11:18:20
-8
-4
0
EAST
WEST

Figure 1

CONLF4
RADIAL: A1
PERCENT CHANGE FROM REFERENCE VALUE AT TIME 111220
REFERENCE VALUE = .141347

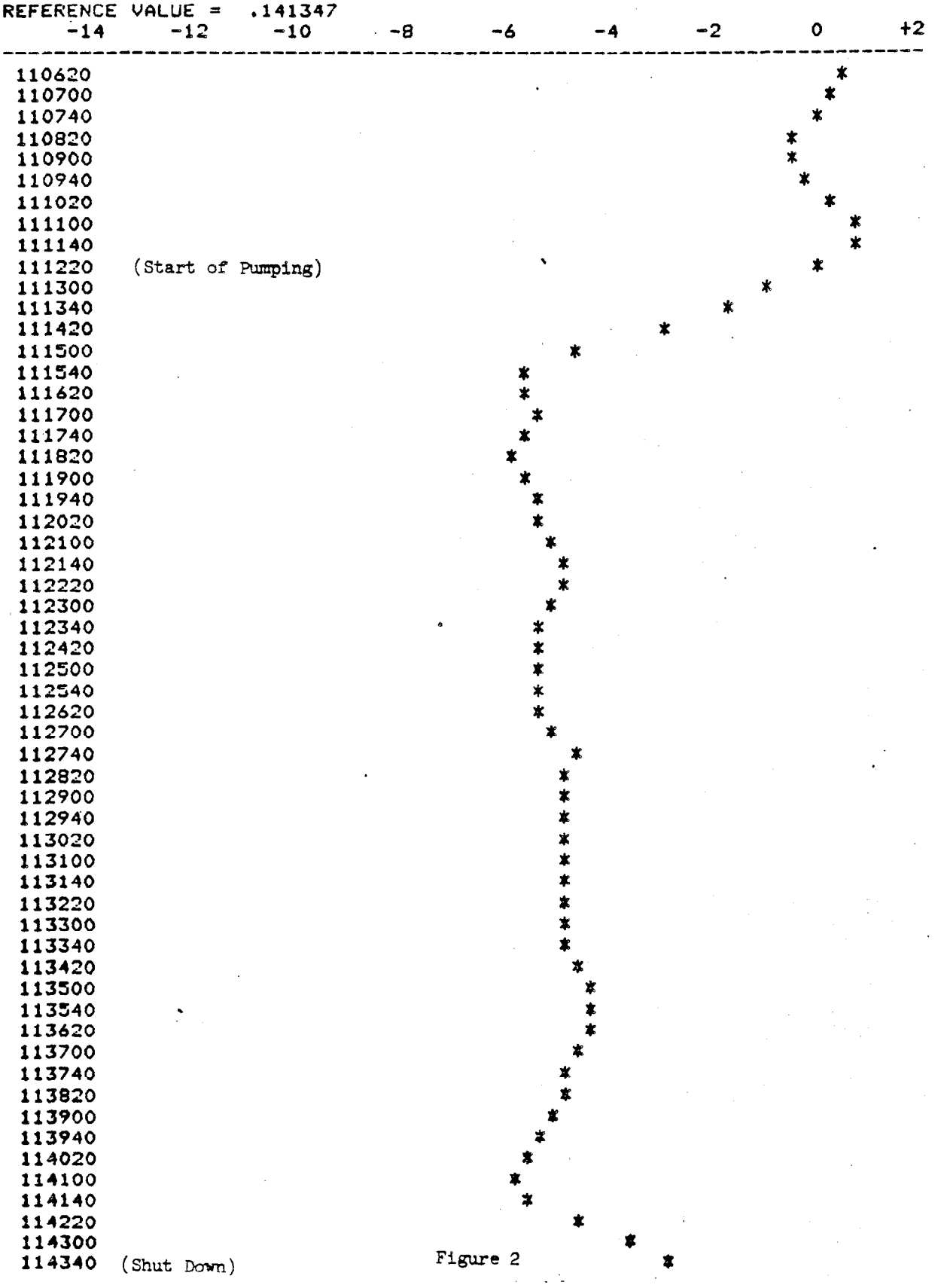

Figure 2

the introduction of layering and lateral inhomogeneity (both in terms of electrical resistivity) in the earth model, imperfect or variable casing-earth electrical contact, or the presence of man-made distortions (other metal well casings in the area) produce mathematical rigors which are not tractable by techniques currently available. As these situations are typically the rule rather than the exception in actual field locations, and as an accurate, quantitative description of the fracture system (length, height, etc.) is desired, an alternate modeling technique was sought which could accommodate those situations met in the field which reduce the applicability of mathematical synthesis. This was the rationale behind the development of an electrolytic model tank.

An electrolytic model tank is basically a water-filled tank with water of variable salinity representing the homogeneous earth. Layering may be simulated by the introduction of sheets of material of varied resistivity into the water. Similarly, casing, ore bodies, cavities or other size-limited bodies may be modeled and placed in appropriate positions within the tank. Scaling of lengths, resistivities, and frequency of applied current from the field to the model is dictated by the following relation (assuming magnetic permeability of model and full scale materials is the same):

$$\frac{\omega' L'^2}{\zeta'} = \omega \frac{L^2}{\zeta}$$

where

ζ' = model resistivity	ζ = full scale resistivity
ω' = model current frequency	ω = full scale current frequency
L' = characteristic model length	L = corresponding full scale length

Our initial interest was to locate an existing model facility and arrange for its use for modeling MHF experiments. To this end, R. P. McCann and T. L. Dobecki visited the electrolytic model facilities at the United States Geological Survey (USGS), Denver and at the Colorado School of Mines (CSM), Golden, Colorado. Both tanks were massive poured cement structures, rectangular in shape, and typically 10 ft. x 15 ft. x 5 to 8 ft. deep. Both tanks were fitted for the performance of electromagnetic model experiments and would therefore require retooling for our galvanic experiments, thereby interrupting the progress of on-going tasts. The USGS facility is in current use with projected heavy use by USGS personnel in the near future. The CSM facility, on the other hand, is being terminated for future office space and will not be available. The situation, therefore, dictated construction of a model tank at Sandia.

The electrolytic model tank currently under development at Sandia is of unique design (Figure 3). The tank is much smaller than those described earlier, measuring 5 ft. x 5 ft. x 3 ft. and utilizes a hemispherical aluminum shell (I.D. = 47.750 in.) as the

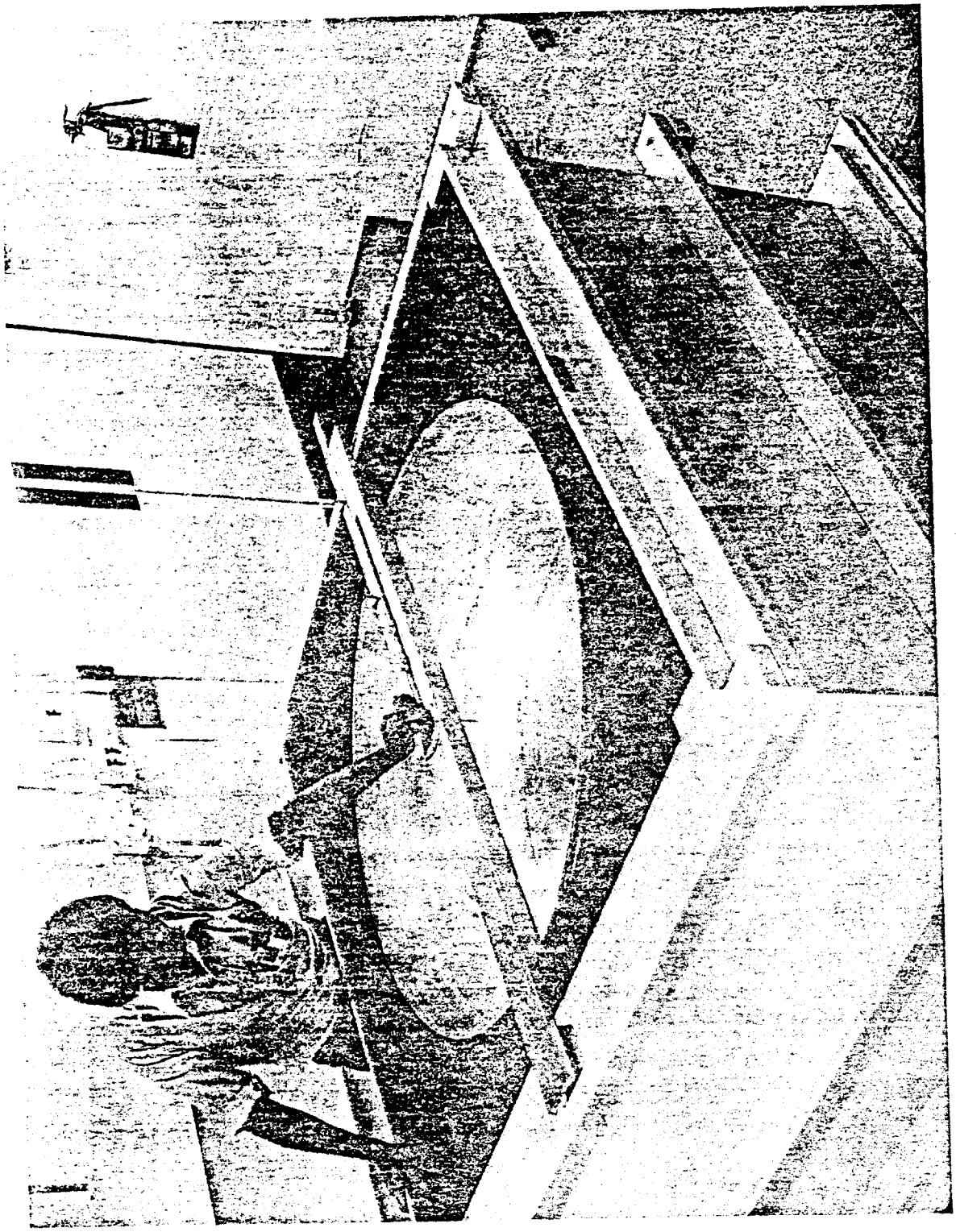

Fig. 3. Electrolytic Modeling Tank Employing a Hemispherical Return Current Electrode.

return electrode. The reasoning behind the choice of a hemispherical electrode may be explained as follows:

The electrical potential field about a point electrode at the earth's surface, if the return electrode is an infinite distance away, is given by

$$V = \frac{I\zeta}{2\pi R}$$

where

I = impressed current
ζ = resistivity of earth material
R = distance to observation point.

All equipotential surfaces are given by R = constant which are hemispheres centered on the point source. If, on the other hand, the return electrode is made a hemisphere centered on the point source, it becomes an equipotential surface and current flow is radial from the point source to the shell. Therefore, again all equipotential surfaces are hemispheres with the same potential distribution as a point source except for an additive constant. For potential difference measurements, this technique is equivalent to having a return electrode at infinity while maintaining a reasonably small sized tank. For standard four-electrode (Wenner or Schlumberger type, e.g.), the aluminum hemisphere may be removed, and experiments may be carried out in the box itself.

An advantage of a large tank is that high precision in placement of electrodes or in lengths of models is not critical. As the size of the tank is decreased, the scaling relation requires greater precision in the measurement of lengths. A scaled track is fit to the top of the hemisphere upon which moveable potential-measuring electrodes may be located with an accuracy of ± 0.005 in. (± 0.12 mm).

The potential measuring and current source electrodes are made of stainless steel hypodermic needles. Several needle diameters and metal platings will be tested and evaluated in the course of preliminary experiments.

The central current electrode (when utilizing the return hemisphere) will simulate the casing and/or fracture. This will be mounted on the track in a calibrated, rotatable mount. In this way, the orientation of the fracture with respect to the surface potential measuring dipole may be varied from 0° to 360°, again to simulate the field configuration of radial dipoles used in MHF mapping programs. Size of the fracture, casing-earth contact, and other situations peculiar to the casing-fracture system may be modeled by changing the size and material characteristics of the current electrode.

The proposed program of experimentation utilizing the electrolytic tank consists of, generally, tests for evaluation of the tank facility followed by experiments to directly model the MHF process. Each individual test could easily lead to numerous other tests of a related nature, but a tentative program may be outlined as follows:

Test the accuracy of the hemispherical shell electrode as an approximation to an infinitely removed point source for a point source at the center of the tank.

Evaluate various current sources and potential measurements systems for consistency and ease of operation.

Evaluate different model materials and metal platings.

Determine the limits of applicability of the hemispherical tank for centrally-located current sources which are not point sources (vertical or horizontal line sources representing fractures and casing).

Model numerous fracture depths and lengths to derive empirical relations between fracture geometry and surface potential measurements.

Model fracture experiments in the presence of subsurface layering, lateral resistivity variation, etc., to observe the effect of these on surface potential measurements.

Other tests may be proposed for future experiments, however, these are felt most applicable to the MHF program.

V. BOREHOLE SEISMIC LOCATOR

The Borehole Seismic Locator (BSL) was assembled and pressure tested. The geophone section which was fabricated from 304 stainless steel failed at 12,000 psi. This housing has been remade from 4340 steel. Stainless steel was initially used because of its proximity to the compass orientation unit. However, it is felt that because of the battery pack separating it from the compass unit, 4340 steel can be used.

During the following quarter surface explosive tests are planned at the test well recently drilled on Kirtland Air Force Base. The test plan is to detonate a number of various size charges at the surface in a number of locations. The charge sites will be in contact with the limestone bed to which the BSL is coupled. The received signals

will be analyzed for wave content and recognition, amplitudes, frequency contact and source location information. Because of the size and weight of the BSL, handling techniques will also be evaluated.

It is also planned to install the BSL on a hydrofracture test at the Nevada Test Site sometime this summer. Seismic events will be recorded in order to obtain information pertaining to the ability of the BSL to map a hydrofracture. Mineback is planned so that precise hydrofracture location will be known.

In late summer or early fall the BSL will be used for recording seismic signals from a hydrofracture of an AMOCO well in the Wattenberg Oil Field in Colorado.

Calibration data has been recorded for the electronic portion of the BSL. Gain and phase characteristics of the amplifiers and voltage controlled oscillators will be determined. This data is still in data reduction but hopefully will be available soon.

VI. DEEP WELL INSTRUMENTATION SYSTEM

Preliminary specifications for the mobile field laboratory for instrumentation to support the western tight gas sands program has been submitted to seven or eight companies. The laboratory will consist of an instrumentation trailer and a mast truck with all of the equipment necessary for long period monitoring of deep wells. Bids have not been received as yet, but are expected shortly. The proposals will be evaluated and an order placed for delivery late fall.

VII. MINEBACK EXPERIMENTS AT THE NEVADA TEST SITE

Mineback operations were conducted during most of the report period on the hydraulic fracture created in Hole U12G10.5 (hole DH-5). This was a vertical hole drilled from the top of Rainer Mesa down to the G tunnel level resulting in a depth of approximately 1395 feet. A multistaged fracture experiment had been conducted in this hole in July 1976, but mineback operations did not commence until early 1977. The first evidence of the fractures were observed in February, and it became readily apparent as mining advanced that a very complex fracture(s) were formed rather than the single vertical fracture that had repeatedly been formed in previous tests at different locations within the tunnel complex.

The complexity of the fracture network made it necessary to slow mining so that sufficient mapping and documentation of the fractures could be accomplished. By the end of April, the injection hole had been reached. At least two fracture systems were induced and the multistaged, colored-sand proppant has shown no consistent transport pattern.

Three diagrams and two photographs (Figure 4-8) are presented to illustrate the complexity of the fracture system. These drawings given here are preliminary as more detailed maps are being compiled from comprehensive data and notes taken during mineback. Figure 4 is a plan view of the mine excavation around Hole DH-5. Figures 5 and 6 are photos showing some of the details of the fractures as they were being exhumed. The fields of view of these two photos are shown on Figure 4 as are the locations of two vertical cross-sections that are presented as Figures 7 and 8.

Figure 5 is looking upwards to the bottom of the drill hole. The position of the hole (hidden in the roof) is located a few feet behind the card being held by the miner. In the right center of the photograph the dark colored face contains sand proppant along what is now one face of the fracture. The width of the fracture was about 3 mm. This fracture terminates abrubtly along a horizontal bedding plane as seen in Figure 7.

Figure 6 shows conditions at the working face when a vertical fault was exposed. A low angle fracture is shown curving in from the left center to a position just below the "+6" mark. The fracture terminated at this fault. A high angle fracture is shown on the right. It also terminates at the fault.

Figures 7 and 8 illustrate the nature of the fractures by cross-section. In Figure 7, the extent of the fracture network is shown. The fault on the left is the one which terminated fracture growth to the north. The horizontal bedding plane at an elevation of 6183' stopped vertical growth. The full extent of the fracture has not been explored below 6158'. Figure 8 is a cross-section looking north. Note the high angle fracture is a composite of echelon type fractures. The low angle fracture dips at about 30 degrees to the north.

Future work is planned at this site so as to better understand why a complex fracture system was induced from what was thought to be a simple hydraulic fracture experiment. In situ stresses may be complicated in this particular area, or the stress field could be almost hydrostatic. In the latter case, subtle changes in rock properties would be the dominant factor on fracture growth. Plans include additional in situ stress determinations into the walls of the excavation using both the overcore and small hydraulic fracture techniques. Cores recovered from this work will be tested for additional physical properties.

Planning of an "interface" experiment was initiated at a joint working group meeting between Halliburton, Dowell, AMOCO Research and Sandia held in Tulsa on February 22, 1977; an additional fracture design meeting was held with Dowell (who holds the present service company contract at the NTS) on March 29, 1977. It was the concensus that the experiment

Preliminary Data

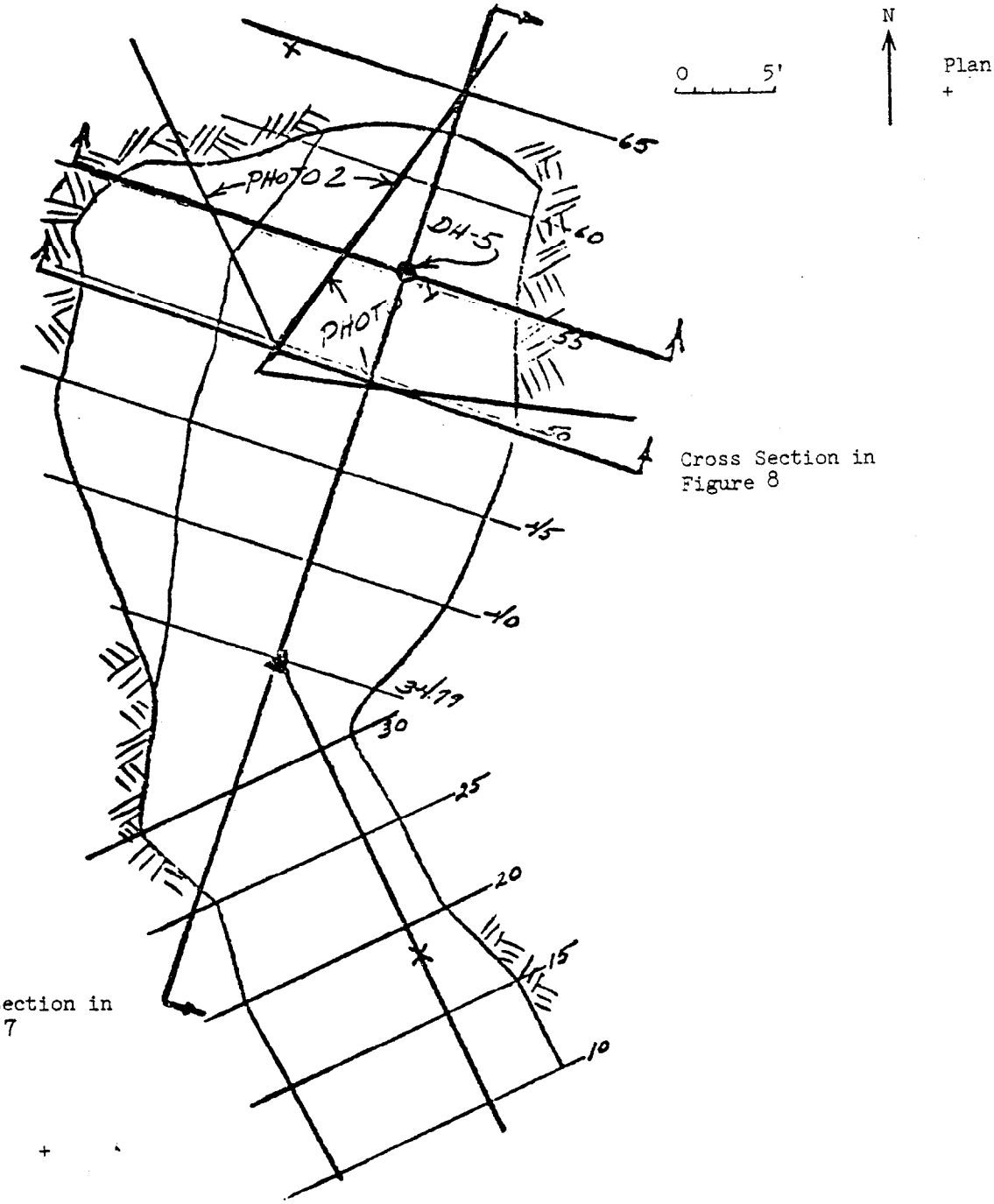

Fig. 4 Plan View of Mineback Operations, Hole DH-5.

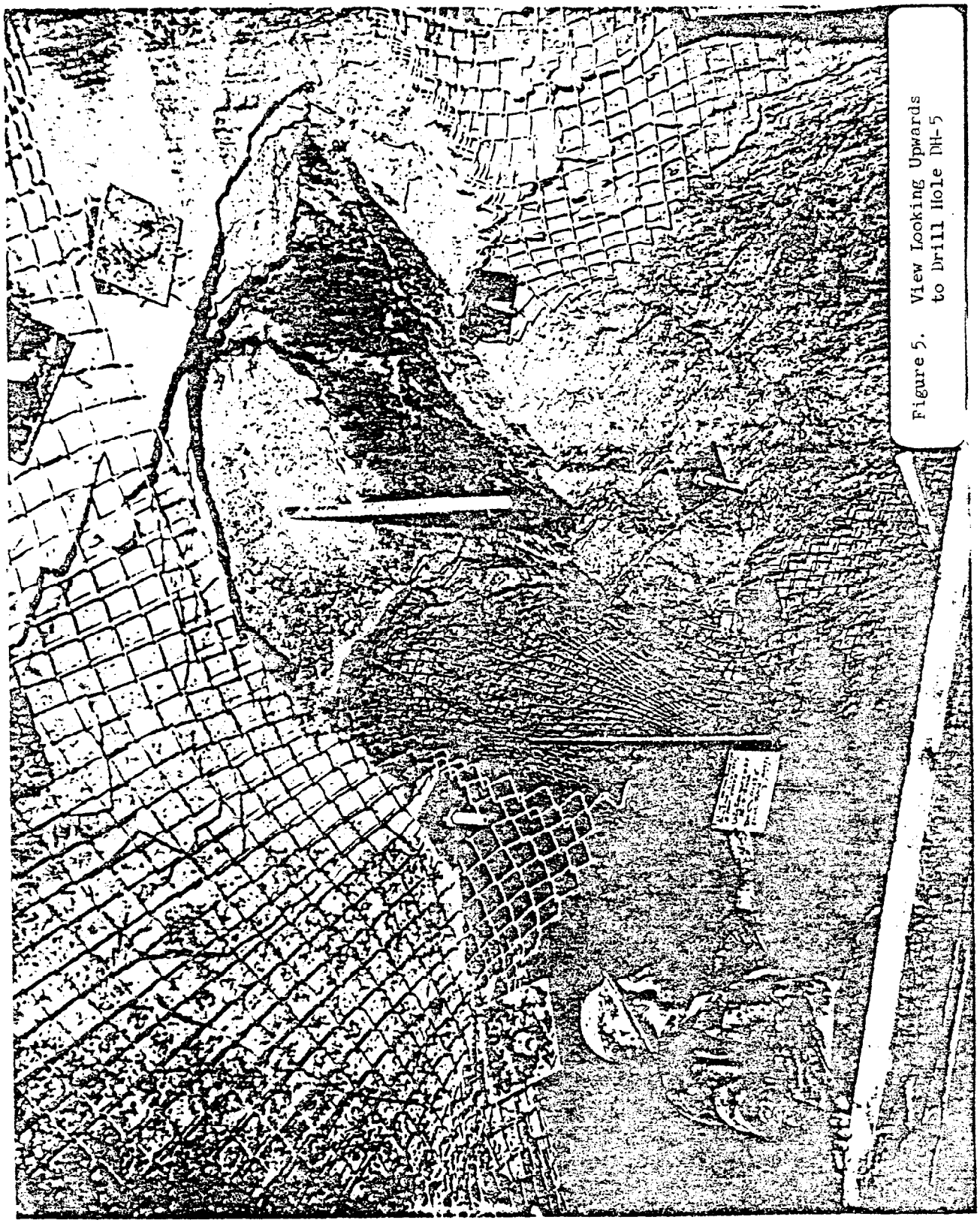

Figure 5. View Looking Upwards to Drill Hole DH-5

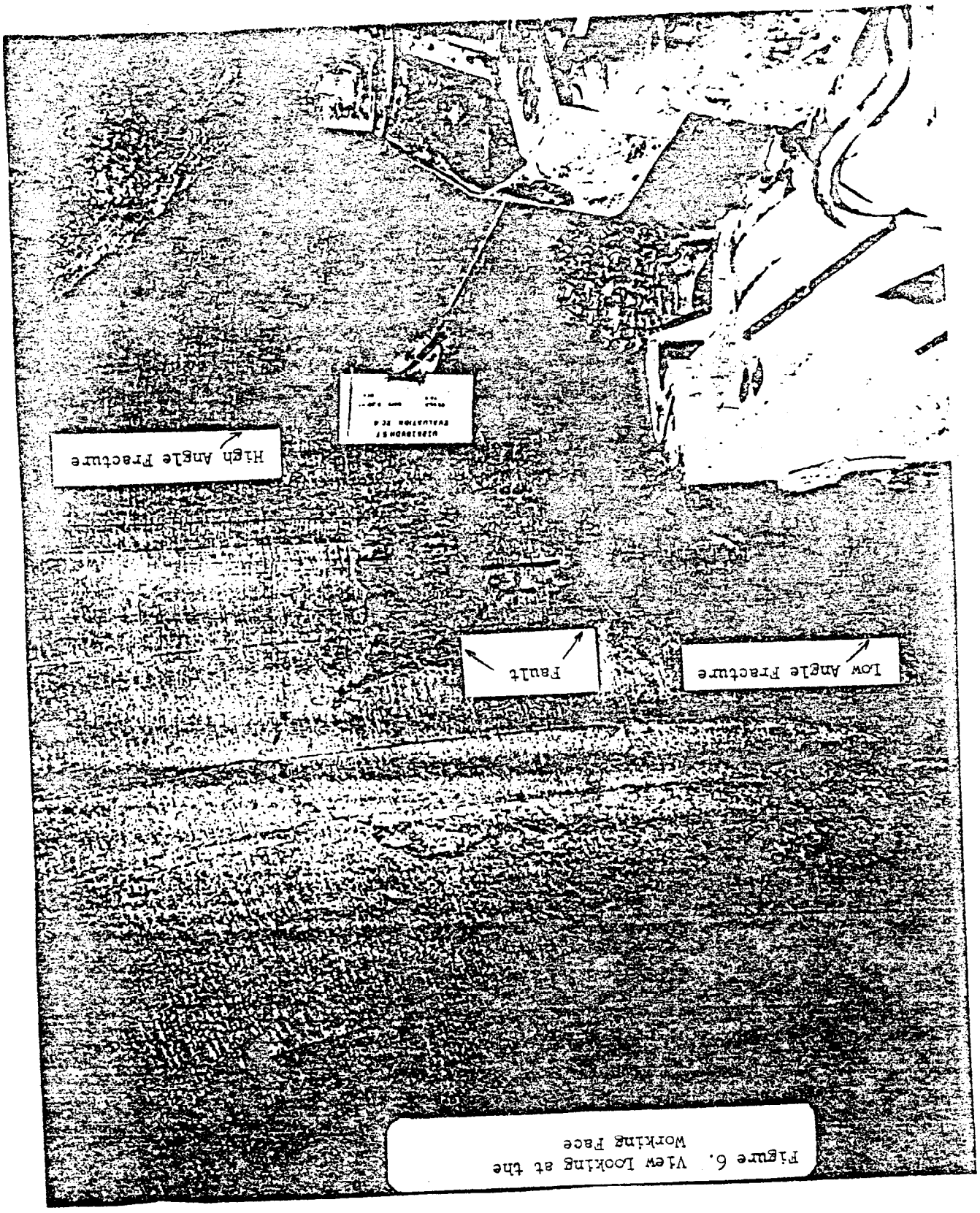

Figure 6. View Looking at the Working Face

UGR File # C073/77Q2
Sandia Laboratories
February 1977-April 1978

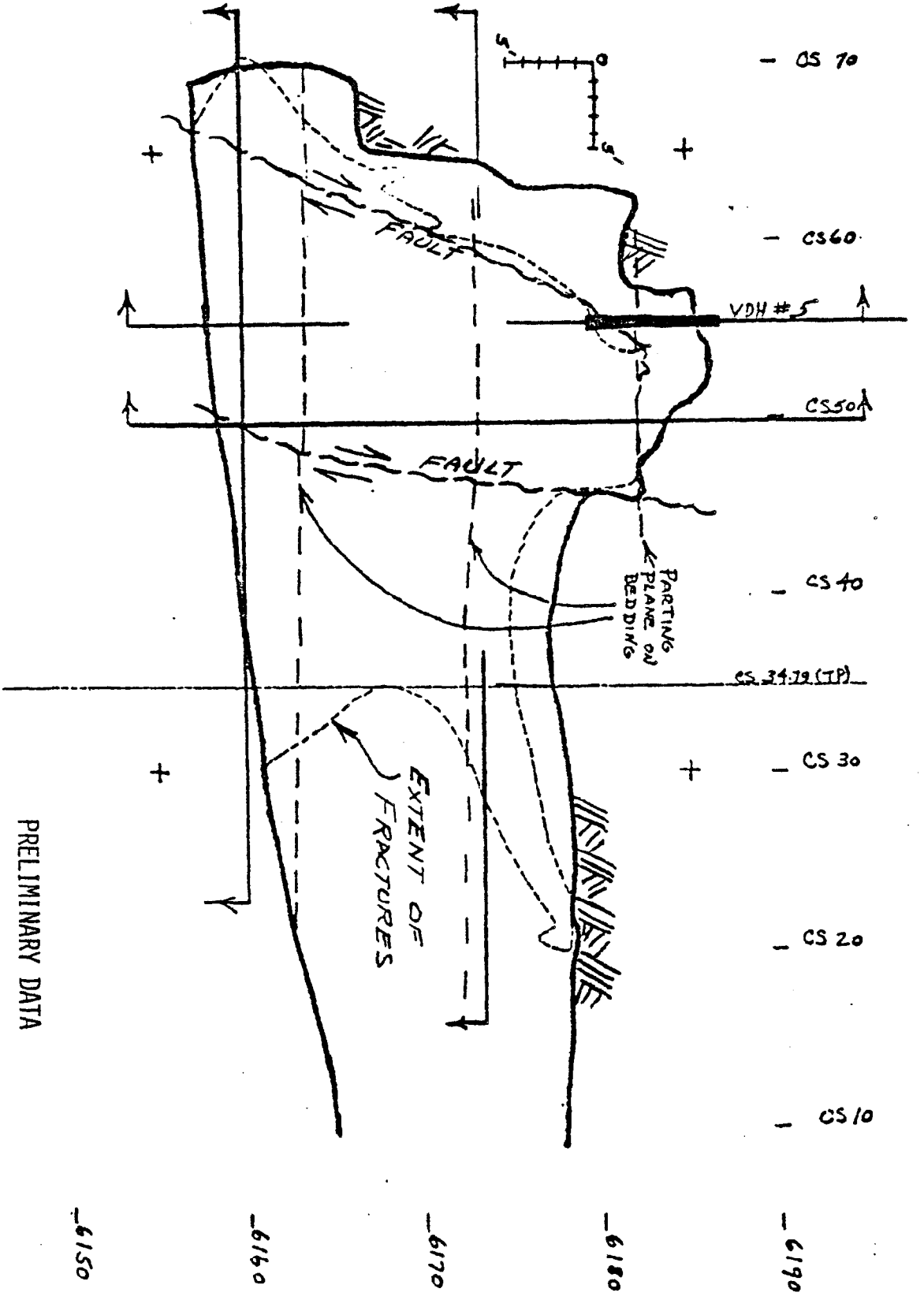

Fig. 7. Vertical Cross-Section Near Hole DH-5.

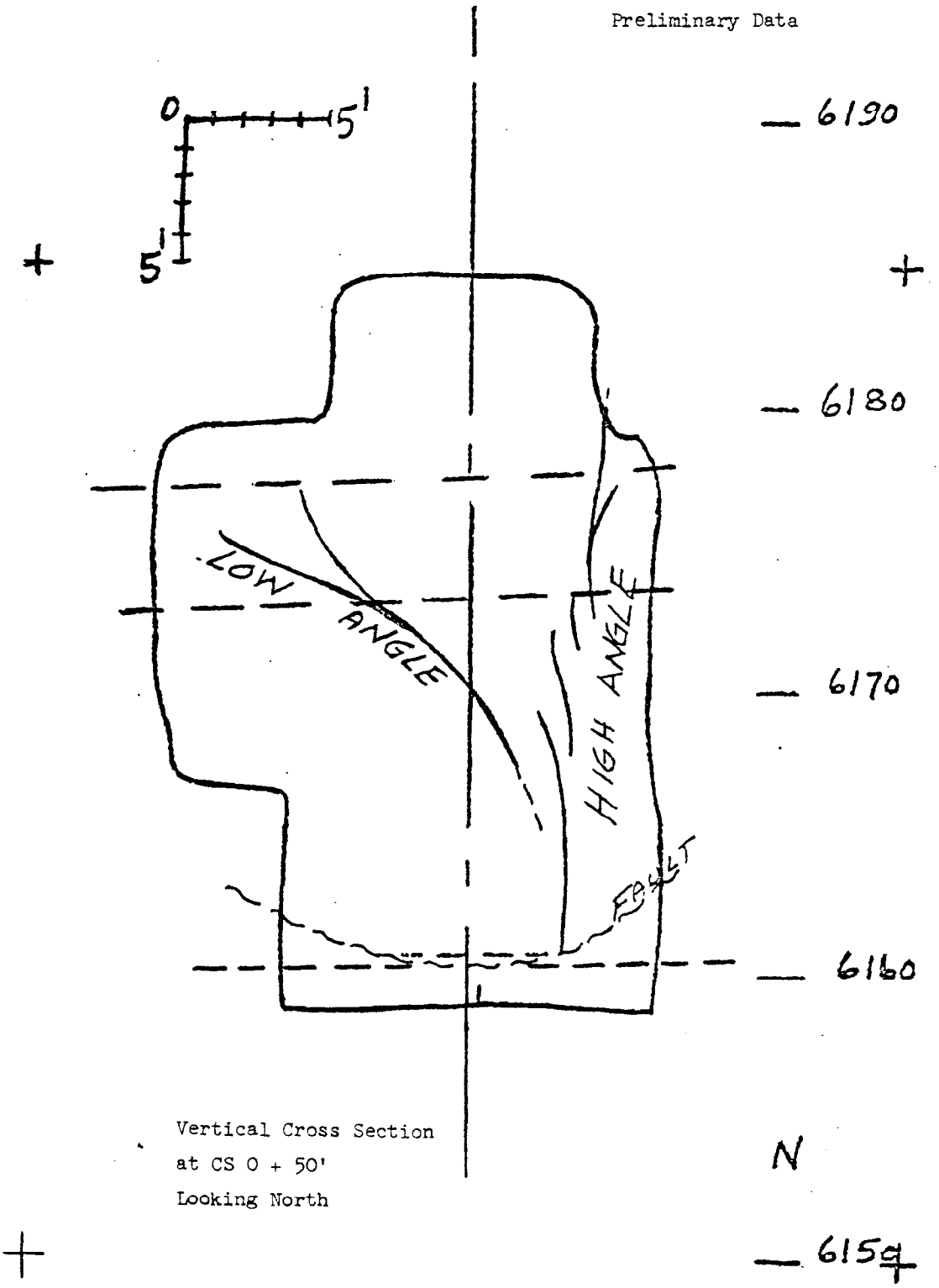

Fig. 8. Vertical Cross Section Near Hole DH-5

should be kept simple in design so as to test fracture growth both above and below a geologic formation interface. This interface consists of a brittle, welded tuff underlain by more porous, softer ash-fall tuff. The plan would be to induce a fracture about 10 feet below the contact followed by a second about 10 feet above. A tentative site for the experiment, designated as Hole U12G10.6 (hole DH-6), has been selected several hundred feet southwest of the staged proppant experiment (Hole DH-5) previously described. Exploratory core drilling to the region is underway. It is anticipated that the west-dipping welded/ash-fall tuff contact will be at tunnel level at this location. Selected core samples of both units will be sent to AMOCO, Halliburton, Dowell as well as commercial testing laboratories.

VIII. TECHNICAL MEETINGS, SYMPOSIUMS & REPORTS

A. Columbia Gas

A meeting on March 8, 1977, at Columbia Gas in Columbus, Ohio was attended by C. Komar, MERC; Darrell Wood, USGS; C. L. Schuster, Sandia; and several local participants. Results from both fracture experiments conducted in 1976 were reviewed and the somewhat unusual results surrounding the screen-out discussed. Still no definitive or substantial results are apparent. Future testing was discussed and three requirements were presented for a meaningful surface electrical potential experiment: (1) add 2% KCl to the frac fluid; (2) resurvey potential probe locations for more optimum locations; (3) provide a downhole current probe. These requirements were reviewed by Columbia and MERC for possible inclusion into the future tests. Their apparent decision was to not go to the expense involved to collect the electrical data for another fracture experiment.

B. AMOCO

A planning meeting was held on April 15, 1977, in Denver with the division office and research personnel of AMOCO. Tentative plans for an experimental series of fractures in the Wattenberg area were formulated. These tests are scheduled for this fall to minimize the interference with the agriculture in the area.

AMOCO is planning to collect orientated cores, run their downhole television system and provide the necessary support for the ERDA experiments.

Sandia will field the surface electrical potential system and hopefully also collect some downhole seismic profiling data. The USGS plans to support these tests with their tiltmeter array. The formation to be fractured is the Sussex at a depth of approximately 4000 feet which is an oil-bearing zone that overlays the deeper Wattenberg gas sands. These tests should provide an intermediate depth for fracture evaluations.

Distribution:

Dr. Phillip C. White
Asst. Administrator for Fossil Energy
U.S. ERDA
20 Mass. Ave., NW
Washington, DC 20545

Edward Lievens, Acting Director
Office of Program Planning and Analysis
U.S. ERDA
20 Mass. Ave., NW
Washington, DC 20545

Mr. Hugh D. Guthrie, Director
Oil, Gas and Shale Technology
U.S. ERDA/Fossil Energy
20 Mass. Ave., NW
Washington, DC 20545

Mr. J. Wade Watkins, Deputy Director
Oil, Gas and Shale Technology
U.S. ERDA Fossil Energy
20 Mass. Ave., NW
Washington, DC 20545

Dr. J. D. Ham, Assistant Director
Oil, Gas and Shale Technology
U.S. ERDA/Fossil Energy
20 Mass. Ave., NW
Washington, DC 20545

Mr. D. C. Ward
Oil, Gas and Shale Technology
U.S. ERDA/Fossil Energy
20 Mass. Ave., NW
Washington, DC 20545

Mr. Jeff B. Smith
Oil, Gas and Shale Technology
U.S. ERDA/Fossil Energy
20 Mass. Ave., NW
Washington, DC 20545

Mr. Alex B. Crawley (10)
Oil, Gas and Shale Technology
U.S. ERDA/Fossil Energy
20 Mass. Ave., NW
Washington, DC 20545

Mr. John S. Ball, Director
Bartlesville Energy Research Center
U.S. ERDA
Bartlesville, OK 74003

Mr. Charles H. Atkinson
Bartlesville Energy Research Center
U.S. ERDA
Bartlesville, OK 74003

Mr. A. A. Pitrolo, Director
Morgantown Energy Research Center
U.S. ERDA
Morgantown, WV 26505

D. K. Nowlin, Director
Special Programs Division
U.S. ERDA
Albuquerque, NM 87115

Dr. Merle E. Hanson
Lawrence Livermore Laboratory
Livermore, CA 94550

Dr. Robert Brownlee
Los Alamos Scientific Laboratory
G-Division
Los Alamos, NM 87544

Dr. William G. Davey
Los Alamos Scientific Laboratory
Q-Division, Mail Stop 570

Dr. M. D. Wood
U.S. Geological Survey
Menlo Park, CA 94025

Louis S. Cook
Columbia Gas System Service Corp.
1600 Dublin Road
Columbus, OH 43215

Mr. James Short
Gas Producing Enterprises, Inc.
2100 Prudential Plaza
P.O. Box 749
Denver, CO 80201

Mr. G. R. Leutkenhans
CER Geonuclear
4220 S. Maryland Pkwy.
P.O. Box 15090
Las Vegas, NV 89114

Mr. Ted Nyquist
Dowell
P.O. Box 21
Tulsa, OK 74102

Mr. Joe P. Pavlich
Dowell Division of Dow Chemical
2200 W. Loop S
Houston, TX 77027

Dr. Robert L. Huggins
Dr. Micheal B. Smith
AMOCO Production Company
P.O. Box 591
Tulsa, OK 74102

C. On April 5, 1977, Sandia participated at the MHF-3 Technical Committee meeting in Las Vegas, Nevada sponsored by CER. L. D. Tyler presented a summary of Sandia mineback activities at the Nevada Test Site where hydraulic fractures are being directly observed and their behavior analyzed. D. A. Northrop briefly discussed future plans for the mineback testing program, described the role that such testing would play in the development of MHF technology, and emphasized the need for, and solicited, industrial participation in all aspects of the program.

The next day Sandia Laboratories sponsored a trip for meeting participants to the Nevada Test Site. The tour included a movie on overall NTS test activities and a visit to Sedan Crater. The afternoon was spent at G tunnel, where L. D. Tyler, W. C. Vollendorf and G. B. Griswold described the on-going test activities: (a) mineback at hole DH-3, a fracture orientation test, (b) mineback at hole DH-5, a proppant distribution test with a complex geometry, (c) coring activities to assess the welded-ashfall tuff interface for a future fracture test (hole DH-6), and (d) contained explosive tests. A great deal of interest was shown by the participants in the on-going work. Especially notable were many comments by industry on the value of such a program; several offers of help, future participation, and support were received.

D. Eric Smith and Steve McKetta of Columbia Gas Company, Columbus, Ohio, visited the Sandia mineback experiments at NTS on April 19, 1977. L. D. Tyler briefed them on the results and activities to date. Their interest stems from a knowledge of Sandia activities on chemical explosive fracturing tests in Devonian shale in West Virginia.

E. David A. Northrop is a member of a working group charged to develop, by the end of FY 77, a program strategy for enhanced gas recovery. ERDA, ERC, and National Laboratory (LLL and Sandia) members are providing technical direction in the formulation and development of this plan. The first meeting was held April 18-19, 1977 in Washington.

UGR File #C073/77Q4
Aug. 1976-Oct. 1976
Sandia Laboratories

FILE

SAND-76-0723
UNLIMITED RELEASE

NATURAL GAS MASSIVE HYDRAULIC FRACTURE RESEARCH AND ADVANCED TECHNOLOGY PROJECT

QUARTERLY REPORT: AUGUST 1976 THROUGH OCTOBER 1976

EDITED BY: C. L. SCHUSTER, SUPERVISOR
INSTRUMENTATION SYSTEMS DIVISION 5733

Prepared by Sandia Laboratories, Albuquerque, New Mexico 87115 and Livermore, California 94550 for the United States Energy Research and Development Administration under Contract AT (29-1)-789

PRINTED JANUARY 1977

EGSP
OPEN FILE # 073/77Q4

Sandia Laboratories

SF 2900 Q(7-73)

UGR File #C073/77Q4
Aug. 1976-Oct. 1976
Sandia Laboratories

Issued by Sandia Laboratories, operated for the United States Energy Research & Development Administration by Sandia Corporation.

NOTICE

This report was prepared as an account of work sponsored by the United States Government. Neither the United States nor the United States Energy Research & Development Administration, nor any of their employees, nor any of their contractors, subcontractors, or their employees, makes any warranty, express or implied, or assumes any legal liability or responsibility for the accuracy, completeness or usefulness of any information, apparatus, product or process disclosed, or represents that its use would not infringe privately owned rights.

SF 1004-DF (3-75)

Printed in the United States of America
Available from
National Technical Information Service
U. S. Department of Commerce
5285 Port Royal Road
Springfield, VA 22161
Price: Printed Copy $4.00; Microfiche $3.00

UGR File #C073/77Q4
Aug. 1976-Oct. 1976
Sandia Laboratories

SAND-76-0723
Unlimited Release

NATURAL GAS MASSIVE HYDRAULIC FRACTURE RESEARCH AND ADVANCED TECHNOLOGY PROJECT

Quarterly Report: August 1976 through October 1976

Edited by: C. L. Schuster, Supervisor
Instrumentation Systems Division 5733
Sandia Laboratories
Albuquerque, New Mexico 87115

Printed January 1977

Abstract

An M.H.F. experiment was conducted in West Virginia that was one of the field demonstrations of the Eastern Devonian Shale Program. It was the largest gelled water and proppant fracture conducted to date in the eastern United States. Halliburton performed the fracture treatment for Columbia Gas as part of the joint/industry contract with the Morgantown Energy Research Center. Sandia installed the revised electrical potential system as a diagnostic to aid in fracture orientation determination. The new system performed according to design goals after some minor revisions. Data analysis of the results are not very definitive for fracture orientation and some improved techniques are being planned for the follow-on experiments.

TABLE OF CONTENTS

		Page
I.	Summary	7
II.	Electric Potential System	9
	A. Potential Measurement Subsystem	9
	B. Current Generator Subsystem	10
	C. Data Control and Collection Subsystem	11
III.	West Virginia Experiment	13
	A. Introduction	13
	B. Experimental Configuration	14
	C. Fracture Design	14
	D. Fracture Characterization Results	16
IV.	Seismic and Pressure Data Analysis	22
	A. Seismic Data	22
	B. Pressure Data	23
V.	Joint AMOCO/ERDA Experiments	27

I. Summary

This is the first quarterly report of the second reporting year for the Sandia Laboratories Program titled "Natural Gas Massive Hydraulic Fracture Research and Advanced Technology Project. The program is funded by the Division of Oil, Gas, and Shale Technology of ERDA. This report summarizes the activities from August 1, 1976 through October 31, 1976.

The principal event during this period was an M.H.F. experiment conducted in West Virginia. Columbia Gas System Service Corporation was the operator and Halliburton performed the fracture treatment. This experiment was a portion of the Eastern Devonian Shale Program administered by the Morgantown Energy Research Center. This was the first Devonian shale hydrofracture in which Sandia participated with our fracture diagnostic system.

Following the January 1976 experiments in Colorado, the electrical potential system was redesigned and this was the first test of the new hardware. After some minor revisions, the system performance was excellent providing good signals with greatly reduced noise levels. Data analysis did not show as definitive a fracture orientation as had been observed in the Wattenberg, Colorado data.

Future testing hopefully will utilize a down hole current probe to more closely resemble the Colorado test configuration.

The other technique being evaluated by Sandia for fracture characterization is to identify and locate seismic signals associated with the fracturing process. The seismic data analysis has been concentrated on the UPRR-22 data from the January 1976 experiment with AMOCO in Colorado. The results from this analysis will probably be available in the following quarter.

Preliminary planning of a shallow fracture experiment with AMOCO near Tulsa, Oklahoma, was completed and the test scheduled for early November. This experiment will allow several techniques for fracture orientation determination to be evaluated and verified by obtaining the ground truth. AMOCO plans to drill into the formation and intercept the fracture to obtain its height and length.

Plans were also initiated for another joint experimental test series for the Wattenberg area in Colorado. These tests are planned to be in the Sussex formation about 4000 feet deep with several different fracture diagnostic techniques utilized. The shallow depth will allow a better interpretation of the various measurement techniques.

II. Electrical Potential System

The electrical potential system is comprised of three subsystems. These are the current generator, the potential measurement boxes (PMB) and the data control and collection system. Based on development tests conducted on M.H.F. experiments performed by the El Paso Natural Gas Company and the Amoco Production Company, a first generation instrumentation system has evolved that is capable of determining fracture orientation. This system will be reported on in a separate publication with sufficient detail to allow the transfer of this technology to industry. The next quarterly report will provide the references for this publication.

A. Potential Measurement Subsystem

Each potential measurement location consists of a pair of stainless steel potential probes driven into the earth and a potential measurement box (PMB). A wire from each probe is fed to a PMB usually located adjacent to the inner potential probe. The output from twelve PMB's are frequency multiplexed onto one coax cable. The coax cable feeds power from the instrumentation van to each PMB and feeds data via the frequency multiplex from each PMB to the instrumentation van. Two coax cables thus feed the

potential data from all 24 locations to the instrumentation van for processing and recording. The potential measurements must be made in the presence of natural and man-made noise.

The PMB is capable of amplifying the desired potential and rejecting the potentials caused by noise currents. The distances from the fracture well to the inner and outer probes are dependent on the well depth and the predicted fracture length. A computer model has been developed which aids in the selection of probe spacings.

B. Current Generator Subsystem

The current generator was designed to provide up to 600 volts and 50 amperes into a load of eight ohms or more with the capability of providing bipolar pulses. The current generator is controlled either manually or by the PDP-11 computer. Monitoring circuits are provided to measure the applied voltage and current and with an output compatible with the PDP-11.

The most critical requirement for the current generator is that at no time shall the source of energy that provides the current come into contact with the earth at any place except the driving points. In this case, these points are the fracture well and the return well.

The design of the current generator requires that batteries be used for the voltage source. The batteries are connected to the drive wells through relays and the current pulse is initiated via the firing of a silicon

controlled rectifier (SCR). In order to provide the bipolar pulse, the SCR is turned off after the desired pulse width has been obtained, relays reverse the load connections and the SCR is fired again. Isolation amplifiers provide for the voltage and current monitoring. Interlock circuits provide a means of removing high voltages when access to the circuitry is required for maintainance or adjustments. Means of charging the batteries are also provided.

C. Data Control and Collection Subsystem

The instrumentation van contains power supplies for the PMB's, the data recording system and the current generator for creating the potential field. The data recording system performs the following functions:

a. Control the current generator during the periods when measurements are being made.

b. Demultiplex and measure the potentials present at all 24 locations simultaneously.

c. Measure the voltage and current levels produced by the current generator simultaneously with the potential measurements.

d. Store the above data on permanent records for post-test analysis.

e. Provide a hard copy output for quick look of test results.

The heart of the data recording system is a PDP 11/10 minicomputer. Peripherals included with the PDP 11/10 are a Lab Peripheral System (LPS11), a printer terminal (LA36), a mass storage disk (RK11), and a cassette tape unit (TA11). The PDP 11/10 operates under the RT11 operating system. All application programs have been written in BASIC. The other major component of the system are the 24 FM discriminators.

III. West Virginia Experiment

A. Introduction

On August 3 and 4, 1976, Sandia participated in a M.H.F. experiment with Columbia Gas in West Virginia. The M.H.F. experiment was a jointly funded ERDA/industry project with the Morgantown Energy Research Center being the technical project office. Sandia's participation was directed at evaluating its fracture characterization geophysical techniques in a variety of geological formations.

Only the electrical potential technique was utilized on this hydraulic fracture mapping experiment as the seismic techniques are continuing to be evaluated.

The surface array was installed and the new electrical potential system checked out during July with the experiment taking place in August. Future plans call for Columbia Gas to conduct two additional fractures in the same well at higher horizons. (Sandia participation to characterize these additional MHF tests will depend on no conflict in schedules and the availability of a down hole current probe to enhance the surface potential measurements). Electrical potential data was recorded, prior to, during and after the August fracture experiments.

B. Experiment Configuration

Figure 1 shows the layout of the fracture well (401), and the current return well (5420) and the potential probes. The site is located approximately 40 miles south of Huntington, West Virginia, or four miles west of Ranger, West Virginia. Potential probes were located at 500 and 3000 feet from the frac well every 15 degrees. This was our most tedious installation as can be seen from the topographic map; the terrain was extremely hilly.

Several roads had to be crossed for the installation and the site was occupied by several head of cattle; both caused problems with broken wires. Several potential lines had to be repaired during the experiment resulting in the loss of some of the data.

The exact locations as given to us by Columbia Gas for each well of interest is given below.

Well Number	Latitude	Longitude
20401	38°5'20"	82°13'35"
20403	38°5'56"	82°13'27"
5420	38°6'59"	82°12'29"

C. Fracture Design

The information presented in this section is intended to provide only a background description of the hydraulic fracturing process. Exact process details, data on the fracturing experiments and/or interpretation of the results

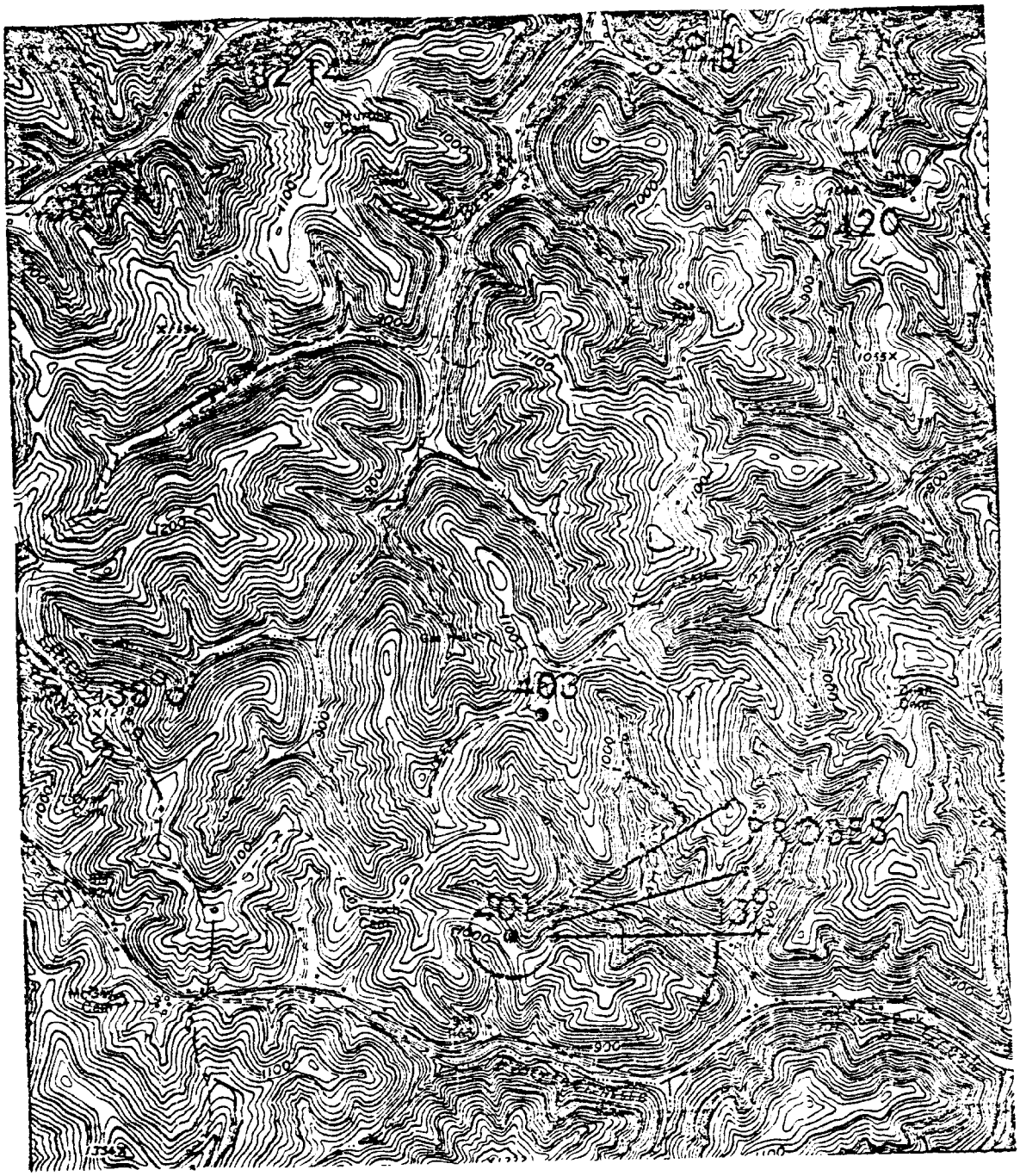

Scale 1 inch = 2000 feet

Figure 1. Columbia MHF Experiment Layout.

should be obtained directly from Columbia Gas or Halliburton.

A breakdown treatment was conducted prior to the main fracture using 1500 gallons of 15% HCl. Good ball action was reported and apparently all perforations accepted fluid.

On August 3, the main fracture treatment was started. Figure 2 shows the volume vs. time curve for that day. Fourteen perforations of 0.49 inches in diameter placed from 3788 to 3860 feet of depth had been shot into the Marcellus shale section. The casing was 5 1/2 inches with a total volume of 3800 gallons in the borehole. Two percent KCl had been added to all the fluid to increase its conductivity. The addition of nitrogen to the fracture fluid evidently resulted in a screenout prior to completing the pumping of all the fluid.

Ten additional perforations were shot from 3750 to 3760 feet of depth on the morning of August 4 and pumping resumed. The volume vs. time for this additional pumping is shown in Figure 3. For both days a total of 506,000 gallons and 930,000 pounds of proppant had been placed into the fracture well.

D. Fracture Characterization Results

Surface electrical potentials collected during the fracture are continuing to be analyzed and will be reported in complete detail in the data analysis report for the experiment. The potentials on all radials decreased during the entire pumping period on August 3. This result is

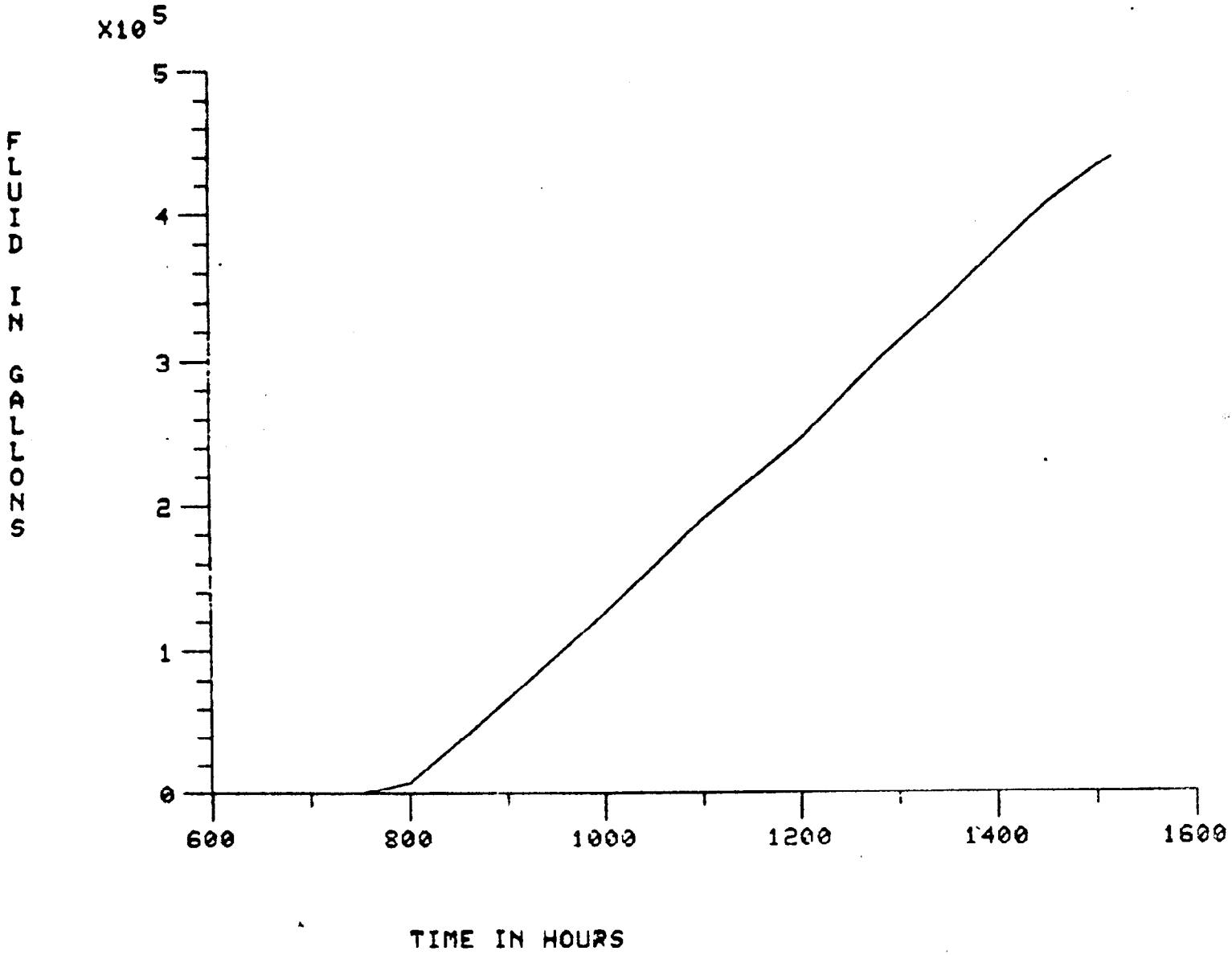

Figure 2. August 3 Fluid Volume

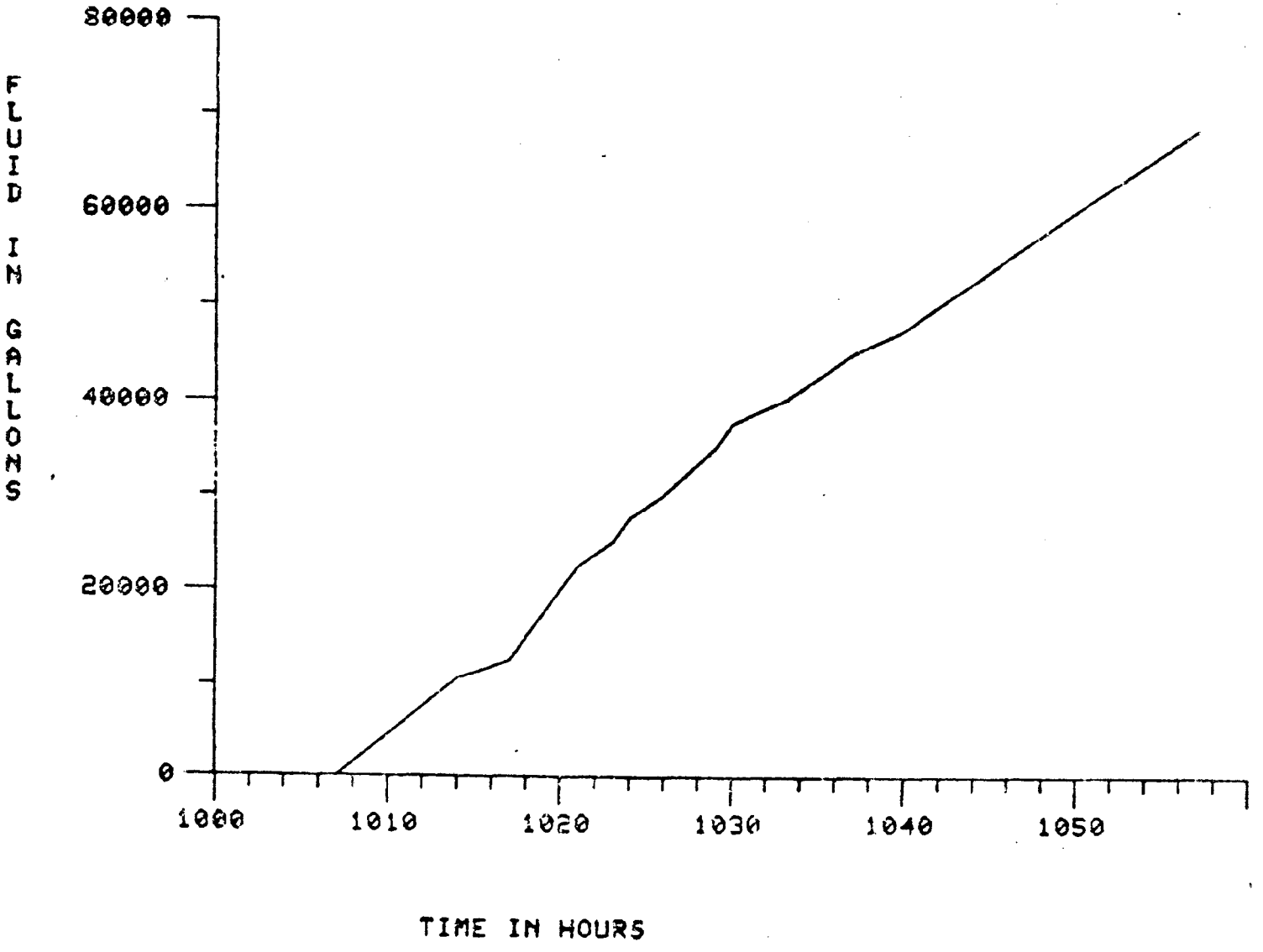

Figure 3. August 4 Fluid Volume

predicted by the theoretical model for a fracture that grows in total length.[1] A typical potential difference for one set of probes is plotted in Figure 4. The initial breakdown causes current to be diverted from the surface to the down hole load, this reducing the surface potentials. This effect continues during the entire time of pumping. Close to the end of pumping (1515) a screenout occurred which caused all the potentials to increase. This can be accounted for by assuming that the sand filled frac increased the resistance into the fracture and unloaded the well casing. This caused the current at the surface to increase. This increase returned the potentials to essentially the pre-frac potentials which effectively gives us a before-to-after comparison.

Plotted in Figure 5 is the potential change in percentage from before-to-after the screenout. As can be seen, the potential changes are about four to five percent on all radials without a clear cut indication of possible fracture orientation. It might be coincidental that the maximum changes are also associated with the radials with the largest absolute potentials. However, if the small differences are caused by the fracture, then the orientation

---

[1] L. C. Bartel, L. J. Keck, R. P. McCann, "Use of Potential Gradients in Massive Hydraulic Fracture Mapping and Characterization," presented at 51st Annual Fall Technical Conference and Exhibition of the Society of Petroleum Engineers of AIME, held in New Orleans, October 3-6, 1976.

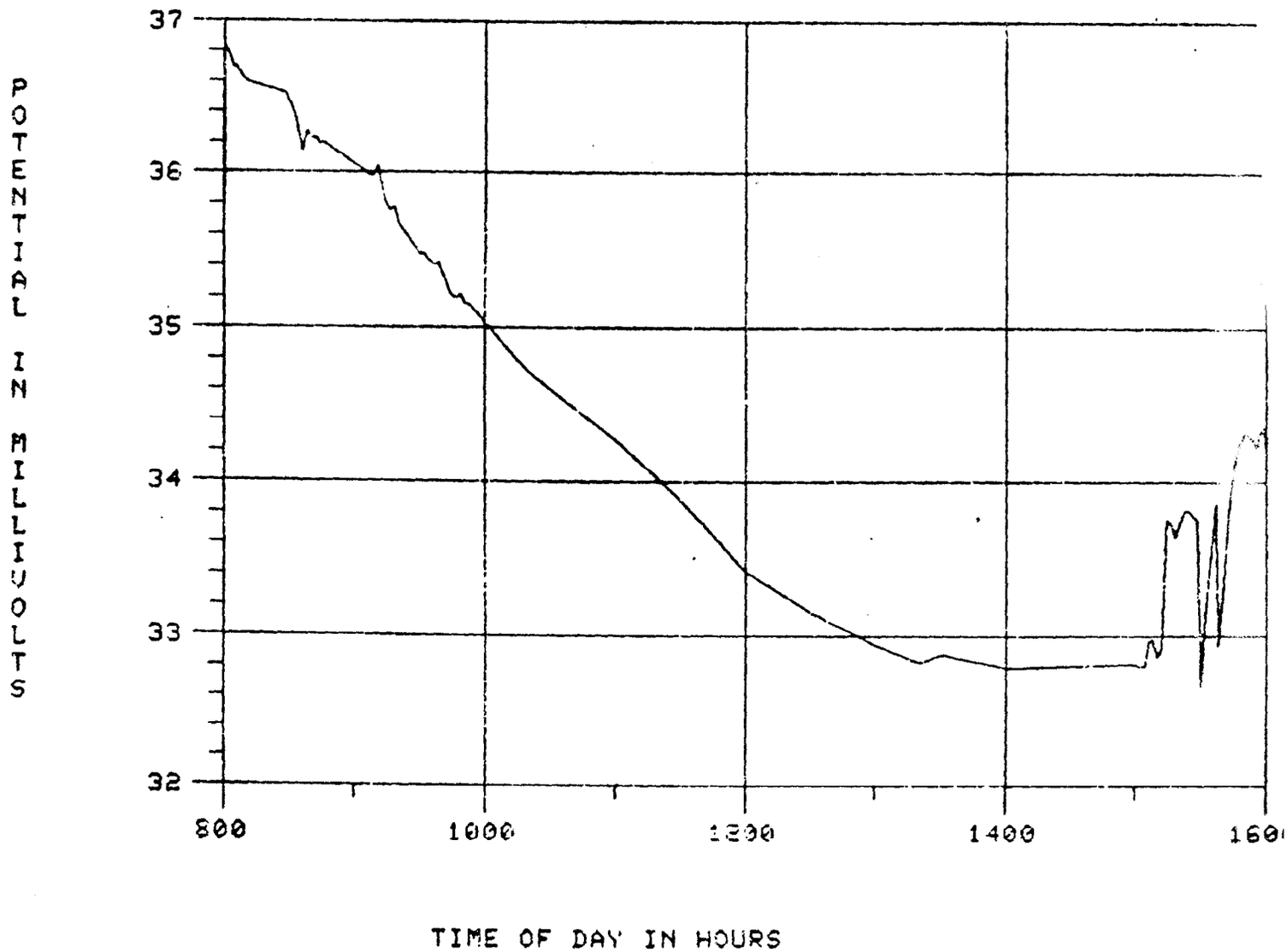

Figure 4. Potentials for Location A-3 on August 3

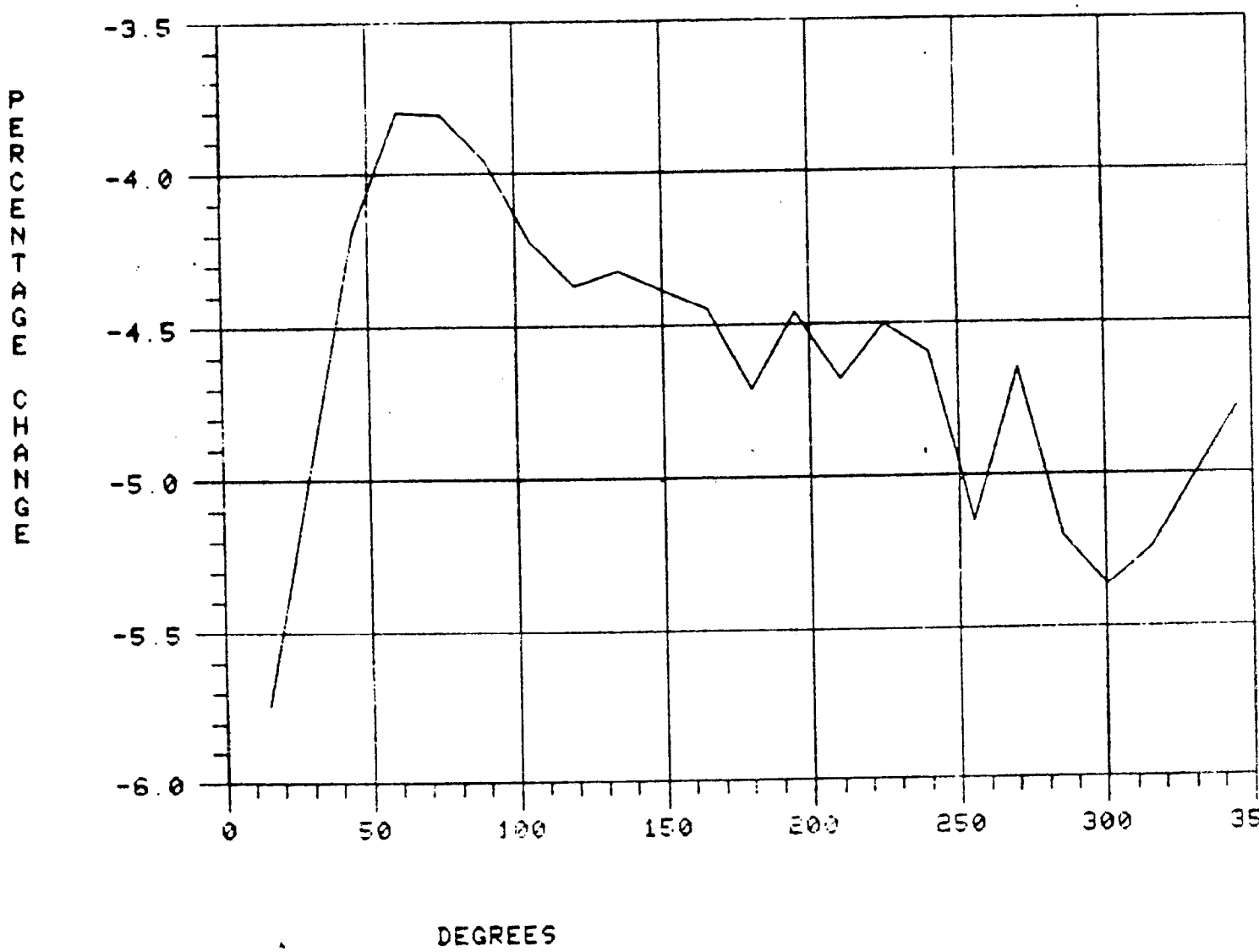

Figure 5. Potential Change During Screenout

would appear to be north-northwest to south-southeast with the longest direction being to the north-northwest.

The large amount of average reduction in all the potentials does not seem consistent with the lack of definitive orientation information. Several unrelated events could have resulted in this happening. Radials separation was increased to 2500 feet with the inner stake at 500 feet which caused a much higher range of potential values. This certainly improved the signal-to-noise ratio but could have masked the frac signal. Also because of the shallow frac depth and casing size restrictions, a down hole current probe was not utilized. If possible future testing should use the down hole current probe to reduce the surface potentials and enhance the signal caused by the frac fluid. Another possible conclusion could be that the fracture was not a long-line source but some other geometry that would appear more like a point source from the surface.

IV. Wattenberg Seismic and Pressure Data Analysis

A. Seismic Data - During this quarter, significant effort was applied to the Wattenberg seismic data. Twe seismic stations were selected for digitizing by data reductions and were sampled at 250 Hz for the ten ho operation. This data was then formated to allow c tional work to be done in the 6600 computer. Ini the data has been divided into six frequency ba

digitized band-pass filtering and then the cross correlations and time difference routines were used. The higher digitizing rate and the increased data has literally swamped the 6600 and some rewriting and stream lining of the routines are currently underway. Hopefully this effort will be completed soon and the surface seismic evaluations can be completed.

B. Pressure Data - The pressure data from the UPRR-22 experiment has been completed and distributed to AMOCO. Hopefully this pressure data was going to reveal some interesting fluctuations that would enhance the seismic data reductions but apparently if they existed they weren't transmitted to the surface. This data was recorded on the surface in a string of tubing that contained the down hole current probe with a frequency response capability of 0 to 2000 Hertz and a range of 0 to 10,000 psi. As there was no flow through this tubing, this pressure plus a static head should accurately reflect the down hole pressure. Figures 6, 7 and 8 show the pressure build up, a typical plot during pumping and shut down. The entire pressure record contains 155 pages and will not be distributed except to AMOCO.

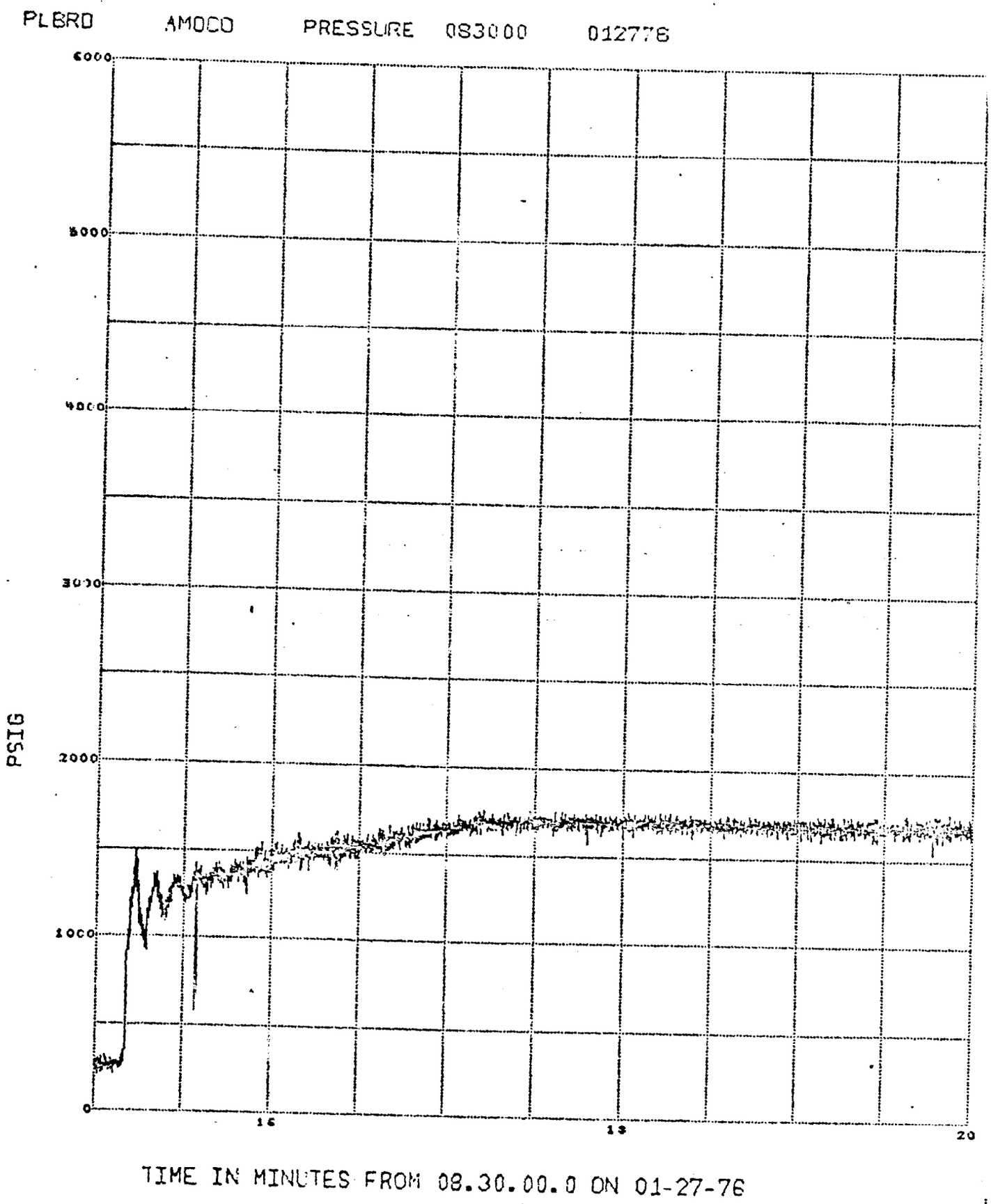
PLBRD AMOCO PRESSURE 083000 012776
6000
5000
4000
3000
2000
1000
0
PSIG
16
18
20
TIME IN MINUTES FROM 08.30.00.0 ON 01-27-76

Figure 6

UGR File #C073/77Q4
Aug. 1976-Oct. 1976
Sandia Laboratories

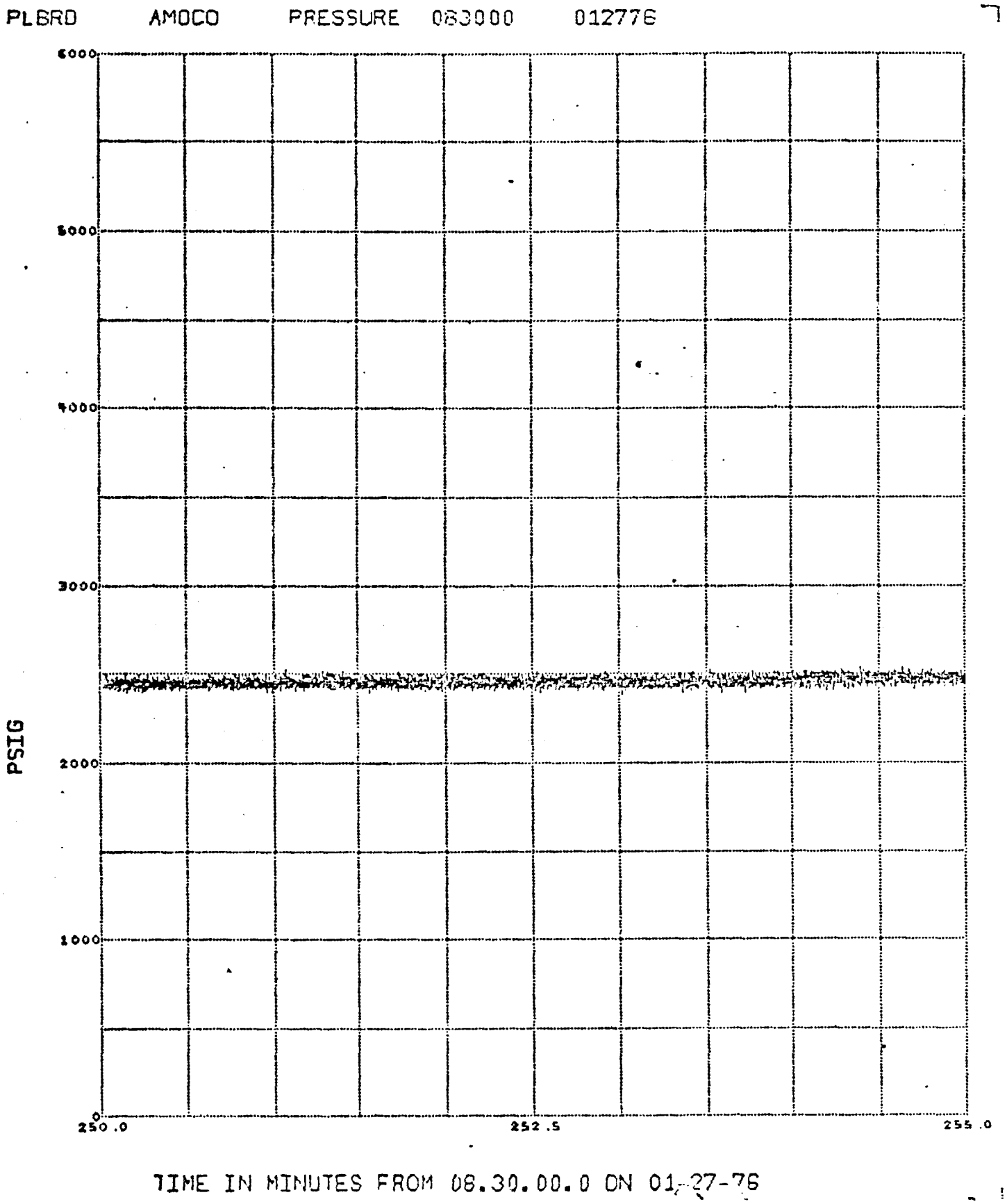

Figure 7

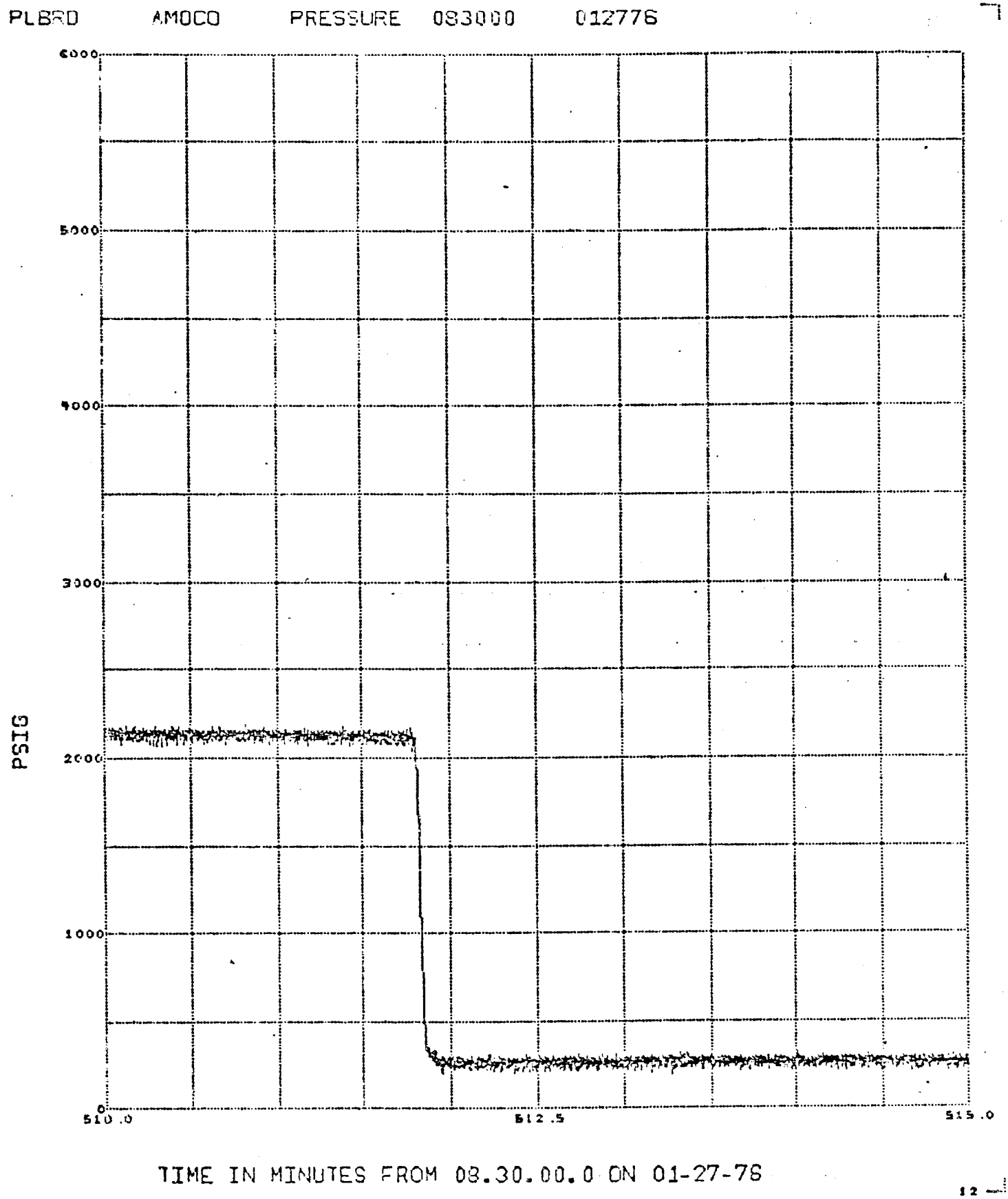
PLBRD AMOCO PRESSURE 083000 012776
6000
5000
4000
3000
2000
1000
0
PSIG
510.0
512.5
515.0
TIME IN MINUTES FROM 08.30.00.0 ON 01-27-78
12

Figure 8

V. Joint AMOCO/ERDA Experiments

A small scale, shallow hydrofrac experiment with AMOCO was planned during October at a meeting attended by Sandia, USGS, ERDA and AMOCO. Plans call for Sandia to install the electrical potential system, USGS to install the tiltmeter array and Sandia will collect their data with the PDP-11 and AMOCO will use their down hole television and televiewer for evaluating the fracture.

Primary goal of the experiment is to allow the various electrical and displacement models to be calibrated and compared with each other. AMOCO plans to drill an offset hole to intercept the fracture and confirm its orientation.

Preliminary discussions were also held regarding a test series for the Wattenberg area. The Sussex formation is going to be in-drilled and the opportunity to monitor several M.H.F. experiments is available. The formation is 4000 feet deep and would be completed with open holes to facilitate both down hole current probes and viewing of the fracture. Planning should be completed during the ensuing quarter.

DISTRIBUTION:

Charles H. Atkinson
Bartlesville Energy Research Center
U. S. ERDA
Bartlesville, Oklahoma 74003

J. S. Ball
Bartlesville Energy Research Center
U. S. ERDA
Bartlesville, Oklahoma 74003

Dr. Robert Brownlee
Los Alamos Scientific Laboratory
G-Division
Los Alamos, New Mexico

Alex Crawley (10)
U. S. ERDA Fossil Energy
20 Massachusetts Avenue NW
Washington, DC 20545

Dr. William G. Davey
Los Alamos Scientific Laboratory
Q-Division, Mail Stop 570
Los Alamos, New Mexico

C. R. Fast
Amoco Production Company
P. O. Box 591
Tulsa, Oklahoma 74102

Hugh Guthrie, Director
Division of Oil, Gas and Shale Technology
U. S. ERDA Fossil Energy
20 Massachusetts Avenue NW
Washington, DC 20545

Dr. J. D. Ham
Assistant Division Director for Petroleum and Natural Gas
U. S. ERDA Fossil Energy
20 Massachusetts Avenue NW
Washington, DC 20545

Dr. Merle Hanson
Lawrence Livermore Laboratory
Livermore, California 94550

D. K. Nowlin
Special Programs Division
U. S. ERDA
Albuquerque, New Mexico 87115

A. A. Pitrolo, Director
Morgantown Energy Research Center
U. S. ERDA
Morgantown, West Virginia 26505

E. J. Ranostaj
Columbia Gas System Service Corp.
1600 Dublin Road
Columbus, Ohio 43215

Don C. Ward
U. S. ERDA
20 Massachusetts Avenue NW
Washington, DC 20545

A. B. Waters
Halliburton Services Inc.
Research Center
Duncan, Oklahoma 73533

Dr. Phil White
U. S. ERDA
20 Massachusetts Avenue NW
Washington, DC 20545

1 Morgan Sparks
1100 C. D. Broyles
1110 J. D. Kennedy
1120 G. E. Hansche
1130 H. E. Viney
5000 A. Narath
5100 J. D. Galt
5160 W. Herrmann
5163 D. E. Munson
5200 E. H. Beckner
5400 A. W. Snyder
5700 J. H. Scott
5710 G. E. Brandvold
5730 H. M. Stoller
5731 R. K. Traeger
5732 D. A. Northrop
5733 C. L. Schuster (25)
5734 A. L. Stevens
5735 M. M. Newsom
5736 A. F. Veneruso

5740 V. L. Dugan
5800 R. S. Claassen
8266 E. A. Aas (2)
9420 T. L. Pace
9422 J. L. Rogers
3141 C. A. Pepmueller (5)
3151 W. L. Garner (3)
for ERDA/TIC (25)
Attn: R. P. Campbell - 3171-1

UGR File #C073/7704
Aug. 1976-Oct. 1976
Sandia Laboratories

Sandia Laboratories
Albuquerque, New Mexico 87115

RS 4733/003

ENCHANCED GAS RECOVERY PROGRAM

MONTHLY INFORMATION LETTER - March, 1980

I. EGR Instrumentation and Diagnostic Program

A. Hydraulic Fracture Characterization

The data obtained in conjunction with the Shell Oil Company's experiment in their Big Mineral Creek field is continuing to be analyzed. The analysis has been complicated by the shortness of the fracture and the large seismic background levels. The pressure and flow data has been analyzed for comparisons with both the tiltmeter and electrical potential data.

The main fracture pump began at 11:13 a.m. and continued through 12:36. Flow rates ranged from 11 to 16 barrels per minute through 12:09 p.m. At 12:09, the average pumping pressure of approximately 3,600 psi began to increase to a maximum value of 4,150 psi while flow rates decreased to a value averaging 4 barrels per minute. The pump was terminated at 12:37 p.m. when the sand had apparently begun to cover the casing perferation. Sandia's current injection probe required several hundred pounds of extra force to break free from the sand even though it was located approximately 100 ft above the perferation.

The seismic signals that occurred during the breakdown pumping from Well 343 have been given a preliminary scan. A large number of seismic signals were recorded and a much closer examination of this data is necessary to gain a confident conclusion as to the fracture orientation.

All seismic signals from the test have been digitized but examination of these signals has not been possible due to equipment malfunction and hardware preparation for a future test.

The next planned mapping test is a breakdown test on Amoco's Patricia Pope Whaley Gas Unit #1 in the Cotton Valley area near Marshal, Texas and is scheduled to take place on April 19, 1980. Further reduction in data will resume after this test.

B. Borehole Resistivity System

The numerical solution to the forward layered one-dimensional borehole resistivity problem was programmed and compared with the continuous solution. The figure shows a comparison of the

Figure I-1

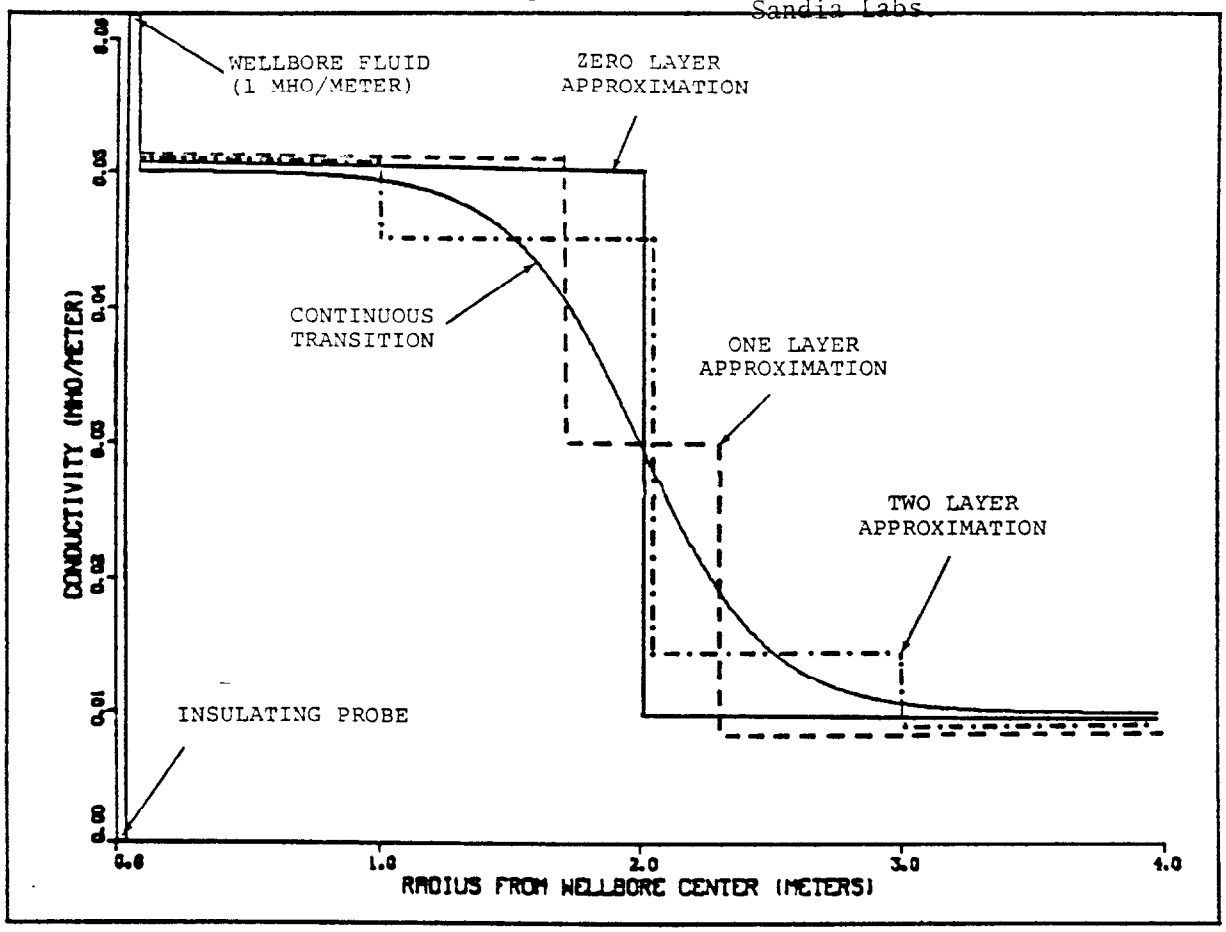
WELLBORE FLUID
(1 MHO/METER)
ZERO LAYER
APPROXIMATION
CONTINUOUS
TRANSITION
ONE LAYER
APPROXIMATION
TWO LAYER
APPROXIMATION
INSULATING PROBE
CONDUCTIVITY (MHO/METER)
0.00
0.01
0.02
0.03
0.04
0.05
0.0
1.0
2.0
3.0
4.0
RADIUS FROM WELLBORE CENTER (METERS)

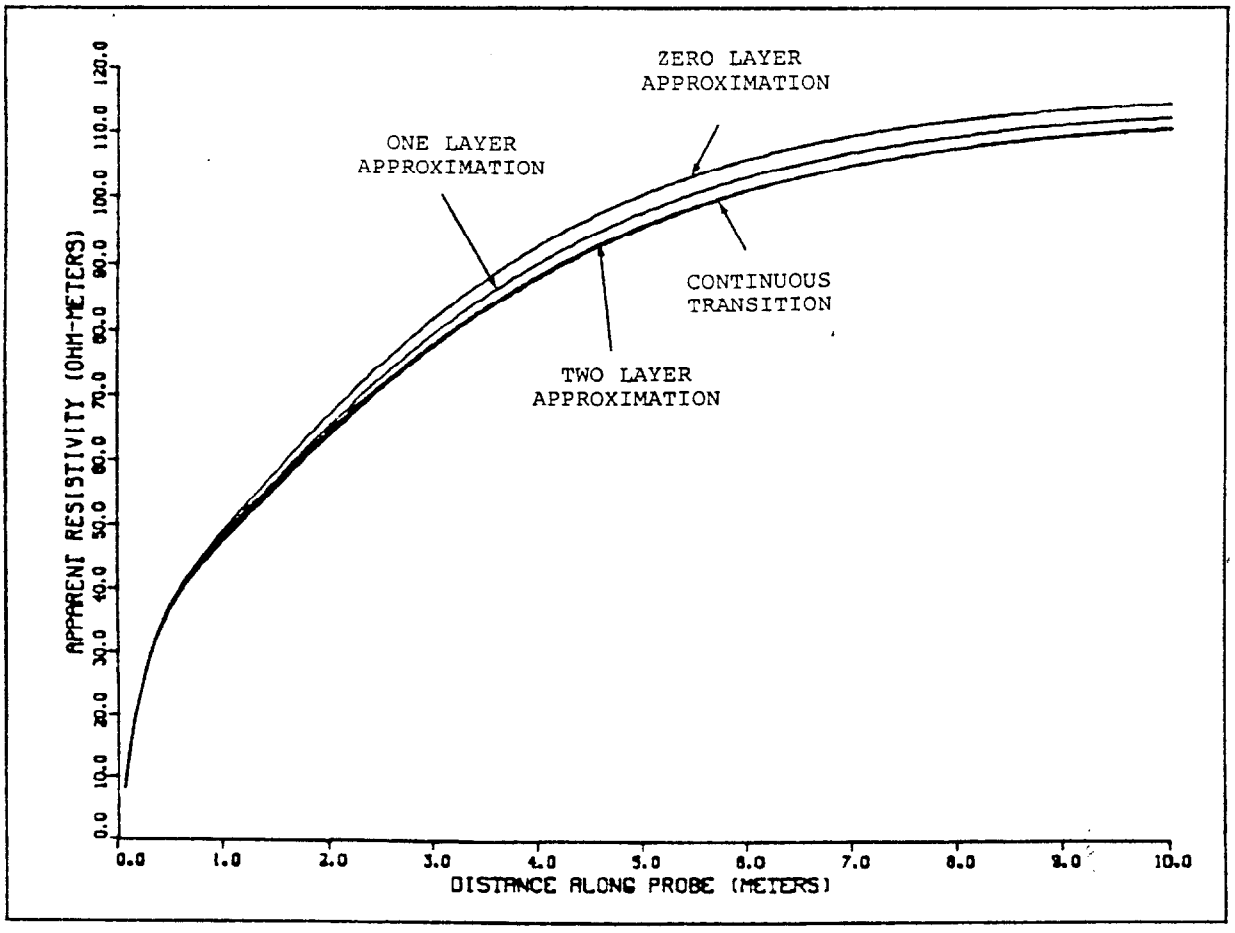
ZERO LAYER
APPROXIMATION
ONE LAYER
APPROXIMATION
CONTINUOUS
TRANSITION
TWO LAYER
APPROXIMATION
APPARENT RESISTIVITY (OHM-METERS)
0.0
10.0
20.0
30.0
40.0
50.0
60.0
70.0
80.0
90.0
100.0
110.0
120.0
0.0
1.0
2.0
3.0
4.0
5.0
6.0
7.0
8.0
9.0
10.0
DISTANCE ALONG PROBE (METERS)

continuous solution with three-layered approximations. The continuous profile is presumed to represent a 3-in-diameter probe emersed in a fluid filled 6-in-diameter wellbore, surrounded by an invaded zone with a hyperbolic tangent type transition to the virgin formation. The apparent resistivity as a function of position along the surface of the probe is given. The two-layer and continuous solutions agree closely but the one- and zero-layer approximations show visually recognizable discrepancies (note that optimization of layer locations has not been attempted). This comparison gives an indication of the resolution obtaining the location of invasion front with typical field measurement accuracies.

C. Electromagnetic Impedance Sonde DE-AT19-79BC10026

(1) Dielectric Modeling

In our previous monthly report we mentioned that our current directions were toward determining water saturations from dielectric measurements. This month computer programs have been developed that augment this task.

At higher frequencies (10^6 - 10^9 Hz) the dielectric response of rocks is particularly sensitive to the water saturation, S_w; the location of the water if S_w <100%; and the pore geometry. To define all of these parameters requires good fits between our model responses and the experimental data for both the real and imaginary components of the current. Past fitting techniques were unsatisfactory since the form of the distribution function, A(k), did not allow for rapid changes in the dielectric response with frequency. The new fitting technique eliminates this problem.

Presently distribution functions based on the data of Poley, et al are being used to generate responses for S_w <100%. Next month's effort will be to understand the significance of these responses.

(2) Laboratory Work

A thorough study of the dielectric properties of rocks must determine the relationship, if present, between rock characteristics such as porosity, permeability, and pore geometry and these properties. The work of Poley, Nooteboom, and de Waal (The Log Analyst, May-June, 1978, p. 8) measured the dielectric properties of "nearly clay-free" sandstones as a function of rock porosity and saturating water salinity. This and other studies are complicated by the unknown effect of impurities such as clays. Therefore, we are investigating the use of a known matrix of materials to simulate the pore geometry of rocks.

For this purpose a useful arrangement would be that of packed glass spheres. A selection of spheres in the diameter range from 38 microns to 1.4 mm has been ordered. Once these are received a program will be initiated with the Sandia ceramics laboratory to prepare sintered samples of different porosities and permeabilities. The possibility of reproducibly producing a sample of given characteristics will be investigated.

(3) Finite-Difference Modeling

A computer code is under development to mathematically model the response of a horizontally and vertically layered earth to a magnetic induction logging tool. Horizontal layers are formed by the geologic structure. Vertical layers are formed by the borehole fluid and by its invasion into the surrounding structure. Understanding the response of the layered earth is expected to aid in determining the permeability of tight-gas-sand reservoirs of natural gas.

The source is assumed to be a point magnetic dipole radiating at constant frequency (or at a set of frequencies) in an azimuthally symmetric, layered earth. The differential equation describing the complex-valued electric field intensity is a second-order equation of the elliptic type. A unique solution exists in a bounded region of space if boundary conditions are available at the edges of the space. These boundary conditions provide the major difficulty in finding a general finite-difference solution to the equation. Once the electric field intensity is found, the magnetic fields can be calculated by differentiation. With all the electromagnetic fields available, receiver response can be obtained. Sensitivity studies are then possible to determine response variation with conductivity and dielectric constant of the various layers of earth.

In a cylindrical (r,z) coordinate system centered on a dipole in a uniform medium, the electric field intensity depends on the factor $f/(z^2+r^2)$. In order to allow larger spatial step sizes (Δz and Δr), we transform to the variable $S \equiv E(z^2+r^2)/r$ to remove a portion of the rapid variation near the source. Along the $r = 0$ axis of symmetry, the Neumann boundary condition $\partial S/\partial r = 0$ is convenient to apply. In the immediate vicinity of the source S is assumed to be identical to that for the same source in a uniform medium. This assumes the outer boundaries and the layering cause only minor perturbations on the electric field intensity very close to the source. At the $z = z_{max}$, $z = z_{min}$, and $r = r_{max}$ boundaries, realistic boundary conditions are not readily available. This is the dominant difficulty encountered. Boundary conditions are necessary to assure uniqueness of the solution inside.

It is expected that Neumann boundary conditions (where normal derivatives are specified) will be easier to apply than Dirichlet conditions (where the electric field is specified) at the outer boundaries.

In an infinite space the fields are zero at infinite distance. The far-boundary conditions are then trivial. Computer memories are not sufficiently large to handle finite-difference solutions out to very large distances from the source. If the medium were uniform, the direction of the waves would be clear at boundary points and outgoing wave equations would be an appropriate analytical form at these boundaries. When layering occurs, reflections form a series of virtual sources greatly complicating the form of any outgoing wave representation. Further experimentation is required to treat the outer boundaries in a reasonable manner. If analytical solutions are available for separate problems of horizontal and vertical layering, perhaps these solutions can be used to approximate the partial derivatives of S at the outer boundary.

Attempts are in progress to solve the differential equation using successive overrelaxation methods. These approaches use a relaxation parameter (between 0 and 2) to regulate the size of the steps taken to lead the solution to convergence. Theory indicates that the converged result is not affected by choice of this parameter. Numerical experiments with a uniform medium (where an analytic result is available), with correct values of S at the boundaries, and with an initial guess of (0,0) for the real and imaginary parts of S everywhere in the mesh indicate the solution converges to the correct result for relaxation parameters in the range 1 to 1.5. It is also encouraging that an initial guess of the correct value was recognized as correct; successive iterations did not wander from the solution. The spatial mesh size chosen was $\Delta r = \Delta z = 0.01$ m. Spatial mesh sizes $\Delta r = \Delta z = 0.06$ m never produced convergence. In addition, relaxation parameters 1.75 and larger appear to never lead to convergence.

There are methods for choosing the optimum relaxation parameter, as discussed by E. L. Wachspress in Iterative Solution of Elliptic Systems, Prentice-Hall, Inc., 1966. There may also be ways of isolating the outer boundary conditions from the solution inside (perhaps by a series of artificial layers of earth with gradually increasing conductivity). These approaches are now being investigated.

(4) Probe and Formation Modeling

The effectiveness of electromagnetic (EM) logging is enhanced by the availability of ancillary relations that accurately express EM parameters in terms of formation parameters.

One pair of such relations has been empirically formulated for 20 to 80 MHz logging based on the published data by Poley, et al. Sandstones of various porosity saturated by water of different salinity are characterized as parametric equations to determine the sensitivity range of EM probe. As it stands, the parametric charts for borehole-coil couplings are able to delineate specific response regions for gas/oil saturated sandstones or limestones. With partial saturations, no ancillary relations are available. However, the loci of sandstones with various porosity and saturating water of various salinity have now become available on the refractive-index charts specifically constructed for coil responses.

Borehole effects due to changes in borehole size, shape, and fluid have a large number of combinational possibilities. Systematic studies have been started from the worst-case scenario; i.e., the borehole is assumed to be flooded by fluid of salinity equal to that of sea water. Coils are first assumed to be emersed in this borehole fluid. Data on 20, 40, and 80 MHz operations have indicated clear trend of larger borehole effects toward higher logging frequencies. More realistic simulations on borehole effects are scheduled for next month. Both analytical and numerical evaluations become rapidly more complex as the number of borehole zones arè increased. A three-zone borehole with variable parametric changes is anticipated as the optimal compromise between the desire to know and the ability to quesstimate realistic parameters.

II. Stilumlation Research for Enhanced Gas Recovery

A. Hydraulic Fracturing

Sandia Laboratories is conducting both basic and applied research to aid in the development of massive hydraulic fracturing as a practical, economic technique for exploiting the resources of the tight gas sands and Devonian shales. Types of research being performed include in situ testing of hydraulic fracturing theory and technology, modeling of hydraulic fracturing behavior, and laboratory testing. The in situ testing is being performed at DOE's Nevada Test Site in a tunnel complex driven through volcanic ash-fall tuff under ~1,400 ft of overburden. This site provides the facilities and equipment for mineback of created hydraulic fractures for direct observation, a capability of determining in situ stresses and obtaining rock samples for testing in regions of interest, and a direct knowledge of the "reservoir" parameters and structure (i.e., permeability, porosity, location of faults, fractures, etc.). Modeling efforts involve many aspects of fracturing, from details of the processes occurring at the fracture tip to numerical codes describing the fluid mechanics/rock mechanics of the entire fracture. Laboratory testing includes the determination of rock properties and the conducting of small scale experiments.

(1) Formation Interface Fracture Experiment

The Formation Interface Fracture Experiment (Hole #6) is an experiment to determine the parameters that influence and control containment of hydraulic fractures. Grout filled fractures were propagated above and below a welded tuff/ash-fall tuff interface and subsequently mined back to examine the behavior of the fractures at the interface. It was found that the fracture that was initiated in the low modulus ash-fall tuff propagated through the interface into the high modulus welded tuff. This suggests that present rock mechanics models, which predict that a bounding higher modulus material will contain a hydraulic fracture, are in error.

An exploratory coring program is currently underway to determine the general shape of the fractures. This shape should reflect the influence of the interface and the in situ stresses on overall fracture propagation and behavior. A total of 31 coreholes have been completed including EV6-34, EV6-35, and EV6-36 in March. The locations of these holes are shown in Figure II-1. this completes the coring program, and we will attempt to use this data to plot fracture width contours. The final work to be performed on this experiment will be several minifracs in two or three of these coreholes in order to determine the in situ stresses in relation to crack growth.

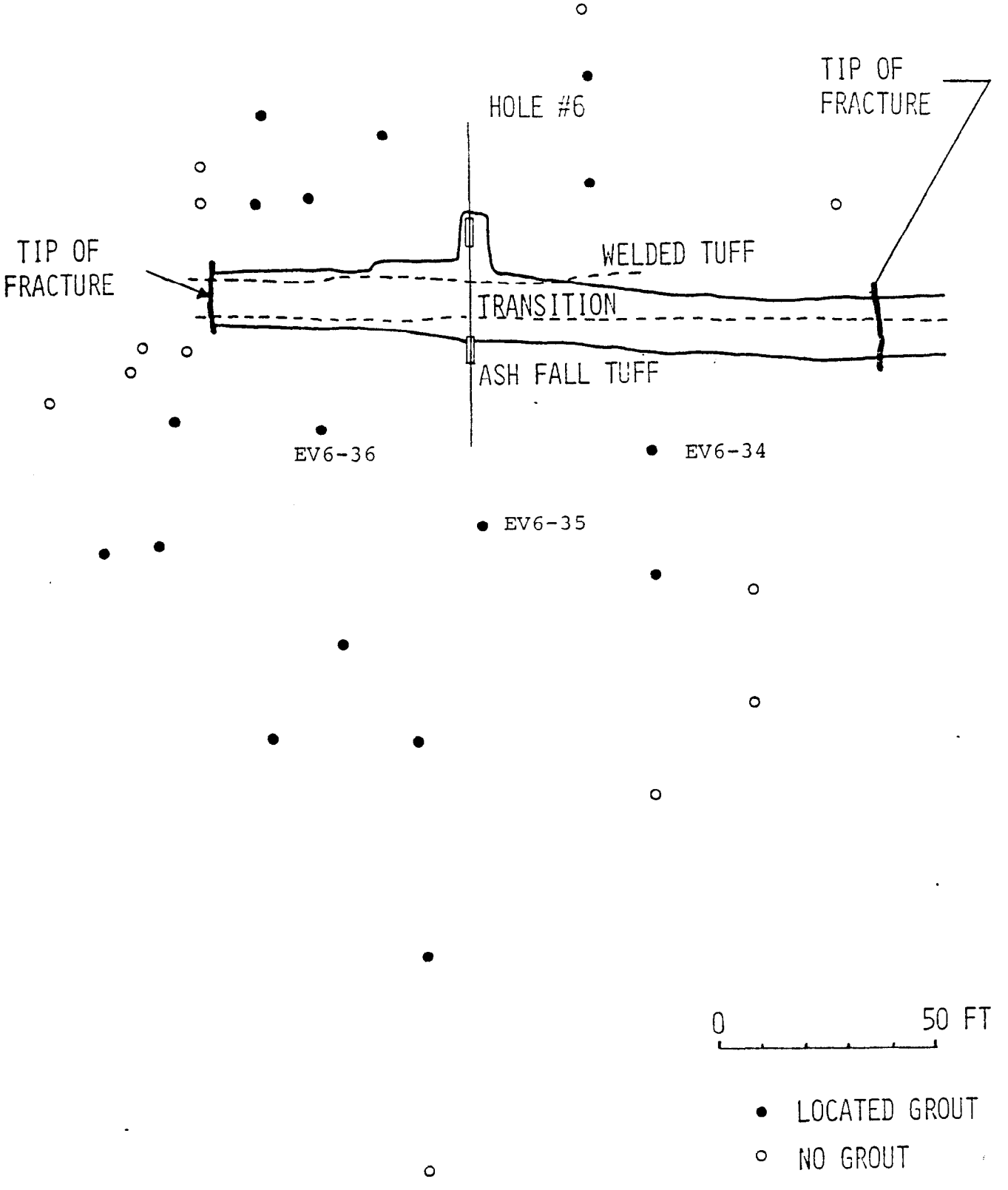

Figure II-1. Exploratory Croing Results of Hole #6 Fractures

(2) Interface Test Series

Work on this activity has been completed.

(3) Fluid Mechanics/Proppant Transport Experiments

The process of hydraulic fracture is recognized to be a complex interaction between rock mechanics and fluid mechanics considerations. In general, however, the fluid mechanics aspects of fracturing are much less understood than the global rock mechanics considerations such as dilation of the crack under a pressure load. The important fluid mechanics processes associated with fracturing can be broadly divided into two categories. The first is basic phenomena, such as the pressure distribution and the width in a propagating fracture. Experiments to measure the pressure and width at various locations in a fracture during propagation are presently being planned. The second area is proppant transport and the resultant conductivity. An in-tunnel pump system is under construction which will pump high viscosity gels with sand concentrations up to 3 lb per gallon. A site for these experiments is presently being prepared, and these tests should begin this year.

(4) In Situ Stress Measurement by Hydraulic Fracturing Through Performations

Mineback Experiments have shown that the most important factor governing containment of hydraulic fractures is differences in the minimum principal in situ stress. Material property differences and interface characteristics (friction) appear to be insignificant. In the Multi-Well Experiment in the Piceance Basin, the distribution of minimum in situ stress will be measured through the Mesaverde Sequence. A large number of in situ stress measurements will be obtained by conducting minifracs through perforations.

In order to be certain that performing these tests through perforations will yield accurate, reliable data, an experiment will be conducted in G-tunnel to compare fracturing through perforations and in an open hole. Approximately five zones in a cased, horizontal borehole will be fractured with a small volume (<10 gal) of dyed water through perforations oriented at different directions to the in situ stress and the important pressure data will be recorded. Afterwards, another hole will be drilled 6-8 ft from and the cased hole, and five comparable zones will be fractured open hole. Differences in the instantaneous shut in pressure (if any) will be compared with dissimilarities in fracture behavior observed during mineback. At present it is not expected that there will be any significant difference, however, the damaged zone due to perforating may result in anomalous fracture behavior near the wellbore and a higher observed closure stress or shut in pressure.

(5) Rock Mechanics

(a) Finite element analyses were done to evaluate the stress distributions resulting from various laboratory experiments for hydraulic fracture propagation in layered media. Whenever an overburden pressure is applied to layered samples with differing strenghts, the horizontal stress state is quite variable with marked contrasts in stress occurring across the boundaries. For example, if a "soft" rock ($E = 4.5 \times 10^6$ psi) is sandwiched between "hard" rocks ($E = 9 \times 10^6$ psi), the horizontal stress in the center of the soft rock will be compressional (16% of overburden pressure) whereas a tensional horizontal stress (13% of overburden pressure) will occur in the hard rock. The stress across the interface will change by a total of 30% of the overburden pressure. If the applied stress is hydrostatic, the horizontal stress of the soft rock is compressional (84% of hydrostatic pressure) with even greater compression in the hard rock (110% of hydrostatic pressure). Since in situ stresses are important in controlling fracture propagation, the results from the apparently simple experiments described above may be difficult to interpret if the in situ stresses are not considered.

(b) In situ stress measurements by an overcoring technique have been made in G tunnel, at NTS, to determine the influence of in situ and residual stresses on the containment of hydraulic fractures. Nine sites were instrumented with delta strain rosettes (three sites on three separate bedding horizons which were 0.28 meters apart) on the central portion of a tunnel wall within one meter of an exposed mined-back hydraulic fracture from the Interface Test Series. All of the sites were in a single bed of ash fall tuff. The lowest bedding horizon which was instrumented corresponded to the horizon in which the hydraulic fracture abruptly terminated. After overcoring, eight of the nine gages were still operational.

Preliminary analysis of the data indicates a significant and consistent increase in the minimum principal strain, ε_3, from 80 $\mu\varepsilon$ tension at the upper horizon, to 140 $\mu\varepsilon$ compression at the middle horizon, to 980 $\mu\varepsilon$ compression at the lower horizon. In all cases, ε_3 was essentialy normal to the plane of the hydraulic fracture. The maximum principal strain showed no significant variation between the three horizons, with an average strain of 2650 $\mu\varepsilon$ compression. Stress calculations from these measured strains will be made once the elastic properties of each core are determined from laboratory compression tests. The results suggest a strong correlation between the large compressive increase in ε_3 and the termination of the hydraulic fracture. Additional work will involve residual stress measurements on each of the cores.

(6) Fluid Mechanics

No March results are reported for this activity.

B. Dynamic Wellbore Fracturing

Dynamic stimulation techniques that produce multiple fracturing in a wellbore are being investigated for enhanced gas recovery. Multiple fracturing appears to be especially promising for stimulating naturally-fractured reservoirs, such as the Devonian shales, since this may be the most effective technique for connecting a wellbore to a pre-existing fracture network. The emphasis in this research study is on tailored-pulse loading techniques that minimize wellbore damage and maximize fracture growth by gas penetration. The focus in this program includes in situ testing at the Nevada Test Site and associated modeling and analysis.

(1) Multi Frac Test Series

All test holes were fished and cleaned out for post-test evaluations. Television logs, caliper logs, and permeability measurements were conducted on each hole.

The post-test evaluations of in situ permeability were made in a manner similar to the pre-test measurements previously discussed. Each test zone was pressurized with dyed water to a constant pressure of 400 psi while recording the decay of flow with time. The pressure decay after shut-in is also recorded. When reduced and analyzed, these data provide two independent values for permeability. The average values, pre-test and post-test, are listed in Table II-1 along with qualitative observations made from the TV logs. Of course, the mineback will provide more direct evidence of fracture extent. A large permeability enhancement is seen for Experiment E which is a clear indication of extensive fracturing. Experiments B, C, and D display a moderate increase in permeability. Experiment A, however, produced a decrease in formation permeability. This is apparently due to the creation of a stress cage even though the explosive was "decoupled" from the formation by an 8 to 1 ratio of hole diameter to charge diameter.

These observations are consistent with the TV log observations. The apparently enlarged borehole for Experiment A was confirmed by the caliper log which showed a 15-35 percent increase in borehole diameter. The other caliper logs showed little alteration of the boreholes except for Experiment E. The caliper record for this hole showed significant fluctuations caused by fractures and misoriented blocks, but overall the hole was not enlarged.

An enlightening comparison can also be made among the three previous Gas Frac shots* and Experiment E. Pressure-time characteristics and observed fracture behavior are compared

*N. R. Warpinski, et al., High Energy Gas Frac," SAND78-2342, December 1978.

TABLE II-1

PERMEABILITY ENHANCEMENT

CASE	TAILORED-PULSE CONCEPT	PRE-TEST PERMEABILITY (md)	POST-TEST PERMEABILITY (md)	FACTOR OF INCREASE	OBSERVATIONS FROM TV LOG
A	DECOUPLED EXPLOSIVE WITH WATER PAD	0.20	0.05	0.25	ENLARGED, DISTORTED BOREHOLE
B	DECOUPLED EXPLOSIVE* WITH PROPELLANT PUSHER (WATER PAD)	0.83	5.6	7	NO FRACTURES APPARENT
C	SMALL DIAMETER PROPELLANT WITH PRESSURIZED WATER PAD	0.0015	0.008**	5**	MULTIPLE FRACTURES (VERY NARROW)
D	THREE SHOTS OF CASE C WITH PRESSURIZED WATER PAD	0.007	0.034	5	MULTIPLE FRACTURES (NARROW)
E	FULL BORE, PROGRESSIVELY-BURNING PROPELLANT WITH AIR PAD	0.014	25.0	1800	MULTIPLE FRACTURES (WIDE)

*EXPLOSIVE DID NOT DETONATE

**SOME PERMEABILITY INCREASE MAY BE DUE TO FRACTURE CAUSED BY EXPERIMENT E

UGR File #C075/SC-5
March 1980
Sandia Labs.

in Table II-2. Note that a good correlation between pressure rate and resulting behavior exists while no such correlation occurs with peak pressure. This indicates that pressure rate may be the governing parameter in determining whether resulting behavior is hydraulic fracturing, multiple fracturing, or explosive compaction. A closed-form analysis was performed that indicates the pressure rates in GF2 and Experiment E were low enough such that tangential stress at the borehole wall begins and remains tensile. On the other hand, the pressure rate of GF3 was sufficiently high to cause tangential compression initially. These initial compressions probably delay the tensile failure until after the compaction process has begun causing the bladder effect. This suggests a multiple fracture criterion that is based on a pressure rate being less than a value that would produce tangential compressive stress at the borehole wall. This criterion was previously suggested by Bligh as a means to avoid explosive compaction.

Mineback was completed in March through Experiments E, C, and D. Experiment E produced both radial and circumferential fractures around the borehole. Two of the raidal fractures extend more than 20 ft from the borehole. The maximum extent of the circumferential fractures was ~1.5 ft from the center of the hole. Most of the radial fractures were propped with rock debris.

Experiments C and D also initiated radial fractures at the borehole, however, these fractures were tight except near the hole. A few fractures in Experiment D were found propped as much as 0.5 in approximately 6 in from the hole. Most of the fractures in C and D extend 1-3 feet from the borehole with one fracture extending a maximum of five feet from Experiment D.

Additional observational evidence will be available next month.

(2) Modeling and Analysis

No March results are reported for this activity.

C. Eastern Gas Shales Analysis

The EGSP data have not yet been received from METC.

D. Petrology and Geochemistry

The petrographic examination of samples of the Mesaverde sandstone from the Pacific Creek Federal 1-3 well (Sweetwater Co., Wyoming) is continuing. As was stated previously, thin sections of these samples will not be available due to a limited amount of sample. The core descriptions (provided by CER) noted that several intervals were visibly outgassing on extrusion from

TABLE II-2

PRESSURE LOADING CHARACTERISTICS VS. OBSERVED BEHAVIOR

	EXPERIMENT	PEAK PRESSURE (MPa)	PRESSURE RATE (kPa/μs)	RESULTING BEHAVIOR
PREVIOUS GAS FRAC TEST SERIES	GF1	43	0.6	HYDRAULIC FRACTURE
	GF2	95	140	MULTIPLE FRACTURES
	GF3	~200	>10,000	EXPLOSIVE STRESS CAGE
	EXPERIMENT E	250	430	MULTIPLE FRACTURES

the core barrel, and these intervals have been the primary focus of the current scanning electron microscope study.

The results obtained so far indicate that diagenetic effects (specifically, the formation of authigenic clays, feldspar, and quartz) are most evident in the "cleaner," coarser-grained sandstone. Conversely, only rarely were authigenic clays observed in the finer-grained silty/organic-rich layers. Although any interpretation is, at this point, highly speculative, this observation may relate directly to the question of in situ methane formation. It is well established that methane formation can occur through the anaerobic decomposition of organic material (e.g., $C_6H_{12}O_6 \rightarrow 3CO_2 + 3CH_4$). The low-Eh environment in which this occurs is reflected in the mineralogy of the sediment by the presence of pyrite (FES_2), siderite ($FeCO_3$), or other reduced-Fe species. The pH may vary depending on whether the environment is fresh, brackish, or seawater, and also on the composition (hence buffering capacity--for example, the presence or absence of carbonate) of the sediment.

The observation of mineral authigenesis in organic-free sandstone versus its absence in the organic-rich silty portion of the sand lenses examined so far suggest that possibly the stability fields of the commonly-observed authigenic minerals are not within the Eh-pH conditions under which methane forms.

Thus, the processes of methane formation and mineral authigenesis appear to be mutually incompatible. The significance of this observation is not immediately obvious at the moment; however, by continuing with detailed petrographic studies, the relationship between the disribution of organic matter and authigenic mineral formation may become part of a regional geochemical pattern.

E. Multi-Well Experiment

This experiment's objectives are (1) to obtain a comprehensive geologic characterization of a lenticular, low permeability reservoir in the Western United States and (2) to evaluate state-of-the-art and developing technology for the recovery of gas from these reservoirs.

A meeting with the MWX Technical Review Panel was held in CER Corporation offices on March 25 and 26, 1980. Representatives from DOE, BETC, METC, Sandia Laboratories, CER Corporation, and industry were present.

The primary purpose of the meeting was to agree on a well site for the Multi-Well Experiment and review the preliminary plans. CER had investigated a number of potential sites, but had narrowed the site selection to three locations:

Exxon Vega Site	Sec 28, T9S, R93W, Mesa County, Colorado
Union Oil Company	In the Buzzard Creek Unit, 2 miles north of Exxon site
Northwest Exploration Company	Sec 20, T6S, R94W Garfield County, Colorado

The latter site was recommended by CER based upon their studies.

After a review of the geology and well control data, the Northwest Exploration Company site was confirmed as the most suitable, not only from a geologic standpoint but also from a year around operational basis. The Exxon Vega site was to be considered as a potential back up site in the case that the primary site was found to be unsuitable during the early phases of the MWX operation. CER is now meeting with Northwest Exploration to obtain the necessary legal agreement so that operations can start as soon as possible. No problems are anticipated in these negotiations. Upon agreement, various operating and drilling permits will be sought. It is believed that drilling of the first well can begin this summer.

The well drilling plans, logging and formation evaluation plans were also reviewed by CER Corporation personnel. Some concern was expressed for the effects on the formation from the fluids which were to be used after the oil-based coring operation. Further consideration of this problem will be made.

Sandia presented the MWX core plan and the stress testing plans for MWX 2. The review panel recommended implementation of the planned core gamma activity and felt that slabbing the core would be necessary for a high quality lithologic description and photographic documentation.

Dr. David Van Alstine of Sierra Geophysics made a presentation of paleomagnetics for possible use in making rough core orientations and determining geologic time of deposition. It was felt that a pilot study, perhaps with appropriate core from the USGS core library, would be useful for an initial display of this technique.

In other MWX-related activities during March:

1) The MWX program plan was distributed in early March. This plan is loose-leaf notebook format and will be continually updated as planning and progress permit.

2) A. R. Sattler visited the Colorado Geological Survey on March 5, 1980, in which further details of their participation on the MWX program, chiefly for coal analyses, were discussed. They also described the coal beds which may

be expected at the MWX site. Finally, additional relevant geologic data in the area of the site was obtained for CER and Sandia.

3) A. R. Sattler visited Core Laboratories on March 11, 1980, in which equipment for slabbing of core was discussed, and their core gamma apparatus was inspected.

4) A. R. Sattler made two short visits to the USGS on March 7 and 20, 1980, to discuss composition and isotope anaysis of desorbed gases and minerological analyses of MWX core. Permission was given to obtain core from the USGS library for study of invasion problems and petrography relevant to MWX.

5) A. R. Sattler made a visit to CER on March 17, 1980, to discuss pressure coring, invasion, and log-core correlations. A special field coring seminar was presented then to CER by Diamond Oil Well Drilling Co. personnel. Problems unique to coring in the Rocky Mountains were discussed.

6) A. R. Sattler made a short visit to Intercomp March 20, 1980, The MWX core program, including revisions made during continuing discussions with Core Laboratories personnel, was reviewed.

7) Additional Sandia help was arranged in the following areas: (a) fielding help in the areas of pressure coring and desorption of gases, (b) mechanical design help for the downhole shut-off tool, and (c) construction of a field core gamma apparatus with special detectors and a core conveyor belt.

III. Other Activities

1) Two papers were prepared for the 1980 SPE/DOE Symposium on Unconventional Gas Recovery in Pittsburgh, PA: "In Situ Evaluation of Several Tailored-Pulse Well-Shooting Concepts," by R. A. Schmidt, N. R. Warpinski, and P. W. Cooper, and "In Situ Stresses: The Predominant Influence on Hydraulic Fracture Containment," by N. R. Warpinski, R. A. Schmidt, and D. A. Northrop.

3) A paper was prepared for the 21st U. S. Symposium on Rock Mechanics, Rolla, MO, entitled "A Microcrack Model and Its Significance to Hydraulic Fracturing and Fracture Toughness Testing," by R. A. Schmidt.

4) H. M. Stoller, C. L. Schuster, and D. A. Northrop participated in a review of Sandia activities within DOE's Unconventional Gas Recovery Program for M. Adams, DOE/Oil and Gas in Morgantown, WV, March 11-12, 1980. A preview of the WGSP portion was held for H. C. Johnson, BETC, in Denver, CO, on March 5, 1980.

5) D. A. Northrop presented aspects of Sandia's Unconventional Gas Recovery Program to Harry Perry (Resources for the Future) and Wade Watkins (Acting Associate Deputy Assistant Secretary for Oil and Gas Technology) in Albuquerque, NM, on March 17, 1980.

UGR FILE #8

Sandia Laboratories
Albuquerque, New Mexico 87115

RS 4733/008

ENHANCED GAS RECOVERY PROGRAM

MONTHLY INFORMATION LETTER - August, 1980

HIGHLIGHTS

- A fracture orientation experiment was conducted with Shell in their Diatomite formation west of Bakersfield, CA.
- Mineback of the experiment and access drifts have been completed and the region determined to be satisfactory for the future fracture mechanics in situ experiments.
- Three studies have been initiated: (a) laboratory determination of the crack-tip process zone, (b) detailed petrographic characterization of a Mesaverde tight gas sand lens and surrounding shale, and (c) determination of oil-based drilling mud invasion in support of the Multi-Well Experiment.

I. EGR Instrumentation and Diagnostic Program

A. Hydraulic Fracture Characterization

Between August 13, 1980 and August 21, 1980 nine intervals were hydraulically fractured in a well in the South Belridge Field, Kern County, California for the Kernridge Oil Company. Sandia National Laboratories provided the Borehole Seismic System for monitoring seismic signals on five of the treatments in an effort to determine quality of seismic signals generated by fracturing diatomaceous earth and to determine fracture orientation if the signals were present.

The Borehole Seismic System was implanted just below the treatment interval and then a set of three near surface explosive charges were detonated for orientation purposes. In between each shot background noise level was recorded. The formation was then hydraulically fractured and shut in immediately after breakdown. Any seismic activity that may have occurred was recorded for ten to twenty minutes while the well was shutin. This was followed by a pre-pad and a pad pump each of which was followed by a quiet period in order to record seismic activity generated by the induced fracture.

Table 1 shows the stages, zones and pumping data for which the Borehole Seismic System was used. During Stage A there were a number of lubrication leaks and a BOP failure. The Borehole Seismic System leaked the first time it was downhole. A backup unit was placed into service but a connector broke. This resulted in the loss of the capability of recording all three geophones. The two horizontal geophones were recorded which will still provide azimuth information but any vertical

height information is lost. A hydraulic packoff unit was used on the lubricator which leaked somewhat. This was replaced by a grease injection unit on the remaining stages. A tape recorder malfunction on Stage A produced a recording that will require extensive playback procedures in order to recover the data.

During Stage D a marsh marine connector leaked which resulted in the geophone amplifiers being forced off center. This results in a loss of dynamic range but it is felt that reasonable signal analysis can be obtained. For the remaining stages (G, H, and I) the geophone amplifiers were ac-coupled and no further problems were encountered.

Table 2 summarizes the status of signal reception by the Borehole Seismic System as well as indicating position. The high noise level for Stage A prevented any signal detection and is in all likelihood due to the leaking hydraulic packoff unit. The high noise level observed during Stages D, H and part of I also prevented signal detection following the pre-pad and pad. The source of this noise is unknown; however, it is probable that the noise was produced by the bridge plug leaking.

Data analysis has not begun and will require a long time period due to other scheduled tests. However, preliminary analysis on some of the data will be started very shortly in order to determine the quality of the signals generated in this type of formation.

The data for the Big Mineral Creek experiment with Shell has been further analyzed and is plotted in Figure I-1. The seismic signals received in the offset well Unit 210 during the main fracture were analyzed for height as well as orientation and then projected onto a plane N37°E to S37°W. This offset well was located 547 ft south and 106 ft west of the treatment well Unit 343. Only the lower solutions are plotted and even these indicate a vertical fracture growth upward of more than 500 ft. Analysis of this possibility is continuing as this is a large departure from the planned fracture height.

A mathematical analysis of the hydrophone system has been initiated in order to determine pulse rise time capability and, under various signal-to-noise ratios, determine the accuracy in measuring the difference in arrival time of two different hydrophone signals. The electronics in the system basically consist of a pressure transducer, a high gain amplifier, which contains a low pass filter, and a frequency modulation (FM) transmission system used to transmit the information to the surface recording equipment. The approach being taken is to analyze the condition of the signal at the output of the high gain amplifier and then determine the effect that the FM system has on passing the signal to the surface recording device.

STAGE	ZONE	TREATMENT INTERVAL	BREAKDOWN PRESSURE	BREAKDOWN ISIP	VOLUME PRE-PAD	PAD
A	Brown Shale	2660-2710	1600	500	350	238
D	Brown Shale	1930-2040	1600	320	300	357
C	Diatomite	1320-1460	500	370	211	476
H	Diatomite	1050-1270	400	200	220	595
I	Diatomite	790-1000	370	150	225	595

TABLE I

NUMBER OF SIGNALS

STAGE	GEOPHONE DEPTH	BACKGROUND	BREAKDOWN	PREPAD	PAD
A	2725	2	3	Note 1	Note 1
D	2056	2	7	61	Note 1
G	1478	10	73	68	40
H	1257	1	0	49	Note 1
I	1020	0	0	25 Note 2	17

1) High Noise Level

2) Several minutes of high noise level prevented signal detection.

TABLE II

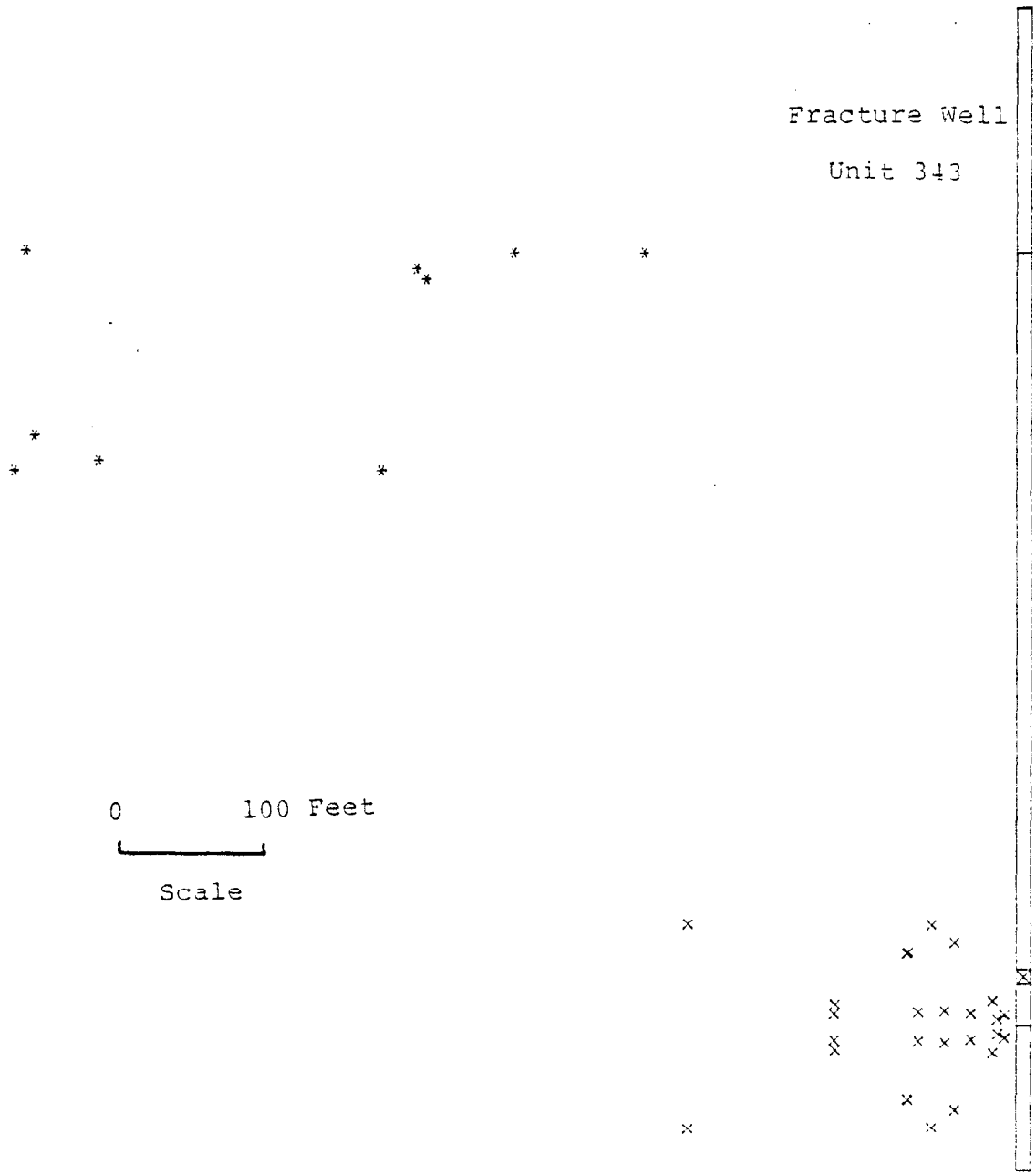

Figure I-1 Plan View of Seismic Events

B. Borehole Resistivity System

The agreement between the one and two-dimensional models was improved by taking a larger number of elements (in the 2-D finite element model) in the direction of large field gradients (radially) rather than along the probe. Figure I-2 shows agreement to within 2%.

The ridge regression inversion algorithm was tested successfully on several simple nonlinear systems of equations. The algorithm is now being integrated with the 1-D forward resistivity solution.

C. Electromagnetic Impedance Sonde (DE-AT19803C10208.501)

(1) Laboratory Work

Work is continuing on the digitization of pore pictures (see last monthly report). From these data it is hoped that parameters useful in the modeling of the electromagnetic, the nuclear magnetic resonance and the fluid flow responses of reservoir materials can be obtained. For example, the orientation of the pores in a rock is not necessarily isotropic, and such an anisotropy can influence the electromagnetic response as well as the fluid flow permeability.

In thin section experiments, a blue epoxy is injected into the pore structure, and thin section photographs obtained by the USGS from CIGE-21 core specimens shows a variation in the depth of the blue coloring. This color variation can be caused by a depth effect, that is deeper pores are a more dark shade of blue, or by a dilution of the epoxy by clay fingers protruding into the pore from its walls. It is possible to include this information in the digitization process. Numbers are given to a pore based on the depth of the blue color in the pore; for instance, numbers would correspond to light blue, medium blue, and dark blue. These numbers then allow pores of different colors to be excluded from the calculations to note the effect. For example, for one sample, if all the pores are included the calculated porosity, which is based on a statistical model, is more than one and a half times too large. If pores of the lightest blue are not counted, however, the porosity approaches that of the measured value. Work is continuing on the pore pictures to determine what other useful parameters may be measured.

(2) Sonde Modeling

This month has successfully implemented the fast-convergence integrations for the generalized N-Zone solution of coaxial-coil logging. After having introduced additional contributions to the previously incomplete solution, preliminary results on two spot-checks have indicated a consistent reduction to both the homogeneous and two-zone solutions.

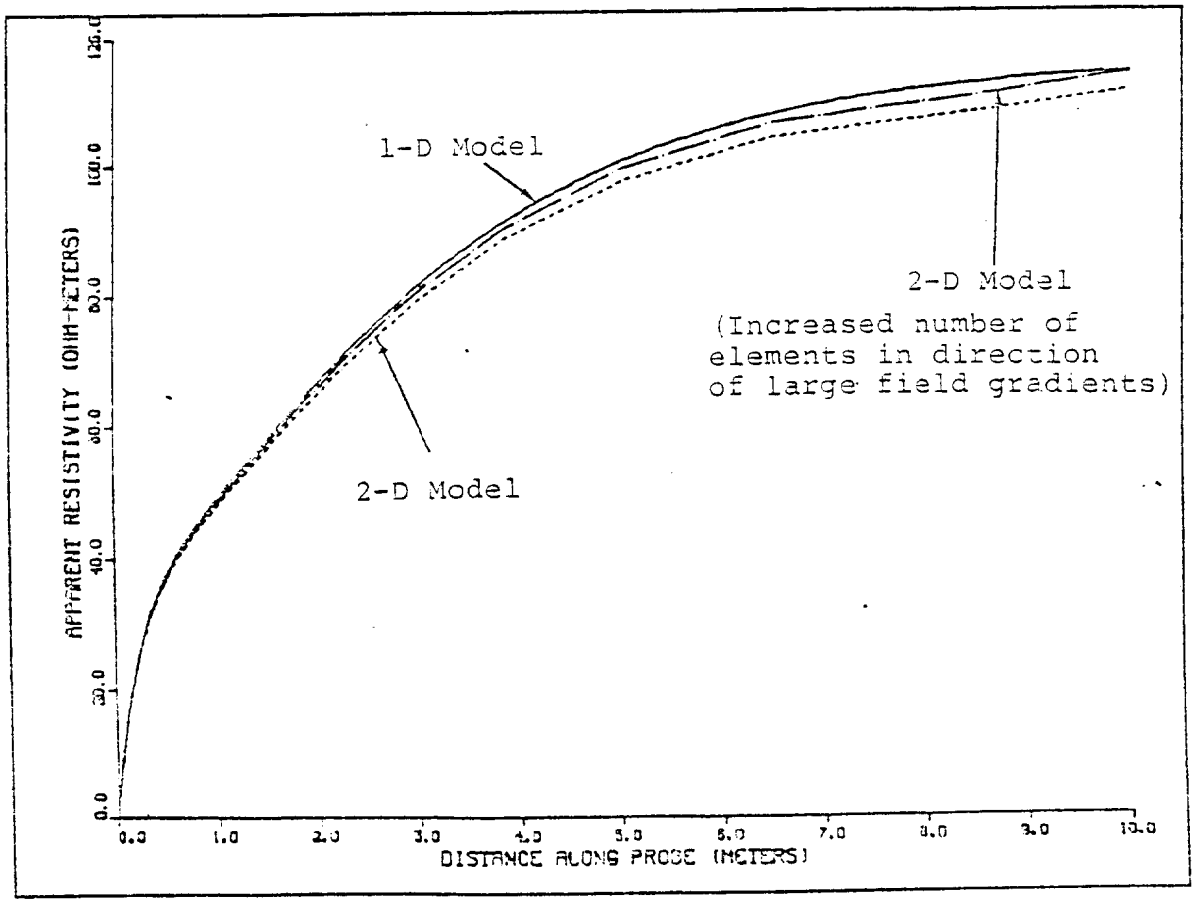

Figure I-2 Comparison of 1-D and 2-D Models

More extensive checks are in progress. The final goal of this generalized solution is to enable a comprehensive study on boundary-layer effects including sonde geometry, borehole fluid, and invaded-formation profile. The complexity of computation seems finally being overcome and useful applications are planned for the coming month.

II. Stimulation Research for Enhanced Gas Recovery

A. Hydraulic Fracturing

Sandia Laboratories is conducting both basic and applied research to aid in the development of massive hydraulic fracturing as a practical, economic technique for exploiting the resources of the tight gas sands and Devonian shales. Types of research being performed include in situ testing of hydraulic fracturing theory and technology, modeling of hydraulic fracturing behavior, and laboratory testing. The in situ testing is being performed at DOE's Nevada Test Site in a tunnel complex driven through volcanic ash-fall tuff under ~ 1,400 ft of overburden. This site provides the facilities and equipment for mineback of created hydraulic fractures for direct observation, a capability of determining in situ stresses and obtaining rock samples for testing in regions of interest, and in direct knowledge of the "reservoir" parameters and structure (i.e., permeability, porosity, location of faults, fractures, etc.). Modeling efforts involve many aspects of fracturing, from details of the processes occurring at the fracture tip to numerical codes describing the fluid mechanics/rock mechanics of the entire fracture. Laboratory testing includes the determination of rock properties and the conducting of small scale experiments.

(1) Formation Interface Fracture Experiment

Measurement of the vertical stress distribution, which is the final work associated with this experiment, has been delayed until September for equipment modifications.

(2) Fluid Mechanics/Proppant Transport Experiments

Hydraulic fracturing is recognized to be a complex interaction between rock mechanics and fluid mechanics considerations. In general, however, the fluid mechanics aspects of fracturing are much less understood than the global rock mechanics considerations such as dilation of the crack under a pressure load. The important fluid mechanics processes associated with fracturing can be broadly divided into two categories. The first is basic phenomena, such as the pressure distribution and the width in a propagating fracture. Experiments to measure the pressure and width at various locations in a fracture during propagation are presently being planned. The second area is proppant transport and the resultant conductivity.

Mineback of the experiment and access drifts were completed in August. The orientation of the in situ stresses in this region were ~ 20° different than expected but still suitable for the experiment. Work on the preliminary fluid mechanics experiment will begin in September or October.

(3) In Situ Stress Measurement by Hydraulic Fracturing Through Perforations

Mineback experiments have shown that the most important factor governing containment of hydraulic fractures is differences in the minimum principal in situ stress. Material property differences and interface characteristics (friction) appear to be insignificant. In the Multi-Well experiment in the Piceance Basin, the distribution of minimum in situ stress will be measured through the Mesaverde Sequence. A large number of in situ stress measurements will be obtained by conducting minifracs through perforations. In order to be certain that performing these tests through perforations will yield accurate, reliable data, an experiment will be conducted in G-tunnel to compare fracturing through perforations and in an open hole.

Five zones in a second cased hole have been perforated with four perforations in the farthest zone and two perforations in each of the other four zones. Orientations of the perforations are staggered horizontally and vertically. Fracturing of these five zones was attempted in August. The zone with four perforations (60' in hole) broke down at 1925 psi, considerably higher than expected (stress cage ?) with a fracturing pressure of about 1200 psi and a shut-in of 930 psi. This shut-in pressure is slightly higher than expected (800 psi), but the value of the minimum principal in situ stress will not be known for sure until several minifracs are conducted open-hole in a nearby (6-8 ft) wellbore. A variable flow rate test showed that the pressure drop through the perfs was insignificant. The second zone (50' in hole) had two perforations and required 2400 psi to break-down and the fracturing pressure remained near 2400 psi. This was clearly due to inadequate perforating and no clear shut-in pressure was seen.

This, of course, shows that good perforating is the foremost requirement if useful, accurate stress data is to be obtained. No further zones were fraced and an attempt will be made to reperforate the other three zones and develop a technique for doing this routinely and adequately at the test site. Perforators, which were supposed to penetrate 7.5 inches into the formation with a 0.5 inch diameter hole, apparently barely ruptured the casing. This will be further investigated.

(4) Rock Mechanics - A

A model of stress distribution surrounding the crack tip of a finite internally pressurized crack approaching a material interface has been extended to include a realistic internal pressure distribution. The realistic distribution causes a significant decrease in the stress intensity factor when compared to the uniformly pressurized case (Fig. II-1).

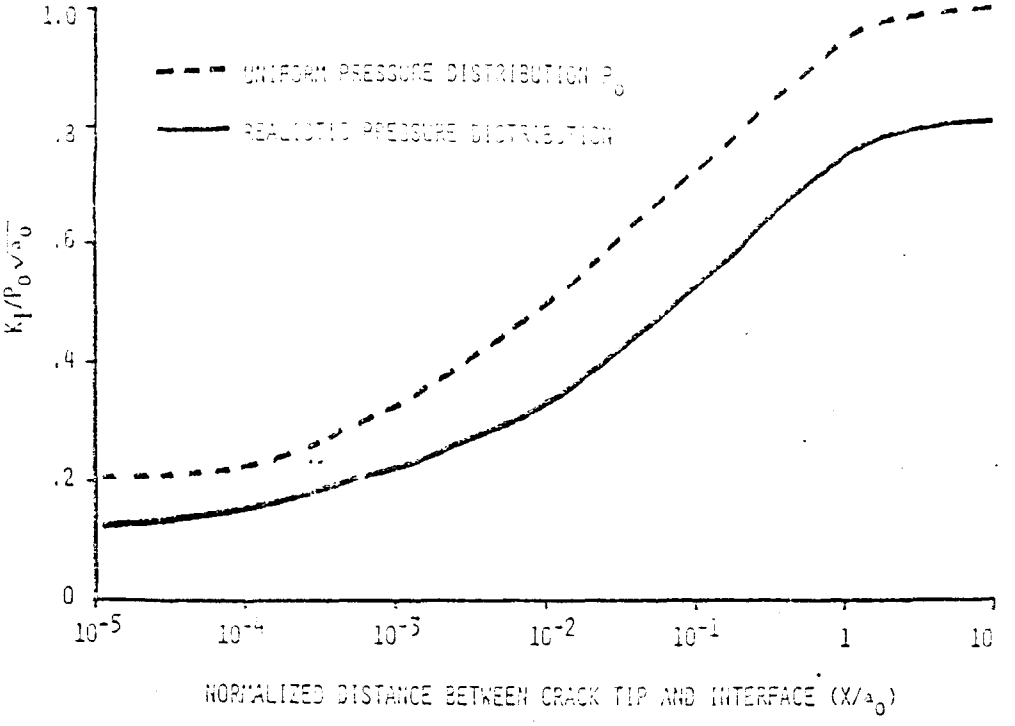

Figure II-1: Stress intensity factor (K_I) for a crack approaching an interface normalized by K_I for a homogeneous material. Stress intensity factors for a crack with a realistic pressure distribution is substantially less than K_I for a uniformly pressurized crack. (See June newsletter for nomenclature).

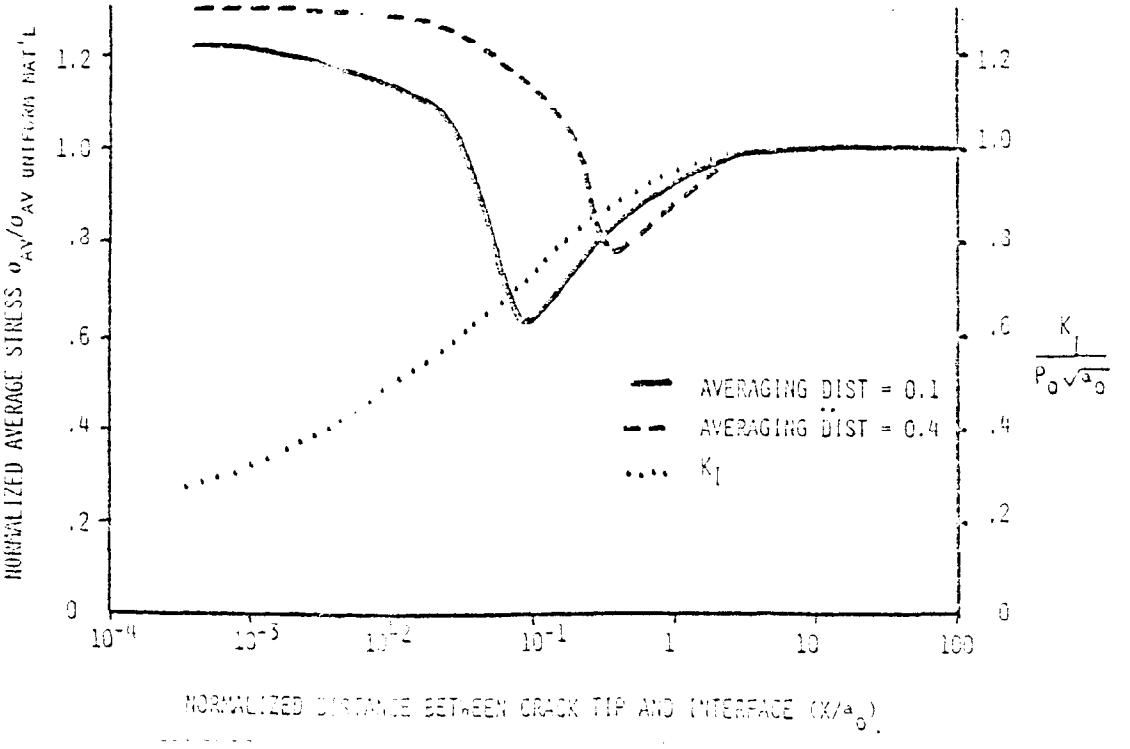

Figure II-2: Average stress fracture criteria compared to stress intensity factor (K_I). For four different averaging distances, the minimum value of the average stress criteria is always greater than that for K_I. If the averaging criteria is an appropriate criteria for fracture growth, these results indicate that a high modulus material may not severely restrict fracture growth as indicated by the K_I criteria.

The stress intensity factor is customarily used as a fracture criteria in homogeneous materials. However, it is not clear that this criteria can be applied to a fracture approaching an interface. An alternative criteria is the average stress over a fixed distance beyond the crack tip. This new criteria gives the same results as the stress intensity factor for homogeneous materials, but it may be applied to cracks approaching an interface as well. For several averaging distances, Fig. II-2 shows the variation in the average stress as a crack approaches an interface. Comparison of the average stress to the stress intensity factor (K_I) indicates that the stress averaging criteria does not inhibit crack growth as severely as the stress intensity factor for distances very close to an interface.

(5) Rock Mechanics - B

The mechanism of crack growth determines the extent of the near crack surface damage that is produced as the crack propagates. The extent of this process zone damage is one of the factors that determines the permeability of the fracture surface and, thus, has a direct bearing on the sizing of a hydrofracture to achieve the desired production rate. In addition, the existence of a process zone provides a mechanism by which cracks can propagate across discrete interfaces between two dissimilar materials. In a joint study with the University of Maryland (D. Barker), we have begun to examine the process zone and to determine its size and shape under simple loading conditions.

In this study, the crack-tip region is examined under load using a surface replicating technique. At various stages of the loading history, an acetate film replica is made of the polished surface of the fracture specimen in the region where the crack intersects the surface. The replicas are then examined using the scanning electron microscope (SEM) to determine the size and shape of the crack-tip process zone. To date, both monotonic loading and cyclic fatigue loading histories have been examined. Preliminary results from the SEM work indicate that the process zone is visible ahead of the crack tip, but apparently not connected to it. This is most likely due to the fact that the crack front is not uniform through the thickness of the specimen and, thus, the measurements made on the surface do not reflect the true three-dimensional character of the problem.

In the next month, measurements of process zone size and shape will be made for the two loading histories. Once this is completed, the effect of hydrostatic pressure on the process zone size will be considered.

(6) Petrology and Geochemistry

Petrographic work has been started on samples of Mesaverde core donated by Mountain Fuel Supply Company. These samples were selected from portions of the core that contained a sandstone-shale contact. It is thought that over geologic time these shales within and adjacent to sand lenses may act as permeability barriers to upward-diffusing interstitial waters. If this is so, then we might expect to see greater evidence of diagenesis at the sandstone-shale interfaces. In fact, this appears to be the case. Carbonate cementation is much more pervasive in these zones and calcite replacement of detrital grains (frequently, plagioclase feldspars) is much more common. Often, these carbonate, replaced grains are surrounded by calcite overgrowths and less frequently, quartz overgrowths are observed. Although this study has only just begun, these preliminary observations suggest that diagenetic alteration in the sand lenses may be analogous to the silicons "hard bands" in the NTS tuffs discussed in the July newsletter.

B. Dynamic Fracturing

Dynamic stimulation techniques that produce multiple fracturing in a wellbore are being investigated for enhanced gas recovery. Multiple fracturing appears to be especially promising for stimulating naturally-fractured reservoirs, such as the Devonian shales, since this may be the most effective technique for connecting a wellbore to a pre-existing fracture network. The emphasis in this research study is on tailored-pulse loading techniques that minimize wellbore damage and maximize fracture growth by gas penetration. The focus in this program includes in situ testing at NTS and the associated modeling and analysis.

A revised proposal for the two-year development of the high energy gas fracturing concept was prepared and sent to John C. Sharer, Gas Research Institute.

C. Multi-Well Experiment

(1) General

The Multi-Well Experiments objectives are: 1) to obtain a comprehensive characterization of a tentacular, low-permeability reservoir in the Western United States and 2) to apply and evaluate state-of-the-art and developing technology for the recovery of gas from this reservoir.

No decision has yet been made by Superior Oil Company concerning the proposed agreement for the use of Superior's lease (Section 34, Township R94W, 6S) as a possible MWX site. Superior has indicated their decision will be available in September.

(2) Core Program

A. R. Sattler, L. W. Teufel and R. W. Ostensen visited IGT on August 14-15, 1980, with the prime purpose of reviewing IGT's contract for the Western Gas Sands Program. As most of the MWX Core Advisory Committee was also present, topics of discussion included:

(a) The importance of determining any deviation from the net stress hypothesis in tight gas sands;

(b) the approach to water saturation measurements in tight gas sands by IGT through the generation of a capillary pressure curve; and

(c) the preliminary work by IGT in consideration of directional permeabilities.

Revisions of the core gamma apparatus have been made based upon several inputs. Some additional design details will be made and it will be ready for fabrication.

The first run of the formation and core drilling mud invasion study was made this month. Dry Tennessee sandstone core was subjected to oil base mud, 150° F, no additives, for four hours at mud pressure of 250 psi. Invasion of slightly over one inch was observed, and the invasion zone in turn was divided into three nearly equal bands, only the middle one fluoresced. A preliminary interpretation is that the intermost zone (greatest invasion) is water, the middle band is oil, and the outer band of the rock (least invasion) seems plugged with some material, asphaltines or paraffin-like material. The oil-based mud which is being used is similar to what will be used on MWX and it has 10% water dispersed throughout. More analyses will be made on these zones. Additional runs will be made to scope the problem.

(3) Reservoir Analysis

The lengths of time needed to perform the well flow and pressure tests desired in the Multi-Well Experiment have been examined. For very low permeability formations, these times may become excessive.

For each promising sand lens, a sequence of four types of pressure tests is to be run: 1) drawdown and pressure build-up of the individual wells; 2) a well-to-well test; 3) a fracture-to-well test, combined with a fracture drawdown; 4) a pressure build-up test in the fractured well.

The testing time is dominated by the well-to-well tests. A multipulse, or pressure signature type of well-to-well test, is only feasible for higher permeabilities (30uD or more). At lower permeabilities, straightforward interference testing is recommended to reduce testing time. Below 3 microdarcies, the well-to-well testing time is too long to be practical. (However, it may be feasible to use a well-to-well tracer technique which would provide data in the interwell region of the gas porosity times the formation height. This possibility will be explored further at a later time).

The sand lenses hit in the Multi-Well Experiment are likely to have a range of permeabilities. If most of the lens are in the 10 to 30 microdarcy range, an average testing time of 1½ months per lens is likely. Then eight lenses could be tested in one year. However, if the permeability range is lower, say 3 to 10 microdarcies, the average testing time could stretch to three or four months per lens. Then eight lenses would need 2 to 2½ years for testing, and even this would involve some sacrifice of the quality of the data for well-to-well tests. The possibility of long test times will have to be kept in mind in our program planning.

(4) MWX Model

An engineering-economic systems analysis of gas production from tight sand lenses has been initiated. It will combine a geologic model, stimulation model and economic model to examine the sensitivity of gas production to various parameters and to identify important factors requiring analysis.

As part of this effort, a number of computer subroutines of reservoir behavior have been written and debugged; their purpose is to calculate gas production rates over time for three situations: 1) production from a massive hydraulic fracture (MHF) well in a sand lens with the fracture running down the length of the lens and contained within the lens; 2) production from an MHF well with the fracture running perpendicular to the lens axis breaking out of the lens and breaking back into neighboring sand lenses; 3) production from a gas-fraced multiple radial fractures well in a sand lens.

The first calculation uses a Fourier series solution for the time-dependent distribution of the real gas pseudo-pressure across the lens. The second calculation uses the standard equation for linear flow to a fracture. The third calculation uses a system of image wells to simulate the sand lens boundary conditions. All of these calculations neglect flow resistence in the fracture.

These routines will be combined with analyses of drilling and well treatment costs, etc., to provide a parametric study of economic performance vs. reservoir and fracture characteristics.

III. Other Activities

(1) D. A. Northrop, N. R. Warpinski, J. A. Clark, R. A. Schmidt, L. W. Teufel and W. E. Warren attended the SPE Forum Series, "Earth Stresses: Their Relation to Petroleum Production" at Colorado Mountain College, Glenwood Springs, Colorado, August 3-8, 1980. Much of Sandia's enhanced gas recovery activities and results were presented during this topical meeting. Sandia activities discussed included: NTS mineback experiments demonstrating that stress is the dominant parameter governing fracture growth, finite element modeling of earth stresses, analysis of packer-induced stresses, the Multi-Well Experiment and its emphasis upon stress, novel stress measurement techniques, and stress measurement by hydraulic fracturing.

(2) D. A. Northrop conducted a tour of G-tunnel and the in situ fracturing experiments on August 12th for the following individuals: John L. Gidley, Exxon Company USA; Alex B. Crawley, U.S. DOE; and Adnan Gumustas and Selcuk Gurpinar of the Turkish Petroleum Corporation.

(3) Henry's Law calculations of methane solubilities at depth in marine sediments were made in response to a request by the USGS, Woods Hole, Maryland.

(4) James B. Jennings of the Bartlesville Energy Technology Center was given a tour of Sandia's electromagnetic laboratory on August 19. Methods of digitizing pore shape and size parameters from thin sections prepared by the USGS were discussed by Len Duda.